

LITHOGEOCHEMICAL AUREOLES TO IRISH MINERALISATION

by

GARY JOHN GRAY B.Sc.

.....oOo.....

Thesis submitted to the University of Strathclyde
for the degree of:

DOCTOR OF PHILOSOPHY.

.....oOo.....

Department of Applied Geology,
University of Strathclyde,
Montrose Street,
GLASGOW,
Scotland.

February 1986

.....oOo.....

**PAGE NUMBERING AS
ORIGINAL**

LIST OF CONTENTS.

Abstract..... i

List of Figures and Tables.....iii

Chapter One - Introductory Chapter..... 1

Chapter Two - Analytical Techniques.....27

Chapter Three - Regional Analytical Data.....43

Chapter Four - Core Geochemistry.....87

Chapter Five - Sample Composition and Inhomogeneity.....105

Chapter Six - Discussion and Genetic Implications:

 Part One - Depositional Processes.....122

 Part Two - Post-Depositional Modification.....192

Chapter Seven - Litho-geochemistry in Exploration.....240

Chapter Eight - Conclusions.....267

Appendix I - Analytical Techniques.....A1

Appendix II - Machine Operating Conditions.....A8

Appendix III - Hanging Wall and Footwall Profiles.....A9

Acknowledgements.....x

References..... xi

LITHOGEOCHEMICAL AUREOLES TO IRISH MINERALISATION.

ABSTRACT.

Examination of the Mn, Fe, Zn and Mg content of host limestones around a number of Irish base metal deposits (Silvermines, Tynagh, Ballinalack, Keel, Moate, Moyvore, Ballyvergin, Aherlow, Courtbrown and Mallow) has shown that all the deposits studied, with the possible exception of Mallow, are accompanied by elevated levels of Mn and Fe in nearby Waulsortian and equivalent limestones. Zinc is also enriched more locally around most of these deposits.

Background values of Mn and Fe are less than 100 ppm in the southwest of the country, rising to over 250 ppm in the north Midlands, and below 10 ppm throughout for Zn.

The enrichments are interpreted as the products of hydrothermal exhalation onto the Waulsortian seafloor, with primary incorporation of trace elements into carbonate sediments.

Careful sampling of host rock is required to avoid secondary (or epigenetic) contamination, or masking by random lithological variation, and analysis is by atomic absorption spectrophotometry, following dissolution of powdered samples in 2M hot acetic acid for 1 hour.

Tynagh has the best developed aureole, with Mn and Fe enriched to 6 km distant and Zn (and Sr) to 5 km, of which over 80% of samples contain anomalously high levels within these limits. Enrichments around the other deposits extend to between 2 and 6 km distant, and are best developed around Ballinalack, Silvermines, Aherlow and Courtbrown, and relatively poorly developed around Ballyvergin, Keel, Moate and Moyvore.

Vertical profiling of boreholes at Silvermines indicates that peak values occur near the base of the Waulsortian, in the same stratigraphic position as the stratiform ore horizon. Enrichments of Mn, Fe and Zn extend up to 100 m into the hanging wall above the ore horizon, and are also present in the immediate footwall sediments. Possible weak basal enrichment of mudbank limestone is also indicated at Keel, but no stratigraphic control is displayed within the host rocks at Ballinalack or Tynagh.

The presence of apparently primary enrichments of Mn and Fe in Waulsortian limestones near to epigenetic deposits at Aherlow, Moate, Moyvore and Ballyvergin indicates that emplacement of sulphide was approximately contemporaneous with mudbank growth.

In the case of Silvermines, severe post-depositional modification (including recrystallisation, dolomitisation, pressure solution and stratigraphic attenuation) has considerably altered the original primary trace element patterns, possibly enhancing the absolute levels of Mn and Fe enrichment in much of the hanging wall dolomite breccias. The extent of diagenetic modification around the other deposits is less well known but probably much less severe.

Application of lithogeochemistry is most useful in early reconnaissance stages of exploration, allowing recognition of areas of local enrichment from possible hydrothermal sources. Stratigraphic profiling of exploration boreholes may also highlight favourable horizons within a sequence.

As part of this study, reconnaissance lithogeochemistry in a number of areas of Waulsortian outcrop has led to the discovery of Pb-Zn mineralisation associated with possible exhalative centres in north County Cork and the Nenagh area in County Tipperary.

LIST OF FIGURES AND TABLES.

Chapter One - Introductory Chapter.

Following page

Figure 1.1 Geology and Carboniferous palaeogeography of Ireland.....6
Table 1.1 Subdivisions of the Dinantian in Ireland.....6
Figure 1.2 Selected stratigraphic profiles from the Irish Lower Carboniferous.....7
" 1.3 Stratigraphic column from the Nenagh area, Co. Tipperary.....7
" 1.4 Simplified model of sediment-hosted, submarine exhalative system.....10
" 1.5 Mid-Dinantian palaeogeography of part of Western Europe.....15

Chapter Two - Analytical Techniques.

Figure 2.1 Summary of laboratory procedures.....28

Chapter Three - Regional Analytical Data.

Figure 3.1 Location of sample areas.....43
Table 3.1 Sample numbers and source.....43
" 3.2 Median values of Mn, Fe, Zn and Mg in all distal outcrop samples.....43
Figure 3.2 Frequency distribution of (Mn+Fe)/2 in all samples.....43
" 3.3 " " " Mn and Fe in Kerry samples.....43
" 3.4 " " " Mn and Fe in all distal outcrop samples.....44
" 3.5 " " " Zn in all distal outcrop samples.....45
" 3.6 " " " Mg in all distal outcrop samples.....45
" 3.7 " " " (Mn+Fe)/2 in all distal outcrop samples.....45
" 3.8 Comparison of Mn and Fe frequency distribution in all distal outcrop samples.....46
Table 3.3 Comparison of means and standard deviations in distal and proximal sites.....46
" 3.4 Median values of Mn, Fe and (Mn+Fe)/2 for each individual area.....46
Figure 3.9 Regional variation in median Mn, Fe and (Mn+Fe)/2 values.....46
" 3.10 Location of Tynagh mine, Co. Galway.....47
" 3.11 Geological sequence at Tynagh mine.....48
" 3.12 North-south geological section of Tynagh deposit.....48
" 3.13 Simplified geology of the Tynagh area, showing sample sites.....50
" 3.14 Manganese content of Waulsortian Limestones around Tynagh mine.....50
" 3.15 Iron " " " " " " "50
" 3.16 (Mn+Fe)/2 " " " " " " "51
" 3.17 Zinc " " " " " " "51
" 3.18 (Mn+Fe)/2 " " " " " " " (outcrop only).....51
Table 3.5 Percentage anomalous values in core and outcrop around Tynagh mine.....51
Figure 3.19 Contoured values of (Mn+Fe)/2 in Waulsortian Limestones around Tynagh mine.....52
" 3.20 Areal distribution of zinc values in " " " " "52

Figure 3.21 Ratio of Mn:Fe in Waulsortian Limestones around Tynagh mine.....52

" 3.22 Strontium content of " " " " "52

" 3.23 Areal distribution of Mn:Fe ratio in Waulsortian Limestones around Tynagh mine.....53

" 3.24 " " " Sr values " " " " " "53

" 3.25 Comparison of Mn and Fe contents of samples from Tynagh area.....53

" 3.26 Simplified geology of Nenagh-Silvermines Basin, Co. Tipperary.....54

" 3.27 Geology of the Silvermines area.....55

" 3.28 Geology of the Silvermines deposits.....56

" 3.29 Outcrop sample locations, Nenagh-Silvermines Basin.....57

" 3.30 (Mn+Fe)/2 content of Waulsortian outcrop samples around Silvermines deposits.....58

" 3.31 Manganese " " " " " " " " "58

" 3.32 Zinc " " " " " " " " "58

" 3.33 Areal distribution of (Mn+Fe)/2 in Waulsortian Limestones of Silvermines area.....59

" 3.34 " " " zinc " " " " " " "59

" 3.35 Contoured values of (Mn+Fe)/2 " " " " " " "59

" 3.36 " " " zinc " " " " " " "59

" 3.37 " " " manganese " " " " " " "59

" 3.38 " " " iron " " " " " " "59

" 3.39 " " " Mn:Fe ratio " " " " " " "59

" 3.40 (Mn+Fe)/2 content of borehole samples from Silvermines area.....60

" 3.41 Average (Mn+Fe)/2 content of each drill hole sampled, Silvermines area.....60

" 3.42 Zinc content of core and outcrop samples, Silvermines area.....60

" 3.43 Location of core and outcrop samples, Silvermines area.....61

" 3.44 (Mn+Fe)/2 content of ore horizon samples, Silvermines area.....61

" 3.45 Zinc " " " " " " " "61

" 3.46 Manganese " " " " " " " "61

" 3.47 Iron " " " " " " " "61

" 3.48 Mn:Fe ratio in " " " " " " "61

Table 3.6 Median values and percentage of anomalous samples, Silvermines area.....61

Figure 3.49 Geology of the North Midlands area.....62

" 3.50 Geology of the Ballinalack area, Co. Westmeath.....64

" 3.51 Geology of the Ballinalack deposit.....65

" 3.52 Comparison of Mn and Fe content of Ballinalack samples.....67

" 3.53 Frequency distribution of (Mn+Fe)/2 in Ballinalack samples.....68

" 3.54 " " " zinc " " " "68

" 3.55 Areal distribution of (Mn+Fe)/2 in Waulsortian limestones around Ballinalack.....68

" 3.56 Location of borehole samples at Ballinalack.....68

" 3.57 Trace element distribution in Ballinalack borehole samples.....68

Figure 4.21 Geochemical profile of X.R.F. data from borehole 77/1 , Silvermines.....97

" 4.22 " " " " " " " " V20 "97

" 4.23 " " " " " " " " G217 and B139 "97

" 4.24 " " " " " " " " V19 and B144 "97

" 4.25 Ratio of acid-soluble to total Mn and Fe in boreholes G217 and V1, Silvermines.....98

" 4.26 " " " " " " " " " " B139 "98

" 4.27 " " " " " " " " " " V19 "98

" 4.28 " " " " " " " " " " B144 "98

" 4.29 " " " " " " " " " " V20 "98

" 4.30 " " " " " " " " " " 77/1 "98

" 4.31 " " " " " " " " " " around the Silvermines deposit.....99

" 4.32 Location of boreholes profiled in Figures 4.33 to 4.36, Ballinalack.....100

" 4.33 Vertical geochemical profiles of boreholes B91, B83 and B89 Ballinalack.....100

" 4.34 " " " " " " " " B64, B51 and B58 "100

" 4.35 " " " " " " " " B33, B11 and BN80/1 "100

" 4.36 " " " " " " " " B101,B100,B99,B98,B97,B80,B2,B75,B74.....100

" 4.37 Location of boreholes sampled at Keel, Co. Longford.....101

" 4.38 Vertical geochemical profiles of boreholes LF9, LF31, LF18, Keel.....101

" 4.39 " " " " " " " " K72, K31, K29 "101

" 4.40 " " " " " " " " K135, K136, LF43 "101

" 4.41 " " " " " " " " K156, K157, K158 "101

" 4.42 " " " " " " " " K162, K164, K163 "101

" 4.43 " " " " " " " " K175, K173, K176 "101

Chapter Five - Sample Composition and Inhomogeneity.

Table 5.1 Correlation matrix for Silvermines core data (X.R.F.).....106

" 5.2 " " " " " outcrop " "106

" 5.3 Statistics of X.R.F. data from Silvermines outcrop and core samples.....106

" 5.4 More statistics of X.R.F. data from Silvermines outcrop and core samples.....106

Figure 5.1 Comparison of geochemical profiles from boreholes LF18 and LF31, Keel.....110

" 5.2 " " " " " " " LF9 "111

" 5.3 Contrasting geochemical results from Silvermines core samples.....112

Table 5.5 Comparison of geochemical results from different sampling methods.....112

Figure 5.4 Geochemical comparison of hand-picked phases from inhomogeneous samples.....115

" 5.5 " " " " " " " " "115

" 5.6 Geochemical comparison of selected phases from inhomogeneous samples.....116

" 5.7 " " " " " " " " "116

" 5.8 Statistical comparison of selected phases from inhomogeneous samples.....116

" 5.9 Electron microprobe traverses of polished sections of inhomogeneous carbonates.....119

Table 6.1	Concentration of selected elements in various hydrothermal systems.....	123
" 6.2	Manganese concentrations in selected hydrothermal and experimental studies.....	123
" 6.3	Temperature and Mn content of brine waters at 21°N, East Pacific Rise.....	123
Figure 6.1	Manganese and iron concentrations above deep sea hydrothermal centres.....	136
" 6.2	Seafloor topography and outline of principal ore zones at Silvermines.....	139
" 6.3	Sketch map of Nenagh-Silvermines Basin.....	141
" 6.4	Comparison of zinc profiles in Silvermines footwall sediments.....	141
" 6.5	Outline of stratiform mineralisation and host rocks at Silvermines.....	146
" 6.6	Diagrammatic cross-section of Silvermines brine pool.....	146
" 6.7	Solubility and stability fields of common Mn and Fe compounds.....	148
" 6.8	Metal contents of sediments of the Red Sea floor.....	152
" 6.9	Origin of the metal enrichments of the Ballyvergin area.....	159
" 6.10	Simplified oxidation potential - pH diagrams for Mn and Fe.....	162
Table 6.4	Ionic radii and electronegativities of selected cations.....	179
" 6.5	Partition coefficients of various trace elements into CaCO ₃	179
Figure 6.11	Interacting parameters affecting primary trace element intake into CaCO ₃	183
" 6.12	Component phases of a typical stromatolite structure.....	183
" 6.13	Interacting parameters affecting chemical exchange during carbonate diagenesis.....	198
" 6.14	Flow diagram of principal trace element movements during carbonate diagenesis.....	198
Table 6.6	Measured Sr contents of various sedimentary carbonate components.....	199
" 6.7	Mean Sr contents of various Silvermines host rocks.....	199
" 6.8	" " " " " " Tynagh " "	199
Figure 6.15	Manganese and iron contents of carbonate components of limestones, Ballybeg Quarry,....	211
Table 6.9	Median values of Mn, Fe and Zn in Silvermines host rocks.....	212
Figure 6.16	Comparison between Na and (Mn+Fe)/2 contents of Silvermines host rocks.....	218
" 6.17	" " Na and Al ₂ O ₃ " " " " "	218
" 6.18	Variation in Na contents of Tynagh host rocks.....	219
" 6.19	Comparison between Na and (Mn+Fe)/2 contents of Kerry samples.....	219
" 6.20	" " " " " " " " North Midlands samples.....	219
" 6.21	Regional variation in Na content in Irish Waulsortian Limestones.....	220
Table 6.10	Mean Na contents of Waulsortian Limestones from various locations.....	220
Figure 6.22	Comparison of Waulsortian and equivalent thickness, Silvermines area.....	226
Table 6.11	Comparison of insoluble content, Mg content and thickness of Silvermines host rocks...	228
" 6.12	Analytical data from I.C.P. analysis of Silvermines host rocks.....	230
Figure 6.24	Sources and sinks of dissolved constituents during diagenesis of Silvermines host rocks.....	238
Figure 6.25	Summary of Mn behaviour in a shallow marine hydrothermal system.....	239

Figure 7.1	Manganese content of host rocks around Meggen deposit, Germany.....	244
" 7.2	Red marble localities and cross section of Irish Waulsortian shelf.....	251
" 7.3	Manganese and iron contents of red marble samples.....	252
Table 7.1	Median (Mn+Fe)/2 contents of red marble samples.....	252
Figure 7.4	(Mn+Fe)/2 litho geochemistry of Waulsortian outcrops in North Co. Cork.....	255
" 7.5	" " " " " " Co. Limerick.....	257
" 7.6	" " " " " " Co. Kerry.....	258
Table 7.2	Comparison of (Mn+Fe)/2 and Zn aureoles around each deposit.....	264

Appendix One - Analytical Tests.

Figure A.1	Comparison of weak acid extraction and X.R.F. results for Mn.....	A2
Table A.1	Results of overnight digestion of calcite and dolomite powders.....	A2
" A.2	Comparison of Mn extraction by various acid attacks.....	A2
" A.3	" " Zn " " " " " "	A2
" A.4	Comparison of Mn and Zn extraction and precision by various acid attacks.....	A4
" A.5	Percentage extraction of Mn, Fe and Zn after 1 hour leach.....	A4
Figure A.2	Temperature of reactants on sandbath during hot digestion	A5
" A.3	Release of Mn, Fe and Zn from impure carbonates, Silvermines.....	A5
" A.4	Release of Mg from Silvermines limestone samples.....	A5
" A.5	" " " " " dolomite samples.....	A5
" A.6	Release of Mn from Silvermines carbonate samples, 50°C leach.....	A5
" A.7	" " Fe " " " " " "	A5
" A.8	" " Zn " " " " " "	A5
" A.9	Comparison between Mn and Fe release, 50°C leach.....	A5
" A.10	Release of Mn from Silvermines carbonate samples, 90°C leach.....	A6
" A.11	" " Fe " " " " " "	A6
" A.12	" " Zn " " " " " "	A6
" A.13	Comparison between Mn and Fe release, 90°C leach.....	A6
" A.14	Precision levels of Zn for 90°C leach.....	A6
Table A.6	Initial analytical precision levels for Mn, 90°C leach.....	A7
" A.7	Analytical precision levels for Mn, Fe, Zn and Mg, 90°C leach.....	A7

Appendix Two - Machine Operating Conditions.

Table B.1	Operating conditions for A.A. analysis.....	A8
" B.2	Operating conditions for X.R.F. analysis.....	A8

Figure C.0	Key for Figures C.1 to C.15.....	A8
"	C.1 Geochemical profile of boreholes W4,W5,W6,W7, Silvermines.....	A8
"	C.2 " " " " V41, V42 "	A8
"	C.3 " " " " S2, S8, S6 "	A8
"	C.4 " " " " V21, V28 "	A8
"	C.5 " " " " 75/2, V23, V24 "	A8
"	C.6 " " " " G217 "	A8
"	C.7 " " " " V17, M5 "	A8
"	C.8 " " " " Y1, K38, K37 "	A8
"	C.9 " " " " B141, B143 "	A8
"	C.10 " " " " 77/1, 76/3 "	A8
"	C.11 " " " " V1, B139 "	A8
"	C.12 " " " " M1 "	A8
"	C.13 " " " " B8 "	A8
"	C.14 " " " " B4 "	A8
"	C.15 " " " " 76/3 "	A8

CHAPTER ONE - Introductory Chapter.

1.1.1. Introduction.

A primary lithogeochemical aureole is the lateral expression of a mineral deposit in which cryptic enrichments of certain associated trace elements become incorporated into surrounding host rock formations during its genesis. One particular type is that formed during sea floor hydrothermal exhalation, and results in a primary aureole related to a sedimentary or sea floor replacement deposit. For example, manganese aureoles of at least five kilometres radius have been found in laterally equivalent beds around some synsedimentary base metal deposits, both ancient and present day, e.g. Tynagh (Russell 1974), Meggen (Gwosdz and Krebs 1977) and the Red Sea (Bignell et al 1976).

Russell (1975) further describes less extensive primary enrichments of Zn and Fe_2O_3 in the vicinity of the Tynagh mine, proposing that (together with Mn) they originated from 'spent' mineralising solutions escaping from the exhalative centre on the sea floor.

Preliminary data from Ballinalack (al-Kindy 1979) and Ballyvergin (Russell, unpublished data), indicated that comparable enrichments were present around other Irish deposits, though on a smaller scale.

After suggesting that the anomalous manganese might be present in the lattice of the calcite in the host limestone, Russell (1974, 1975) proposed that such a feature might be common to all sedimentary base metal

deposits in calcareous host rocks. Thus, exploration companies might routinely analyse samples of limestone host rock for anomalous trace element content, as a means of improving success rate in regions of variable outcrop and thick drift cover, where blind orebodies may not be easily detectable by conventional exploration methods.

From published information, previous application of lithogeochemistry to base metal exploration has been confined largely to non-carbonate terrains, such as the volcano-sedimentary basins of the Northern Cordillera (Goodfellow et al 1980a, 1980b) and the mafic volcanic sequences associated with ophiolite complexes (Govett 1976).

Investigation of alteration haloes associated with submarine mineralisation of volcanic affiliation (e.g. Whitehead and Govett 1974, Goodfellow 1975, Riverin and Hodgson 1980), deep-seated porphyry-style mineralisation (Gunton and Nicholl 1975, Olade and Fletcher 1976), and epigenetic vein deposits (Boyle 1965, Bailey and McCormick 1974) in numerous parallel studies, reflects a similar approach utilising epigenetic dispersion of elements in a primary mineralising environment. Govett and Nichol (1979, p.358) state that "within the past ten years in the western world, lithogeochemistry has advanced from an essentially academic involvement to a technique used sparingly by the mining industry in mineral exploration.

They conclude that they are not aware of any mineral discovery to date that can be attributed to lithogeochemical analysis.

1:1.2 Aims and Motivation.

This thesis is about the nature of primary trace elements aureoles associated with mineralisation in the Irish Carboniferous. Its aim is to test whether such aureoles are a feature common to all sedimentary 'Irish-type' mineralisation, and to assess their potential as an exploration tool in geochemistry. On top of this, it aims to determine where possible, the site of the various anomalous trace element species, whether sited in the carbonate lattice of the host limestone, or associated with separate oxide, sulphide or clay mineral phases.

The study is motivated by a need to provide the mineral exploration industry with a new approach to identification of potential mineralisation in terrains with erratic exposure, thick drift cover and peat bog, and to add to our knowledge of the geochemistry of ore deposits in general, as well as the origin of the particular deposits under research.

Any scientific study should commence with a working hypothesis which can be put to test. In this case, it is stated quite simply: that lithogeochemical analysis is a useful tool in mineral exploration in the Irish Carboniferous, and yields valuable information on the

genesis of mineral deposits.

1.1.3. Methodology.

This research was undertaken with a view towards the development and practical application of new techniques for the mineral industry in Ireland.

The first approach was to perfect an analytical technique which allowed rapid analysis of mudbank limestone samples by atomic absorption spectrophotometry for some commonly occurring trace elements, followed by application of this technique to a suite of samples from the stratiform ore horizon around the Silvermines base metal-baryte deposit.

Combination of this data with reanalysed sample data from Tynagh and Ballvergin (Russell 1975, unpublished work) and new samples from the Irish Waulsortian Limestone enable me to draw a general picture of the distribution of trace elements in the host rocks of known deposits and prospects. The method was then tested in an area of unknown mineral potential, with the co-operation of an interested exploration company.

Parallel studies on the nature of the trace element enrichments were undertaken by the use of discriminative atomic absorption spectrophotometry, X-ray fluorescence and electron microprobe analyses, to determine any association between individual trace elements and mineral phases.

From the results of this work, inferences on the

genesis and origins of the mineralisations studied are discussed, and suggestions made concerning the application of the technique of lithogeochemistry in the mineral exploration industry.

1.2.1. Geological Background.

Most of central Ireland is underlain by relatively undisturbed Lower Carboniferous shelf sediments forming a peneplain, through which inliers of Lower Palaeozoic rocks and unconformable Upper Devonian to Lower Carboniferous Old Red Sandstone facies cover protrude, to form areas of higher ground.

The Lower Palaeozoic rocks are dominated by turbiditic greywackes, slates and siltstones, which have suffered low grade metamorphism during the Caledonian Orogeny. The overlying Old Red Sandstone (O.R.S.) facies is dominated by non-marine sandstones, siltstones, mudstones and conglomerates, often strongly reddened.

Summary of the Lower Carboniferous Geology of Ireland.

The broad environment of deposition in central Ireland during Dinantian times is of a shelf sea located between the diminishing Old Red Sandstone continent to the north, with associated fluvial/deltaic deposition, and the deep water turbidite facies of the Culm to the south (Figure 1.1.). Subdivision of the Dinantian in Ireland is depicted in Table 1.1.

Although sedimentation within this shelf was fairly uniform throughout early Dinantian times, considerable variation in facies and thickness of individual sequences in subsidiary basins and structural highs (allied to tectonic movements) from mid-Tournaisian onwards, led to marked contrast between different basins on a local scale.

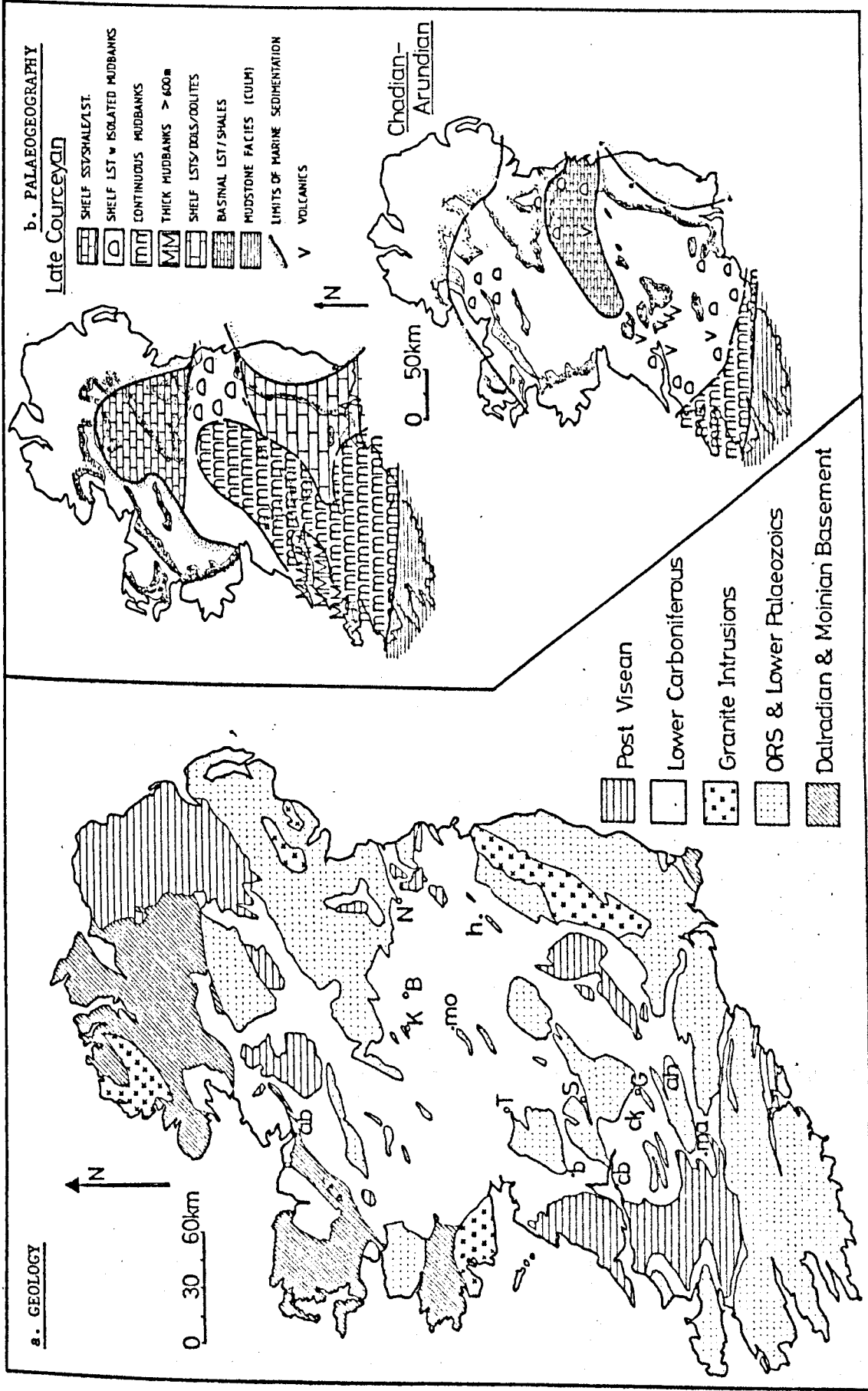


Figure 1.1a: Simplified geology of Ireland, showing principal Lower Carboniferous base metal deposits. (B = Ballinalack, G = Gortdrum, K = Keel, N = Navan, S = Silvermines, T = Tynagh, ab = Abbeystown, ah = Aherlow, b = Ballyvergin, cb = Carrickittle, ck = Courtbrown, h = Harberton Bridge, ma = Mallow, mo = Moate).

Figure 1.1b: Lower Carboniferous palaeogeography of Ireland, after Sevastopulo (1979, 1981). Stippled areas represent pre-Carboniferous rocks.

STAGE	VAUGHAN'S ZONES	BELGIUM	RADIOGENIC AGE (my)	MUDBANKS
Brigantian	D ₂	↑	325	
Asbian	D ₁			thick mudbanks in SW
Holkerian	S ₂			also patchy development in North Midlands
Arundian	C ₂ S ₁			345
Chadian	C ₁	VISÉAN		thick mudbanks in SW
Courseyan	(C ₁)	TOURNAISIAN	360	Waulsortian
	Z			
	K			

Table 1.1: Subdivisions of the Dinantian in Ireland, and approximate equivalents in U.K. and Belgium. Approximate age range of Waulsortian and younger mudbank limestones is also indicated. After Sevastopulo (1981).

Over most of the region, facies boundaries are diachronous and frequently transitional in nature, so that rarely can one lithological change or unit be taken to represent a time plane over any great area. A selection of stratigraphic profiles through the lower part of the Dinantian from various prospects and deposits is shown in Figure 1.2.

The earliest part of the Courceyan is represented by shallow marine deltaic clastics and carbonates of the Lower Limestone Shales, in transition from the fluvial regime of the Upper Old Red Sandstone to the marine shelf facies of the Ballysteen Limestone (Figure 1.3.). The Carboniferous sea rapidly transgressed northwards and deposited shallow marine ('lagoonal') limestones and shales quite uniformly over most of the Midland Plain.

The Ballyvergin Shale is a laterally persistent, distinctive, grey or green, non-calcareous mudstone or siltstone, of widespread use as a marker horizon over much of southern and central Ireland. The ensuing Ballysteen Limestone includes thick, well-bedded, argillaceous bioclastic limestones, interbedded with variable amounts of shale. These beds are nodular and cherty in places, especially towards the top, and culminate in a change to the massive, pure carbonate mudbanks of the Waulsortian Complex. Brück (1982) divides the Ballysteen succession into six units on the basis of varying contents of chert, shale, limestone and

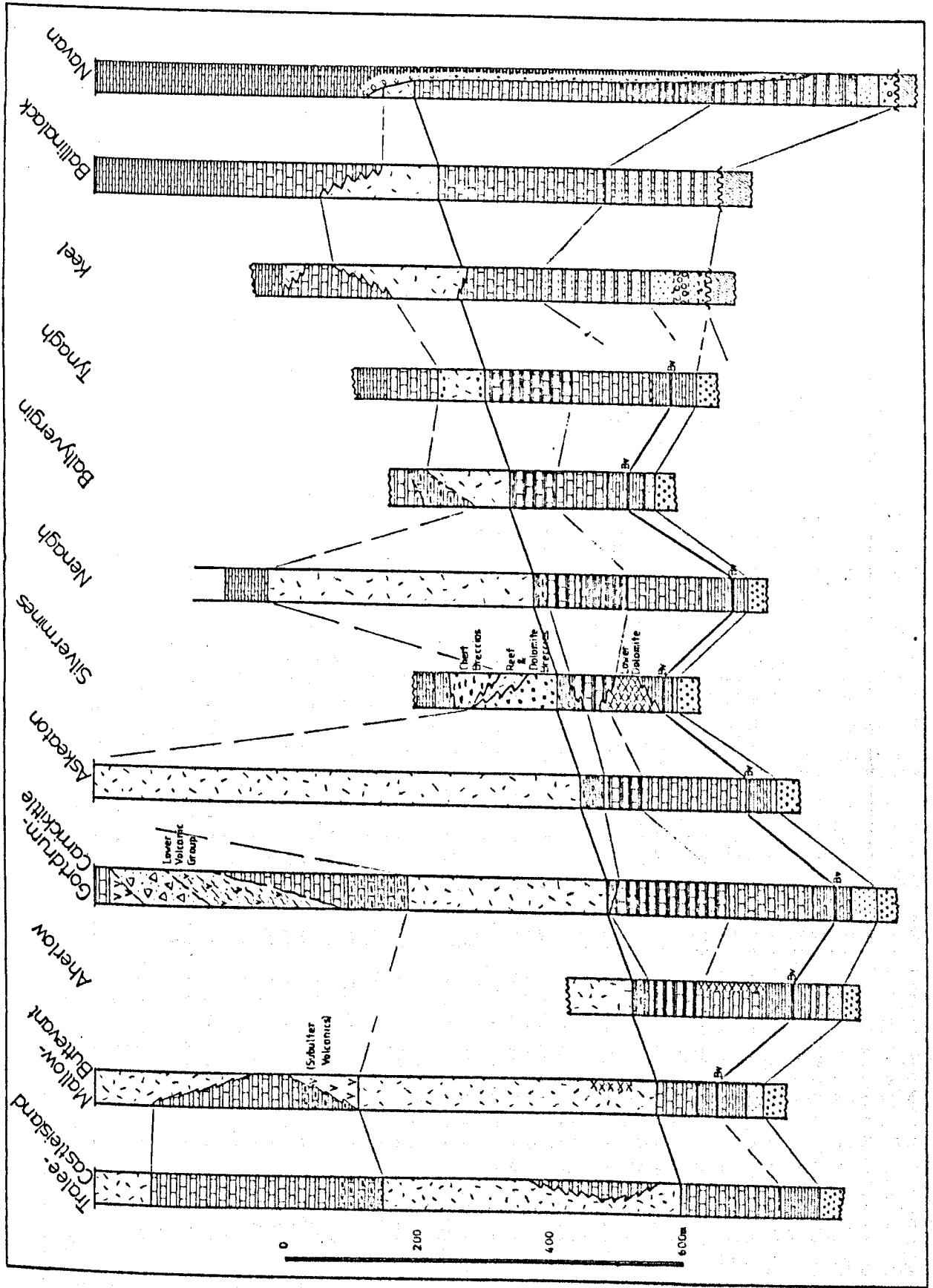


Figure 1.2a: Selected stratigraphic profiles from a number of locations across Southern and Central Ireland and Central Ireland, showing broad correlations from southwest to northeast. For key, see Figure 1.2b. Data from many sources.

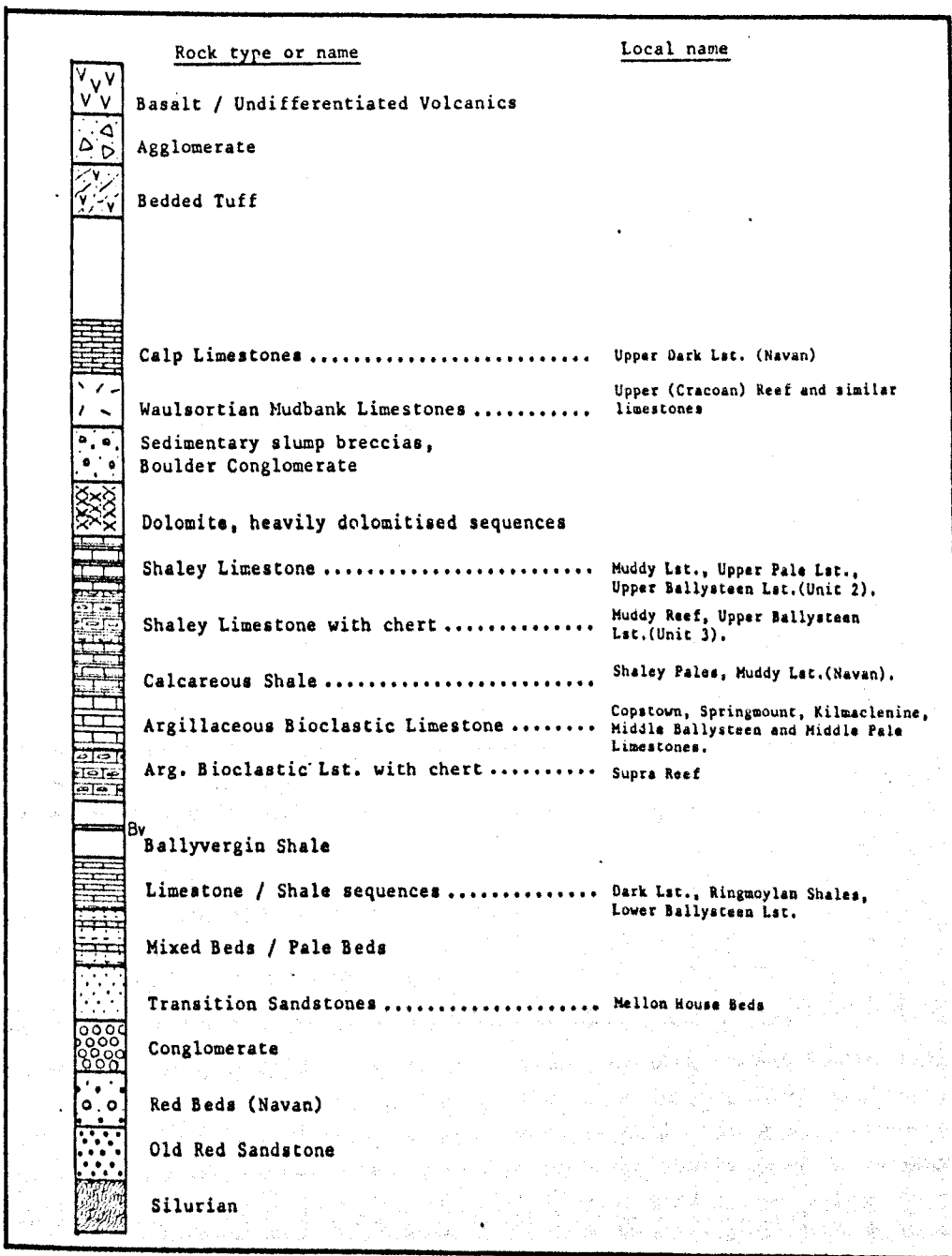


Figure 1.2b: Key for Figure 1.2a, showing variations in local nomenclature.

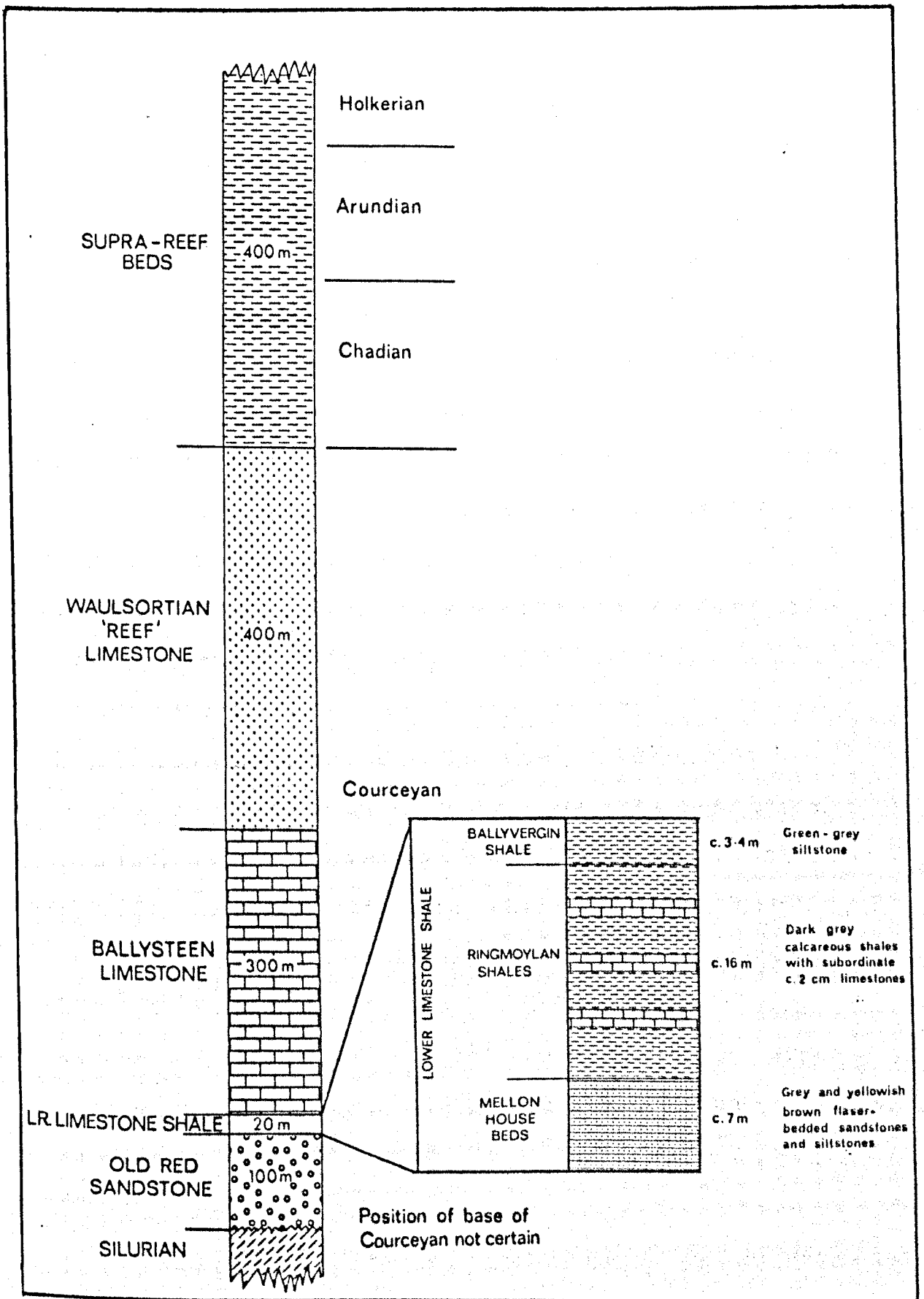


Figure 1.3: Stratigraphic column from Nenagh area, Co. Tipperary, showing thicknesses and local nomenclature for each unit. Inset shows the subdivision of the Lower Limestone Shale unit. From Brück (1982).

bioclastic debris.

The Waulsortian Mudbank or 'Reef' Limestone is a thick, relatively massive, poorly bedded, micritic limestone, with textures ranging from pure calcite mudstone (characterised by the presence of irregularly shaped stromatactis cavities (Lees 1961, 1964)), to coarse encrinite with subordinate, locally well-bedded, cherty 'reef equivalent' or 'off-reef' limestone. It is on this sequence (and its equivalents) that the majority of the work has been carried out. Towards the northeast of the country, greater variation is present in the Lower Carboniferous stratigraphic sequence. For instance, the Waulsortian Limestones are only sporadically developed, and diachronously younger than in the south and west (Nevill 1958, Lees 1964, Sevastopulo 1981).

Deposition of Waulsortian Limestones is generally followed in the Chadian stage by a variable succession of thick, dark mudstones and basinal limestones with turbidite characteristics, in subsiding basins (Calp Limestones, Sevastopulo 1981), and elsewhere a variety of shelf limestones, oolites and mudstones, in which pronounced lateral and vertical facies variations are observed (Brück op cit). This is followed in the Arundian by more widespread 'Calp' facies deposition.

Post-Dinantian Geology.

Post-Dinantian rocks are preserved in two main areas of southern and central Ireland, one in the west, extending from County Kerry northwards through Limerick

into Clare, the other in the east, entered on the Leinster Coalfield, in Counties Kilkenny, Carlow and Tipperary. These formations (mainly Namurian in age) are dominated by cyclothemmic sandstones, siltstones and mudstones deposited in subsiding basins, separated by positive structural highs.

Coal bearing strata of Westphalian age are preserved in both these areas. No significant post-Carboniferous rocks are preserved onshore in South Central Ireland, although further to the north, approximately 600 metres of Permo-Triassic sediments are preserved in the Kingscourt Graben.

The main structural influence on the Carboniferous of Central Ireland was the imposition of Hercynian stresses at the end of the Carboniferous period, often relieved by reactivation of northeast trending Caledonoid structures. Hercynian deformation took place mainly along E/W to NE/SW axes, reflecting N/S compression, and increases in intensity southwards. An axial planar cleavage is well developed towards the south, thrust faulting is exhibited, and folding becomes tighter in the same direction.

Glacial and Recent Cover.

As a result of at least two major Quaternary glaciations (Synge 1979), large areas of Central Ireland are covered by boulder clay, kame and esker deposits. Extensive peat bog development (with an average thickness of 7 metres, overlying lacustrine clays and marls),

covers much of the lower lying ground, with less extensive upland bog on the higher ground.

1.2.2. Mineralisation in the Irish Carboniferous.

Large (1980) includes the Irish deposits in his description of sediment hosted submarine-exhalative deposits, along with major base metal mineralisation in the North Australian Proterozoic (Mount Isa, McArthur River, Lady Loretta), the Canadian Cordillera (Sullivan, Tom), and the Central European Variscan (Rammelsberg, Meggen). Large (op cit) distinguishes them from volcanogenic submarine-exhalative and Kupferschiefer styles of mineralisation. Attempts by other authors to classify the Irish deposits as Mississippi Valley type (Watling 1976, Williams and McArdle 1979, Carter 1982) are refuted by the fluid inclusion evidence of Samson and Russell (1982).

The principal mineral deposits of the Irish Lower Carboniferous are not wholly identical in style, but have many features in common with sediment hosted, submarine-exhalative deposits, as described by Large (op cit), the major characteristics of which are summarised in Figure 1.4. On the other hand, certain features are not well displayed in the Irish deposits, such as the juxtaposition and arrangement of the sulphide, baryte and oxide facies of the third order basin environment.

At Silvermines, the baryte and weakly developed oxide facies appear to coincide; at Tynagh, the baryte and sulphide facies coincide within the feeder-zone,

epigenetic domain, and genuine stratiform sulphides are minor in importance; at Navan, the baryte and oxide facies are essentially absent, as is any recognisable feeder-zone or obvious development of a third order basin.

In addition, footwall alteration zones are apparently absent in the deposits, with the exception of extensive footwall dolomitisation at Silvermines, and some reduction of iron oxides in sandstones nearby at the replacement deposits of Shallee.

The principal Irish deposits are hosted by relatively undisturbed Lower Carboniferous carbonate shelf sediments in a major first order basin (over 200 km x 100 km), straddling a major NE/SW trending lineament, the Iapetus Suture (Phillips et al 1976). All the major Pb+Zn deposits are of approximately the same age, occurring during a period of widespread subsidence and marine transgression, with deeper water Waulsortian mud-bank deposition having replaced littoral, sub-littoral and shallow water marine shelf facies in the stratigraphic succession.

Boyce et al (1983) propose that extensional stresses during the late Courceyan gave rise to rapid subsidence of second order sedimentary basins up to a few tens of kilometres across (such as the North Tynagh Basin and the Silvermines-Nenagh Basin), locally bounded by active normal faults. Within these basins, individual deposits are located in small, low energy, reducing, third order

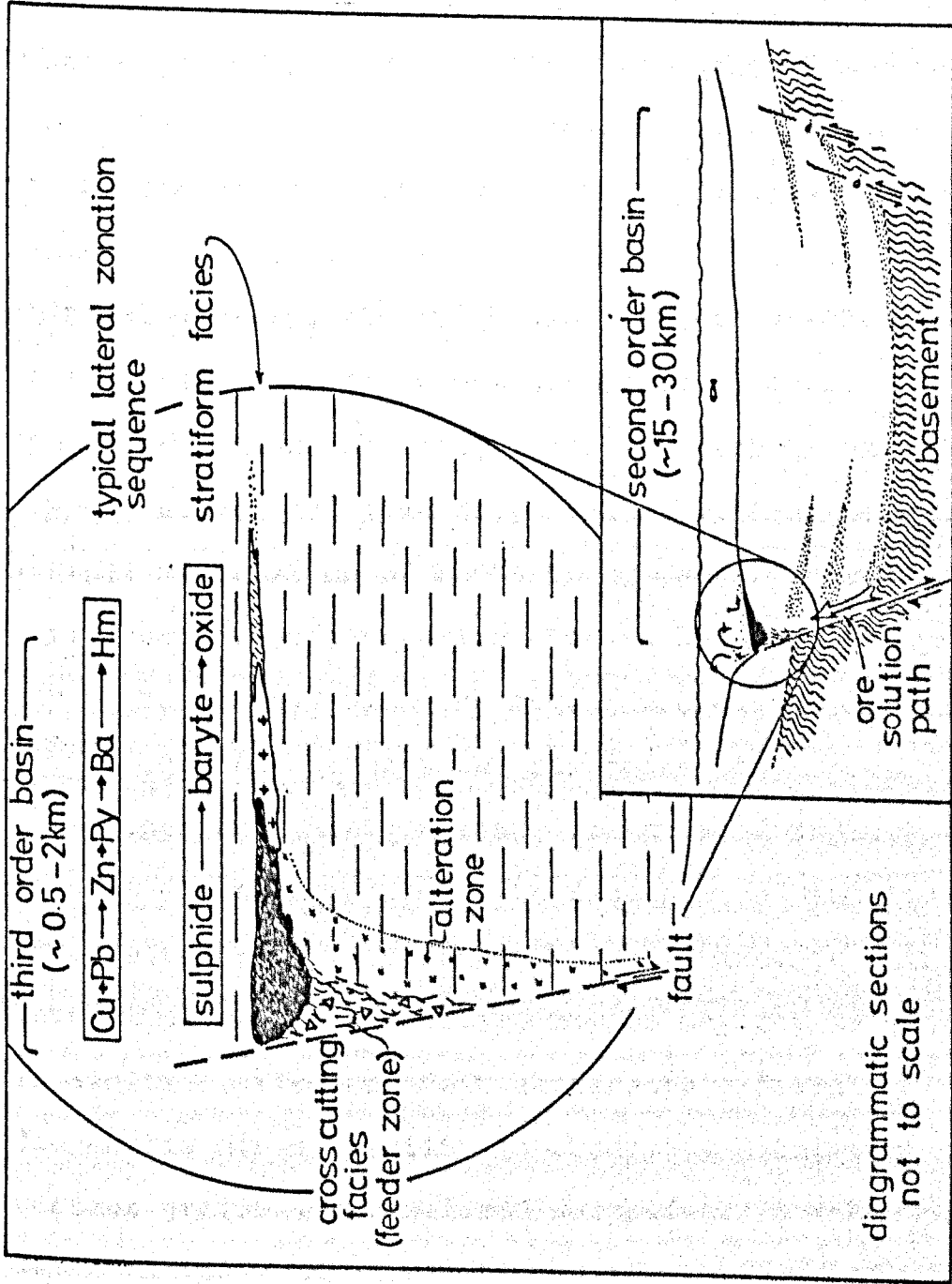


Figure 1.4: Simplified model of sediment-hosted, submarine exhalative system, based on Large (1980), showing many features in common with Irish base metal deposits. Enlargement of inset shows typical facies arrangement and mineral zonation within the third order basin. Cu = chalcopyrite, Pb = galena, Zn = sphalerite, Py = pyrite, Ba = baryte, Hm = hematite.

basins, adjacent to active fault zones, in which the products of hydrothermal exhalation accumulated, along with allochthonous lithologies formed by syndepositional fault movements (submarine sedimentary breccias and slumping).

The larger stratiform orebodies in rocks of Courceyan age contain features which suggest that at least part of the ore was deposited contemporaneously with other sediments on the sea floor.

Mineralogically, the Irish deposits are simple, comprising varying proportions of pyrite, galena, sphalerite, minor chalcopyrite and lesser amounts of copper, silver and lead sulphosalts, with an overall element association of Pb-Zn-Cu-Hg-Cd-Ag. Massive, stratiform cryptocrystalline baryte and massive pyrite may be associated with the sulphide ore, and dolomitisation frequently affects the carbonate host rocks.

The deposits exhibit a range of textural styles, from massive and structureless, to fine grained and laminated often with intimately intermixed sulphide, in which a lateral or vertical zonation may or may not be present. In addition, frequent vein and fracture-filling diagenetic mineralisation is observed, along with coarser grained, remobilised sulphides. A stockwork or disseminated vein or cavity replacement type of mineralisation, interpreted by Samson and Russell (1983) as remains of a hydrothermal feeder zone. This may be all that is preserved of the original exhalative system at

deposits such as Aherlow, Ballyvergin and Mallow.

The Navan deposit is almost an order of magnitude greater in size than the other major deposits of Silvermines or Tynagh, comprising approximately seventy million tonnes of ore at over 12% combined lead and zinc. It is hosted in a shallow water argillaceous limestone sequence, on the northern flank of a NE trending anticlinal structure (Andrew and Ashton 1982, Ashton et al 1984). The bulk of the ore occurs in a number of stacked, shallow-dipping lenses with fine-grained sulphides, low in pyrite, in which sedimentary textures are largely masked by later post-depositional and diagenetic modification. Sphalerite and galena dominate the ore mineralogy and metal zonation is expressed in an upward increase in Fe and Zn/Pb through the ore lenses. Zinc, Mn, As and Pb are enriched in the host rocks, stratigraphically equivalent to the ore zones, and in the hanging wall. A proportion of the orebody is truncated by an erosion surface with overlying mineralised and pyritic debris flow breccia, interpreted by Boyce et al (1983) as a large scale slump.

Many other smaller deposits and occurrences of base metals are known throughout central and southern Ireland, exhibiting a whole range of genetic styles, including vein, cross-cutting, disseminated, replacement and breccia-hosted. Of similar age, style and tectonic setting to the larger Irish deposits, the Gays River Pb+Zn deposit (Akande and Zentille 1984), and related

minor occurrences in Nova Scotia, probably belong to the same metallogenic province (Russell 1976).

For a number of reasons, the host rocks surrounding the Navan deposit were not investigated in this study, in particular, the fact that a comparable study was at that time already initiated, the results of which are now published (Finlay et al 1984). On top of this, the host rocks at Navan are very different from the Waulsortian Mudbank, which is relatively poorly developed locally, and significantly younger than the main sedimentary mineralisation.

The geology of each deposit investigated will be described individually in more detail at the relevant section in Chapter 3, preceding the presentation of analytical results.

As the Waulsortian Mudbank Limestone forms the principal sample medium in this study, a more detailed description of its origin and composition is called for, before any further discussion of analytical procedures or results.

1.2.3. The Waulsortian Mudbank Limestone Facies.

Well documented developments of Waulsortian bryozoan-crinoid carbonate mud mounds are present in the Central Irish Carboniferous Basin and the Belgian Dinant Syncline (Lees and co-workers 1961, 1964, 1977, 1980). Between these areas, sporadic occurrences are known in South Wales, Southwest England and Northern England (Miller and Grayson 1982, Lees 1982, Lees and Hennebert 1982). In addition, examples from the North American continent have been described (Pray 1958, Cotter 1965, Ross et al 1975, McQuown and Perkins 1982).

Comparable and mound facies range in age from Cambrian to Jurassic (Pratt 1982) but the best known examples are confined to the Lower Carboniferous from the Upper Tournaisian to the Lower Visean.

Paleogeographic setting - Waulsortian mudbanks formed on subsiding shelf seas around major contemporary land masses, notable the Wales-Brabant Ridge (Figure 1.5), but at some distance from the shoreline, in clear open marine water, and beyond the influence of terrigenous sediment input (Lees 1961). Towards the shoreline, shallower water with highly variable lagoonal and clastic facies presided, whereas in deeper waters to the south, the basinal mud belt of the Culm facies was located. In this basin, thick developments of flysch-like shale, sandstone and calcareous mudstone accumulated, with clastic material derived from the south (Wilson 1975).

Palaeomagnetic evidence indicates that the Dinantian succession of this area developed only a few degrees north of the palaeo-equator (Miller and Grayson op cit).

Lees (1964) shows how the mudbank complex in Ireland changes from one of thick, laterally and vertically continuous mudbank developments through more patchy, discontinuous buildups to isolated reef mounds and clusters across the country from southwest to northeast.

Descriptions of the more isolated developments in the northern and east-central parts of the country are to be found in Nevill (1958), Schwarzacher (1961) and Philcox (1963).

The Galway and Leinster Granite Massifs form stable zones flanking the main zone of basin subsidence, centred on the Shannon Estuary, where mudbank accumulations are greatest (over 1000m, Lees 1961).

The base of the Waulsortian in Ireland is known from fossil evidence to be diachronous, becoming younger to the northeast (Lees op cit). This trend appears to continue eastwards into the Craven Basin area of Northern England, where Miller and Grayson (op cit) note that the development of mudbank sedimentation did not commence until post-Tournaisian times, later than elsewhere. They also note that (as in Ireland) Waulsortian developments are concentrated in the areas of greatest continuing subsidence, where underlying successions are thickest.

Origins and environment of deposition - Typical mud-

Mid Dinantian Palaeogeography

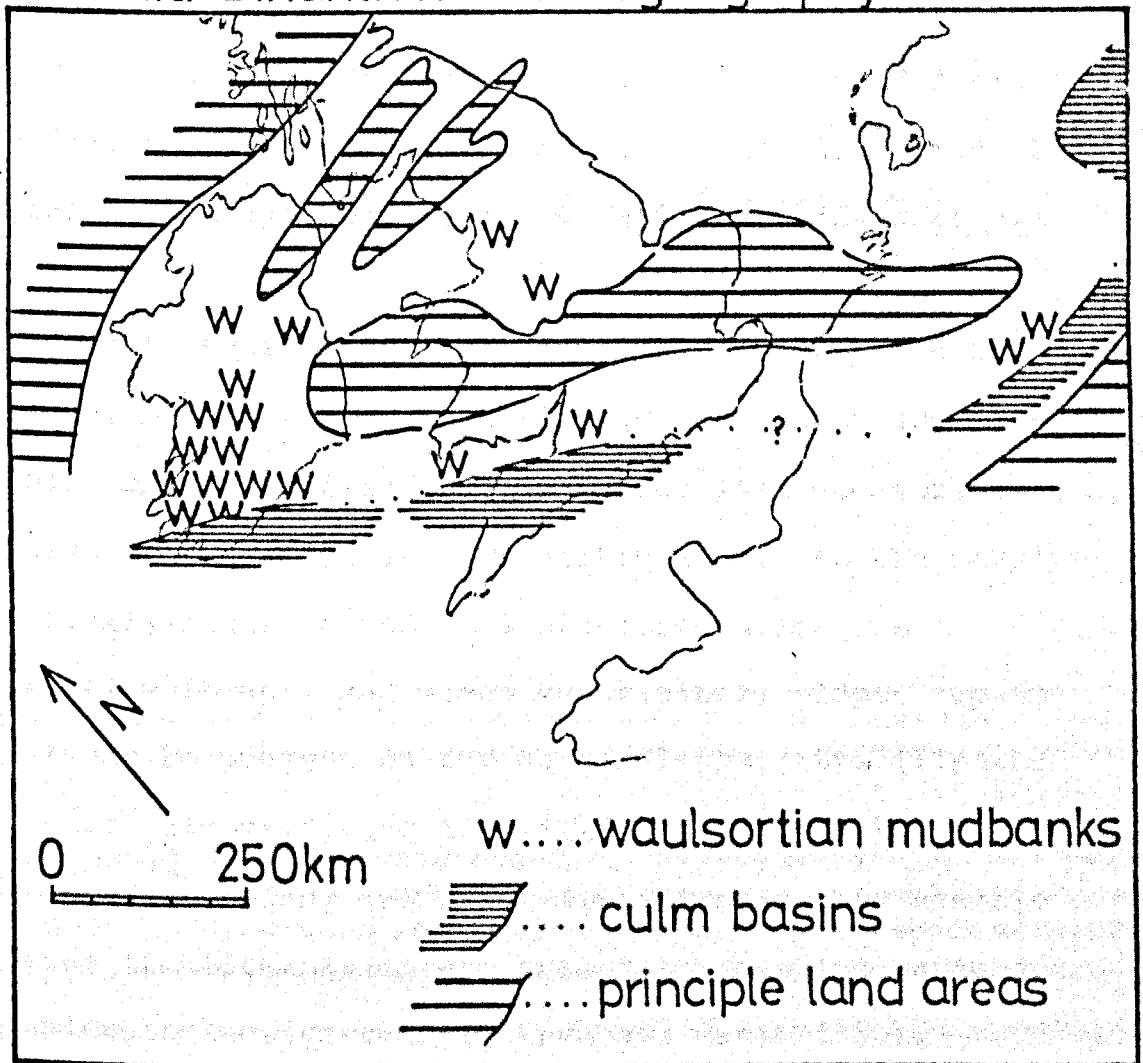


Figure 1.5: Palaeogeography of part of Western Europe during Mid-Dinantian, showing distribution of Waulsortian mudbank developments relative to land areas and deeper basins.

mounds form lenticular masses up to more than 1 kilometre across and up to 300 metres thick, composed of varying amounts of carbonate mud, recrystallised carbonate mosaics (including stromatactis) and varied fossil debris, notable fenestellid bryozoans and disarticulated crinoids. Algal remains are notably rare (Lees et al 1977).

Laterally equivalent formations tend to be thinner bedded, bioclastic grainstones, grading into argillaceous, cherty-nodular or thin-bedded lime mudstones, shales and wackestones. Transitions between the massive to weakly-bedded mounds and off-reef facies are typically abrupt, and steep depositional slopes (up to 50°) may be present on the mound flanks. Stabilisation of these slopes during deposition probably takes place by organic binding and rapid lithification, as visible traces of bioturbation are absent, as are indications of microboring (Pray 1969, Lees and Conil 1980).

The ratio of mound thickness to surrounding equivalent facies thickness may be as great as 5:1 (J. Miller, pers. comm. 1981), and the height of individual mound facies may be up to, or even more than, 200 metres above the sea floor. However, the sedimentary characteristics remain comparable with the lateral facies equivalent, without any indications of emergence or proximity to wave base, suggesting deeper water origins for the mud mounds.

The lack of evidence for algal influence, combined with

the comparative absence of turbid depositional features led Pray (1969) to propose such a deeper water marine origin, perhaps even below the photic zone. This idea is backed up by Wilson (1975) and others (e.g. Lees et al 1977, Lees and Conil 1980), although Miller (pers. comm. 1981) disputes this with descriptions of filamentous algae preserved in ancient mounds, which suggest that the water must at least have been clear and un-turbid. Such photosynthesising biota may of course merely form part of a death assemblage from shallower water origins.

Lees et al (1984) describe the wider environment of deposition as a broad, sloping ramp or shelf, in which mudbanks are best developed distally, isolated and scattered proximally, and absent in the shallows. They reject the suggestion by Newmann et al (1977) that present day lithoherms in the Straits of Florida, at a depth of 700 metres or more, are modern day analogues of ancient Waulsortian buildups, on the basis of many differences, including geometry, structure, fabrics, skeletal frameworks, associated facies and settings.

Stromatactis and mudbank origins - Many detailed descriptions of stromatactis cavity systems, and discussions on their origin have been published, for example Schwarzacher (1961), Philcox (1963), Lees (1964) Ross et al (1975), Bathurst (1980, 1982) and Pratt (1982). Stromatactis structures usually consist of a reticulate network of sparry or fibrous calcite infill,

enclosed in the host micrite-microspar of the mudbank limestone. The elongate and subhorizontal outline of the former cavities often includes irregular to digitate upper contacts and a smooth lower contact with the host, commonly with a geopetal internal sediment.

Usually more than one generation and type of calcite cement infill is present, viz. an earlier radiaxial fibrous calcite mosaic, followed by a later, equant sparry calcite infill. Dimensions vary from finely intricate, sub-centimetre sized networks, to large, open, metre-long cavity fillings.

Most recent theories on their origin are based on rapid lithification of mound carbonates and suggest that winnowing of unbound or unlithified sediment has taken place from underneath, or between, solid (i.e. bound and/or lithified) crusts or carbonate mud. Resulting cavities become filled with varying proportions of radiaxial fibrous calcite of marine origin, geopetal carbonate mud or other internal sediment, and may be followed by later generations of diagenetic spar in remaining voids. The early or rapid formation of stromatactis infilling is indicated by their presence, intact, in reworked boulders in mound talus deposits (Wilson 1975).

Bathurst (1980, 1982) favours origin by lithification of carbonate crusts which form episodically and may be reworked during bioturbation and burial, with loss of unlithified sediment from between these crusts

to form elongate cavity systems.

Recently, Pratt (1982) has proposed that organic binding of locally generated sediment suspensions was facilitated by the activity of blue-green algae in stabilising the carbonate mud fraction. Subsequent cementation formed a reef framework of unlaminated stromatolite (thrombolite), now represented by the carbonate mud mounds. Winnowing of unbound sediment from the algal mat created the network of cavity structures through the framework, now represented by stromatactis fillings. Morphology of the resulting network is dependent on the extent of algal binding and supply of unconsolidated mud.

The ability of blue-green algae to grow at considerable depths (beyond light penetration), and perhaps accelerate CaCO_3 precipitation by CO_2 consumption, allows rapid growth of mudbanks to keep pace with rapid subsidence. This, combined with the protective function of the algae on preventing microboring by other organisms is compatible with solving many of the previously unanswered questions on Waulsortian mudbank origins. Recognition of these origins leads Pratt (op cit) to classify the mudbanks as genuine reefal framework, which may exert some control on the surrounding environment. This control is highlighted by Taylor (1984) in the Silvermines brine pool, where mudbank growths influence host mineral lithologies by ponding of denser, stratified hydrothermal solutions.

Local form, setting and influence - Lees and Conil (1980) have established that Waulsortian reef mounds formed positive structures with relief often over 100 metres, in deeper water perhaps over 200 metres, tens of kilometres distant from the shoreline. Rapid subsidence of basin floors allow thick buildups to form (Pray 1969, Wilson 1975). An association with active faulting is suggested by Miller and Grayson (1982) in their 'tilt-block' model for Dinantian sedimentation in the Craven Basin area of Northern England. In this model, Waulsortian mudbanks grow on relatively narrow carbonate ramps in deeper water.

The upper surfaces of the mounds were probably craggy and uneven (Pratt 1982), with carbonate mud bound in places by thrombolitic algal growths, and providing a source of unbound sediment to the immediate surrounds by current winnowing. Some laterally equivalent facies of massive, micritic carbonate sediment may have arisen in this manner, for example, the 'Leffe' facies of both Lees and Conil (1980) and the 'off-reef' facies of Philcox (1967). In both cases, thick sequences of structureless, fine-grained, detrital carbonate sediments abound adjacent to 'true' Waulsortian-type limestone with as little as 10% original micrite framework, and large proportions of secondary sparry calcite infill (the 'veines-bleues' of Lees and Conil (op cit) and the 'bryozoan reef' of Philcox (op cit)).

Termination of reef growth may take place by shallowing

and increased energy levels (e.g. Craven Basin (Miller and Grayson (1982) and Belgium (Lees et al 1977)), by increased argillaceous input in continuing deep water regimes (e.g. the Calp Limestones of the Irish basins), or perhaps, as will be discussed in Chapter 6, by inhibition of CaCO_3 nucleation or growth, or algae poisoning in a brine pool environment.

Clearly, for the hypothesis proposed in Section 1.1.2. to stand, growth of the Waulsortian mudbanks must have been approximately contemporary with exhalative hydrothermal activity, otherwise genuine primary syngenetic trace elements aureoles could not develop within the mudbanks. Even if this is the case, initial mound frameworks often contain later stages of carbonate infill (e.g. stromatactis), and have generally suffered a certain degree of diagenetic modification or replacement.

Aspects of the composition and diagenesis of the mudbanks, and the suitability of the Waulsortian Limestones as a host for stratiform mineralisation, will be considered further in the discussion towards the end of this study.

1.2.4. Mineral Exploration Practice in Ireland.

Considerable evolution of mineral exploration techniques and approach has taken place in the last three or four decades, in the search for economic base metal deposits. This has involved increasing expense and sophistication, through surface prospecting, surface geochemistry, geophysical methods, deep overburden sampling and diamond drilling (Schultz 1971, Irish Association for Economic Geology 1979).

The Lower Carboniferous rocks have been the focus of the most intense exploration activity in Ireland, bearing in mind that most of the principal known deposits are hosted therein, virtually all suboutcropping beneath a thin but variable cover of overburden.

Increased application of new or combined techniques is required to locate those deposits which may be under thick Quaternary cover or younger rock formations. Lithochemical prospecting is one such approach.

CHAPTER TWO - Analytical Techniques.

2.1.1. Introduction.

This chapter outlines the sampling and analytical procedures utilised in the collection of data from each locality in Ireland. Techniques used in more detailed micro-examination of trace element distribution, in particular the electron microprobe, will be discussed in Chapter Five.

It should be borne in mind that, as development of a technique for application to the mineral exploration industry was one of the principal aims of this study, complications in both laboratory and analytical procedure were kept to a minimum. Techniques used were designed both for cheapness and rapidity, whilst handling large numbers of samples with relatively untrained staff.

2.1.2. Sampling Strategy.

In order to outline a pattern of trace element distribution around a particular deposit, as wide and continuous a spread of sample points is clearly desirable. Three principal sources of rock samples are available, viz:-

- i) surface outcrop;
- ii) drill core;
- iii) underground exposures in mine workings.

Of these, the second was preferred where possible, because of the greater control afforded by drill core

on stratigraphic positioning, less oxidation of rock sample, and more rapid sampling routines when core from a wide area is stored in a single shed. Unfortunately, drill cover is generally available only for the immediate vicinity of known prospects and mines (usually within about one kilometre of mineralisation), consequently surface outcrop sampling was utilised to cover a wide area around each deposit. Similarly, underground workings are even more confined to the area of mineralisation, and offer very restricted areal coverage.

It should also be borne in mind that in reconnaissance geochemical exploration, outcrop samples are usually the only available source of sample material. Therefore, recognition of the surface expression of trace element aureoles is of premier importance.

As natural outcrop is scarce in many areas of Ireland, due to extensive mantling by drift, peat bog, or because of agricultural activity, additional sample sites are provided by man-made exposures (quarries, ditches, road and rail cuttings). The former tend to suffer more from surface weathering, depending on durability of the rock type, whereas the latter usually offer a greater area of fresh rock for sample selection.

There is an inherent problem in relying upon natural, unweathered outcrops, as there is a danger of creating a sample bias because of possible differential weathering rates of different sample types. This situation cannot really be avoided without widespread use of

diamond drill and sub-outcrop sampling, and must be taken into account during interpretation of results.

Maximum sample density is usually determined by availability of outcrop. In areas of more or less continuous outcrop, required sample density would obviously depend on the dimensions of the trace element aureoles being sought.

2.2.1. Sampling Procedure and Laboratory Preparation.

In the study of primary trace element distribution in host rocks to stratiform mineralisation, one obvious requirement is that only primary material should be analysed, i.e. all secondary oxide coatings should be avoided. In addition, as the quest is for cryptic trace element patterns, visible sources of contamination, or abnormal enrichment of any sort, should be avoided where at all possible. Such sources include visible mineralisation (including pyrite), dolomitisation and stylolites. Where unavoidable, any abnormality in rock appearance or mineral content was recorded for future reference, so that any spurious value obtained could be quickly traced to its source.

2.2.2. Sampling Routine.

Sampling of clean, Waulsortian-type mudbank limestones, and their local equivalents, involved collection of both whole rock and chip samples, in each case devoid of secondary contaminants. With drill core, a 10 to 15 centimetre length of core (depending on diameter) was selected as representative of a given length of core, or alternatively, 50 to 100 grammes of selected centimetre-sized chips were taken to represent such a length of core. In outcrop locations, either a fist-sized piece of fresh rock was collected using a 1 kg. hammer (or 4 kg. sledge hammer if required), or 50 to 100g of randomly selected rock chips were taken to represent as wide an

area as possible of the exposed rock face. In general, more than one sample was taken from each locality, the total number depending on the total outcrop area.

Chip sampling was eventually adopted as standard procedure, mid-way through the sampling programme, because of the time saved in laboratory preparation (in spite of greater time required in the field), smaller bulk yet greater representation of outcrop, and the difficulty in some instances of obtaining a single uncontaminated rock or core sample. This matter is discussed further in Chapter 5.

In each case, samples were stored in individual sealable polythene or stiff paper sample bags for transport to the laboratory.

2.2.3. Laboratory Preparation of Rock Powders for Analysis.

Laboratory procedures undertaken were standard in approach for both whole rock and chip samples (see Figure 2.1.), with the following additional comments:

- 1) Initial sieving of powders to -200 mesh was discontinued, being considered time consuming and unnecessary. Approximate grain size of powder in the Tema mill could be judged by Tema noise. Beales (1976) compares sieved -200 samples with unsieved and +200 mesh samples (of similar Waulsortian carbonates) and concludes that sieving is not really necessary. He observes that the difference between analytical results of sieved -200 samples and unsieved samples lies within statistical

limits of precision and prefers to omit this stage, influenced also by the considerable time saving;

2) Grinding by Tema disc mill was only done for short lengths of time, usually less than 90 seconds, by which time a sufficiently fine grain size had been attained, thereby avoiding clogging up of the mill by annealing carbonate powder. Thus we avoid slowing down of cleaning routines or deleterious and destructive effects on carbonates at high temperatures, brought about by long grinding times (Reay 1981);

3) Cleaning of the jaw crusher and Tema mill between each sample was by use of a stiff brush and warm water. Where necessary, pure quartz sand was used in the Tema mill if annealing minerals such as sulphides were present.

2.3.1. Analytical Procedures.

For analysis by atomic absorption spectrophotometry, Russell (1974, 1975) used overnight dissolution of 0.25g of rock powder by 25 ml of cold 0.2M acetic acid to determine Mn content, digestion in 3M HCl at greater dilution for Mg, and concentrated HNO₃ digestion for Zn. All other elements were determined by X-ray fluorescence.

For this study, and any practical application to mineral exploration, a rapid analytical method was sought that would preferably allow determination of carbonate-associated trace elements from a single digestion of limestone rock powder, at the same time leaving intact

any impurities present, such as clay minerals, sulphides and iron-manganese oxides.

Although every attempt is made during sampling to avoid these non-carbonate impurities, this is not always possible if samples from close to mineralisation, or non-mudbank sediments are involved.

There is no reason, however, why trace elements associated with hydrothermal input may not be locked in some non-carbonate phase, particularly if precipitation took place under more oxidising conditions. Examination of the 'total' trace element content of an impure carbonate leads to problems in discriminating between those elements leached from any insoluble minerals associated with hydrothermal input and those derived from detrital sources.

In this study, the quest is essentially for cryptic trace element enrichments, rather than those associated with visible impurities.

The effect of non-discriminative analysis of multi-lithology profiles is examined in Chapter 5.

2.3.2. Method of Digestion of Rock Powder for A.A.

Analysis.

Background - By definition, pure carbonate rocks contain less than 10% mineralogical impurities such as clay minerals and oxides, in which the majority of trace element concentrations in the whole rock are located. The principal carbonate-associated cations are those which form common, naturally occurring carbonate minerals such as Mg^{2+} , Fe^{2+} , Mn^{2+} and Sr^{2+} . Other elements which might be expected to occupy Ca^{2+} lattice positions in calcite are divalent cations such as Ba^{2+} , Zn^{2+} and Pb^{2+} (Milliman 1974).

Many attempts have been made to study the problem of separating trace elements associated with the carbonate phase of limestones and dolomites from those associated with the non-carbonate phase (e.g. Barber 1974, Robinson 1980). None of these have been completely satisfactory, as some degree of leaching of trace elements from clays, sulphides or oxide minerals always takes place to distort the normally low values of these elements in the carbonate fraction (Martin and Chabot 1981).

Before selecting any one technique for application, it was considered necessary to examine the alternatives available, and apply some experimentation on a few representative samples. Chemical dissolution, with various degrees of attack on pulverised rock, may be attained by the use of either weak acids, dilute strong acids, or cation exchange resins. Examples of the use

of each of these methods are outlined in the following pages.

Weak acid digestion - Ray et al (1957) showed that 25% V/V acetic acid effectively breaks down carbonate in limestone - clay mineral - quartz mixtures, whilst apparently leaving intact the clay mineral lattices, using the relatively unstable hectorite as a reference clay mineral. They overcome the inability of cold acetic acid to digest dolomite by heating the reactants to 80 to 85°C for 3½ hours with no appreciable effects on the clay mineral fraction. The stronger hydrochloric and formic acids were shown to break down the clay minerals, unless acid strengths were reduced and temperatures kept low, such that reaction rate was very slow.

The same technique of using 25% V/V acetic acid was adopted by several authors in distinction between 'detrital' and 'non-detrital' fractions of various limestones and sediments (Hirst and Nicholls 1958, Chester 1965, Chester and Hughes 1967). To digest a variety of limestone types, Barber (1974) likewise used 25% V/V acetic acid, dissolving dolomitic samples by heating the reactants to above 60°C for 12 hours with 'minimal alteration to the non-carbonate fraction'. He gives comparative analyses for the same samples using atomic absorption on the insoluble fraction (by H₂O₂ dissolution) and X-ray fluorescence on the whole rock and insoluble fraction, to evaluate mineralogical associa-

-tions of trace and major elements.

Renard and Blanc (1972) studied the problem relative to acid strength and type, and duration and temperature of the reaction, concluding that 1N acetic acid at 55°C for 2 hours was the optimum for maximum leaching of carbonate and minimum leaching of non-carbonate.

In dealing with Recent marine and estuarine sediments, Loring (1976, 1979) states that the 25% V/V acetic acid digestion is useful to remove elements:

- i) held in carbonate minerals;
- ii) held in easily soluble amorphous compounds of Mn and Fe;
- iii) weakly held in ion exchange positions and attached to organic matter;

whilst leaving intact silicate lattice structures and resistant ferromanganese oxides.

On the other hand, Pomerol (1977) shows that leaching of clay minerals even by cold 1N acetic acid causes release of ions which are atypical of the carbonate phase of a limestone, although the elements liberated depend on a number of parameters, notably the structural position within the clay mineral (whether intra- or inter-layer elements) and nature and relative abundance of that element. The elements most in question were Al, Fe, Mg, K, Na and Ca, with Mg and K leached easily by weak acids, and Fe only if present in great quantity. Pomerol (op cit) also stresses the importance of grinding, filtration and consistency during application of

the technique, which should also be clearly monitored and described.

Robinson (1980) prefers the use of 1M HCl because of reasons of greater rapidity over the weak acid methods, although in comparison with hot 0.3M acetic acid digestion, notes that Fe tends to be leached from certain non-carbonate fractions in the former method.

Martin and Chabot (1981) point out the problem created by trace quantities of sulphide and oxide, which often cannot be avoided during sampling, due to thorough dissemination or invisibility. This problem is not easily overcome by selective dissolution techniques as the low background values for many elements in the carbonate phase means that even very slight leaching of tiny proportions of sulphide minerals will lead to a significant release of metal to distort analytical results. In spite of this, by comparing hydrochloric and acetic acid-leached Mn with total Mn content (from X-ray fluorescence analysis), Bencini and Turi (1974) show that most of the Mn present in clay minerals is absorbed, and not lattice bound, therefore very easily leached. However, with relatively pure limestones, the proportion of Mn contributed to the analyte is negligible, and within the precision limits of analytical procedure. This holds true even in a limestone with 10% of insoluble clay mineral residue.

Stronger acid treatments - The use of weak HCl has been briefly mentioned in the previous section.

More concentrated HCl has been utilised by several authors in similar discriminative studies, looking at trace elements in the carbonate fraction of limestones.

Wagner et al (1979) used concentrated HCl to determine carbonate-associated elements and 'soluble impurities', as distinct from 'insoluble residue', whereas Parekh et al (1977) also used 6N HCl, heated until all effervescence ceased.

That HCl and other strong acids (e.g. HNO_3 , HClO_4 , HF) attack such 'insoluble' minerals as sulphides, oxides and clay minerals is in no doubt (Angino and Billings 1972). Thus their use in digestion of carbonate rocks may be acceptable if the samples involved are of pure dolomite or calcite rhombs, for example, from fossil tests, where contaminating substances are at a minimum (possibly located along cleavage traces as fine films).

On the other hand, if examining fine-grained to micritic limestones containing significant argillaceous impurity (10% or more), often disseminated through the matrix, contamination by leaching from these constituents becomes a real problem. Because of this, Brand (1981) proposes that monomineralic components such as fossils, rather than multicomponent and multiphase matrix samples, are best suited as geochemical indicators in studies of carbonate rocks.

Other treatments - In their experiments on attack of calcite - dolomite - quartz - hectorite mixtures, Ray et al (1957) include the effect of cation exchange

resins (in this case Amberlite IRC-50 and IR-120). They noted that the effects on clay minerals were very similar to those of hot 25% V/V acetic acid, but that some of the hectorite may have been destroyed by prolonged heating (8 hours), in the leaching of dolomitic mixtures by the cation exchangers.

Deurer et al (1978) used a strong acid exchanger (MERC-1) on pulverised lake sediment samples (after treatment with 0.2N BaCl₂ - triethanolamine and 0.1N NaOH to remove exchangeable heavy metals and cations bonded to humic acids) to separate carbonate material from clay substances. Regeneration of the solution by 10% HCl was undertaken (while ensuring no carbonate remained) before atomic absorption analysis was performed.

In a five step procedure, Forstner and Stoffers (1981) use an acidic cation exchanger to extract carbonate-associated trace elements from Recent pelagic sediments. This step is undertaken before dissolution of the remaining acid-soluble phases (mainly hydrous ferric-manganese oxides and hydroxides) to prevent buffering to the extractive solutions by carbonate. They conclude, however, that the techniques utilised are as yet too inaccurate to decide between 'easily' and 'moderately' acid-soluble phases.

Boyle (1981) uses overnight dissolution in pH5.5 ammonium acetate/acetic acid buffer to dissolve the carbonate, while keeping the pH high to minimise the solubility of other phases. He also utilises several

methods of 'cleaning' the samples with basic complexing agents prior to dissolution, but casts doubt on the ability of acetate buffers to selectively leach only the carbonate fraction of calcareous sediments. Along similar lines, the initial treatment of pulverised marine sediments for four hours with 1M $MgCl_2$ solution is undertaken by Grieve and Fletcher (1976) to remove water-soluble and exchangeable metals before acid attack.

Discussion - Although careful attempts are made both in the field and laboratory to ensure purity of the sample collected, host rocks in and around centres of mineralisation generally suffer from pervasive dolomitisation, argillaceous impurities and disseminated, fine-grained or microscopic mineralisation. This creates the need for an analytical technique which is selective in revealing the carbonate-associated trace elements as accurately as possible, without appreciable effect on non-carbonate minerals, yet sufficiently potent to break down the more stable or resistant carbonates.

In separation of carbonate-associated trace elements from those associated with the non-carbonate fraction, reaction between the weak acid and non-carbonate minerals depends on:

- 1) the type and concentration of acid used;
- 2) the temperature and duration of the reaction;
- 3) particle size, solubility and crystallinity of the rock powder being digested.

Prior treatment of pulverised sediments with various weak solutions or basic complexing agents to 'clean' or remove water-soluble exchangeable metals, as undertaken by Grieve and Fletcher (1976) and Boyle (1981) was not considered suitable or necessary for consolidated and fairly pure ancient limestones which have undergone diagenesis and recrystallisation. Likewise, as the use of various cation exchangers is not shown to be any more effective than weak acid attack in isolating carbonate-associated trace elements from pulverised limestone or carbonate sediments, (in spite of relatively high cost and time demands), their application here is not considered advantageous.

As no single acid treatment has been proven as entirely satisfactory in leaching only those metals associated with carbonate phases of limestones, a number of short experiments were conducted to determine which method was optimum for the samples collected for this study, and the elements sought. These are described in Appendix I.

Trial experiments showed that heating of acetic acid improved dissolution rate, percentage extraction (for Mn), and reduced analytical error (Figure A.1, Tables A.1. to A.5.). Use of acetic acid rather than hydrochloric or nitric acids, reduced the degree of attack on sulphides and other 'insoluble' minerals. This agrees with the conclusions made by Beale (1976), who used heated acetic acid rather than cold, stronger acids

on similar rock types.

Following the experiments outlines in Appendix I, the technique adopted for application in regional and local surveys utilises 2M acetic acid, with higher temperature attack (90°C) preferred, to permit breakdown of any dolomitic, ankeritic or sideritic components. Duration of the reaction was kept to the minimum necessary to break down all the carbonate, whilst ensuring that sufficiently fine grain size had been achieved during grinding. Prolonged attack at high temperatures would cause significant release of metals from small amounts of clay minerals and (especially) sulphides present in the rock, as well as increasing the risk of contamination from external sources (Robinson 1980).

Outline of method used - Digestion of rock powder was conducted in a test-tube, at 100x dilution (0.2g into 20ml of 2M acetic acid); simmered at 90°C for one hour on a sand bath; rapidly cooled in cold water and made up to 20ml with deionised water; then decanted into a fresh tube (Figure 2.1).

The 100x dilution allows direct determination of the elements being sought, although further dilutions were made if required, in samples with anomalously high concentrations of any of these.

Analyses were performed on an I.L. 251 Atomic Absorption Spectrophotometer in the Applied Geology Department, University of Strathclyde. Standard preparation and machine operating conditions are given in

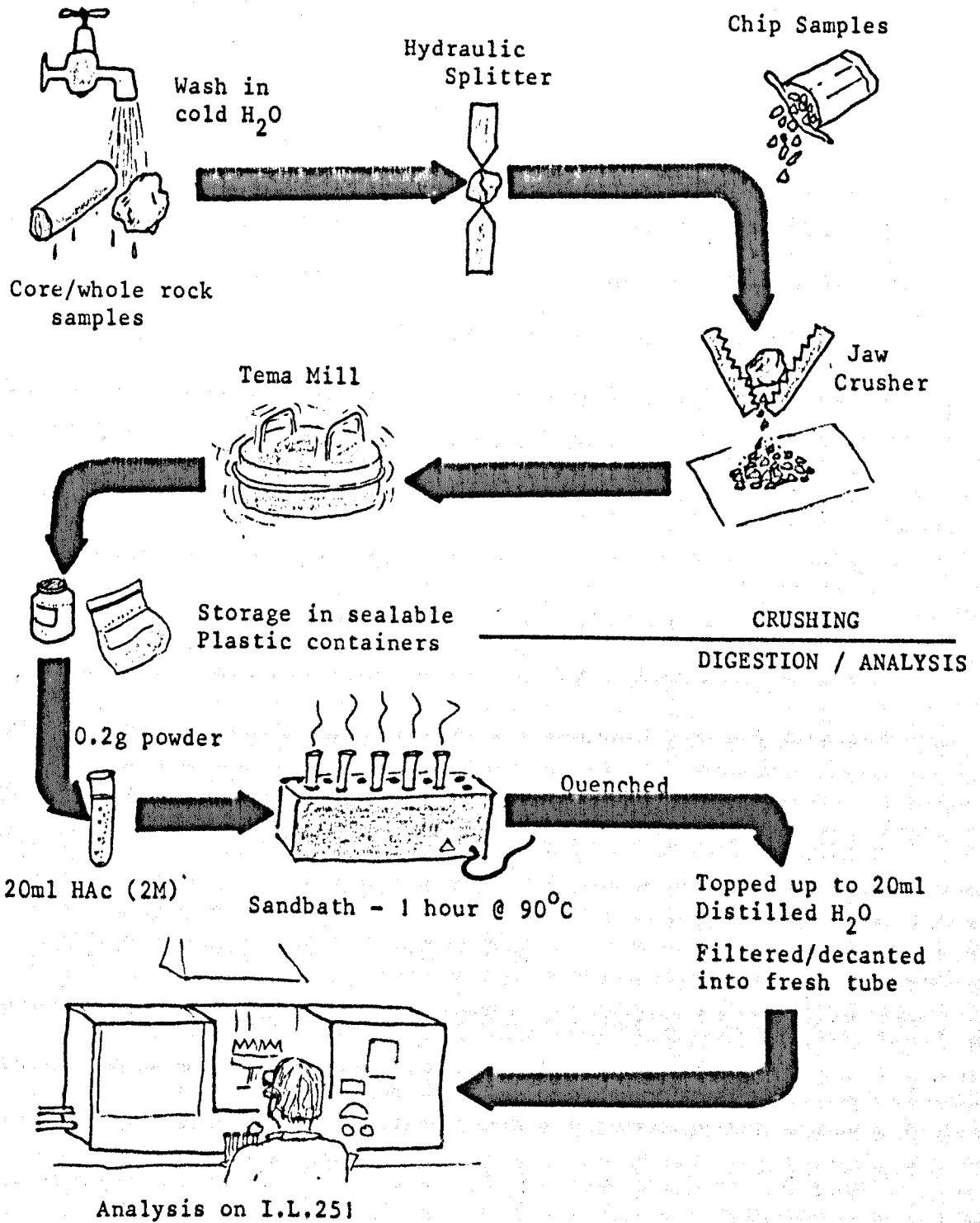


Figure 2.1. Summary of laboratory procedures for preparation and analysis of carbonate rock samples by atomic absorption.

Appendix III. Before analysis, one percent of pure CaCO_3 powder was added to the standard and blank solutions so as to match the relatively high CaCO_3 content of the sample solutions.

Analysis of samples containing visible sphalerite resulted in considerable enhanced Zn values, reflecting gradual breakdown of the sulphide at higher temperature. Likewise, samples of semi-massive pyrite subjected to the same treatment began to show excess Fe values after prolonged heating indicating breakdown of the sulphide and release of Fe into solution (Figures A.2. to A.13.).

The elements Mn, Fe, Zn and Mg were analysed by atomic absorption spectrophotometry (A.A.S.) in all samples. Some other elements were analysed by X-ray fluorescence (X.R.F.) in a selected number of samples. Most importantly, the number of elements chosen was kept to a minimum to ensure rapid, uncomplicated (and therefore inexpensive) procedures, all four being handled by the single method outlined above.

Manganese and Iron are commonly occurring trace elements in carbonate lattice positions of limestones and dolomites, and both are associated almost universally with hydrothermal solutions. Both are present in the limestones of the Irish Lower Carboniferous near to the optimum concentrations for A.A.S. sensitivity (after 100x dilution) at between 0.5 and 5 ppm in solution.

Magnesium is analysed as an index of the degree of

dolomitisation suffered by the mudbank limestone samples (often difficult to determine in hand specimen), and to investigate any control this may have over other trace elements. Manganese and iron levels may vary directly with Mg, as predicted and exemplified by many authors (See Chapter Six.). In pure limestone samples with less than 0.5% Mg, direct readings may be taken from the analyte, whereas if appreciably higher than this value, further dilution is required.

Zinc is analysed as a direct indicator of hydrothermal input, and probably reflects the amount of microscopic sphalerite present in the rock, rather than purely carbonate-associated zinc. When present at background levels (10 ppm or less in the rock), it is towards the lower limit of detection of the analytical method, and poorer precision levels are encountered (Figure A.14). Any advantage of utilising lower dilution factors is outweighed by the increased interference effects from major elements, particularly calcium. Use of the hydrogen continuum is made to combat background absorption at such low levels.

Although commonly occurring as trace constituents in carbonate rocks and minerals, the elements Ba, Sr and Pb were not analysed by A.A.S. because of the unsuitability of the acetic acid digestion, and complications which may arise, particularly with Ba and Pb (e.g. Campbell and Ottaway 1974). Without the use of a carbon furnace, Ba and Pb analyses by A.A.S. suffer from severe

Ca interference problems (Billings 1965), and difficulty is experienced in maintaining Ba in solution for aspiration. Instead, these three elements (Ba, Sr, and Pb) were analysed by X.R.F., along with a number of other major and minor constituents (CaCO_3 , SiO_2 , Al_2O_3 , K_2O).

A number of analyses for Na were made using the same solution as for routine Mn, Fe, Zn and Mg analysis.

Although not attempted in this study, direct analysis of Ca and Mg at 100x dilution can be undertaken, without further dilution, by utilising spectral overlap of nearby non-resonance lines (Ge 422.66nm, for Ca 422.67nm; V285.17nm, for Mg 285.21nm) to reduce A.A.S. sensitivity for these elements (Robinson 1980).

3.1.1. Introduction.

This chapter is concerned with the presentation of analytical data from sample suites collected throughout central and southwest Ireland. Each section commences with an outline of the principal geological features and mineral deposits of the area under investigation. This is then followed by presentation of the relevant data in summarised form, by means of graphs, maps and tables.

A total of 2300 outcrop and 770 core samples of Waulsortian Mudbank Limestone and its local equivalents, were collected from the eleven areas shown in Figure 3.1. and Table 3.1. All were analysed for Mn, Fe, Zn and Mg. Comparison of their Mn and Fe contents reveals a significant difference between the core and outcrop samples (Figure 3.2.). The former contain a wide range of Mn and Fe contents, whereas the latter are concentrated towards the lower end of the scale, below 500 ppm. The most probable cause of this is that all the core samples originate from within 3 kilometres of known mineralisation, and have therefore been influenced by primary enrichments, as outlined in the introduction to this study. Outcrop samples, on the other hand, range from within one kilometre of known mineralisation to many tens of kilometres distant. Because of this, only a small proportion of them have been influenced by primary trace element enrichments.

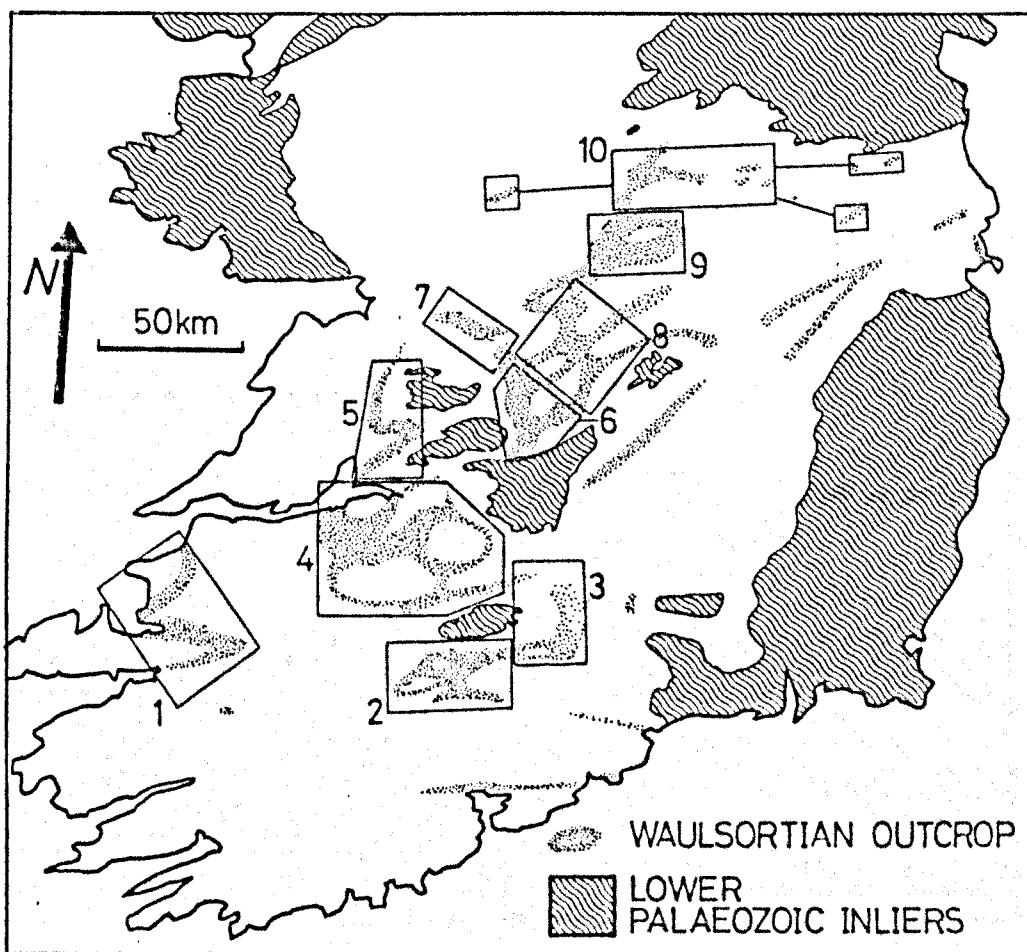


Figure 3.1: Location of sample areas in this study, for Key see Table 3.1. Not shown is Craven Basin sample area, Northern England.

TABLE 3.1 LOCATION	(N) CORE	(N) OUTCROP	(N) DISTAL OUTCROP*
1. Kerry	-	234	234
2. North Cork	-	489	441
3. Aherlow / South Tipperary	29	42	42
4. Limerick	-	217	195
5. Ballyvergin / East Clare	-	159	94
6. Silvermines-Nenagh	387	292	132
7. Tynagh-Loughrea	62	139	94
8. South Midlands	-	82	82
9. Moate-Athlone	-	116	110
10. North Midlands	292	286	169

TABLE 3.2	(n)	(Mn+Fe)/2	Mn	Fe	Mg (%)	Zn	Mn:Fe
All distal outcrop	1593	115	108	111	0.32	(3.8)	0.97

Table 3.1: Sample distribution for each area in Figure 3.1. * Distal outcrop from at least 4 kilometres distant from centres of known mineralisation (see text).

Table 3.2: Median values of Mn, Fe, Zn and Mg for all distal outcrop samples. Data in ppm except where indicated.

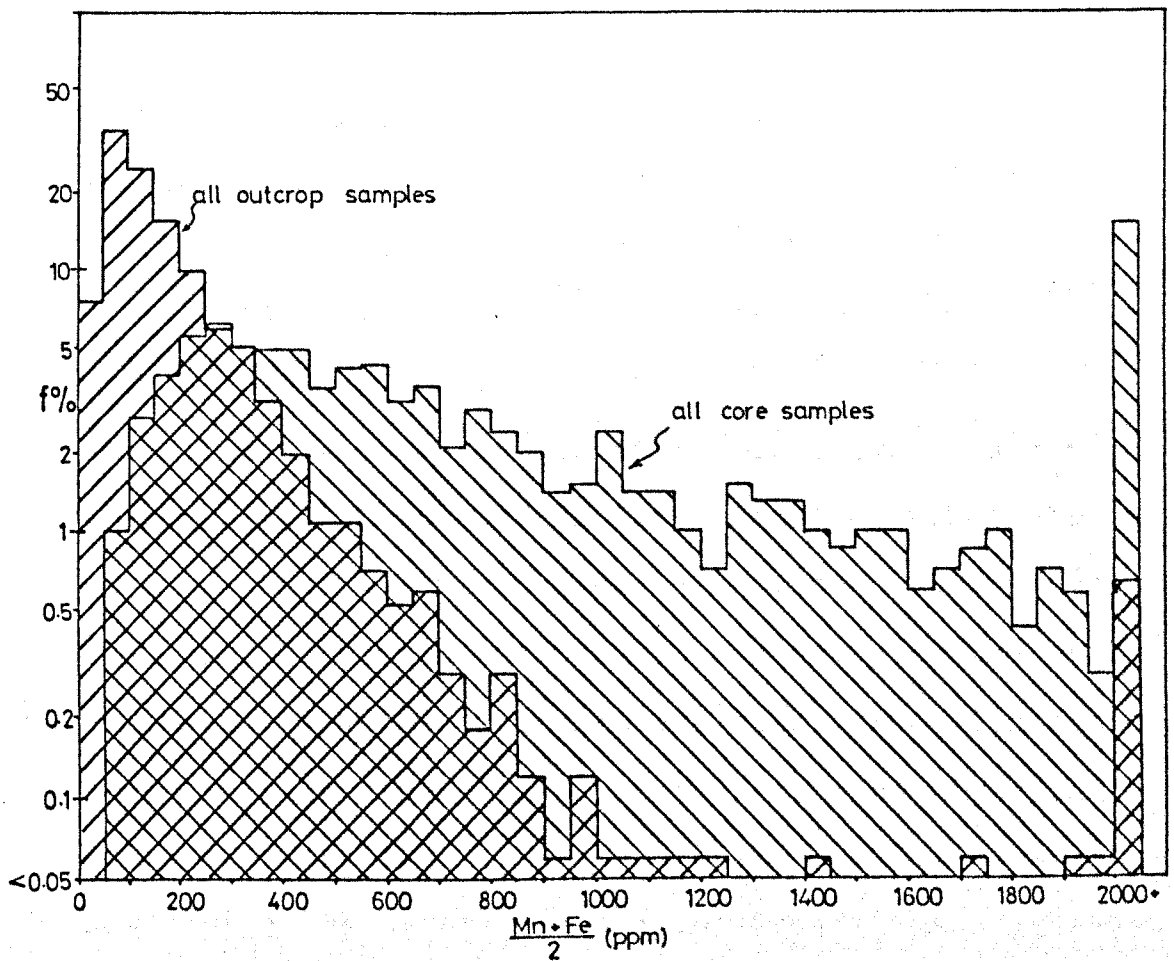


Figure 3.2: Comparison of frequency distribution of $(Mn+Fe)/2$ between all core samples ($n = 770$) and outcrop samples ($n = 2300$) from Ireland. Note vertical log scale.

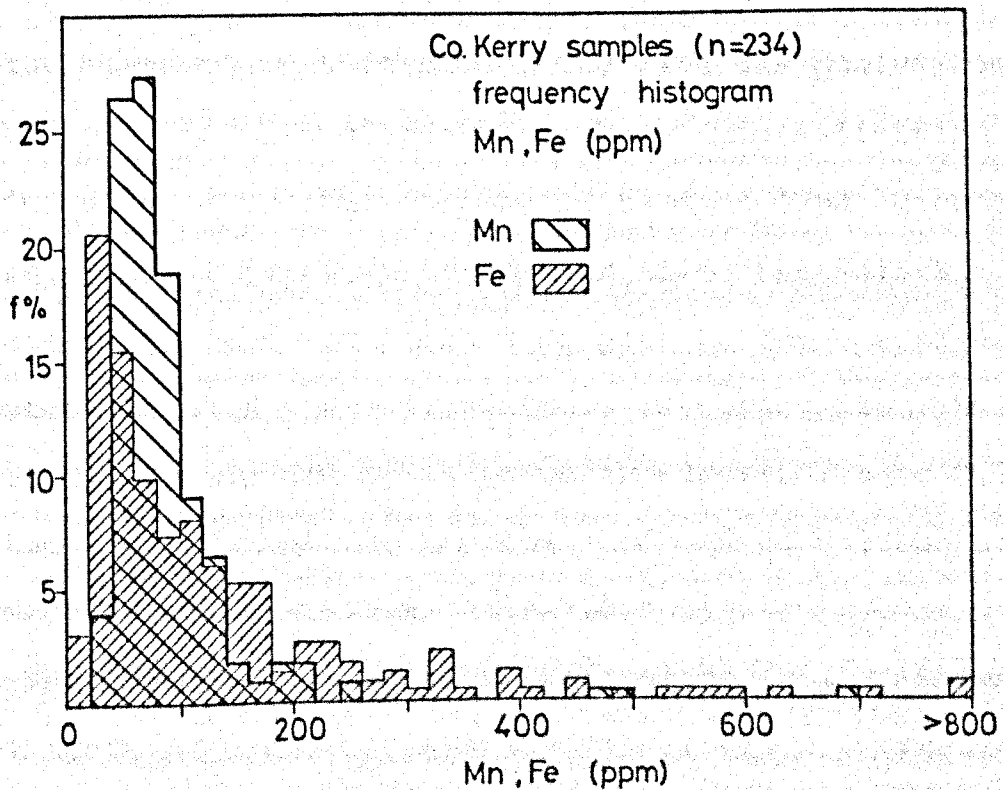


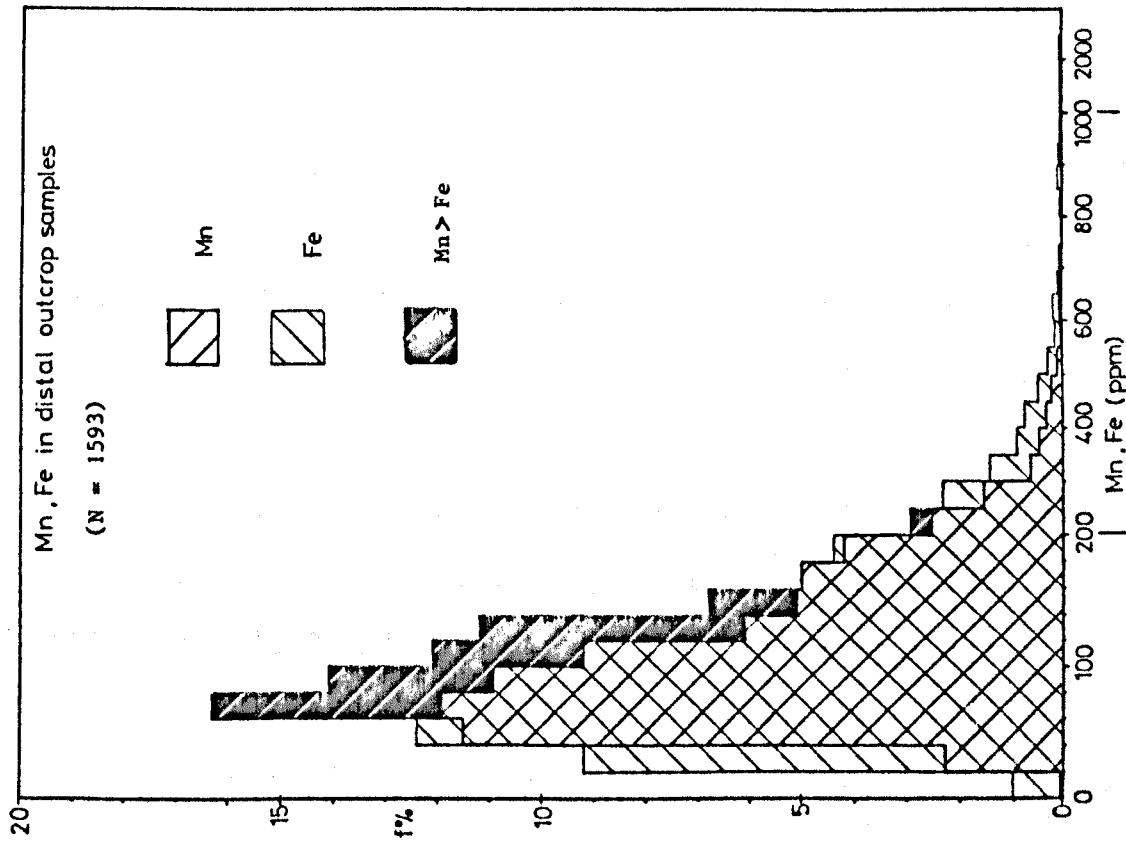
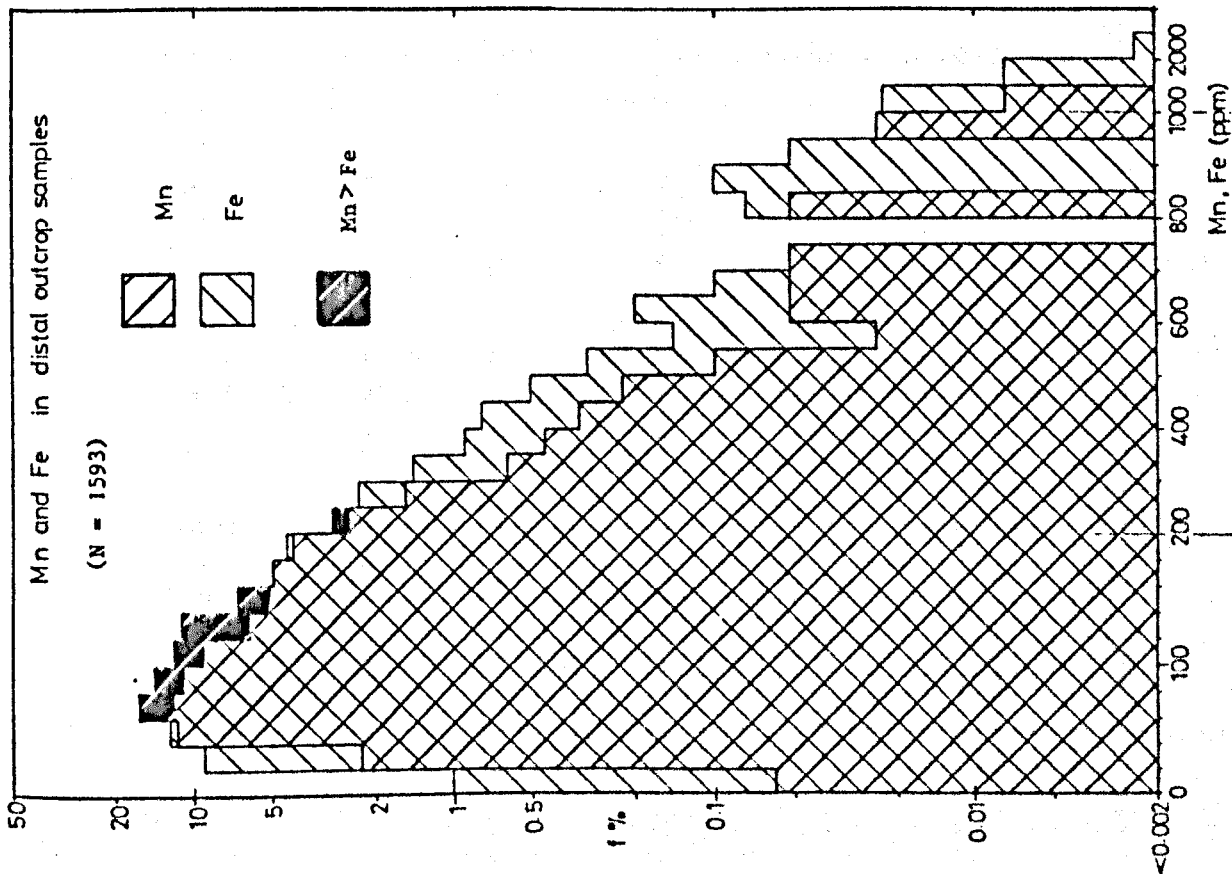
Figure 3.3: Frequency histogram of Mn and Fe in Co. Kerry samples (Area 1), where no significant exhalative mineralisation is known in the Carboniferous. Only a small proportion contain over 100 ppm Mn or Fe. Note also the comparison between Mn and Fe.

Comparison between the core samples and those outcrop samples collected only from areas where no mineralisation is known, provides a more pronounced contrast between 'distal' and 'proximal' samples (e.g. Co. Kerry, Area in Table 3.1, see Figure 3.3.).

In all the samples collected for this study, a strong sample bias exists towards 'anomalous' or trace element-enriched samples, because patterns around known deposits are under scrutiny. At Tynagh, for example, over half of the total outcrop samples are taken from within the seven kilometre zone of primary enrichment described by Russell (1974). Because of this, 'proximal' samples are excluded from statistical evaluation, when attempting to define background trace element levels for Waulsortian Mudbank Limestones.

In order to determine background levels for each of the elements in this study, the data was pooled together, and only samples distant from known mineralisation were included. For this purpose, data from 1593 outcrop samples collected at least four kilometres distant from mineralisation was plotted on probability curves and median values were calculated. Frequency distribution of Mn, Fe, Zn and Mg is shown in Figures 3.4 to 3.7 for these distal outcrop samples, and median values for each are tabulated in Table 3.2.

The distribution of $(\text{Mn}+\text{Fe})/2$ values is also shown (Figure 3.7) as this average represents a convenient means of combining the two sets of results. Preliminary



Figures 3.4a,b: Frequency distribution of Mn and Fe in all distal outcrop samples from Ireland. Note that Mn frequency is greater than Fe frequency only in mid-range, between 60 and 200 ppm (shaded). Both diagrams show the same data, the vertical scale in 3.4a is logarithmic, but linear in 3.4b. Note also the change in horizontal scale (Class Interval size) at 200ppm and 1000ppm in both diagrams.

examination of the data indicates that Mn and Fe essentially follow very similar, related patterns in their distribution in mudbank limestones (e.g. Figure 3.4). Some of the reasons for this are discussed in Chapter 6. Their relationship can be displayed by measuring the ratio Mn:Fe, which averages 1.03 in distal outcrop samples, or by graphing Mn against Fe (e.g. Figure 3.25). Use of the averaged value $(\text{Mn}+\text{Fe})/2$ effectively smoothes out the distribution patterns of the two individual elements. Comparison of means and standard deviations for Mn, Fe and $(\text{Mn}+\text{Fe})/2$ from ten outcrop samples from a single site (Table 3.3) indicates that σ/\bar{x} is lower for the averaged value than for the individual elements.

The most obvious difference between their distribution is that Fe tends to follow more extreme patterns, being slightly lower than Mn at background levels in the rock, and higher at anomalous levels. This is displayed in Figure 3.4, where the frequency distribution of Mn exceeds that of Fe only in 'mid-range' between 60 ppm and 160 ppm, further emphasised by Figure 3.8, in which Fe frequency (f_{Fe}) has been subtracted from Mn frequency (f_{Mn}) for each class interval of the same population. In Table 3.3, σ/\bar{x} is also greater for Fe than Mn, although median values for distal samples are very similar to Table 3.2.

Over 90% of zinc values in distal outcrop samples are below 10 ppm, and over 99% below 20 ppm (Figure 3.5).

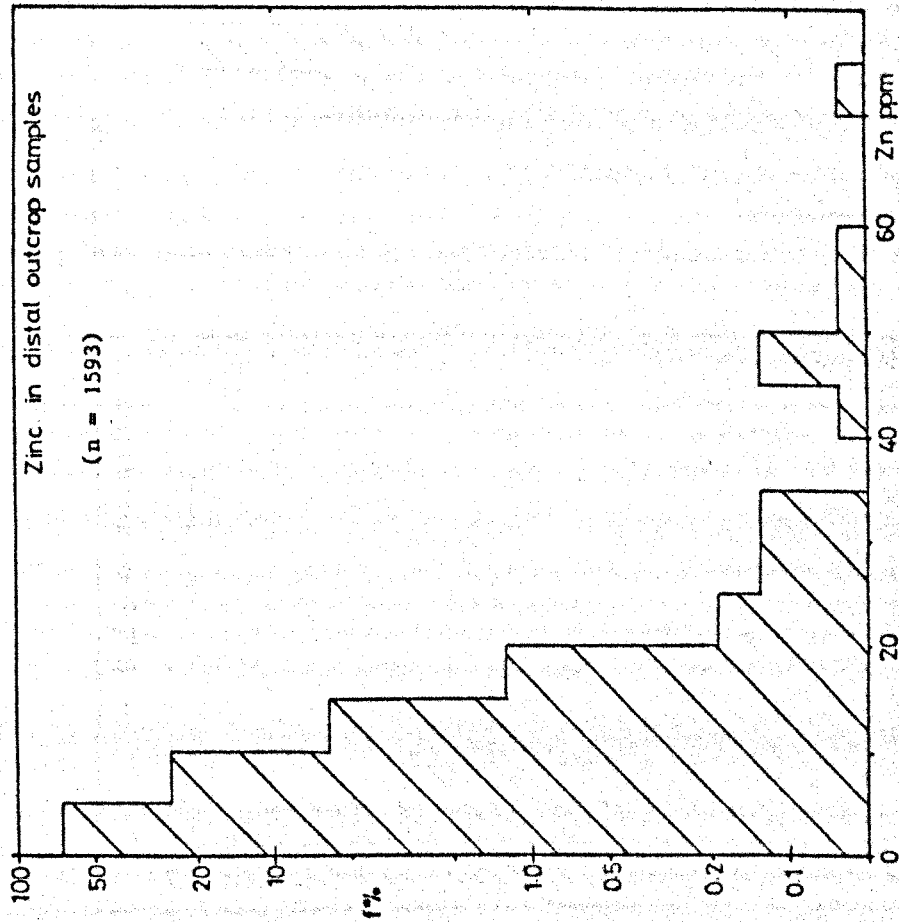


Figure 3.5: Zinc frequency distribution in all distal outcrop samples in Ireland. Note vertical log scale.

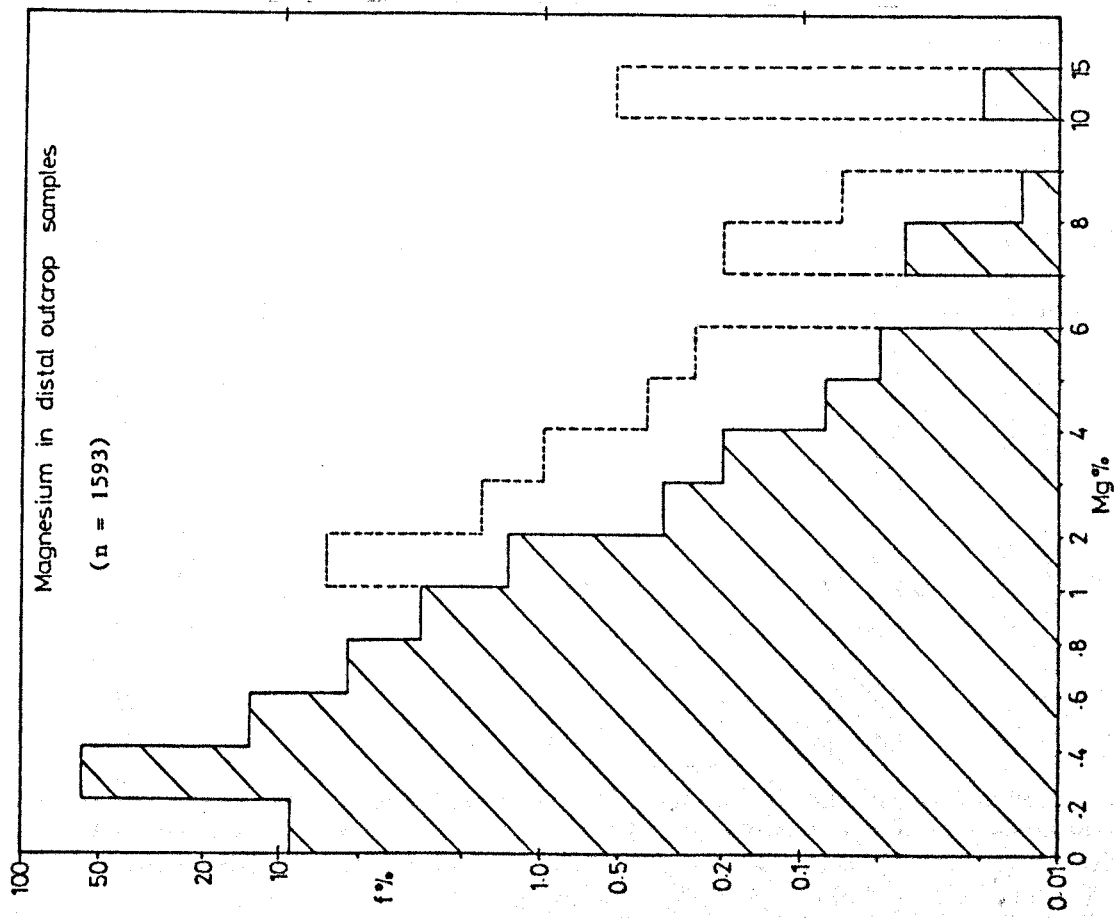
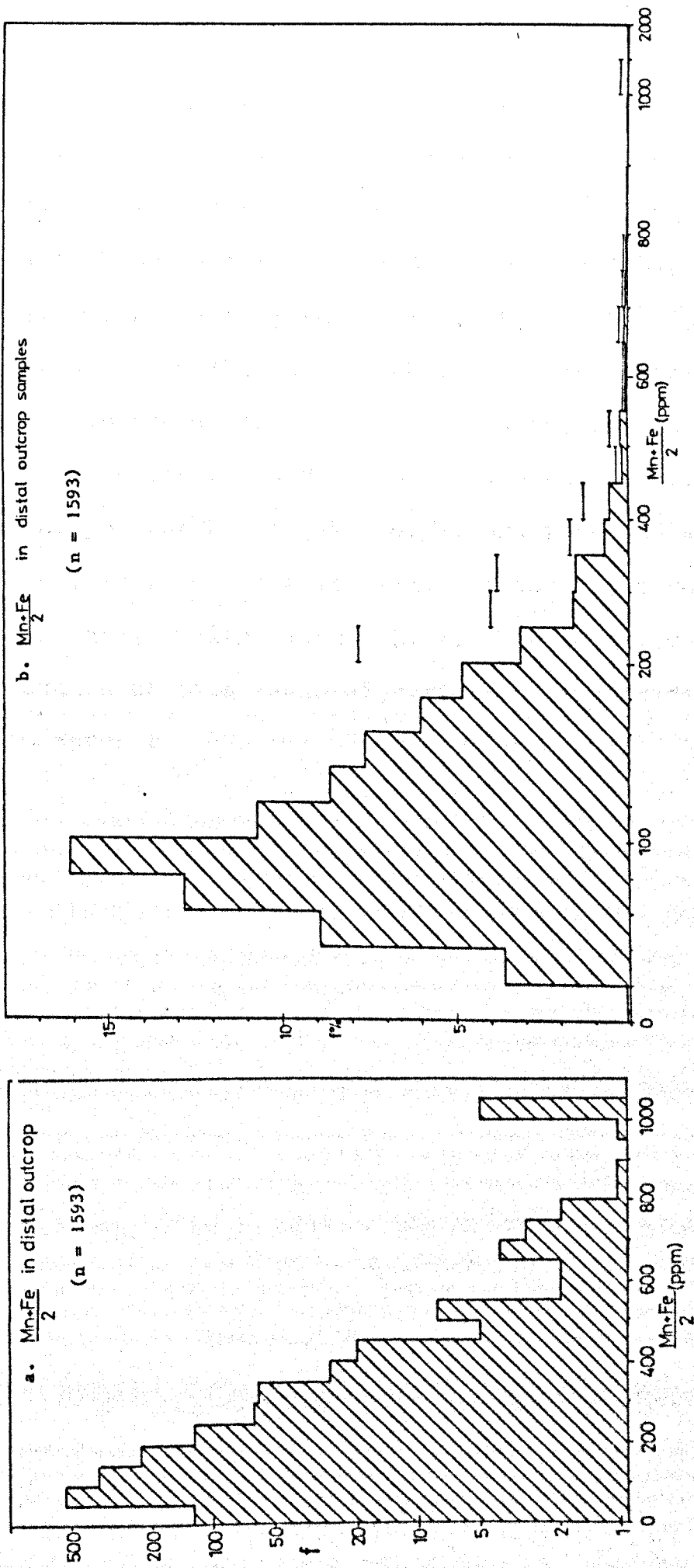


Figure 3.6 (right): Magnesium frequency distribution in all distal outcrop samples in Ireland. Note change in horizontal scale at 1% and 10%, dotted line represents actual frequency values, solid lines represent 'equal area' histogram. Note also vertical log scale.



Figures 3.7a, b: Frequency distribution of $(\text{Mn}+\text{Fe})/2$ values in all distal outcrop samples from Ireland. Figure 3.7a has vertical log scale, Figure 3.7b has 'equal area' representation, with vertical scale adjusted to match changing horizontal scale (larger class intervals) at 200ppm and 1000ppm (horizontal bars represent actual frequency percent (f%) values).

As well as the differences between Mn and Fe, median values of Mn, Fe and $(\text{Mn}+\text{Fe})/2$ vary slightly between study areas, leading to slightly different background levels for each individual area. These values are tabulated in Table 3.4 and the regional variation they represent is contoured in Figure 3.9 for $(\text{Mn}+\text{Fe})/2$, Mn and Fe. This shows how values range from below 100 ppm in the southwest of the country, to 200 ppm or more in the North Midlands. Even higher values (over 300 ppm for Fe and $(\text{Mn}+\text{Fe})/2$) are recorded still further to the east in similar Waulsortian Mudbanks in Northern England (Table 3.4). The significance and origin of this regional variation is considered in Chapter 6.

TABLE 3.3 SAMPLES ELEMENT (N) \bar{x} μ μ/\bar{x}

Tynagh	(Mn+Fe)/2	10	502	134	0.27
T26 - T35	Mn	10	471	188	0.40
(proximal)	Fe	10	533	156	0.29
Tynagh	(Mn+Fe)/2	10	98	15.1	0.15
T158 - T167	Mn	10	117	22.5	0.19
(distal)	Fe	10	79	15.5	0.20

Table 3.3: Comparison of means and standard deviations for Mn, Fe and (Mn+Fe)/2 from ten outcrop samples from two individual sites, one proximal, one distal to Tynagh Orebody.

TABLE 3.4 LOCATION (N) (Mn+Fe)/2 MN FE

1. Kerry	234	84	71	83
2. North Cork	441	90	101	74
3. Aherlow - S. Tipperary	42	73	84	51
4. Limerick	195	125	107	130
5. Ballyvergin - E. Clare	94	110	96	117
6. Silvermines - Nenagh	132	114	123	103
7. Tynagh - Loughrea	94	137	127	142
8. South Midlands	82	161	126	185
9. Moate - Athlone	110	173	177	172
10. North Midlands	169	202	172	223
All distal outcrop	1593	115	108	111
North England	244	321	228	394

Table 3.4: Median values of Mn, Fe and (Mn+Fe)/2 for each sample area, distal samples only. Also shown are median values from Northern England Waulsortian Limestone samples.

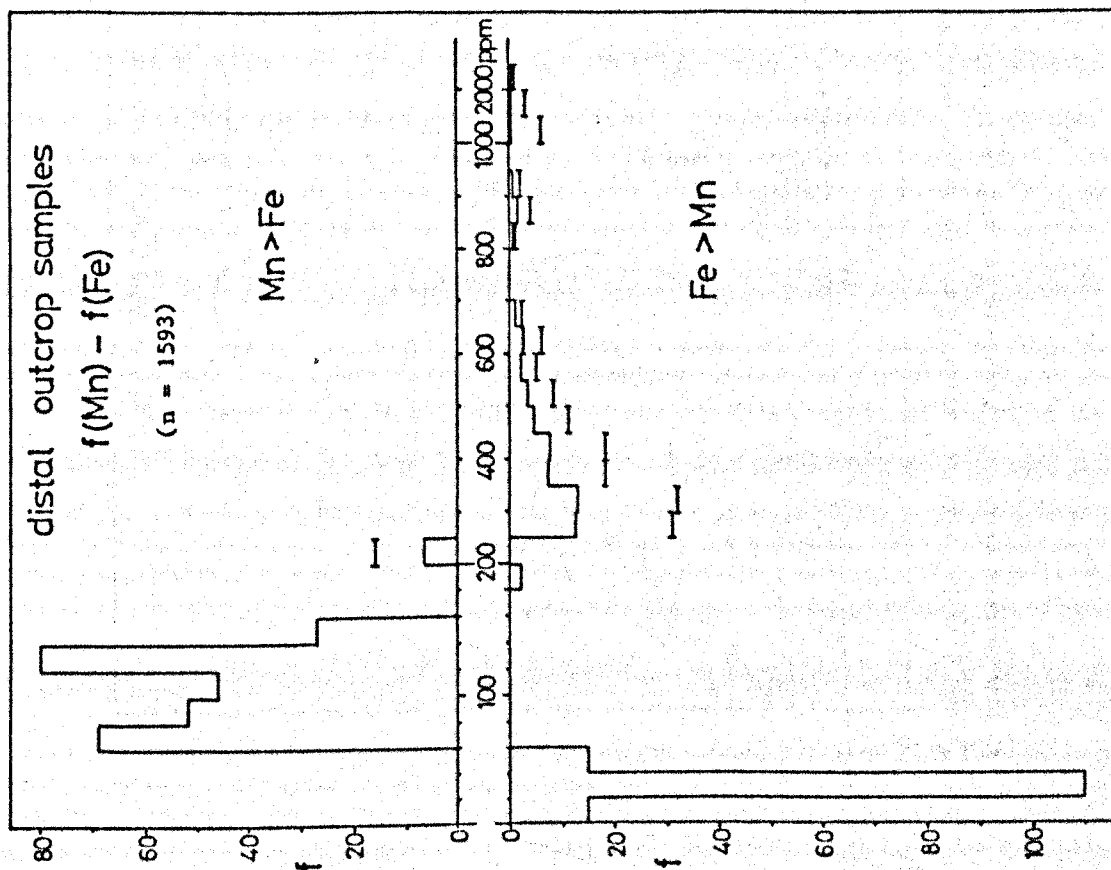


Figure 3.8: Comparison between Mn and Fe frequency distribution in all distal outcrop samples, achieved by subtracting Fe frequency from Mn frequency for each class interval. Note changes in horizontal scale at 200ppm and 1000ppm, with adjustment of vertical scale to preserve 'equal area' (bars represent actual frequency values).

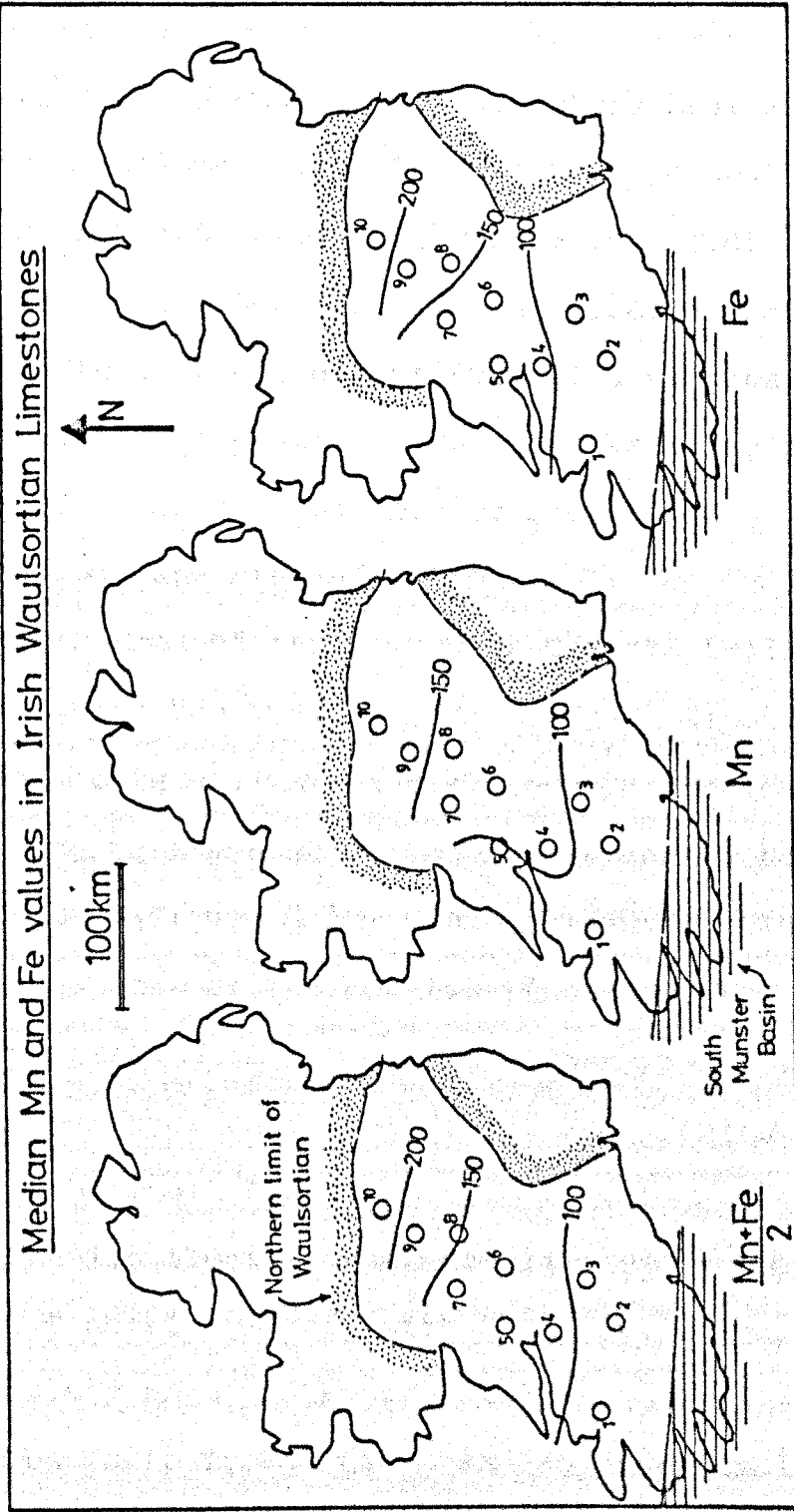


Figure 3.9: Regional variation in median Mn, Fe and $(\text{Mn}+\text{Fe})/2$ values in Irish Waulsortian Limestones. Values contoured in ppm. Median values for Northern England (not included on map), are 228, 394 and 321 ppm, respectively (see Table 3.4).

3.2.1. Tynagh.

Introduction.

Russell (1974, 1975) presented results of a lithogeochemical study of 200 samples from Tynagh Mine and surrounding area, in which manganese was shown to be enriched in Waulsortian Limestone host rocks up to seven kilometres distant from the mine. Concentration of Zn, Al_2O_3 and Fe_2O_3 were also enriched in the surrounding host rocks to a lesser extent.

In this study, all of Russell's samples were re-analysed using the technique described in Chapter 2. No further samples were collected.

Geology and Mineralisation.

This area of study in West Central Ireland, which includes the Tynagh Pb+Zn+Cu+Ag+Ba deposit, is underlain by a shallow-dipping Lower Carboniferous strata, lying to the east of the Slieve Aughty Lower Palaeozoic inlier (Figure 3.10). Discontinuous outcrop of a broad belt of Waulsortian Limestones trends approximately NW-SE, parallel to the NE margins of the inlier, offset by a number of NE trending faults, notably the North Tynagh Fault.

The lithological sequence is similar to that elsewhere in Central Ireland, with local variations and terminology noted in Figure 3.11.

The North Tynagh Fault and adjacent small suboutcropping Old Red Sandstone inlier separate the carbonate rocks of two adjacent sedimentary-structural basins -

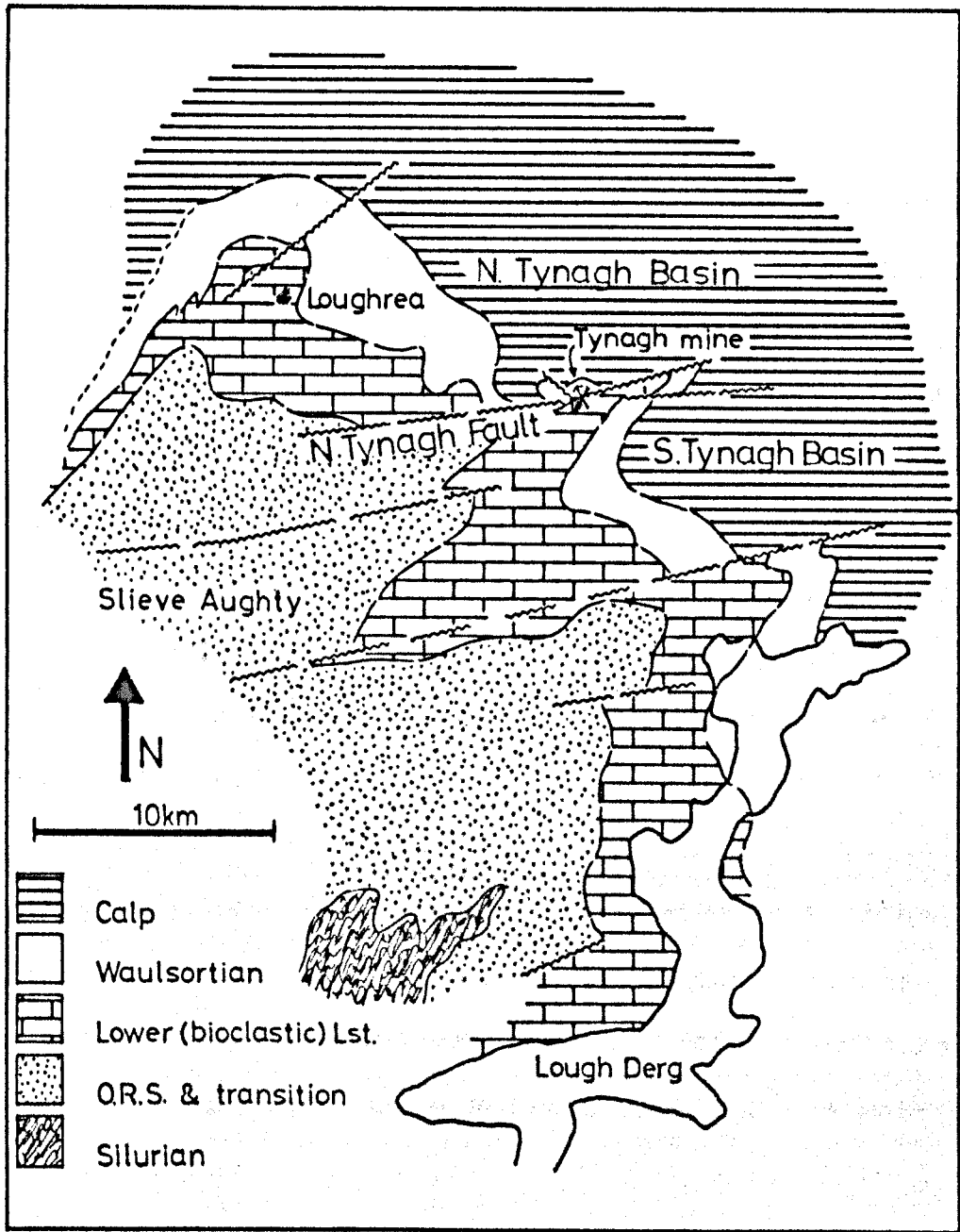


Figure 3.10: Location of the Tynagh Mine, County Galway, with outline of the geology of the area. See also Figure 3.1.

- the North Tynagh Basin (which hosts the Tynagh orebodies) and the South Tynagh Basin (which has no known economic mineralisation, except for the old trial workings close to the Tynagh Mine).

The Tynagh primary orebody (Figure 3.12) is hosted in a fault-bounded wedge of Waulsortian Mudbank Limestones and equivalent lithologies, the latter consisting of iron formation, slump breccias and dolomitised mudbank limestone (Derry et al 1965). Although mineral textures are dominated by fracture- and cavity-fill styles of cross-cutting and epi-genetic and epi-diagenetic mineralisation, a sedimentary exhalative origin is favoured for the bulk of the ore material. Several features support this view:-

- 1) the coincidence of the sedimentary iron formation and laterally extensive primary trace element enrichments with base metal mineralisation (Russell 1975);
- 2) sedimentary slumping and reworking of both mineralised and unmineralised mudbank limestones and ore material, including banded sulphide (Schultz 1966, Riedel 1980);
- 3) the occurrence of laterally persistent, very finely laminated sphalerite mineralisation in L₂ Limestone; footwall sulphide, baryte and oxide layers in L₃ (cf. banded footwall mineralisation in Muddy Reef at Silvermines (Taylor 1984)); and zinc rich microspherules, similar to present day, Lake Kivu mineralisation in East Africa (Degens et al 1972), within the orebody

REGIONAL NAME	ORE	SYMBOL	LOCAL STRATIGRAPHY (thickness)
MIDDLE LIMESTONE (CALP)	SECONDARY ORE	L1a	Upper Calp (up to 270m)
		L1b	Lower Calp
WAULSORTIAN MUDBANK COMPLEX	PRIMARY ORE	L2a	Reef Limestone (crinoidal biomicrite) (0-170m)
		L2b	(slump breccia)
		L2c	(calclutite) → Iron Formation
		L2b	(slump breccia)
LOWER LIMESTONE		L3	Lower Muddy Limestone } (200-270m)
		L4	Lower Bioclastic Limestone
LOWER LIMESTONE SHALE		L5	Lower Limestone Shale (50m)
		S	Old Red Sandstone
			Silurian

Figure 3.11: Geological sequence of Tynagh Mine, with thickness variation and local terminology. After Hutchings (1979).

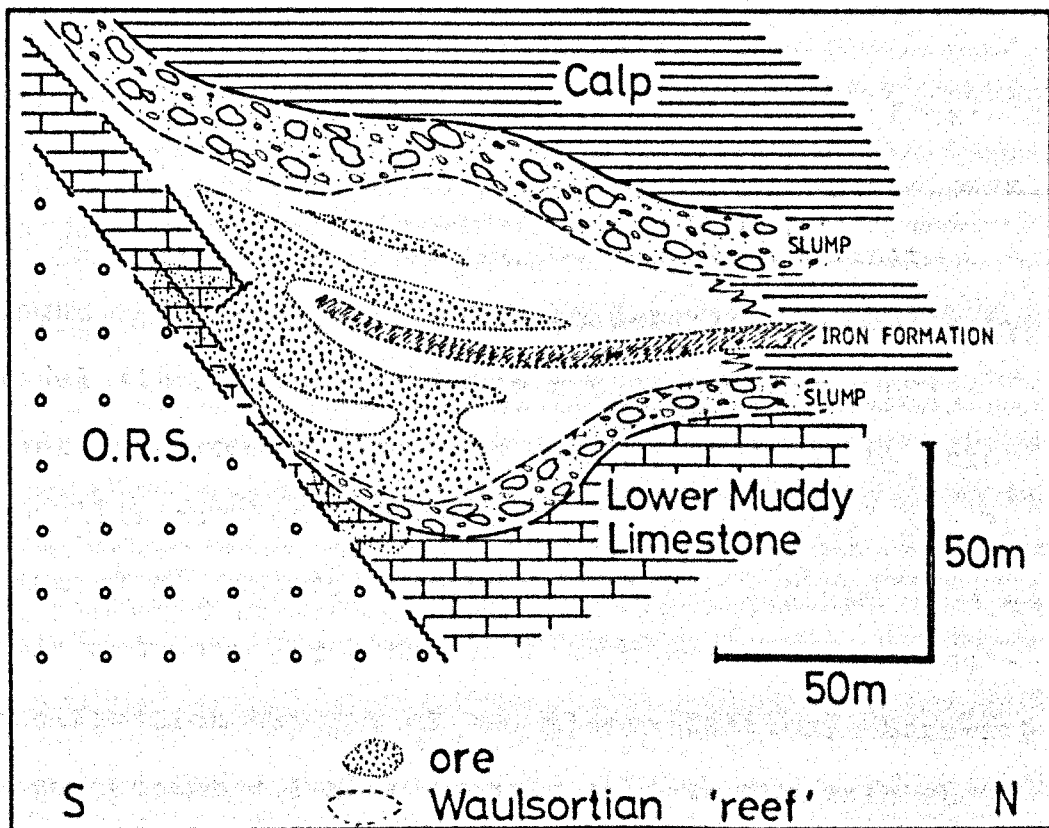


Figure 3.12: Generalised North - South geological section of Tynagh Mine. Modified from Hutchings (1979).

(Riedel 1980a, b).

Although the main North Tynagh Fault is probably a reactivated Caledonoid structure, movements have taken place periodically, and in more than one episode in the Carboniferous (Moore 1975). Syndepositional fault movements in the Lower Carboniferous are indicated by the abundance of submarine slump material, sedimentary breccias and turbidite deposits associated with the ore and sediments, together with thickness changes of various sedimentary units towards the fault (Derry et al 1965).

Mineralisation at Tynagh occurs at the point of maximum syndepositional throw (about 700 metres, northwards), and maximum fault plane steepness (dip 60 to 80° northwards, increasing with depth) along the North Tynagh Fault (Russell 1972, Hutchings 1979).

The primary mineralogy consists essentially of galena, sphalerite and pyrite, with subordinate copper minerals and sulphosalts in a baryte, dolomite and calcite gangue. Ore textures have been described recently by Riedel (1980), who envisages syngenetic and syndiagenetic introduction of ore metals, modified by later remobilisation on both large and small scales, and by Boast et al (1981), who present stable isotope data in their argument for a multi-stage diagenetic and post-lithification history of ore mineralisation. Late-stage, cross-cutting dolomite plugs post-date the main Pb+Zn mineralisation and contain traces of copper (Hutchings

op cit). These are the subject of a study by Banks (in preparation).

Sampling and Results.

The majority of the 137 outcrop samples analysed come from the tract of outcrop between Tynagh Mine and Loughrea, supplemented by 62 core samples from within a few kilometres of the mine itself (where outcrop is scarce), and a limited number of samples from the south-east continuation of reef outcrop towards Lough Derg (Figures 3.13a,b).

Examination of the analytical data indicates that iron accompanies manganese in its lateral enrichment patterns around the Tynagh deposit. Figures 3.14 to 3.15 show the lateral distribution of Mn and Fe content of Waulsortian Mudbank Limestone outwards from the approximate centre of the economic mineralisation, this point having been chosen as an approximation for the exhalative centre. Note that beyond 6 kilometres of this centre, Mn values generally do not exceed 250 ppm, whereas within 4 kilometres, they do not drop below this level (Figure 3.14). Although background values for Fe are slightly higher than Mn, beyond 6 kilometres they rarely exceed 300 ppm, whereas within 5 kilometres, they do not drop below 200 ppm (Figure 3.15). The distribution of $(\text{Mn}+\text{Fe})/2$ follows a similar pattern of enrichment to 6 kilometres, remaining above 250 ppm within 4 kilometres of the mine (Figure 3.16). Plotting of $(\text{Mn}+\text{Fe})/2$ values in outcrop samples alone is equally

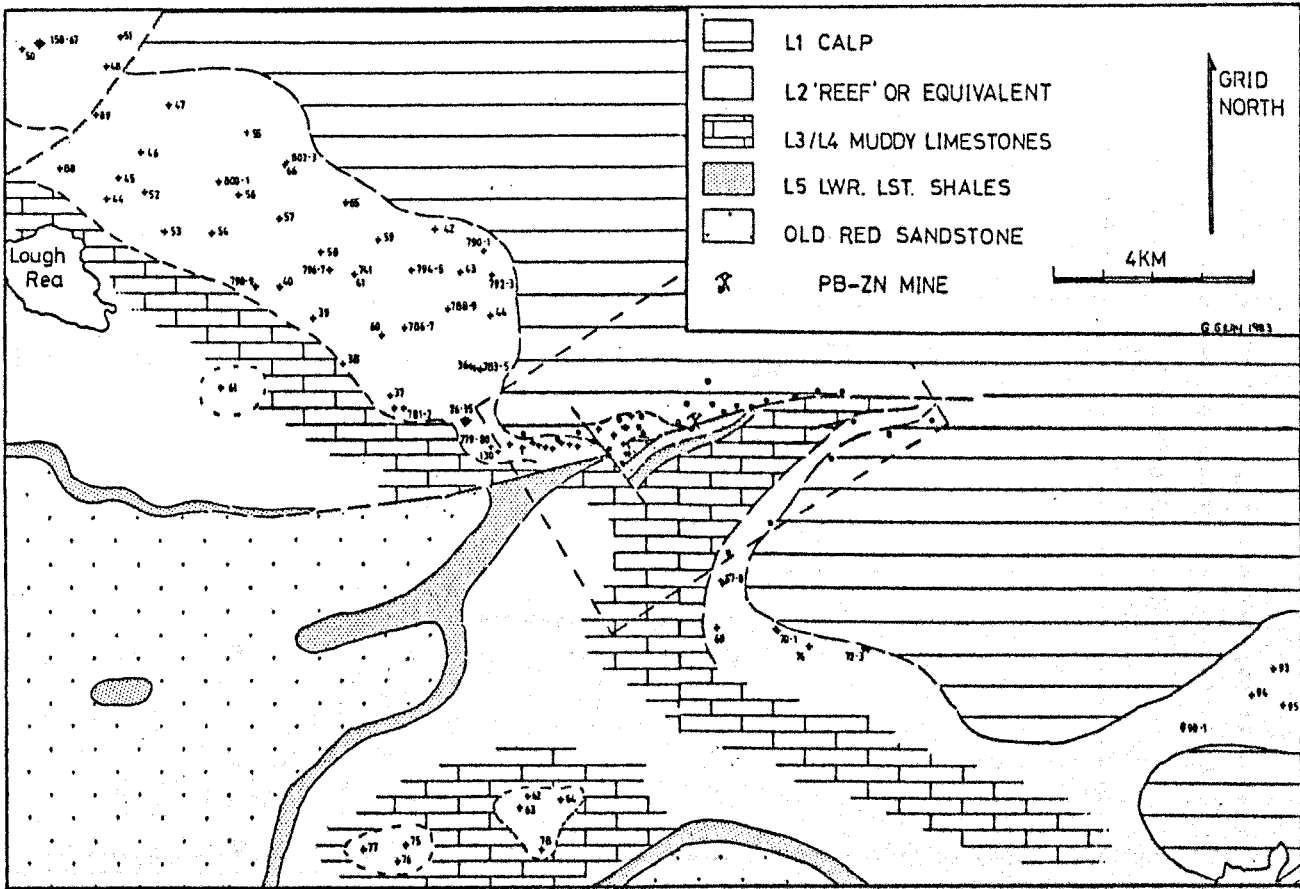


Figure 3.13a: Simplified geology of Tynagh - Loughrea area, showing sample sites in Waulsortian Muddbank or L2 Limestone. Circles represent core samples, crosses outcrop. For dashed inset area, see Figure 3.13b.

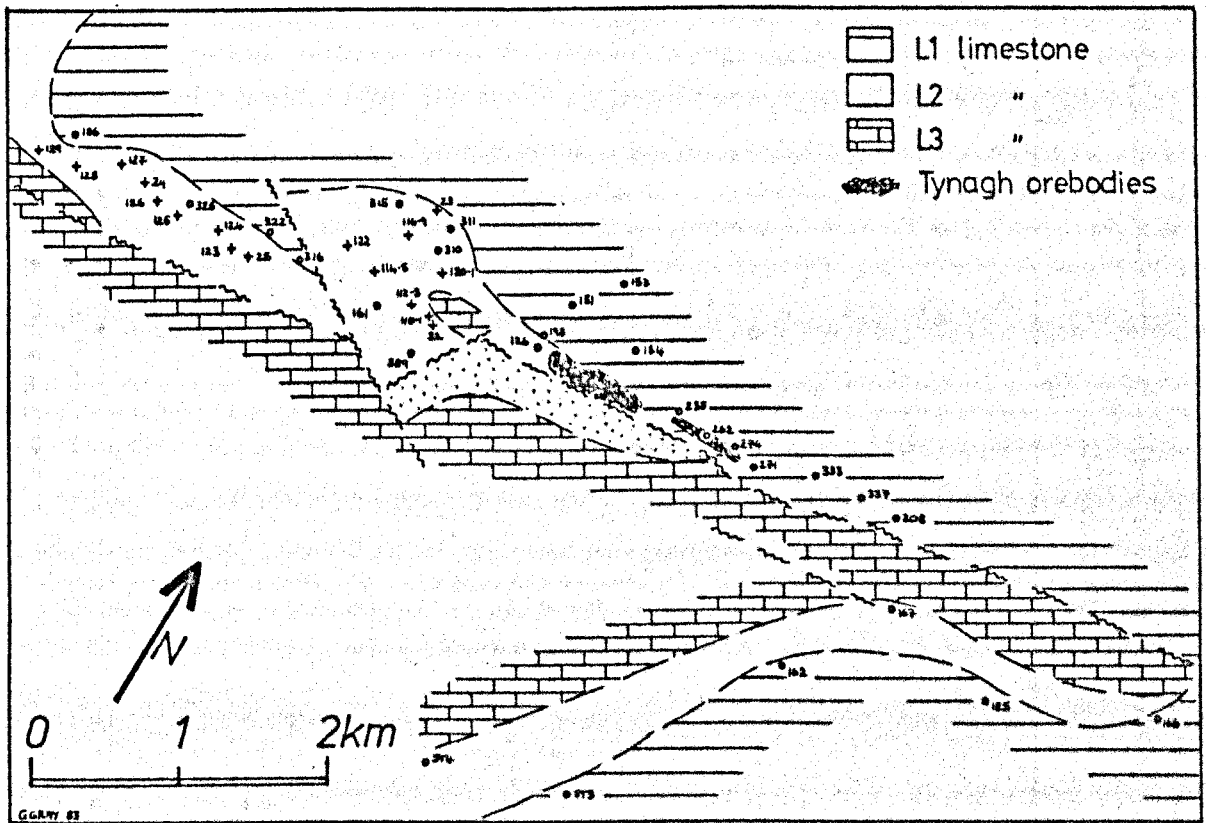


Figure 3.13b: Simplified geological map of area around Tynagh Mine, showing sample sites. Circles represent drill core, crosses outcrop samples.

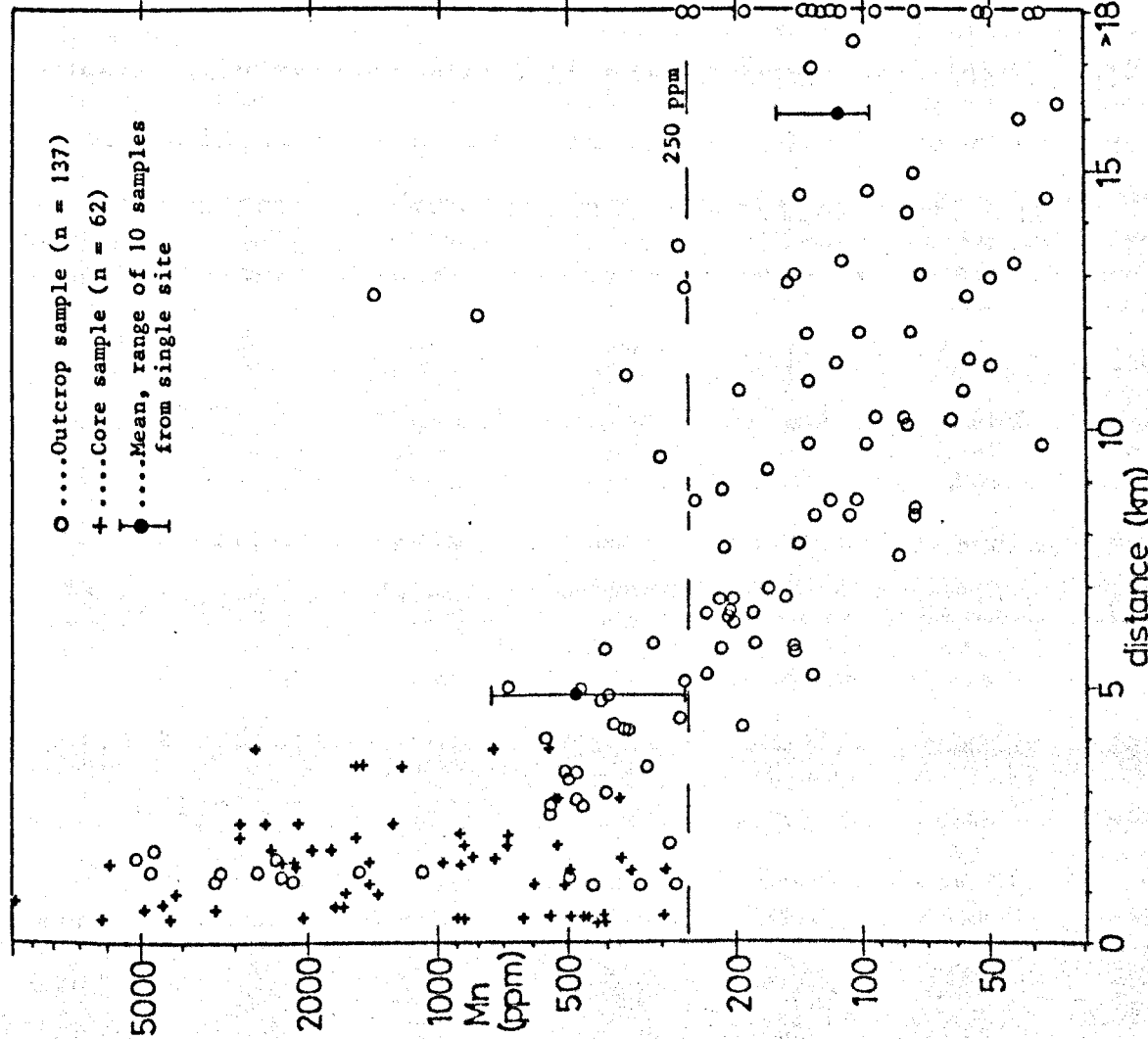


Figure 3.14: Manganese content of Waulsortian Limestones around Tynagh deposit. Note vertical log scale.

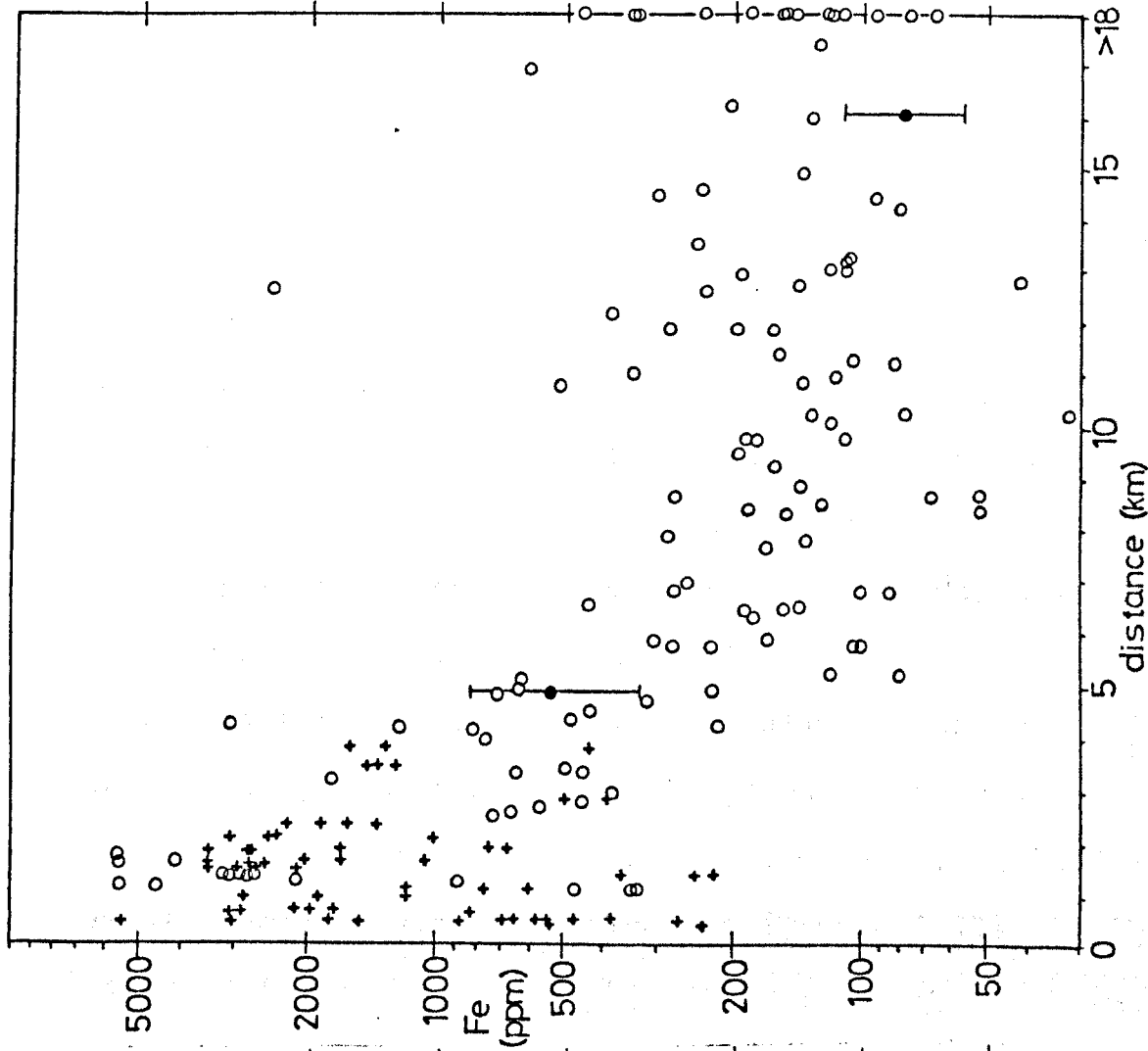


Figure 3.15: Iron content of Waulsortian Limestones around Tynagh deposit. Note vertical log scale. For key, see Figure 3.14.

effective in displaying the anomalous levels up to 6 kilometres distant (Figure 3.18).

By selecting a threshold value of 250 ppm for Mn, Fe and $(\text{Mn}+\text{Fe})/2$, and a lateral cut-off at 6 kilometres from the mine from visual examination of Figures 3.14 to 3.16, the dimensions of the Mn and Fe aureole can be crudely quantified. Within these limits, 94% of the samples from the aureole carry enriched Mn, and 90.5% carry enriched Fe (Table 3.5).

Zinc distribution also shows laterally extensive enrichments, remaining below 10 ppm only beyond 5 kilometres from the mine, although similar background values occur to within 1 kilometre (Figure 3.17), effectively to the edge of the orebody itself. Within a one kilometre radius of the chosen centre, zinc generally remains above 15 ppm in apparently unmineralised micrites. Looking at Table 3.5, 61% of core and outcrop samples from within 5 kilometres of the mine contain over 10 ppm zinc, whereas only 4% of distal samples from beyond this distance exceed this value.

A number of exceptions to the above patterns are present in the study area, in the form of anomalous Mn, or Fe or Zn values outwith the defined aureoles to 6 kilometres (for Mn and Fe) and 5 kilometres (for Zn). These account for 8% of Mn, 17% of Fe and 4% of Zn in all the distal outcrop samples (Table 3.5), and include both isolated and groups of two or more adjacent samples. One of these groups of enriched Mn and Fe lies to the

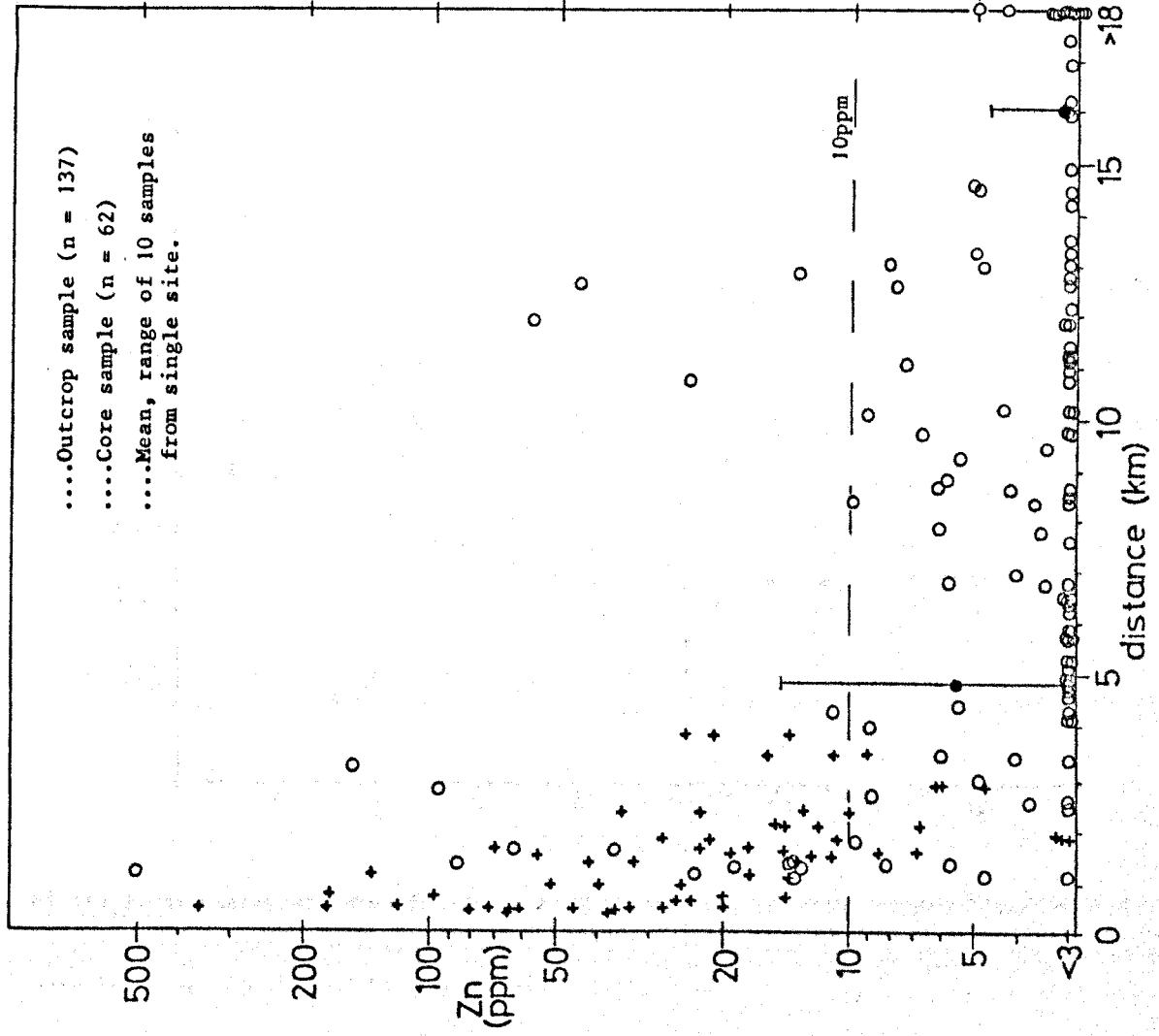
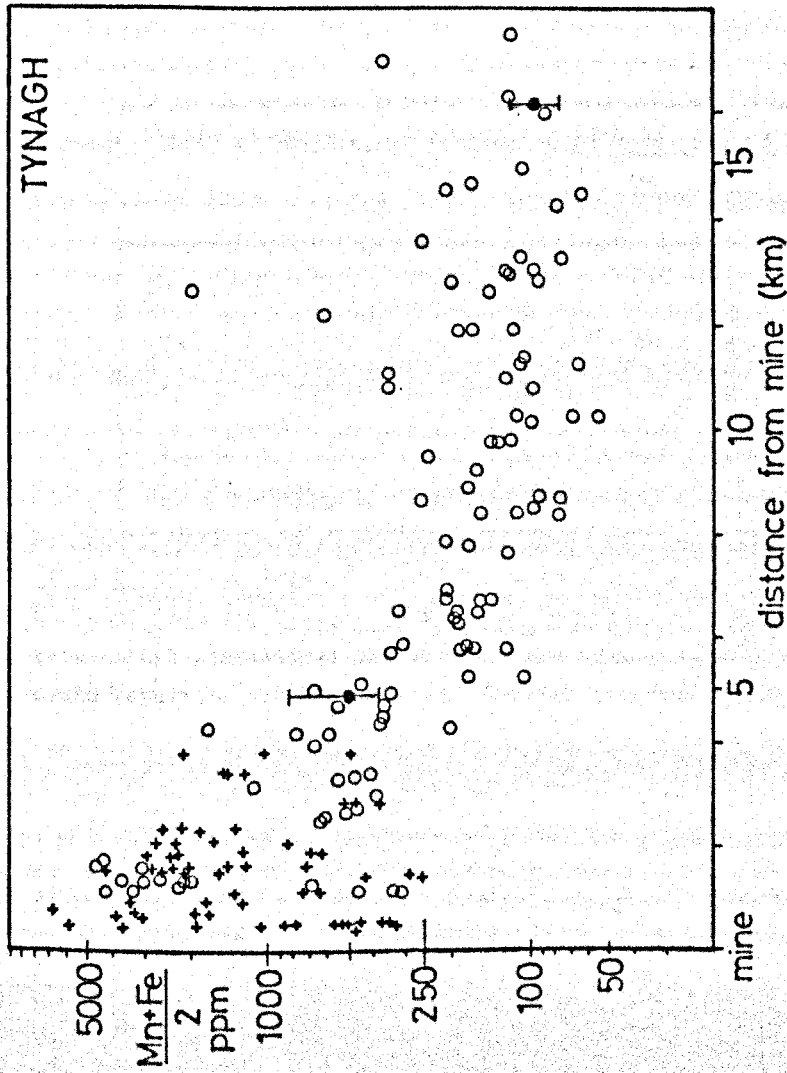


Figure 3.16: Distribution of $(Mn+Fe)/2$ in Waulsortian Limestones around Tynagh deposit. Note log scale on vertical axis. Key as for Figure 3.17.

Figure 3.17: Zinc distribution in Waulsortian Limestones around Tynagh deposit. Note log scale on vertical axis.

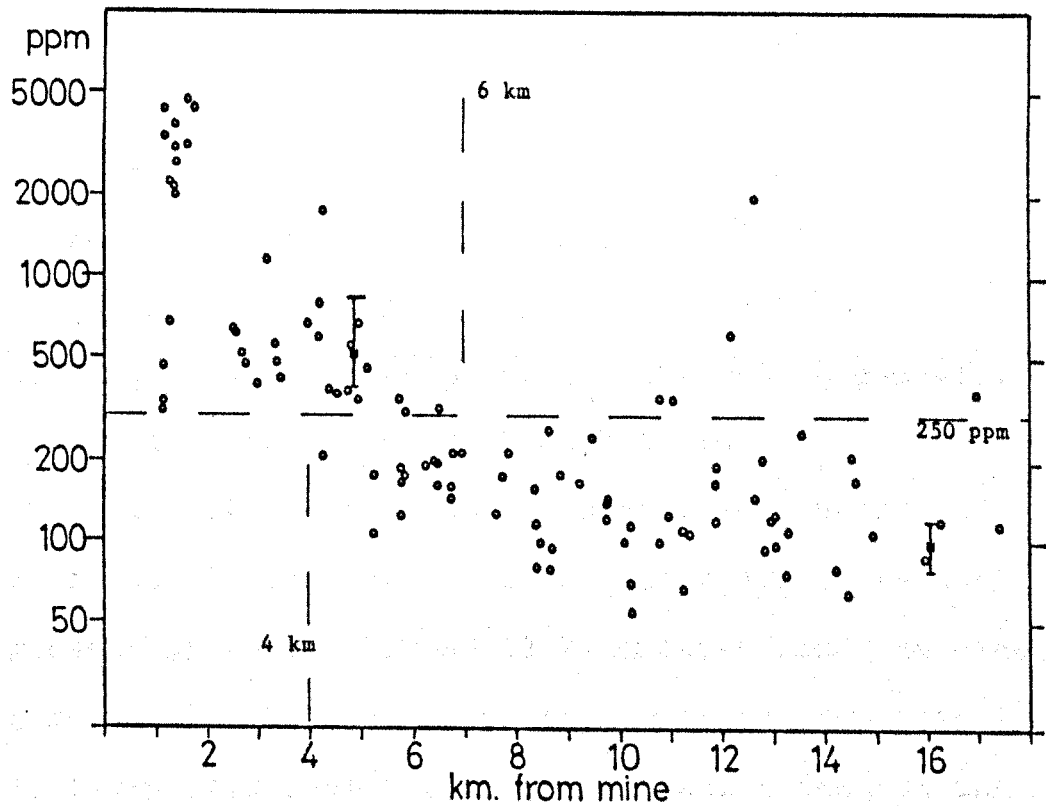


Figure 3.18: Distribution of $(\text{Mn}+\text{Fe})/2$ in Waulsortian Limestones around Tynagh deposit. Only outcrop samples are displayed ($n = 137$). Filled squares with vertical bar represent mean and range of 10 samples from single outcrop site.

ELEMENT	THRESHOLD (PPM)	DISTANCE (KM)	ANOMALOUS SAMPLES (PERCENTAGE)				
			(PROXIMAL)			(DISTAL ONLY)	(ALL SAMPLES)
			ALL	CORE	OUTCROP		
$(\text{Mn}+\text{Fe})/2$	250	6	94.0	100	87.0	9.6	54.8
Mn	250	6	94.0	100	87.0	8.4	54.8
Fe	250	6	90.5	95.2	85.2	16.9	52.7
Zn	10	5	61.1	82.3	52.6	4.4	33.2
Sr	200	5	60.2	72.1	40.0	0	42.8

Table 3.5: Percentage of anomalous samples for given threshold values up to given distance from the Tynagh deposit, for each element analysed. Note that if normal geochemical statistical threshold levels were utilised, much higher cutoff values would result.

southeast, near Lough Derg, and is described by Russell (1975), and another (enriched Zn) lies in the North Tynagh Basin, towards Loughrea (Figure 3.20a).

The areal dispersion patterns defined by all the sample data are shown in Figures 3.19 and 3.20, both locally in core and outcrop around the Tynagh deposit, and distally into the North Tynagh Basin.

Comparison between Mn and Fe distributions using Mn:Fe ratio, demonstrates that a wide range of values is present up to and beyond 18 kilometres from the mine (Figure 3.21). No obvious pattern emerges from this data, except for a higher Mn concentration towards the centre of the North Tynagh Basin, to the north of Tynagh Mine, and extending into the northern flank of the Waulsortian outcrop in Figure 3.23a. This may represent enrichment of Mn over Fe in a stratigraphically younger part of the mudbank limestone formation, although the absence of mudbank development in core or outcrop any distance to the north of the mine precludes further investigation of this possibility. Russell (1975) and Riedel (1980) describe high manganese concentrations, centred on the manganiferous iron formation, along the central axis of the sedimentary basin during deposition, near to the northern margin of the orebody.

Direct comparison between Mn and Fe values at Tynagh (Figure 3.25) reveals that up to an order of magnitude variation between the two may exist, throughout the

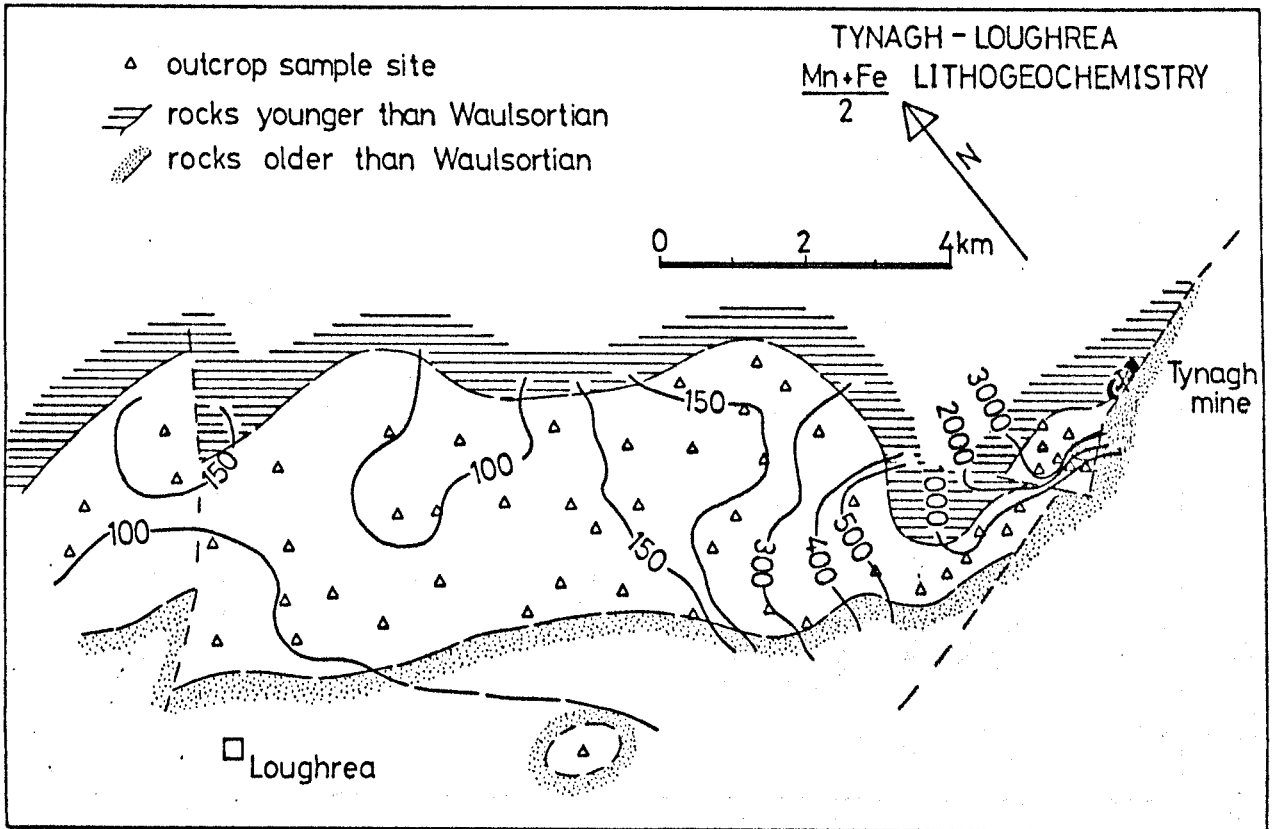


Figure 3.19a: Map of Tynagh - Loughrea area showing contoured values (in ppm) of $(Mn+Fe)/2$, using a rolling mean. Only outcrop samples are included.

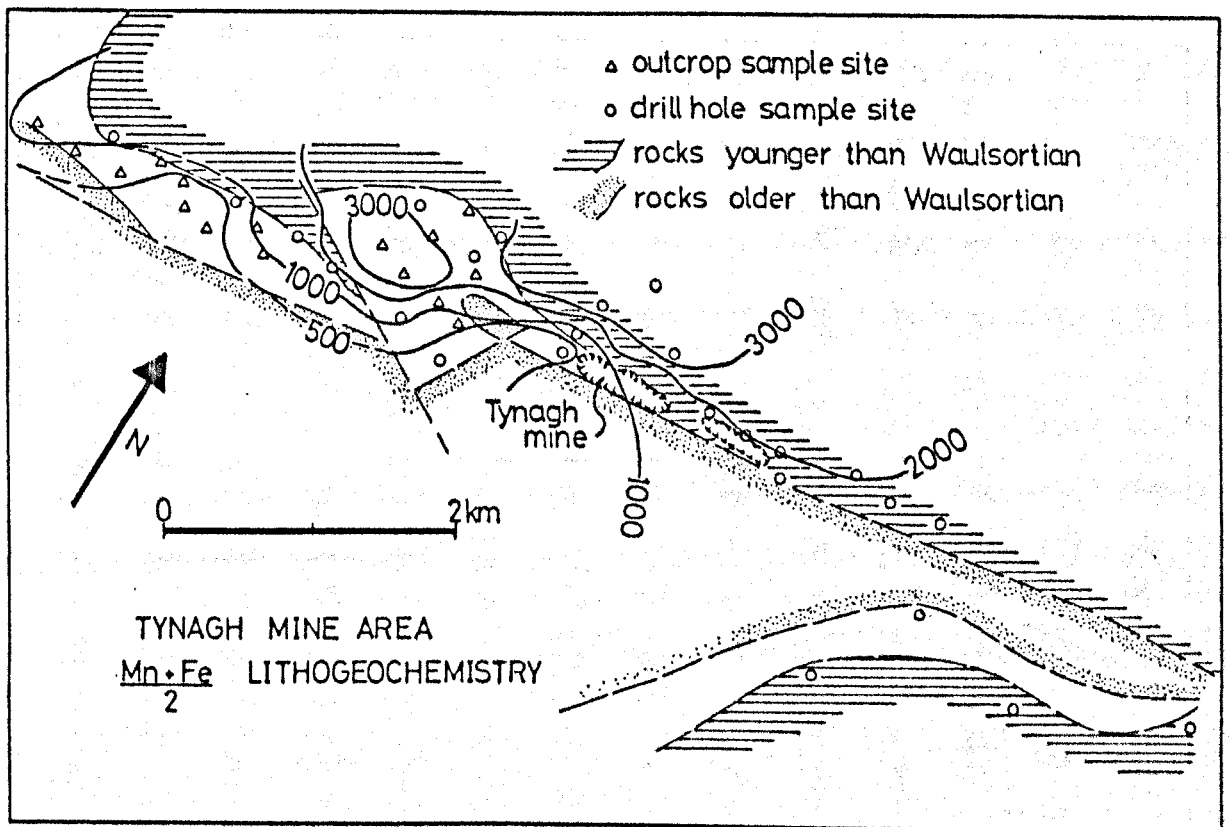


Figure 3.19b: Map of Tynagh Mine area showing contoured values of $(Mn+Fe)/2$ (in ppm), using a rolling mean. Both outcrop and core samples are included.

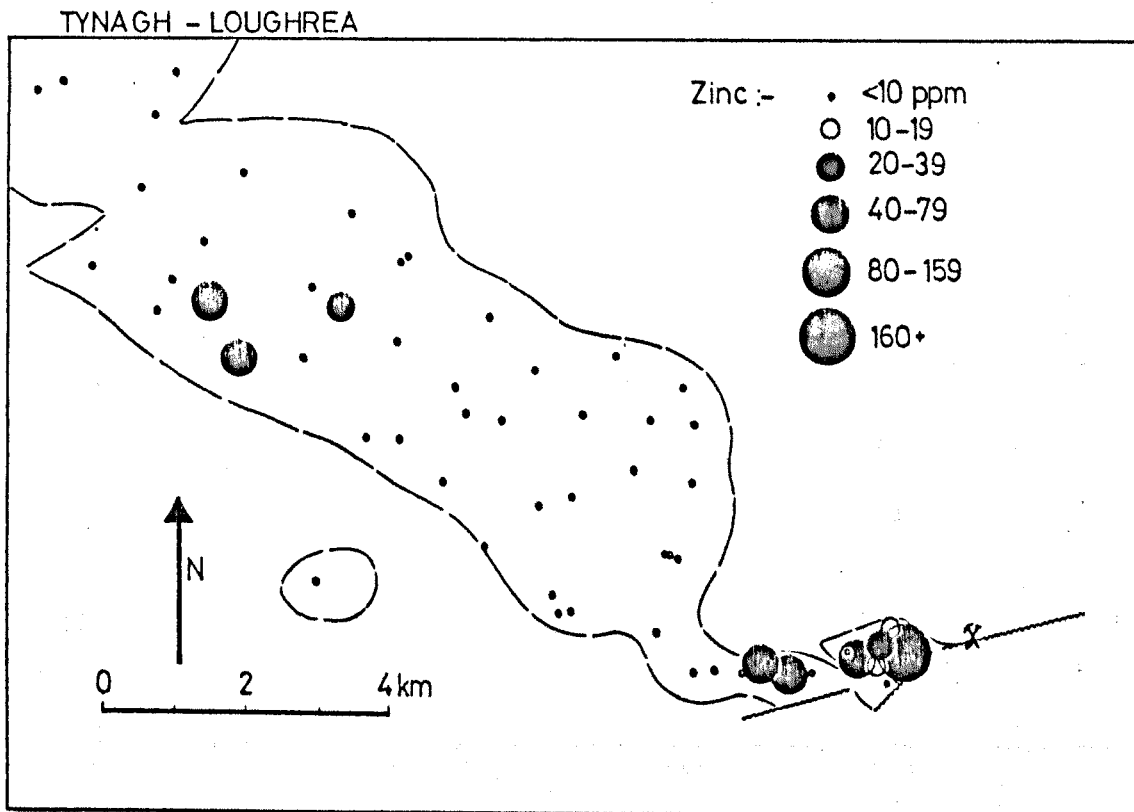


Figure 3.20a: Map showing zinc content of Waulsortian Limestones between Tynagh and Loughrea. Spot size represents zinc concentration in ppm.

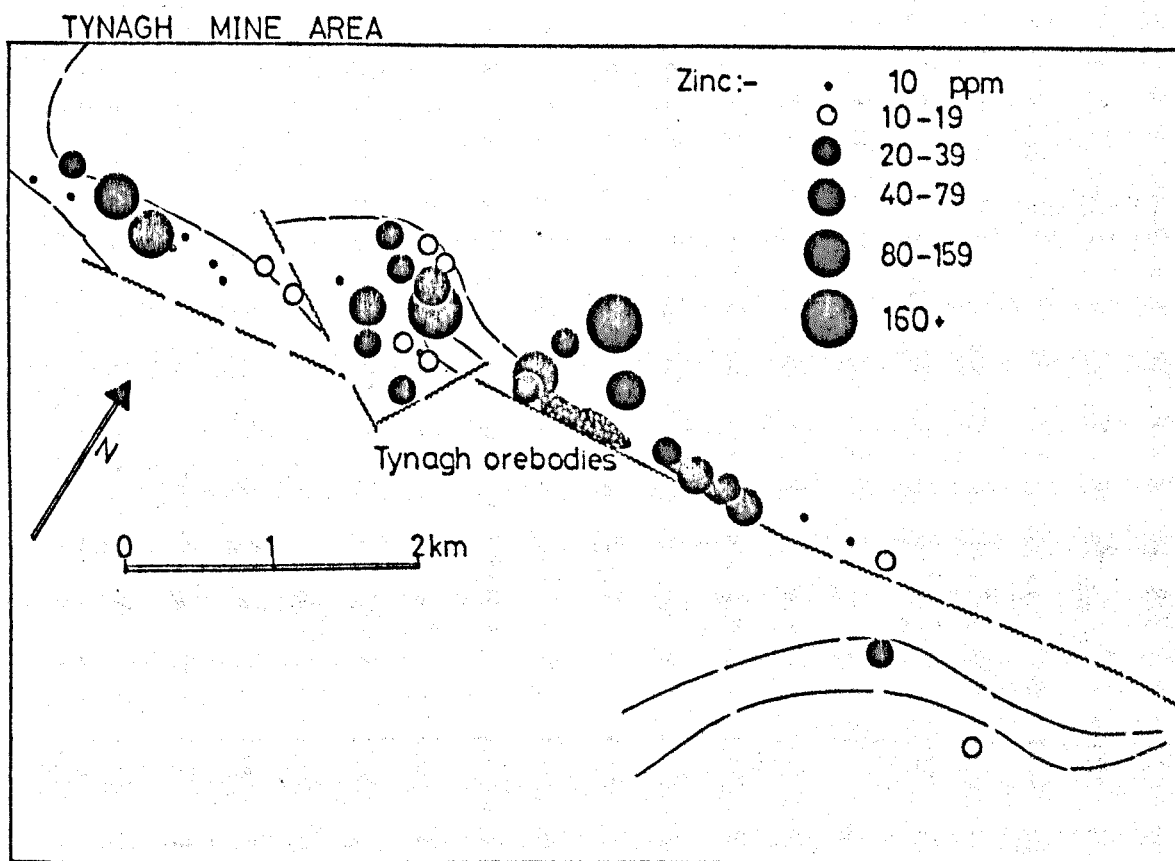


Figure 3.20b: Map of Tynagh Mine area showing zinc content of Waulsortian Limestone in both outcrop and core samples.

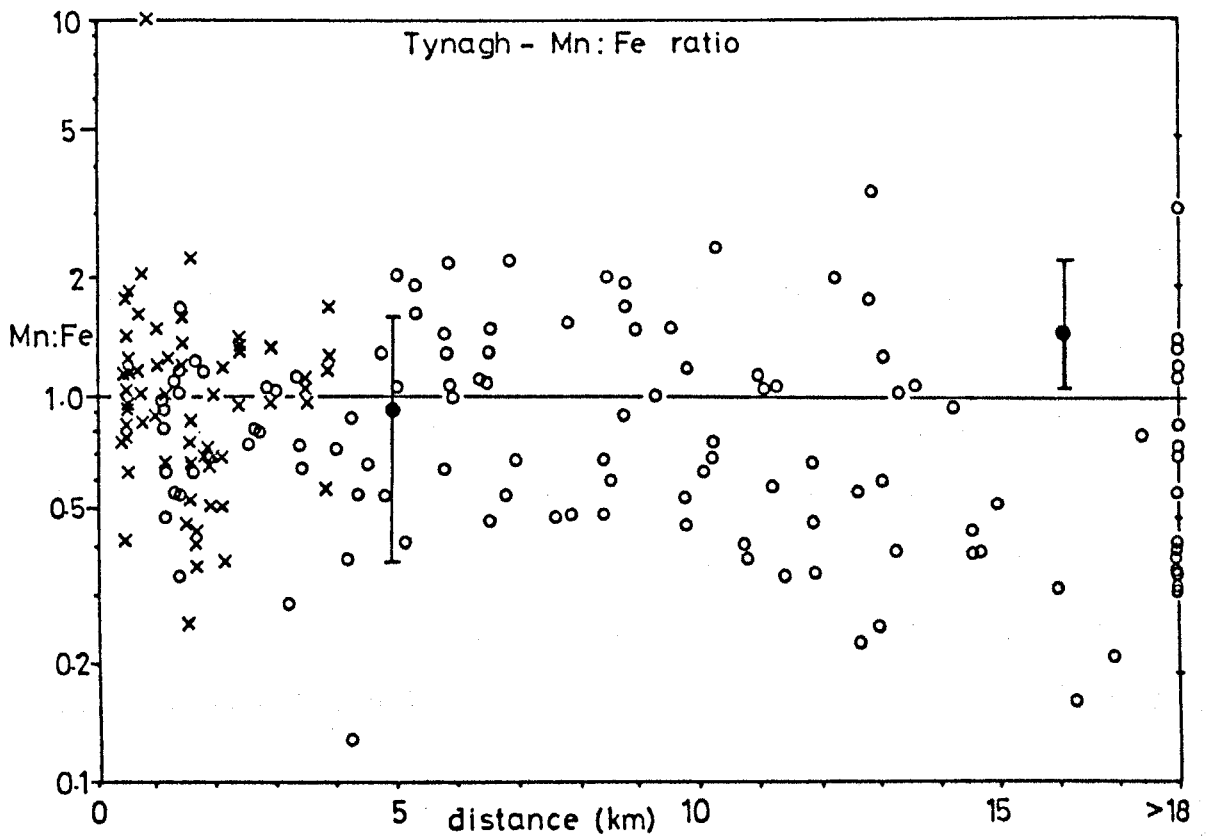


Figure 3.21: Ratio of manganese to iron in Waulsortian Limestones around the Tynagh deposit. For key see Figure 3.22.

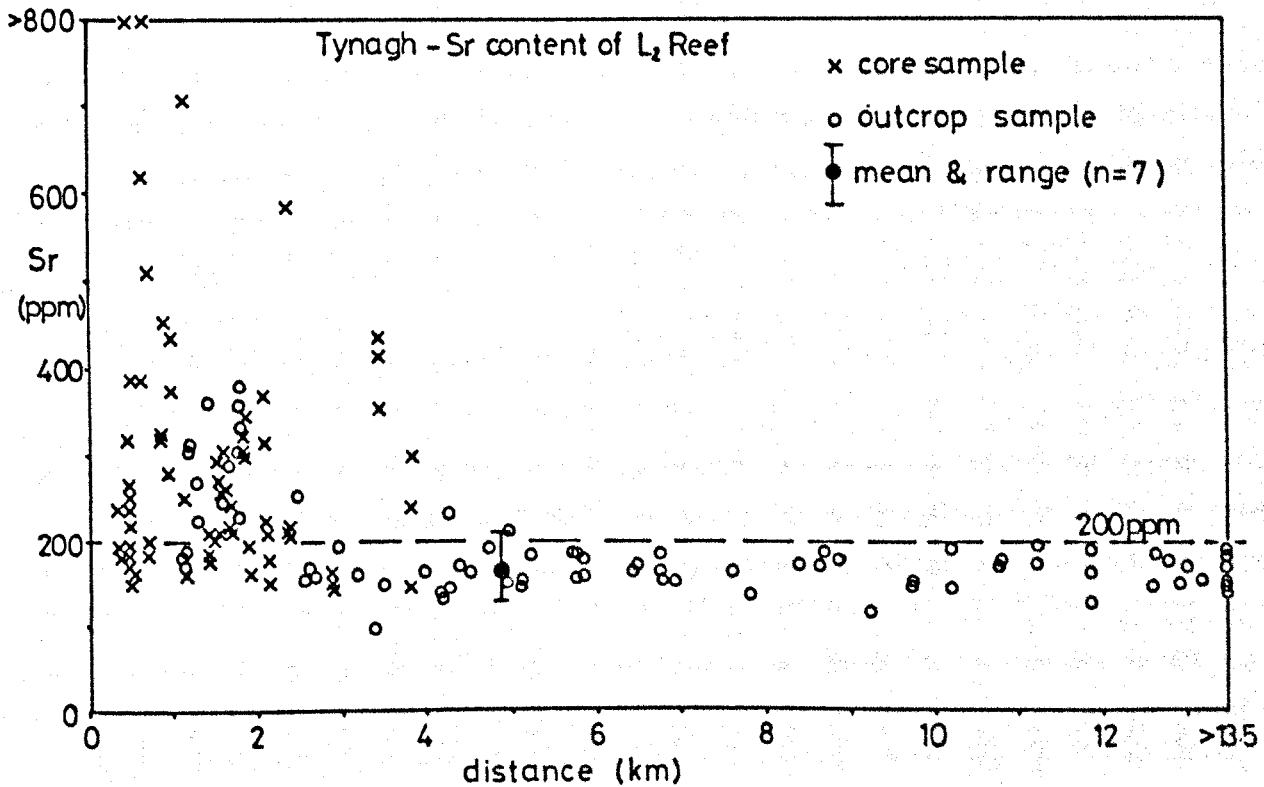


Figure 3.22: Strontium content of Waulsortian Limestones around the Tynagh deposit. (61 core samples, 86 outcrop samples).

entire concentration range.

For comparison with Mn, Fe and Zn data, Figure 3.22 displays strontium values determined by Russell (unpublished data), using X.R.F. analyses on the same samples. This illustrates that Sr also increases in a regular fashion towards the mineralisation. Beyond 5 kilometres, values remain between 100 and 200 ppm, whereas within 5 kilometres, approximately 60% of core and outcrop samples contain more than 200 ppm Sr (Table 3.5, Figures 3.24a,b).

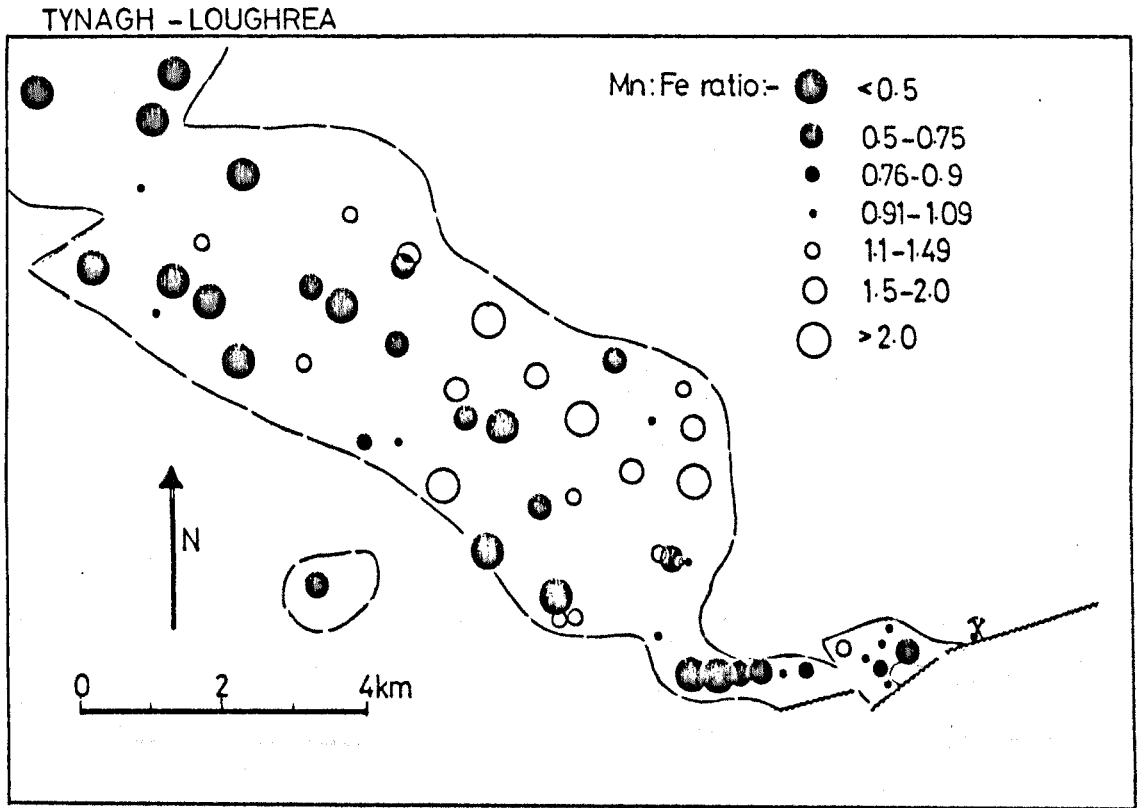


Figure 3.23a: Map showing ratio of manganese to iron in Waulsortian Limestones between Tynagh and Loughrea. Only outcrop samples included.

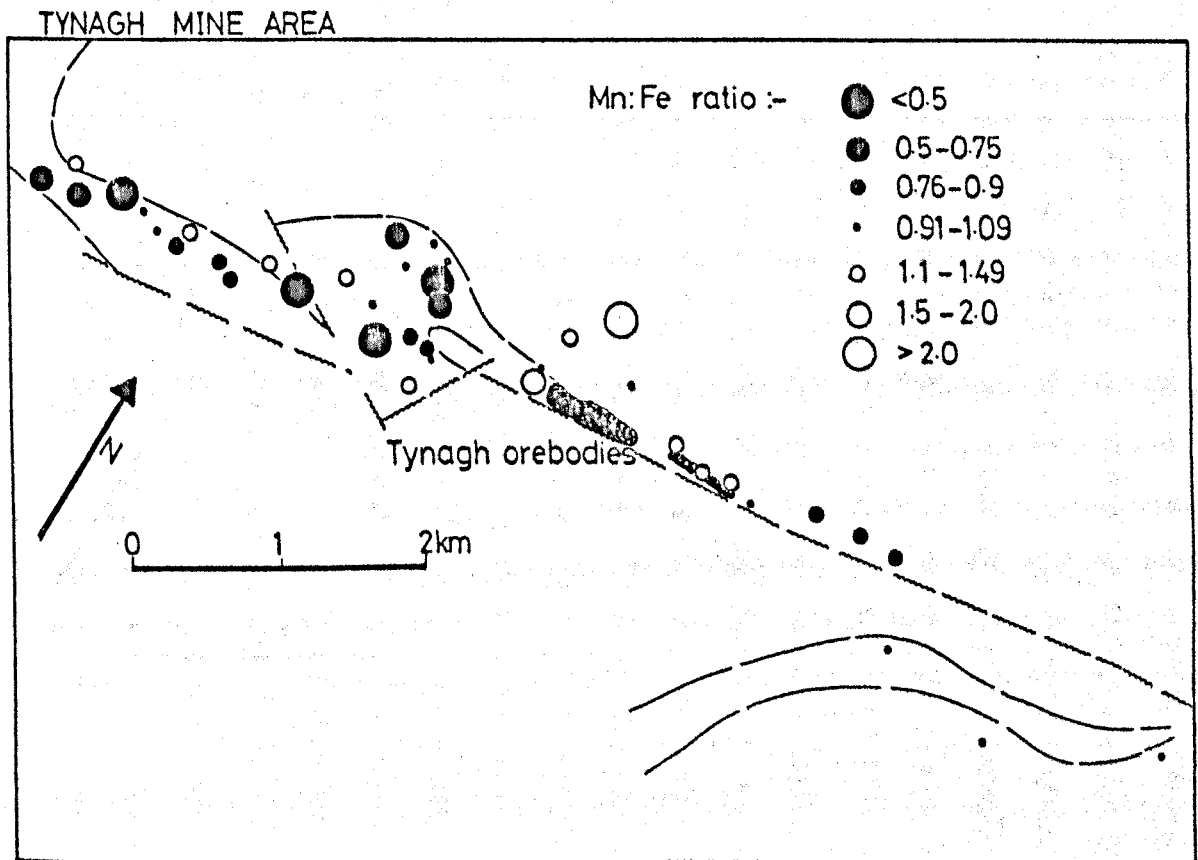


Figure 3.23b: Map of Tynagh Mine area, showing ratio of manganese to iron in Waulsortian Limestones. Both outcrop and core samples included.

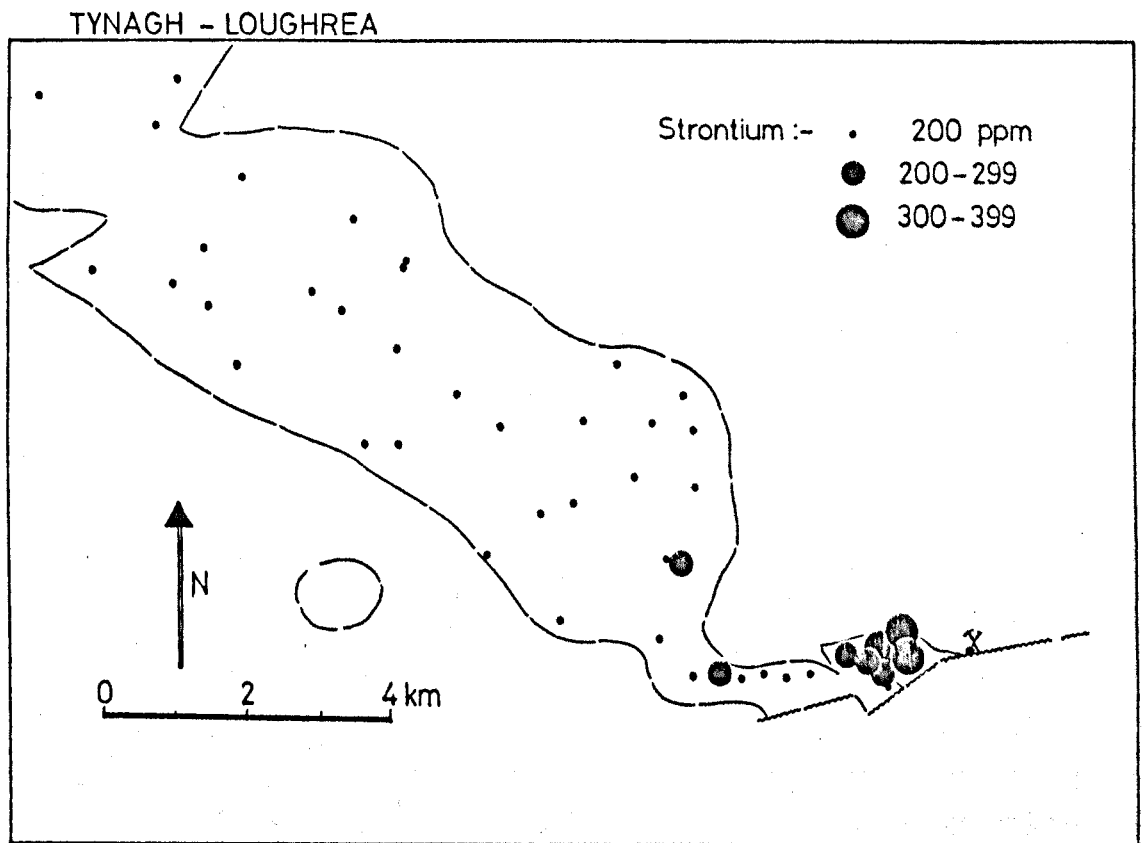


Figure 3.24a: Map showing strontium content of Waulsortian Limestones between Tynagh and Loughrea. Only outcrop samples included.

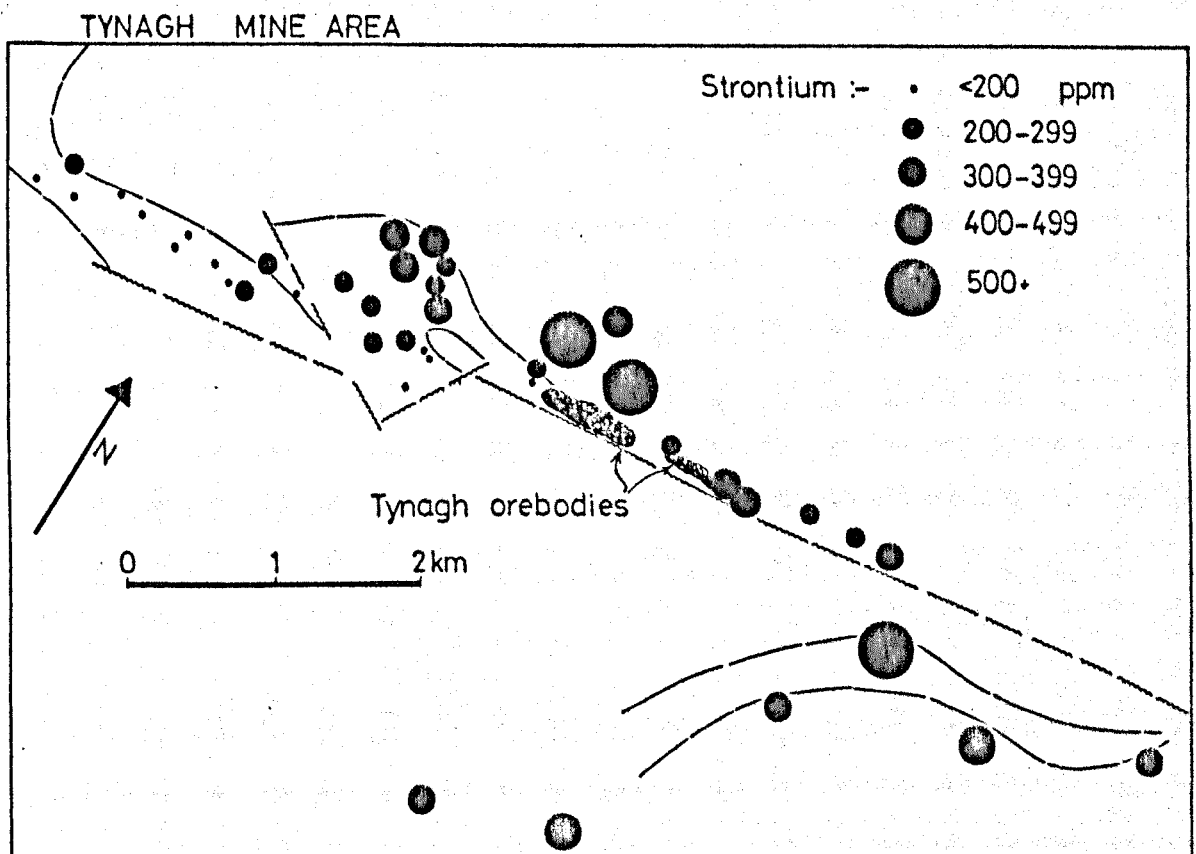


Figure 3.24b: Map of Tynagh Mine area showing strontium content of Waulsortian Limestones. Both outcrop and core samples shown.

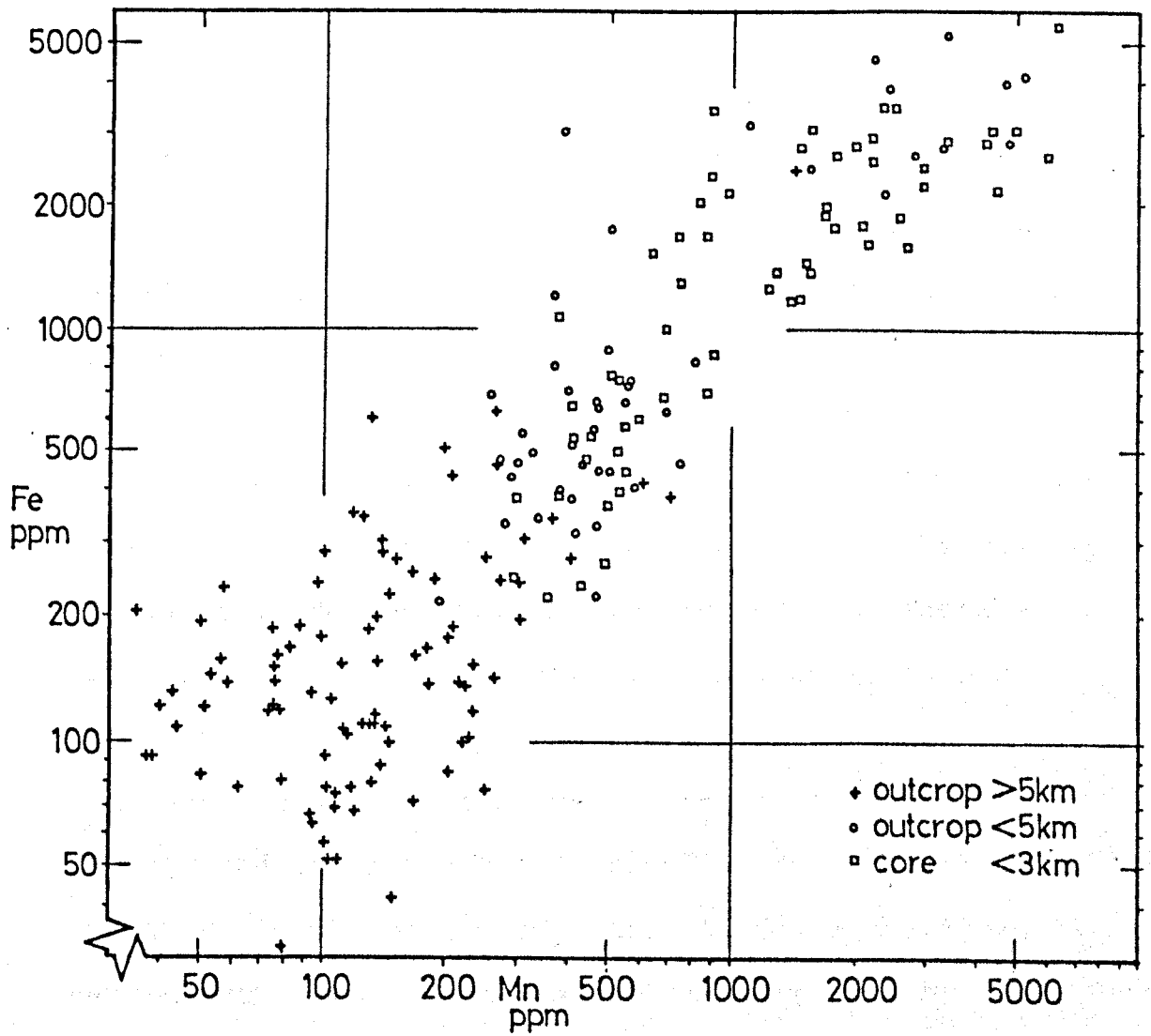


Figure 3.25: Graph of manganese against iron in Waulsortian Limestone samples from Tynagh area (137 outcrop, 62 core samples).

3.3.1. Silvermines.

Introduction.

Following his success at Tynagh, Russell (unpublished work) failed to recognise any obvious manganese halo at Silvermines in a preliminary study of approximately 100 outcrop samples from the Nenagh Basin.

Barrett (1975) refuted the presence of widespread primary enrichments in the form of a trace element aureole, by stating that "Mn content of wall rocks quickly falls below 800 ppm within 100 feet of the mineralised horizon". Significantly, he had confined his study to material only from the immediate mine environment and was thus unable to recognise any lower background levels in the surrounding carbonate rocks. However, in the same study, Barrett describes footwall and hanging wall 'enrichments' of Mn, Fe and Si from the Baryte orebody at Ballynoe, without examining their lateral extent.

Reanalysis of Russell's samples (using the method outlined in Chapter Two) indicated that enriched Mn, Fe and Zn were present, but not so extensively as at Tynagh.

Geology.

The regional geology of this study area is well described by Brück (1982). Essentially it consists of a single, arcuate syncline, open to the northeast, and flanked by Lower Palaeozoic inliers to the west and southeast. The latter is separated from the younger

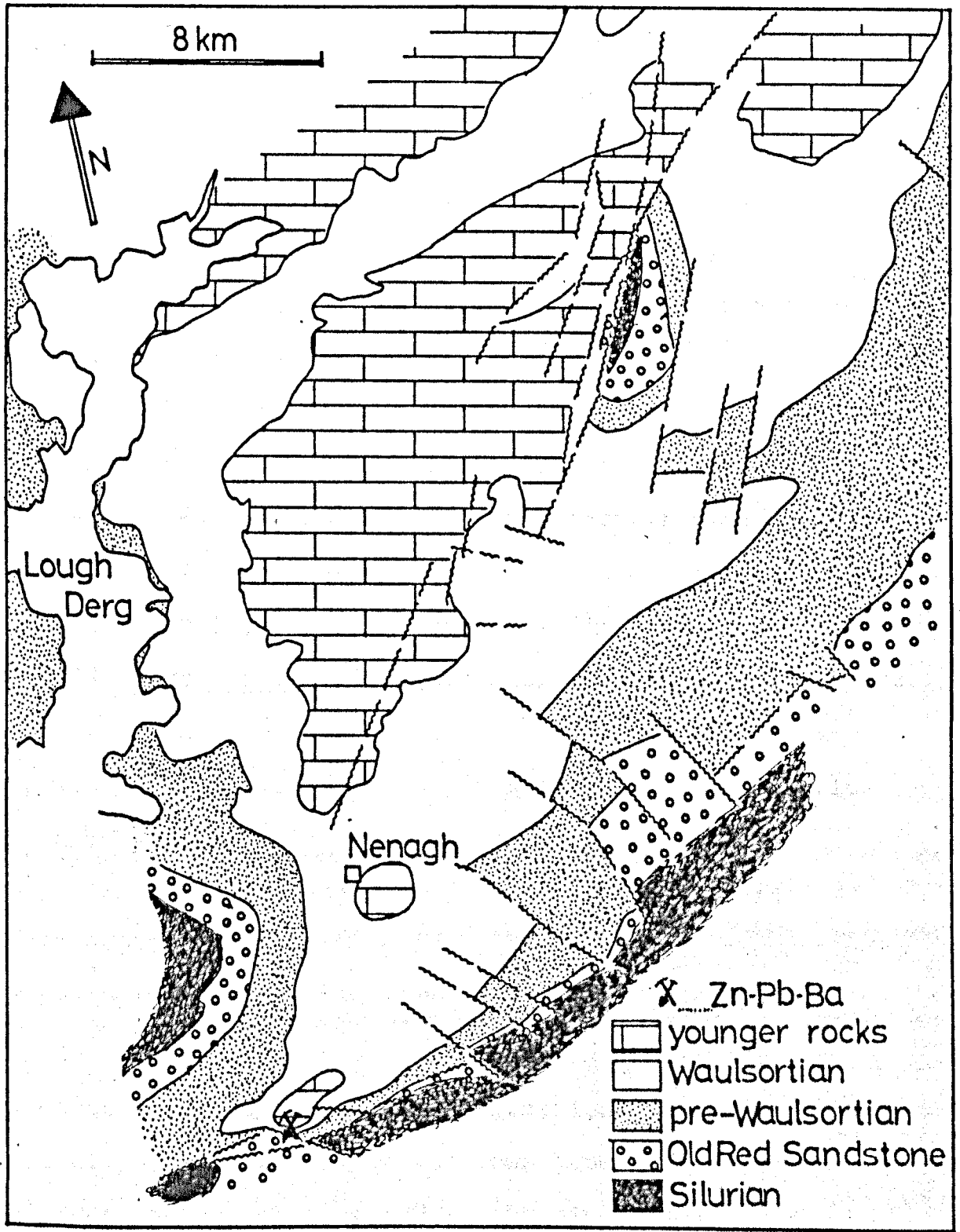


Figure 3.26: Simplified geology of the Nenagh - Silvermines Basin, mainly after Brück (1982).
 For location, see also Figure 3.1.

rocks of the basin by the Silvermines Fault Zone and its northeasterly continuation (figure 3.26). Dips are generally shallow and towards the synclinal axis. Younger, post-Waulsortian rock cover is confined to northern parts of the area, north of Nenagh, except for two small outliers of Calp-like limestones, one overlying the base metal deposit itself.

The geology of the Silvermines Zn+Pb+Ag+Ba deposit has been described by Taylor and Andrew (1978) and Taylor (1984). Further aspects of the mineralisation, such as fluid inclusion characteristics (Samson 1983; Samson and Russell 1983), sulphur isotopes (Coomer and Robinson 1976; Boyce et al 1983), structural geology (Coller 1982; Larter, in preparation), the presence of fossil sea-floor vent material in the form of hydrothermal pyrite chimneys (Larter et al 1981; Boyce et al 1983), and genesis and origin of the mineralising fluids (Russell et al 1981) have been covered satisfactorily to proscribe further lengthy description here.

In summary, the stratiform deposits at Silvermines occur in small third order depressions (each less than 1 kilometre across), on the downthrown side of a major ENE-trending (locally E-W at the mine) fault zone, the Silvermines Fault, where intersected by smaller NW and NNW trending cross faults (Taylor and Andrew 1978, Coller 1982, Andrew 1984). Movements on these faults during sedimentation in Upper Tournaisian times resulted in lateral thickness changes and extensive

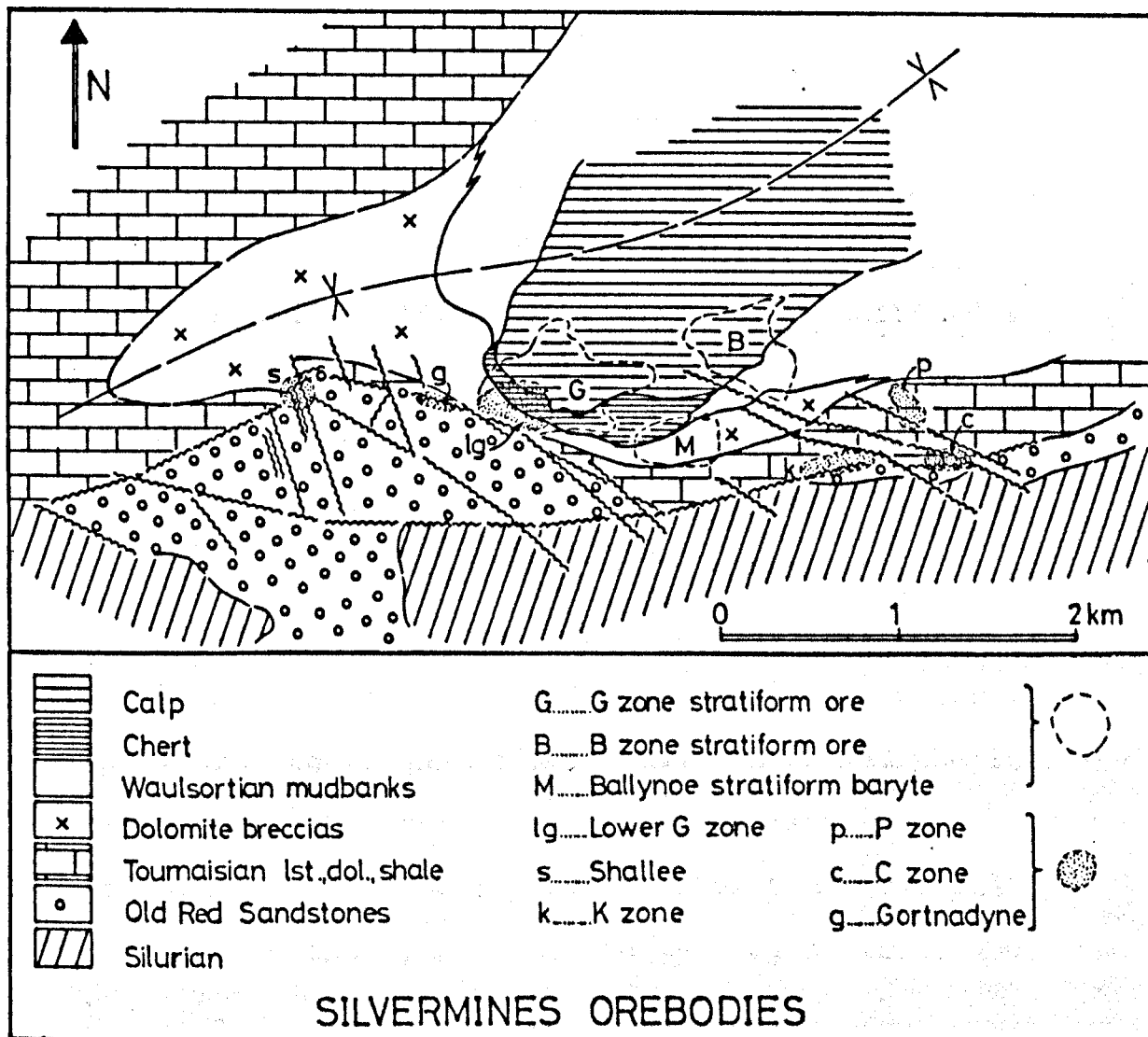


Figure 3.27: Geology of the Silvermines area, showing location of the principal base metal and baryte orebodies. After Taylor and Andrew (1978) and Taylor (1984).

slumping and reworking by sedimentary breccias (Graham 1970, Boyce et al 1983, Taylor 1984).

Epigenetic styles of mineralisation, interpreted as replacement features alongside the main feeder zones (Larter et al, op cit; Samson 1983; Taylor op cit) also occur in older sandstones, shales and dolomitised limestones adjacent to the fault, and over a distance of at least six kilometres from east to west (Figure 3.27).

The importance of the NW trending cross faults in controlling ore mineralisation is stressed by Taylor and Andrew (op cit). Of particular note is the way in which sea floor topography, allied to structural movements and mudbank growth, has controlled the location of the richest sedimentary ore zones, ore isopachytes, and the distribution of the principal host rock lithologies (massive pyrite, siderite and baryte).

This emphasises the direct sedimentary aspects of the stratiform mineralisation (Taylor op cit).

Ore mineralisation is dominated by fine grained galena and sphalerite, in a gangue of massive pyrite and dolomitic reef limestone and breccias. Massive, stratiform baryte is present in economic quantities up-dip, and along strike from the sulphide orebody, on the same stratigraphic horizon (Barrett 1975, Grennan 1979). Sedimentary slumping and mass movements, triggered by synchronous tectonic events, have created some overlap of individual host rock lithologies, because

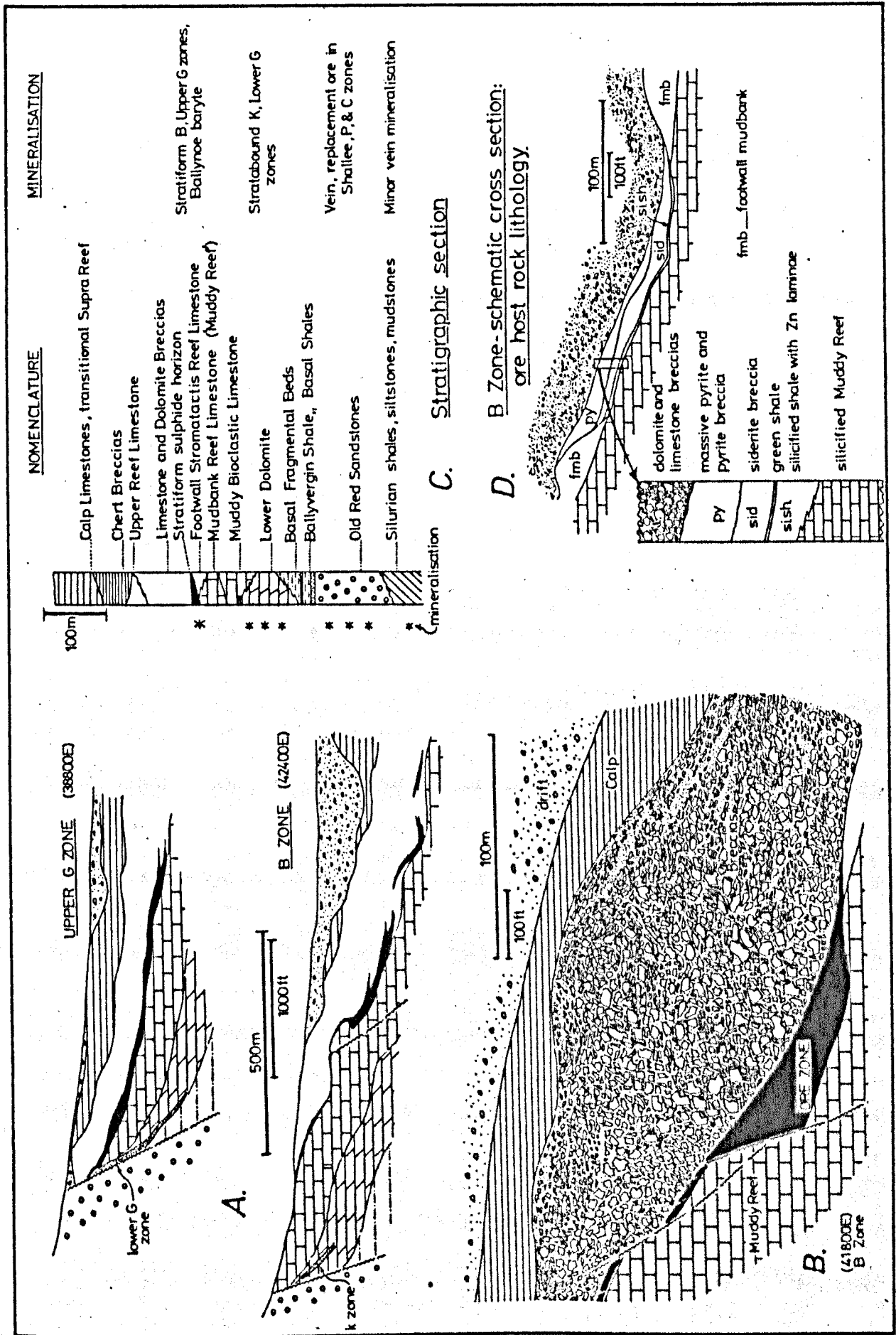


Figure 3.28: Geology of the Silvermines deposits: A) N-S cross sections through G and B zones; B) N-S cross sections through G and B zones; C) Generalised stratigraphic section; D) Schematic cross section, B zone ore horizon. Source: Taylor and Andrew (1978); Taylor (1984); Company sections.

of reworking of material. Figure 3.28 summarises some of the geology of the deposits.

Sampling.

In this study, 220 outcrop samples were combined with Russell's 96 samples, and 441 samples of drill core from the mine area, to give an overall picture of the lateral trace element distribution in the Nenagh-Silvermines area. The location of the outcrop samples is given in Figure 3.29 and the boreholes samples on Figure 3.43.

Limitations to the areal sampling programme arose because of a number of reasons:-

- 1) limited surface outcrop, especially in the mine area, because of thick overburden;
- 2) limit of drilling generally within a kilometre of economic mineralisation;
- 3) much of the core has been disposed of, particularly those holes from areas now mined out;
- 4) a large area to the NW of the mine has suffered from deeply penetrating oxidative weathering.

Vertical profiles of selected diamond drill holes were also investigated in an attempt to add a third dimension (representing time) to trace element patterns. These are described in the following chapter.

Results.

For the purpose of measuring the distance of each outcrop (or borehole) site from the hydrothermal source, the centre of mineralisation is chosen as the approx-

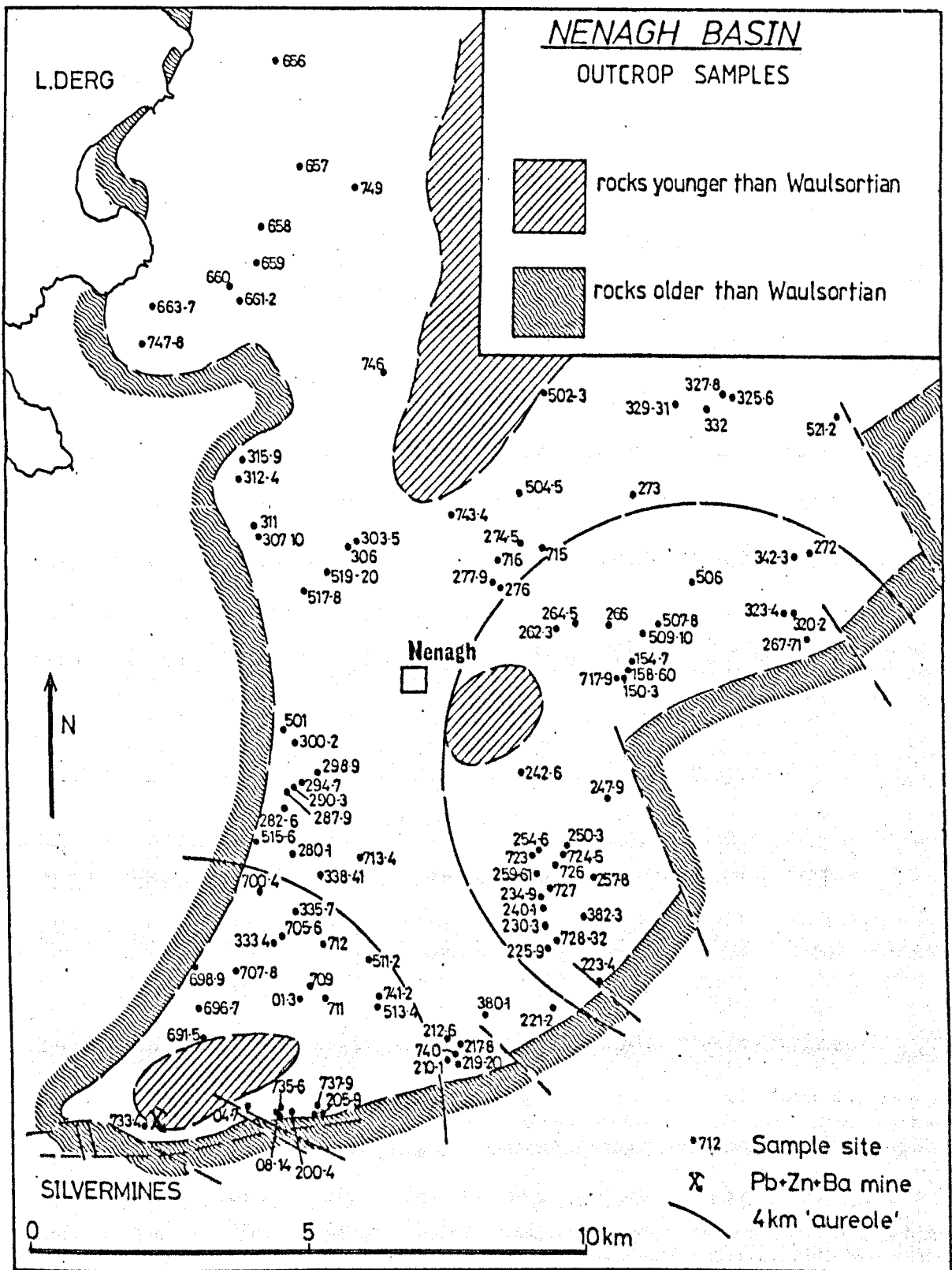


Figure 3.29: Outcrop sample locations, Nenagh - Silvermines Basin. Also shown are outlines of 4 km. aureoles defined around both Silvermines and Nenagh centres (see text).

imate centres of the B and Upper G zones, whichever is closer.

Graphs depicting the concentration of Mn, Fe and Zn with distance from the mine (Figures 3.30 - 32) do not present such a clear picture of decreasing concentration with increasing distance, as they do at Tynagh (Figures 3.15 - 18). High concentrations, comparable with those at Tynagh, are present close to the mineralisation, but assuming background and threshold values to be also comparable, anomalous concentrations of each element appear to be present up to 15 kilometres or more from the deposit, with several peaks.

Examination of the areal distribution of trace element contents throughout the basin partly elucidates the nature of these anomalous concentrations (Figures 3.33 - 39). In these diagrams, suboutcrop samples from drill core in the Silvermines area have been included to supplement the sparse surface outcrop available there. Higher values of the three elements Mn, Fe and Zn appear to be confined largely towards the margins of the synclinal basin (i.e. the lower part of the mudbank complex), especially along the southern limb. This suggests that enrichments are therefore confined to the basal part of the mudbank succession, over a distance of perhaps ten kilometres or more from the mine, and outcrop sampling has failed to express this adequately, because of poor exposure of basal mudbank in certain areas. With the location of the stratiform mineral-

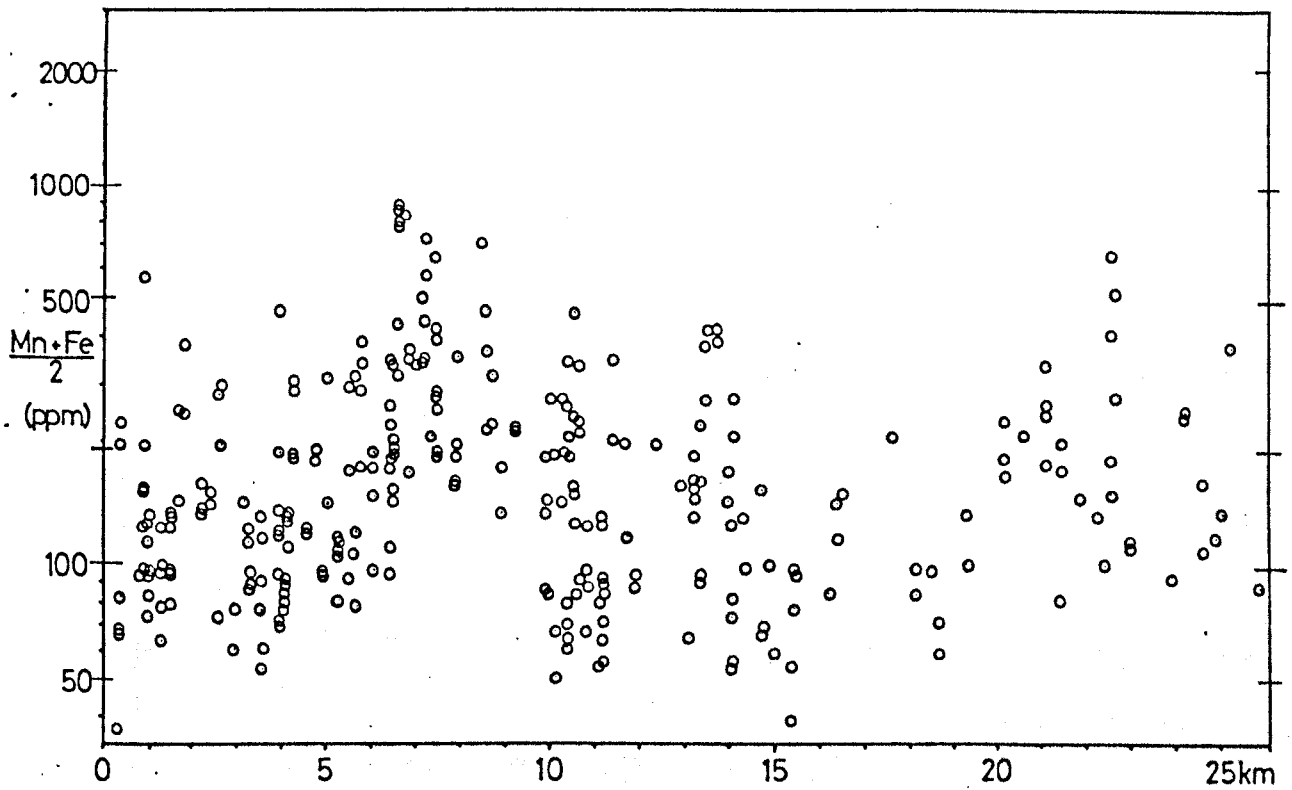


Figure 3.30: $(\text{Mn}+\text{Fe})/2$ content of Waulsortian Limestone samples around the Silvermines deposits. Only outcrop samples are included on this graph, with distances measured from the approximate centre of the B zone (n = 220).

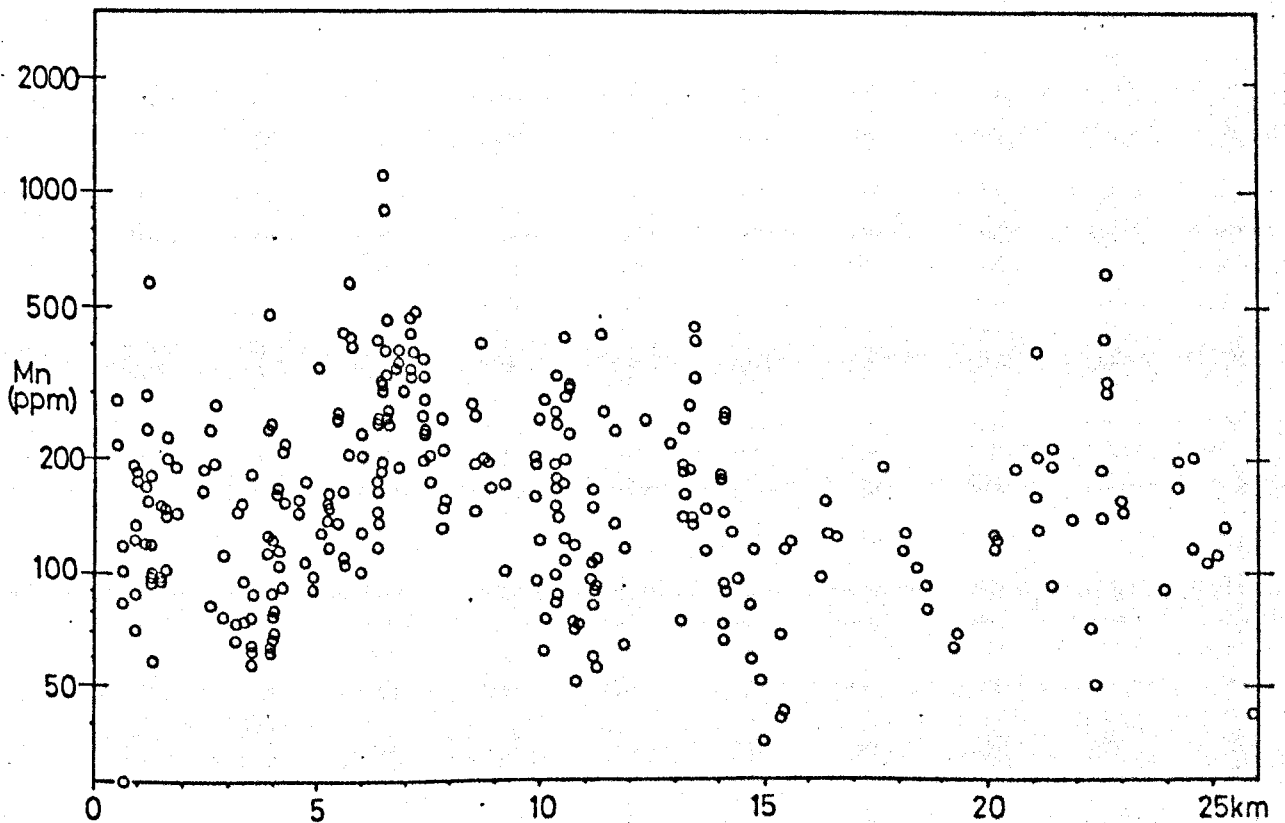


Figure 3.31: Manganese content of Waulsortian Limestones around the Silvermines deposits, outcrop samples only (n = 220).

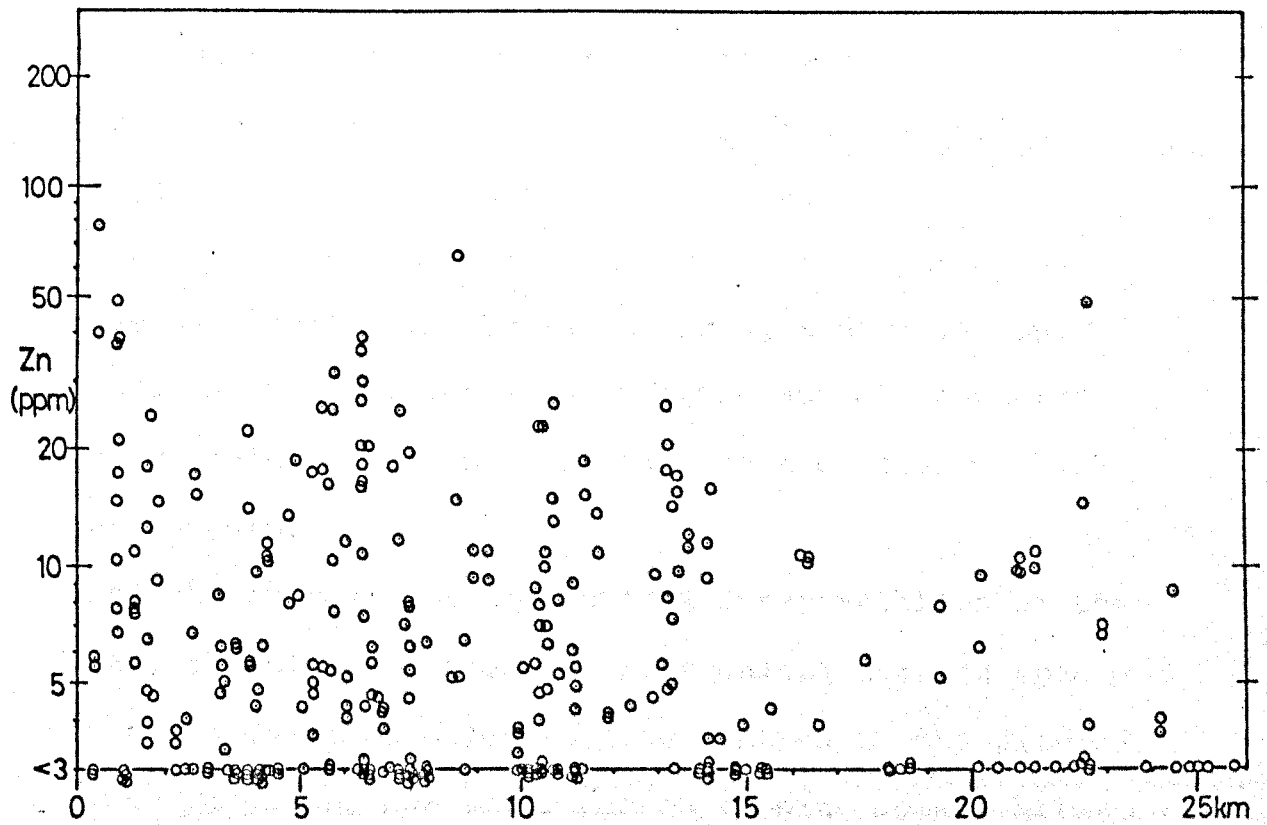


Figure 3.32: Zinc content of Waulsortian Limestones around the Silvermines deposits, outcrop samples only (n = 220).

isation at Silvermines near to the base of the mudbank succession, it is not surprising therefore, that the associated primary enrichments appear to be confined largely to the same part of the succession.

Alternatively, more than one exhalative centre may have been active in the basin during sedimentation, producing two (or more) interfering aureole patterns, and explaining the apparent gaps in the basal mudbank enrichments.

For the purposes of statistical interpretation of the data, the elevated trace element values were grouped into two distinct aureoles, one centred on the Silvermines deposits, and the other on a point some 4 kilometres to the east of Nenagh (Figure 3.29). The reasons for this are based on the discovery of in-situ lead and zinc mineralisation at this second location, 12 kilometres from, and unrelated to, the Silvermines deposits (Gray 1982).

Examination of the distribution of trace elements in core and outcrop samples from around the Silvermines centre, on a more local scale, allows some quantification of the dimensions of the zone of enrichment (Figures 3.40 - 42). Almost 80% of all samples from within 4 kilometres of the centre of mineralisation contain over 200 ppm $(\text{Mn}+\text{Fe})/2$, and over 60% of the same samples contain over 10 ppm Zn (Table 3.6a). Similarly, of the 83 outcrop samples falling within 4 kilometres of the postulated Nenagh centre, 68% contain over 200 ppm

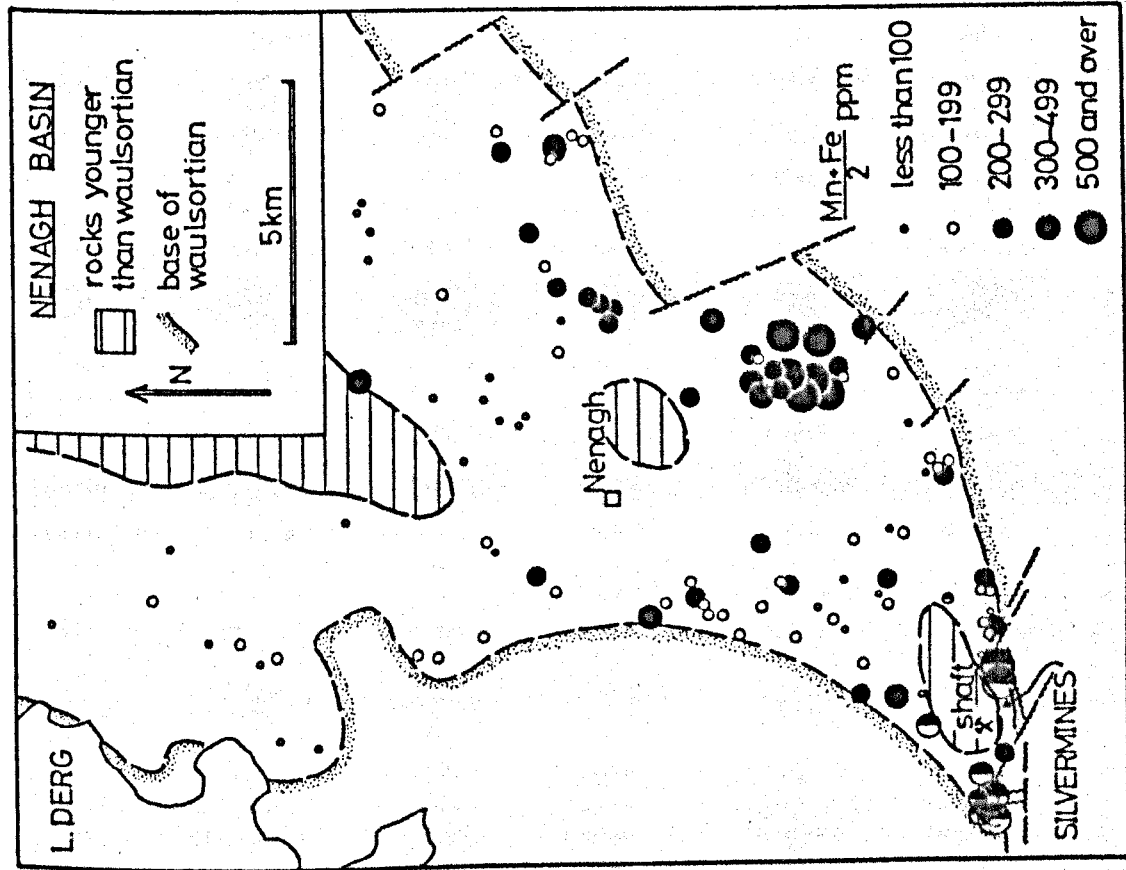


Figure 3.33: $(Mn \cdot Fe)/2$ content of Waulsortian Limestones in Nenagh-Silvermines area. Half-filled circles near Silvermines represent suboutcrop samples from drill core.

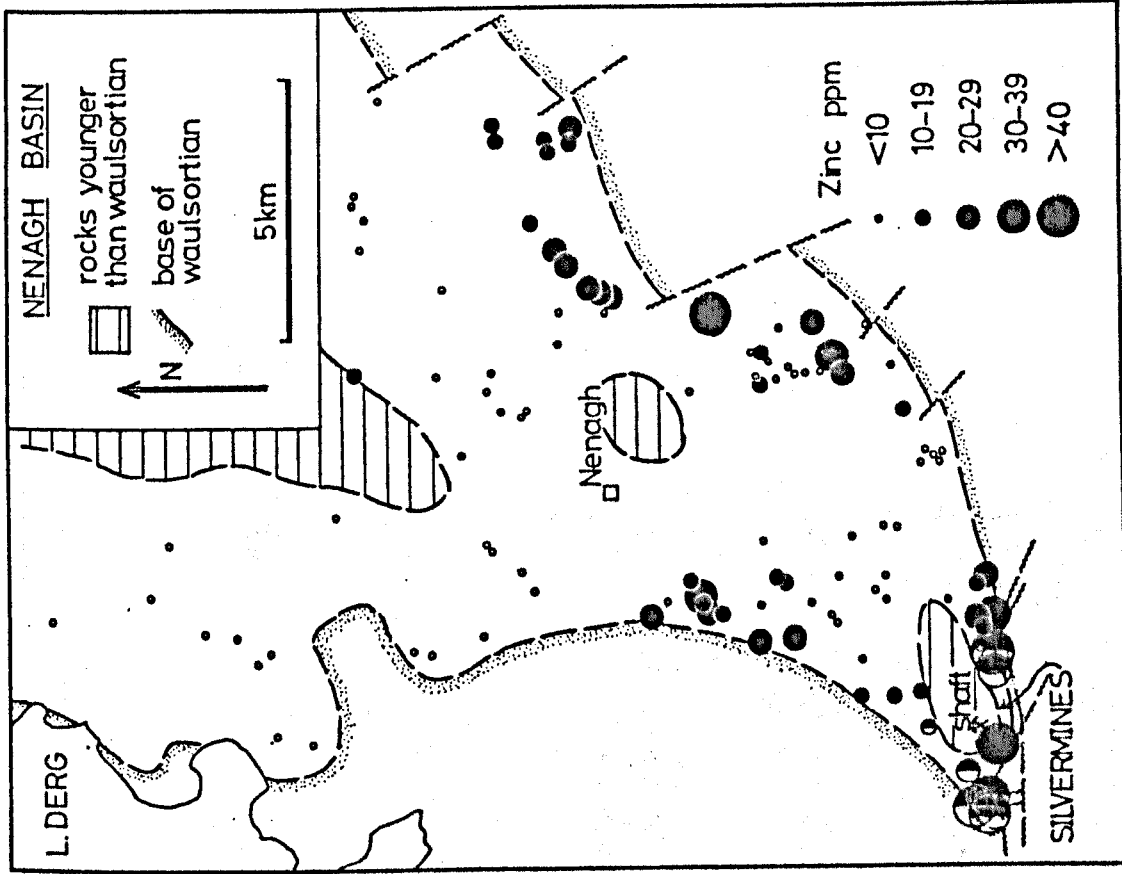


Figure 3.34: Zinc content of Waulsortian Limestones in Nenagh-Silvermines area. Half-filled circles near Silvermines represent suboutcrop samples from drill core.

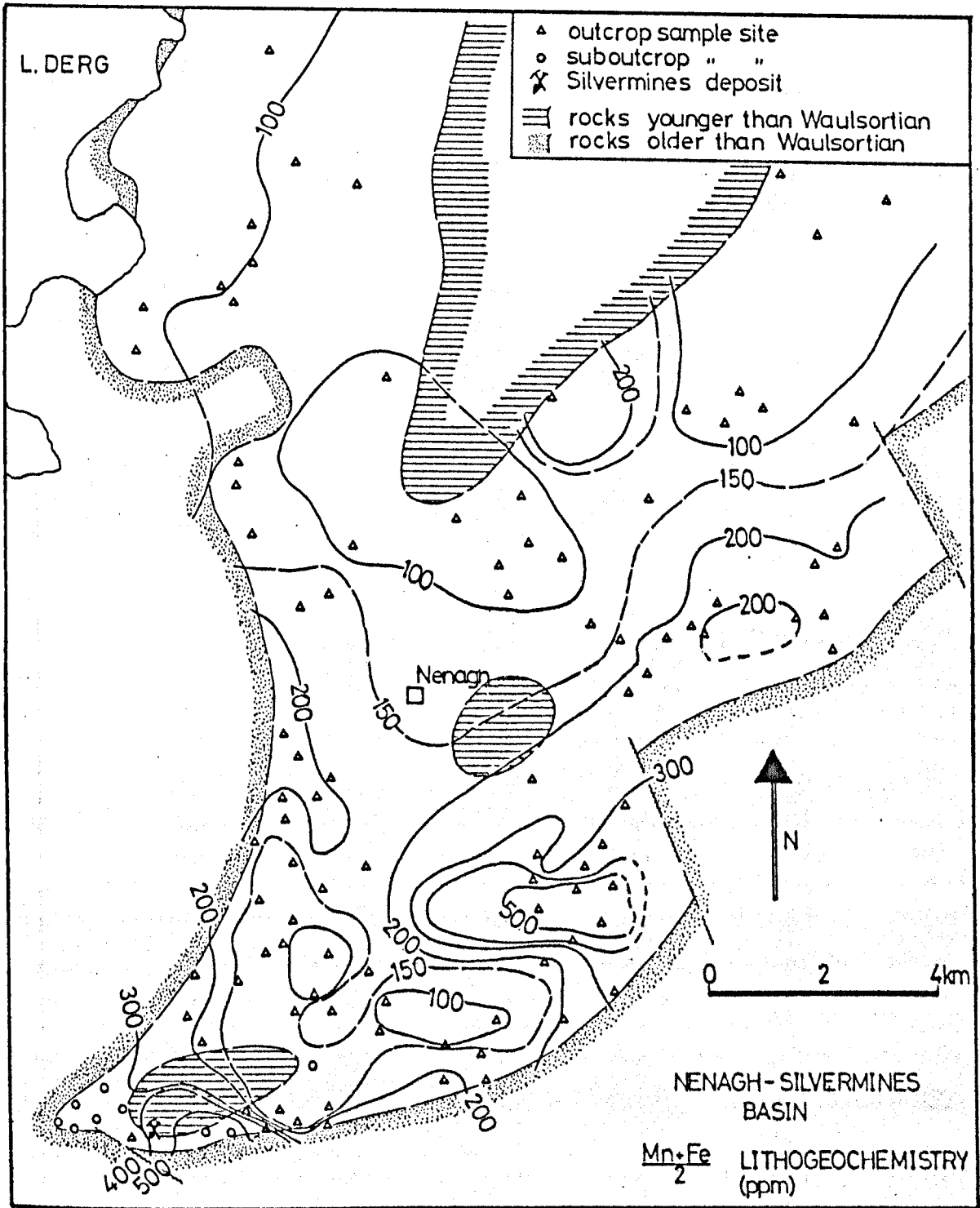


Figure 3.35: $(Mn+Fe)/2$ content of Waulsortian Limestones in Nenagh - Silvermines area. Values contoured using a rolling mean.

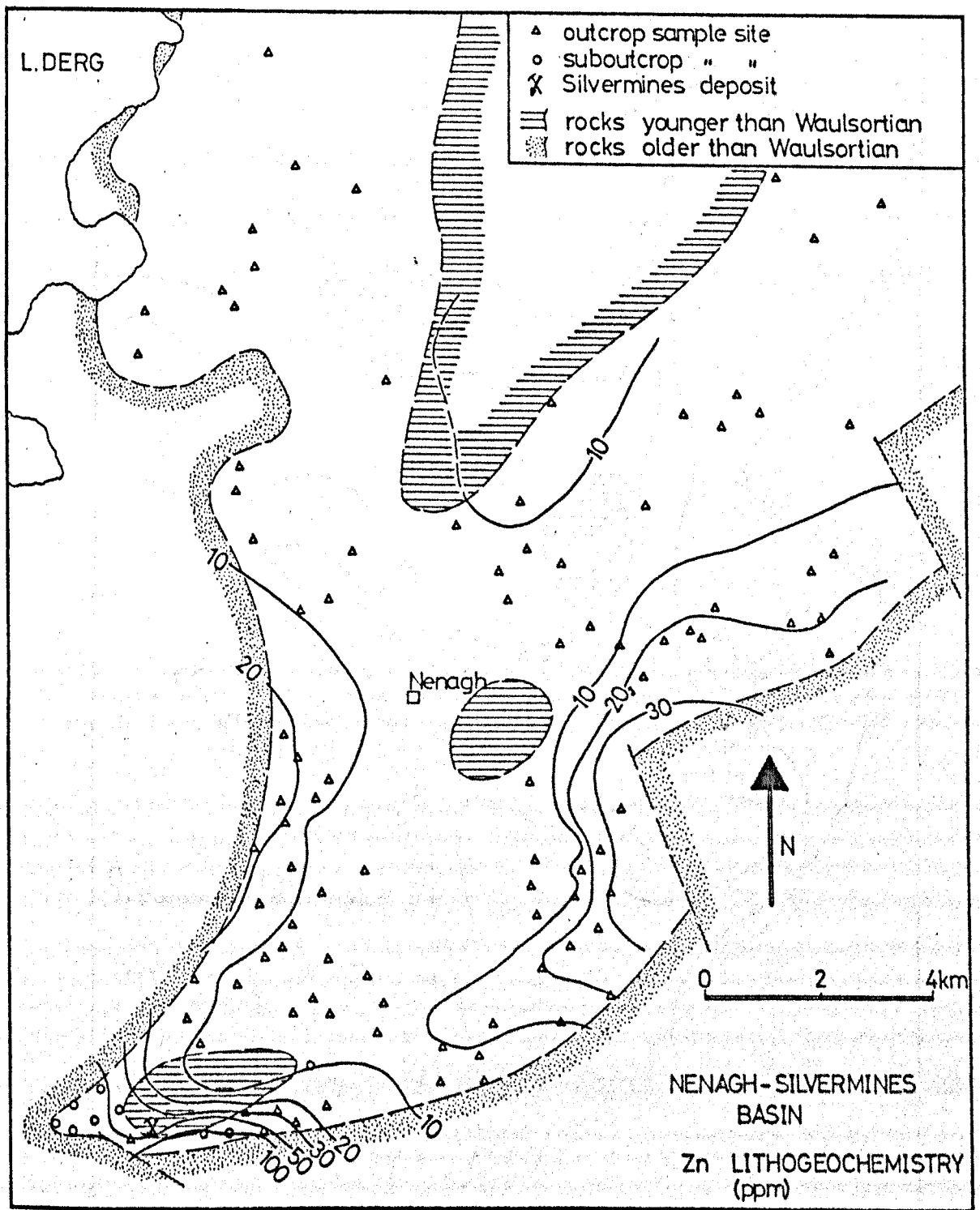


Figure 3.36: Zinc content of Waulsortian Limestones in Nenagh-Silvermines area. Values contoured using a rolling mean.

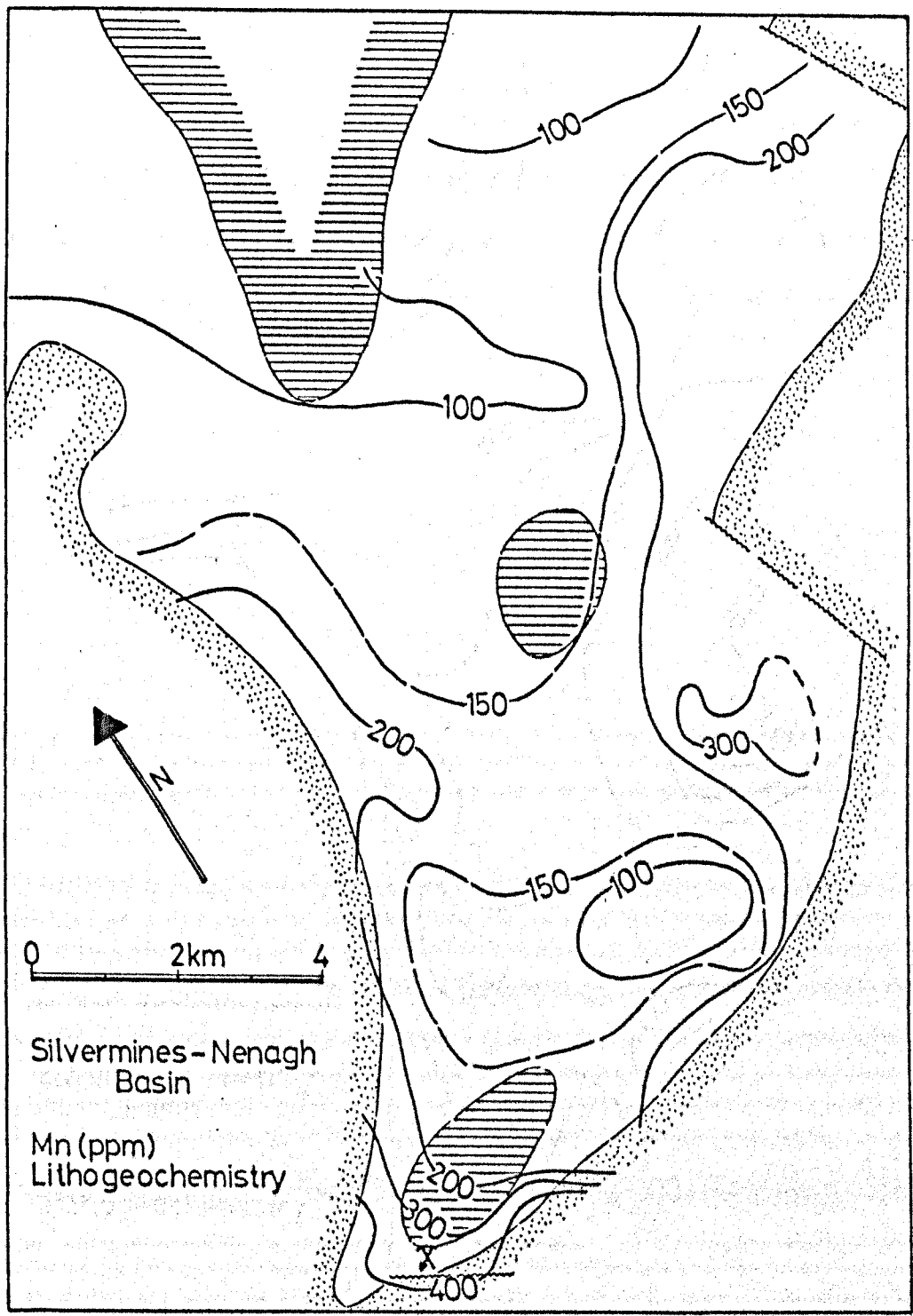


Figure 3.37: Manganese content of Waulsortian Limestones in Nenagh - Silvermines area, contoured using a rolling mean.

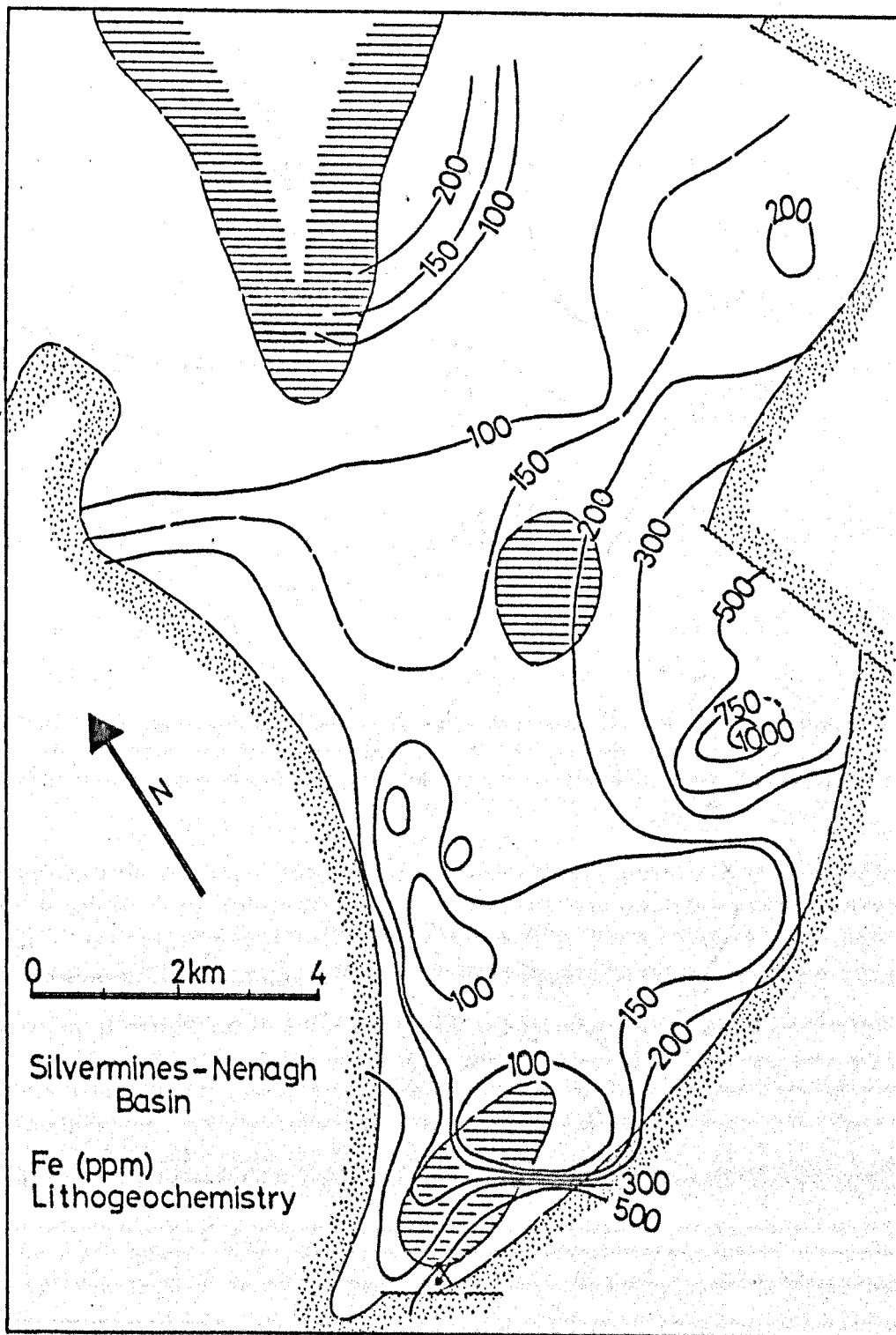


Figure 3.38: Iron content of Waulsortian Limestones of Nenagh-Silvermines area, contoured using a rolling mean.

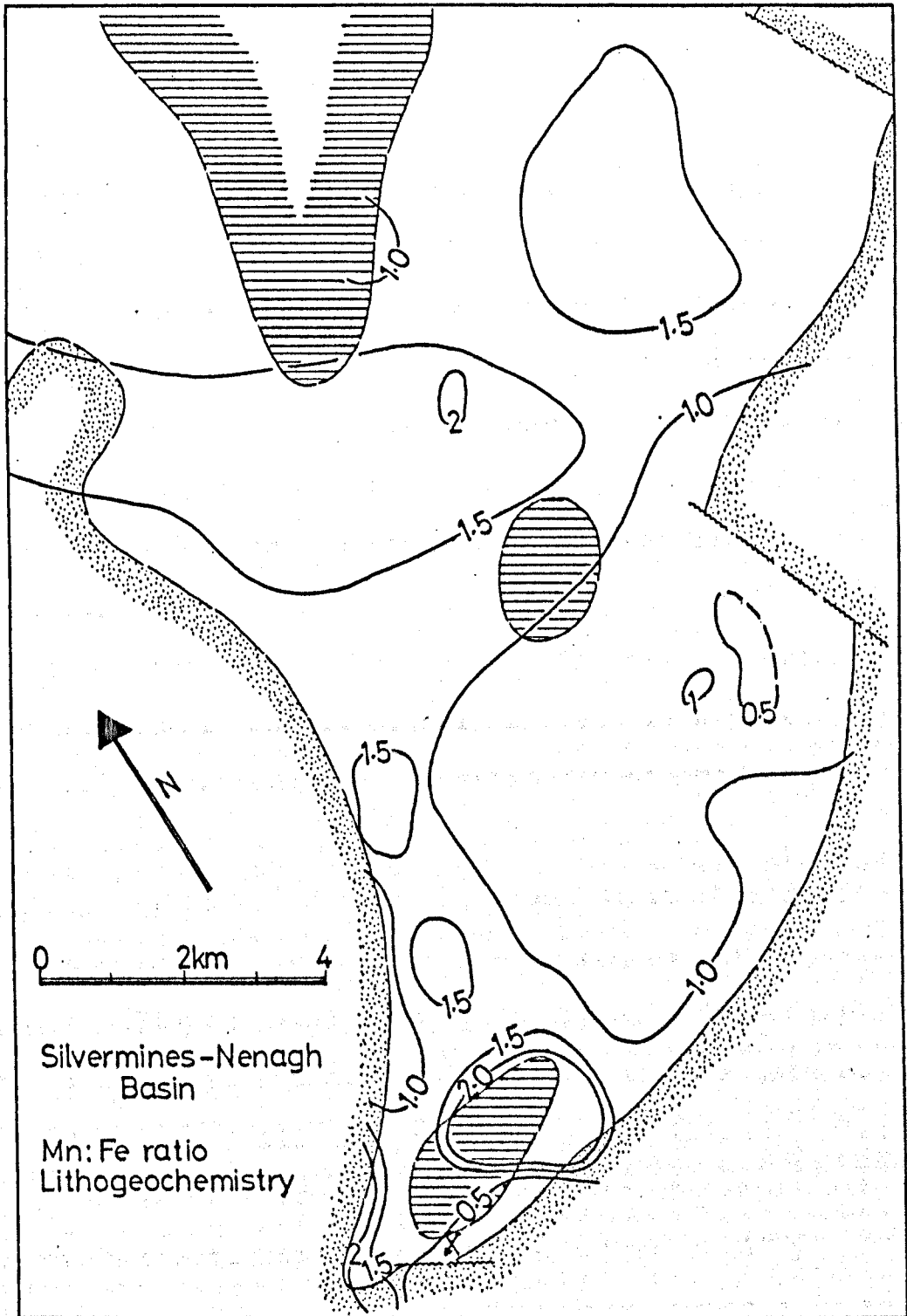


Figure 3.39: Manganese to iron ratio in Waulsortian Limestones of Silvermines - Nenagh area, contoured using a rolling mean.

(Mn+Fe)/2, and 41% contain over 10 ppm Zn (Table 3.6a). However, in the former case, utilising only outcrop samples around the mine is less effective than in the latter, as the proportion of anomalous samples drops to 27% for Zn, and less than 20% for (Mn+Fe)/2 (Table 3.6a). For comparison, of the 132 samples from more than 4 kilometres from either centre, 15% contain more than 200 ppm (Mn+Fe)/2, and 16% contain more than 10 ppm Zn, indicating how easy it would be to miss the Silvermines centre in surface reconnaissance sampling. Comparison of the median values of Mn, Fe and Zn in outcrop samples from the three areas (Silvermines proximal, Nenagh proximal and all distal samples) illustrates how poorly expressed the Silvermines centre is in surface outcrop (Table 3.6b).

It is possible to contour the areal distribution of trace elements in the area close to the Silvermines deposits (Figures 3.44 - 48). In these, only sample data from the stratiform ore horizon, and its lateral equivalents in drill core samples, are utilised. Also included are data from surrounding outcrop sample sites, for which stratigraphic control is not so readily determined with any degree of certainty, especially in the absence of nearby borehole information. These diagrams enable patterns of trace element distribution to be compared with the distribution of stratiform ore and host rocks more directly. Several zones of high Mn, Fe and Zn content are outlined in the immediate vicinity

core samples, n>5

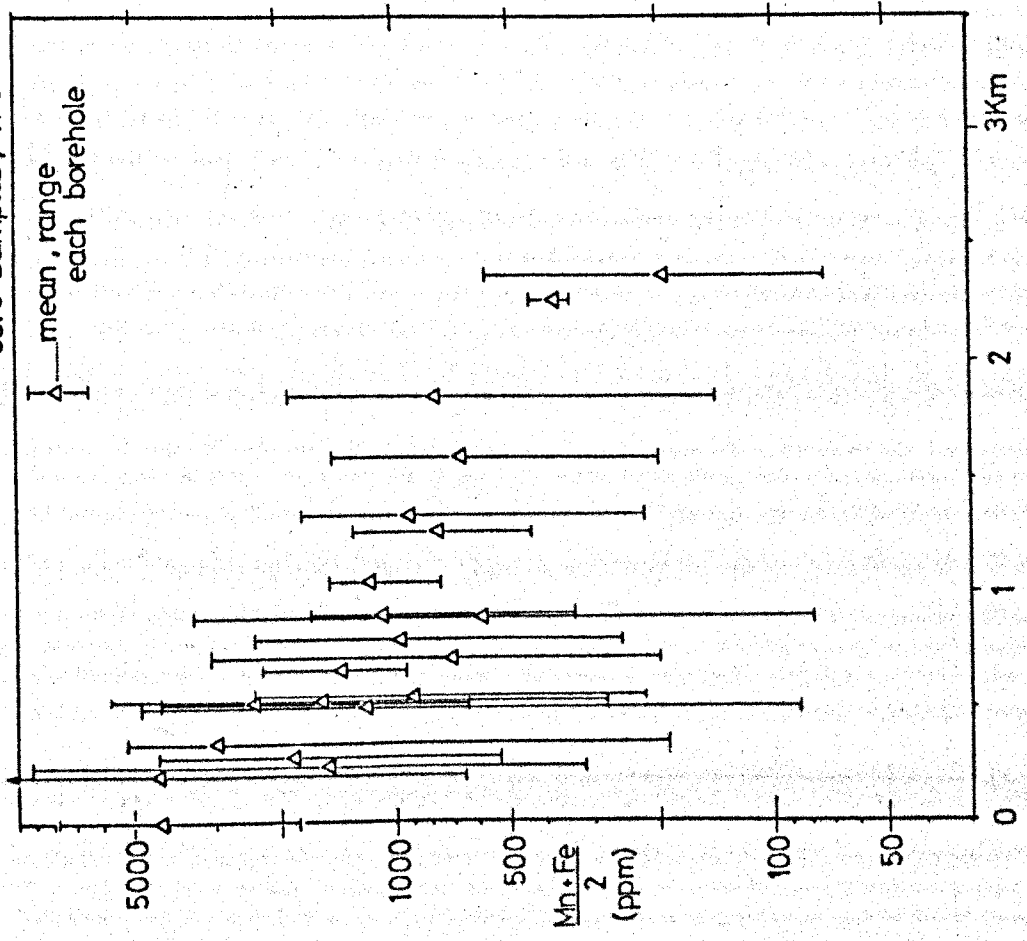


Figure 3.40a: Mean and range of $(Mn+Fe)/2$ contents from borehole samples close to the Silvermines deposits. Only holes with over five samples are displayed.

undolomitised core samples

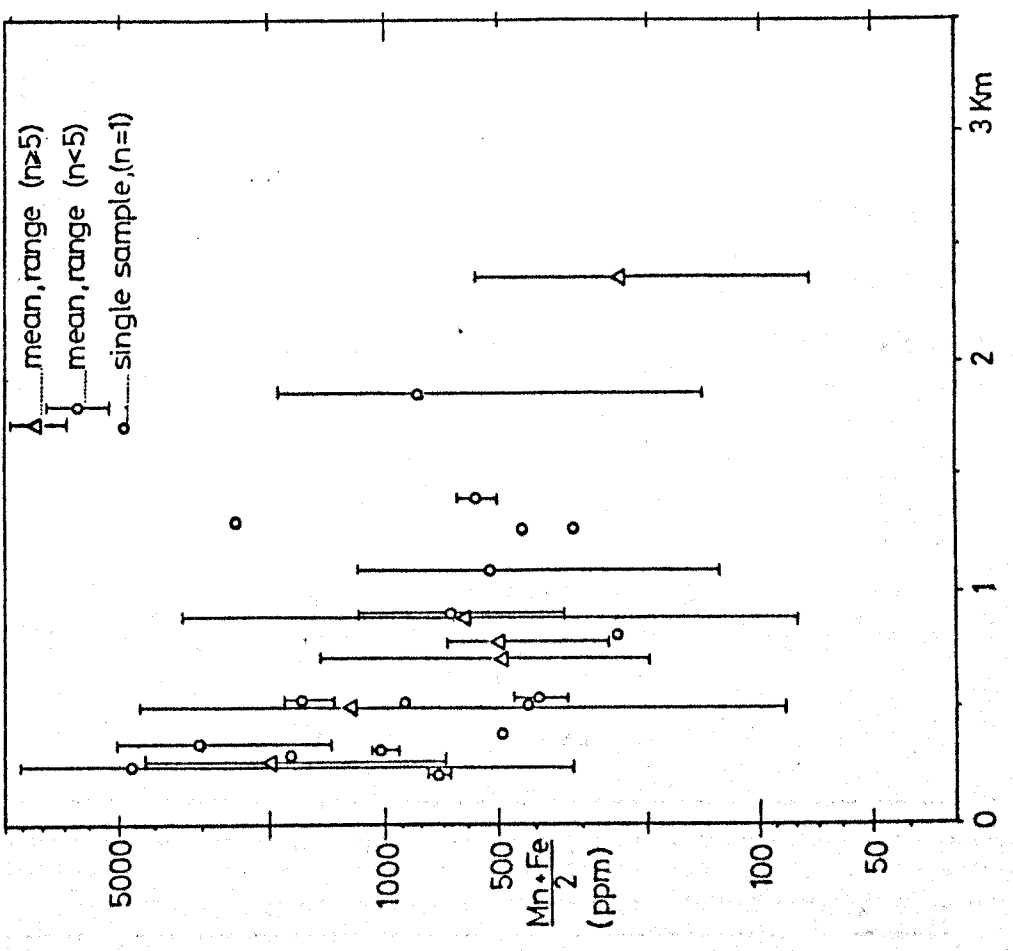


Figure 3.40b: Mean and range of $(Mn+Fe)/2$ contents of undolomitised core samples from close to the Silvermines deposits.

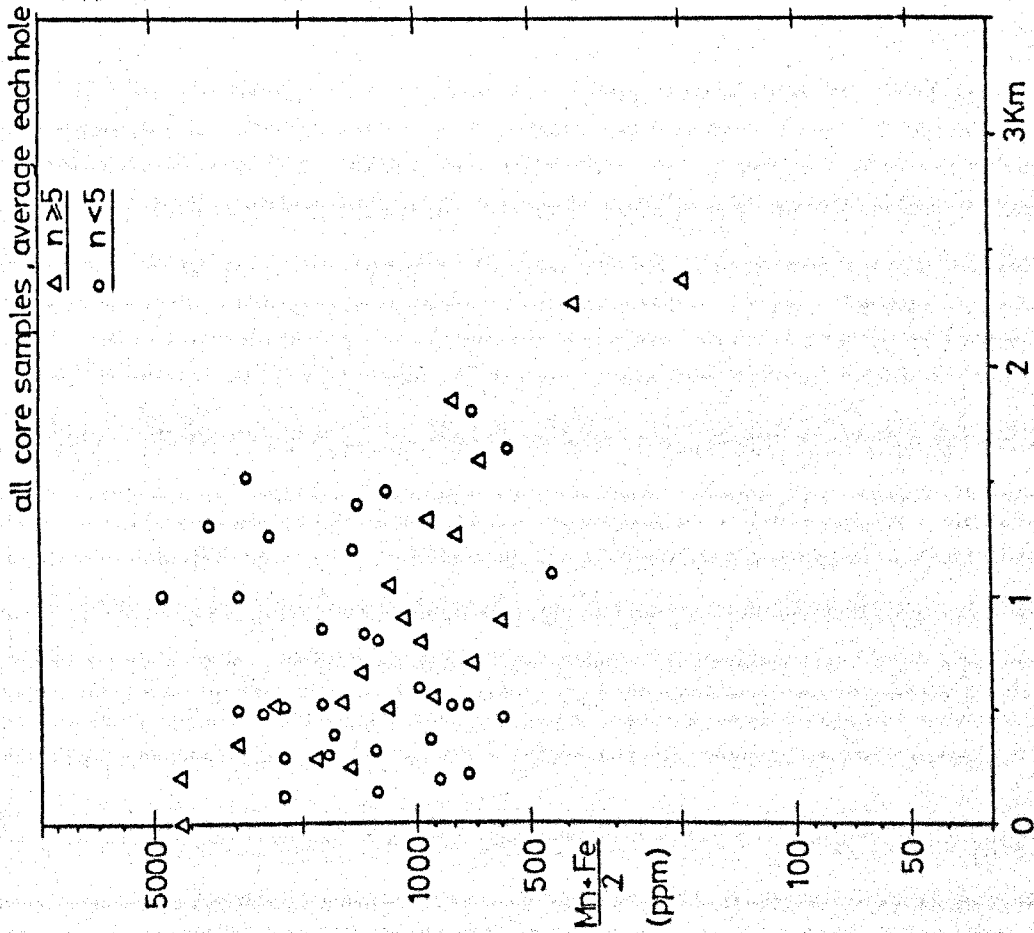


Figure 3.41: Average $(Mn+Fe)/2$ content in each drill hole sampled from around the Silvermines deposits.

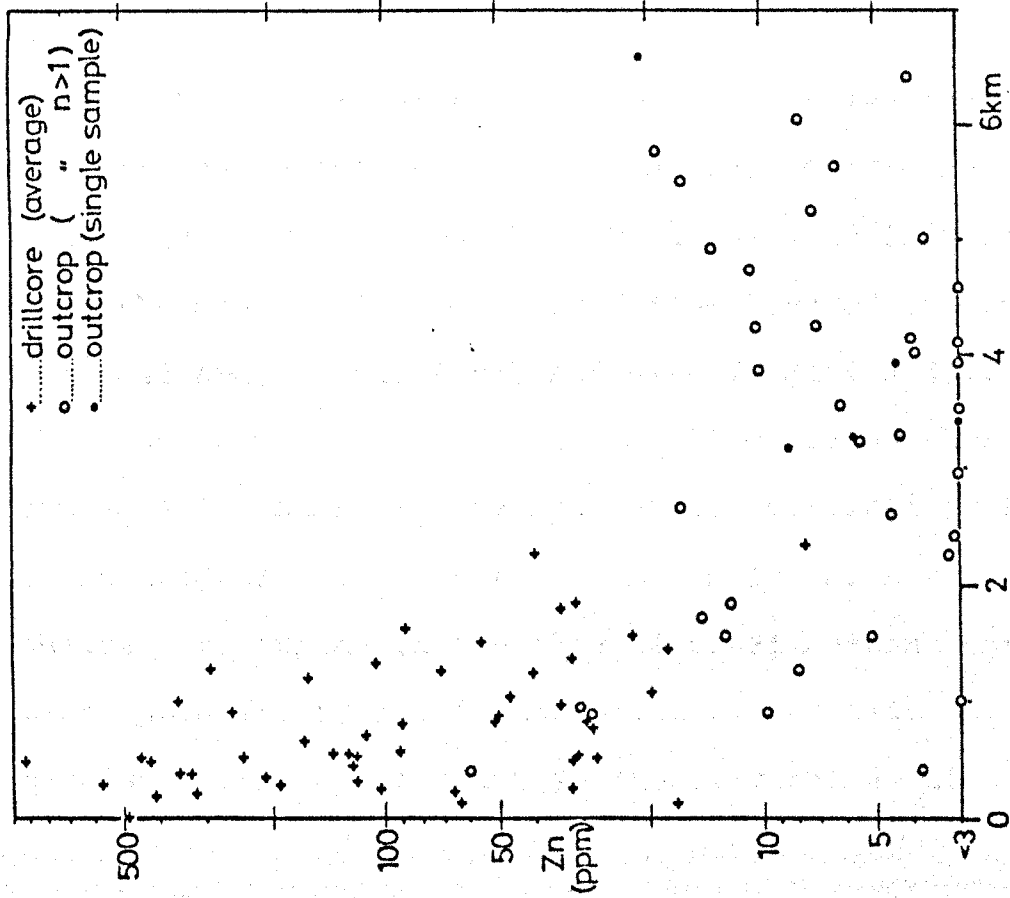


Figure 3.42: Zinc content in core and outcrop samples from close to the Silvermines deposits.

of the stratiform B and Upper G zones, particularly around the margins of the economic mineralisation, falling off rapidly towards the northeast (Figures 3.44 - 48). The ration of Mn:Fe appears to increase from the western and southern extremities of the ore zone outwards to the north and east (Figure 3.48).

Discussion of the origin and significance of these patterns is undertaken in Chapter 6. Vertical profiles of individual boreholes are examined in the next chapter, to expand on the idea of basal mudbank enrichments paralleling the localisation of economic base metals at the same horizon in the Silvermines deposits.

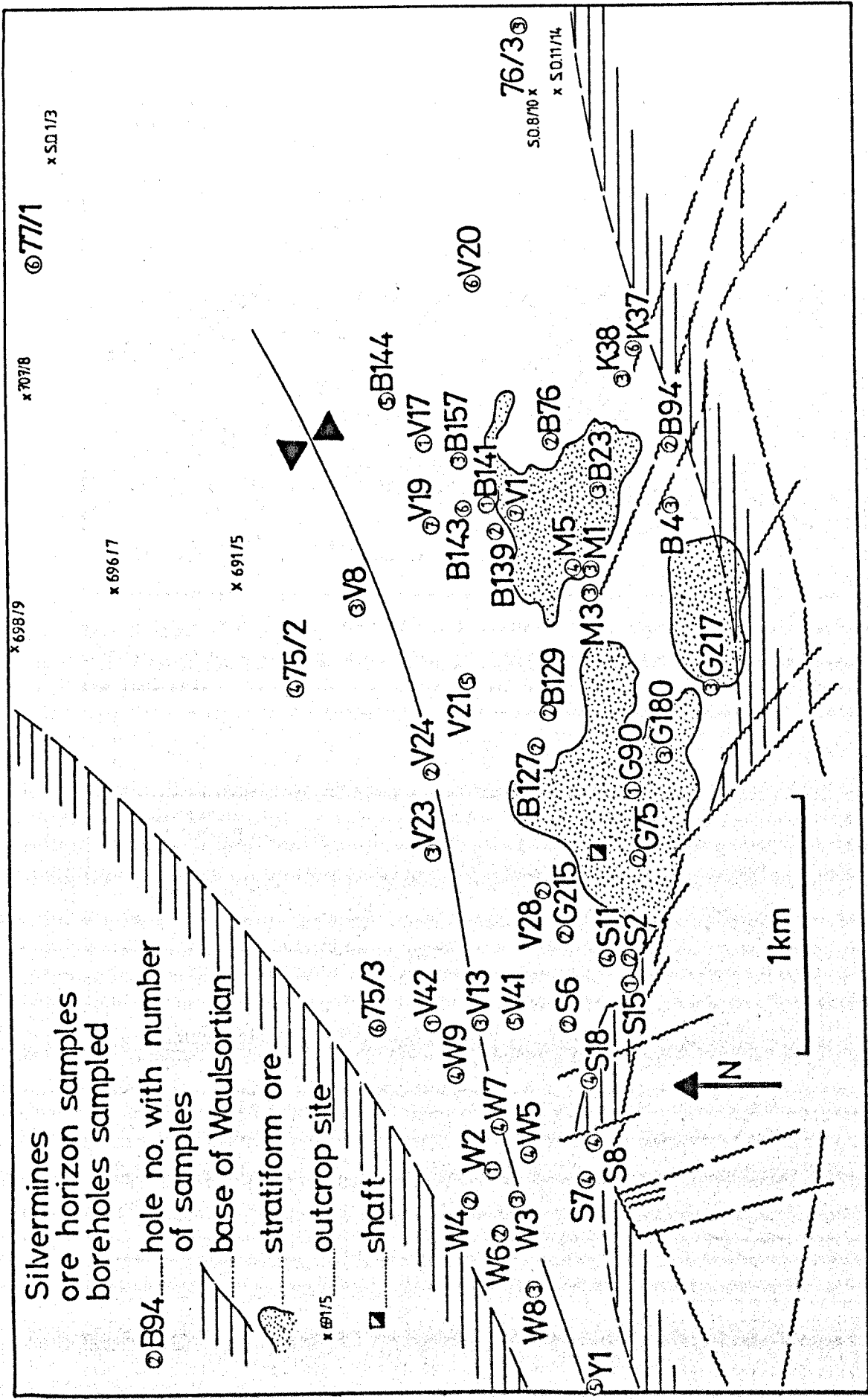


Figure 3.43: Location of core and outcrop samples from the vicinity of the Silvermines deposits, also showing outline of geology.

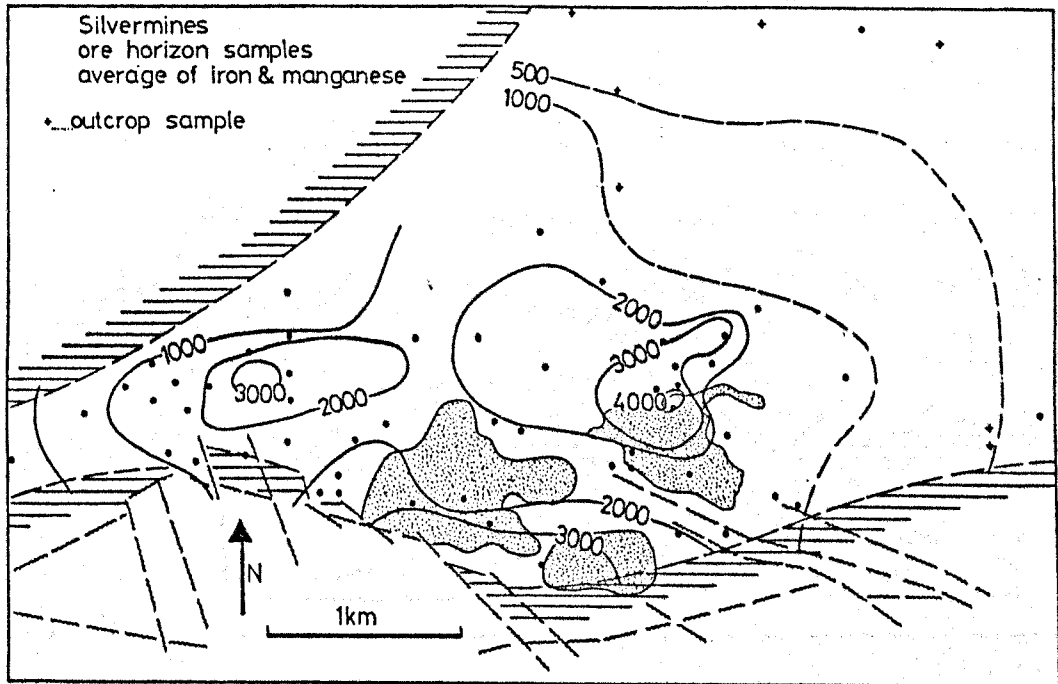


Figure 3.44: $(Mn+Fe)/2$ content of ore horizon samples around Silvermines deposits, contoured using a rolling mean. Only outcrop samples from beyond drill coverage are included.

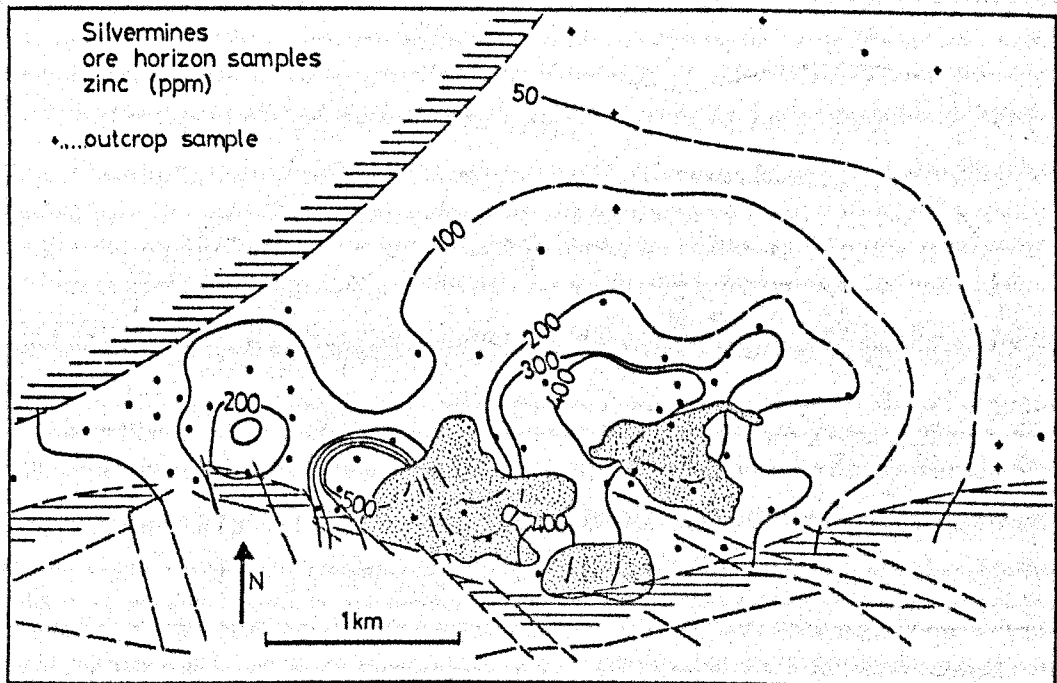


Figure 3.45: Zinc content of ore horizon samples around the Silvermines deposits, contoured using a rolling mean. Only outcrop samples from beyond drill coverage are included.

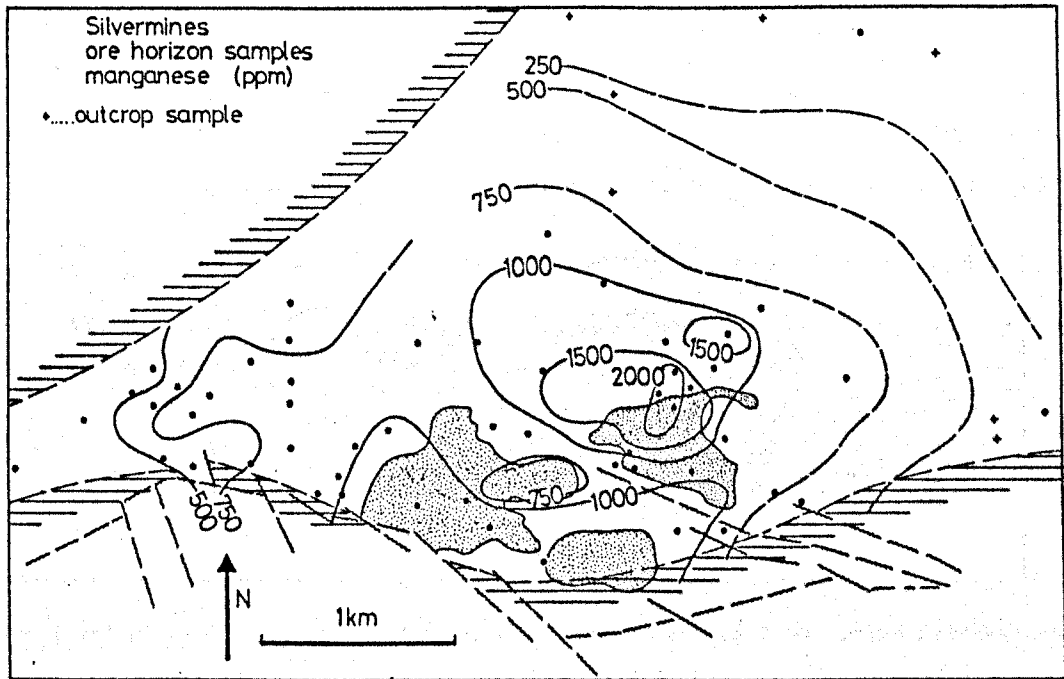


Figure 3.46: Manganese content of ore horizon samples from around the Silvermines deposits, contoured using a rolling mean. Only outcrop samples from beyond drill coverage are included.

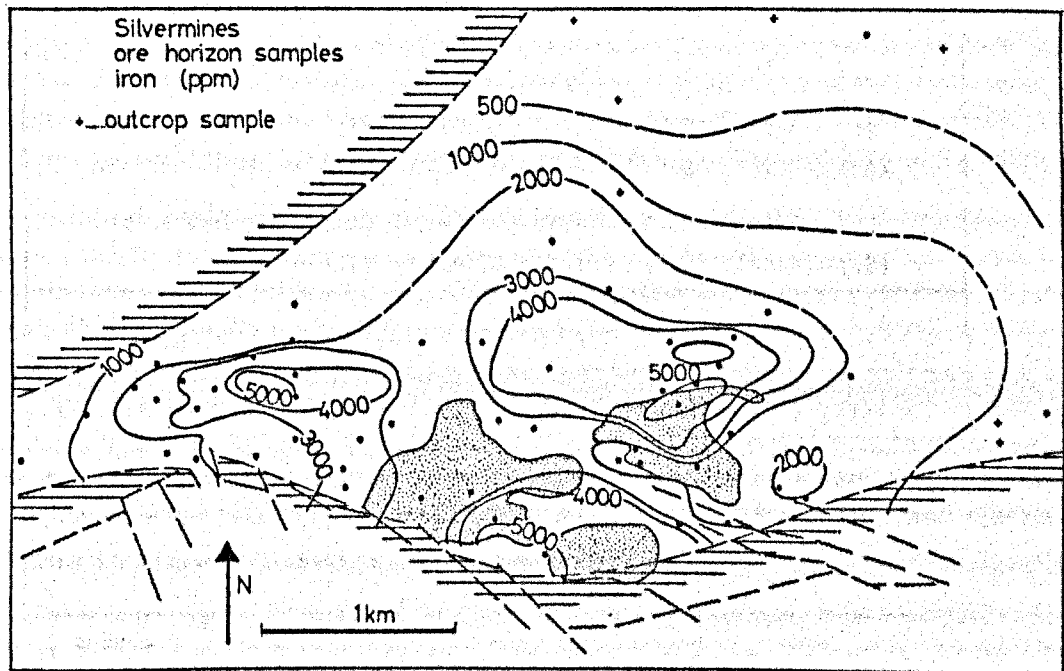


Figure 3.47: Iron content of ore horizon samples from around the Silvermines deposits, contoured using a rolling mean. Only outcrop samples from beyond drill coverage are included.

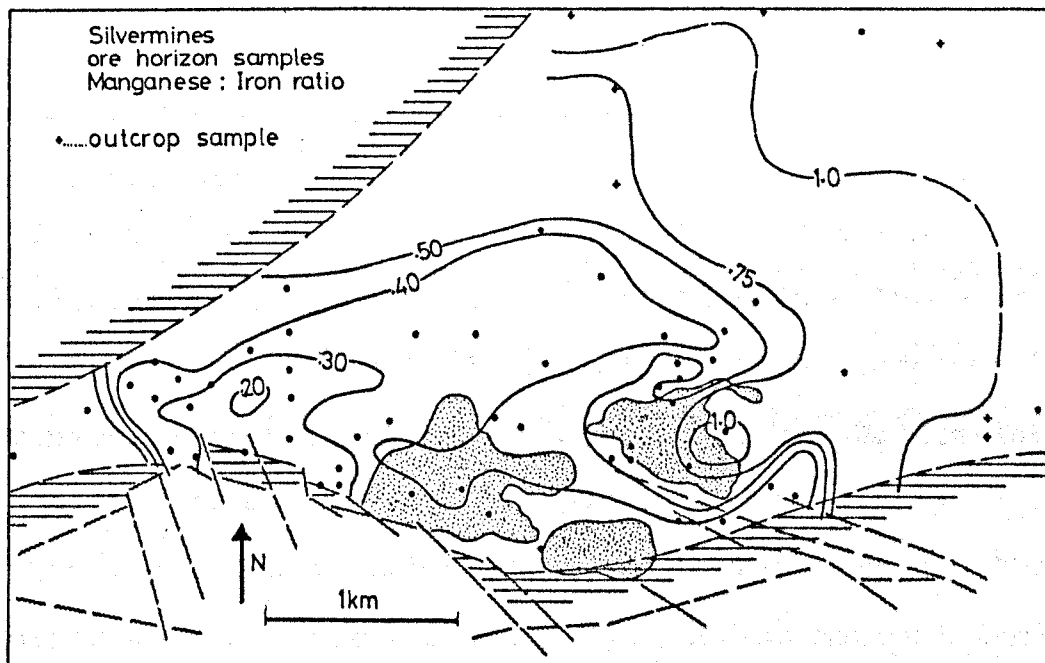


Figure 3.48: Manganese to iron ratio in ore horizon samples from around Silvermines deposits, contoured using a rolling mean. Only outcrop samples from beyond drill coverage are included.

Sample description	n	Percentage anomalous samples				
		$\frac{Mn+Fe}{2}$	Mn	Fe	Zn	Sr
Silvermines proximal						
Outcrop	63	15.9	15.9	12.7	27.0	10
Core	386	89.6	89.1	87.0	69.4	19
	* (114)	(82.5)	(78.1)	(79.8)	(52.6)	(22)
Core + outcrop	449	79.0	78.3	76.1	63.1	15
	* (177)	(58.3)	(55.0)	(55.0)	(42.8)	(18)
Nenagh proximal outcrop	83	67.5	66.3	59.0	41.0	0
All distal outcrop	132	15.2	17.4	18.2	15.9	10

Table 3.6a: Percentage of anomalous samples out of total from around the Silvermines and Nenagh centres (see text). Threshold of 10ppm for Zn, 200ppm for other elements.

* Figures in brackets exclude dolomitic samples.

MEDIAN VALUES (PPM), OUTCROP SAMPLES ONLY.

SOURCE	n	$\frac{Mn+Fe}{2}$	Mn	Fe	Zn	Sr
Silvermines proximal	63	110	130	88	6.1	168
Nenagh proximal	83	245	255	235	7.5	163
All distal	132	114	123	103	(3.5)	174

Table 3.6b: Median values of each element in outcrop samples from Nenagh-Silvermines area. Note the poor expression of the Silvermines aureole in outcrop samples.

3.4.1. Athlone - Longford - Mullingar.

Introduction.

This part of the study was initiated to examine patterns of trace element distribution in a large area of North-Central Ireland, containing known base metal mineralisation in several places, viz. the Ballinalack, Keel, Moate and Moyvore prospects (Figure 3.49).

One significant difference between this area and the other areas studied, is that Waulsortian mudbank facies is only patchily developed here, in an otherwise 'lagoonal' limestone sequence, representing the northern edge of the main central zone of continuous reef development (McDermott and Sevastopulo 1972; Sevastopulo 1979). Mudbanks here appear to form more localised sheet forms grading northeast into isolated mound or 'knoll' forms, before disappearing altogether (Nevill 1958; Lees 1964).

A large proportion of this area is underlain by weakly folded rocks of Carboniferous age, with very poor outcrop characterising the post-Tournaisian strata (Calp and later formations). A few small inliers of pre-Carboniferous or basal Carboniferous sediments outcrop and tend to display northeasterly-trending Caledonoid features. These may be fault-bounded by similar-trending normal fault systems.

A number of preliminary studies of the lithogeochemistry of parts of this area, initiated following the publication of results from Tynagh (Russell 1974, 1975),

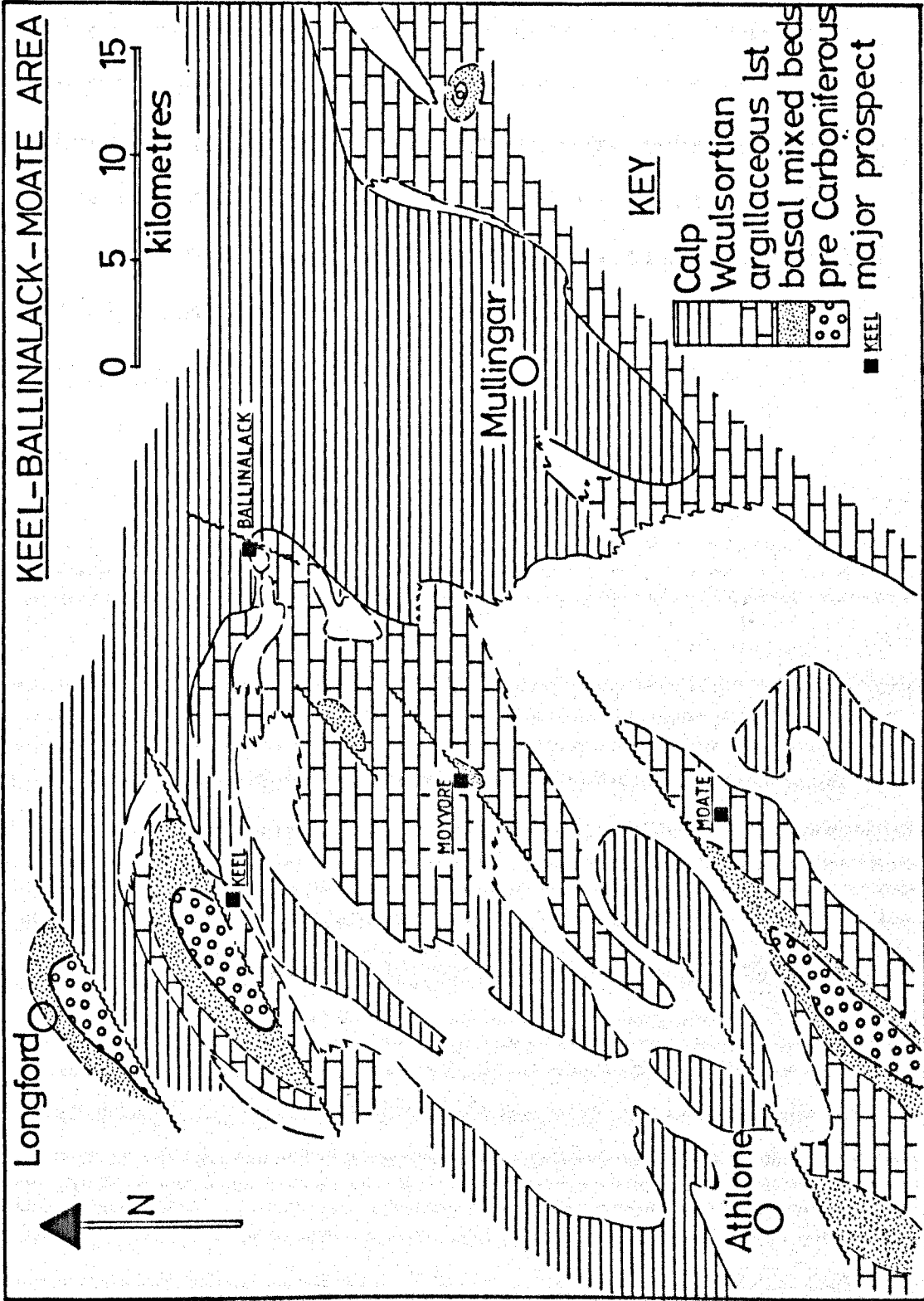


Figure 3.49: Outline of regional geology of North Midlands area (for location see also Figure 3.1). Location of base metal prospects discussed in text is also shown.

are described by Beale (1976) and Al-Kindi (1979) for Ballinalack, and by Martin and Chabot (1981) for Moate. Each of these authors report local enrichments of manganese around the base metal mineralisation, up to several kilometres distant.

Outcrop samples from this area were supplemented by core material from both Keel and Ballinalack, and by outcrop samples collected by Russell (unpublished work) from the Moate - Athlone area.

3.4.2. Ballinalack.

Introduction.

Beale (1976) examined core from the Ballinalack Pb+Zn prospect and outcrop from the surrounding area, and reported primary enrichments of manganese up to 3 kilometres from the deposit, with local zinc enrichments in drill core to half a kilometre. A number of outcrop samples collected by Al-Kindy (1979) from the vicinity of the mineralisation yielded high values of Mn compared to the background values from elsewhere in Ireland.

As discussion on the genesis of the Ballinalack mineralisation suggests a range of possible modes of introduction of ore material from syngenetic, through syndiagenetic, to post-lithification or epigenetic (Beale op cit; McArdle 1978; Halls et al 1979; Jones and Bradfer 1982), lithogeochemistry was seen as one method for proving or disproving syn-genetic introduction of base metals and associated trace elements into a submarine environment.

Geology.

The bedrock geology of this area consists almost entirely of rocks of Lower Carboniferous age. The oldest rocks at the surface are located in a small NE-trending inlier of basal Carboniferous Mixed Beds and clastics at Ballinacarrigy, to the southwest of the Ballinalack prospect (Figure 3.50). Discontinuous Waulsortian mudbanks are surrounded by dark, impure lagoonal limestones (Argillaceous Bioclastic Limestone).

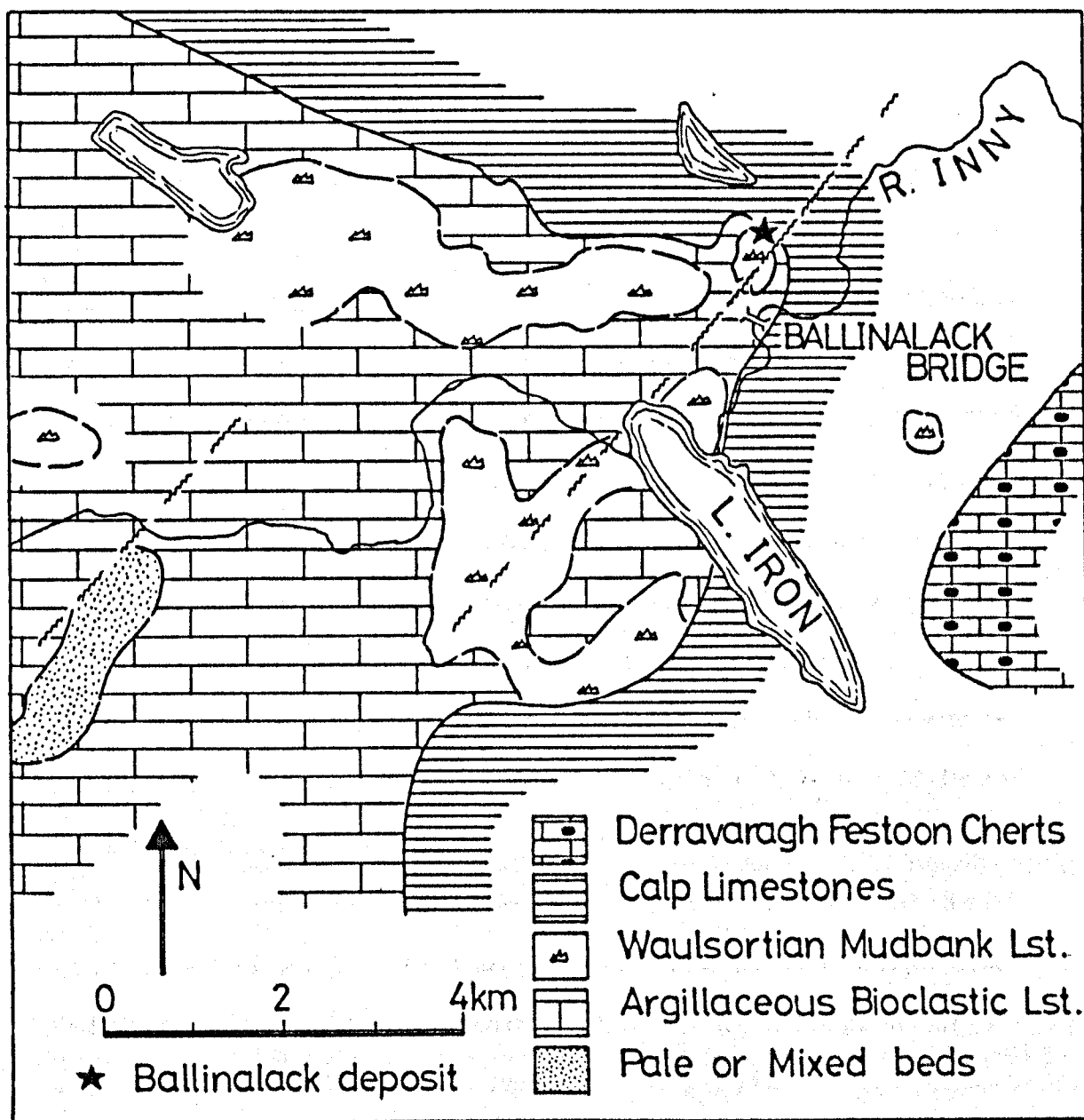


Figure 3.50: Geology of Ballinalack area, Co. Westmeath, showing location of Ballinalack deposit. Inlier of Mixed Beds on western edge of map is Ballinacarrigy Inlier (see text).

and thick 'Calp' limestones (over 300 metres thick) cover large areas to the north and east (Jones and Bradfer op cit). Thicker, sheet-like developments of Waulsortian 'Reef' outcrop to the southwest, between Ballinacarrigy and Moate, whereas only isolated 'knoll reefs' of Waulsortian and younger age occur sporadically to the northeast (Nevill 1958; Lees 1964).

Regional dips are generally shallow ($5-10^{\circ}$) and towards the east or southeast, and although a number of major fault trends have been postulated for the area (N-S, Russell 1968; NW-SE, Horne 1979; NE-SW, Deeny 1982), little evidence for these is seen at the surface. A northeasterly Caledonoid trend is indicated by structural alignment of basal Carboniferous inliers and borehole information on fault patterns.

The apparent absence of Old Red Sandstone or Red Bed lithologies in this area may be real or apparent, due either to palaeogeographic variation or faulting in the sequence (Jones and Bradfer op cit).

Mineralisation.

The mineralisation at Ballinalack is associated with a NNE trending normal fault, but differs from other Irish deposits in that it does not lie adjacent to any major inlier of Lower Palaeozoics or Old Red Sandstone. Movement on the fault is of the order of 200 to 250 metres downthrown to the west, increasing northwards (from which we may infer a hinged movement), with smaller cross-cutting faults trending WNW, with

BALLINALACK E-W SECTIONS

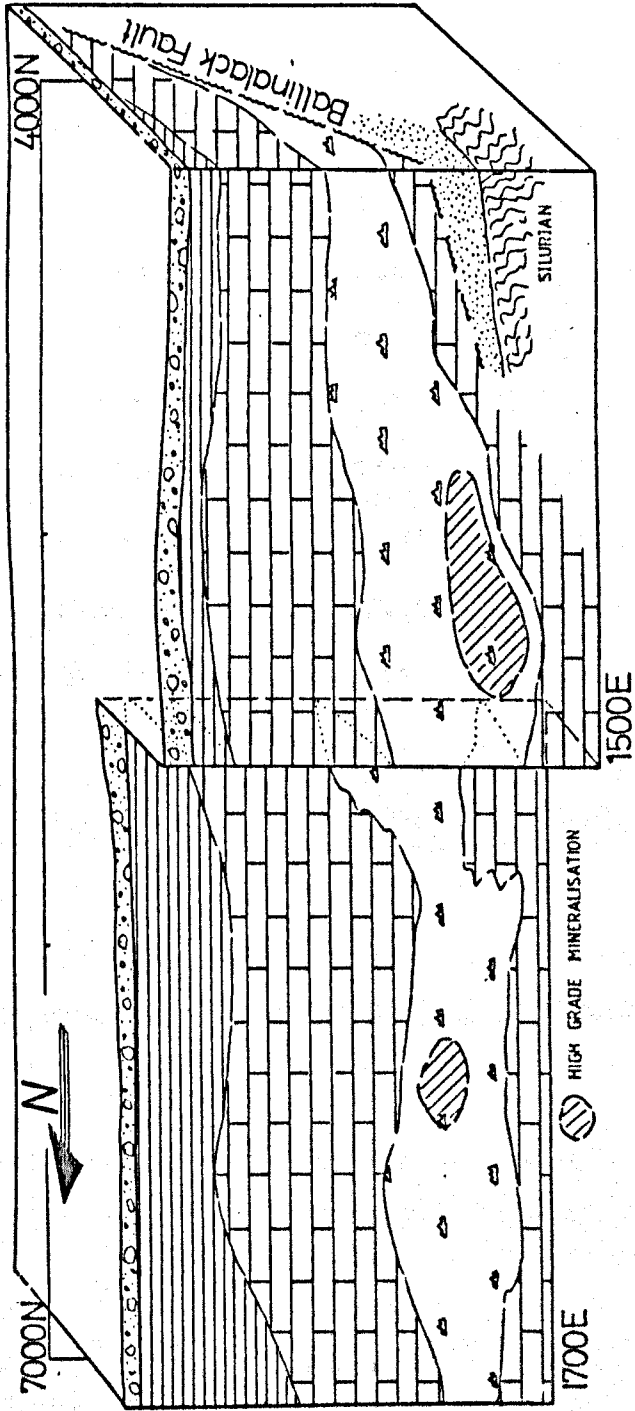


Figure 3.51a: Sketch block diagram of Ballinalack deposit, constructed from company sections.
Key as for Figure 3.50.

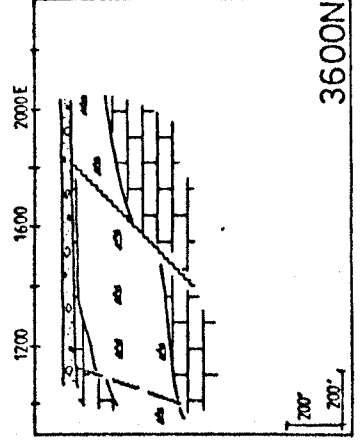
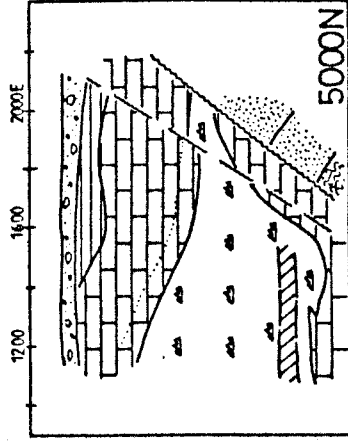
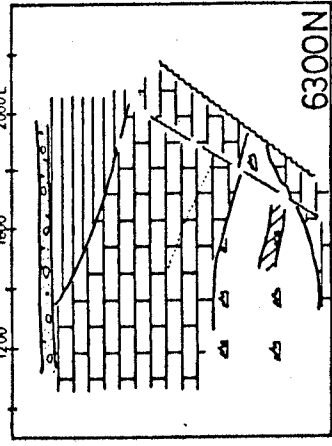


Figure 3.51b: Simplified E-W cross sections of Ballinalack deposit, constructed from company sections. Key as for Figure 3.50.

a NE downthrow and relatively minor amounts of movement.

Three, or perhaps four, mudbank 'knolls' are strung parallel to, and along the fault, and considerable thinning of these is observed eastwards across the structure. This is coincidental with localised reef breccias of uncertain origin, possibly indicating contemporaneous movements on the fault (Jones and Bradfer op cit). These knolls are up to approximately 200 metres thick, elongated parallel to the fault, and thin to less than 25 metres between maximum developments, and also to the east of the fault, where 'off-reef' argillaceous bioclastic limestone facies predominated.

The most important sulphide mineralisation is centred on the mudbank limestones (Figure 3.51), with minor concentrations in older strata at depth, notably the 'Navan Micrite' unit of transitional mixed beds.

Sulphides are present as sporadic concentrations of galena and sphalerite, with pyrite and bravoite, in primary (notably stromatolites) and secondary cavities in the mudbank framework, deposited from evolving hydrothermal fluids during diagenesis (Halls et al 1979). The principal gangue minerals are calcite, dolomite and baryte.

A possible textural control on deposition, according to permeability of individual mudbank microfacies and interbedded argillaceous layers, is indicated by Jones and Bradfer (op cit). They give detailed descriptions

of host carbonate mudbanks. listing four generations of cement and internal sediment within stromatactis cavities, along with late-stage calcite and pink dolomite veinlets.

Sampling and Results.

Fist-sized samples were collected from available outcrop locations of Waulsortian mudbank at Ballinalack, and probably contemporaneous knolls in the surrounding area. A small number of samples collected by Al-Kindi (1979) were also used, and the data was complemented by a suite of core samples from the deposit itself.

Initial examination of Mn and Fe data from outcrop within 5 kilometres of the Ballinalack deposit indicated that a range of values, from below 200 to over 1000 ppm was present (Figure 3.52a). Analysis of distal outcrop samples, mostly taken from some 15 to 20 kilometres to the south towards Ballymore, and sporadic outcrops to the south and east of Mullingar, suggested that an extensive aureole of Mn and Fe was present around the mineralisation, as average distal values were generally less than 250 ppm. Absence of outcrop in the region from 5 to 12 kilometres distant (except towards the neighbouring deposit at Keel, see Section 3.4.3.) reduces the effectiveness of simple graphing of the data against distance from the deposit, to determine the lateral extent of the enrichments.

Plotting the analytical results of core samples from within 2 kilometres of the centre of mineralisation

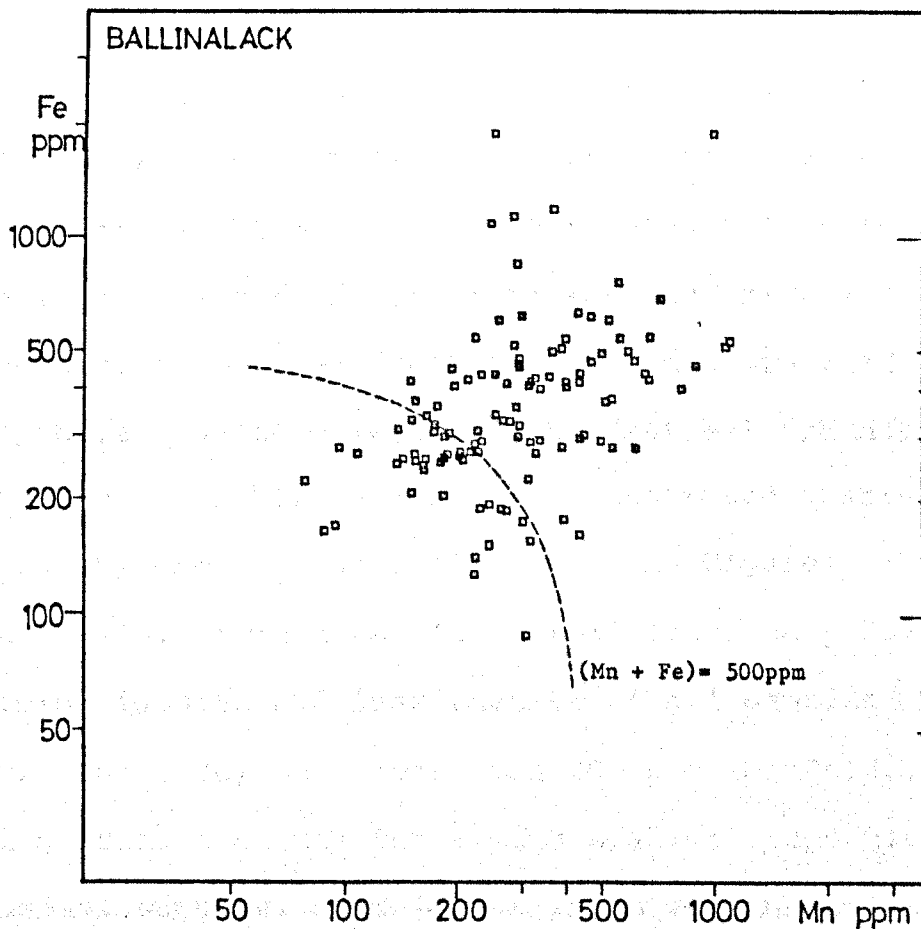


Figure 3.52a: Graph of Mn against Fe for outcrop samples from within 5 km of Ballinalack deposit (n = 106). Note log scale.

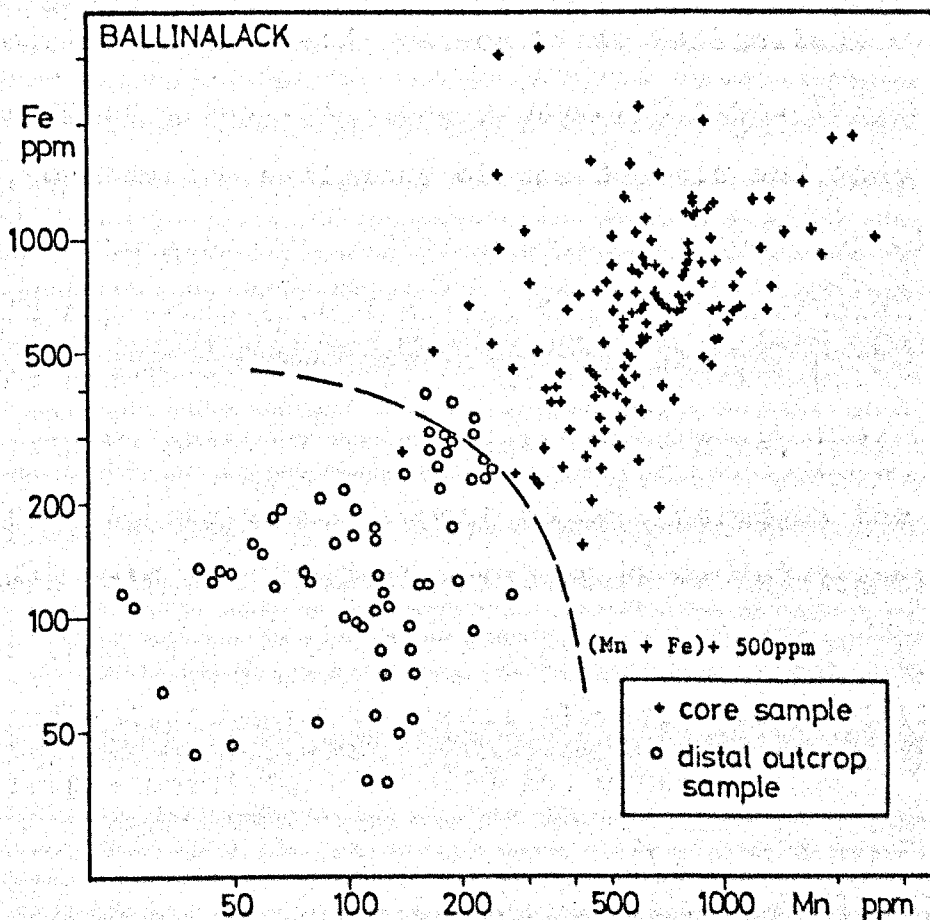


Figure 3.52b: Graph of Mn against Fe for core and distal outcrop samples from Ballinalack area. All core samples (n=136) from within 3 km, all distal outcrop samples (n=63) from beyond 10 km of mineralisation. Note log scale.

alongside the distal outcrop samples from Ballymore and Mullingar (Figure 3.52b) indicates the differentiation between the two sets of samples, effectively separated by the curved line representing $Mn+Fe = 500ppm$.

The comparison between $(Mn+Fe)/2$ and Zn content in core, proximal outcrop (within 5 kilometres) and distal outcrop (beyond 5 kilometres), is illustrated quantitatively by the frequency histograms in Figures 3.53 and 3.54. Within the 'proximal' zone, only 12% of outcrop samples and less than 6% of all samples (outcrop and core) have less than 200 ppm $(Mn+Fe)/2$. Anomalous zinc accounts for a much smaller proportion of proximal samples, over 74% of which retain background values of less than 10 ppm (including 90% of all proximal outcrop samples).

Contouring of $(Mn+Fe)/2$ values in the Ballinalack - Ballymore area outlines two pronounced highs (Figure 3.55), one on the periphery of the deposit and one close to the southern end of the drill grid. Included on this map are averaged values from each borehole.

Closer examination of Mn and Fe distribution within the vicinity of the deposit, using core data, indicates that the highest values appear to be centred on the northern half of the drill grid, where Mn is slightly higher than Fe (Figures 3.57a-b).

Vertical distribution of trace element data in drill core is presented in the following chapter.

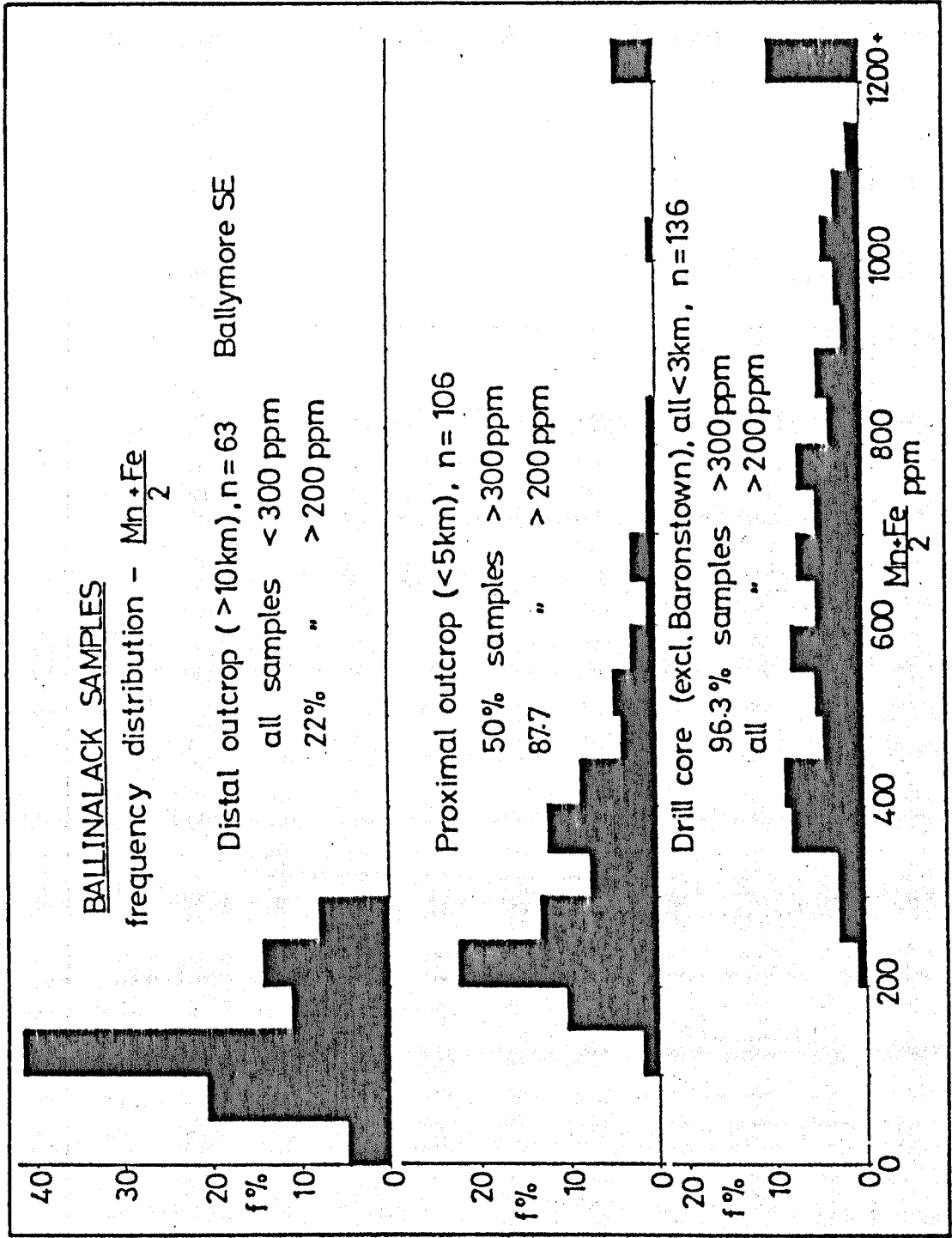


Figure 3.53: Comparison of frequency distribution of $(Mn+Fe)/2$ in distal outcrop, proximal outcrop, and proximal core samples from Ballinalack area.

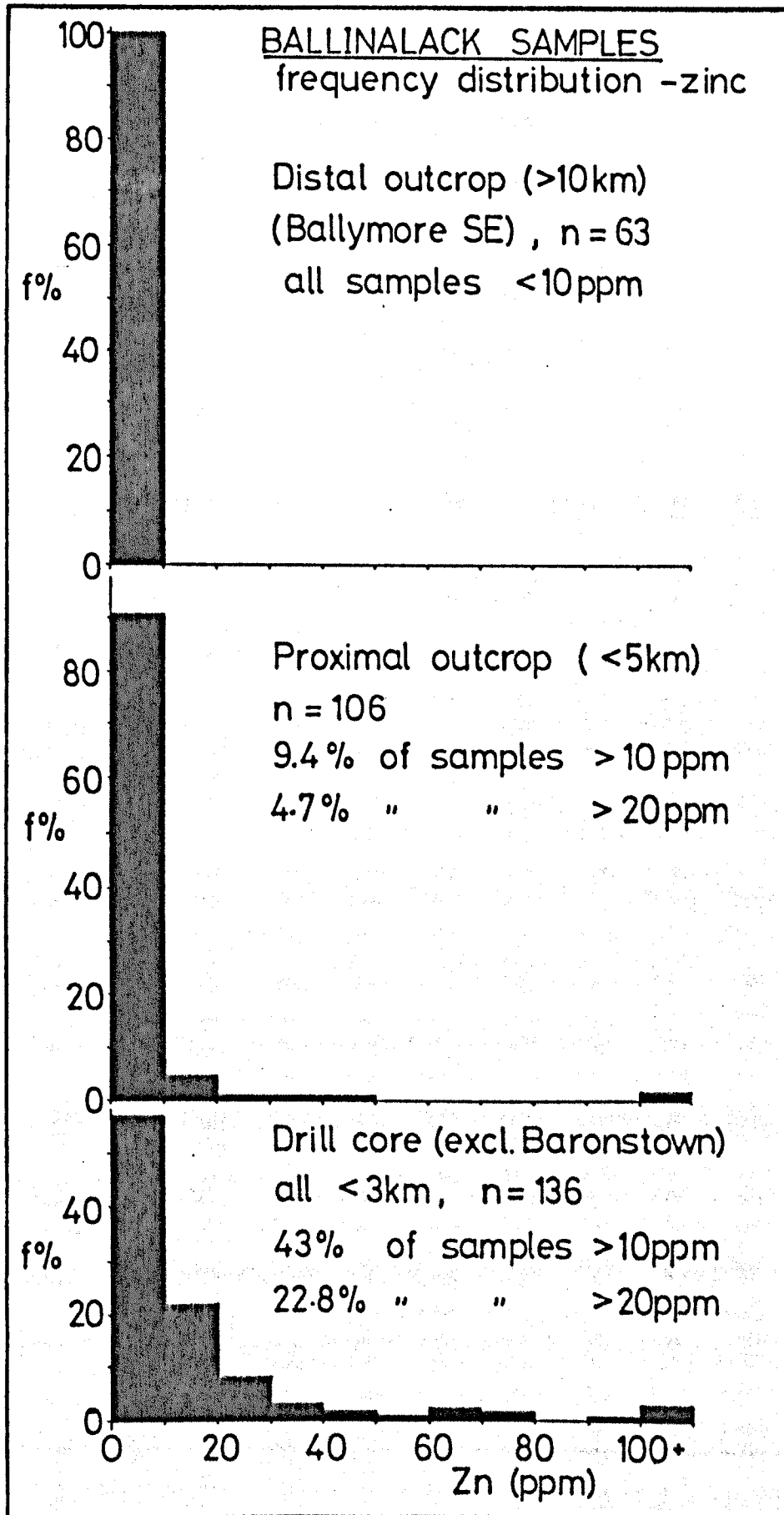


Figure 3.54: Comparison of frequency distribution of zinc in distal outcrop, proximal outcrop and proximal core from Ballinalack area.

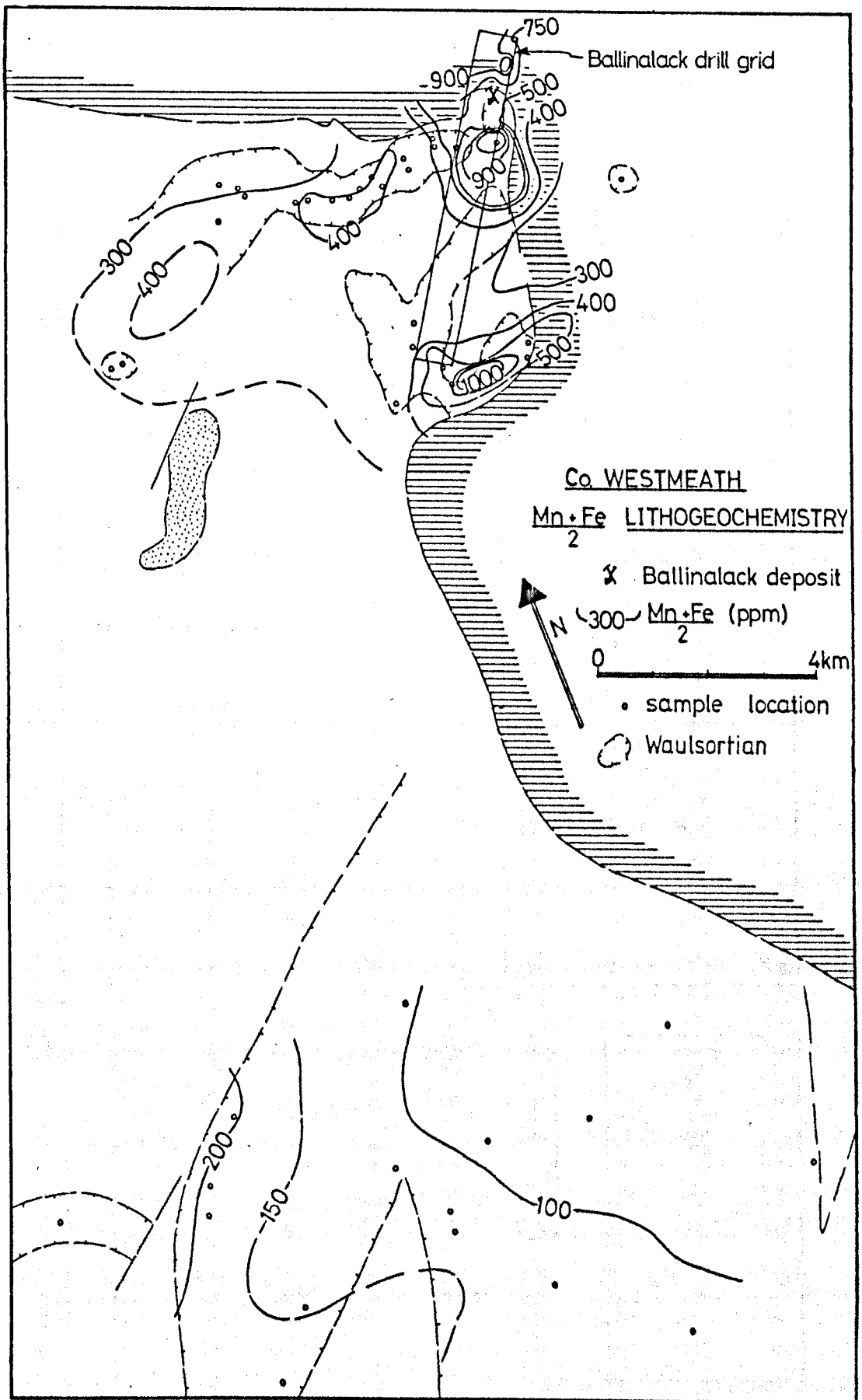


Figure 3.55: Distribution of $(Mn+Fe)/2$ in Waulsortian Limestones in Ballinalack area, contoured using a rolling mean. Stippled area is Basal Carboniferous of Ballinacarrigy inlier, horizontal ruling is Calp outcrop. Immediately to the west of the map lies the Keel sample area.

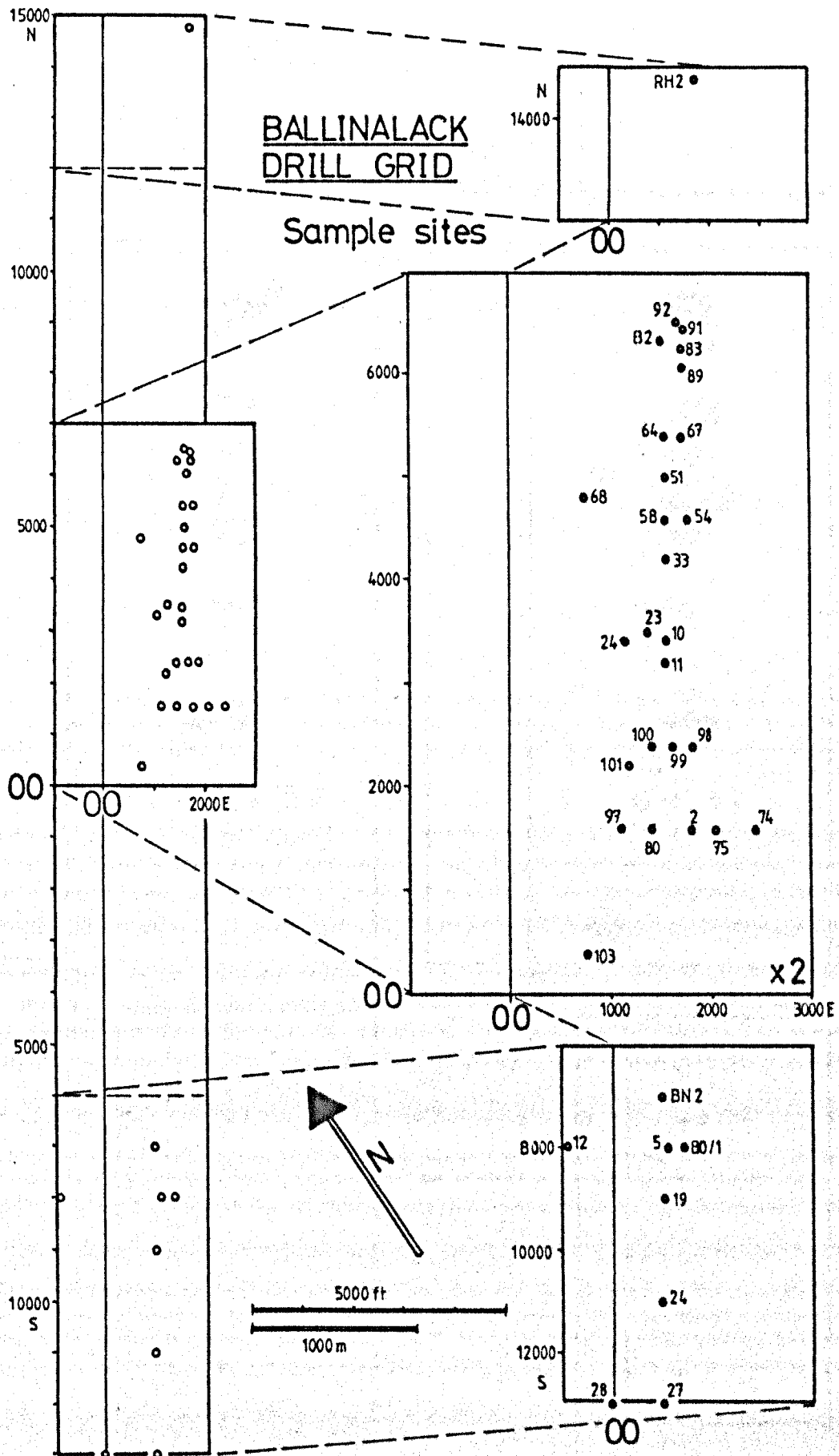


Figure 3.56: Location of boreholes sampled on Ballinalack drill grid, and arrangement as displayed in Figure 3.57.

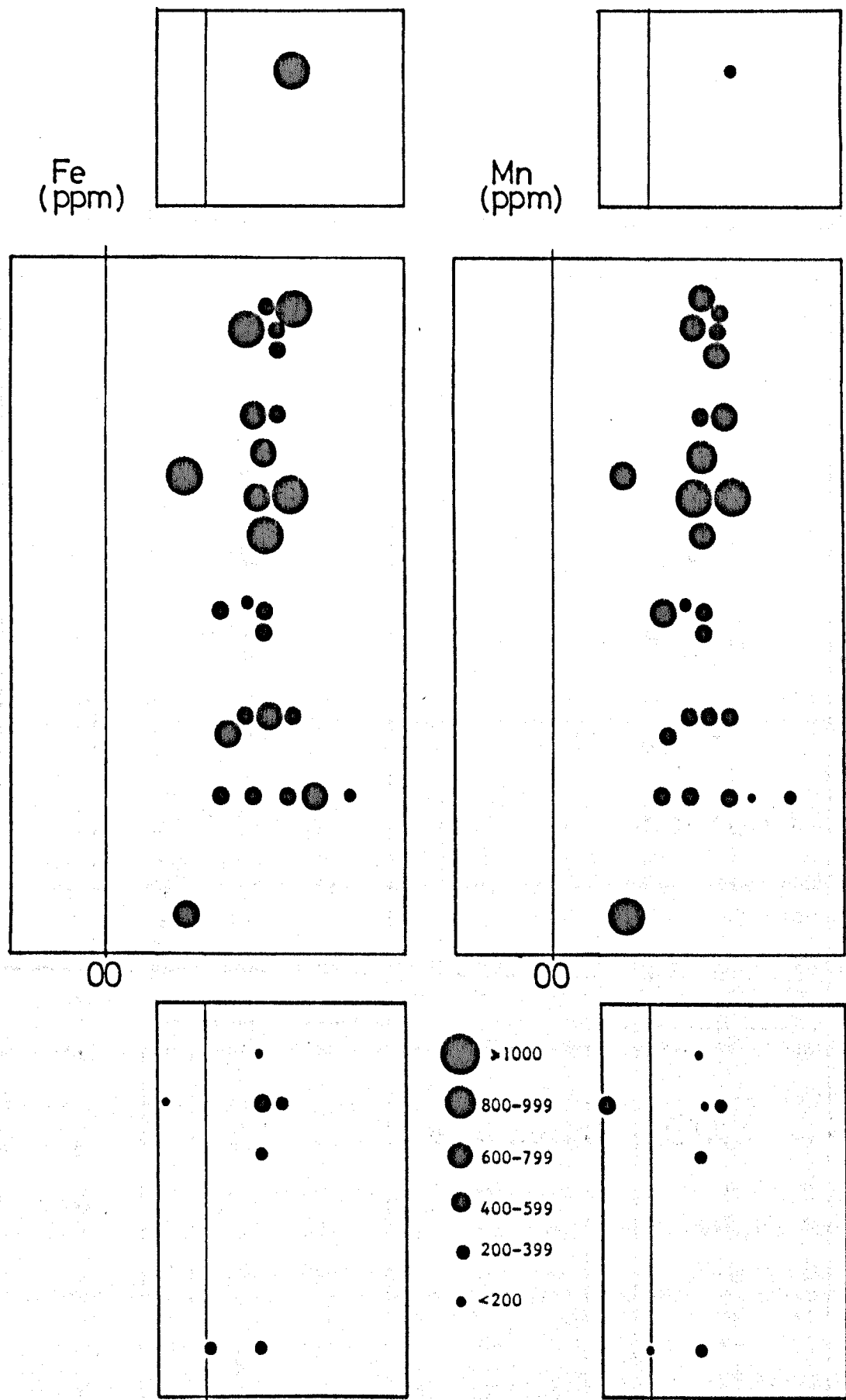


Figure 3.57a: Distribution of iron (left) and manganese (right) in boreholes sampled at Ballinalack. Results averaged from two or more samples for each hole.

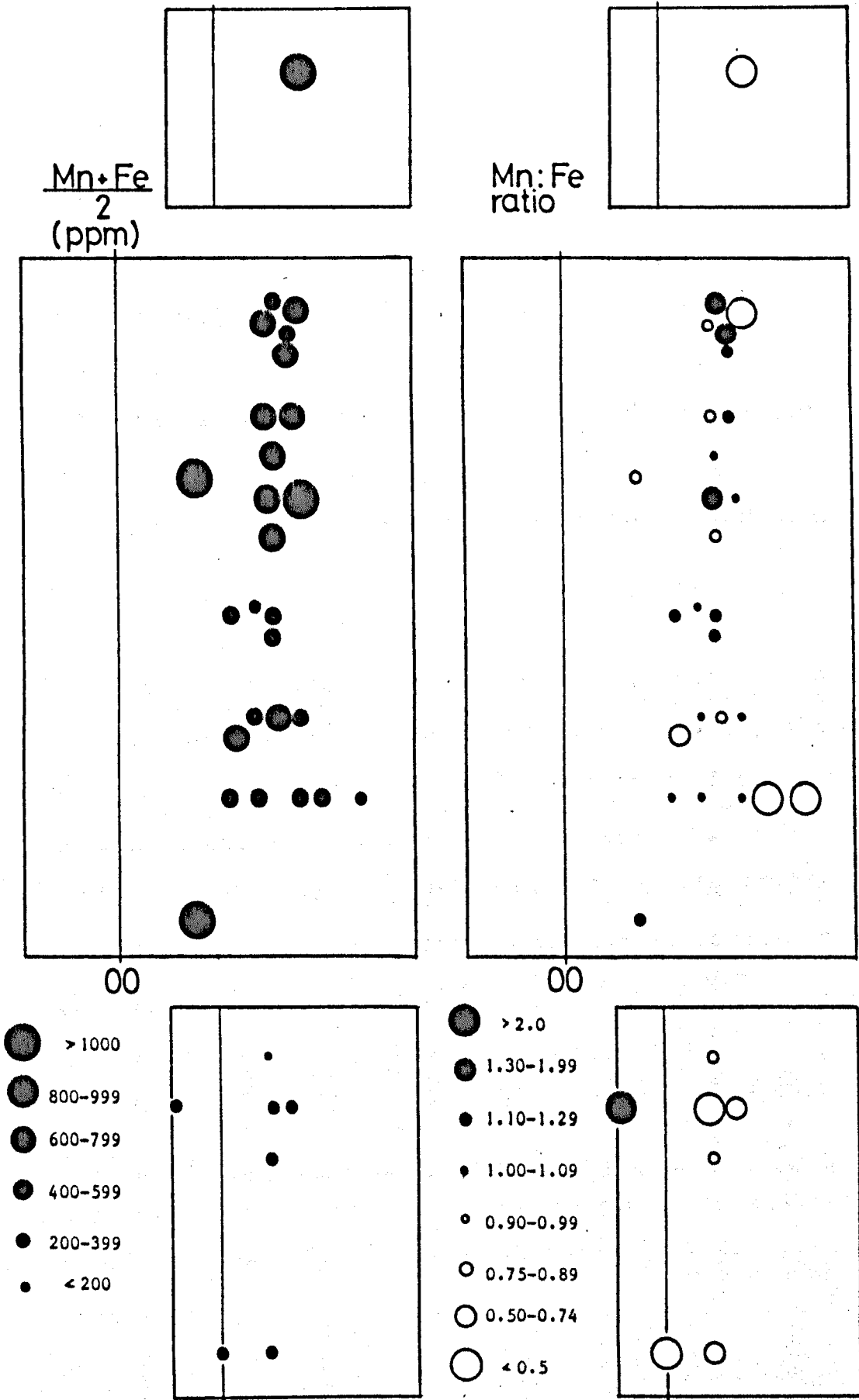


Figure 3.57b: Distribution of $(Mn+Fe)/2$ (left) and $Mn:Fe$ (right) in boreholes sampled at Ballinalack. Results averaged from two or more samples for each hole.

3.4.3. Keel.

Introduction.

The Keel Zn+Pb+Cd deposit is situated some 15 kilometres to the WNW of the Ballinalack deposit, on the opposite margin of the same shallow basin (Figure 3.49).

Unpublished lithogeochemical work undertaken by RioFinEx, on groove and chip samples from drill core, indicated apparently elevated levels of a number of trace elements, notably Mn, Zn and Ba, in the vicinity of the deposit. Background values were not determined for the surrounding area.

Geology and Mineralisation.

The geology of the epigenetic mineralisation at Keel was the subject of a study by Patterson (1970), although his results were not published. Outlines of the geological setting are included in general reviews by Morrissey et al (1971), Williams and McArdle (1978), and in papers by Meyers and Evans (1973), Lovell et al (1979) and Slowey (1984).

The local setting of the Keel deposit bears many resemblances to Silvermines, in that epigenetic feeder-zone mineralisation occurs in veins and replacing basal Carboniferous clastics and conglomerates. A major normal fault (the Keel Fault) separates this from stratabound massive baryte and pyrite, with zinc and minor lead, at the base of the Waulsortian mudbank (Slowey op cit). Economic quantities of stratiform base metals have not yet been encountered.

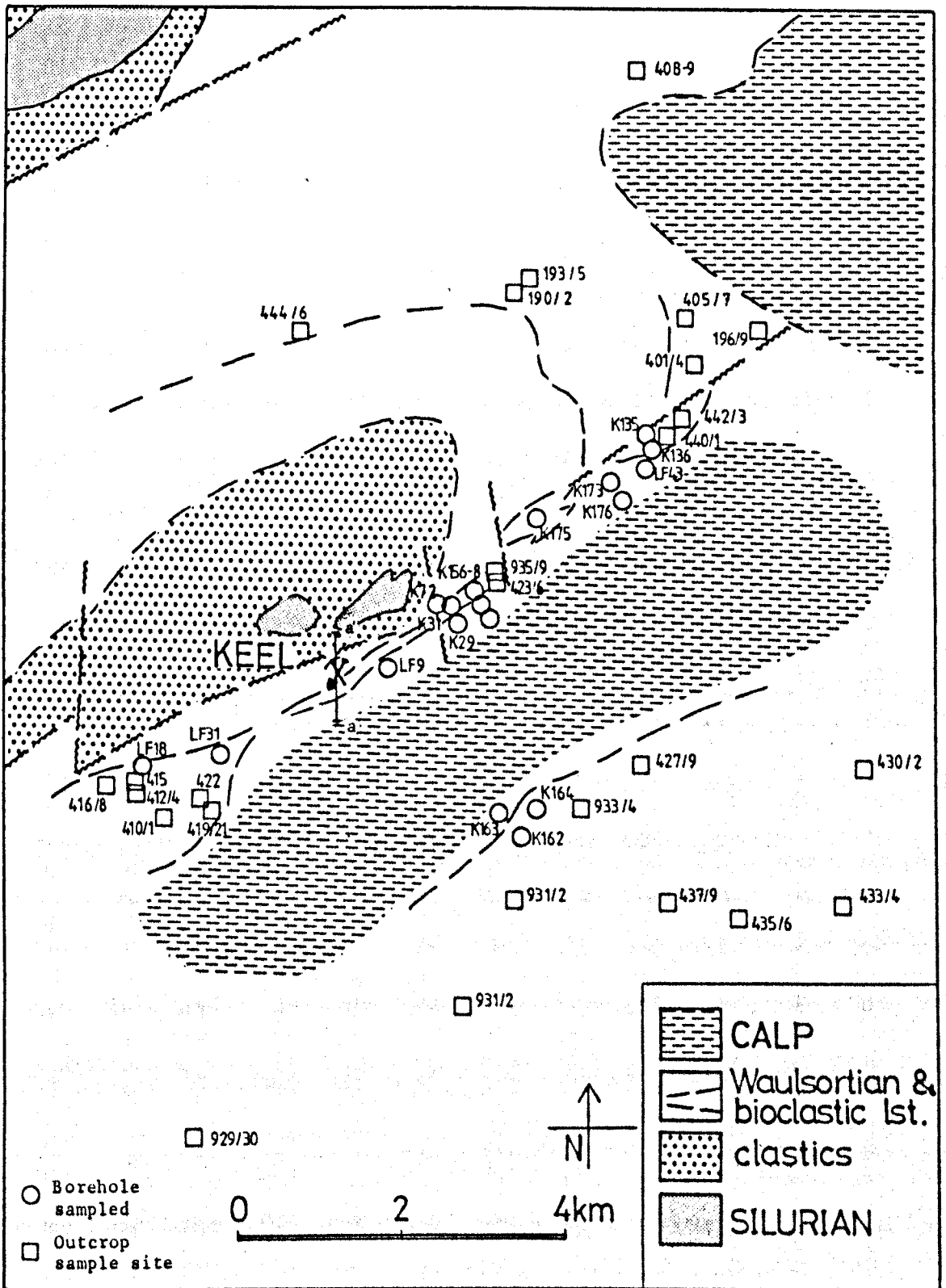


Figure 3.58: Geology and sample sites of Keel area. Line a - a' is approximate line of section in Figure 3.59. Mine symbol is location of Keel shaft.

The mineralisation is situated in a NE-SW fault system, on the southeastern margin of a small Lower Palaeozoic inlier (Figures 3.58 - 59).

The youngest rocks known to host mineralisation are the Waulsortian mudbanks, which are up to about 200 metres thick, and located on the downthrown side of this fault system. The mudbank complex thickens to the south, where outcrops become more frequent, and more or less dies out to the north. Virtually no Waulsortian-type mudbank developments of similar age are known to the north of this area (D.C.Smith, personal communication 1981).

Apart from minor thinning of stromatactis reef lenses away from the fault, high up in the succession, and very minor occurrence of sedimentary breccia (or possible reef talus), little evidence is seen to support substantial synchronous movements on the fault during Lower Carboniferous times. This is in apparent contrast to other major deposits in Ireland, although if basin subsidence was rapid and approximately matched by the fault movements, deposition of slump breccias would not necessarily arise. Fault movements may thus have been more or less insignificant, or else very gradual and non-catastrophic, absorbed largely by minor folding and bedding plane slips. In comparison with Ballinalack, however, much greater movement overall is indicated by the close proximity of Lower Palaeozoic rocks to post-Waulsortian Calp Limestones along the fault zone.

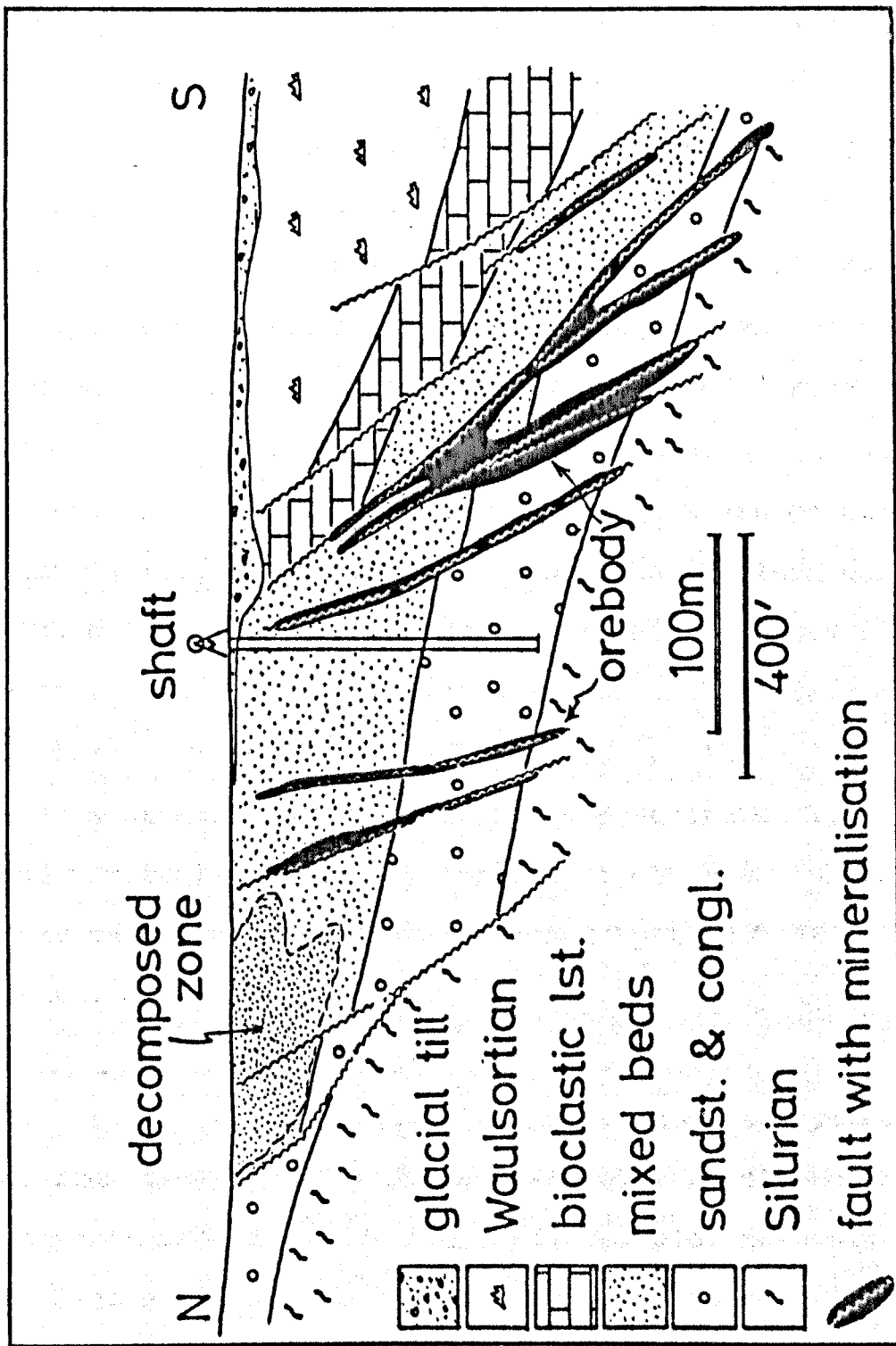


Figure 3.59: Cross section through Keel epigenetic mineralisation (for location see Figure 3.58), after Patterson (1970). Decomposed zone is probably a result of intense weathering during Tertiary (cf. Tynagh secondary orebody).

Thickness and form of the mudbank appears to be similar to Ballinalack, with perhaps four main 'knolls' up to 200 metres thick, strung along the downthrown side of the fault. They consist almost entirely of stromatactitic calcilutite, with only minor, thin, shaley or bioclastic intercalations and inter-reef tongues of argillaceous limestone. Dolomitisation, although present, is not important, and even the stratiform baryte and pyrite concentrations at the base of the mudbank are hosted by relatively unaltered stromatactitic calcilutite (D.C. Smith, personal communication 1981).

Boundaries within the mudbanks may be sharp or somewhat indistinct, interbedded and probably diachronous with neighbouring 'reef-equivalent' argillaceous bioclastic limestones. Individual reef knolls are composed of stacked mudbanks or reef mounds, and individual lenses of mudbank may or may not be separated laterally and vertically by shaley tongues or other peripheral detrital lithologies, as described by Lees (1964) from nearby Carrickboy Quarry.

Sampling and Results.

A total of 69 outcrop and 134 core samples were collected from the area to examine trace element dispersion patterns around the deposit, with sample sites displayed in Figure 3.58. Although high values are recorded close to the mineralisation, simple plotting of Mn and Fe concentration against the distance from the deposit does not allow recognition of any pronounced trace

element aureole. Only a vague distinction can be made between samples from near the mineralisation and those distant, in terms of compositional average and range.

If areal distribution of $(\text{Mn}+\text{Fe})/2$ content is examined (Figure 3.60a), a more suitable 'centre' can be chosen to allow the definition of proximal and distal sample populations for statistical comparison. A zone of higher Mn and Fe concentrations is apparent, averaging over 250 ppm, enclosed to the northwest and straddling the Keel Fault. This is centred approximately 2 kilometres to the N.E. of the Keel shaft (which was sunk into the epigenetic mineralisation), closer to the existing stratiform ore zone, at the base of the mudbank. A point central to these enrichments, on the main Keel Fault, was selected as a centre for measuring distance to the sample sites.

In Figure 3.61, $(\text{Mn}+\text{Fe})/2$ contents of distal samples (from over four kilometres from the chosen centre) are compared to those of proximal samples, indicating the slightly higher range of values in the latter. Over twice as many distal samples as proximal contain less than 200 ppm $(\text{Mn}+\text{Fe})/2$, and the converse is true of those samples containing more than 300 ppm. The threshold between the two sets of data appears to be around 250 ppm.

Areal expression of Mn and Fe values includes a weak suggestion of basal mudbank enrichment along the flanks

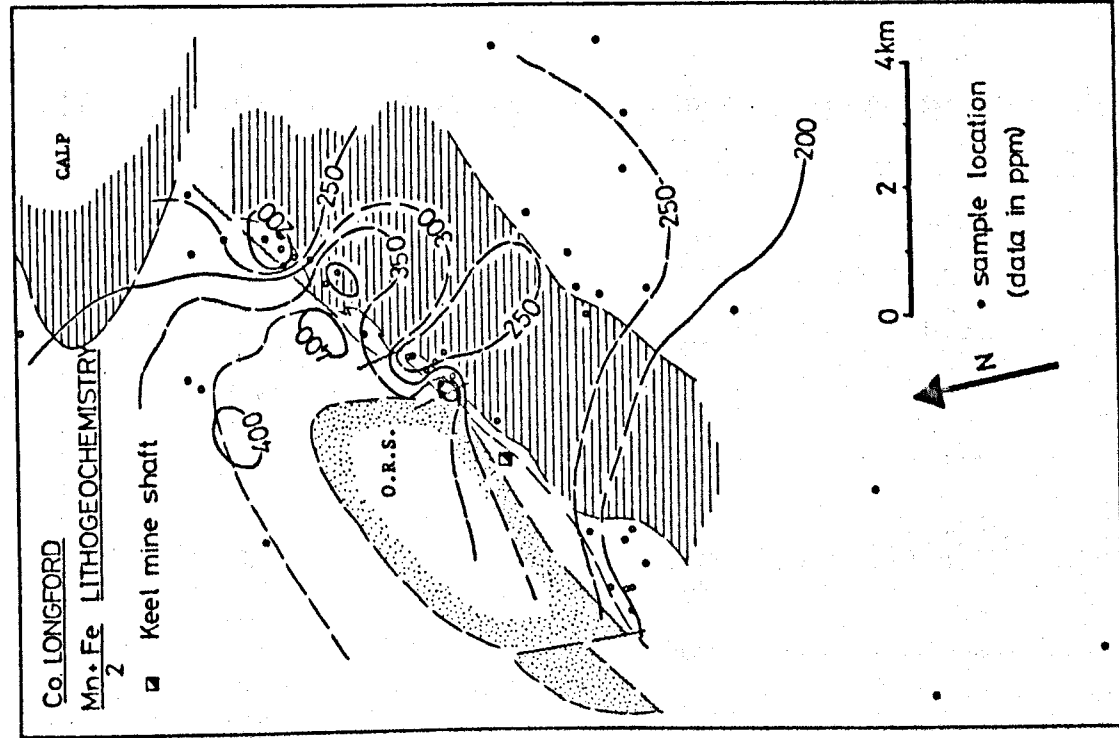


Figure 3.60a: Distribution of $(Mn+Fe)/2$ in Waulsortian Limestones of Keel area, contoured using a rolling mean. Both core and outcrop samples included.

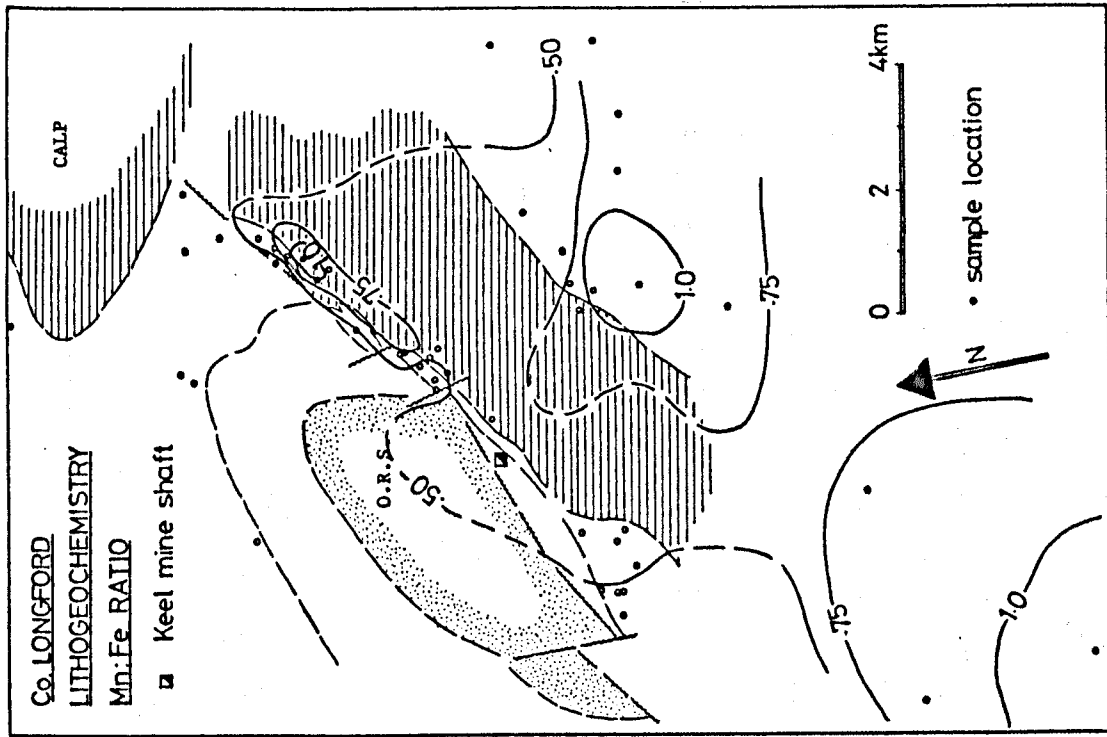


Figure 3.60b: Distribution of Mn:Fe in Waulsortian Limestones of Keel area, contoured using a rolling mean. Both core and outcrop samples included.

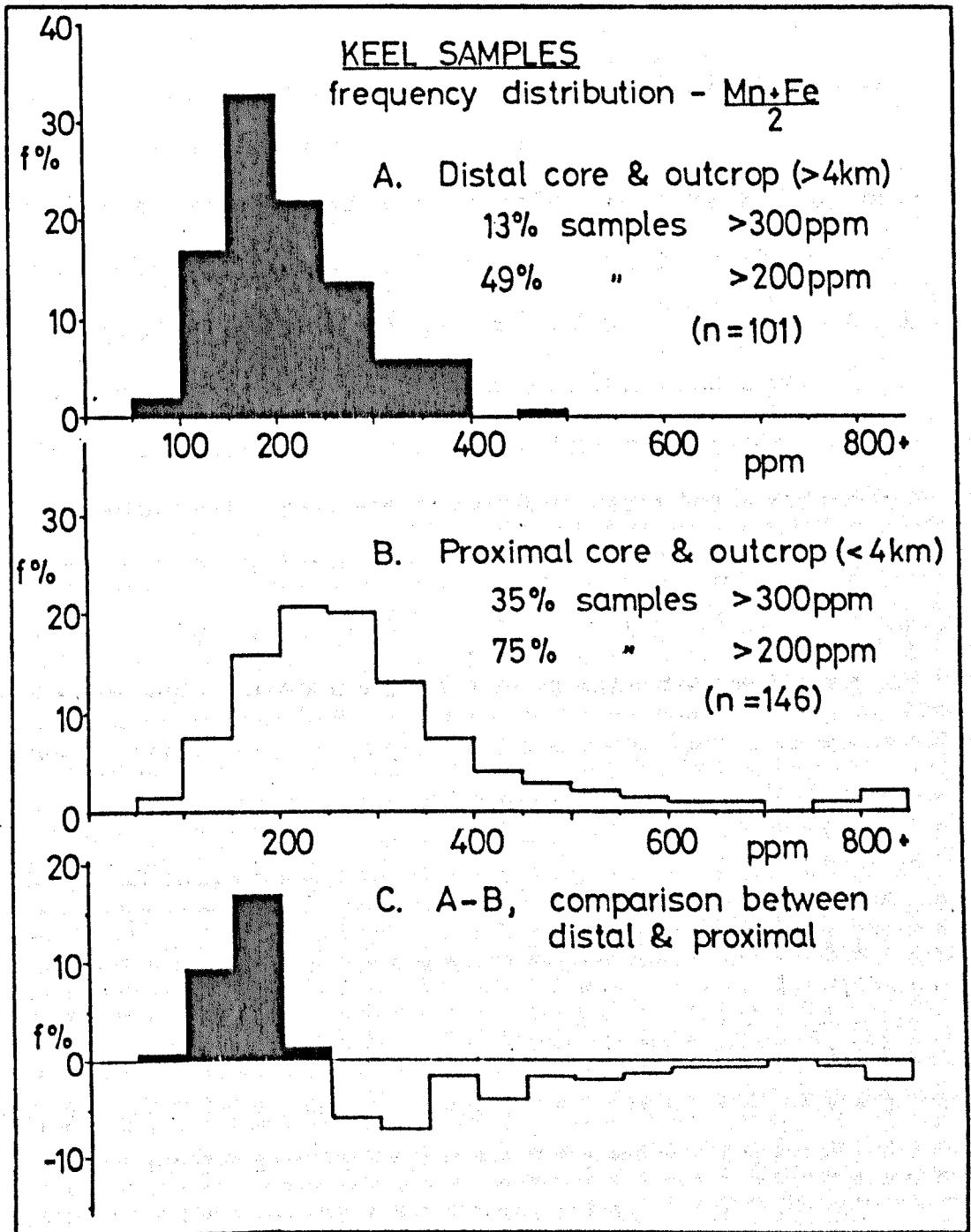


Figure 3.61: A) Frequency distribution of $(Mn+Fe)/2$ in distal samples - core and outcrop from beyond 4 kilometres of chosen centre (see text); B) Frequency distribution of $(Mn+Fe)/2$ in proximal samples - core and outcrop from beyond 4 kilometres of chosen centre; C) Comparison of distal and proximal samples, achieved by subtracting frequency distribution of B from A.

of the Lower Palaeozoic inlier (Figure 3.60a). This is apparently similar to the situation at Silvermines, and could perhaps be expected, as the known stratiform mineralisation is also located in the lowest part of the mudbank sequence. This suggestion is investigated further in vertical profiles of drill holes in the following chapter.

Areal distribution of Mn:Fe ratios (Figure 3.60b) outlines a general increase in Fe over Mn from the south and southeast towards the north and west, with a small Mn high (relative to Fe) situated along the Keel Fault, coinciding with the main $(\text{Mn}+\text{Fe})/2$ peak.

Zinc values at Keel are generally very low, and only 11 samples (both core and outcrop) from within 4 kilometres of the centre contain over 10 ppm zinc, representing less than 10 percent of the total proximal sample population.

3.4.4. Moate and Moyvore.

The southern part of the area studied contains two known base metal prospects, those at Moate and Moyvore, the locations of which are indicated on Figure 3.49.

Moate.

Martin and Chabot (1981) have described primary manganese and iron enrichments in lowermost Carboniferous calcareous sediments associated with fault controlled Zn+Pb mineralisation at Moate.

The mineralisation here occurs in gently folded,

shallow-dipping Carboniferous Mixed Beds and shallow water carbonates, in numerous steeply dipping minor faults, associated fractures and fissures, and stratabound zones in adjacent carbonate rocks (Schultz 1971, Poustie and Kucha 1984). Mineralogy is primarily sphalerite and pyrite, with galena, in a calcite and baryte gangue. Knowledge of the stratigraphic range of the mineralisation is limited by the removal, by erosion, of much of the overlying Argillaceous Bioclastic Limestone and Waulsortian mudbanks in the immediate vicinity.

Moyvore.

Nawrocki and Romer (1979) document the discovery of a zone of low grade (up to 5% combined metals) Pb+Zn mineralisation associated with a NE trending normal fault, with a vertical displacement of approximately 250 metres. As at Moate, knowledge of the texture and composition of the mineralisation is limited to borehole material and mineralised float, but it does appear confined to sub-Waulsortian strata, in essentially epigenetic styles.

The Moyvore prospect occurs in an area of very poor outcrop, several kilometres to the north of Moate, where most of the Waulsortian and underlying Argillaceous Bioclastic Limestones have likewise been removed by erosion.

Sampling of Waulsortian Limestones has included outcrops within a few kilometres of both of these

localities.

Results.

A total of 116 outcrop samples were collected from the Moate-Athlone-Ballymore area. Analytical results of those outcrop samples from the nearest ten outcrop sites to the Moate and Moyvore prospects were compared with the remainder. These 23 samples came from sites up to about 6 kilometres from either of the prospects.

Comparison of the Mn and Fe contents of the two sets of samples (Figure 3.62a) reveals a large area of overlap in concentration range. In the same way as at Keel, however, proximal samples contain significantly higher levels than distal samples, as displayed in Figure 3.62b, with median values of 240 and 163 ppm respectively, for $(\text{Mn}+\text{Fe})/2$.

These same results are displayed in contoured map form in Figure 3.63. An extensive area of weak enrichment of Mn and Fe stretches northwards from the Moate inlier and westwards from the southern end of the Moyvore inlier. In addition, distal samples from east of the two inliers appear to contain lower levels than those from the west (see also Figure 3.62a).

As at Keel, zinc levels are low, generally below 10 ppm, in both proximal and distal samples.

Sampling in this area was undertaken more to determine regional background levels and variation, rather than dispersion around either of these two centres. As a result, sample density is generally on the sparse side

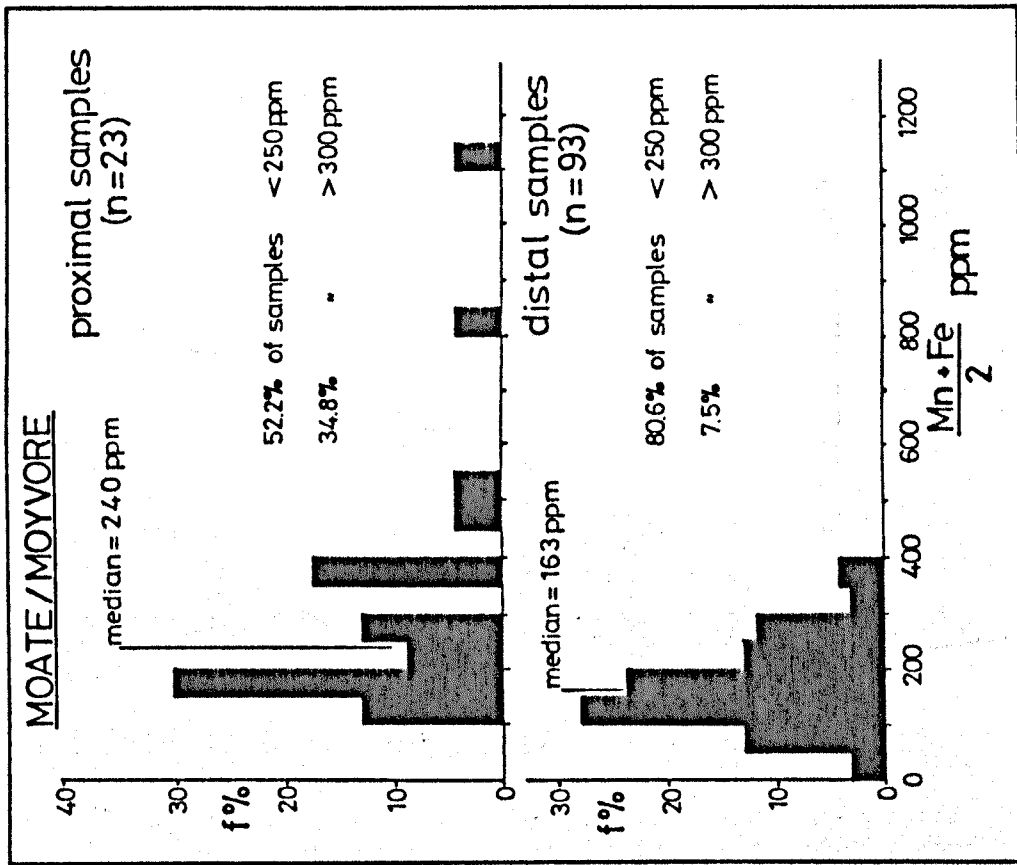


Figure 3.62b: Comparison of frequency distribution of $(Mn+Fe)/2$ in proximal samples (within about 6 kilometres of either prospect) and distal samples.

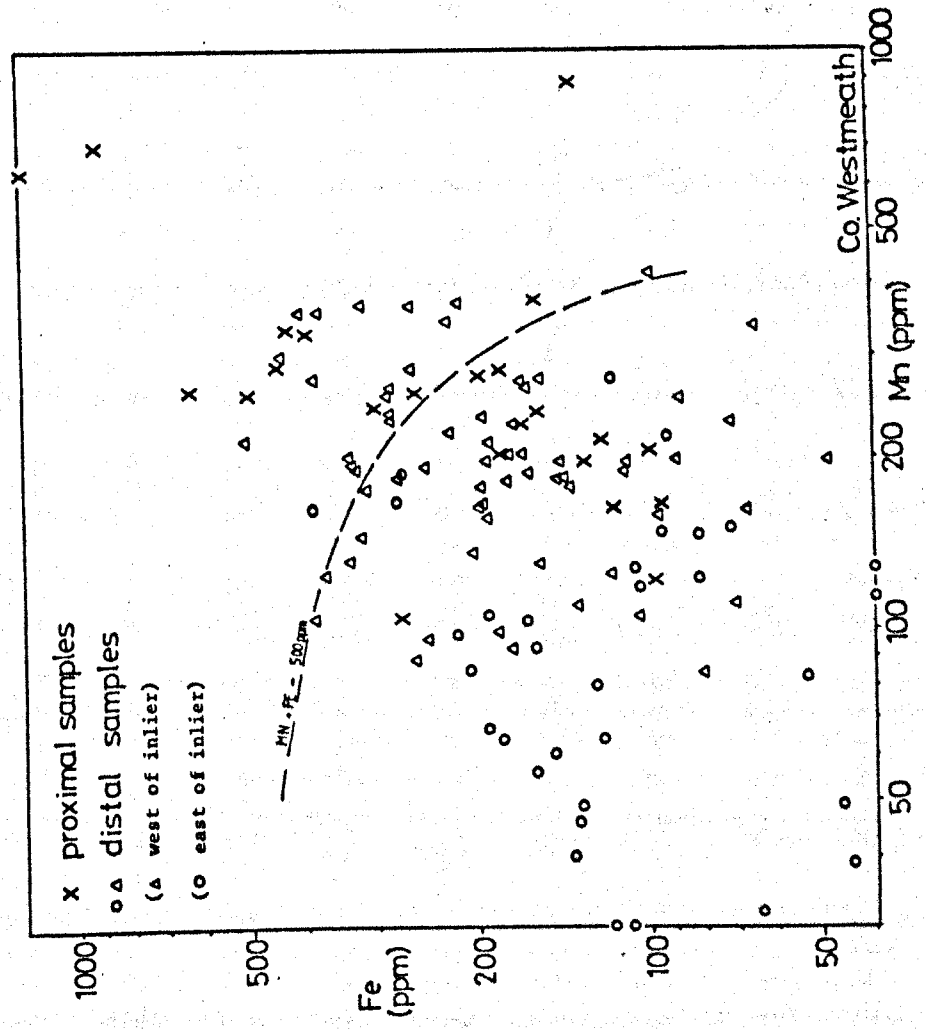


Figure 3.62a: Graph of Mn against Fe for outcrop samples from Moate-Athlone area. Proximal samples originate within about 6 kilometres of either Moate or Moyvore prospects (see text). Note log scales.

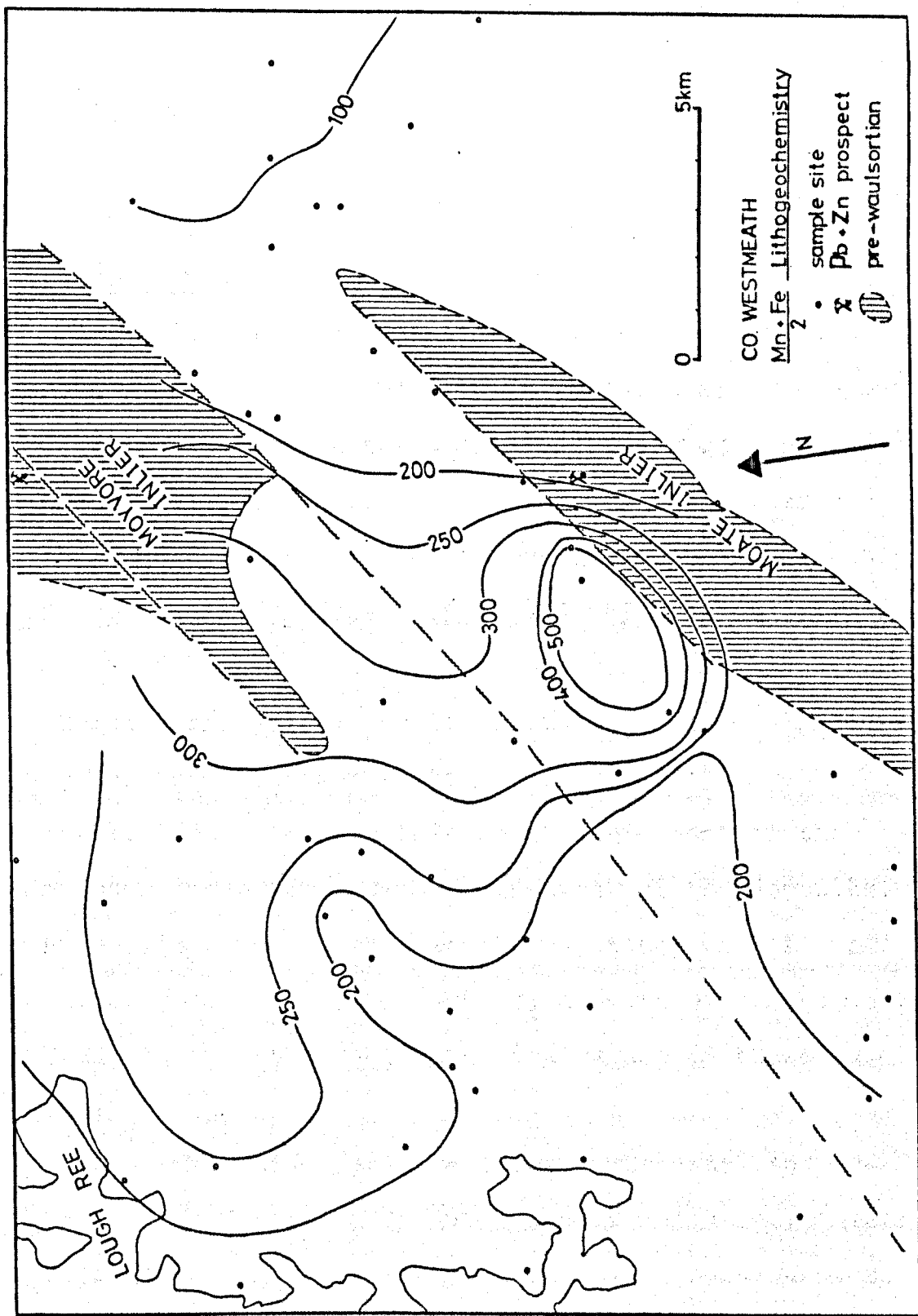


Figure 3.63: Distribution of $(Mn+Fe)/2$ in Waulsortian Limestones of Moate - Athlone area, contoured using a rolling mean. Geology much simplified, and unshaded areas include Waulsortian equivalent ('off-reef') and possible Calp Limestones, as well as Waulsortian Limestones.

to delineate specific patterns, and insufficient samples from close to either prospect were collected to permit a clear definition of trace element aureoles around them.

3.5.1. Ballyvergin.

Introduction.

The Waulsortian Mudbank Limestone outcrops of East County Clare were sampled to investigate trace element distribution around the small Pb, Zn and Cu deposits of the Ballyvergin area. These deposits are largely epigenetic in style, and are considered to be probably Hercynian in age (Sevastopulo and Phillips 1984), post-dating the mudbank deposition by over 50 million years.

Initial analytical results from the area were encouraging, though somewhat ambiguous (Russell, unpublished work), indicating possible local enrichment of the mudbanks associated with emplacement of the deposits. Russell's samples were reanalysed, along with a small number collected by the author, as part of the present study to investigate further the nature of these enrichments.

Recognition of apparent primary enrichments in mudbanks around supposedly much younger, epigenetic mineralisation would necessitate a change in opinion over the genesis of the deposits (that they were contemporaneous with mudbank growth), or reconsideration of the processes thought to control primary, syngenetic trace

element aureole formation.

Geology of the area.

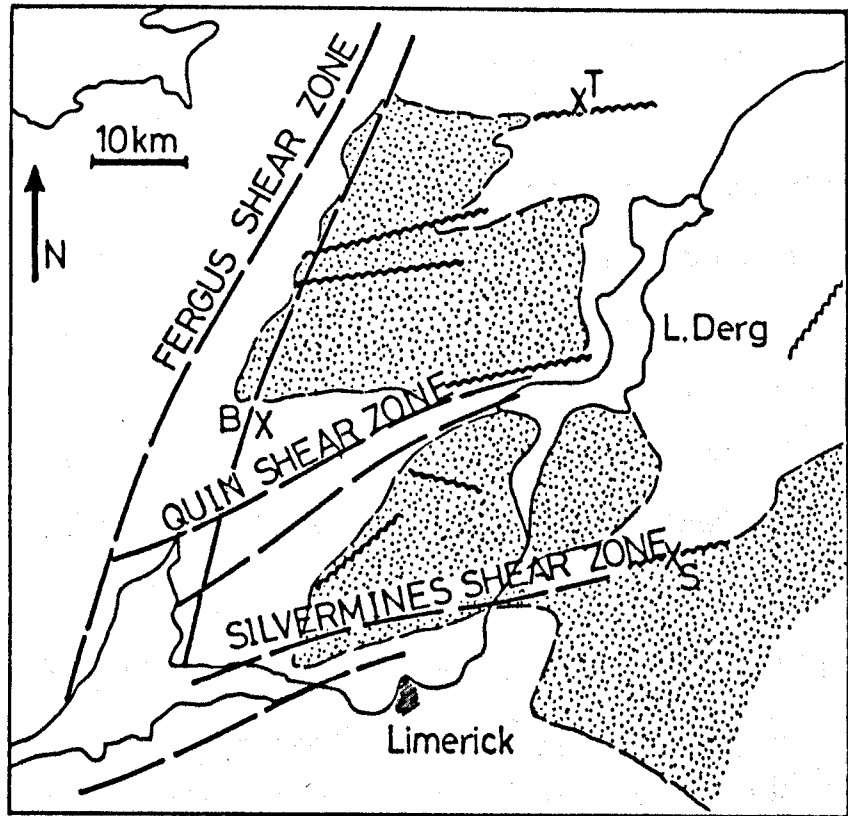
The Pb+Zn+Cu occurrences of the Ballyvergin area are situated on the northern limb of a broad shallow syncline, with shallow axial plunge to the southwest. In the northwestern part of this limb, strike swings round from westerly, through north, to northeasterly, forming a counterpart anticlinal or domal structure, on which the deposits are located (Figure 3.65). The Waulsortian mudbank outcrop forms an S-shaped pattern with shallow dips, rarely exceeding 15° (Hallof et al 1962).

Coller (1982) describes this area structurally as occurring in a local zone of dilation at the intersection of the NNE-trending, sinistral Fergus Shear Zone, and the ENE-trending, dextral Quin Shear Zone, which in turn lies parallel to the major Silvermines Shear Zone to the south, also dextral (Figure 3.64). Surface expression of these large scale features is represented by minor fold and fault patterns, and pressure solution cleavage. It appears that some of these features may have been generated along pre-existing Caledonoid lines of weakness.

Intersection and terminal dilation zones on these shear zones are favourable sites for potential mineralisation (Phillips 1983).

Geology of the deposits.

Obtaining most of their information from old Survey




- | | | | |
|---|-------------|---|---------------------------------|
| B | Ballyvergin |  | Major pre Carboniferous inliers |
| T | Tynagh | | |
| S | Silvermines | | |

Figure 3.64: Principal structural features of West Central Ireland, after Collier (1982). T = Tynagh, S = Silvermines, B = Ballyvergin.

Memoirs, Hallof et al (1962) briefly describe three of the deposits, those of Ballyvergin, Ballyhickey and Kilbreckan, which occur in sub-Reef, Reef and supra-Reef formations respectively. They consist of varying proportions of galena, sphalerite, chalcopyrite and pyrite, with trace amounts of other sulphides in a mainly calcitic gangue, cross-cutting the host limestones in irregular veins and pockets. These are associated, in part, with dolomitisation of the host rocks.

Although generally considered to be epigenetic in nature (e.g. Williams and McArdle 1978, Phillips 1983), visual inspection of dump material from two of the smaller occurrences (Carrahin and Crowhill), both situated within the mudbank complex, reveals fine-grained intergrowths of common sulphide minerals, similar texturally to ore from the upper stratiform zones at Silvermines.

With this in mind, and no detailed information available on morphology, setting or textural work, the origin of these deposits was approached with an open mind.

Results.

The location of the outcrop samples is shown on Figure 3.65, along with the salient features of the geology of the area. Analytical results of these samples indicate that enriched Mn and Fe values (above 250 ppm) are present locally around the mineralisation, extending

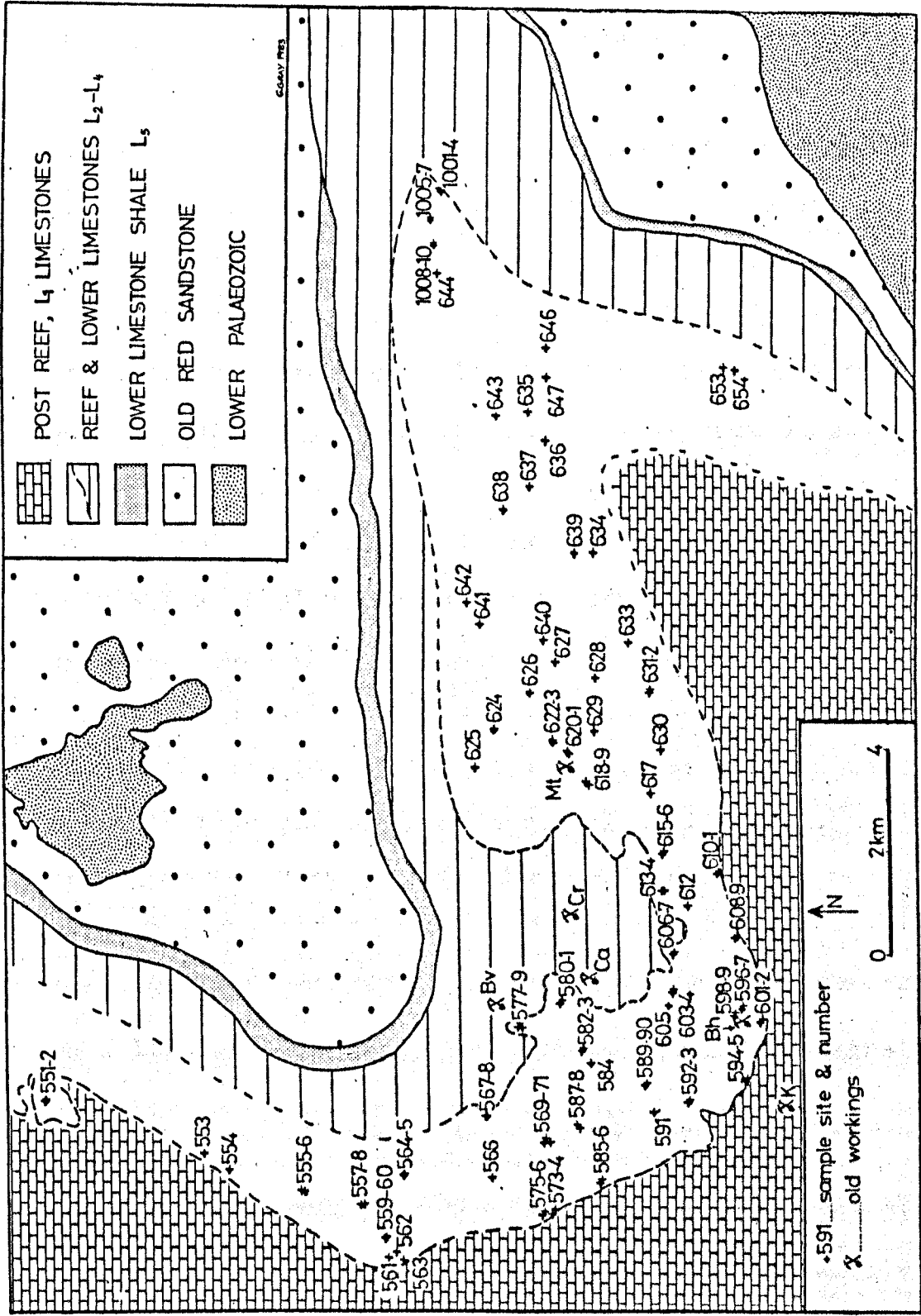


Figure 3.65: Simplified geology of the Ballyvergin area, showing sample sites and location of deposits mentioned in text. Bv = Ballyvergin, Ca = Carrabin, Cr = Crowhill, Mt = Milltown, Bh = Ballyhickey, K = Kibreckan.

up to about six kilometres from the arbitrarily chosen centre of the deposits (Figures 3.66a - c). Within this 6 kilometre zone of enrichment, only 26% of the samples contain over 250 ppm $(\text{Mn}+\text{Fe})/2$ (Table 3.7), and more Fe than Mn values rise above this threshold level (32% and 14.5% respectively). In other words, within the sphere of the suggested aureole, over 70% of samples still contain background levels of the trace elements. Only a small proportion of samples (5%) from outside the 6 kilometre aureole contain over 250ppm Fe, and none of them contain anomalous levels of Mn or $(\text{Mn}+\text{Fe})/2$. Only a few samples from close to the individual prospects contained more than 10 ppm zinc.

A vague suggestion of basal enrichment of the mudbank complex is implied by the data on either side of the anticlinal structure which hosts mineralisation, except on the very nose of the structure, where peak values are observed towards the top of the mudbank (Figure 3.67). More detailed stratigraphic distribution on a local scale, using drill core, sections for instance, has not been undertaken here.

The presence of Mn and Fe enrichments of apparent primary aspect (although relatively poorly developed), implies that hydrothermal emanation associated with the mineralisation supplied trace metals into the mudbank environment, contradicting a Hercynian age for the deposits. The significance of this implication is discussed further in Chapter 6.

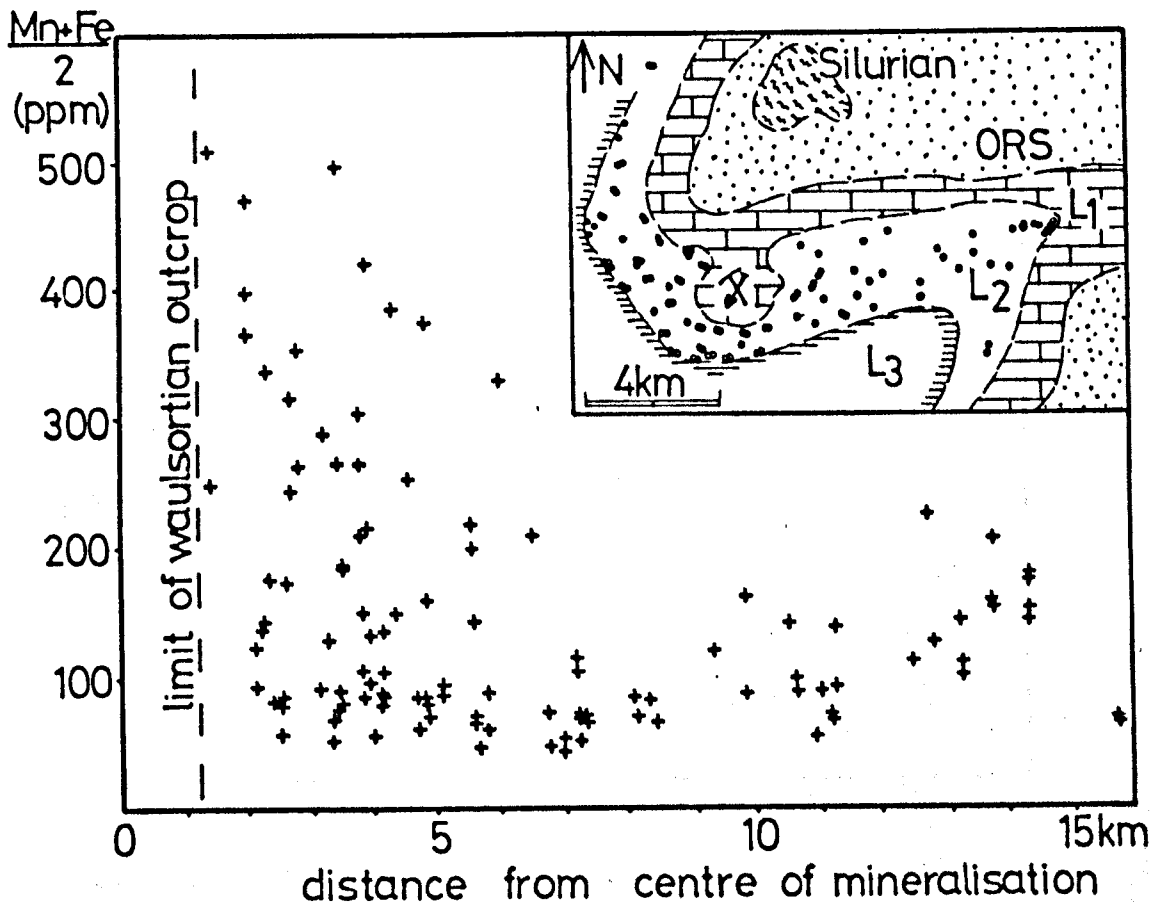


Figure 3.66a: Distribution of $(Mn+Fe)/2$ contents of Waulsortian Limestones around Ballyvergin deposits ($n = 112$). Distance measured from the arbitrarily chosen central point (see text).

BALLYVERGIN SAMPLES	n	Percentage anomalous		
		$\frac{Mn + Fe}{2}$	Mn	Fe
Proximal samples (within 6 km)	69	26.1	14.5	31.9
Distal samples (beyond 6 km)	44	nil	nil	4.5

Table 3.7: Percentage anomalous samples both near to, and distant from, the Ballyvergin deposits. Threshold chosen at 250 ppm Mn, Fe or $(Mn+Fe)/2$.

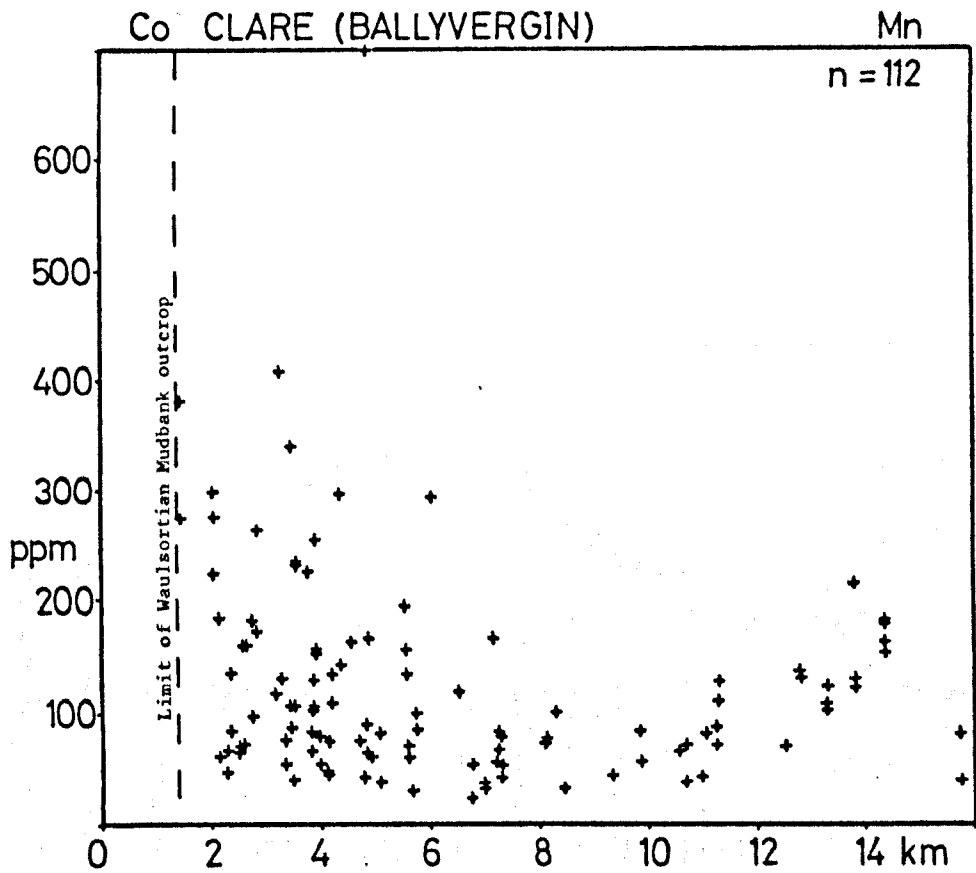


Figure 3.66b: Distribution of Mn contents in Waulsortian Limestones around the Ballyvergin deposits, distance measured from the arbitrarily chosen central point.

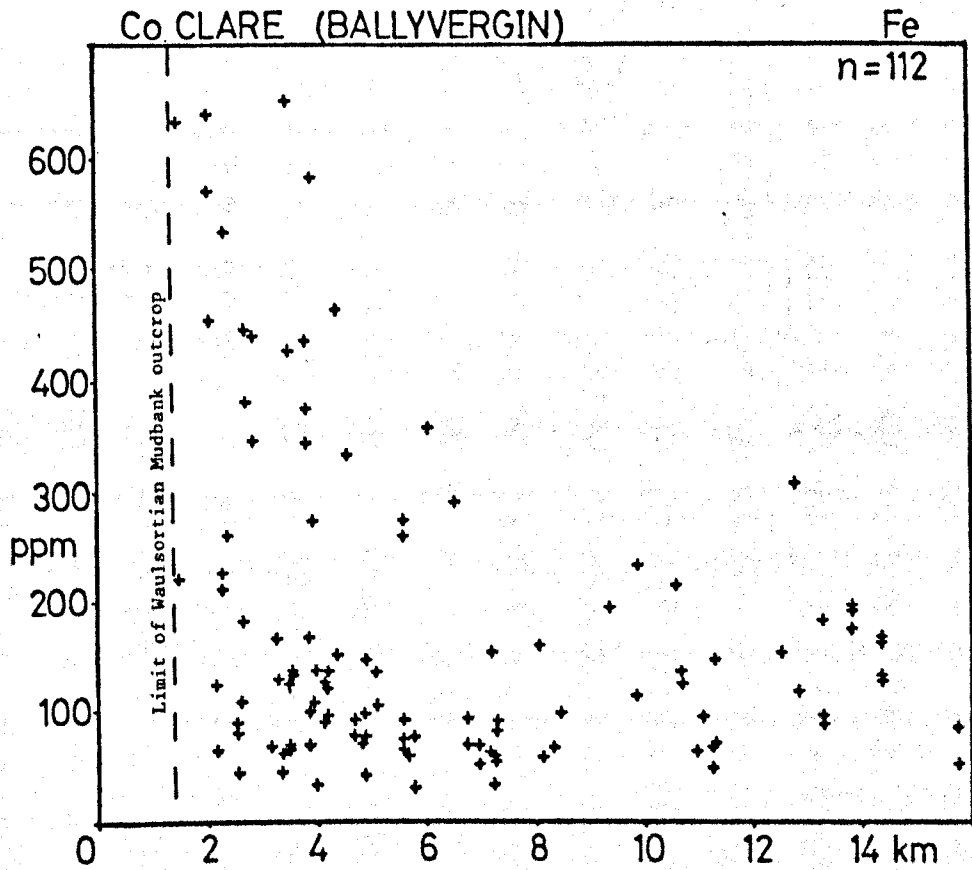


Figure 3.66c: Distribution of Fe contents in Waulsortian Limestones around the Ballyvergin deposits, distance measured from the arbitrarily chosen central point.

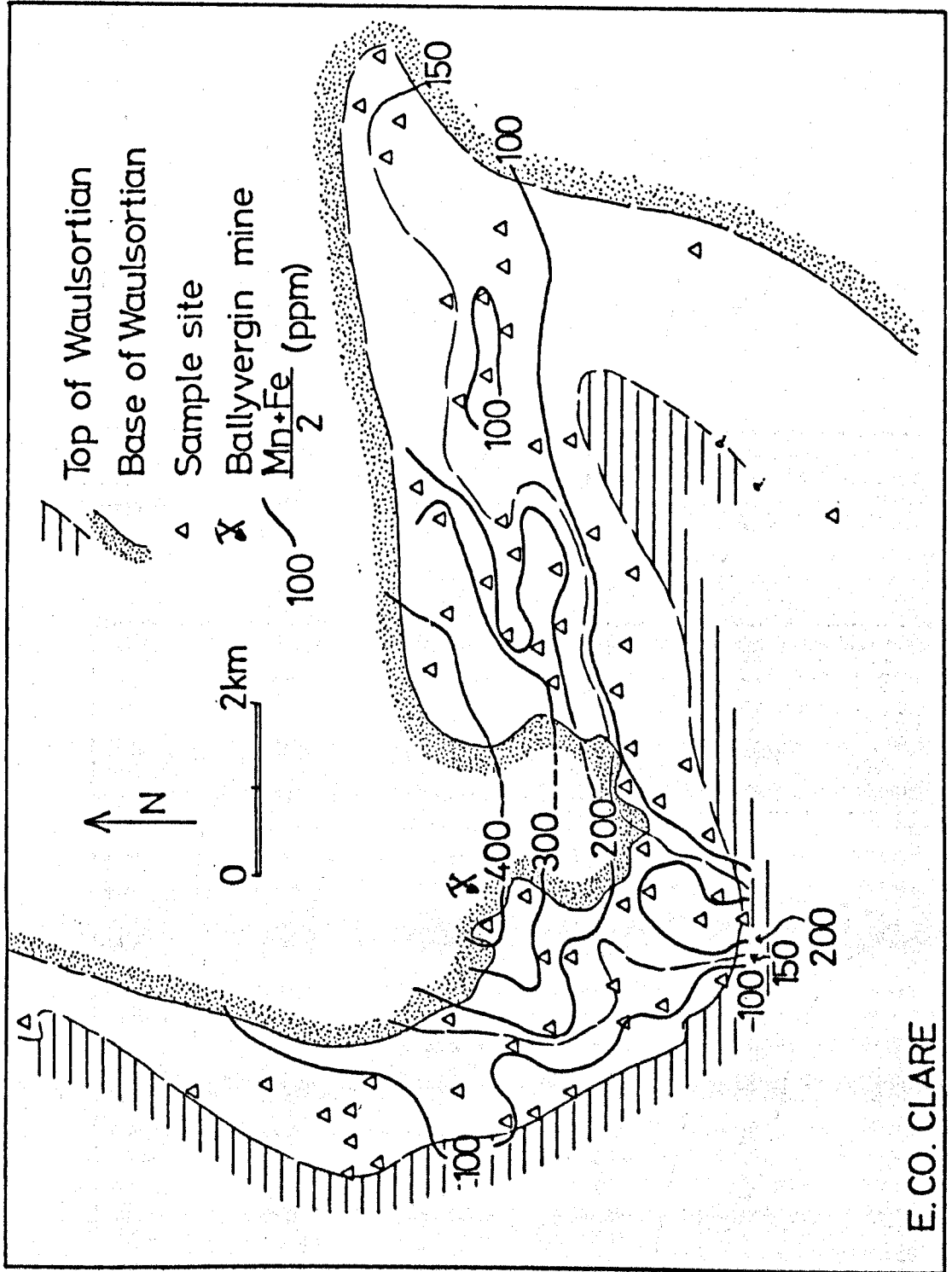


Figure 3.67: Areal distribution of $(\text{Mn}+\text{Fe})/2$ contents of Waulsortian Limestones of Ballyvergin area, contoured using a rolling mean.

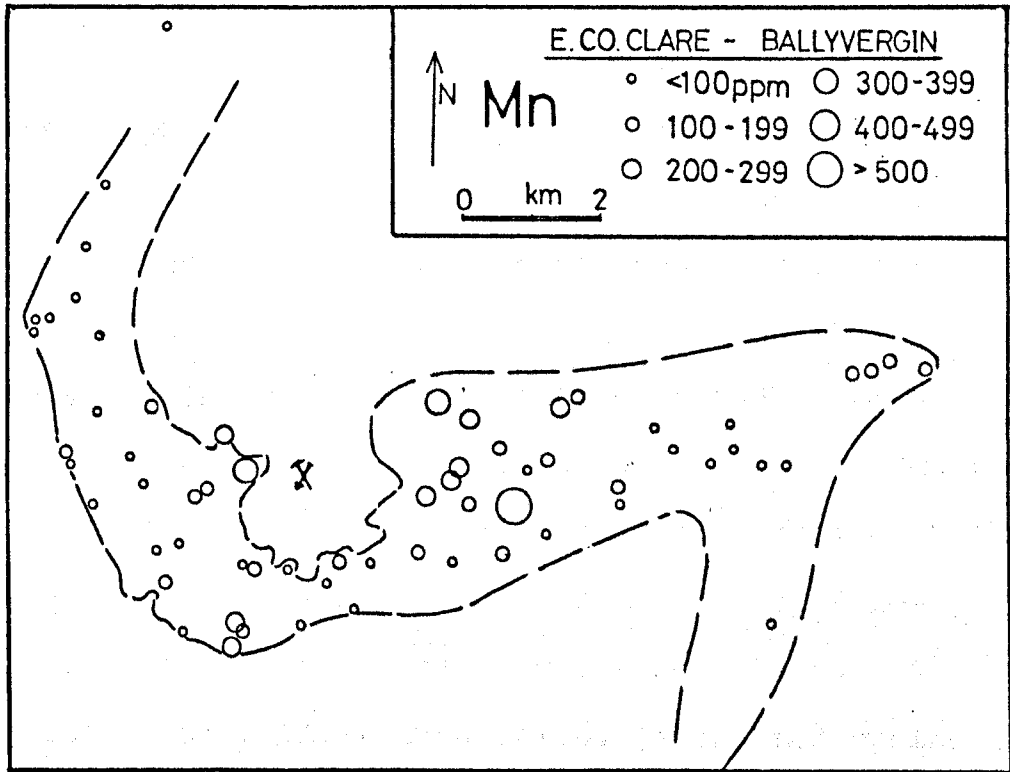


Figure 3.68a: Areal distribution of Mn contents of Waulsortian Limestones of the Ballyvergin area, dashed line represents boundary of Waulsortian outcrop.

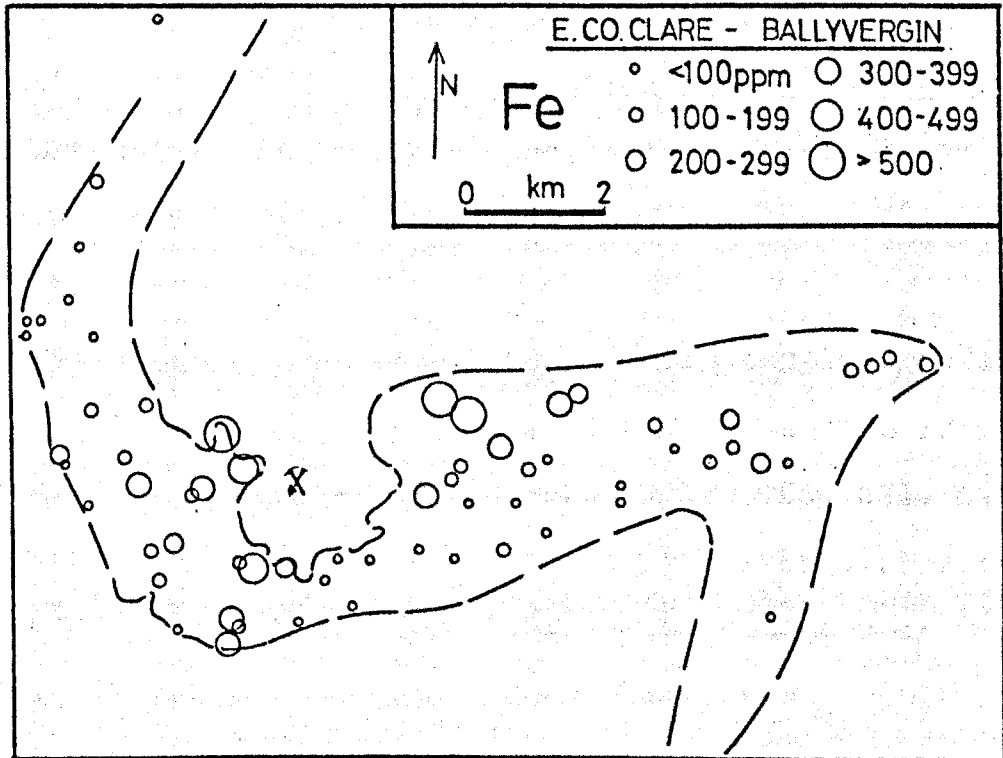


Figure 3.68b: Areal distribution of Fe contents of Waulsortian Limestones of the Ballyvergin area, dashed line represents boundary of Waulsortian outcrop.

3.5.2. Aherlow.

Introduction.

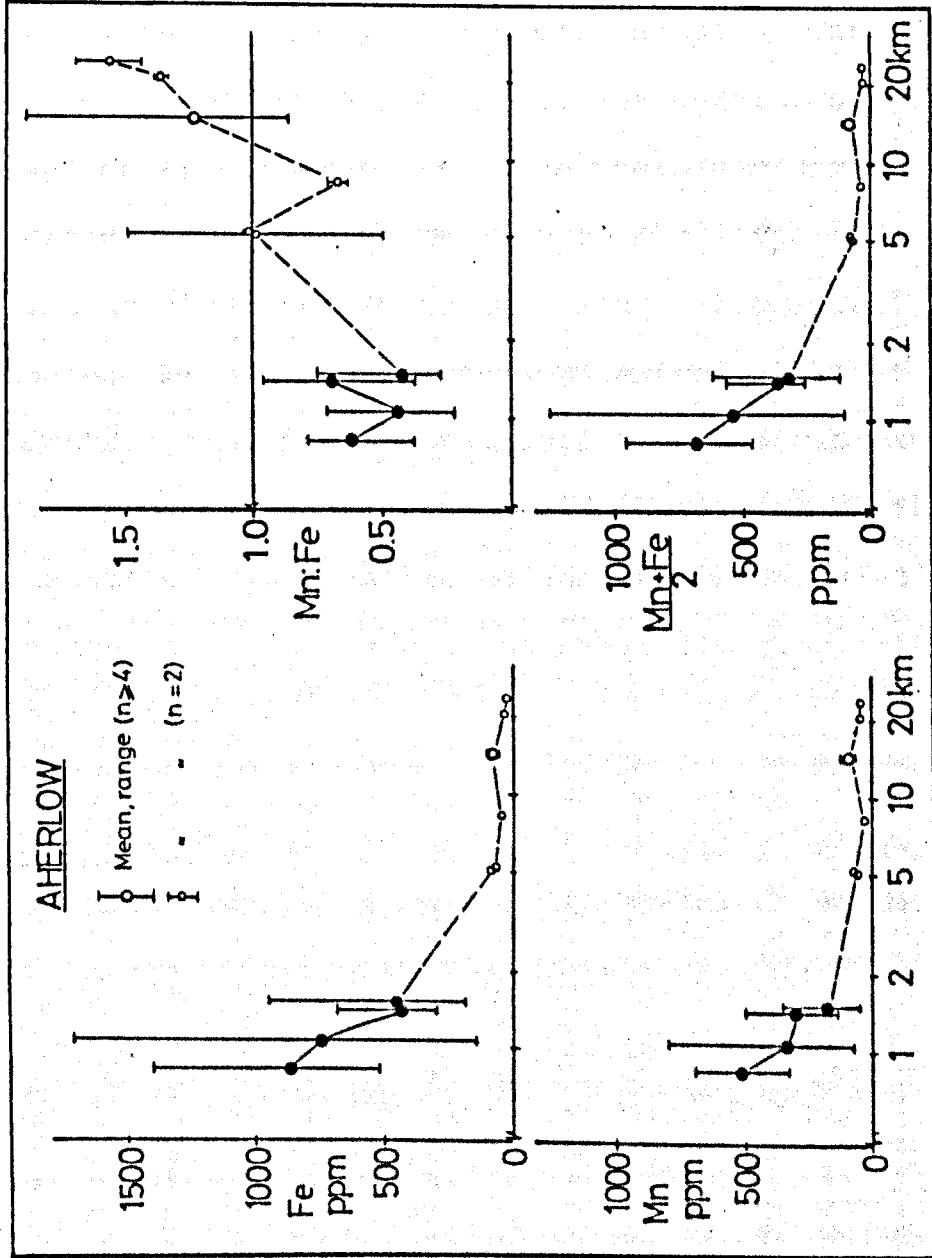
The location of the Aherlow base metal deposit is shown in Figure 1.1. This deposit consists of epigenetic Cu-Ag mineralisation in an E-W trending, steeply dipping zone of deformation hosted in sub-Waulsortian argillaceous bioclastic limestones (Cameron and Romer 1970). There is a strong structural control on the mineralisation, which is dominated by fine-grained, disseminated chalcopyrite, bornite and chalcocite, with minor sphalerite, galena and pyrite peripheral to the copper. The gangue is calcite - dolomite, with lesser amounts of baryte and quartz.

A 25 metre thick chert horizon is present at the base of the Waulsortian Limestone, 500 metres to the west of the sulphide zone, and the mineralisation is associated with extensive recrystallisation, dolomitisation and brecciation of the host rock sequence.

Results.

Analytical data from 29 'proximal' core samples and 16 'distal' outcrop samples were examined. The core samples were all obtained from four boreholes (C5, C6, D21, D22) all within 1.5 kilometres of the sulphide zone, whereas the outcrop samples were collected from a number of sites, between 5 and 25 kilometres distant.

The proximal samples are enriched in Mn and Fe compared to the distal ones, which generally contain less than 100 ppm, and Fe is more consistently enriched than



Zn	Core	Outcrop
> 10ppm	51.7%	nil
> 20ppm	20.7%	nil
> 50ppm	13.8%	nil

Table 3.8: Zinc contents of Aherlow samples, expressed as the percentage of total samples with concentration in the range shown. All core samples from within 2 kilometres, all outcrop from beyond 5 kilometres of the deposit.

Figure 3.69: Graphs showing Mn and Fe contents of Waulsortian Limestones around the Aherlow deposit. Filled circles are core samples, unfilled circles are outcrop samples. Note logarithmic horizontal scale.

Mn (Figure 3.69). In the nearest borehole to the mineralisation (at approximately 0.8 kilometres), Mn and Fe both remain above 300 ppm.

Individual $(\text{Mn}+\text{Fe})/2$ values in each borehole do not fall below the level of the highest value in the distal samples (110 ppm). In addition, iron levels are higher than manganese closer to the mineralisation, but generally lower in the outcrop samples, as indexed by the Mn:Fe data (Figure 3.69).

Zinc is also enriched close to the mineralisation, in approximately one half of the core samples (Table 3.8), and remains below 10 ppm in all the outcrop samples.

Although the lateral extent of these enrichments cannot be defined accurately, because of the large gap in the sample sites (between 2 and 5 kilometres), anomalous Mn, Fe and Zn contents extend at least 1.5 kilometres from the mineralisation. On top of this, post-depositional thrusting during Hercynian earth movements may have shortened some of the original distances between the site of mineralisation and present distal outcrop sites.

3.5.3. Courtbrown.

The Pb+Zn prospect at Courtbrown, County Limerick (Figure 1.1) comprises approximately one million tonnes of low grade Pb-Zn-Ag mineralisation, hosted in micrites near the base of the Waulsortian Mudbank Limestone. Semi-massive pyrite, sphalerite and galena are present,

along with disseminated, vein and stylolitic sulphides (Grennan 1984). Traces of lead and zinc sulphides are also present in outcrop and float at Rineanna Point, on the opposite bank of the Shannon Estuary, some 6 kilometres to the north. Both occurrences of sulphide mineralisation are associated with nearby developments of hematitic mudbank limestone or 'red marble'.

Outcrops in the vicinity of both occurrences were sampled and analysed as part of a wider, regional sampling programme, and $(\text{Mn}+\text{Fe})/2$ results are displayed in map form in Figure 3.70. Contoured values indicate that elevated levels are present around the mineralisation on both sides of the estuary, and for some distance along strike.

Six core samples of mudbank from the Courtbrown prospect were analysed by M.J. Russell (unpublished work) using cold acetic acid digestion (Russell 1974), and contained an average of 425 ppm manganese. Digestion in HCl for zinc analysis indicated that some high Zn values were also present, but possibly associated in at least one case, with weak mineralisation in stylolites. Although these samples were not available for reanalysis, extrapolation from other data indicates that manganese levels of approximately 600ppm would be attained by hot acetic acid digestion, with iron values presumably higher, in line with the outcrop data.

Of some significance perhaps in influencing the considerable lateral extent of enrichments along strike

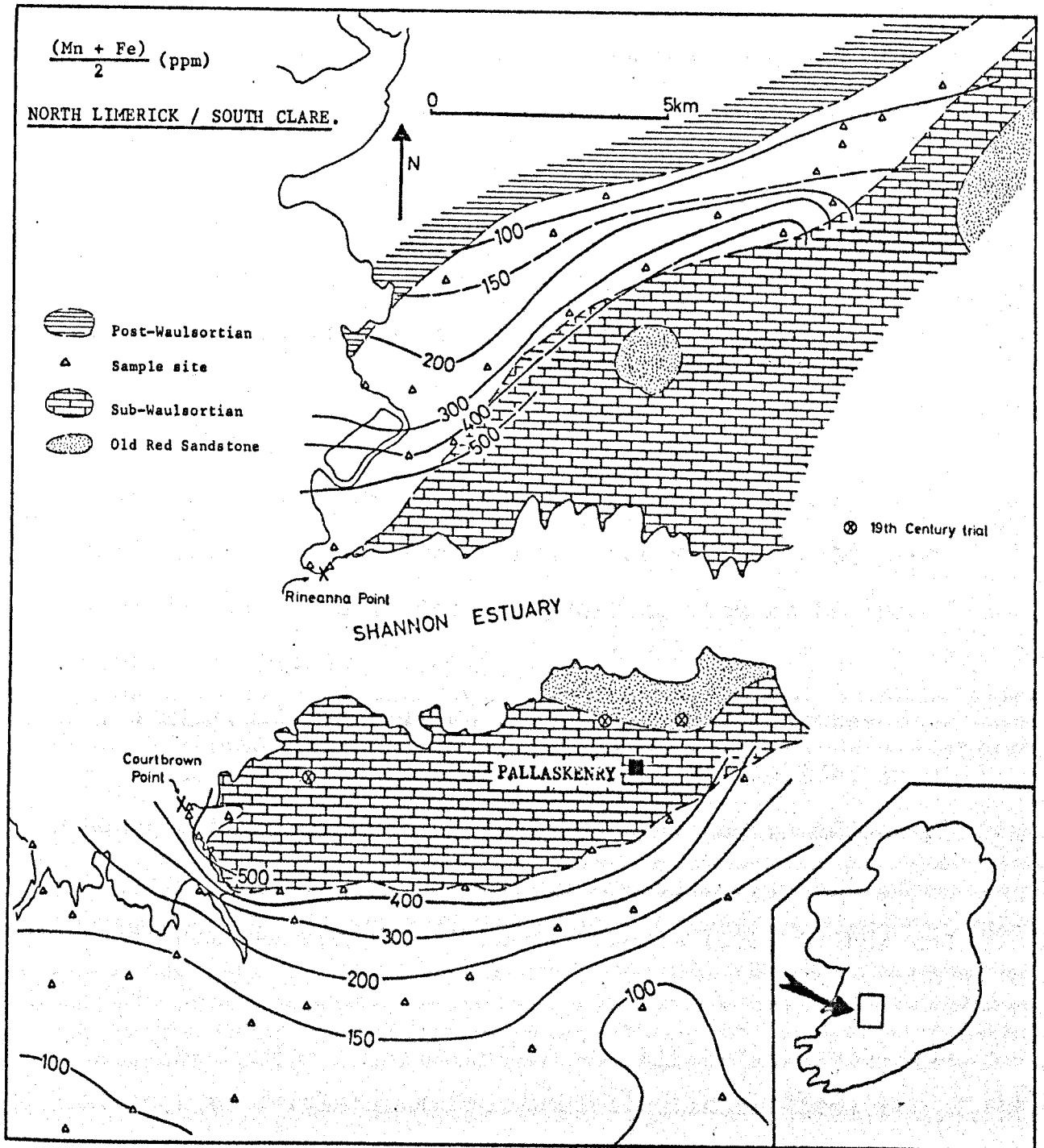


Figure 3.70: Areal distribution of $(Mn+Fe)/2$ in Waulsortian Limestones of South Clare and North Limerick, contoured using a rolling mean. Also shown are locations of Courtbrown Point (Pb + Zn), Rineanna Point (minor Pb, Zn) and numerous old trial workings for Cu, Pb and Zn.

are a number of small, 19th century workings and trials (for Cu, Pb, Zn) situated within the sub-Reef inlier to the south of the estuary (Figure 3.70). These are more central to the anomalous mudbank samples and may represent a remnant feeder zone, an idea which will be pursued in Chapter 6.

3.5.4. Mallow.

Al-Kindi (1979) records restricted Zn, Mn and Hg enrichments in host rocks around the Mallow Cu-Ag prospect in north County Cork, suggesting them to be epigenetic in origin.

The mineralisation at Mallow consists of a cross-cutting, steeply dipping zone of copper sulphides in Lower Carboniferous (sub-Reef) strata, and an adjacent silver-rich stratabound zone in transitional Old Red Sandstone sediments (Wilbur and Royale 1975, Wilbur and Carter 1984).

Samples collected by Al-Kindi (op cit) were reanalysed along with further outcrop samples collected from surrounding areas, undertaken as part of a regional study. Contoured results of $(Mn+Fe)/2$ outline a possible very weak anomaly centred close to the Mallow deposit (Figure 3.71). Some doubt is cast on this, however, by the fact that one crucial sample site of Al-Kindi's relies on probable not-in-situ material, apparently lying within the boundary of sub-Waulsortian limestones. It would therefore seem that, on the basis

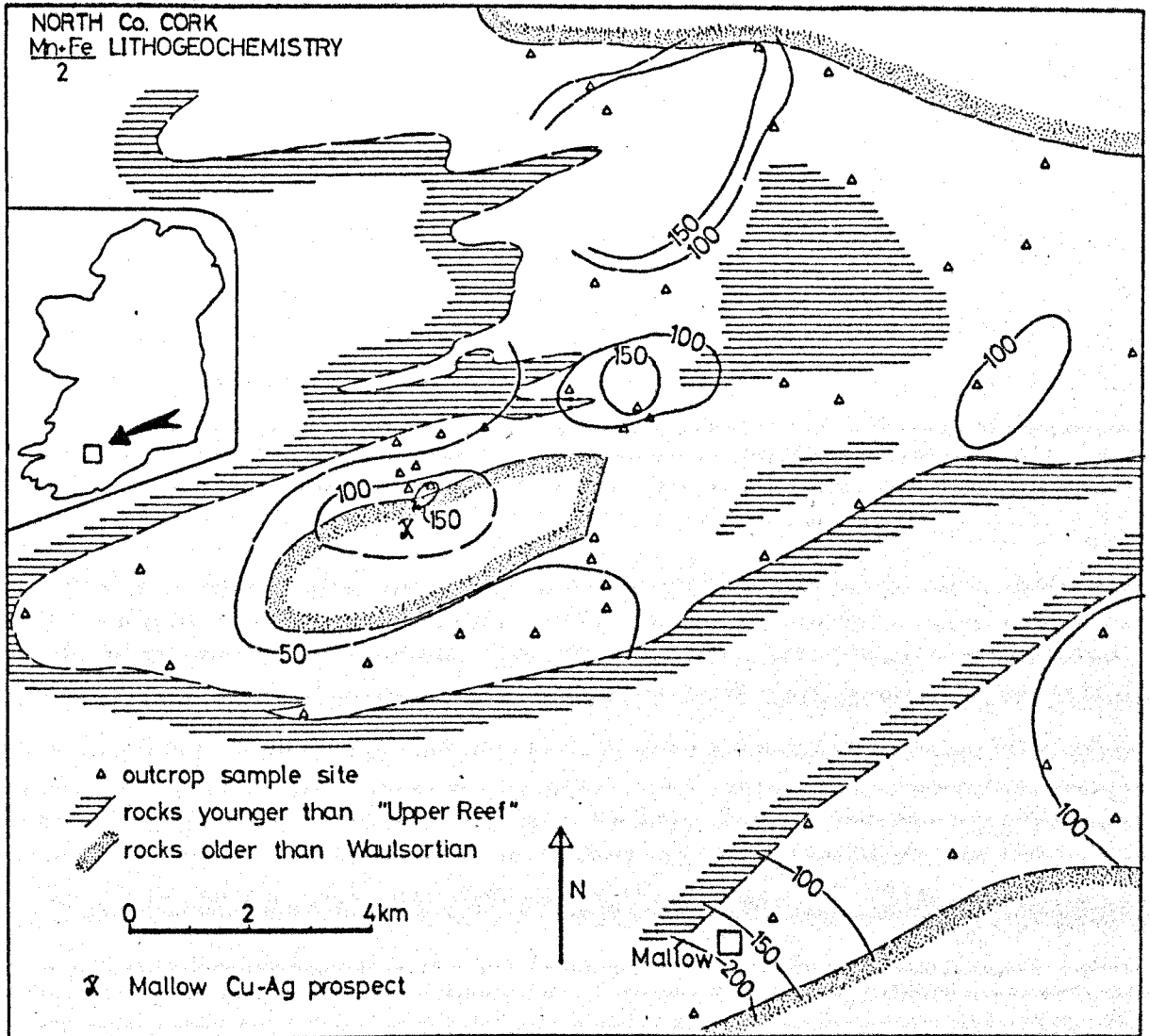


Figure 3.71: Areal distribution of $(Mn+Fe)/2$ content of Waulsortian Limestones (and Upper Reef) of Mallow area, contoured using a rolling mean.

of the data illustrated here, the Mallow base metal prospect is not accompanied by significant enrichments of Mn or Fe in the surrounding mudbank limestones. Virtually all the samples yielded background levels of Zn, only two of those analysed contained more than 10 ppm of the element.

3.6.1 Summary.

Analysis of pure, unaltered Waulsortian Mudbank Limestones from around known base metal deposits hosted in the same, or nearby older or equivalent rocks, indicates that elevated levels of Mn, Fe and Zn accompany them.

The base metal deposit at Tynagh is surrounded by a pronounced Mn and Fe aureole to at least 6 kilometres distant, with elevated Zn (and Sr) values to about 5 kilometres.

Enriched Mn, Fe and Zn levels are present within at least 3 kilometres of the Silvermines deposits, although further elevated levels of these three elements encountered some distance away may be associated with a separate exhalative centre somewhere to the east of Nenagh.

The Ballinalack deposit is associated with elevated levels of Mn, Fe (and some Zn) up to perhaps 5 kilometres distant.

The deposits at Keel, Moate and Moyvore are associated with subtle increases of Mn and Fe locally, although Zn remains essentially at background levels in unmineralised limestones.

Although apparently epigenetic in style, the deposits of the Ballyvergin area are also surrounded by a 6 kilometre-wide zone of weak primary enrichments, with more locally enriched zinc.

Deposits at Aherlow and Courtbrown are both associated with elevated Mn, Fe (and Zn) levels, decreasing out-

wards, extending to at least 1.5 kilometres at Aherlow, and considerably further (over 5 kilometres along strike) at Courtbrown.

Only at Mallow, are surrounding host rocks apparently free of primary trace element enrichments.

Threshold levels vary slightly between each area, but are of the order of 200 to 250 ppm for Mn and Fe, and 10 ppm for Zn.

CHAPTER FOUR - CORE GEOCHEMISTRY.

4.1.1. Introduction.

Sampling of drill core from Silvermines, Ballinalack and Keel was undertaken to complement the relatively scarce surface outcrop around the deposits, when examining lateral dispersion patterns, as outlined in Chapter 3. It was also undertaken to provide a stratigraphic profile of trace element patterns within the Waulsortian Mudbank Limestone, its equivalents and immediate stratigraphic neighbours. This vertical profiling introduces a third dimension, representing the passage of time during sedimentary and hydrothermal processes, provided of course, that post-depositional geochemical redistribution was negligible.

In this chapter, the results of these stratigraphic profiles are presented separately for each of the three deposits.

4.2.1. Silvermines Hanging Wall.

Initially at Silvermines, samples were collected from the ore horizon and lateral equivalents, later supplemented by samples from varying intervals (from less than 1 metre to over 50 metres) throughout the remainder of the mudbank sequence. In total, 58 holes were sampled, and their locations are shown in Figure 4.1. Holes were selected to allow a good three dimensional coverage of the mine area beyond, limited by availability and condition of core.

SILVERMINES - VERTICAL PROFILES

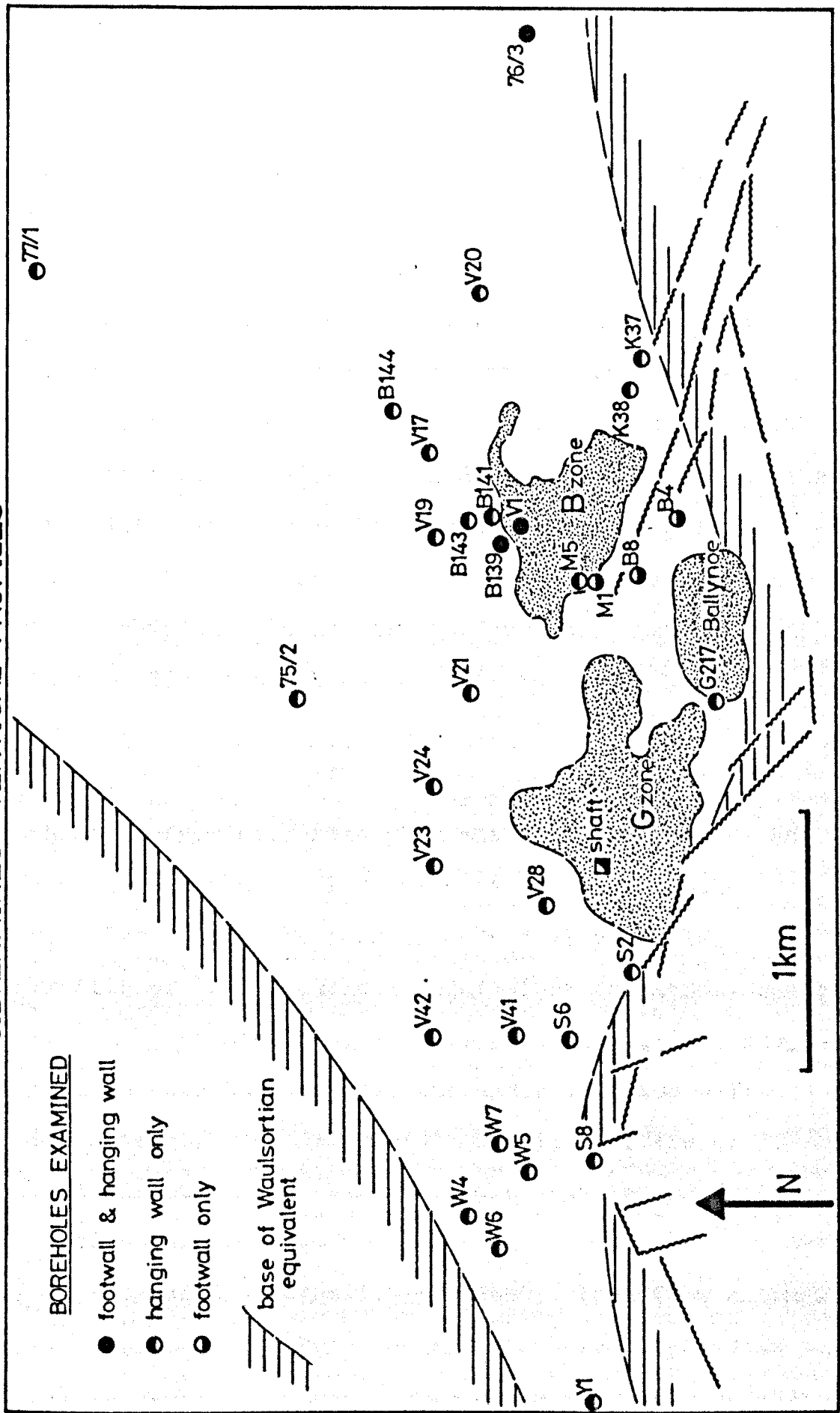


Figure 4.1: Location of boreholes sampled for vertical profiling, showing outline of main stratiform ore zones (stipple).

At Silvermines, the dominant Waulsortian equivalent lithologies are dolomite and limestone breccias, with varying degrees of recrystallisation and argillaceous impurity, in which fine-grained pyrite is fairly ubiquitous, forming a vague envelope above and around the stratiform sulphide (Graham 1970).

During sampling of core, unlike regional outcrop sampling, visible impurities such as fine-grained pyrite, argillaceous mud or stylolites (both of which are often rich in fine grained sulphides) and dolomite, are virtually unavoidable because of their pervasive nature. However, it should be stressed here that no vugh, veinlet or other obvious secondary material was taken. Siderite formed part of the sample medium in several of the holes close of the deposit (V1, B139, B141).

Samples from each hole were analysed for Mn, Fe, Zn and Mg, and the results drawn as vertical geochemical profiles. Some sections allow a fairly complete profile of the Waulsortian equivalent formation, whereas others examine only a small part of it, for example, from the ore horizon into the underlying footwall Stromatactis Reef Limestone. Profiles of the Muddy Reef Limestone are examined separately in the following section (4.2.2.)

Of the vertical sections examined, those from which 20 or more samples were taken are displayed in Figures 4.2 to 4.8. Those with between 5 and 20 samples are

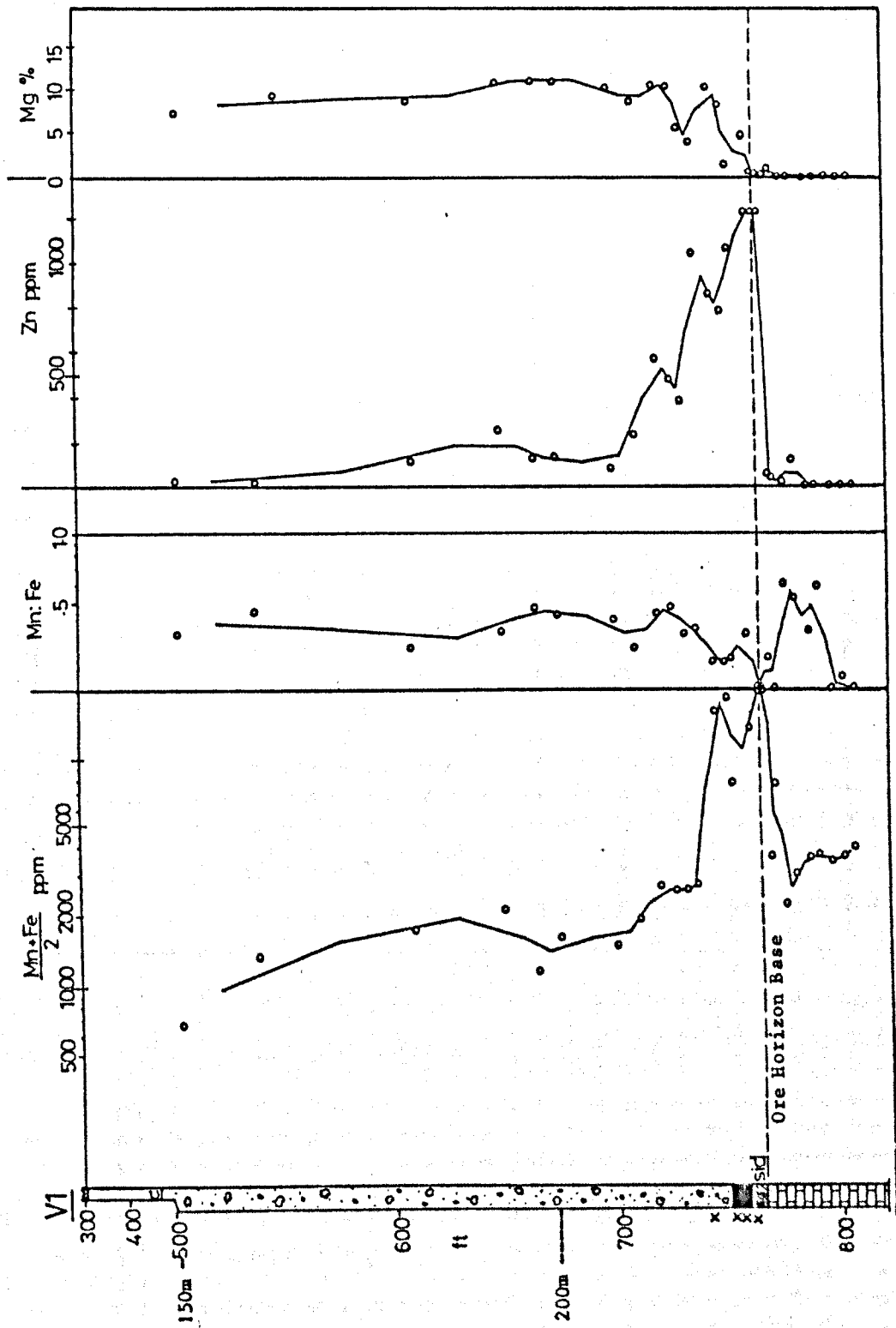


Figure 4.2: Vertical geochemical profile of borehole V1 at Silvermines. Solid lines join mid-points between each sample. Note log scales for (Mn·Fe)/2 and Mn:Fe. For key see Figure 4.3.

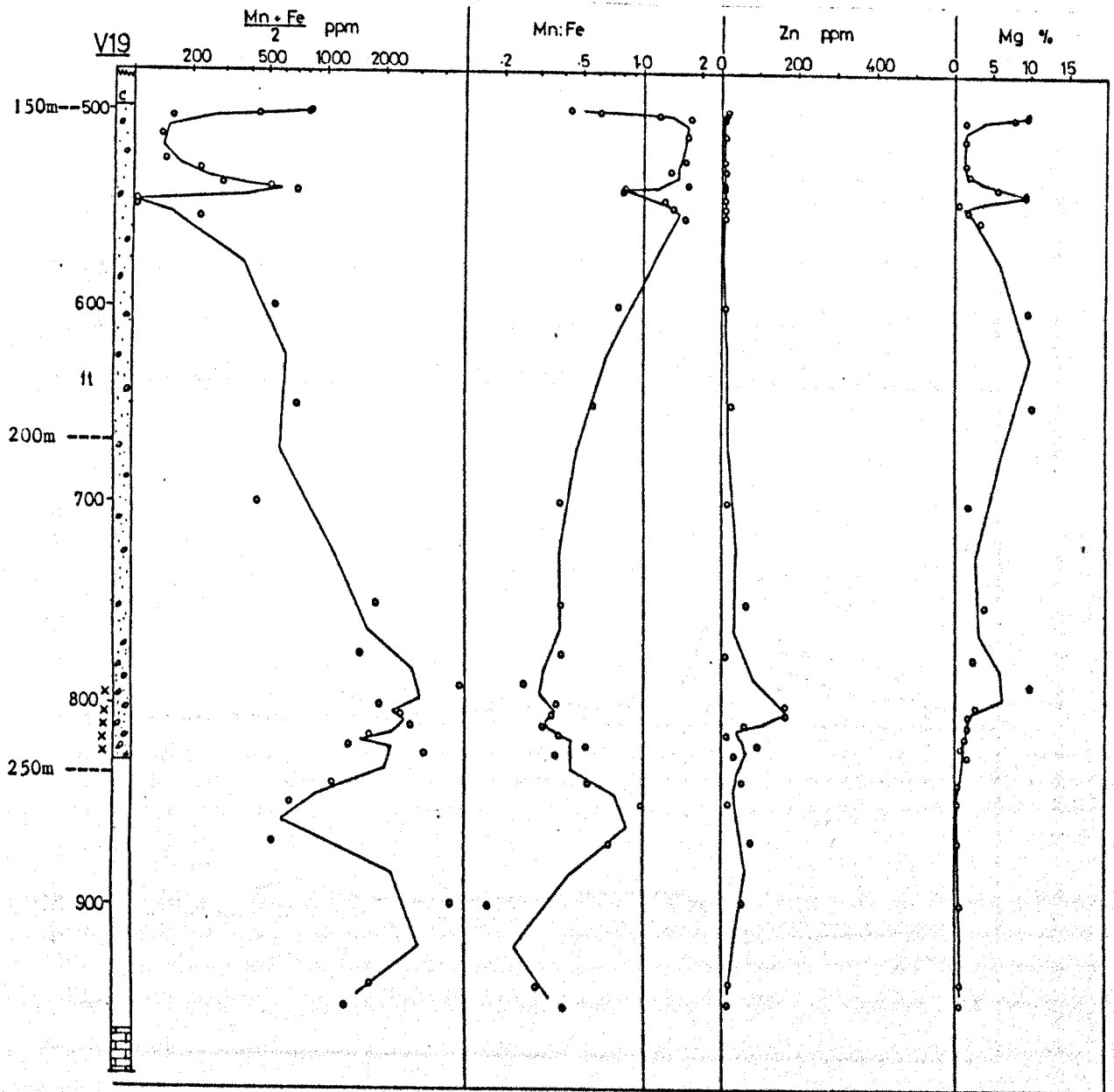
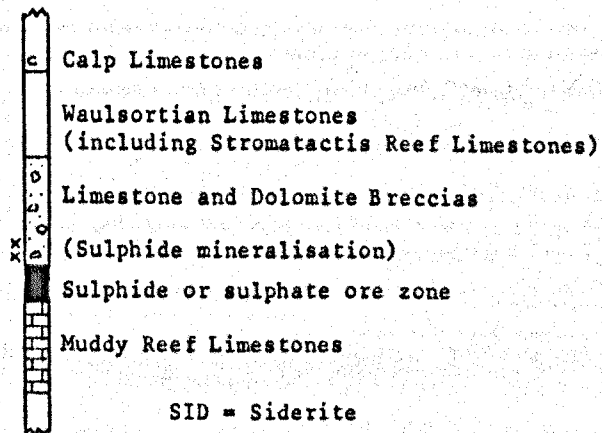


Figure 4.3: Vertical geochemical profile of borehole V19 at Silvermines. Solid lines join mid-points between each sample. Note log scales for $(Mn+Fe)/2$ and Mn:Fe. For key see below.



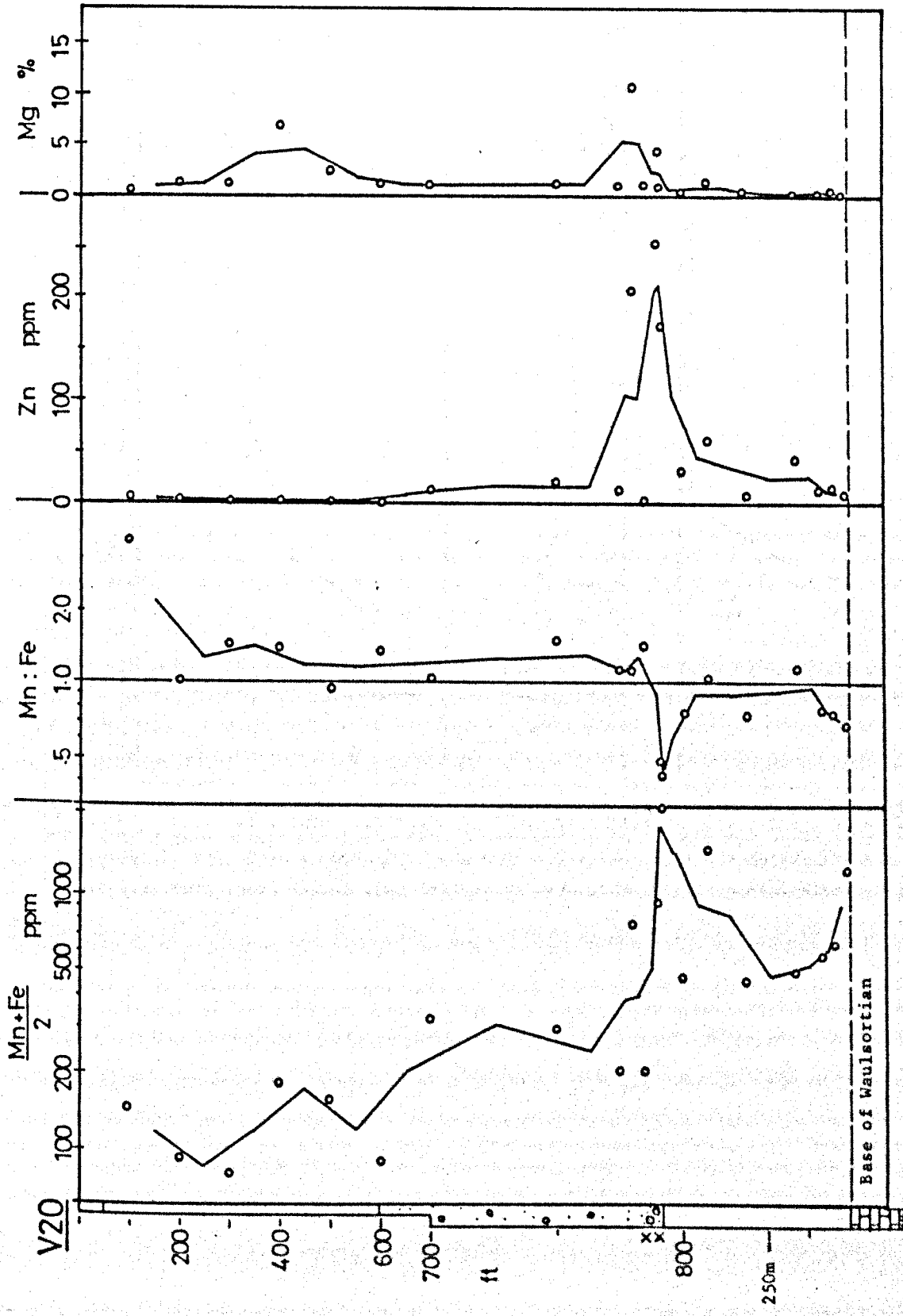


Figure 4.4: Vertical geochemical profile of borehole V20 at Silvermines. Solid lines join mid-points between each sample. Note log scales for (Mn+Fe)/2 and Mn:Fe. For key see Figure 4.3.

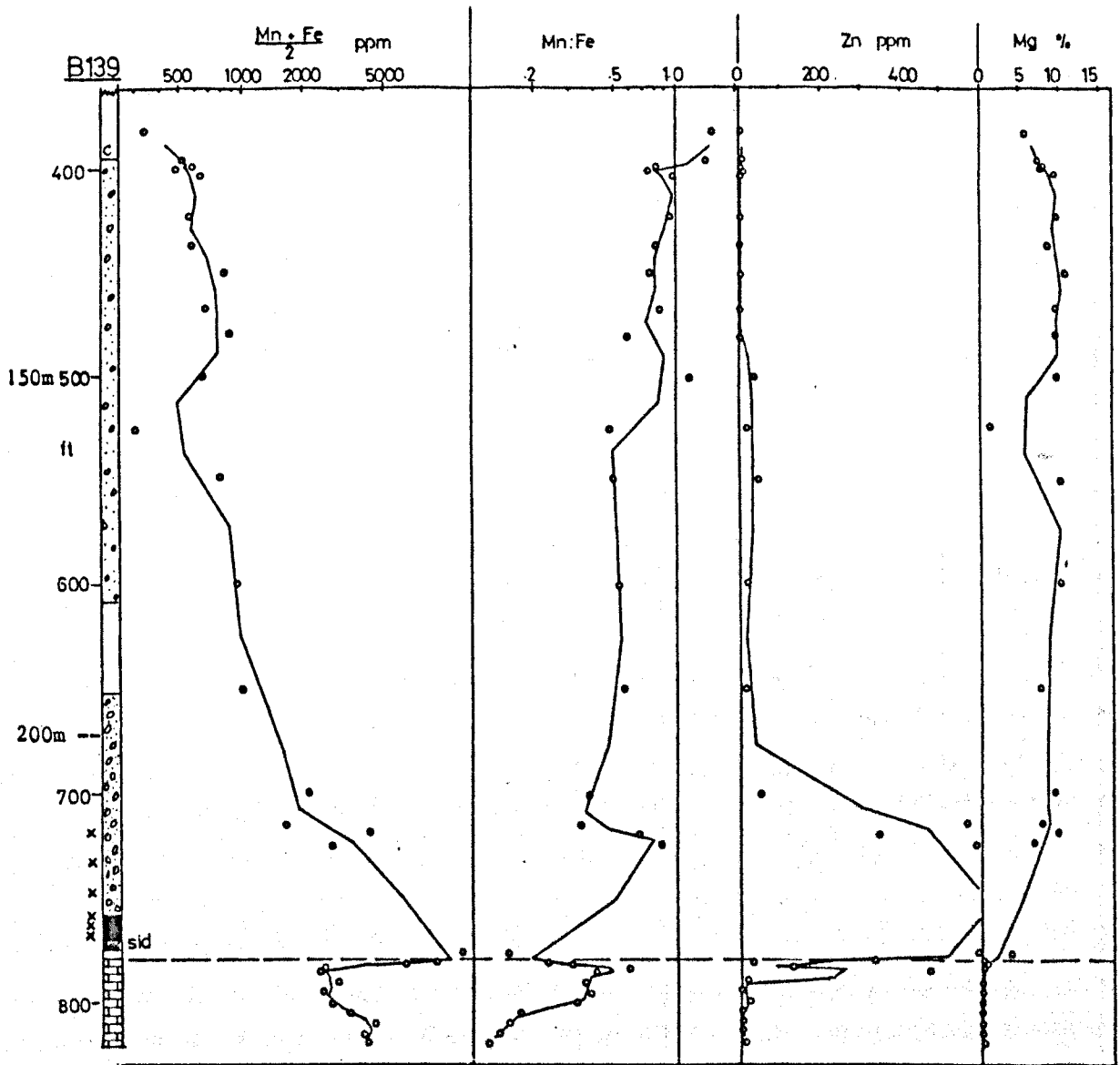


Figure 4.5: Vertical geochemical profile of borehole B139 at Silvermines. Solid lines join mid-points between each sample. Note log scales for $(Mn+Fe)/2$ and Mn:Fe. For key see Figure 4.3. Horizontal dashed line represents base of Waulsortian equivalent.

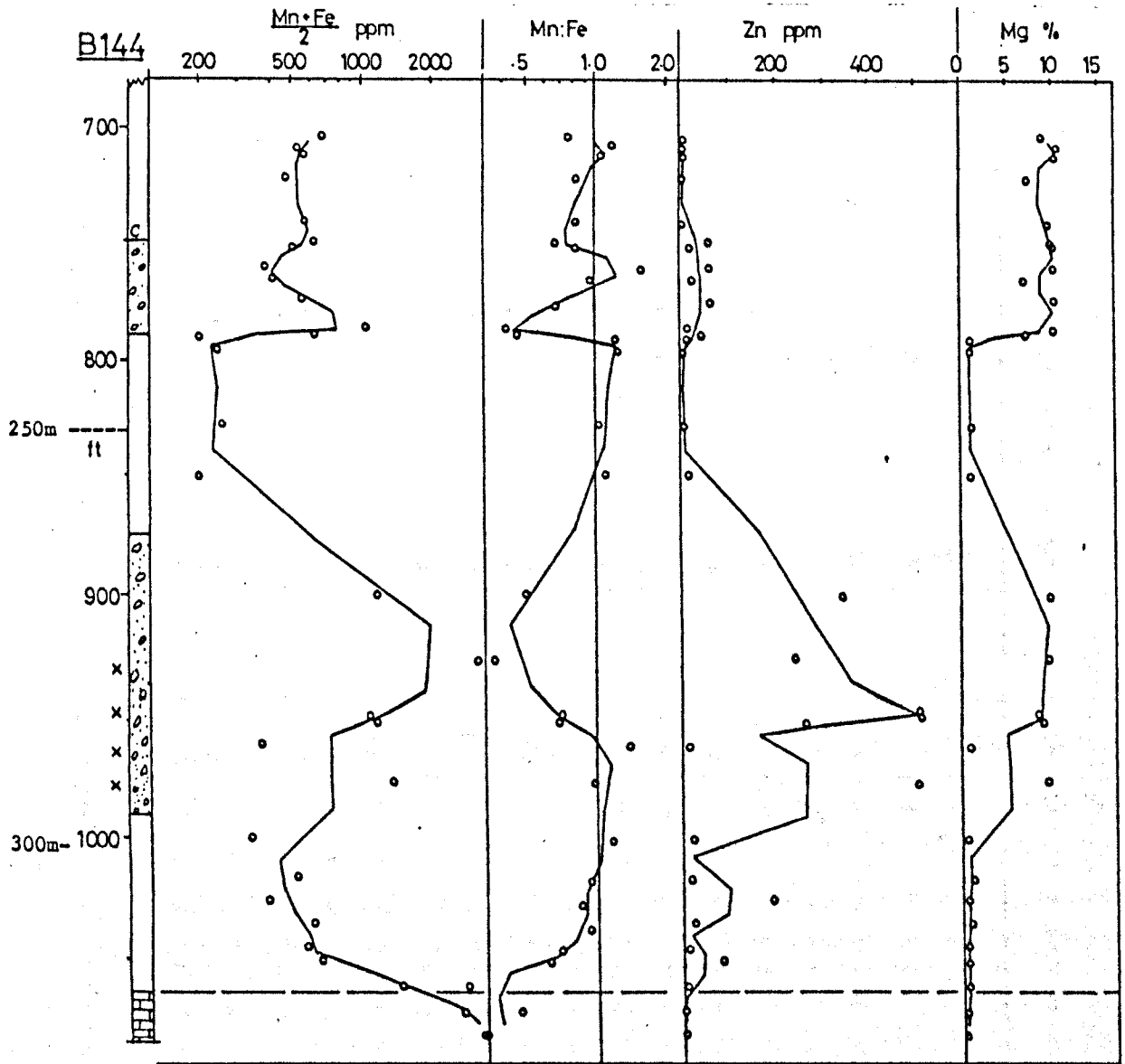


Figure 4.6: Vertical geochemical profile of borehole B144 at Silvermines. Solid lines join mid-points between each sample. Note log scales for $(\text{Mn}+\text{Fe})/2$ and $\text{Mn}:\text{Fe}$. Horizontal dashed line represents base of Waulsortian equivalent. For key see Figure 4.3.

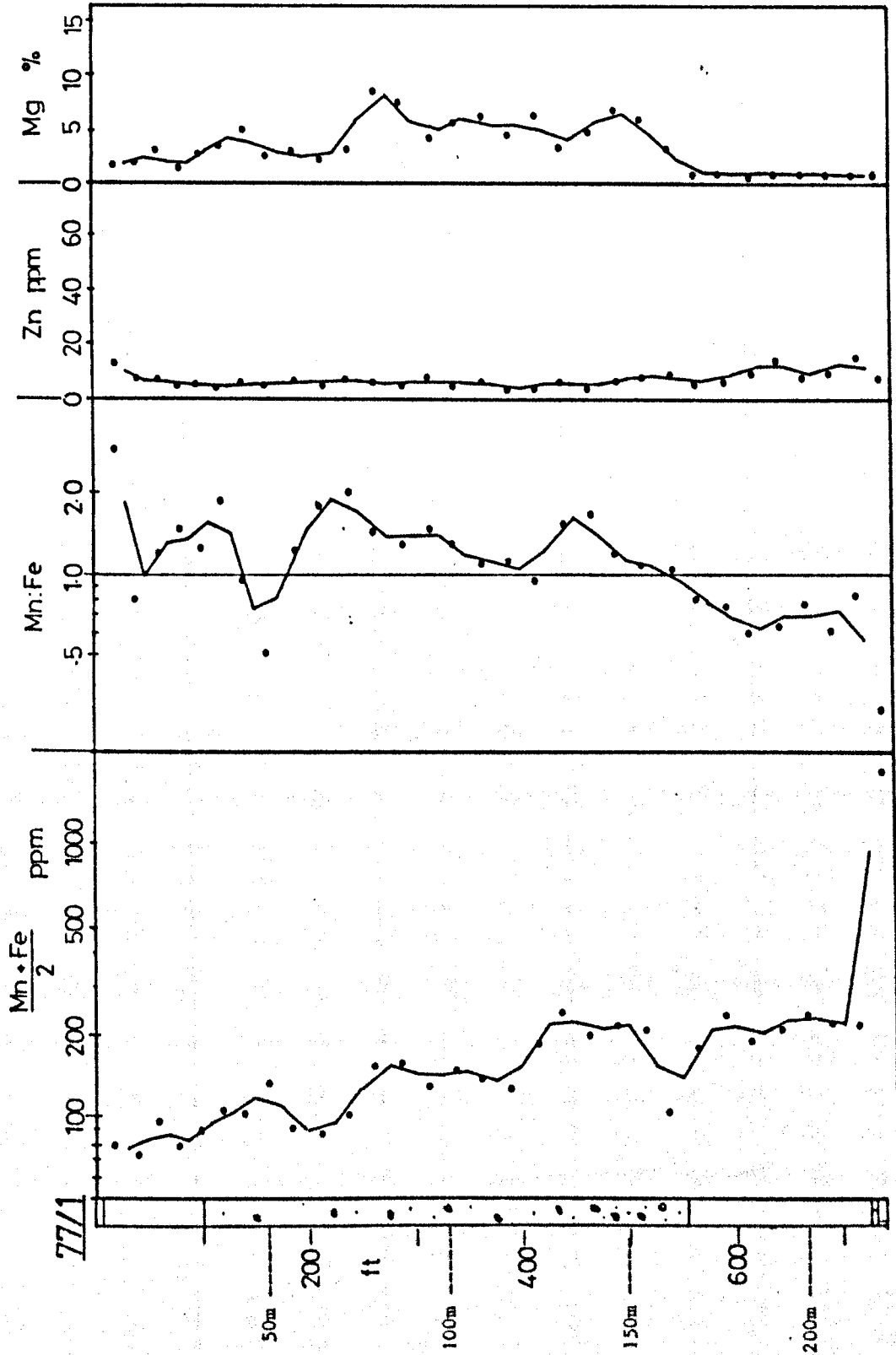


Figure 4.7: Vertical geochemical profile of borehole 77/1 at Silvermines. Solid lines join mid-points between each sample. Note log scales for $(Mn+Fe)/2$ and Mn:Fe. For key see Figure 4.3.

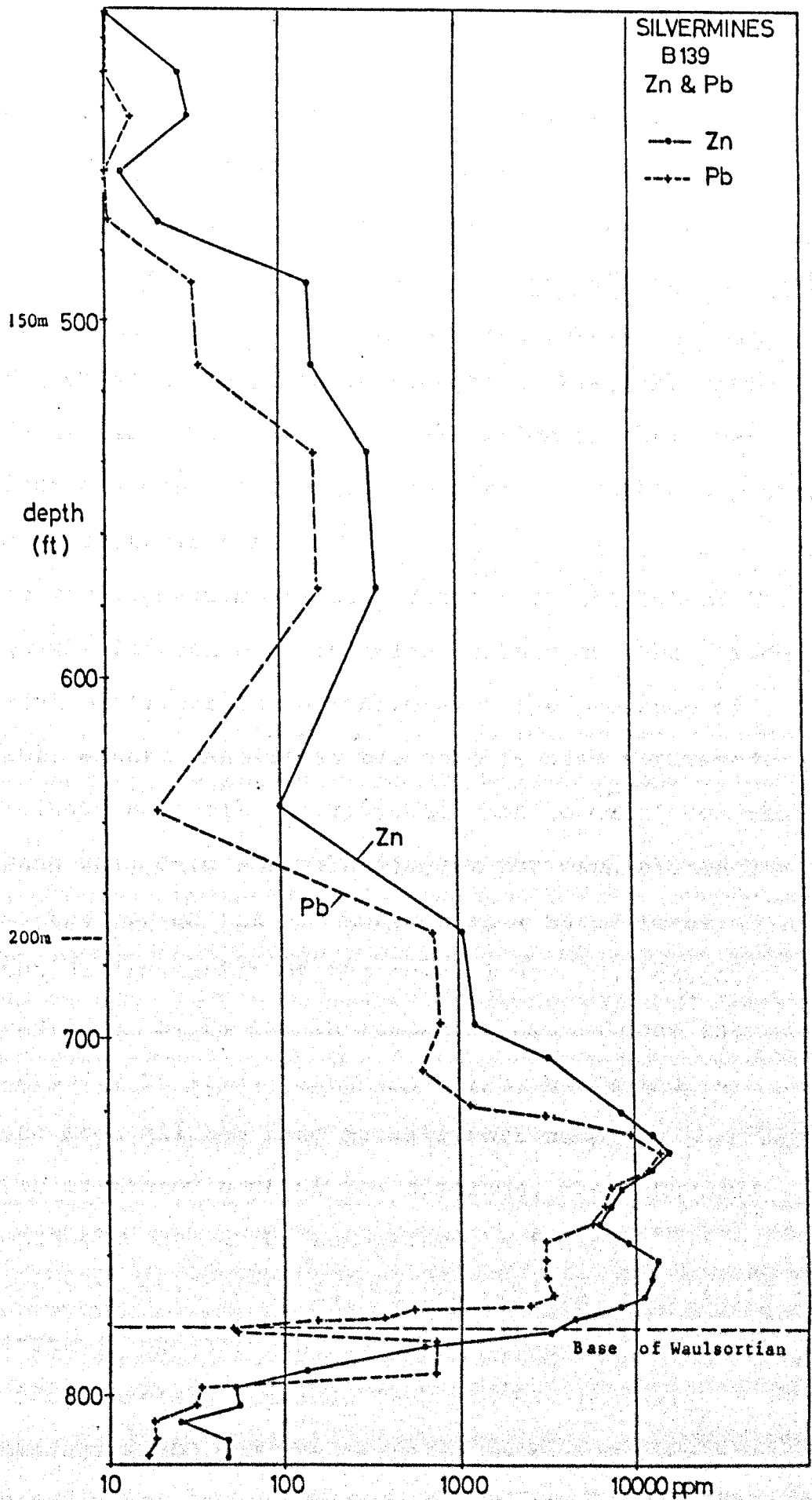


Figure 4.8: Vertical profile of Zn and Pb levels in borehole B139 (see Figure 4.5 also) using X.R.F. results. (Note between 725' and 775' Mogul assay results used since this core was dumped). Note also log scale.

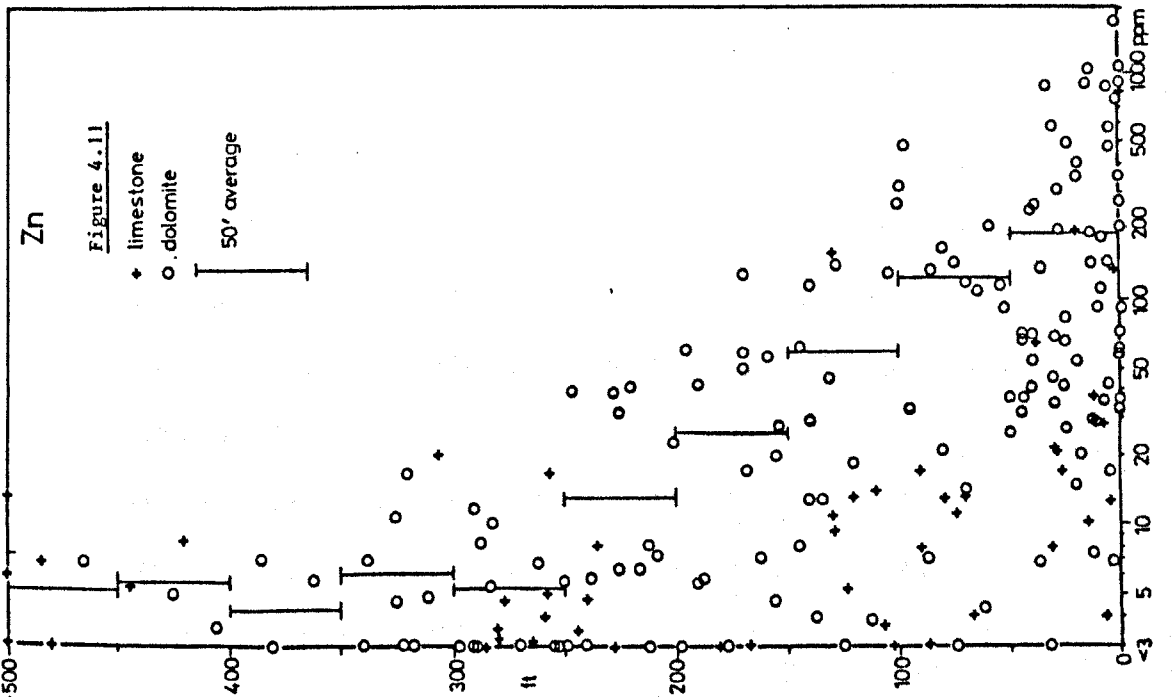
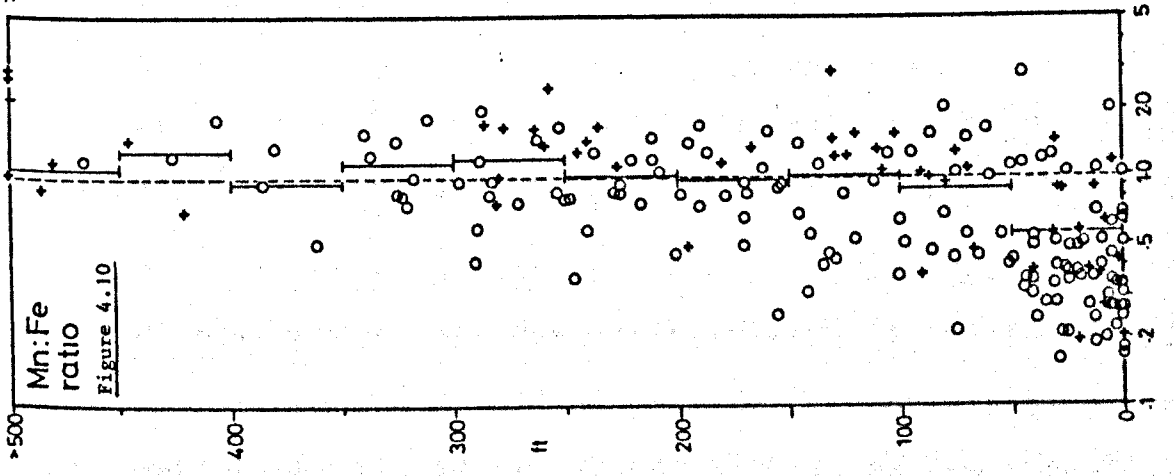
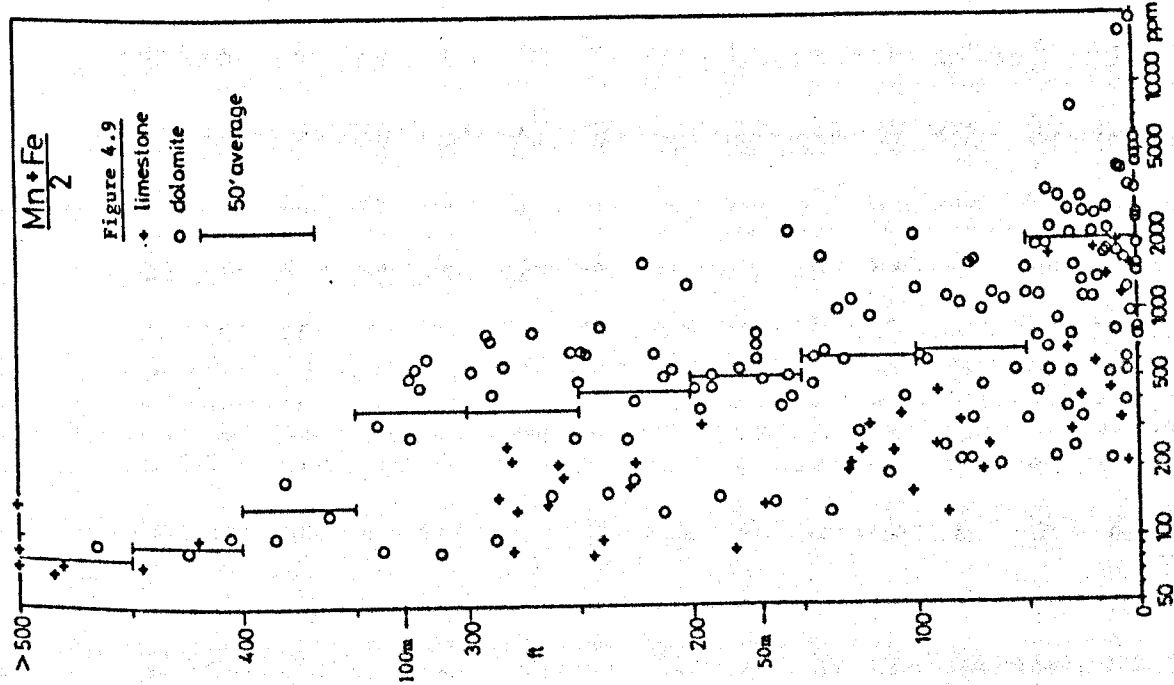
displayed in Appendix II. Each profile includes a simplified geological log to allow visual correlation between lithology and trace element content. Each diagram shows $(\text{Mn}+\text{Fe})/2$ content of core samples, as both Mn and Fe behave in a roughly similar manner in the Reef equivalent formation. Alongside this, the ratio Mn:Fe is displayed, as subtle variation in their behaviour may otherwise escape detection. Both are plotted on a logarithmic scale.

Zinc and magnesium are also displayed, the latter to allow the influence of dolomite content on other trace element behaviour to be monitored. The presence of visible mineralisation in the core is also portrayed.

Combination of all the vertical profile data from the hanging wall onto a single diagram for each element, using the top of the ore horizon as a datum level, allows determination of the overall vertical extent of elevated Mn, Fe and Zn values. This is done in Figures 4.9 to 4.12, using $(\text{Mn}+\text{Fe})/2$, Mn:Fe and Zn values from all the hanging wall core samples.

After examining each of the diagrams, the behaviour of each element can be summarised as follows:

$(\text{Mn}+\text{Fe})/2$: This peaks in the ore horizon, especially if siderite is present, where values may exceed 10000 ppm, and drops steadily upwards into the hanging wall. Values above 200 ppm are recorded up to 120 metres (400 ft.) above the top of the ore horizon. However, low values, below 200 ppm, are recorded throughout much



Figures 4.9 to 4.11: Geochemical profiles of hanging wall at Silvermines, using all core samples. Vertical scale is height above top of ore horizon. Vertical lines represent average of all samples in each 50' interval. Note also log concentration scales.

of the hanging wall sequence, to within 15 metres (50 ft.) of the top of the ore horizon. The influence of Mg is fairly obvious, and where levels are high, Mn and Fe are seen to increase also. The median value of $(\text{Mn}+\text{Fe})/2$ in all hanging wall samples is 582 ppm, but 740 ppm in dolomites and only 240 ppm in limestones (Table 4.1).

Note here that the locations of the boreholes sampled range from within the orebody to almost three kilometres distant (Figure 4.1). The majority of samples with low values of $(\text{Mn}+\text{Fe})/2$ (below 200 ppm) within 60 metres (200 ft.) vertically of the ore horizon, originate from over one kilometre from the mine. Likewise, only beyond two kilometres, do dolomitic samples appear to contain less than 400 ppm $(\text{Mn}+\text{Fe})/2$.

Mn:Fe: This mirrors the distribution of $(\text{Mn}+\text{Fe})/2$, i.e. the ratio drops when $(\text{Mn}+\text{Fe})/2$ is high, reflecting much higher levels of Fe than Mn. Mn:Fe tends to remain low, below 0.40, in ore horizon samples, and rises to approximately equal proportions over 30 metres (100 ft.) above.

Zinc: As would be expected, Zn peaks within the ore horizon and drops towards background levels upwards into the hanging wall. Values over 10 ppm are recorded up to 90 metres (300 ft.) above the ore horizon, with less obvious preferential enrichment of dolomitic samples than is the case for Mn and Fe. Background values of below 10 ppm are recorded throughout the hanging wall

Median values (Mn+Fe)/2 (ppm) (n in brackets)	All samples	Limestone (< 2% Mg)	Dolomite (> 2% Mg)
All Hanging Wall	582 (161)	240 (47)	740 (114)
Upper Hanging Wall over 30 m	450 (78)	170 (26)	570 (52)
Lower Hanging Wall below 30 m	1250 (83)	350 (21)	(2000) (62)

Median Values zinc (ppm) (n in brackets)	A.A.	X.R.F.	A.A./X.R.F. ratio
All core samples	38 (426)	88 (150)	0.43
Outcrop samples	(5.4) (291)	12.5 (48)	0.43
Core and Outcrop	14 (717)	48 (198)	0.29
Core:			
All Hanging Wall	24 (164)	50 (81)	0.48
Upper Hanging Wall (>30m)	(5.8) (76)	18 (58)	0.32
Lower Hanging Wall (<30m)	50 (88)	(75) (23)	(0.67)
Hole 77.36.1 (@ 2.5 km)	(5.4) (41)	25 (11)	0.22

Table 4.1: Median (Mn+Fe)/2 and Zn values in outcrop and core samples from Silvermines area (n = number of samples).

right down to the top of the ore horizon, both close to, and distant from the orebody. Median Zn values are 24 ppm in all hanging wall samples, but only 5.4 ppm in hanging wall samples from over 30 metres (100 ft.) above the ore horizon (Table 4.1).

Lead: Lead levels in the core appear to closely follow those of zinc, as illustrated by Figure 4.8, which portrays the total (from X.R.F. analysis) Pb and Zn levels in Borehole B 139. This shows how the two elements fall off more rapidly below the ore horizon into the footwall (within 7 metres or less), than into the hanging wall, possibly reflecting either pronounced differences in the rate of base metal supply, or in the rate of sediment accumulation.

Magnesium: The Mg content reflects directly the amount of dolomite in the sample, and varies from below 1% in pure mudbank samples to over 12% maximum in the hanging wall dolomites. Footwall samples contain more consistent, relatively low levels, generally below 1%.

These vertical traceelement profiles are summarised further and compared in Figure 4.12, where the mid point of each 15 metre (50 ft.) average (from Figures 4.9 to 4.11) is joined to portray the overall hanging wall Mn, Fe and Zn behaviour. From this it can be stated that, within 30 metres (100 ft.) of the top of the ore horizon, $(\text{Mn}+\text{Fe})/2$ content averages over 1000 ppm, with Fe higher than Mn, and Zn content averages over 100 ppm.

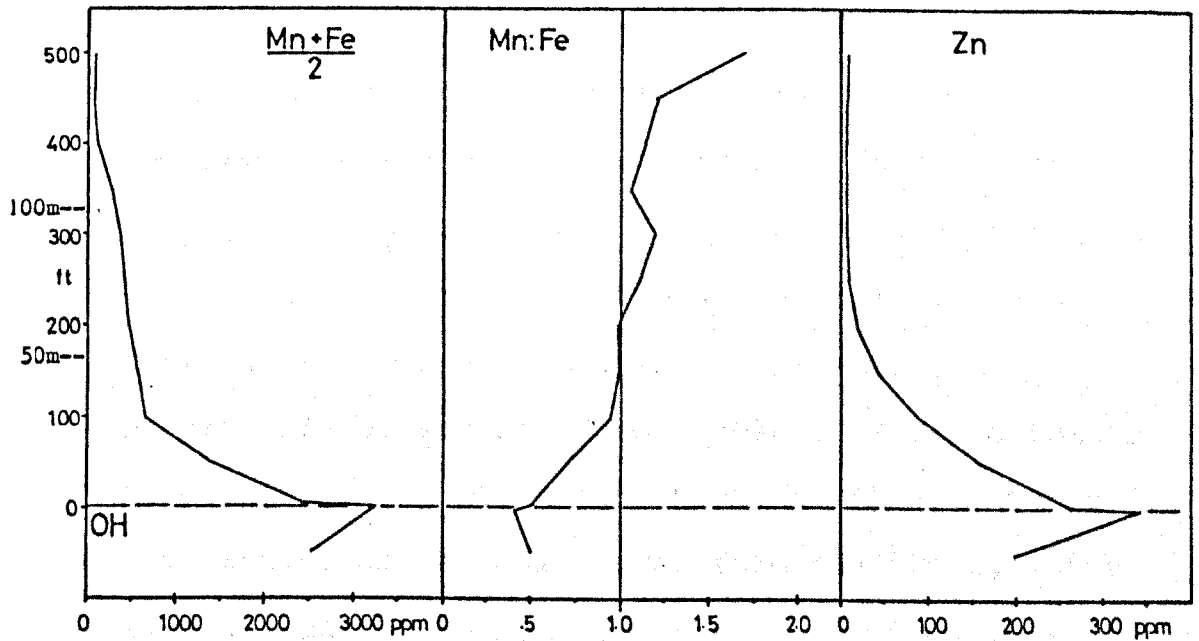


Figure 4.12: Summary of Silvermines hanging wall geochemistry, drawn by joining all averages from each 50' interval. Total number of samples = 335 (hanging wall = 174, ore horizon = 110, Stromatactis Reef Limestone = 51). OH = Ore horizon.

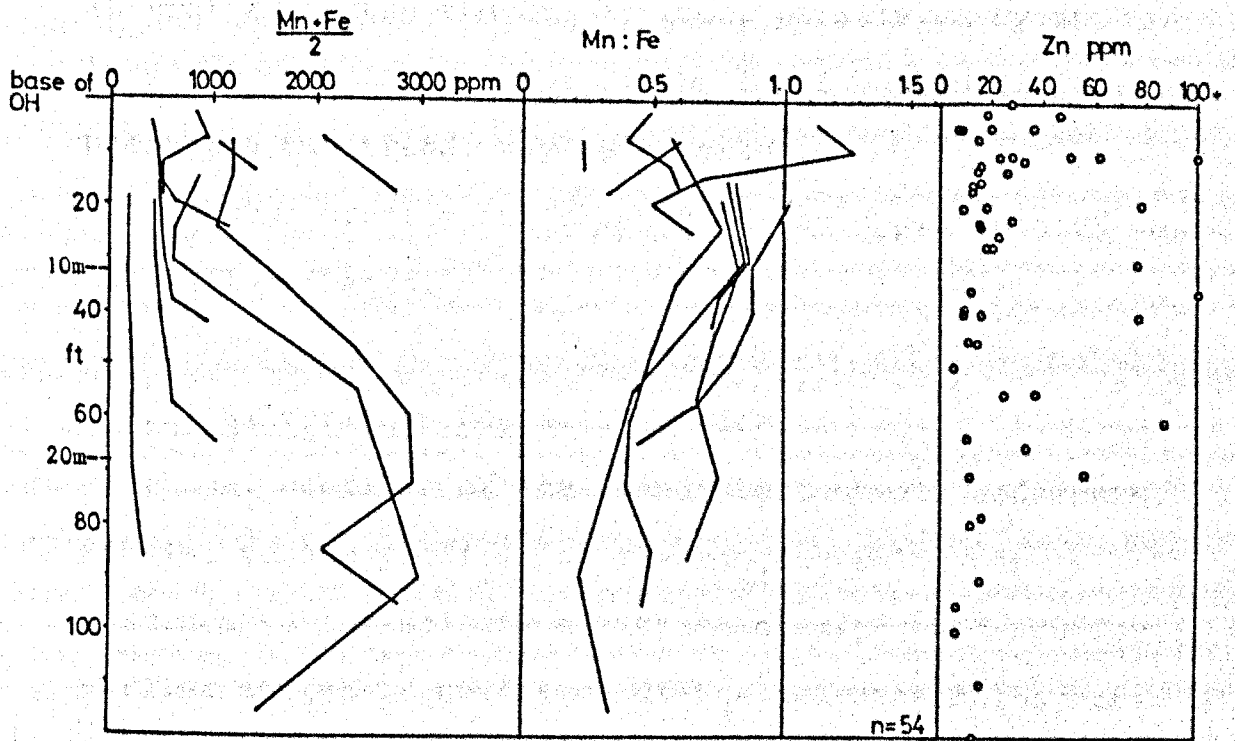


Figure 4.13: Geochemical profiles of footwall Stromatactis Reef Limestone. Individual solid lines join mid-points between samples from individual boreholes.

Footwall Stromatactis Reef Limestone.

The trace element content of Waulsortian limestones from stratigraphically below the ore horizon (the footwall Stromatactis Reef Limestone of Taylor and Andrew (1978)) was also examined separately, in approximately 50 samples from 9 holes. These mudbanks are up to at least 30 metres thick in places, around the periphery of the main stratiform ore zones, which post-date them.

Vertical profiles of $(\text{Mn}+\text{Fe})/2$ content and Mn:Fe ratio of these samples is shown in Figure 4.13, using the base of the ore horizon as a datum level, each line representing the trend from a single borehole. Overall patterns are suggestive of an upward decrease in $(\text{Mn}+\text{Fe})/2$ towards the ore horizon, paralleled by an increase in Mn:Fe, except in the top 6 metres (20ft.), where the two trends may be reversed.

Zinc shows erratic enrichments in the upper half of the footwall mudbanks.

4.2.2. Silvermines Footwall Profiles.

Vertical profiles of the immediate footwall sediments, similar to the profiles of the hanging wall, were examined to investigate any trace element evidence for earlier stages of evolution of the hydrothermal system. Six boreholes were profiled from the base of the ore horizon downwards to varying depths, each of the holes chosen containing negligible or non-existent

footwall Stromatactis Reef Limestone developments between the ore horizon base and the top of the Muddy Reef.

Holes V1 and B 139 are situated in the depths of the B Zone hollow, at the northern margin of the economic mineralisation; holes M1, B8 and B4 are situated on the southern margin of the B Zone hollow, progressively further onto the flanks of the Silvermines Basin; and hole 76/3 is situated approximately two kilometres to the east of the B Zone, still on the margin of the Silvermines Basin (figure 4.1).

A vertical profile through almost 300 metres (1000 ft.) of strata in borehole 76/3 allows a general insight into large scale patterns in both the hanging wall and footwall (Figure 4.14), particularly since no secondary dolomite (Lower Dolomite) is developed in this hole, unlike those from the mine area. In 76/3, the hanging wall enrichments are less well pronounced, because of the distance (over 2 kilometres) from the centre of mineralisation. However, a large peak is present in the immediate footwall, with values rising to over 1500 ppm. This peak is approximately 30 metres (100 ft.) thick, and corresponds with the intersection of the Muddy Reef Limestone, values falling back down to around 300 ppm in the underlying Muddy Limestone. Although Fe shows close similarities to Mn in the hanging wall part of the sequence, comparable with other borehole profiles in the mine area, a much broader

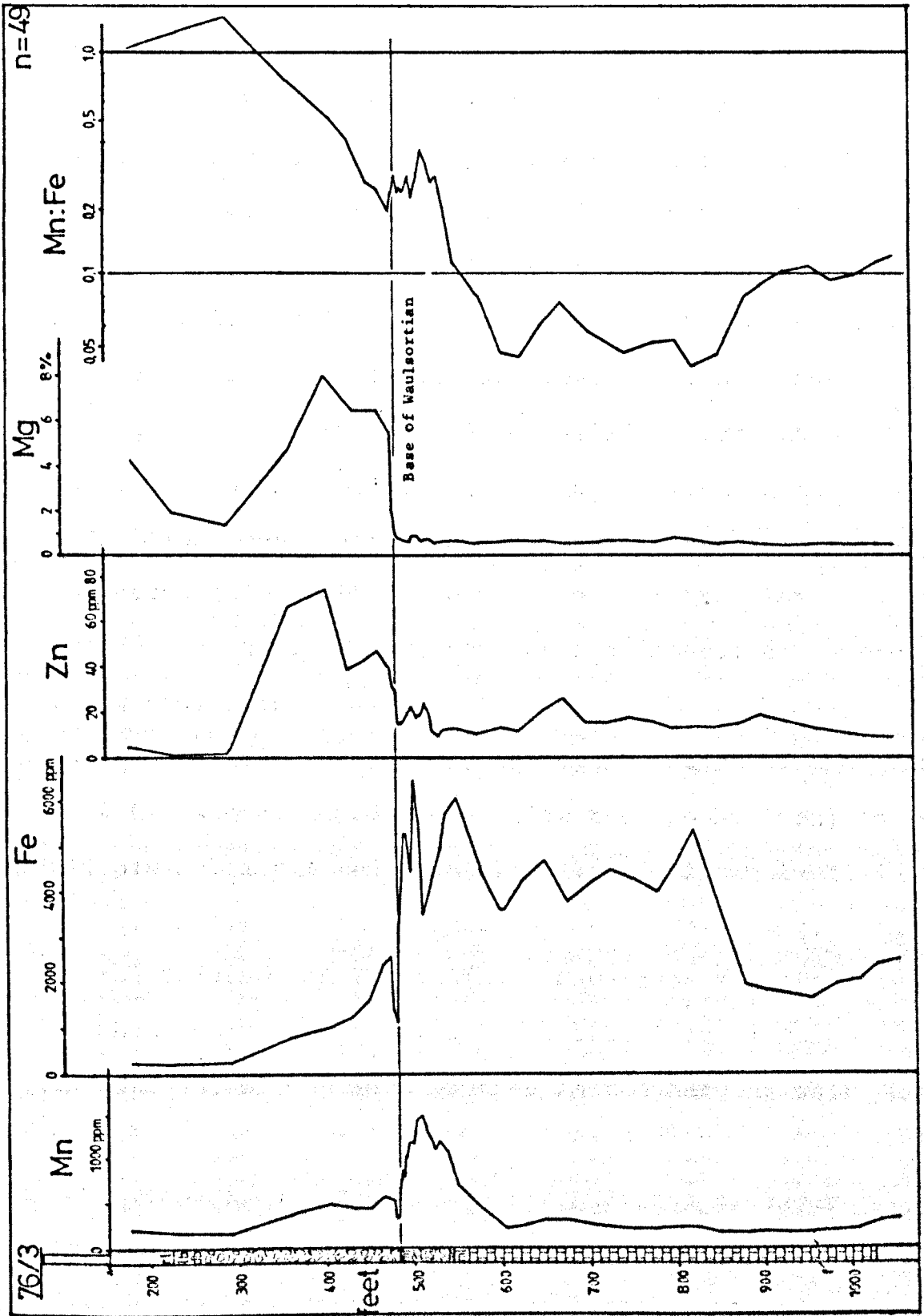


Figure 4.14: Vertical geochemical profile of borehole 76/3 at Silvermines, including large part of the footwall succession. Solid line joins mid points between each adjacent sample. Note log scale for Mn:Fe. (Key: rl = Waulsortian Limestone; lb,db = Limestone and Dolomite Breccias; ml = Muddy Reef Limestone; al = Muddy Limestone; f = fault).

peak, some 120 metres (400 ft.) thick, is observed in the footwall sediments down to almost 270 metres (900 ft.) depth. Values in this zone of enrichment rise to over twice the level of the highest hanging wall or ore horizon values, at over 6000 ppm Fe.

Partly as a result of this, Mn:Fe levels are very low in the footwall, between 0.1 and 0.05 throughout much of the Muddy Limestone, and rise towards 1.0 in the hanging wall, in line with elsewhere in the mine area.

Magnesium and zinc levels are low, and consistent throughout the footwall sediments, Mg at less than 1% and Zn below 20 ppm, right down to the base of the Muddy Limestone. Both elements peak in the lowermost 45 metres (150 ft.) of the hanging wall breccias, corresponding to the ore horizon and immediately overlying sediments.

More detailed profiles of the top 30 metres of the Muddy Reef Limestone, immediately below the ore horizon, in all six holes sampled, are displayed in Appendix II, Figures A.11-15. These show Mn, Fe, Mn:Fe and Mg, with Mn and Fe drawn on log scales. Manganese and iron are graphed separately because their behaviour is more independent of one another than in the hanging wall sequence.

For comparison, each of the six profiles is superimposed onto a single graph for each element in Figures 4.15 and 4.16. In an attempt to simplify matters further, and give an overall picture of footwall trace

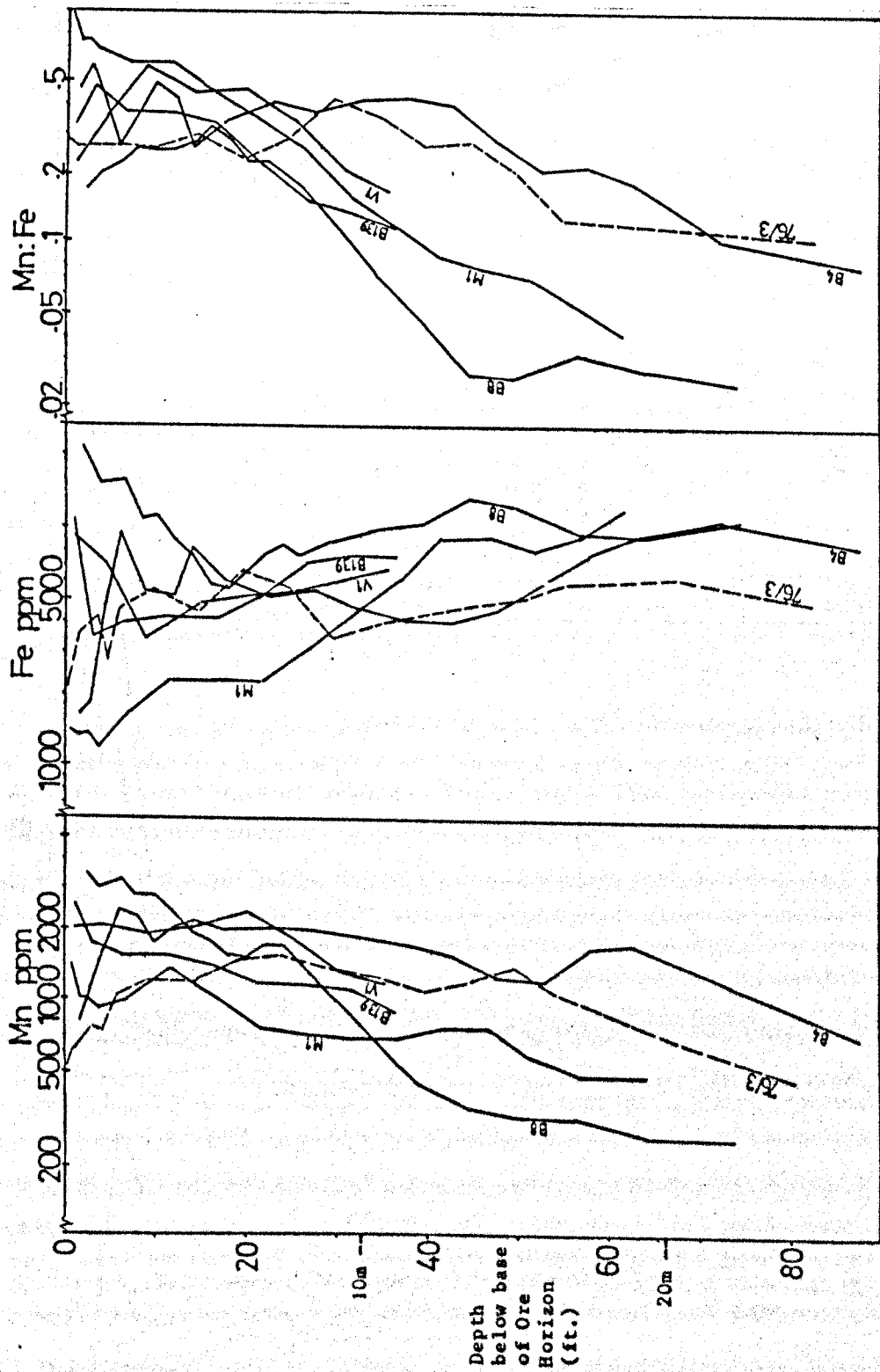


Figure 4.15: Vertical profiles of Mn, Fe and Mn:Fe content on borehole sections of Silvermines footwall Muddy Reef Limestone. Each line joins mid-points between individual samples in each hole. Note log scales.

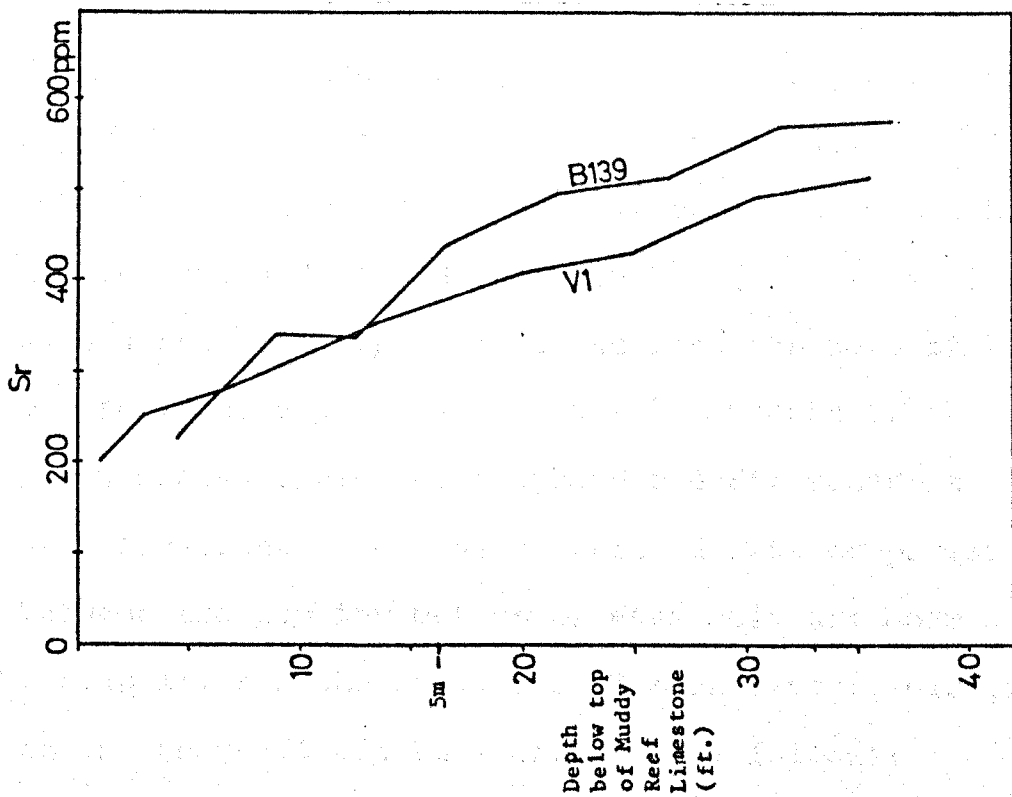


Figure 4.17: Vertical profile of strontium content of boreholes VI and B139 in Muddy Reef Limestone at Silvermines. Solid lines join mid-points between each sample.

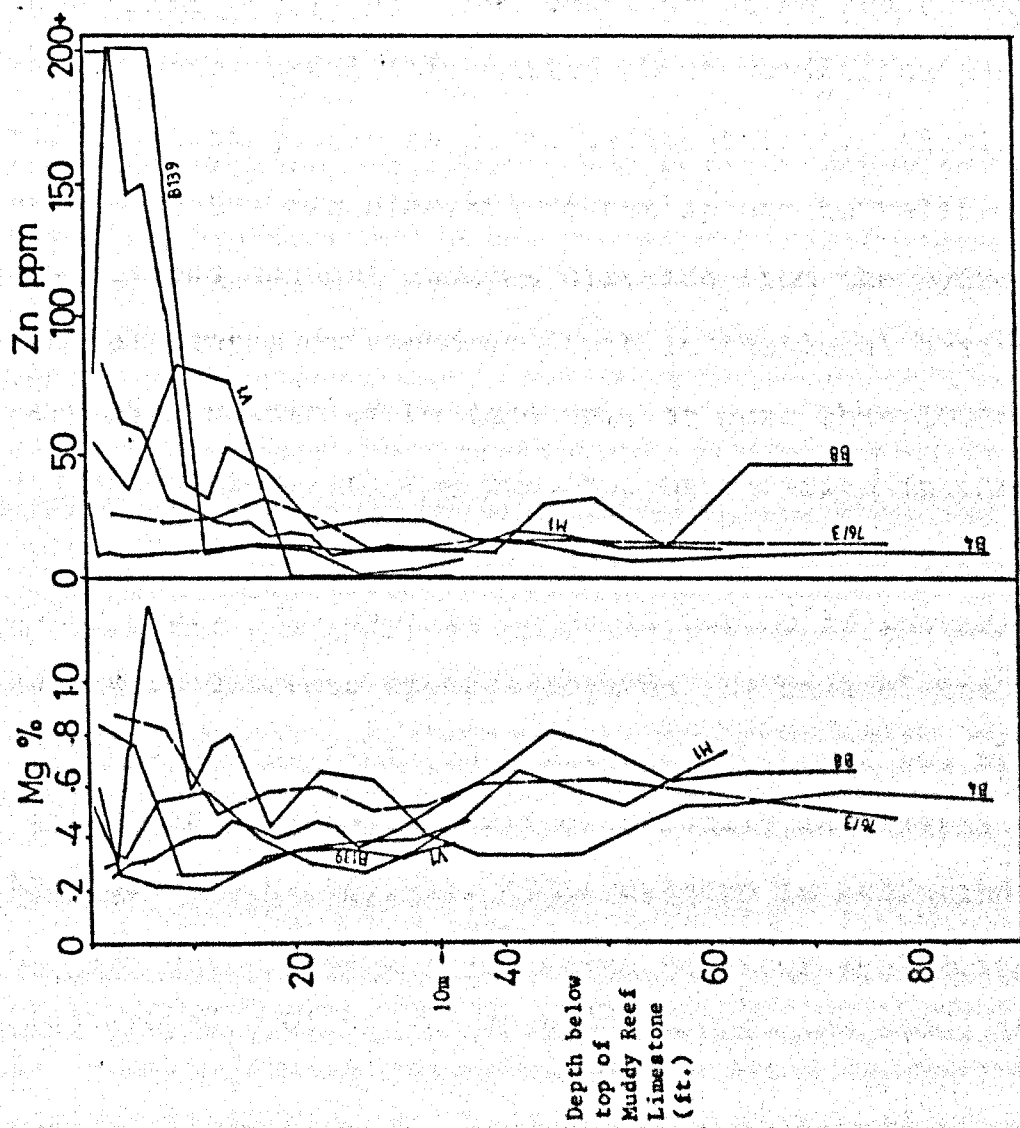


Figure 4.16: Vertical profiles of Mg and Zn in footwall Muddy Reef Limestone at Silvermines. Lines join mid-points between individual samples in each hole.

element patterns, data from each 1.5 metre (5 ft.) interval below the ore horizon base is averaged and represented by a single line in Figures 4.18 and 4.19.

The thickness of the Muddy Reef varies from one hole to another, and considerable lithological variation exists over the top metre or so into the base of the ore horizon, expressed by variable amounts of chert, green shale, siderite, sulphide and Stromatactis Reef Limestone. Because of this, direct comparisons between the top few metres of each hole are more difficult, and the behaviour of each element elsewhere in the footwall can be summarised as follows:

Manganese and iron: The behaviour of Mn and Fe may reveal some useful information about conditions prevailing during pre-ore phase sedimentation. Absolute values of the two elements do not appear to relate to any obvious control such as distance from the hydrothermal centre or supposed depth in the local basin. Very high values of Fe (and Mn), at more than 10000 ppm, are associated with the presence of siderite in three holes (V1, B8, B139) at, or very near to the top of the Muddy Reef. The overall trend is for Mn to increase and Fe to decrease upwards towards the base of the ore horizon, except over the top three metres or so, where Fe also appears to increase erratically in several of the holes (e.g. B8, V1). This pattern is reflected in average Mn:Fe ratio, which shows a steady increase from around 0.05 to 0.5 upwards through the Muddy Reef.

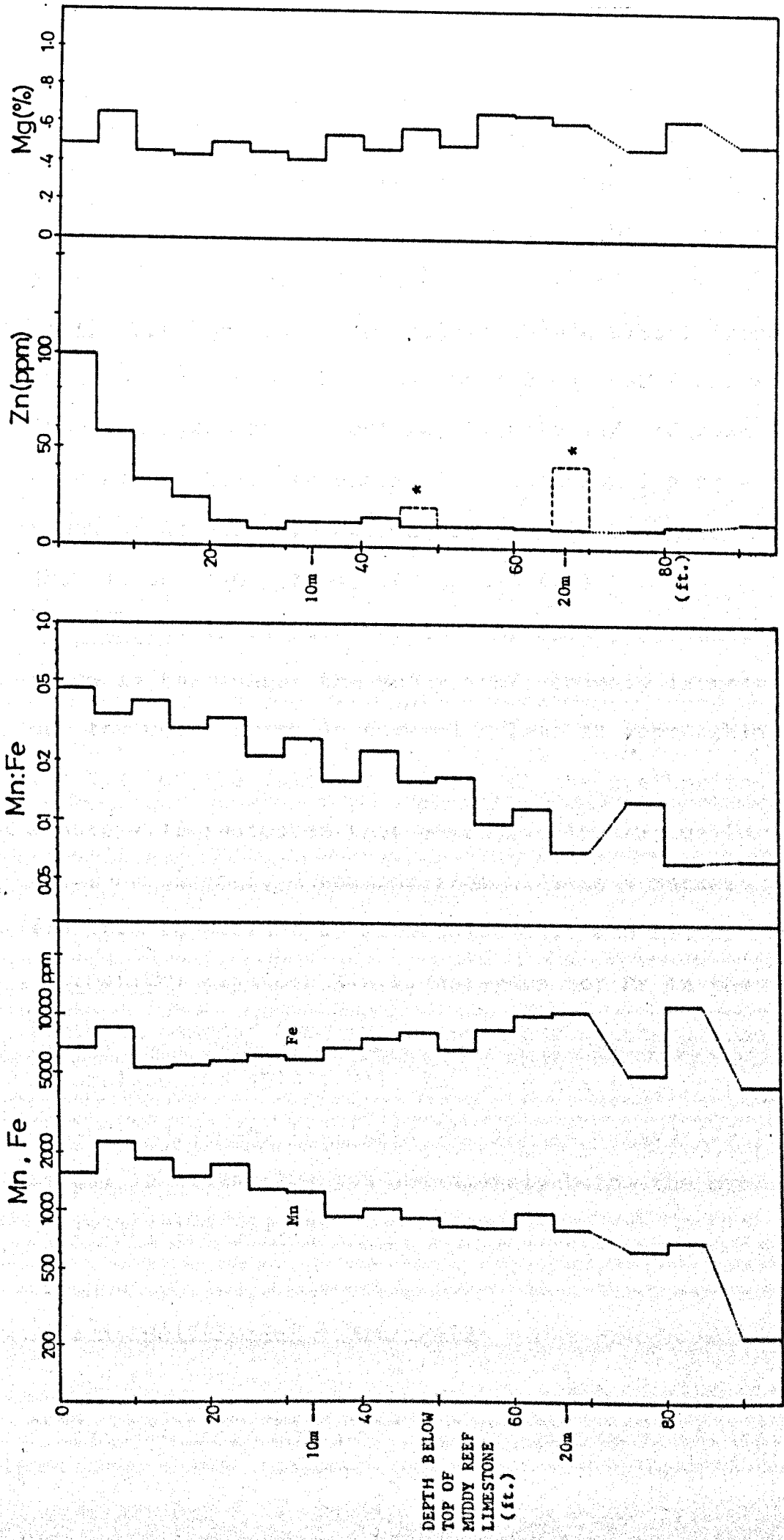


Figure 4.18: Averaged vertical profiles of Mn, Fe and Mn:Fe in footwall Muddy Reef Limestones at Silvermines. Average for each 5 foot interval below top of formation (= base of ore horizon). Note log scales.

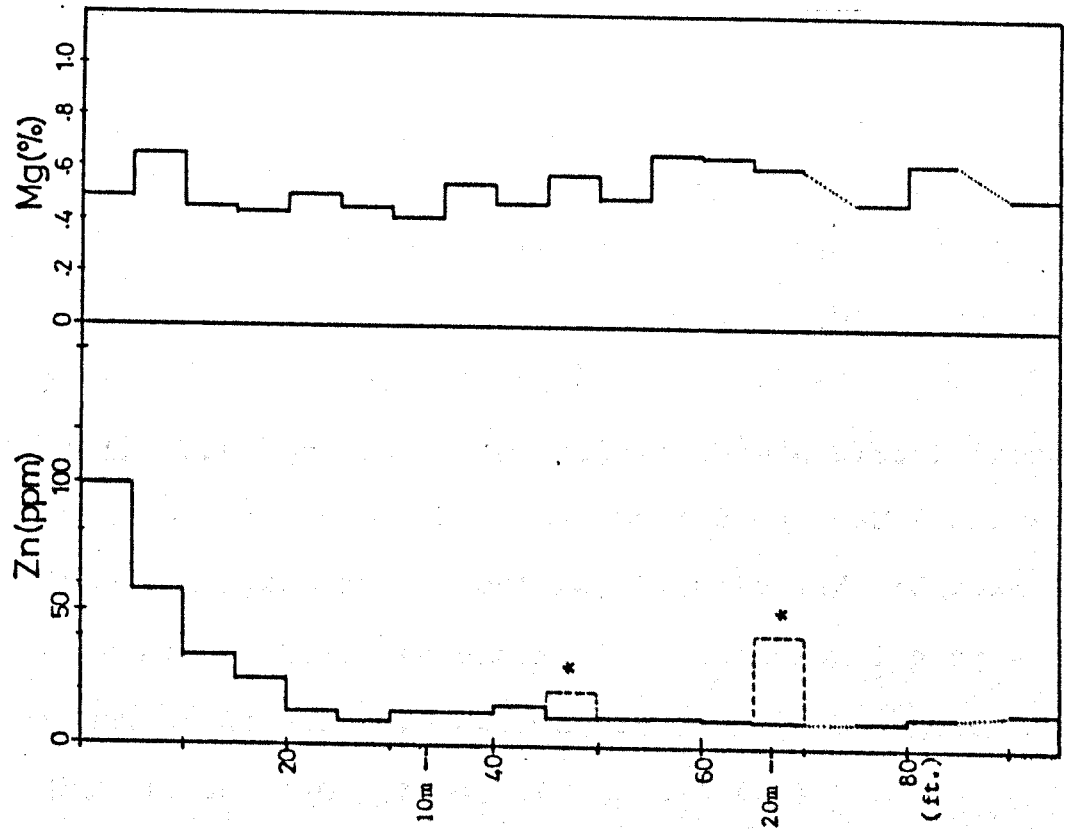


Figure 4.19: Averaged vertical profiles of Zn and Mg in footwall at Silvermines. Dotted lines (*) indicate single spurious values.

Zinc: Zinc generally remains below 20 ppm throughout the footwall rocks, except for the top 6 metres (20 ft.), where higher values are recorded. In Figure 4.19, the average Zn values increase steadily in this zone, from below 20 ppm to over 100 ppm in the immediate footwall to the ore horizon. Zinc values show a slight increase towards the top of the Muddy Reef even over 2 kilometres from the hydrothermal centre, in hole 76/3 (Figure 4.16, also Figure A.15, Appendix II). Occasional single spot highs of Zn are recorded deeper down in one hole (B8, around 110 metres, 360 to 380 ft.).

Magnesium: In all six vertical profiles, Mg remains below 1% throughout the Muddy Reef, and only increases in the top metre or so in several holes, on approaching the base of the dolomite breccia of the ore horizon. Figure 4.19 indicates that average values actually increase slightly downwards from 0.4% at 6 metres (20 ft.) to 0.6% at 18 metres (60 ft.) and below.

Strontium: Eighteen X.R.F. analyses for Sr in the footwall samples from two holes close to the B Zone mineralisation (B139, V1), indicate a steady drop in level upwards, from over 500 ppm 11 metres (35 ft.) below, to around 200 ppm immediately below the ore horizon (Figure 4.17).

4.2.3. Silvermines X.R.F. Data.

X-ray Fluorescence data for Mn, Fe, Zn, Pb, Ba, Sr, CaCO₃, Mg, SiO₂, Al₂O₃ and K₂O in six boreholes was

examined to allow comparison between individual elements and between A.A. and X.R.F. data for the four elements Mn, Fe, Zn and Mg. The locations of the six boreholes samples, along with the main geological features of the Silvermines deposits, are given on Figure 4.20.

Figures 4.21 to 4.24 summarise the vertical profiles of each of the elements on X.R.F., and allow a number of particular element associations to become apparent, linked in mineral phases or related minerals.

Good visual correlation exists between Zn, Pb and Ba, through their presence in sulphide and sulphate phases, in or near the mineralised horizon. Likewise, Al_2O_3 , SiO_2 and K_2O behave in similar fashion, linked via the presence of clay mineral impurities in the carbonates. Only in the presence of chert do they appear to show any independence (e.g. Bl44 @ 210-220m (700-750ft.)). Manganese and iron are linked mainly through their presence in carbonates, especially dolomite.

Calcium and magnesium show strongly contrasting behaviour, reflecting the varying proportions of calcite and dolomite, one substituting directly for the other, except to some degree in very argillaceous sediments (e.g. footwall Muddy Reef Limestone, Figure 4.23b), where mud content replaces a significant proportion of both carbonates.

Comparison between A.A. and X.R.F. analyses from the same samples was made by examining the ratio between the two, for each individual element, e.g. Mn(A.A.) :

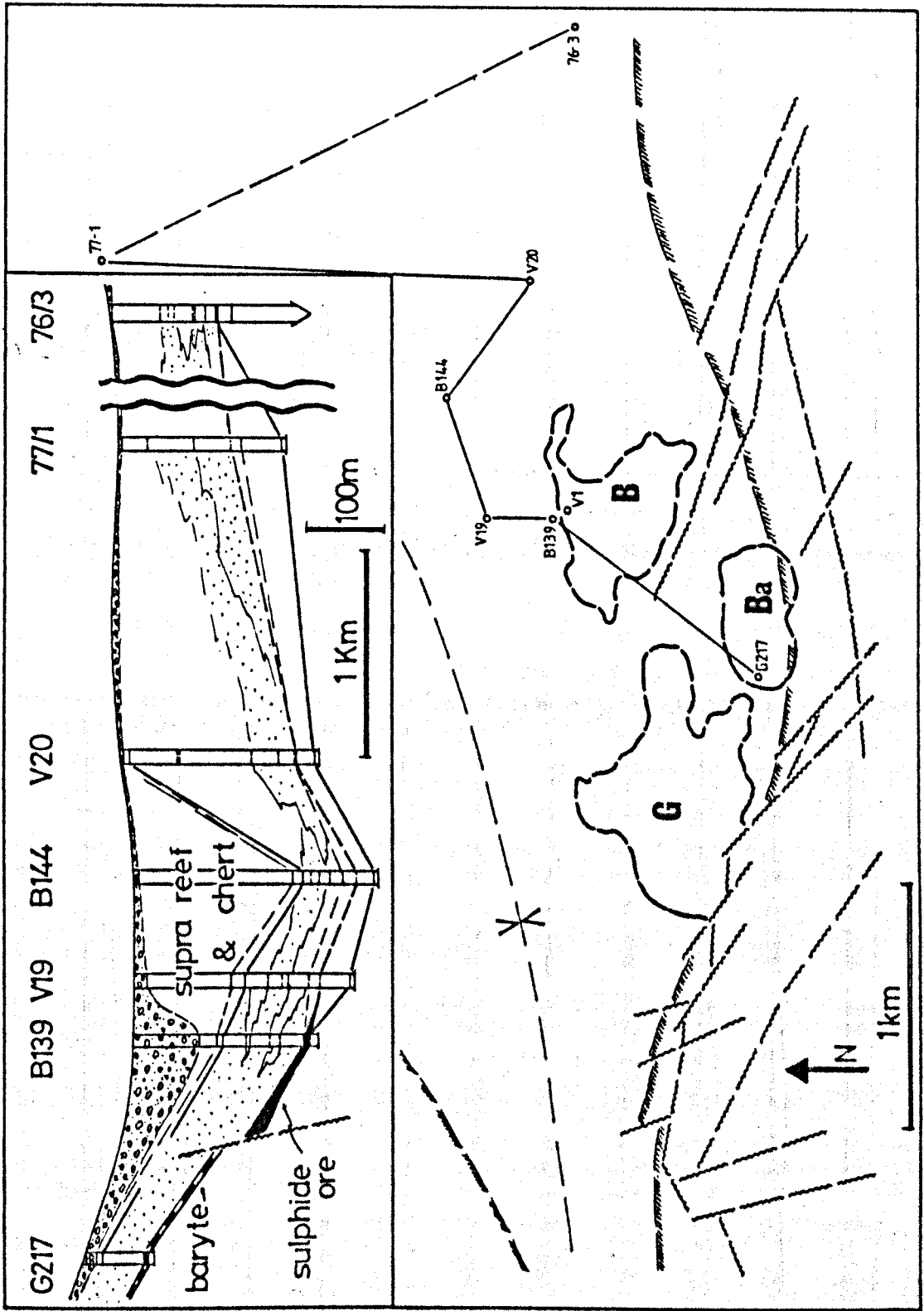


Figure 4.20: Location of borehole sections shown in Figures 4.21 to 4.31, with outline of main stratiform ore zones and suboutcrop of base of Waulsortian equivalent succession. Inset shows diagrammatic section joining each borehole (stipple is breccia horizon).

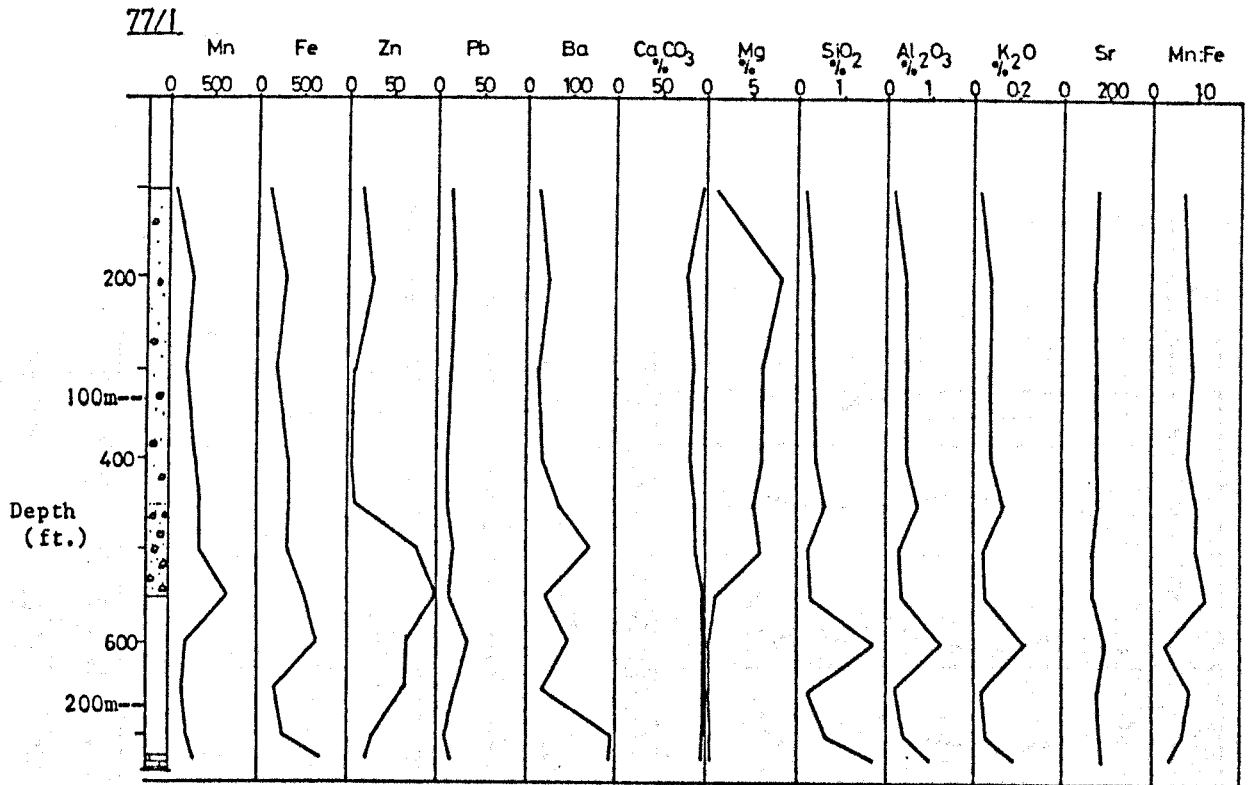


Figure 4.21: Vertical geochemical profile of X.R.F. data from borehole 77/1 at Silvermines. Lines join mid-points between adjacent samples. Data in ppm except where indicated. For key see Figure 4.3.

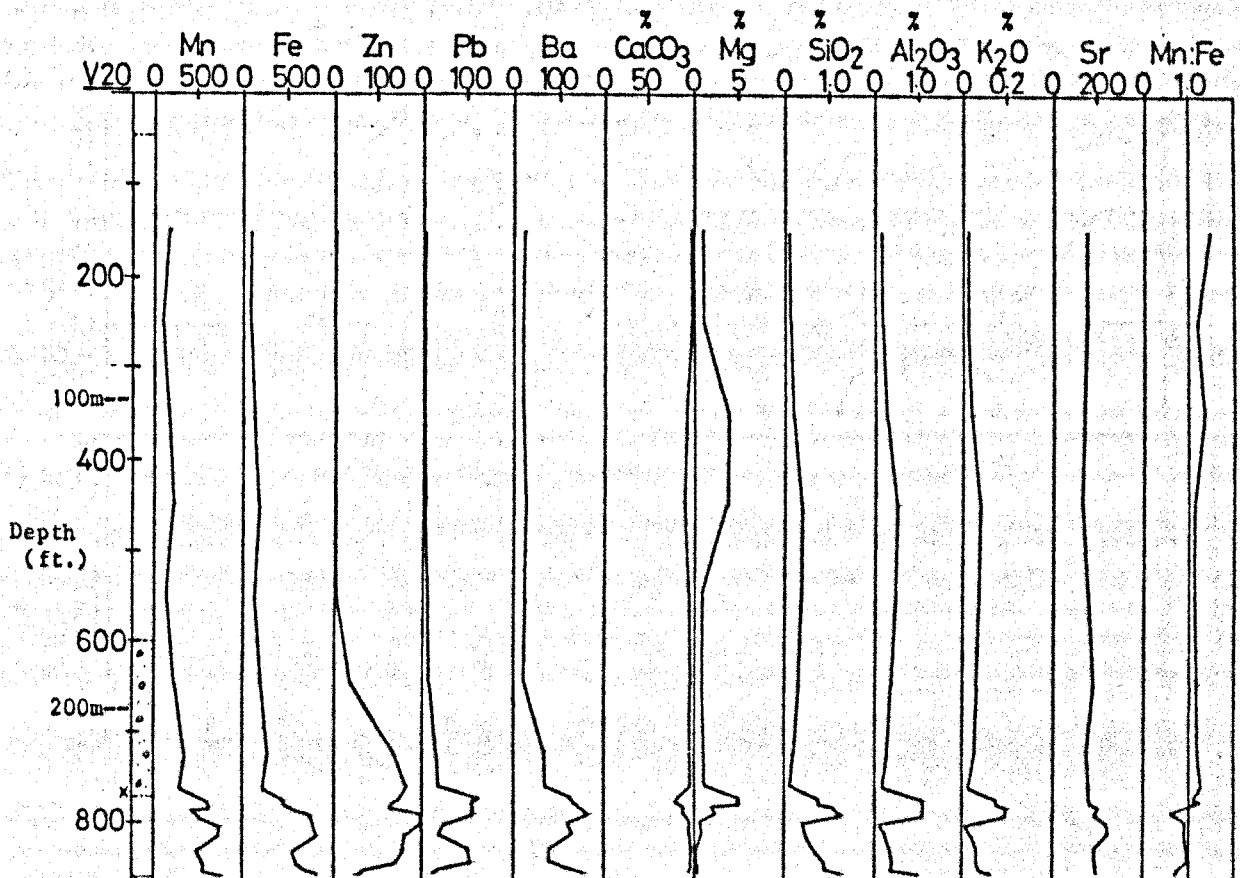


Figure 4.22: Vertical geochemical profile of X.R.F. data from borehole V20 at Silvermines. Lines join mid-points between adjacent samples. Data in ppm except where indicated. For key see Figure 4.3.

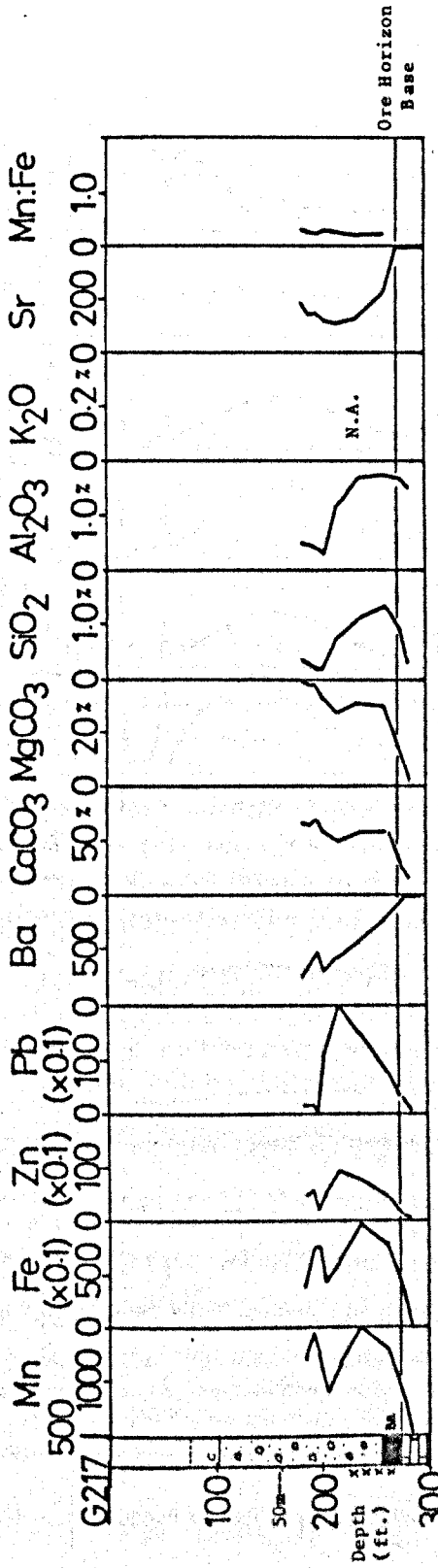


Figure 4.23a: Vertical geochemical profile of X.R.F. data from borehole G217 at Silvermines. Lines join mid-points between adjacent samples. Data in ppm except where indicated. For key see Figure 4.3.

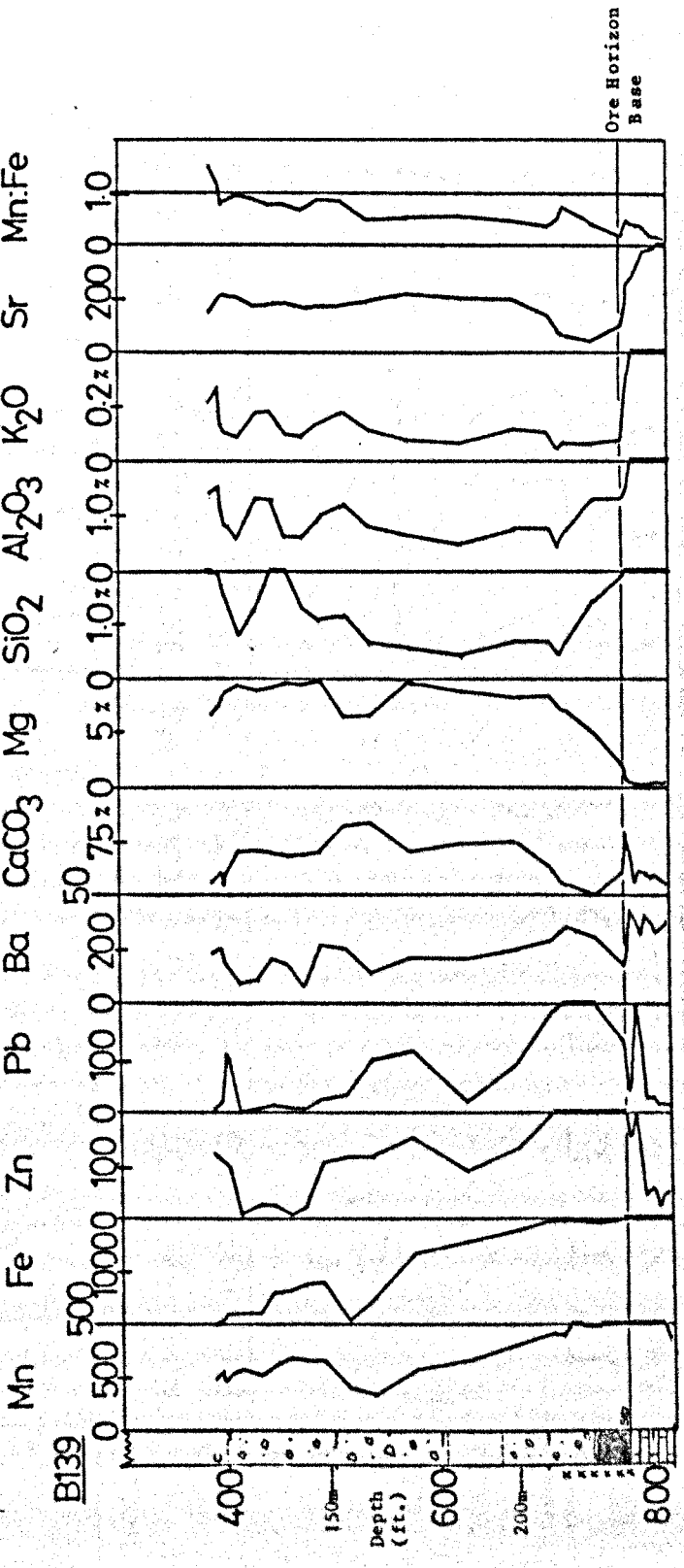


Figure 4.23b: Vertical geochemical profile of X.R.F. data from borehole B139 at Silvermines. Lines join mid points between adjacent samples. Data in ppm except where indicated. For key see Figure 4.3.

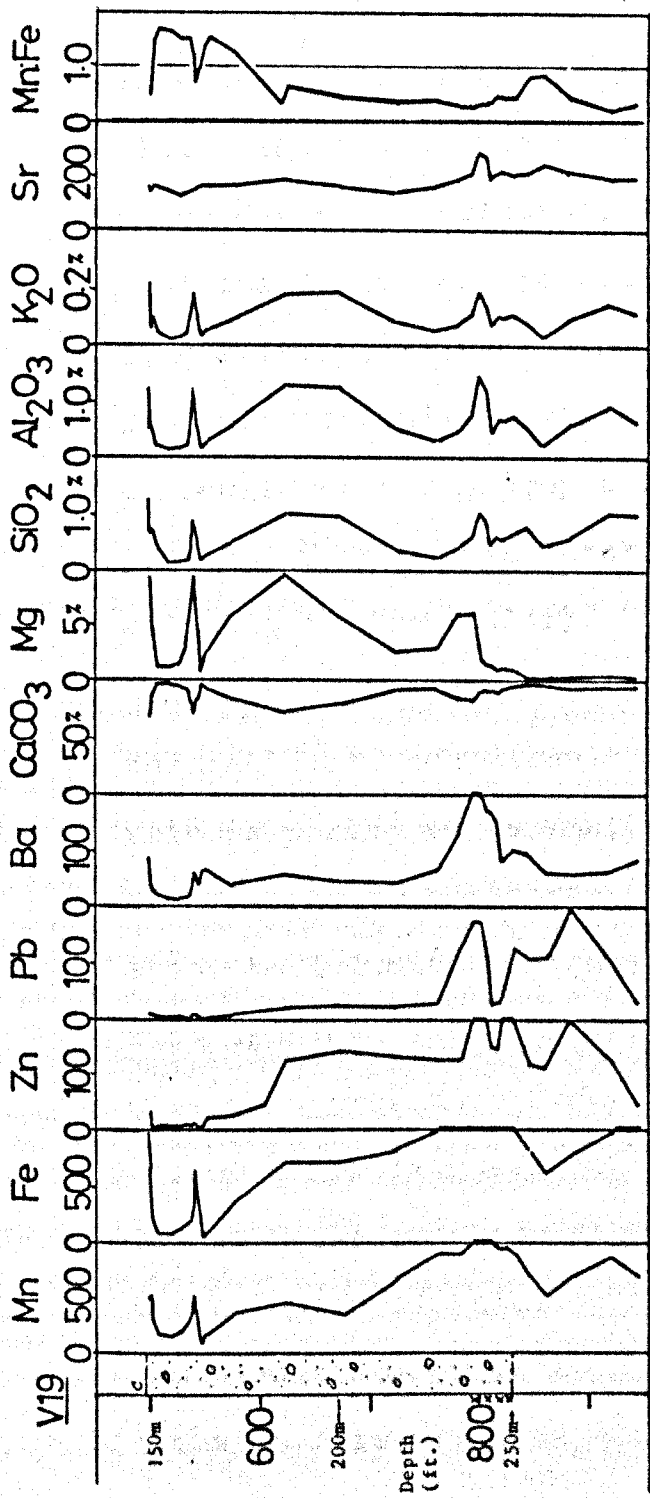


Figure 4.24a: Vertical geochemical profile of X.R.F. data from borehole V19 at Silvermines, for key see Figure 4.3.

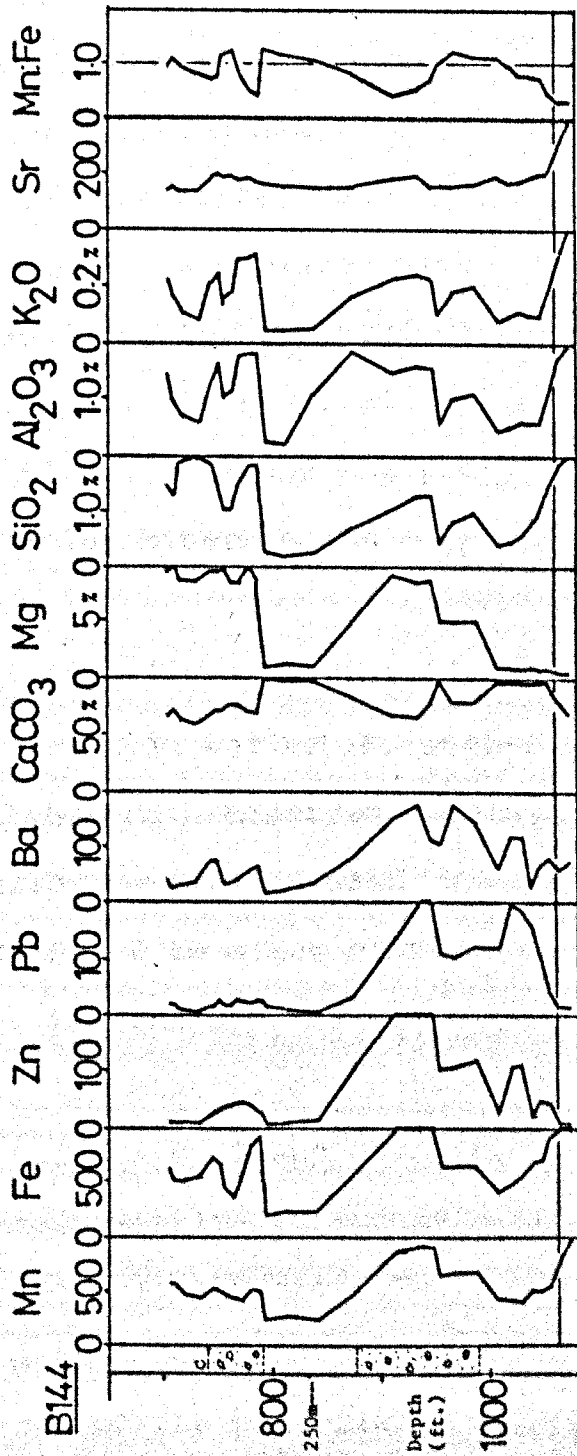


Figure 4.24b: Vertical geochemical profile of X.R.F. data from borehole B144 at Silvermines. For key see Figure 4.3.

Mn(X.R.F.). This follows the assumption that the X.R.F. analysis represents the total content in the rock, and the A.A. analysis the acid-soluble portion. This ratio is not consistent between samples, and varies from 1 (where both results are the same) to less than 0.2. The former case indicated that complete leaching of the element in question has taken place during dissolution, whereas the latter case indicated that most of the element is associated with some relatively insoluble phase (e.g. Fe with pyrite). The main controlling variables appear to be total carbonate content, proportion of dolomite and the proportion of insoluble material (clay minerals and sulphide in particular).

In each of the sections examined (Figures 4.25 to 4.30), the ratio of each element between A.A. and X.R.F. analysis is portrayed as r_{Mn} , r_{Fe} and r_{Mg} . Recorded levels of Mg are also presented to allow comparison with absolute dolomite content, $(Mn+Fe)/2$ to allow comparison with absolute levels of Mn and Fe, and $SiO_2+Al_2O_3$ to give an approximate index for clay mineral content.

Zinc is not examined because of its dominant association with the sulphide phase, only weakly leached by the hot acid dissolution technique (see Chapter Two).

No single, clear patterns emerge from these comparisons as often two, or all three of the potential controlling variables are closely related. For instance, increased Mg content is usually accompanied by parallel

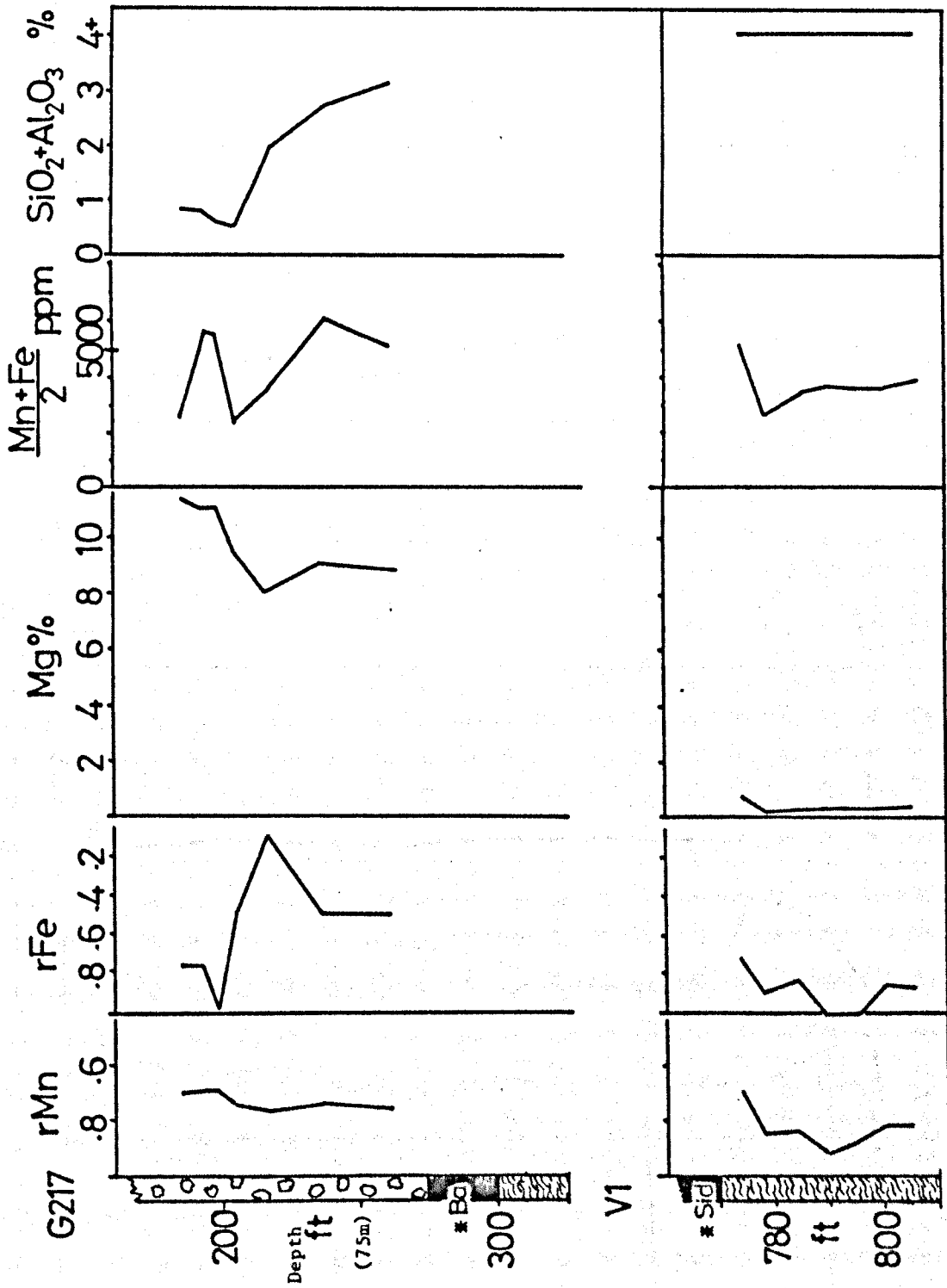


Figure 4.25: Ratio of acid-soluble to total Mn and Fe (represented by rMn and rFe, see text) in vertical profiles of Boreholes G217 and V1 at Silvermines. For key see Figure 4.31.

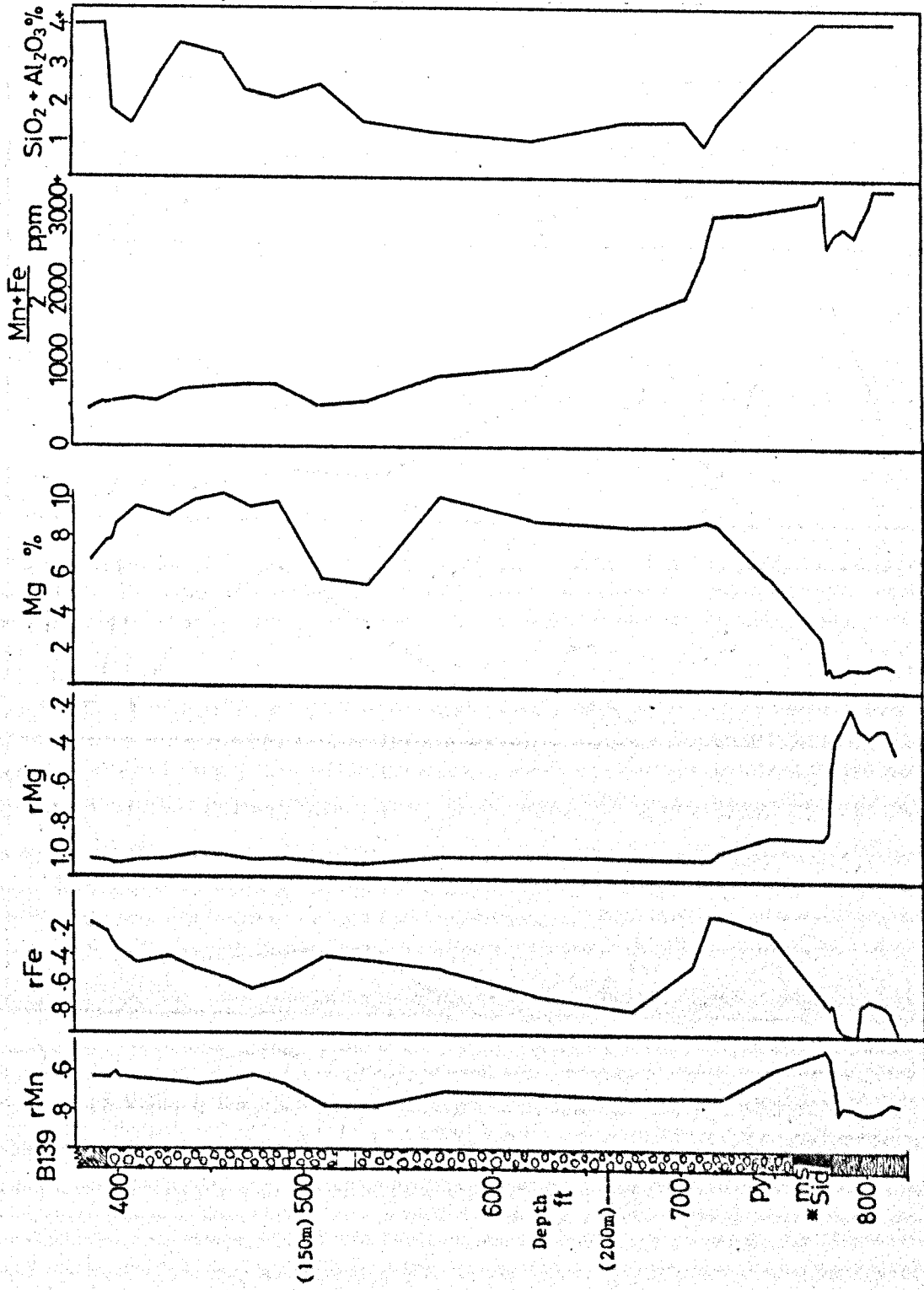


Figure 4.26: Ratio of acid-soluble to total Mn, Fe and Mg (represented by rMn, rFe and rMg, see text) in borehole B139 at Silvermines. Lines join mid-points between adjacent samples. For key see Figure 4.31.

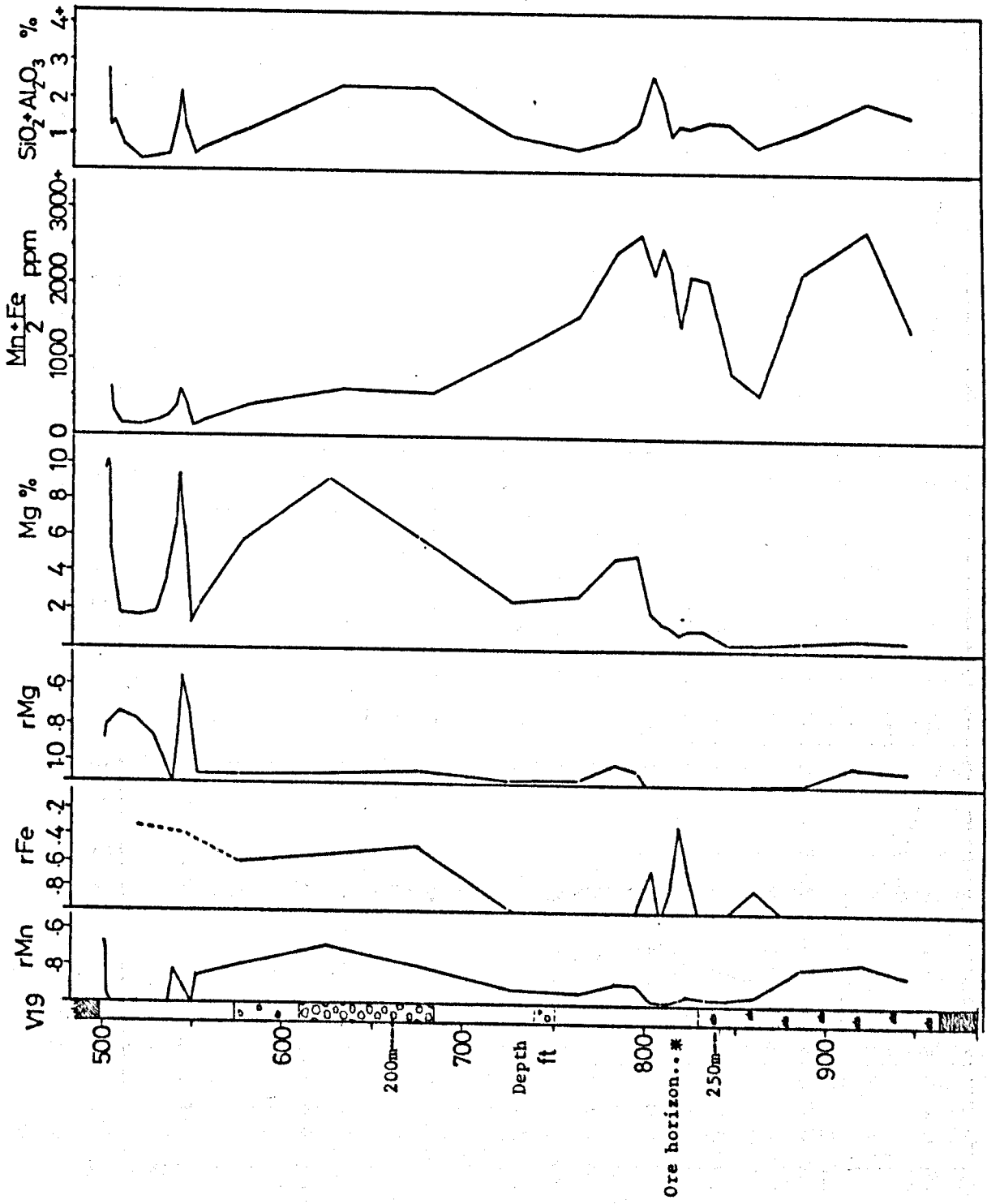


Figure 4.27: Ratio of acid-soluble to total Mn, Fe and Mg (represented by rMn, rFe and rMg, see text) in borehole V19 at Silvermines. Lines join mid-points between adjacent samples. Not all samples analysed for Fe, hence broken line at top of profile. For key see Figure 4.31.

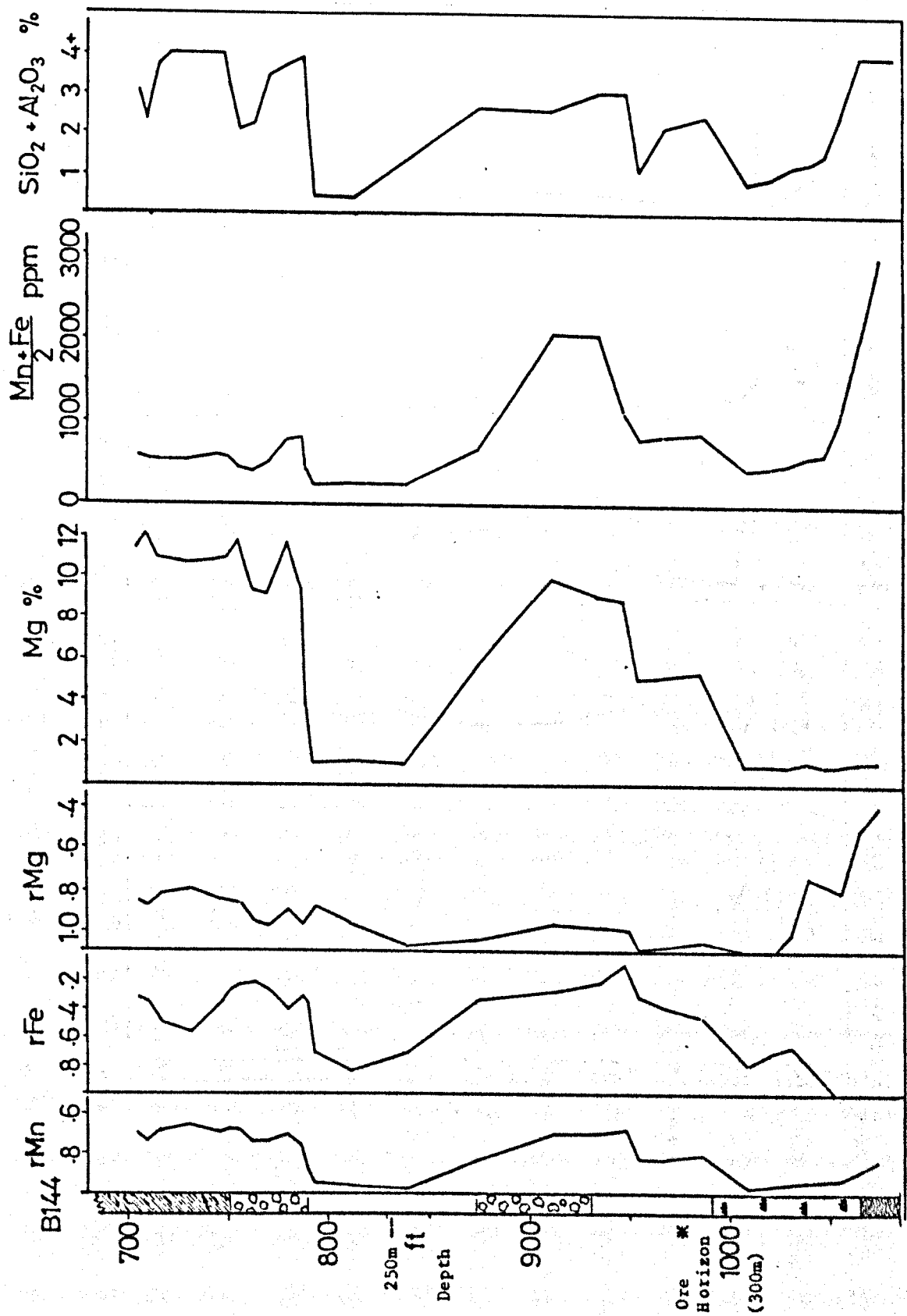


Figure 4.28: Ratio of acid soluble to total Mn, Fe and Mg (represented by rMn, rFe and rMg, see text) in borehole B144 at Silvermines. Lines join mid-points between adjacent samples. For key see Figure 4.31.

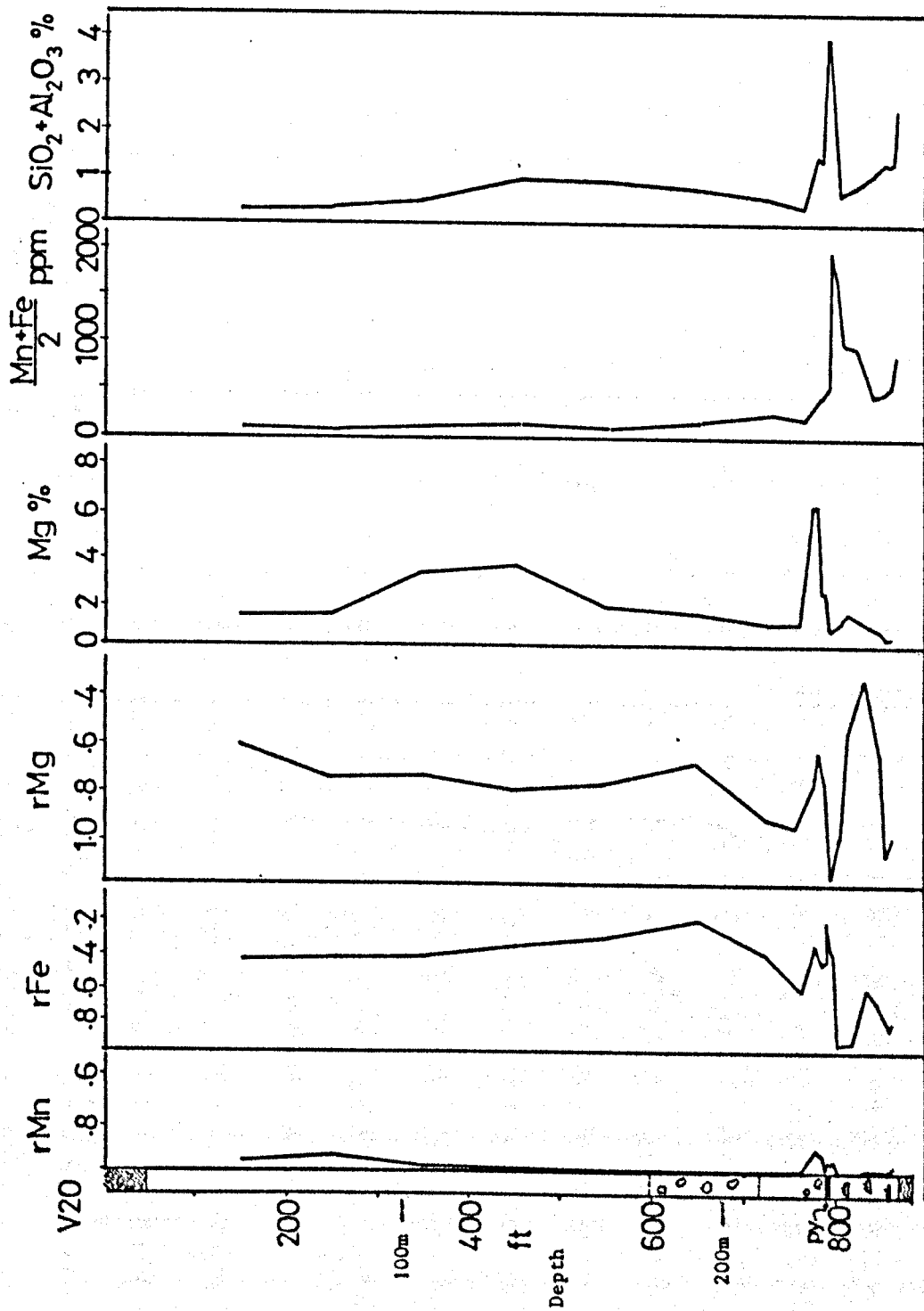


Figure 4.29: Ratio of acid soluble to total Mn, Fe and Mg (represented by rMn, rFe and rMg, see text) in borehole V20 at Silvermines. Lines join mid-points between adjacent samples. For key see Figure 4.31.

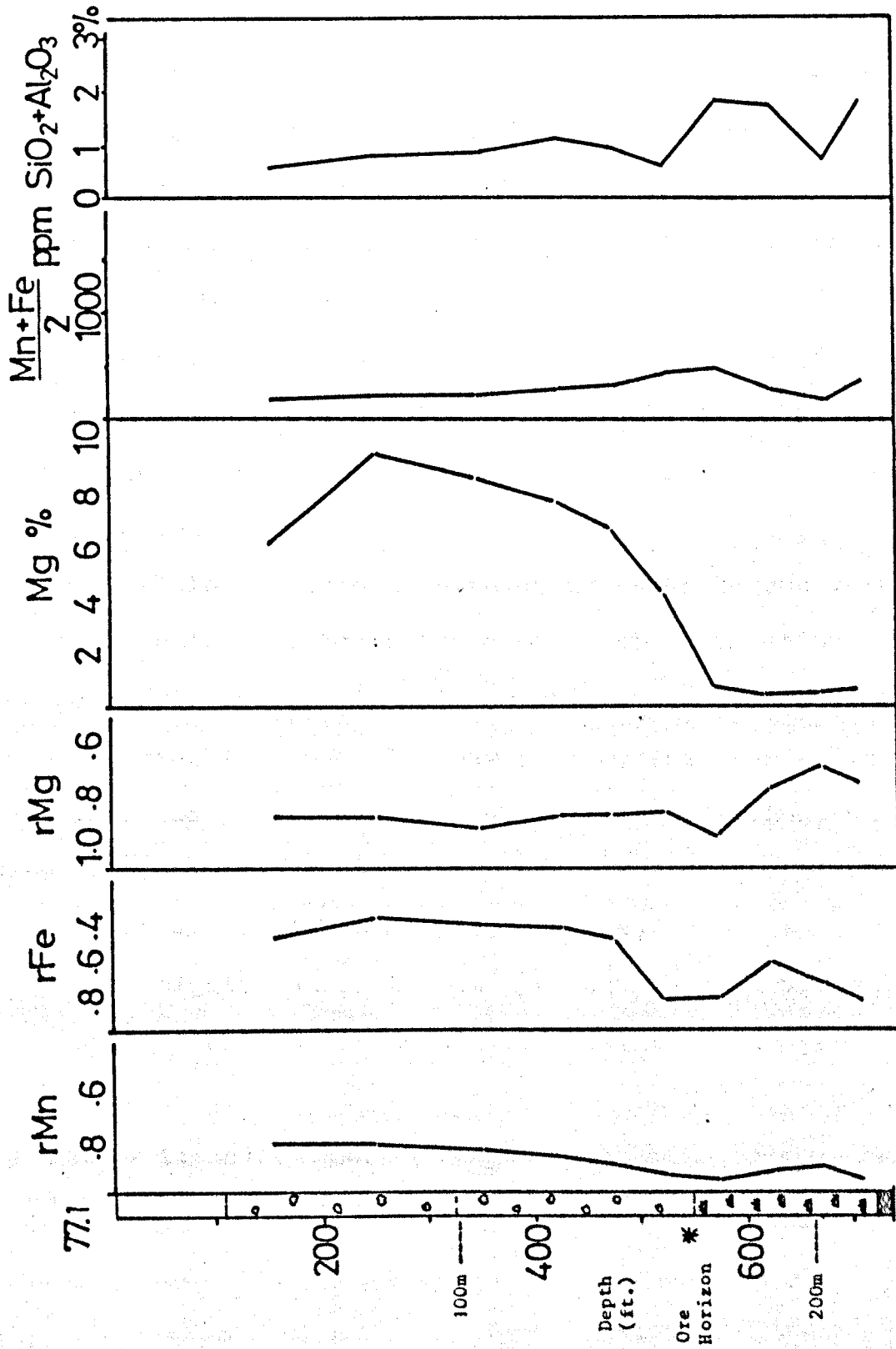


Figure 4.30: Ratio of acid soluble to total Mn, Fe and Mg (represented by rMn, rFe and rMg, see text) in borehole 77.1 at Silvermines. Lines join mid-points between adjacent samples. For key see Figure 4.31.

increases in clay content ($\text{SiO}_2 + \text{Al}_2\text{O}_3$) and $(\text{Mn} + \text{Fe})/2$.

The ratio r_{Mn} is high, almost one, in most limestone samples, and drops when the dolomite and/or clay content increases. The behaviour of iron is similar, but more erratic, probably because of minor pyrite content in some samples. Although the pyrite content is not indexed, its presence is generally signified by a drop in r_{Fe} .

The ratio r_{Mg} remains high in the majority of samples, both limestone and dolomite, and only drops significantly in the footwall Muddy Reef and Stromatactis Reef Limestones.

Possible differences between the average r_{Mn} value in each hole (and for outcrop samples), indicating a gradual decrease in acid-soluble manganese close to the mine (Figure 4.31) may reflect the overall increase in dolomite and mud content in this direction, whether from primary or other sources. Iron does not appear to behave in the same way, however,

The significance of this apparent lateral variation in acid-soluble Mn is considered further in Chapter 6, and statistical correlation between the X.R.F. and A.A. data is undertaken in Chapter 5.

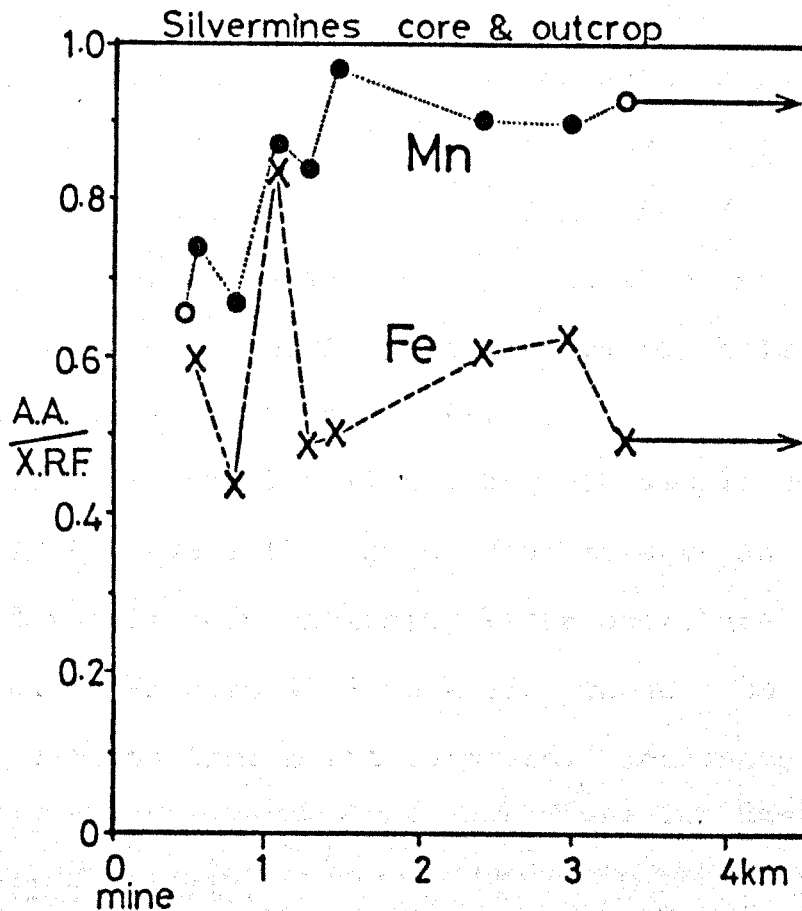
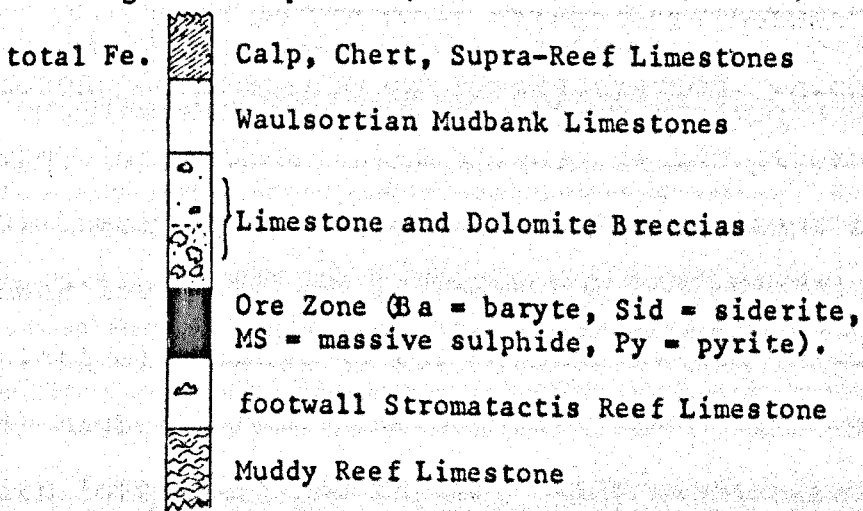


Figure 4.31: Ratio of acid soluble to total Mn and Fe (represented by A.A./X.R.F. values) variation with distance from the centre of the Silvermines deposit. Core data from samples portrayed in Figures 4.25 - 4.30, solid line represents average of distal outcrop samples, and single outcrop site (hollow circle near mine) not analysed for total Fe.



Key for Figures 4.25 to 4.30.

4.3.1. Ballinalack.

For comparison with the Silvermines data, a number of boreholes at Ballinalack were examined to investigate the vertical distribution of Mn, Fe, Zn and Mg within the host mudbanks. Sodium was also investigated in this instance. The location of each borehole sampled is given in Figure 4.32.

Nine vertical profiles with 5 or more sample points at irregular intervals throughout the Waulsortian Mudbank and immediately enclosing limestones, are displayed in Figures 4.33 to 4.35. These also represent a crude section from north to south. Manganese and iron data for two short east-west sections are also shown (figure 4.36).

No obvious pattern emerges in the vertical distribution of Mn and Fe, in contrast to the Silvermines data:

- 1) there is no obvious basal enrichment, except perhaps in boreholes B83, B89 and B51;
- 2) there is no apparent direct link between the trace element enrichments and mineralisation, which are both irregularly distributed throughout the mudbank;
- 3) there is no apparent N-S trend, except for the lower levels at the southern end, in BN80/1, which is relatively distal to the mineralisation (Figure 4.32);
- 4) higher levels, particularly of Fe, are associated with 'off-reef' and the enclosing bioclastic limestones, represented on the sections by unfilled bars;
- 5) magnesium is consistently low, below 1% throughout

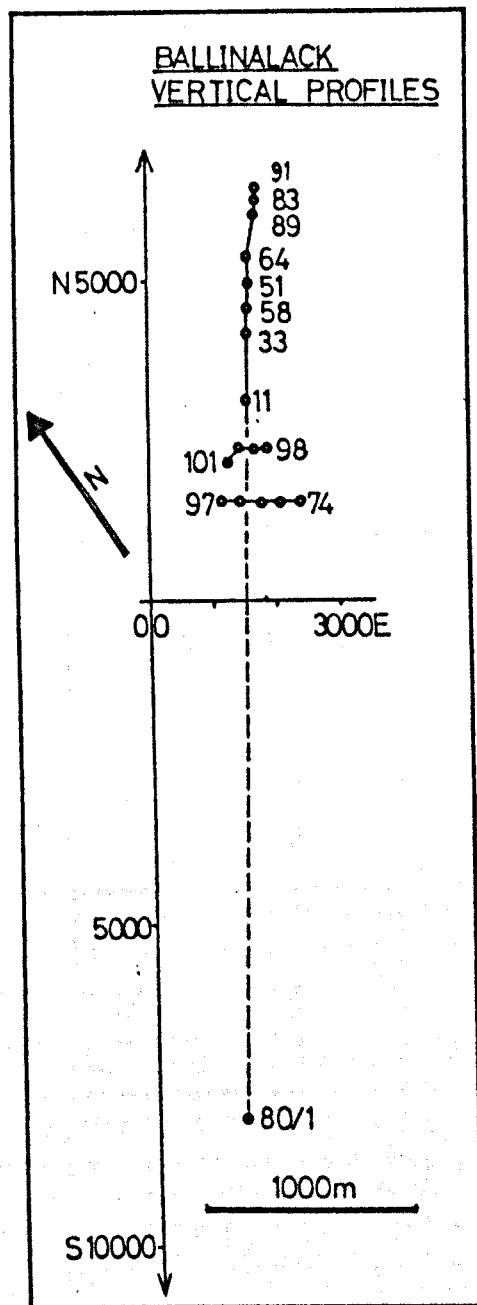


Figure 4.32: Location of boreholes profiled in Figures 4.33 to 4.36 on Ballinalack drill grid. Below is key for these diagrams.

- CCalp Limestones
- U.B.L.Upper Bioclastic Limestones
- M.B.Waulsortian Mudbank Limestones
- XMineralisation
- DolDolomite
- L.B.L.Lower Bioclastic Limestones

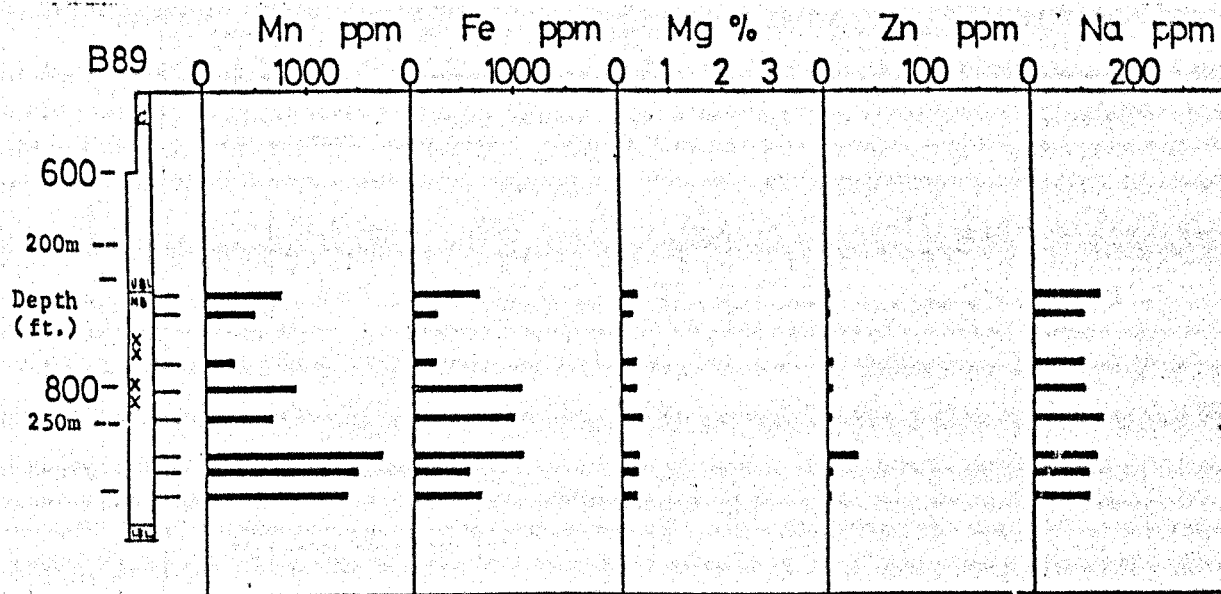
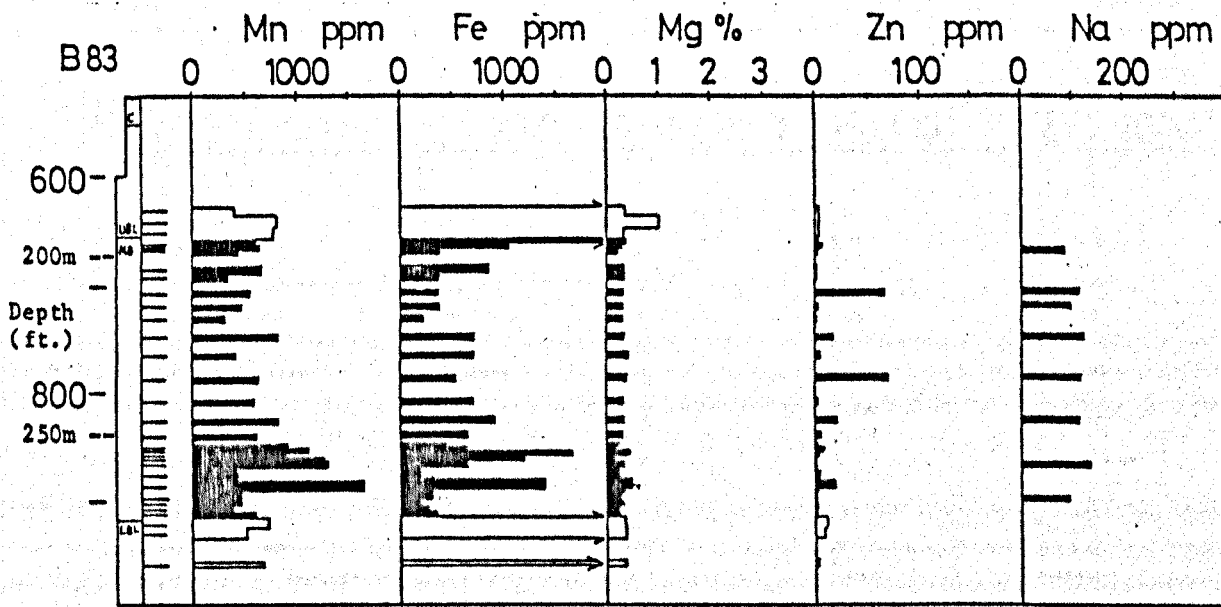
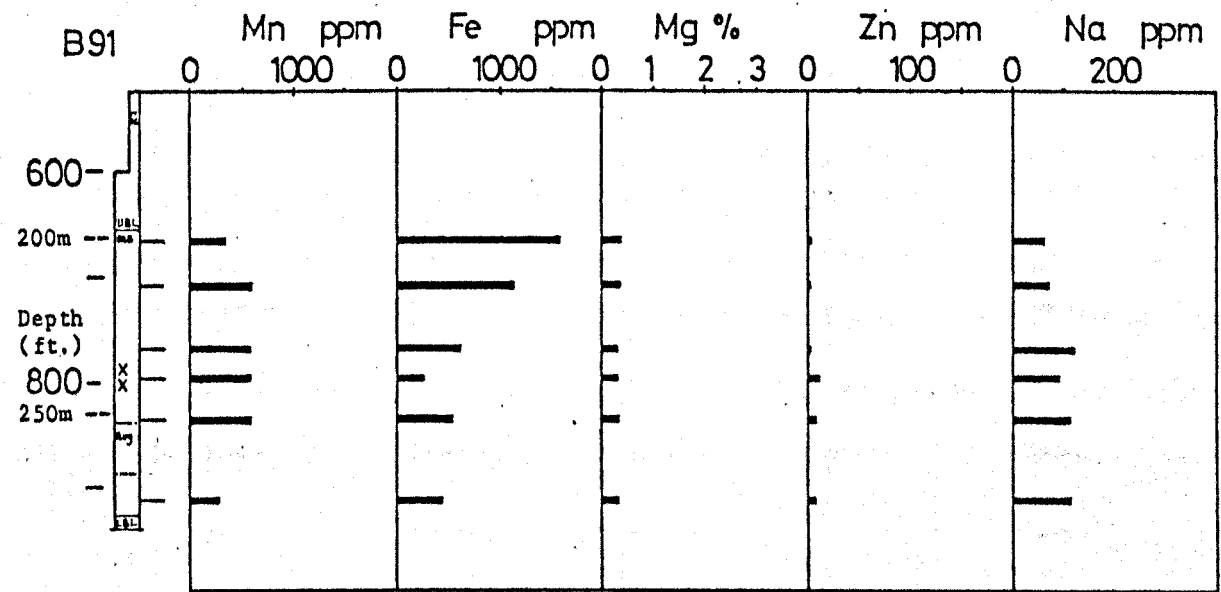


Figure 4.33: Vertical geochemical profiles of boreholes B91, B83 and B89 at Ballinalack. For key, see Figure 4.32.

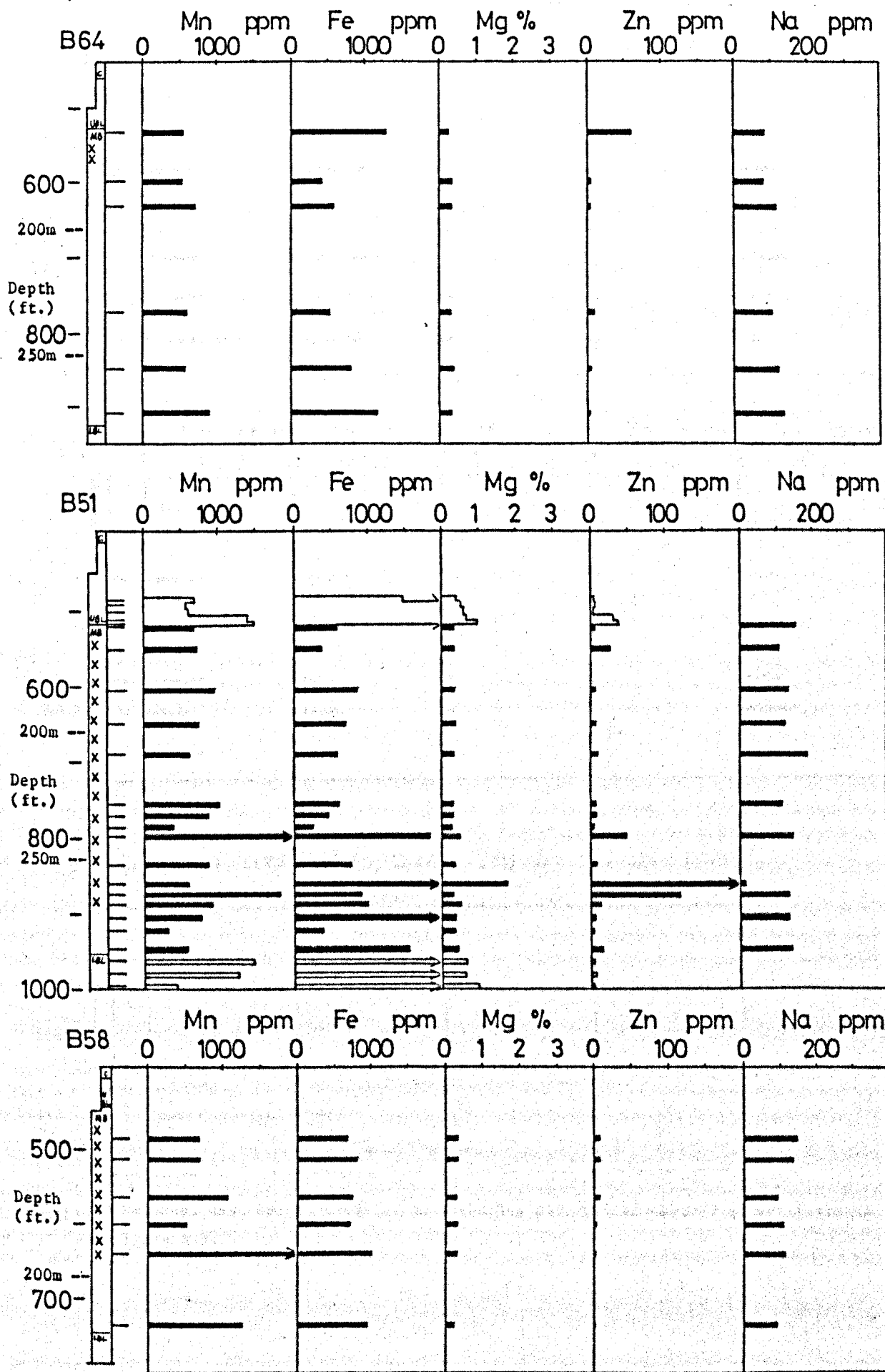


Figure 4.34: Vertical geochemical profiles of boreholes B64, B51 and B58 at Ballinalack. For key see Figure 4.32.

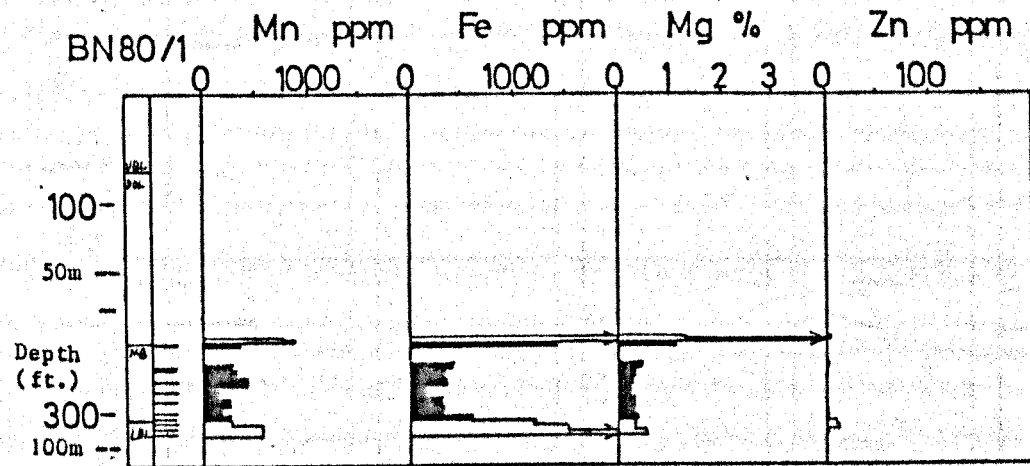
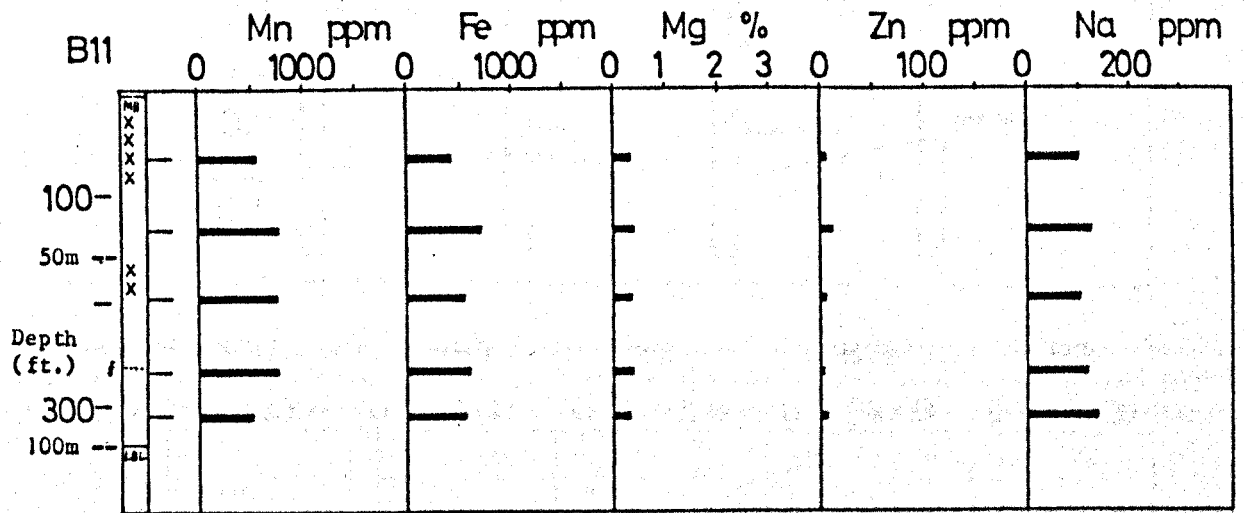
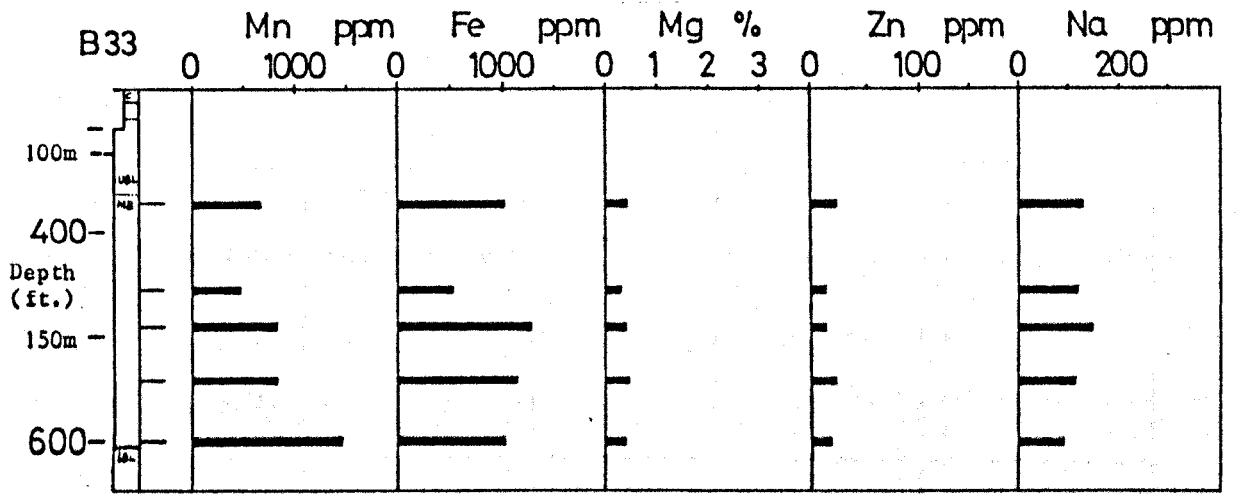


Figure 4.35: Vertical geochemical profiles of boreholes B33, B11 and BN80/1 at Ballinalack. For key see Figure 4.32.

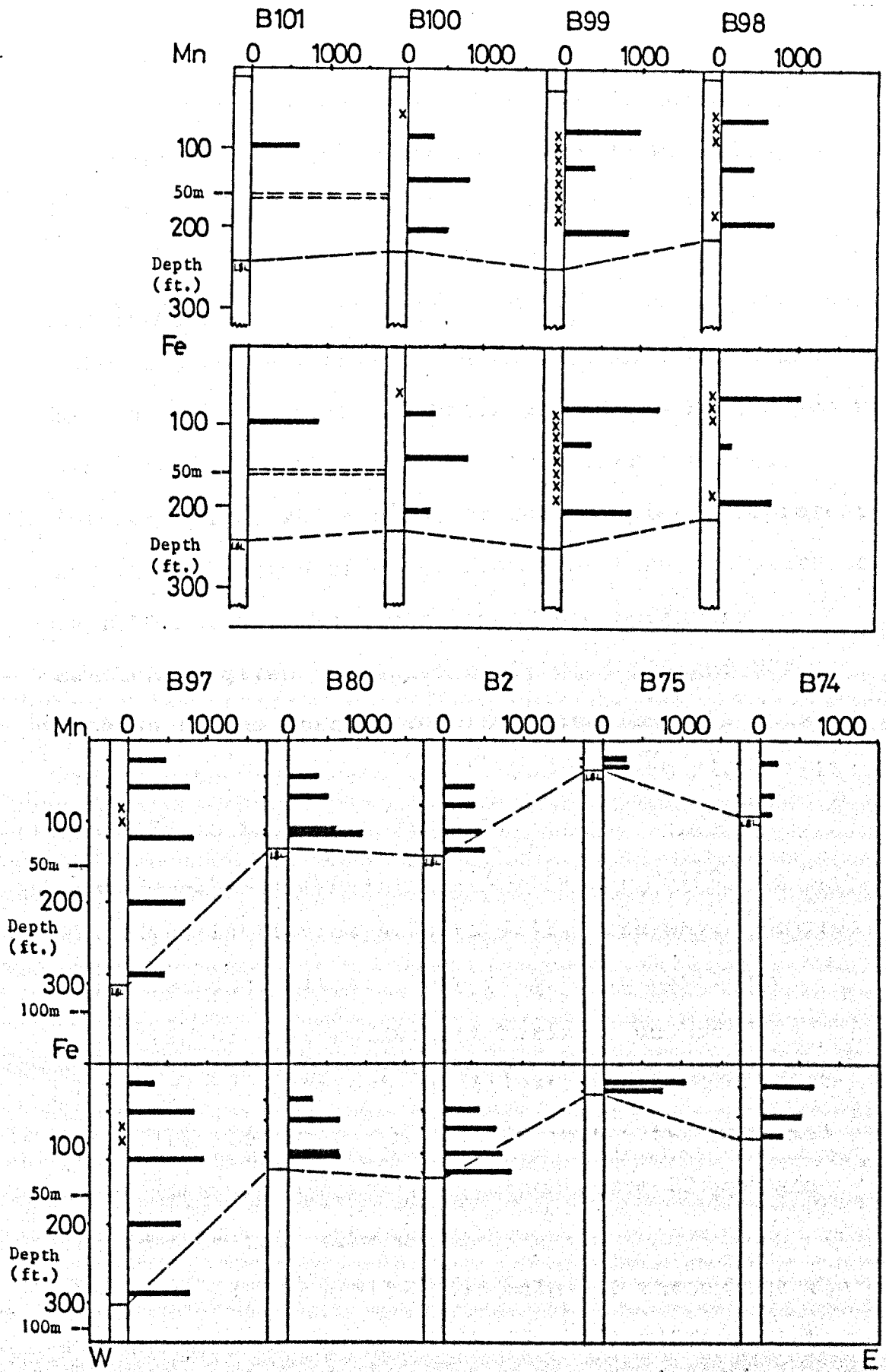


Figure 4.36: Vertical profiles of boreholes B101, B100, B99 and B98 (above), and B97, B80, B2, B75 and B74 (below) at Ballinalack, arranged as E-W sections. Only Mn and Fe data shown. For key see Figure 4.32.

the mudbank, and no regular patterns emerge from the Zn or Na data. Considerably reduced Na content is observed in the one sample with over 1% Mg (B51 @ 870 ft.).

4.4.1. Keel.

Also for comparison with the Silvermines and nearby Ballinalack deposits, 18 holes around the Keel deposit were profiled with samples at irregular intervals (either split, whole core, or chip samples), representing given lengths of core, from less than one metre to over 50 metres. The location of the boreholes sampled is given in Figure 4.37, with LF9 and K72 closest to the stratiform mineralisation (LF9 coincident with the baryte zone), and K162 to K164, LF18 and K135 to K136 most distant.

The analytical results for $(\text{Mn}+\text{Fe})/2$, Mn:Fe and Mg are displayed in Figures 4.38 to 4.43, with whole samples shown as single lines, chip samples as bars, and dolomitic or Reef Equivalent horizons unshaded.

Zinc values, although not illustrated, are consistently low, below 10 ppm, except in the two proximal holes (LF9 and K72), where values above 20 ppm are recorded in four samples.

Magnesium is generally low, below 1% throughout the mudbank samples, except in a few holes (LF43, where a thick dolomite zone is present, K135, K136, K137).

In the $(\text{Mn}+\text{Fe})/2$ data, there is a vague suggestion of basal enrichment of the mudbank in several holes.

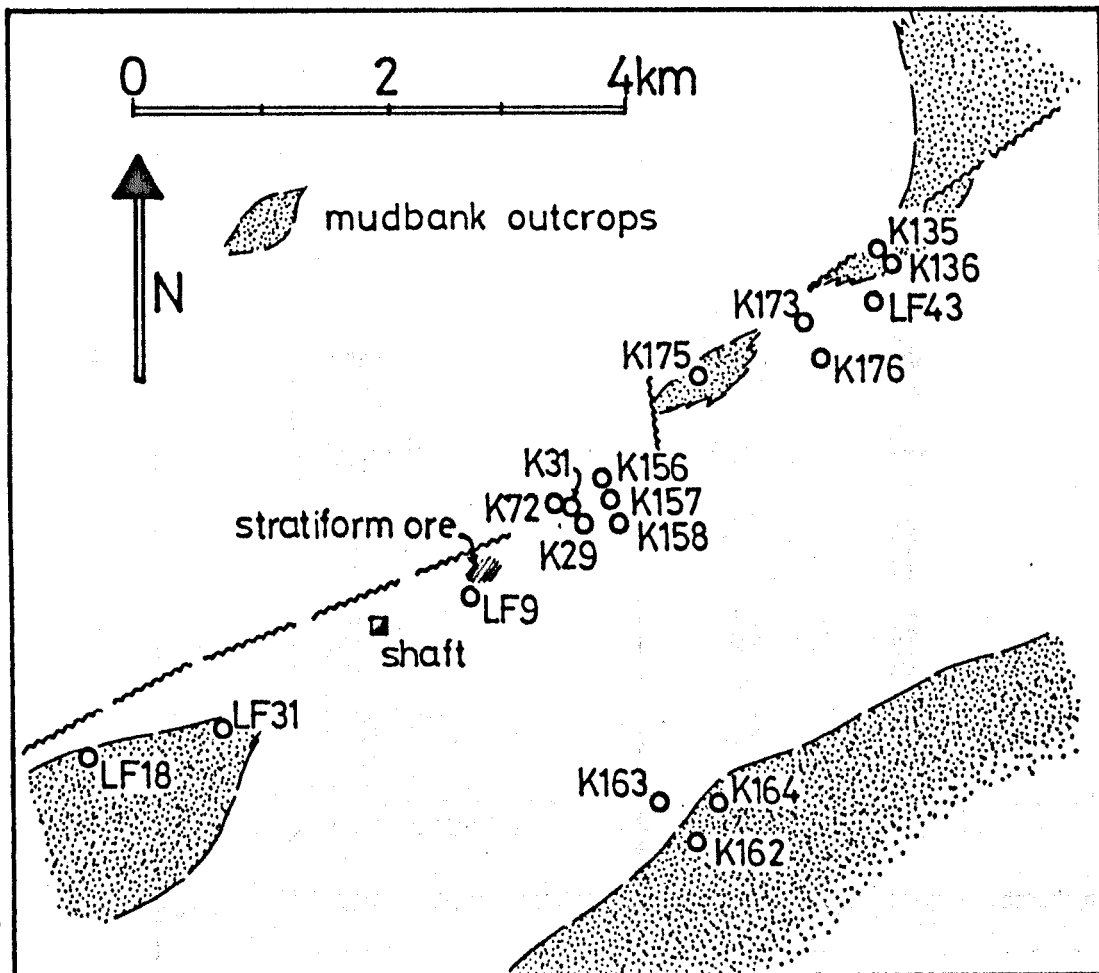
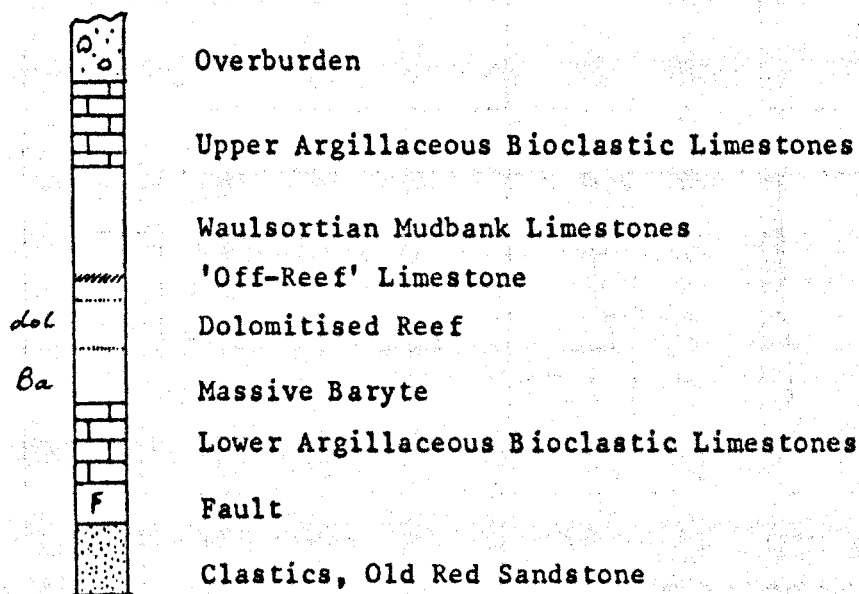


Figure 4.37: Location of boreholes sampled at Keel, displayed on Figures 4.38 to 4.43, with outline of mudbank outcrops and Keel Fault. Below is key for these Figures.



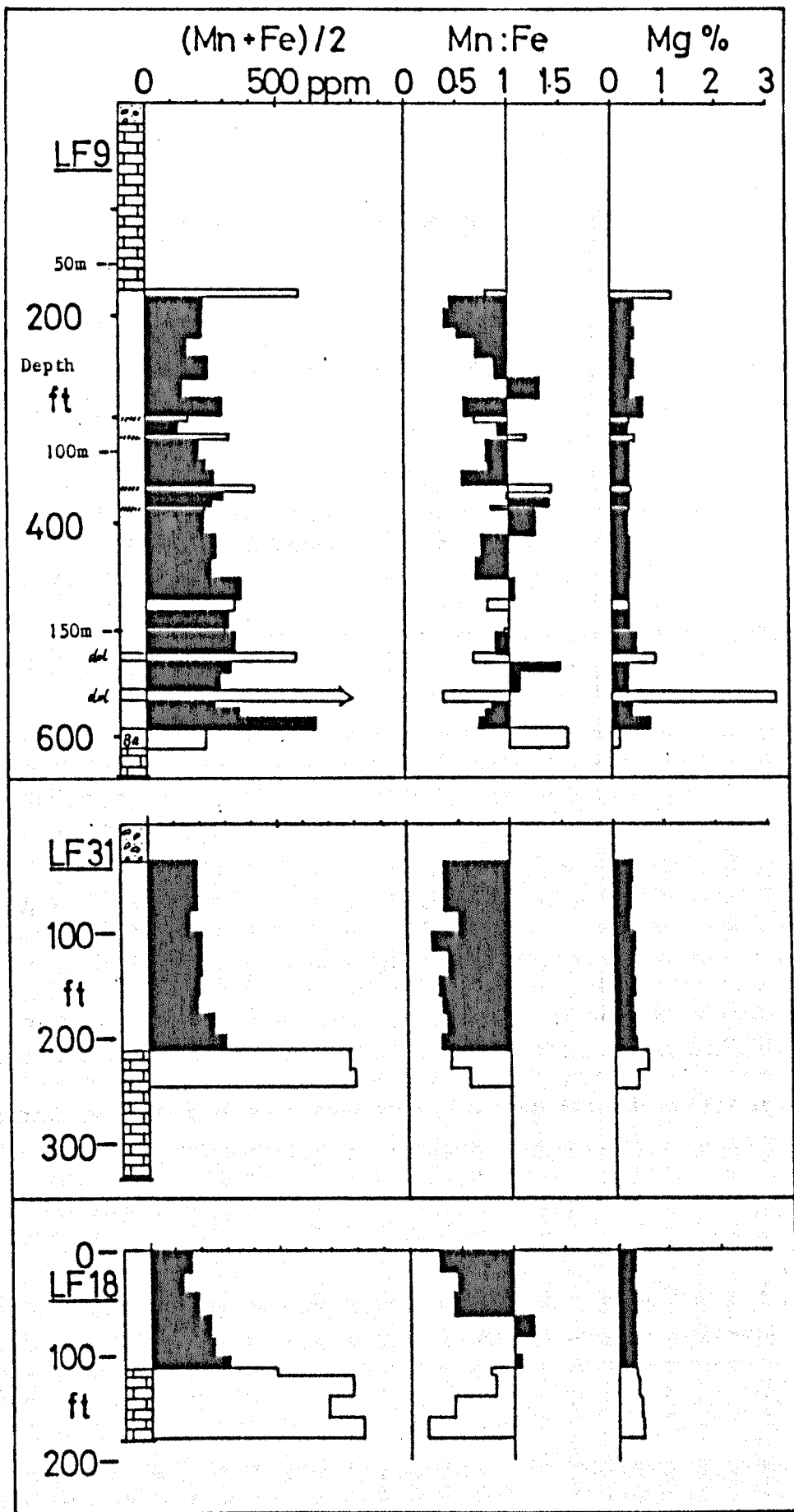


Figure 4.38: Vertical geochemical profiles of boreholes LF9, LF31 and LF18 at Keel. For key see Figure 4.37. Only Waulsortian Mudbank bars are shaded.

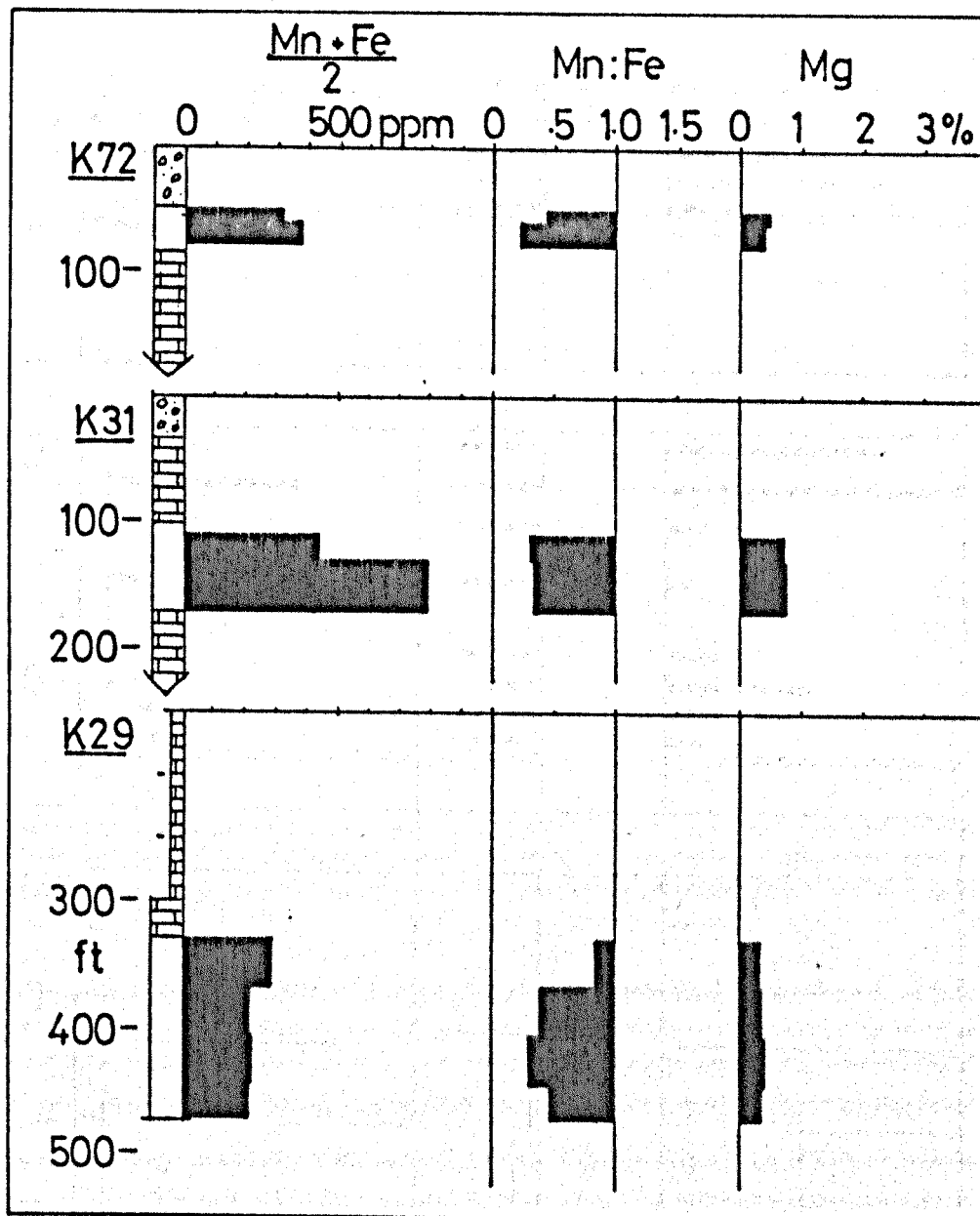


Figure 4.39: Vertical geochemical profiles of boreholes K72, K31 and K29 at Keel. For key see Figure 4.37.

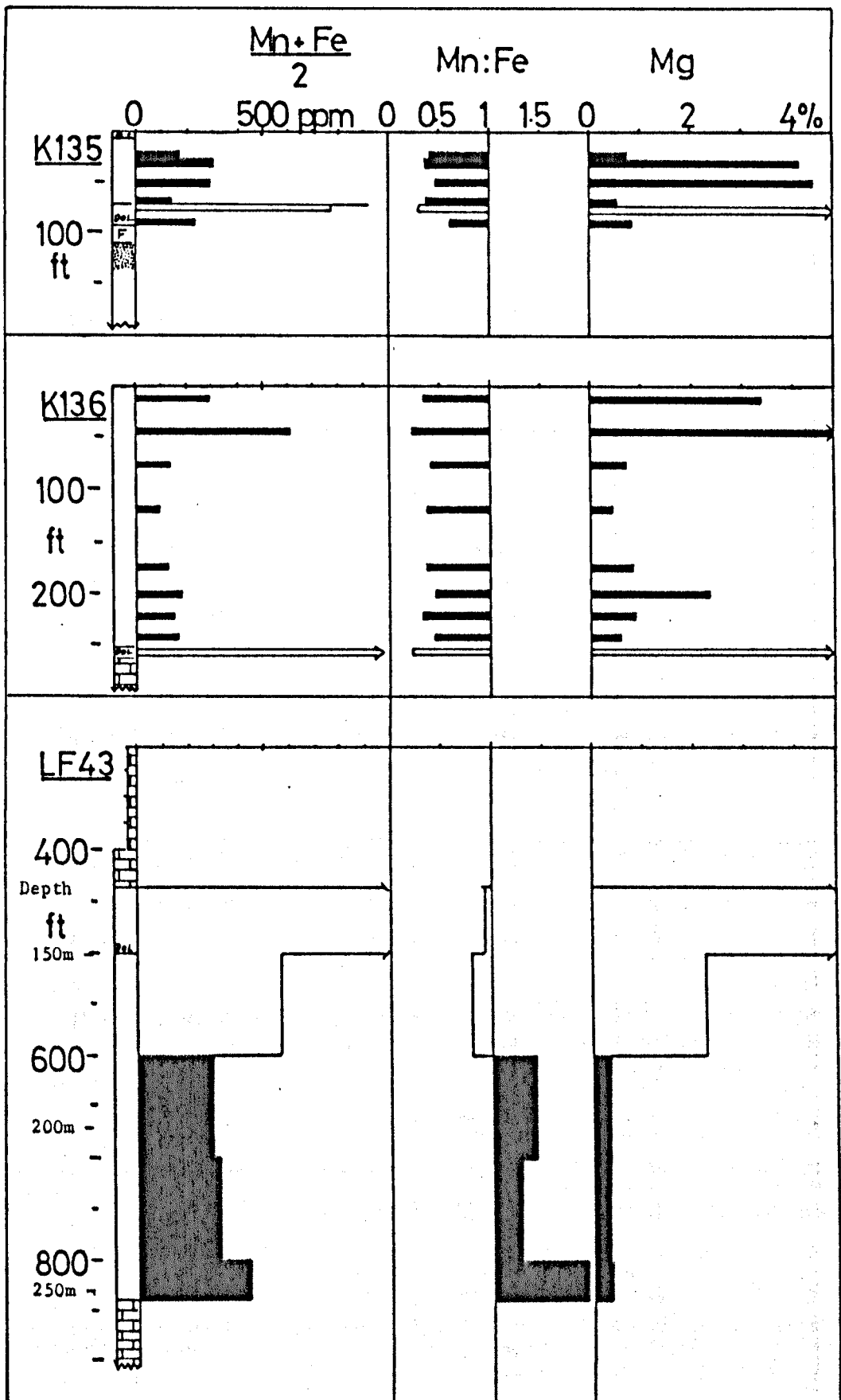


Figure 4.40: Vertical geochemical profiles of boreholes K135, K136 and LF43 at Keel. For key see Figure 4.37. Only Waulsortian Mudbank bars are shaded.

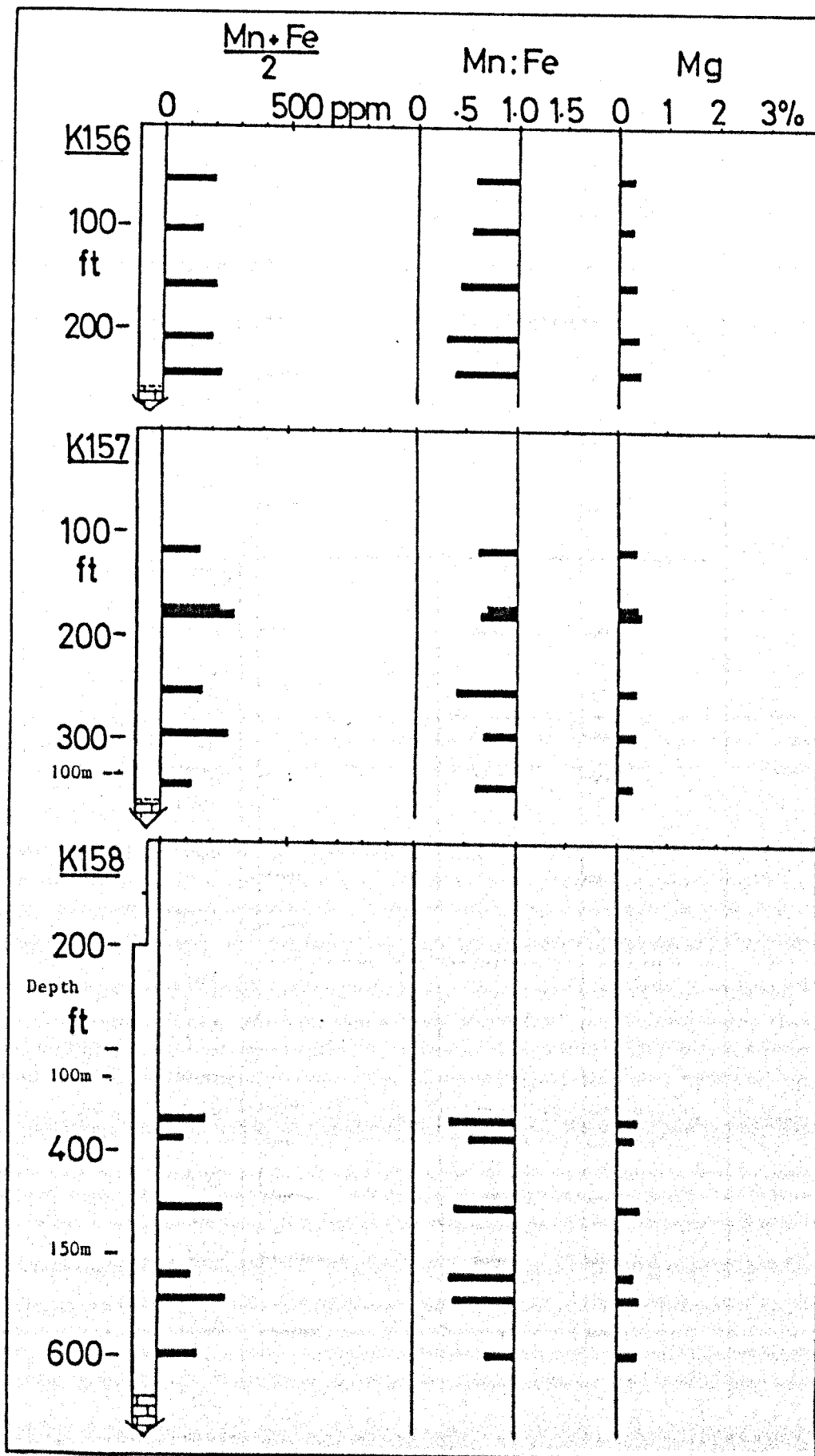


Figure 4.41: Vertical geochemical profiles of boreholes K156, K157 and K158 at Keel. For key see Figure 4.37.

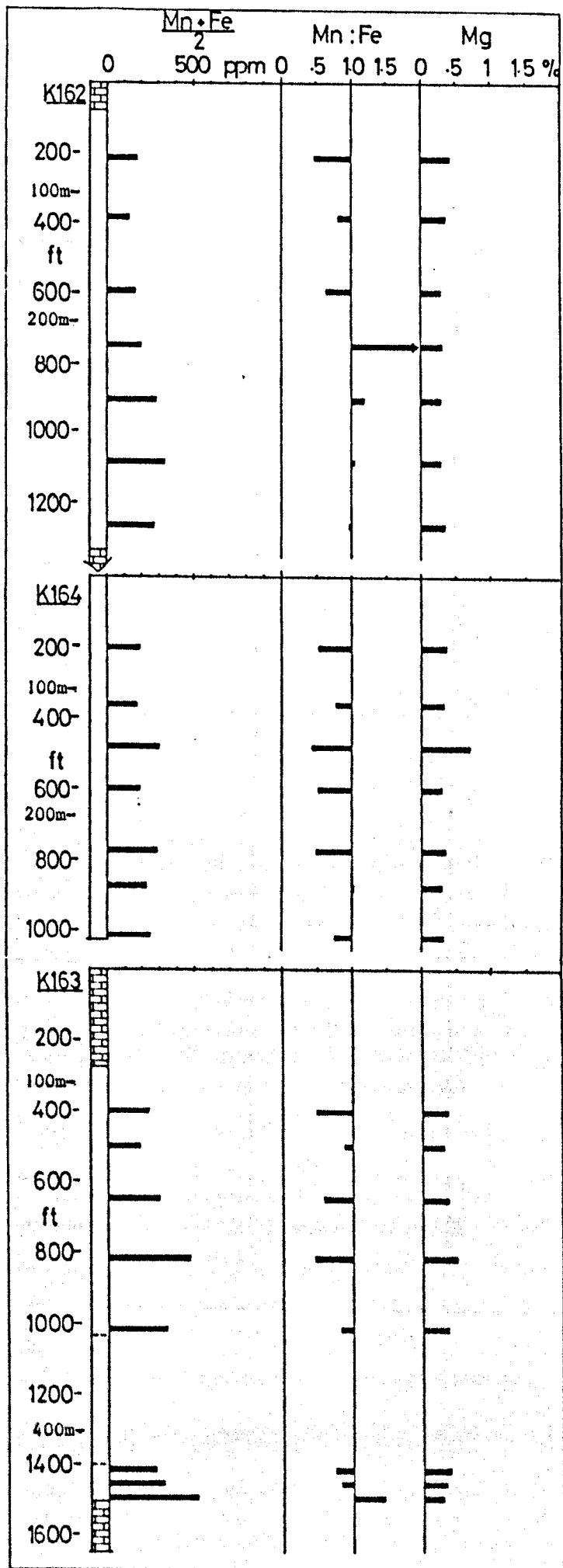


Figure 4.42: Vertical geochemical profiles of boreholes K162, K164 and K163 at Keel. For key see Figure 4.37.

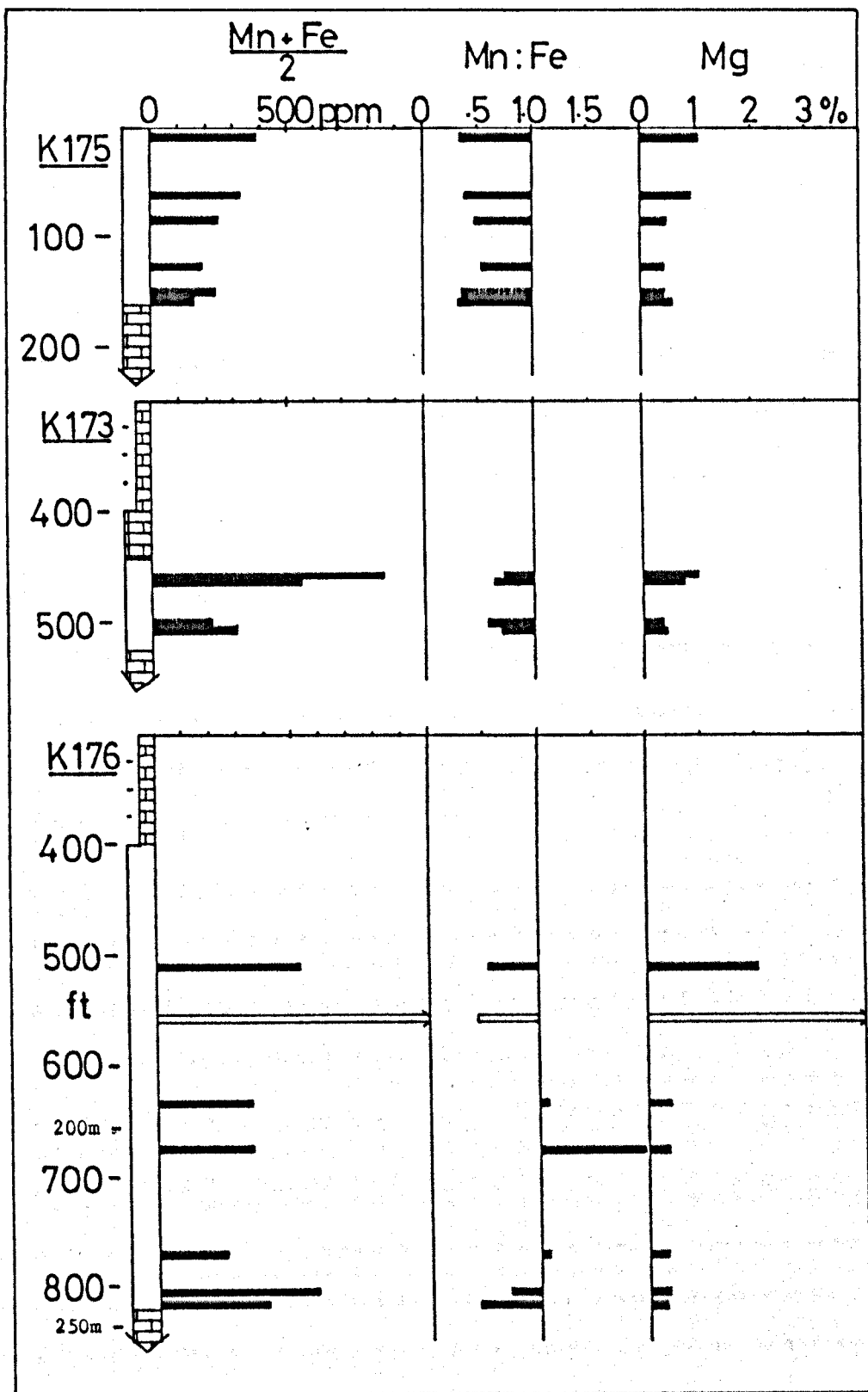


Figure 4.43: Vertical geochemical profiles of boreholes K175, K173 and K176 at Keel. For key see Figure 4.37. Unfilled bar is Reef Equivalent limestone.

(LF9, LF18, LF31, LF43 and K162), agreeing with the results of outcrop sampling (Chapter 3.4.3). This pattern is not very strongly developed compared to Silvermines, and in the majority of boreholes examined, no regular pattern emerges.

The ratio Mn:Fe is generally low (around 0.5), except in LF43, inconsistently in LF9, and rarely elsewhere, where values greater than one are recorded.

4.5.1. Summary.

Examination of drill core geochemical profiles at Silvermines reveals a number of trace element patterns which may relate to hydrothermal processes that formed the stratiform orebody.

At Silvermines, Mn, Fe and Zn are enriched in the Waulsortian equivalent formation and underlying Muddy Reef Limestone. Peak values are recorded at the base of the Dolomite Breccia, the same horizon as the stratiform ore, and average levels decrease away from it, above and below.

In the hanging wall, enriched $(\text{Mn}+\text{Fe})/2$ values are recorded up to 105 metres (350 ft.) above the top of the ore horizon, especially associated with dolomite breccia samples, but background values of below 200ppm are recorded from 15 metres above, increasing in frequency upwards.

Zinc levels fall off steadily above the ore horizon. Enriched values are recorded up to over 90 metres

(300 ft.) above the top of the ore horizon, but background values of 10 ppm or less are also recorded throughout the hanging wall, right down to the ore horizon.

The ratio Mn:Fe is low, 0.5 or less, within the ore horizon, and up to 20 metres above, and increasing upwards, averaging 1.0 or more beyond 30 metres (100ft.) from the ore horizon top.

Footwall enrichments are present, but have not been fully delineated in the mine area. An extensive Fe (and less extensive Mn) anomaly is developed in the Muddy Reef Limestone and part of the underlying Muddy Limestone, at a distance of over 2 kilometres from the mine, in the only large scale, undolomitised footwall intersection examined. More detailed profiling of the immediate footwall (Muddy Reef Limestone) around the mine indicated that Mn and Fe are both high in the 30 metres or so beneath the base of the ore horizon, but only Mn increases upwards, whereas Fe decreases upwards, reflected in a steady upward increase in Mn:Fe ratio, from less than 0.1 at 30 metres below the base, to 0.5 immediately below the ore horizon. This reflects the changing bottom conditions during sedimentation (see Chapter Six).

Enriched zinc is present only in the topmost 6 metres (20 ft.) of the footwall, where Mn and Fe levels become very erratically distributed. Strontium values also show a pronounced upwards decrease in the top 10 metres of the footwall, from 500 ppm or more, to

around 200 ppm at the base of the ore horizon.

Examination of X.R.F. data from the same samples indicates the close relationship between high absolute trace element levels, high insoluble trace element levels, dolomite content and clay mineral impurities in the host carbonates.

At Ballinalack and Keel, examination of vertical profiles of trace element data indicates that no real comparison with Silvermines exists, with only vague suggestions of basal enrichment of mudbank limestones at Keel.

Apart from the coincidence of trace element enrichments with mineralisation in the mudbanks at Ballinalack no obvious direct link between the latter, and the patterns exhibited by the former has emerged.

CHAPTER FIVE - SAMPLE COMPOSITION AND INHOMOGENEITY.

5.1.1. Introduction.

In the previous chapter, comparison of A.A. and X.R.F. data indicated the effect that visible insoluble material may have on trace element geochemistry. In this chapter, several aspects of sample composition and inhomogeneity are examined which may effect geochemical analysis or interpretation.

Firstly, simple correlation of A.A. and X.R.F. data from Silvermines is undertaken to investigate individual and group element associations. This is followed by a comparison of selective and non-selective sampling and dissolution techniques on material from Silvermines and Keel.

The results of simple separation techniques are then described from distinctly inhomogeneous core and outcrop samples from the Ballinalack area, to compare visual compositional heterogeneities with geochemical contrasts.

Finally, this examination is carried a step further by investigation of the heterogeneous character of samples on a micro-scale, by profiling a number of polished thin sections from Silvermines and Keel on the electron microprobe.

5.2.1. Correlation of Trace Element Data.

In Chapter 4, vertical profiles of A.A. and X.R.F. data from Silvermines drill core indicated that certain

elements appear to vary directly with one another, whereas others show an inverse variation. With the aid of EMAS (Edinburgh University Central Computer Link), a simple correlation matrix was drawn up using a limited set of A.A. and X.R.F. data from both outcrop and drill core from the Silvermines area. This allows any links between the elements to be quantified, and the results, along with average values for each element, are presented in Tables 5.1 to 5.3. Outcrop and core data are presented separately because of their significantly different composition, the latter all from within 3 kilometres of the mine representing 'proximal' samples, and the former (mostly from sites some distance away) as a crude representation of 'distal' samples.

Some useful information on trace element associations and behaviour during sample digestion can be gleaned from the correlation matrices.

Not surprisingly, the highest positive correlation values occur between analyses for the same element on A.A. and X.R.F. (Table 5.3c). High values are also recorded between SiO_2 , K_2O , Al_2O_3 and Rb, and between Zn and Pb. A strong negative correlation is observed between Mg and Ca.

In comparing A.A. and X.R.F. data for Mn, Fe, Zn and Mg, Fe shows a much poorer correlation between the two methods in both outcrop and core samples (Table 5.3c), than the other three elements. This reflects the

	A.A. Mn	Mn	A.A. Fe	Fe ₂ O ₃	A.A. Zn	Zn	A.A. Mg	Mg	Ba	Pb	Sr	Rb	SiO ₂	Al ₂ O ₃	K ₂ O	CaCO ₃
A.A. Mn	.	.98	.83	.57	.49	.41	.35	.35	.38	.49	-.13	.06	.10	.18	.23	-.53
Mn	.	.	.85	.55	.51	.42	.42	.42	.33	.48	-.18	.06	.11	.19	.25	-.58
A.A. Fe42	.49	.41	.22	.24	.31	.40	-.10	.11	.09	.18	.17	-.40
Fe ₂ O ₃49	.44	.22	.20	.27	.48	-.24	.03	.02	.17	.19	-.52
A.A. Zn97	.34	.26	.12	.70	-.19	-.01	-.02	.10	.32	-.40
Zn31	.22	.07	.72	-.21	-.05	-.03	.03	.24	-.34
A.A. Mg99	.11	.23	-.21	.09	.14	.19	.43	-.83
Mg11	.21	-.26	.14	.13	.18	.39	-.84
Ba36	.33	-.03	-.00	.09	.09	-.20
Pb	-.16	-.09	-.03	.06	.07	-.37
Sr11	.13	.06	-.04	.23
Rb84	.96	.77	-.37
SiO ₂57	.29	-.40
Al ₂ O ₃97	-.44
K ₂ O	-.50
CaCO ₃

Table 5.1: Correlation matrix for analytical data in 202 core samples from Silvermines area. All analyses by X.R.F. except where indicated.

	A.A. Mn	Mn	A.A. Fe	Fe ₂ O ₃	A.A. Zn	Zn	A.A. Mg	Mg	Ba	Pb	Sr	Rb	SiO ₂	Al ₂ O ₃	K ₂ O	CaCO ₃
A.A. Mn	.	.98	.51	.78	.40	.34	.14	.12	-.05	.48	-.28	.00	.47	.58	.46	-.36
Mn	.	.	.49	.80	.47	.45	.34	.34	-.06	.59	-.27	-.02	.56	.64	.50	-.52
A.A. Fe75	-.03	-.03	.04	.01	.15	.17	-.16	.19	.55	.56	.65	-.21
Fe ₂ O ₃48	.33	-.02	.03	.13	.70	-.19	.30	.82	.86	.80	-.74
A.A. Zn97	.46	.50	.08	.71	-.08	-.10	.47	.37	.12	-.54
Zn59	.60	.16	.80	-.10	-.09	.53	.34	.19	-.63
A.A. Mg99	.05	.73	-.10	-.20	.54	.40	.31	-.98
Mg03	.74	-.01	-.18	.53	.39	.29	-.98
Ba05	.01	.13	.27	.25	.27	-.09
Pb	-.11	.37	.68	.68	.36	-.79
Sr01	-.14	-.27	-.30	.14
Rb49	.57	.54	-.23
SiO ₂88	.85	-.70
Al ₂ O ₃97	-.63
K ₂ O	-.45
CaCO ₃

Table 5.2: Correlation matrix for analytical data in 55 outcrop samples from Silvermines area. All analyses by X.R.F. except where indicated.

OUTCROP					CORE				
A.A.	Mn	Fe	Zn	Mg	A.A.	Mn	Fe	Zn	Mg
Mn	.	.51	.40	.14	Mn	.	.83	.49	.35
Fe	.	.	-.03	.04	Fe	.	.	.49	.22
Zn46	Zn34
Mg	Mg

Table 5.3a: Correlation matrix for A.A. analyses for Mn, Fe, Zn and Mg in outcrop (55) and core (202) samples from Silvermines area.

OUTCROP					CORE				
A.A.	n	\bar{x}	σ	range	n	\bar{x}	σ	range	
Mn	55	186	102	15 - 578	202	546	511	15 - 3233	
Fe	55	198	232	18 - 1298	202	1367	2316	18 - 15435	
Zn	55	14.0	14.7	2 - 78.6	202	83.8	236	0 - 2500	
Mg %	54	1.37	2.06	.26 - 10.8	182	3.83	3.95	.26 - 11.50	

Table 5.3b: Mean, standard deviation and range of A.A. analyses for Mn, Fe, Zn and Mg in outcrop and core samples from Silvermines area. Data in ppm except where indicated.

A.A. v X.R.F.		Correlation coefficient	
		Outcrop	Core
Mn	v Mn	0.98	0.98
Fe	v Fe	0.75	0.42
Zn	v Zn	0.97	0.97
Mg	v Mg	0.99	0.99

Table 5.3c: Correlation between A.A. and X.R.F. results for Mn, Fe, Zn and Mg in outcrop (55) and core (202) samples from the Silvermines area.

Element	OUTCROP SAMPLES				CORE SAMPLES			
	n	\bar{x}	σ	range	n	\bar{x}	σ	range
Mn ppm	55	205	120	15 - 668	202	709	728	15 - 4590
Fe ₂ O ₃ %	34	.054	.041	.02 - .21	171	.67	1.60	.02 - 10.74
Zn ppm	48	24.8	34.3	1.9 - 180	193	979	3891	1.9 - 44000
Mg %	45	1.41	2.41	.16 - 12.8	192	4.70	4.36	.16 - 12.80
Ba ppm	51	54.7	67.8	10 - 368	192	186	543	10 - 4461
Pb ppm	55	11.8	19.2	0 - 105	192	295	1125	0 - 8986
Sr ppm	48	172	41.2	120 - 399	158	169	44.9	49 - 399
Rb ppm	27	2.0	2.5	0 - 9	122	6.5	11.6	0 - 112
SiO ₂ %	55	.385	.46	.05 - 2.36	200	1.44	3.62	.05 - 30
Al ₂ O ₃ %	55	.334	.32	.05 - 1.56	202	0.92	1.42	.05 - 15.1
K ₂ O %	48	.059	.05	.01 - .23	160	0.11	0.12	.01 - .78
CaCO ₃ %	55	96.14	6.02	69.4 - 99.7	202	84.97	14.84	45.0 - 99.7

Table 5.4: Mean, standard deviation and range of X.R.F. analyses in outcrop and core samples from Silvermines area. Data in ppm except where indicated otherwise.

association between relatively insoluble phases (such as pyrite, oxides and clay minerals), particularly near to the mine, in core samples. Although zinc is almost entirely associated with the relatively insoluble sulphide phase, weak but consistent leaching of the element during weak acid attack, accounts for its good correlation between the two analytical methods. Both Mn and Mg are principally associated with the carbonate minerals, explaining the good correlation between A.A. and X.R.F. results.

The association between SiO_2 , Al_2O_3 , K_2O and Rb reflects the presence of clay mineral (and possibly minor feldspar) impurities in the carbonates. The slight reduction in correlability between silica and the other three elements in core samples is caused by the presence of chert in some hanging wall samples.

A comparison between Mn, Fe (Mg, Zn, Pb) and the 'insoluble association' (SiO_2 , Al_2O_3 , K_2O , Rb) is present in the outcrop samples but absent in the core samples. This suggests that anomalously high Mn and Fe content (and Mg, Zn and Pb) is associated with relatively impure mudbank in the outcrop area, away from known mineralisation. On the other hand, in the mine area, no direct association between trace element content and insoluble material is implied, or else it is obscured by overall higher levels of both components, or some other, stronger control.

Good positive correlation between Pb and Zn in both

populations, and between Ba and Sr in the core samples, reflects the coexistence of sphalerite and galena throughout, and the presence of baryte in the mine area, respectively.

The strong negative correlation between Mg and Ca is due to the direct substitution of the latter by the former in dolomite. The negative correlation which Ca displays with all elements except Sr, indicates the fact that introduction of any other trace element (or major constituent) into the carbonate, occurs at the expense of Ca, either by direct substitution in the CaCO_3 lattice, or by sulphide or clay mineral impurities in the rock. Strontium occupies only the Ca lattice sites in carbonates, and avoids the Mg sites, explaining its parallel behaviour with Ca, and negative correlation with other elements.

The significance of this data is further considered in Chapter 6.

5.3.1. Non-Selective Sampling and Digestion.

In Chapter 2, the need to be selective in both sampling technique and sample dissolution was expressed. Figures 5.1 to 5.3 illustrate the results of a comparison between selective sampling coupled with partial dissolution (as outlined in Chapter 2) and a less selective sampling technique (i.e. groove sampling), coupled with a strong acid digestion.

The material used was a variety of mineralised and unmineralised, pure and impure mudbank limestone and equivalent 'off-Reef' carbonates from the Keel prospect, in the form of vertical borehole sections.

The 'non-selective' data was from part of a study by RioFinEx, involving groove sampling of entire sections (in 1 to 8 metre lengths), and aquaregia digestion for a variety of trace element analyses on A.A. For comparison, similar sections of the same drill core were selectively chip sampled (following the parameters outlined in Chapter 2) and analysed for the elements Mn, Fe, Zn and Mg, following dissolution in weak acid.

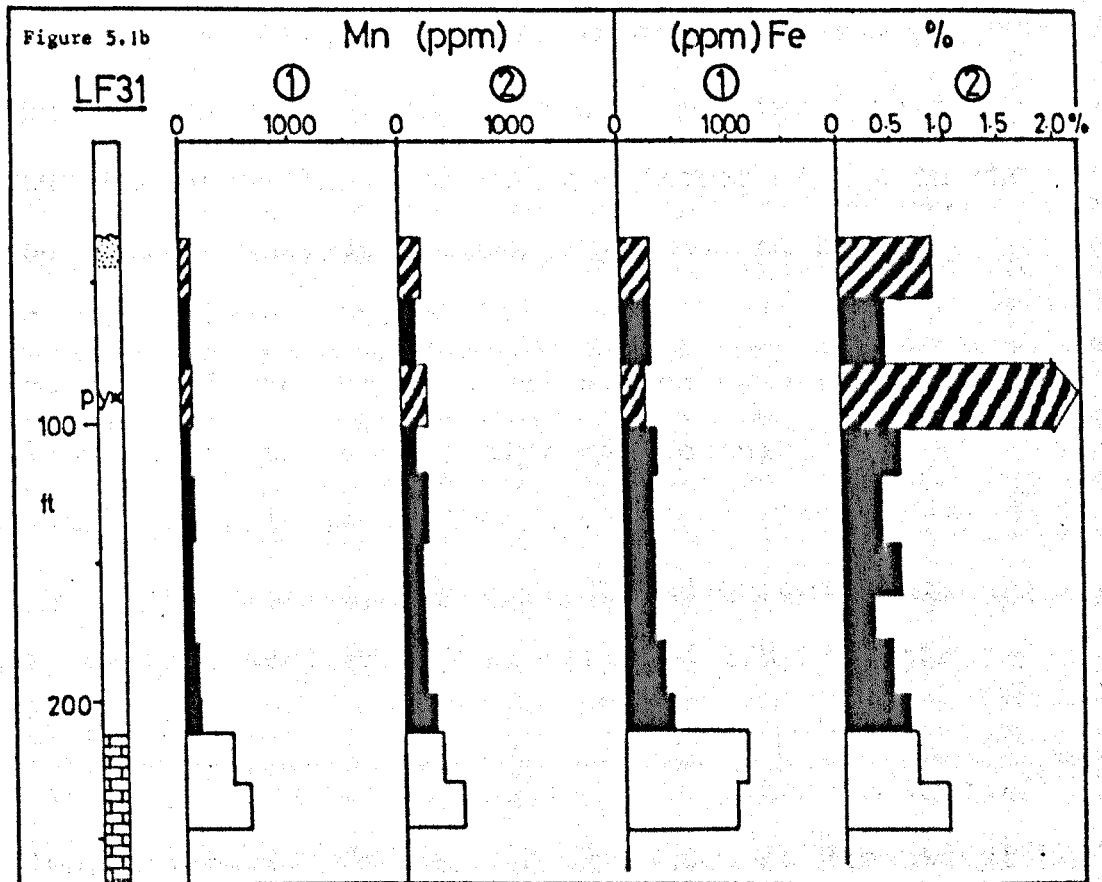
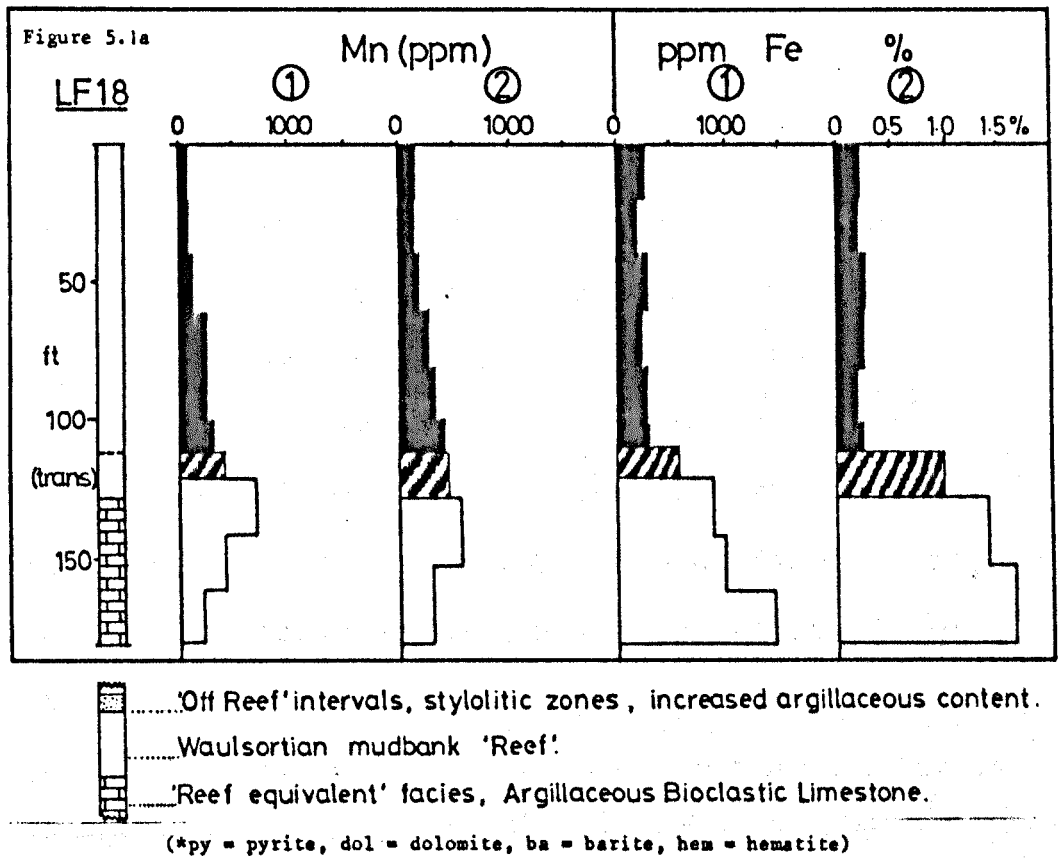
Comparisons between the two indicate that, except in the purest of Waulsortian mudbank intersections, the non-selective technique provides little more than a geochemical log of the section which closely matches the lithological log. In particular, the presence of visible dolomitic, pyritic or clay mineral impurities (such as mud seams or stylolites) and off-Reef horizons is highlighted by the Mn and Fe data. The combined

effect of this is to thickly disguise any subtle enrichments which may be present in the carbonate fraction.

In Figure 5.1a, LF18 is a fairly pure mudbank limestone section, in which comparison between the two techniques is good, and contrasting patterns are restricted to the sub-Reef argillaceous limestones. Absolute values, however, differ by a factor of 1.3 for Mn and 12.5 for Fe.

Borehole LF31 (Figure 5.1b) is a section of mainly pure mudbank limestone with some pyritic impurities and off-reef intercalations. Significant iron release is noted for both these intervals in the right hand column, leached from the non-carbonate impurities by the stronger acid digestion. Even small, centimetre-wide pyritic zones can lead to a significant contamination in the analytical result from a larger 6 metre (20 ft.) interval. Slightly increased occurrence of stylolite zones throughout this section (which are sufficiently far apart to be avoidable in chip sampling) has led to higher and more erratic Fe values in the right hand column. Even in pure mudbank samples, Fe is higher in the non-selective analyses by an average factor of 14.3. Manganese is relatively unaffected by minor facies or compositional changes, but is still higher in the non-selective analyses by an average factor of 1.8.

Section LF9 (Figure 5.2) contains a mixture of pure mudbank, impure mudbank, off-reef intervals stylolite



Figures 5.1a,b: Vertical geochemical profiles of boreholes LF18 and LF31 at Keel, in which analytical results from selective sampling and weak acid digestion (1) are compared with results from non-selective sampling and strong acid digestion (2), for both Mn and Fe. Pure Waulsortian samples are represented by black shading, transitional or pyritic by stripes, and off-Reef or sub-Reef limestones by unshaded bars.

zones, dolomite, pyrite and hematite. In the non-selective analyses (Column 2), Mn peaks appear in several of these zones (especially the dolomite, some off-reef and pyrite, but rarely in the stylolite zones), where they may or may not be present in the selective analyses (Column 1). This indicates that Mn is not always associated with the carbonate phase.

Iron peaks in Column 2 are associated with virtually all the impure mudbank zones, but are confined mainly to the dolomite zones in Column 1. In nearly all of the strong acid digestions of stylolite zones, off-reef intervals, dolomite and pyrite zones, higher Fe levels are accompanied by anomalous values of Zn, Pb and Ba, although this is not illustrated on the diagrams.

In pure mudbank samples, Fe values are higher by an average factor of 12.3 and Mn by a factor of 1.4 in the non-selective analyses (Column 2), compared to the selective analyses (Column 1).

Comparison of whole core sampling and selective chip sampling, using the same analytical technique for both, also reveals some pitfalls.

The following experiment was conducted on one Silvermines borehole section (77/1, situated 2.5 kilometres to the northeast of the mine) consisting mainly of relatively pure mudbank limestone with patchy dolomitisation, stylolite zones and brecciation (sedimentary) throughout its upper half.

Eleven 15-centimetre long samples of BQ core were

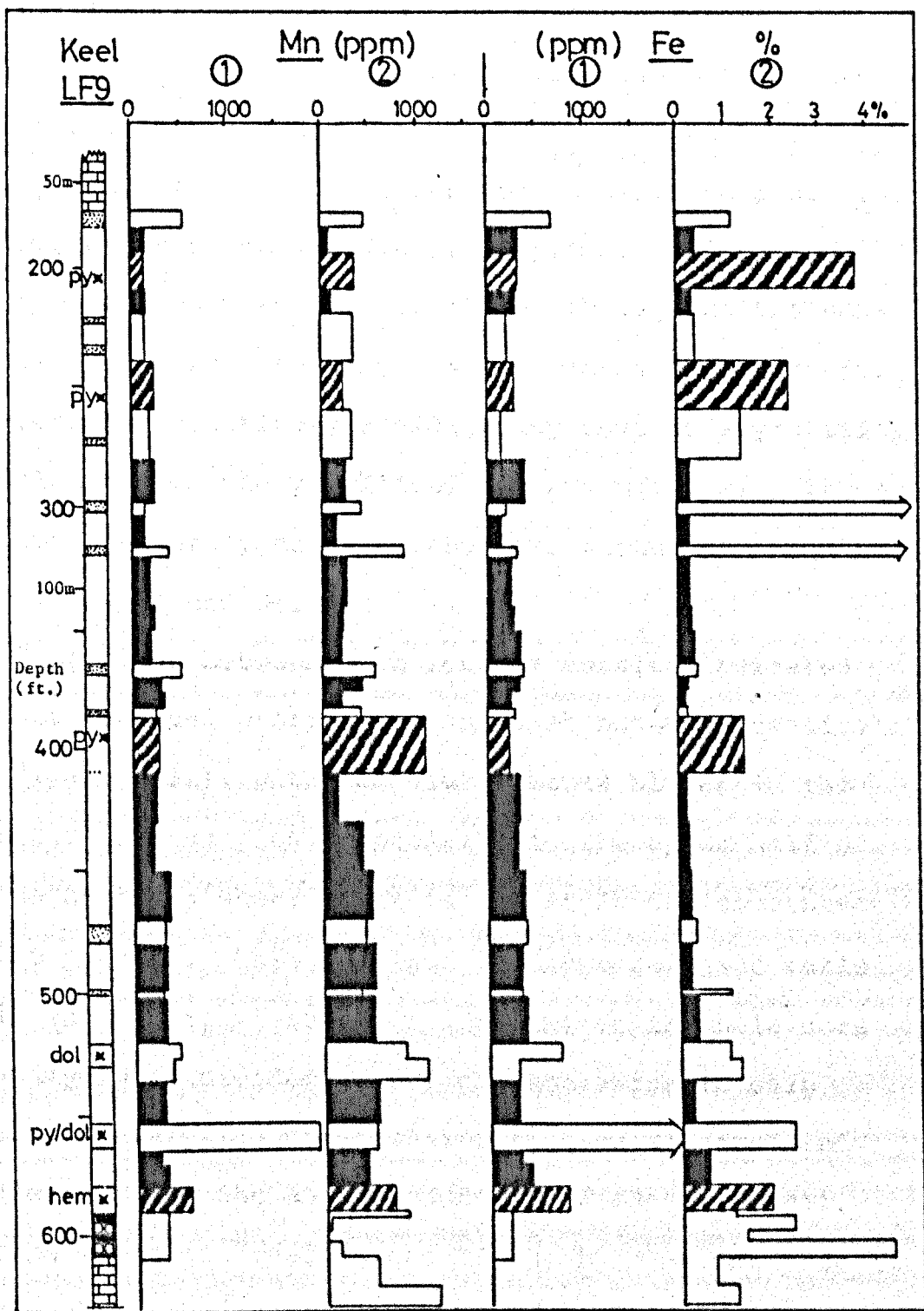


Figure 5.2: Vertical geochemical profile of borehole LF9 at Keel, in which analytical results from selective sampling and weak acid digestion (1) are compared with results from non-selective sampling and strong acid digestion (2), for both Mn and Fe. Pure Waulsortian samples are represented by black shading, transitional or pyritic Waulsortian by diagonal stripes, and off-Reef or sub-Reef Limestones by unshaded bars. For key see Figure 5.1.

collected at intervals of 15 to 30 metres (50 to 100 ft.) throughout the hole, and analysed for Mn, Fe, Zn and Mg, using the hot 2M acetic acid method outlined in Chapter 2. Because of the intensity of stylolite formation, it was not possible to avoid them completely on this scale of sampling. Thirty-one chip samples were collected from throughout the same hole, each representing a 6 to 8 metre (20 to 25 ft.) section, selectively avoiding any obvious stylolitic, dolomitic or recrystallised mudbank material. These were then analysed using the same technique, also for Mn, Fe, Zn and Mg.

Comparison between both sets of results indicated that vertical profiles are similar but not identical (Figure 5.3a), with absolute values higher in the whole core samples, especially in the upper half of the section, where dolomite and stylolite concentrations are present. This increase is expressed as a ratio in Table 5.5, where the concentration in whole core analysis is divided by the concentration in chip sample analysis (for the same section of core, and averaged for the entire section for each element).

The whole core values are higher by over 50% than in the chip sampled core, in the upper half of the section (above 550 ft., 165 metres), whereas in the lower half of the section, the ratios are lower for each element, and much closer to one (Table 5.5).

The upper part of the section corresponds to the

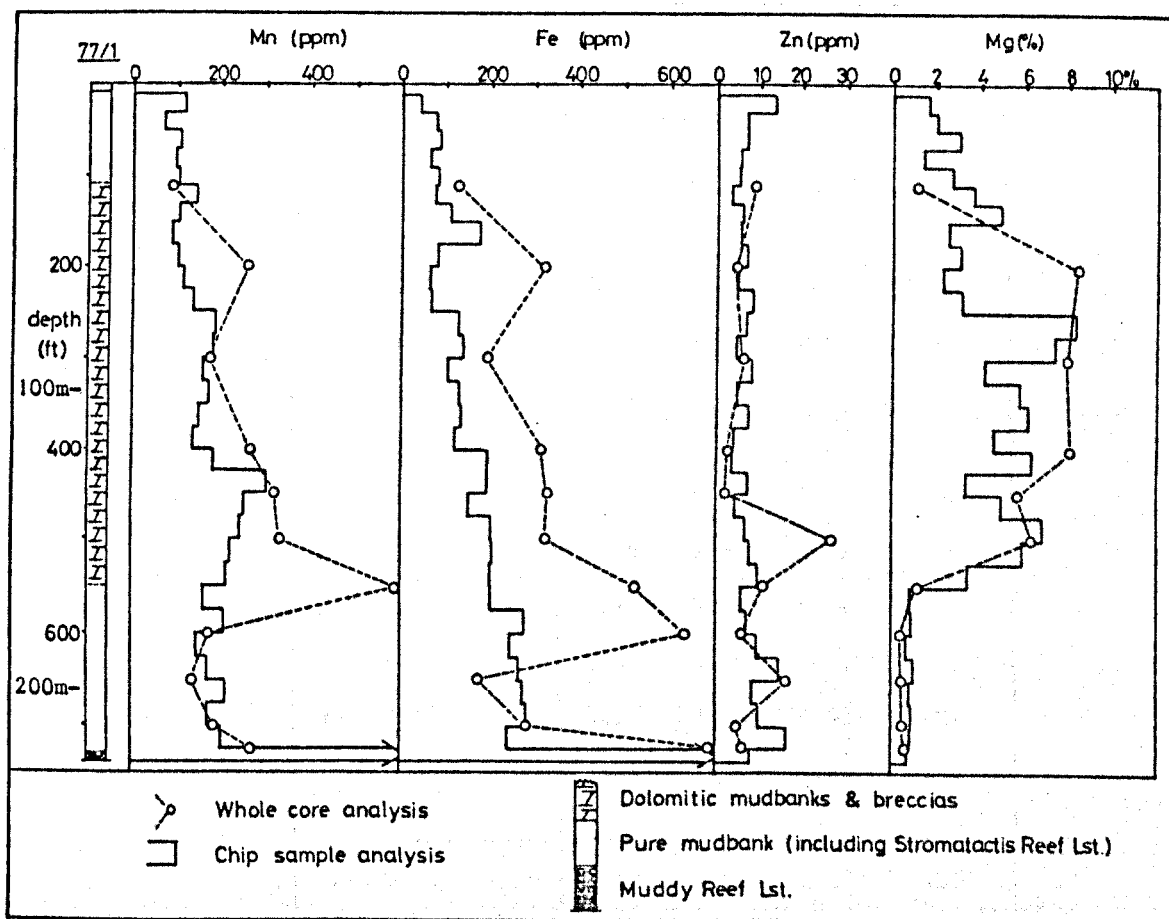


Figure 5.3a: Comparison of whole core (11) and chip samples (31) in A.A. analysis in borehole 77/1 at Silvermines. This illustrates how whole core sampling may yield higher levels of some trace elements, especially Fe. The scale of chip sampling allows insoluble seams to be avoided, unlike in whole core sampling.

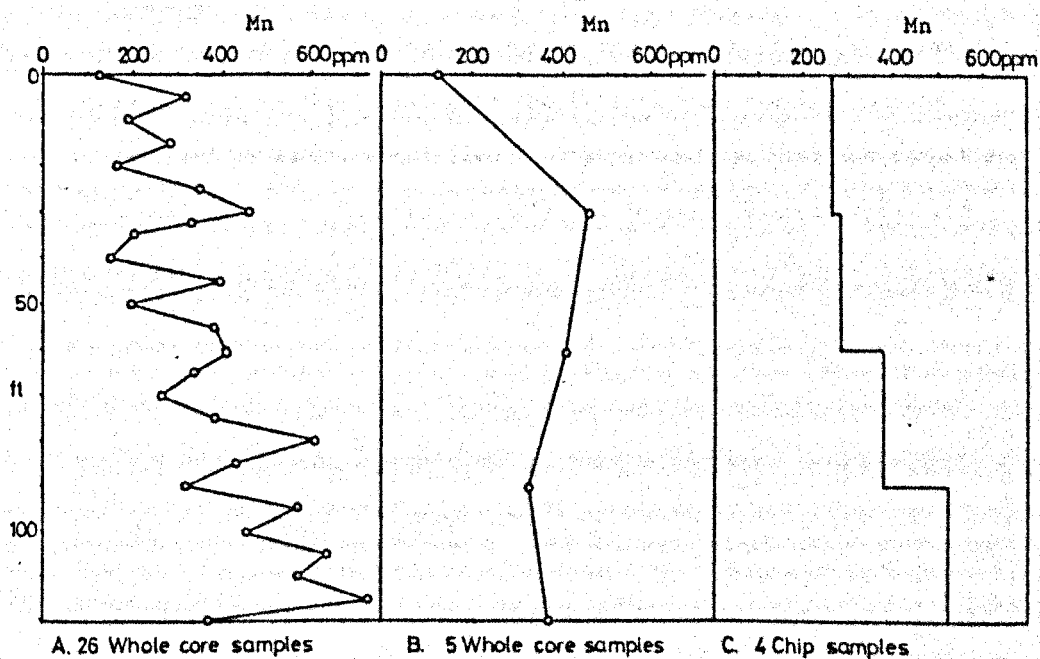


Figure 5.3b: Comparison of whole core (both frequent (A) and infrequent (B) sample intervals) with chip samples (C) in borehole K38, using Mn data from A.A. analysis. This shows how too few whole sample points (B) can lead to distortion of vertical geochemical trends, avoidable by taking relatively few chip samples of entire core section (C).

Sample Depth		Ratio (whole core/chip sample)			
		Mn	Fe	Zn	Mg
1	105'	0.82	1.54	1.74	0.39
2	200'	2.39	4.40	0.77	3.17
3	300'	1.01	1.55	0.95	1.38
4	400'	1.66	2.04	0.65	1.47
5	450'	1.14	1.89	0.36	1.37
6	500'	1.41	1.60	3.67	0.99
7	550'	3.25	2.58	1.39	0.57
-----		-----			
8	600'	0.96	2.41	0.74	0.60
9	650'	1.00	0.66	1.41	0.45
10	700'	0.97	1.08	0.38	0.63
11	720'	1.32	2.96	0.40	0.70
Average above 550' (Hanging Wall)		1.67	2.23	1.36	1.33
-----		-----			
Average below 550' (Stromatactis Reef)		1.06	1.78	0.73	0.60

Table 5.5: Comparison of analytical results from whole core and chip samples from equivalent depths in borehole 77/1, expressed as a ratio of the former over the latter. Both types of sample analysed by atomic absorption spectrophotometry. Note the comparison between hanging wall (above 550') and footwall Stromatactis Reef samples.

hanging wall dolomite breccias of the mine area, represented by partly dolomitic and stylolitic mudbank limestone and some breccia. The lower half corresponds to the footwall Stromatactis Reef Limestone of the mine area, where pure mudbanks predominate. The implications from this data are several, and relate to both genetic and analytical aspects of trace element distribution.

Firstly, a chip sample of a given length of core represents an 'averaged' sample of that core, effectively smoothing out small scale irregularities in trace element distribution, caused by sample heterogeneity, which may dominate individual whole core samples. This situation is further illustrated by Figure 5.3b, which portrays a set of Mn results obtained from borehole K38 (Silvermines). In this, four chip samples of the top 120 ft. of core were collected to compare with 26 whole core samples from the same section of dolomite breccias. Had only the 5 samples in Column B been collected, a misleading vertical profile would have resulted, yet with only 4 chip samples (Column C), a more accurate representation of the overall pattern is achieved. This illustrates the way in which insufficient sample density may create distortion or misleading patterns.

Secondly, regarding the nature of the hanging wall carbonates, it is possible that the stylolite seams concentrate small amounts of dolomite, which in turn

harbour excess Mn and Fe (as well as possible small quantities of Zn). Because of this, chip sampling, which is sufficiently selective to avoid stylolite material in this case, avoids the problem of possible secondary enrichments by post-depositional processes. This problem does not apply to the majority of mine host rocks, where the pervasive nature of the stylolitic dolomite (unavoidably by any hand sampling method) results in similar analytical levels in both whole core and chip samples. Instead, interpretation of results should be made with these implications borne in mind, and this is undertaken in the following two chapters.

5.4.1. Sample Separation.

Two simple techniques of separating different phases of core and outcrop mudbank samples from Ballinalack were implemented to compare trace element contents of each individual phase with those of whole rock analysis.

Samples from Ballinalack were utilised because of the striking inhomogeneity of much of the mudbank, which consists of a micrite phase and at least one sparry phase. This latter constituent may be a stromatactis filling, cross-cutting sparry veins, or a later, iron-stained infill in either. These secondary phases are present over a wider area than the mineralisation, but are probably closely associated with the mineralising

solutions (Jones and Bradfer 1982).

Hand-picked separations were analysed from samples with fairly coarse inhomogeneity (after initial jaw crushing to gravel sized chips), whereas hand-held dentist-drill separations were performed on more finely intermixed phases.

5.4.2. Hand Picking.

Comparison was made between micrite phases, secondary spar (including several generations of vein and stromatactis fillings, and darker recrystallised carbonate), surface oxidation products, fossil spar and whole rock samples. The main sparry phases were calcitic, with only a few dolomitic samples.

Figure 5.4 compares the analytical results (Mn and Fe) of each micrite phase and corresponding whole rock analysis from the same sample. This shows that, with few exceptions, the micrite portion contains less Fe and Mn than the whole rock. Therefore, as would be expected, comparison of the micrite phases with the various contaminating phases from the same sample (Figure 5.5) shows that the majority of the latter contain higher values, particularly of iron.

Manganese contents remain similar in some of the contaminating phases, for example, in recrystallised portions.

Hand-picked separations of inhomogenous samples

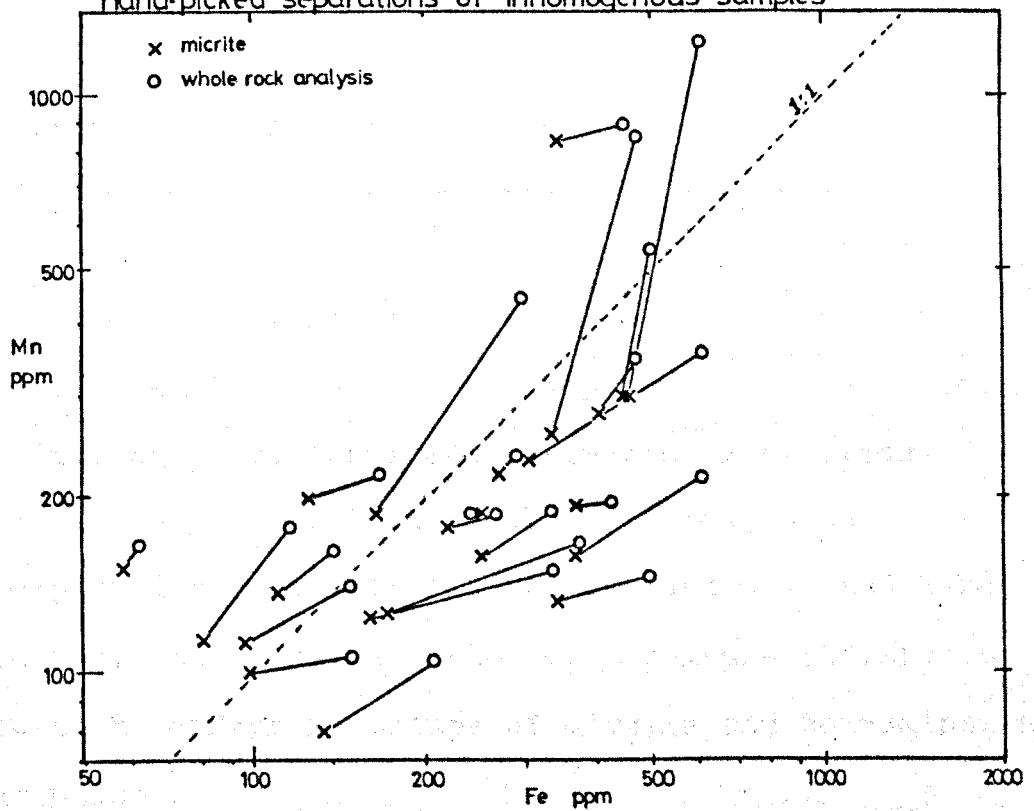


Figure 5.4: Comparison of Mn and Fe levels in whole rock and hand-picked micrite phases, using mudbank samples from Ballinalack. In virtually every case, reduction of Mn and especially Fe is recorded in the micrite phase. Note log scales.

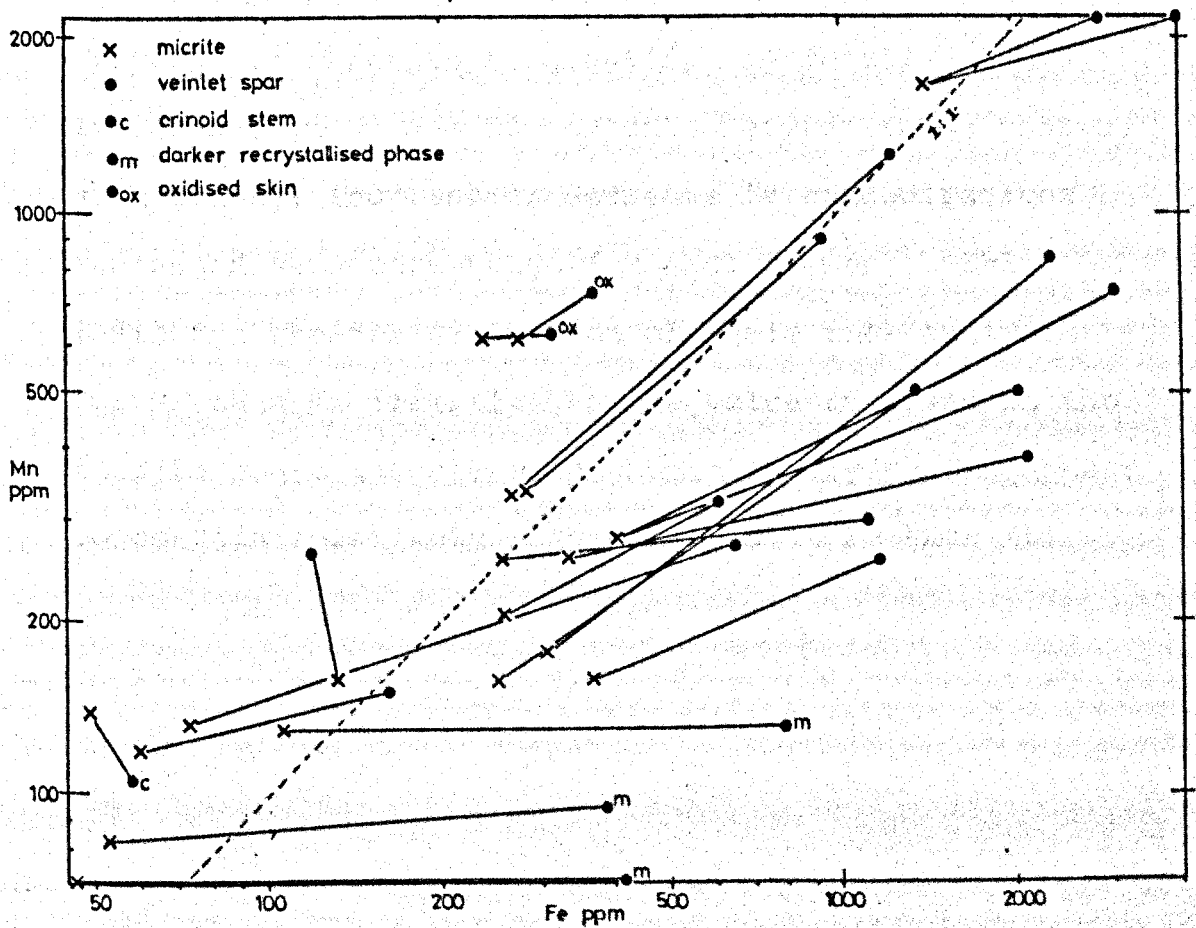


Figure 5.5: Comparison of Mn and Fe levels in hand-picked micrite phases and associated contaminant or other phases, using mudbank samples from Ballinalack. In most cases, increased Mn and especially Fe levels are recorded in the contaminating phase. Note the log scales.

5.4.3. Dentists Drill.

Use of a hand held dentist drill allows more careful selection of any single phase, particularly if used with binocular microscope. This was used with more finely-intermixed heterogeneous phases, such as thinner veinlets and more intricate stromatolite fillings. Results are presented in similar fashion to those of hand-picked samples, in Figures 5.6 and 5.7, and likewise indicate almost an order of magnitude difference between Mn and/or Fe values of micrite and contaminating spar phases.

The significance of this data is that whole rock analytical results may depend almost entirely on the relative proportions of contaminant to matrix.

Figure 5.8 attempts to quantify the relative difference in Mn and Fe contents between these phases, with average increase or decrease in concentrations expressed as a percentage for each element. This indicates greater distortion of whole rock analysis for Mn than Fe (relative to the value recorded in the micrite phase alone), even though sparry phases appear to contain relatively higher levels of Fe than Mn.

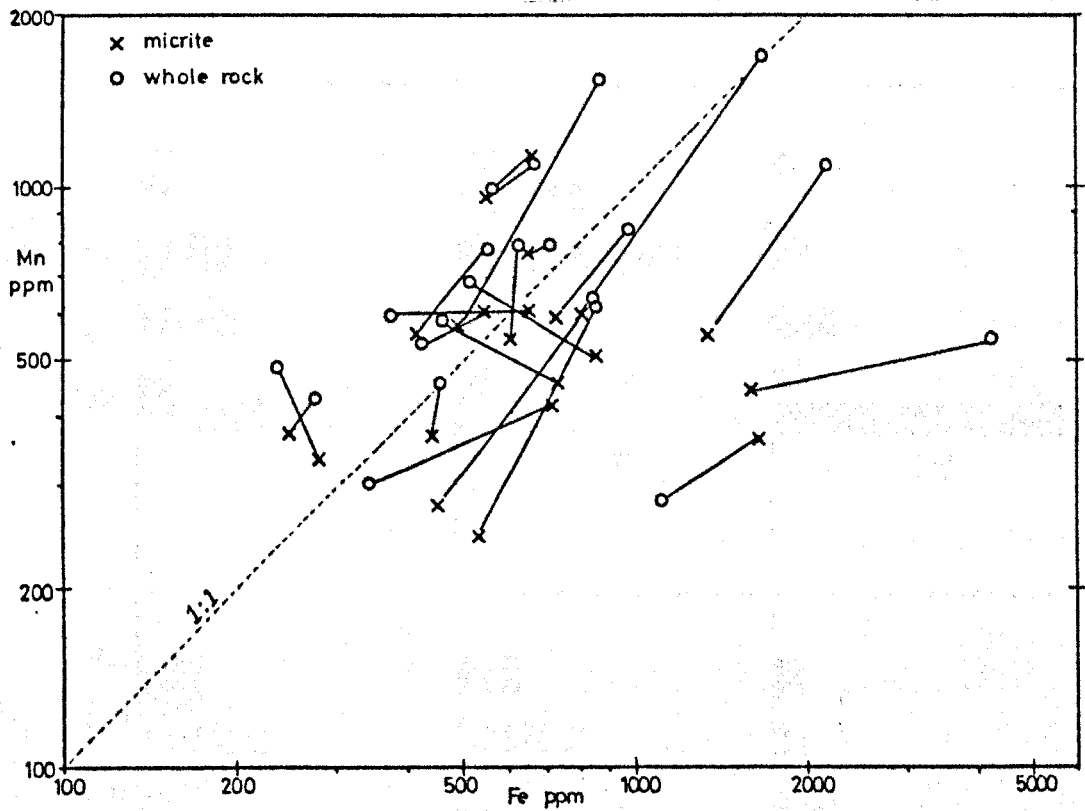


Figure 5.6: Comparison of Mn and Fe levels in micrite and corresponding whole rock samples, using dentist drill separation of mudbank samples from Ballinalack. Note log scales.

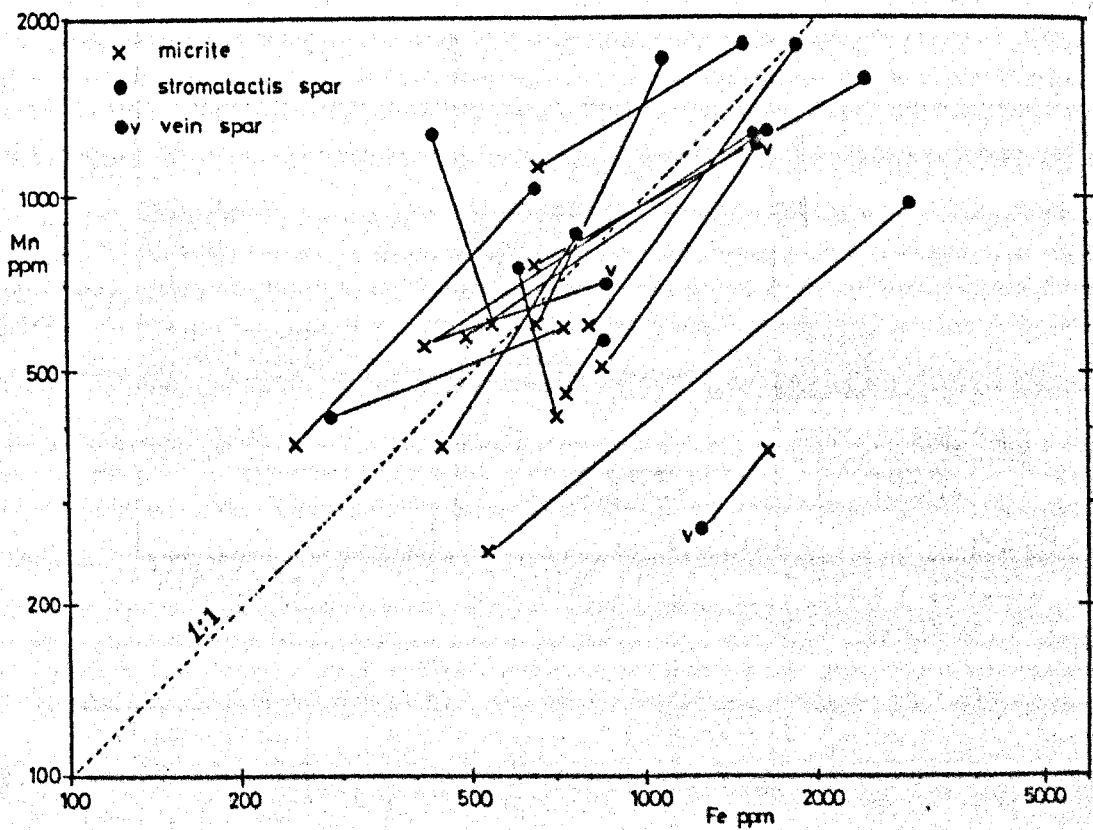


Figure 5.7: Comparison of Mn and Fe levels in micrite and associated sparry phases, using dentist drill separation on mudbank samples from Ballinalack. Note log scales.

Dentist drill separation of inhomogenous samples

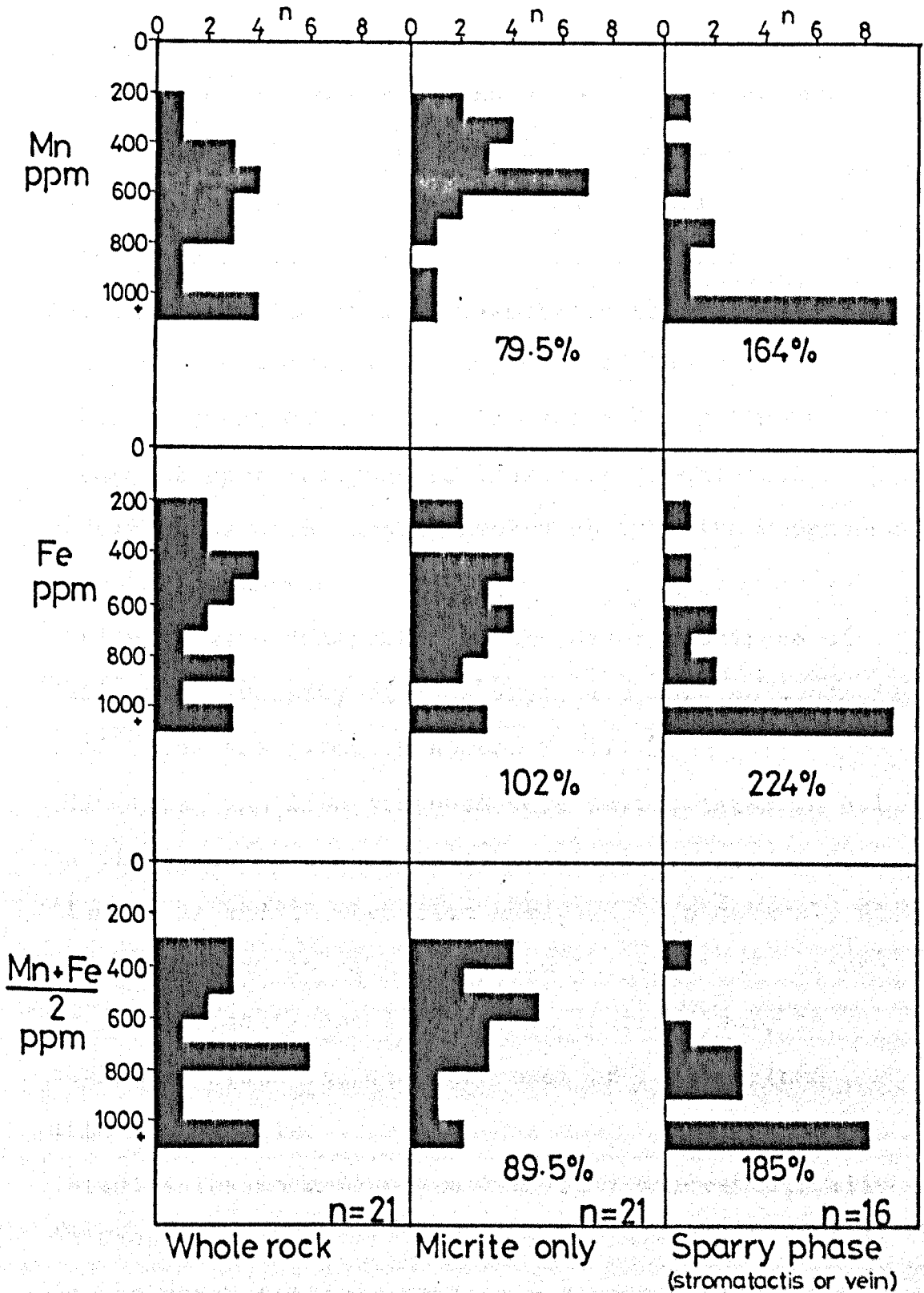


Figure 5.8: Comparison between Mn, Fe and (Mn+Fe)/2 contents of whole rock and corresponding micrite and sparry phases, using mudbank samples from Ballinalack. Figures quoted are average increase or decrease of values as percentage of whole rock value.

5.5.1. Electron Microprobe Profiles.

Electron microprobe analyses of polished sections of host rock carbonates from Silvermines and Keel were undertaken to examine the inhomogeneity of the samples on a micro-scale, and also in an attempt to determine the location of respective trace element sites within the individual phases of the rock.

Trace element content was investigated by linear arrays of spot analyses to construct geochemical traverses of each sample, broken up into its representative components.

Analyses were undertaken at the Grant Institute of Geology, University of Edinburgh, and machine operating conditions are given in Appendix III.

Manganese and iron contents were investigated in all samples, and in the majority of samples, Mg, Ca, Si, Al, Sr, Ba and Zn were also analysed. In general, Si, Al, Sr, Ba and Zn remained below the limit of detection, and significant levels were recorded only in stylolite seams and muddier zones of fine grained dolomitic matrix.

Results for Mn and Fe are displayed diagrammatically in Figures 5.9b-p, with Mg content displayed crudely in the ornamentation, whether the sample is dolomitic (over 3% Mg) or calcitic. The sections illustrated are all simplified reconstructions of the original sectioned sample, showing only the relevant and important features of each, with respect to the individual

component phases.

The manganese and iron data reinforce the observation from other work in this chapter, that considerable heterogeneity exists within the samples.

After examining each section, it can be stated generally that dolomite matrix contains much higher Fe levels than Mn, whereas limestone contains lower absolute levels of both elements, but slightly more Mn than Fe. Comparative levels of these two elements in secondary phases, especially veinlets, are much more erratic and changeable. An order of magnitude or more difference frequently exists between the matrix and contaminant phases, with the latter usually containing much higher absolute values.

A relative concentration of Fe in stylolite seams is observed, probably mainly as fine grained pyrite (e.g. W4-167', S.O.241, Figures 5.9e,c), whereas Mn is only rarely concentrated significantly in stylolite zones.

Certain fossil remains also contain very high concentrations of Mn and/or Fe, especially bryozoan fronds and crinoid central columns (e.g. Figures 5.9i,k, m). In addition, trace element inhomogeneity is not only confined to different phases within each sample, but is also present in the matrix of some samples (e.g. Figures 5.9c,g,i).

The presence of Zn and Ba in the calcite or dolomite lattice sites is not substantiated by this examination, as they are generally present below the detection limits

of the microprobe (which are not very low), or absent altogether from these phases. Alternatively, they may be confined entirely to very fine-grained sulphide or sulphate phases dispersed throughout the matrix.

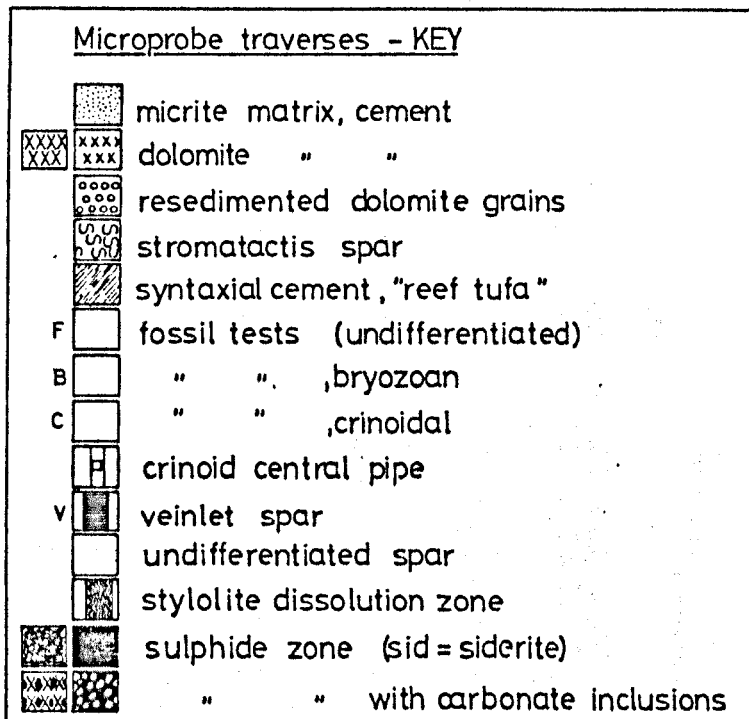


Figure 5.9a: Key for Figures 5.9b - p.

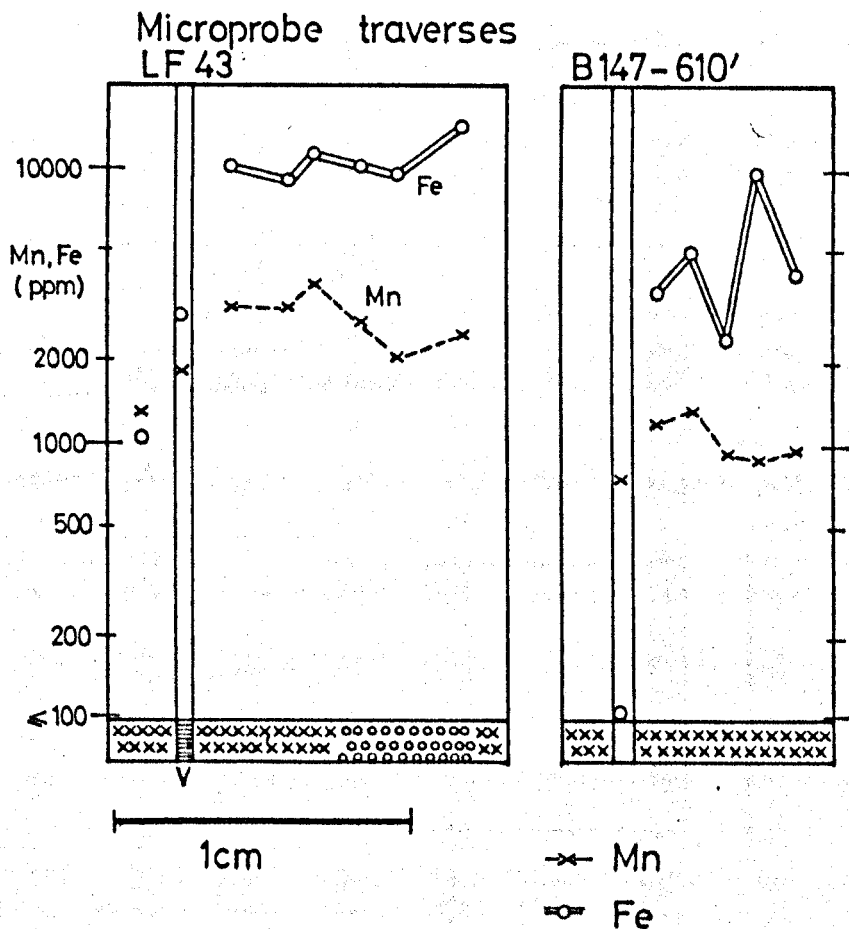


Figure 5.9b: Electron microprobe traverse of samples LF43 (Keel) and B147-610' (Silvermines). For key see Figure 5.9a.

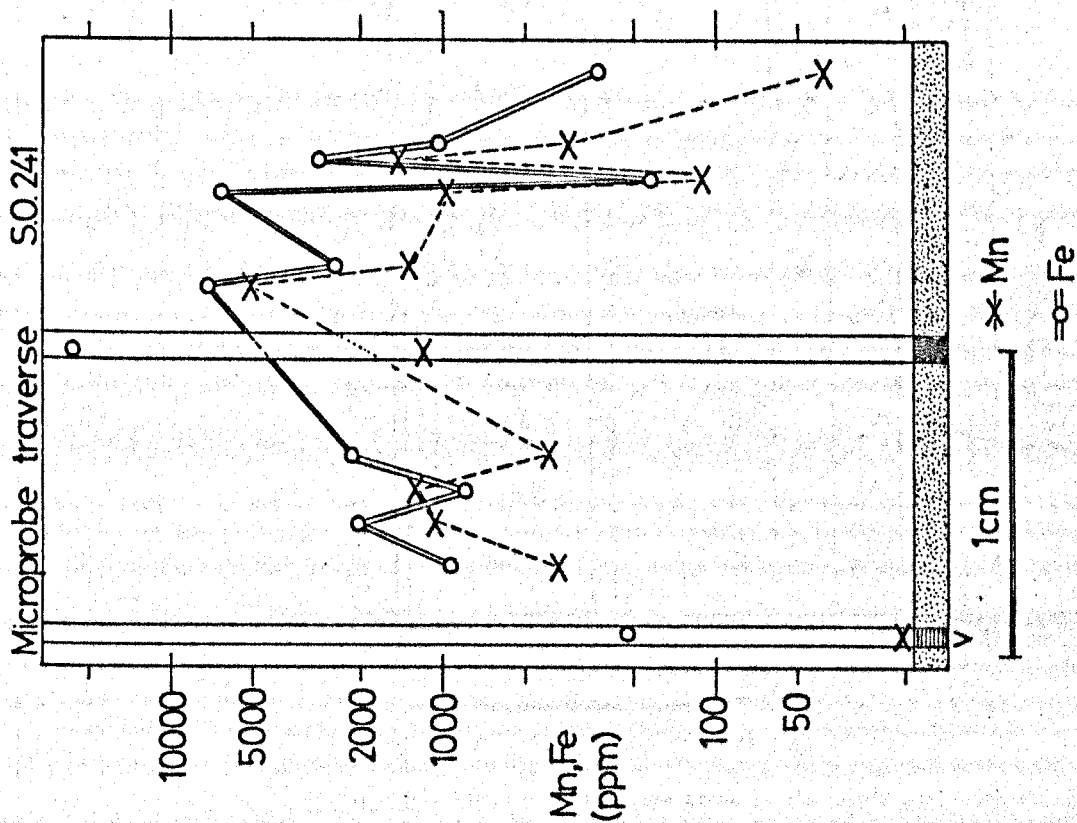


Figure 5.9c: Electron microprobe traverse of sample S.O.241 (Silvermines). For key see Figure 5.9a.

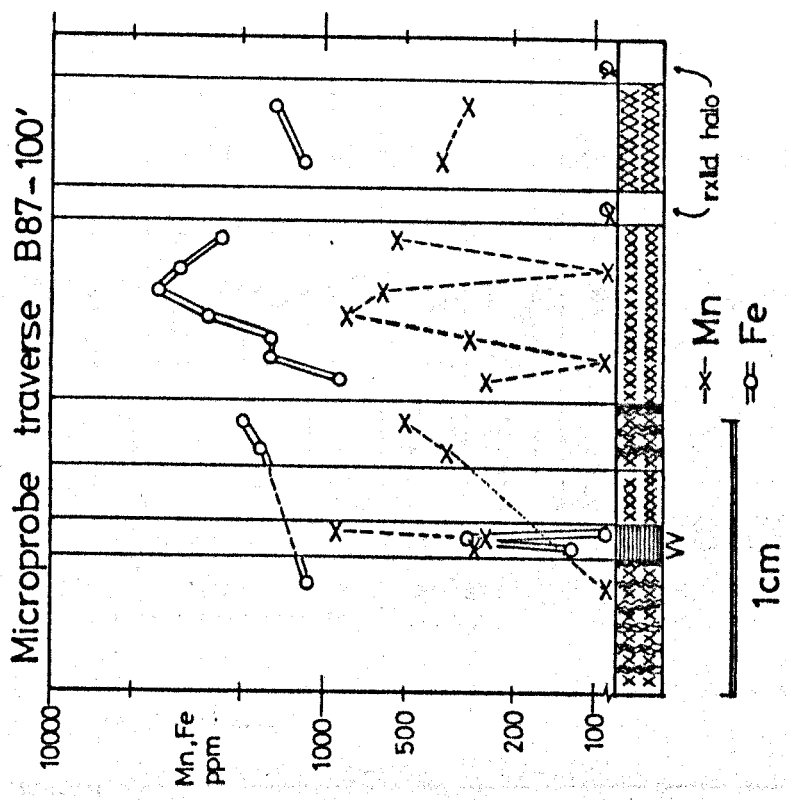


Figure 5.9d: Electron microprobe traverse of sample B87-100' (Silvermines). For key see Figure 5.9a.

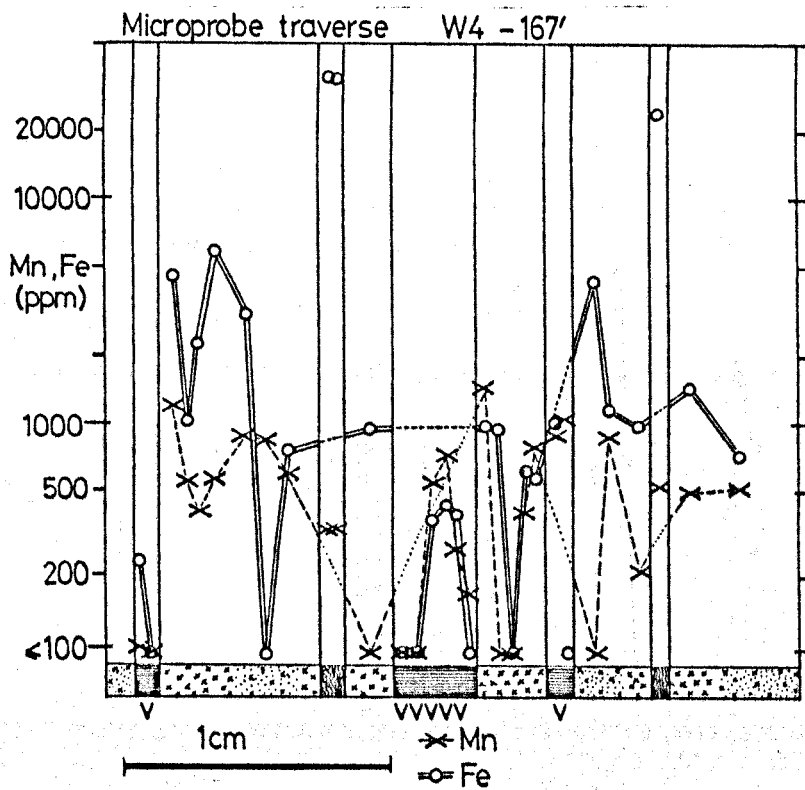


Figure 5.9e: Electron microprobe traverse of sample W4-167' (Silvermines).
For key see Figures 5.9a.

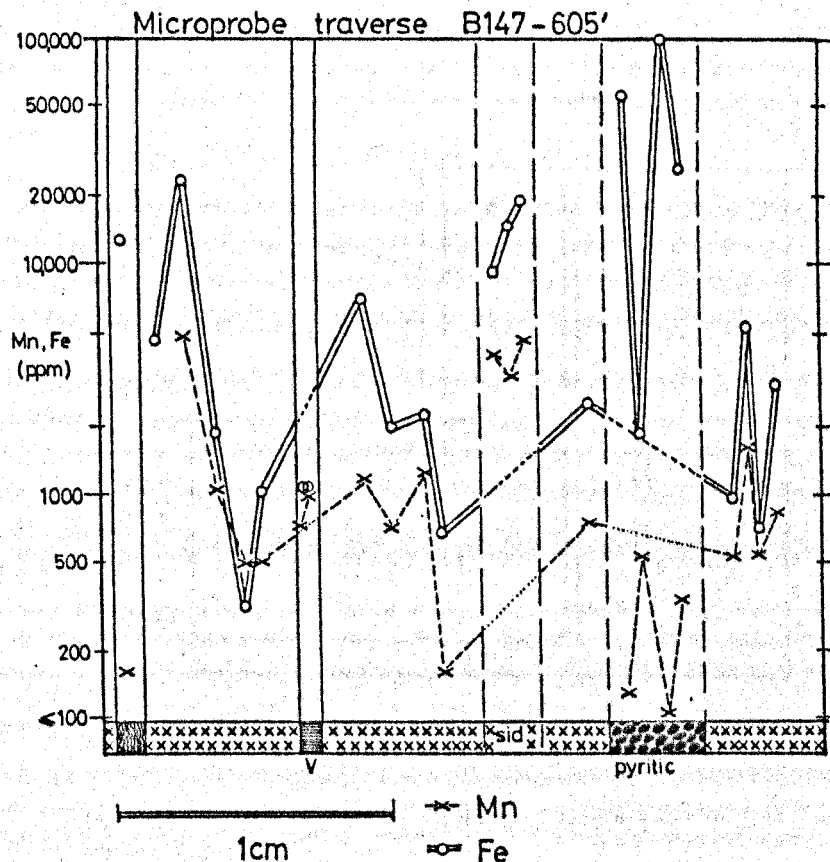


Figure 5.9f: Electron microprobe traverse of sample B147-605' (Silvermines).
For key see Figure 5.9a.

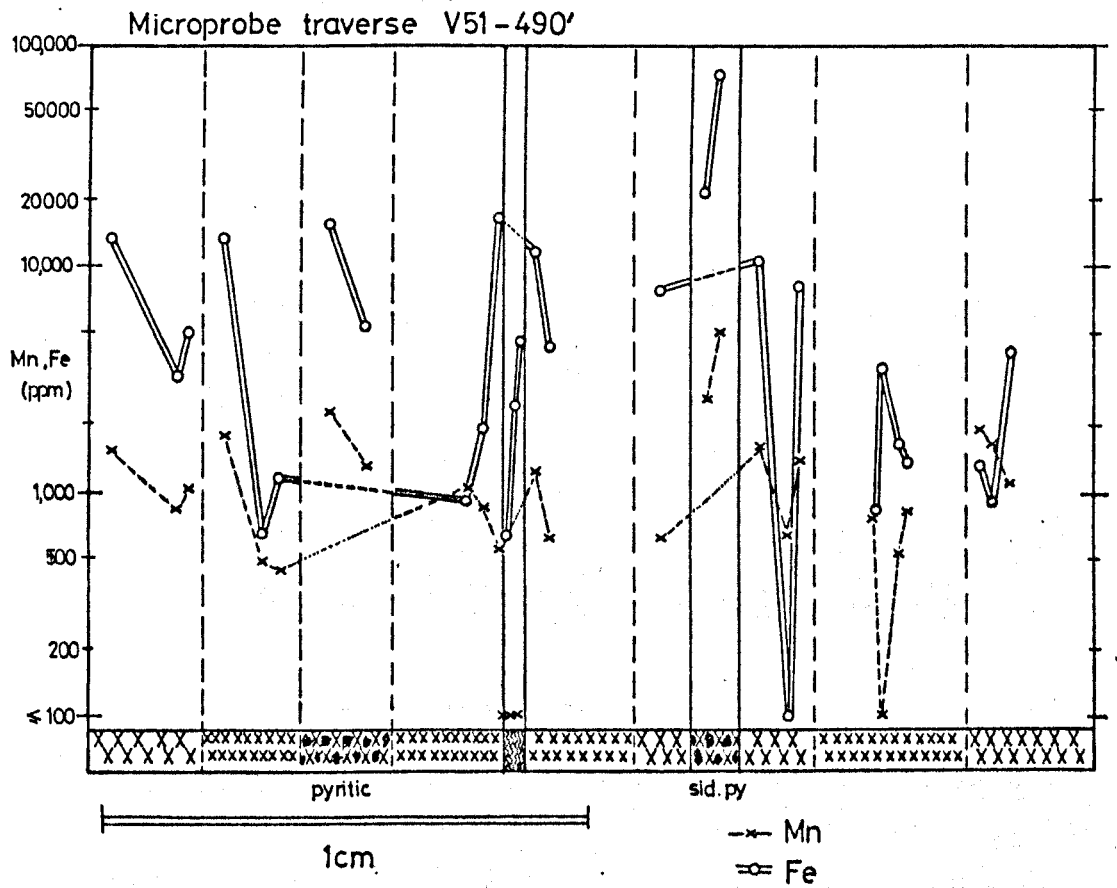


Figure 5.9g: Electron microprobe traverse of sample V51-490' (Silvermines). For key see Figure 5.9a.

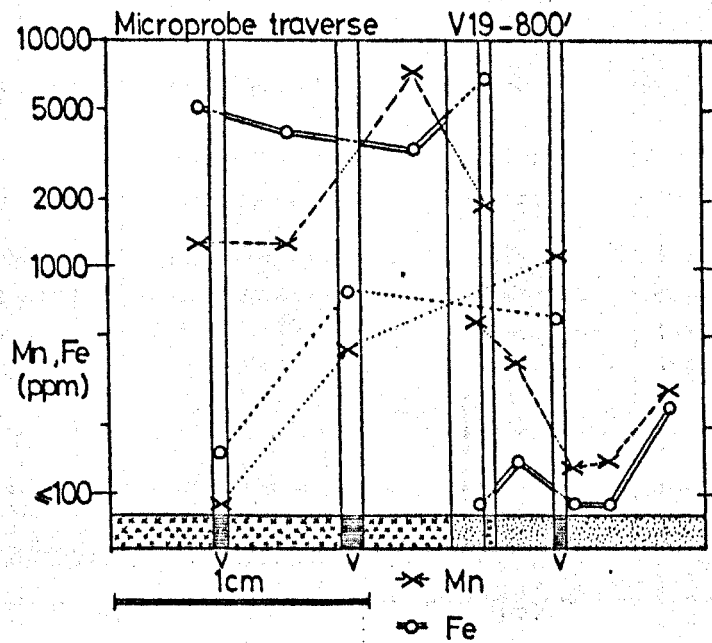


Figure 5.9h: Electron microprobe traverse of sample V19-800' (Silvermines). For key see Figure 5.9a.

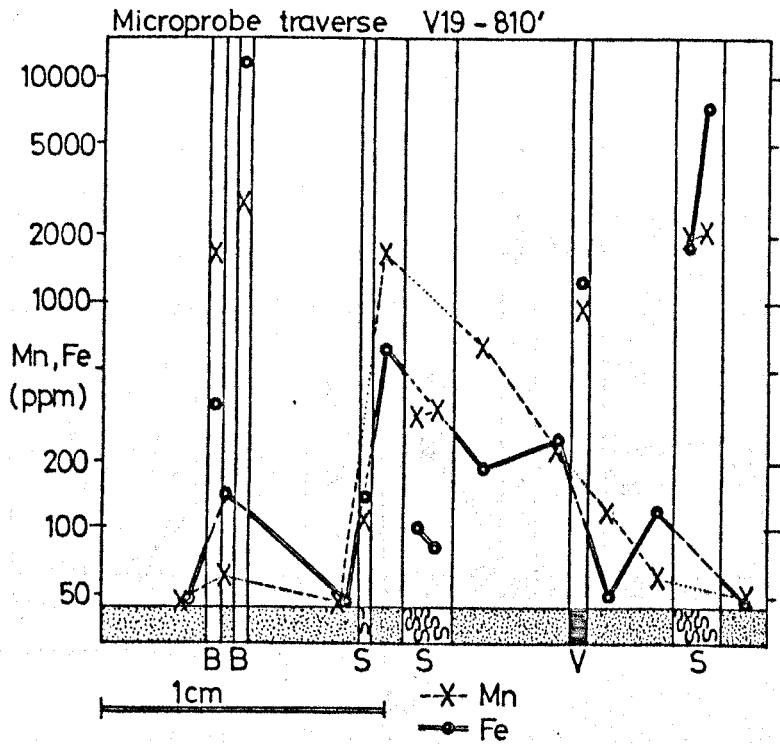


Figure 5.9i: Electron microprobe traverse of sample V19-810' (Silvermines). For key see Figure 5.9a.

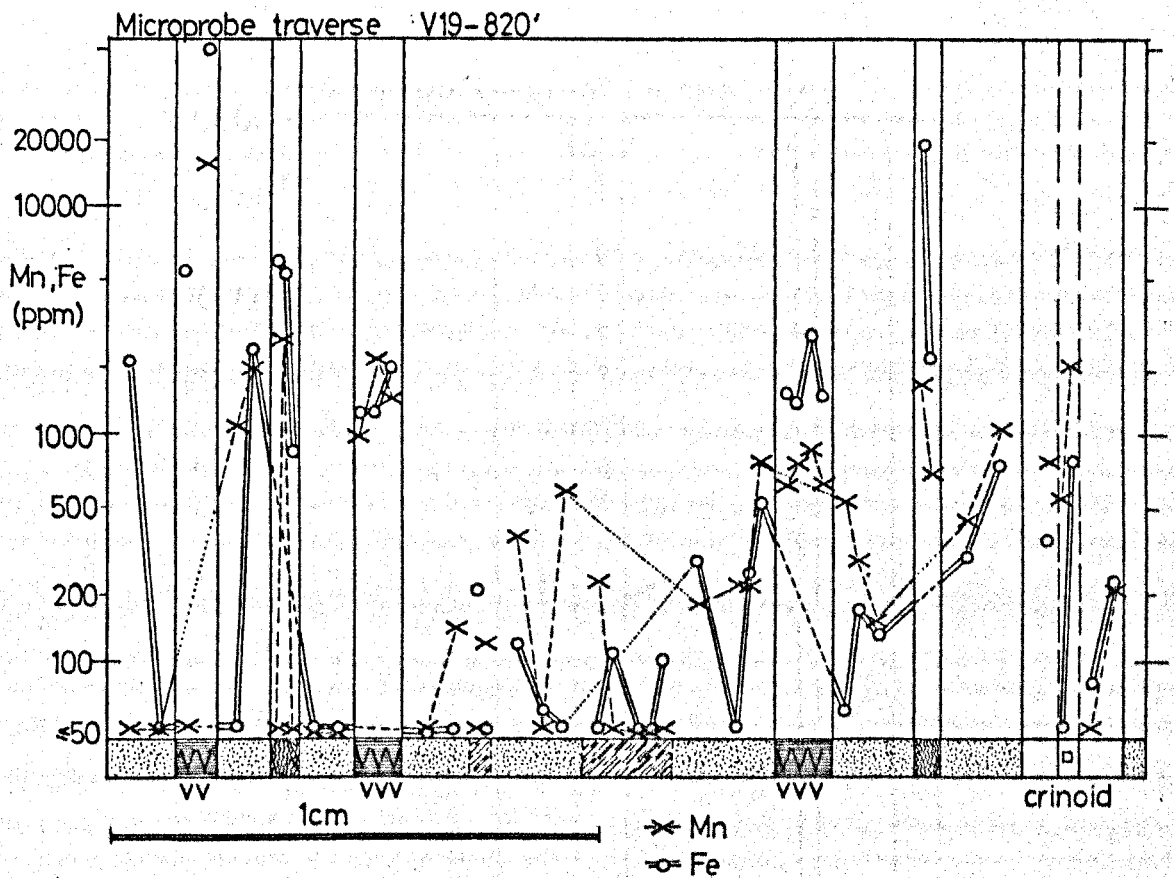


Figure 5.9j: Electron microprobe traverse of sample V19-820' (Silvermines). For key see Figure 5.9a.

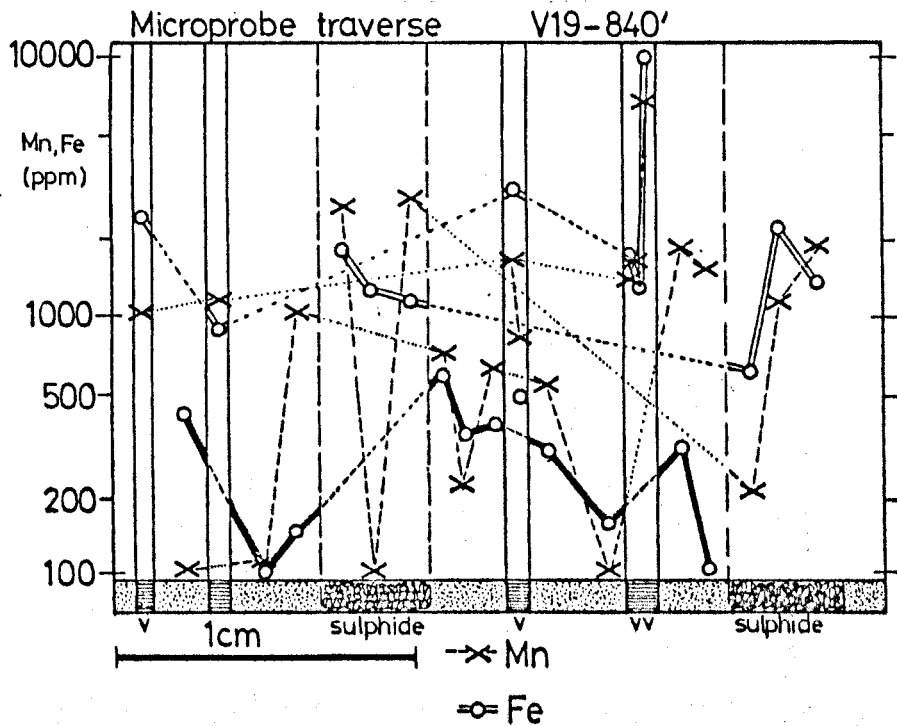


Figure 5.9k: Electron microprobe traverse of sample V19-840' (Silvermines).
For key see Figure 5.9a.

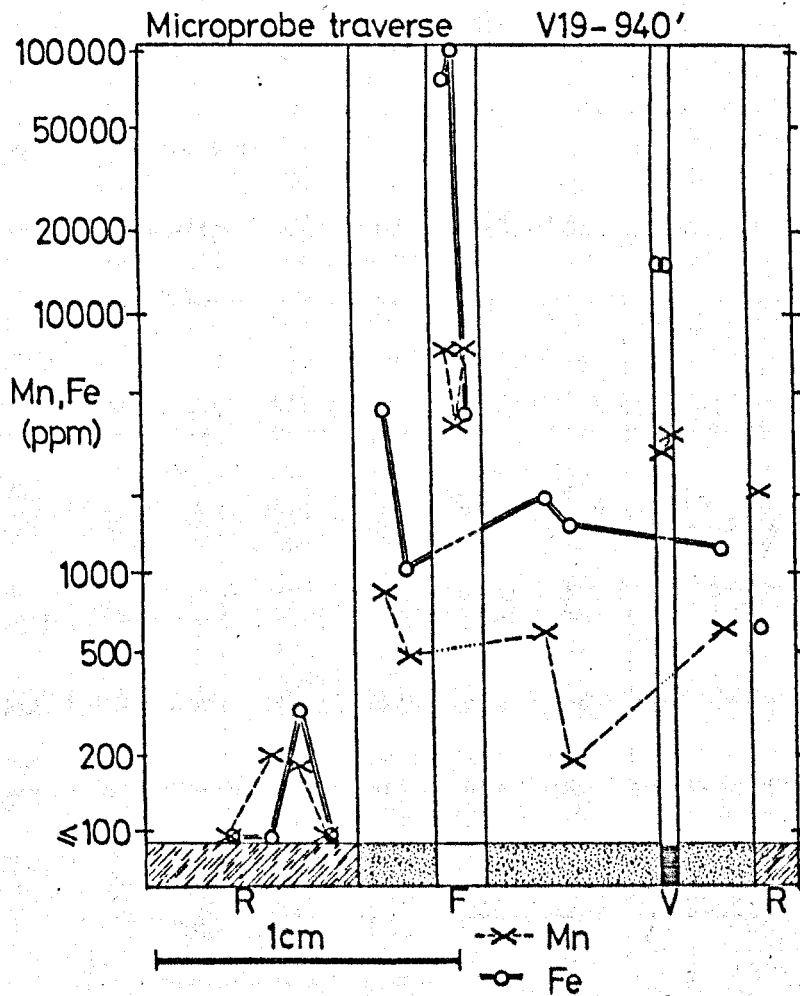


Figure 5.9l: Electron microprobe traverse of sample V19-940' (Silvermines).
For key see Figure 5.9a.

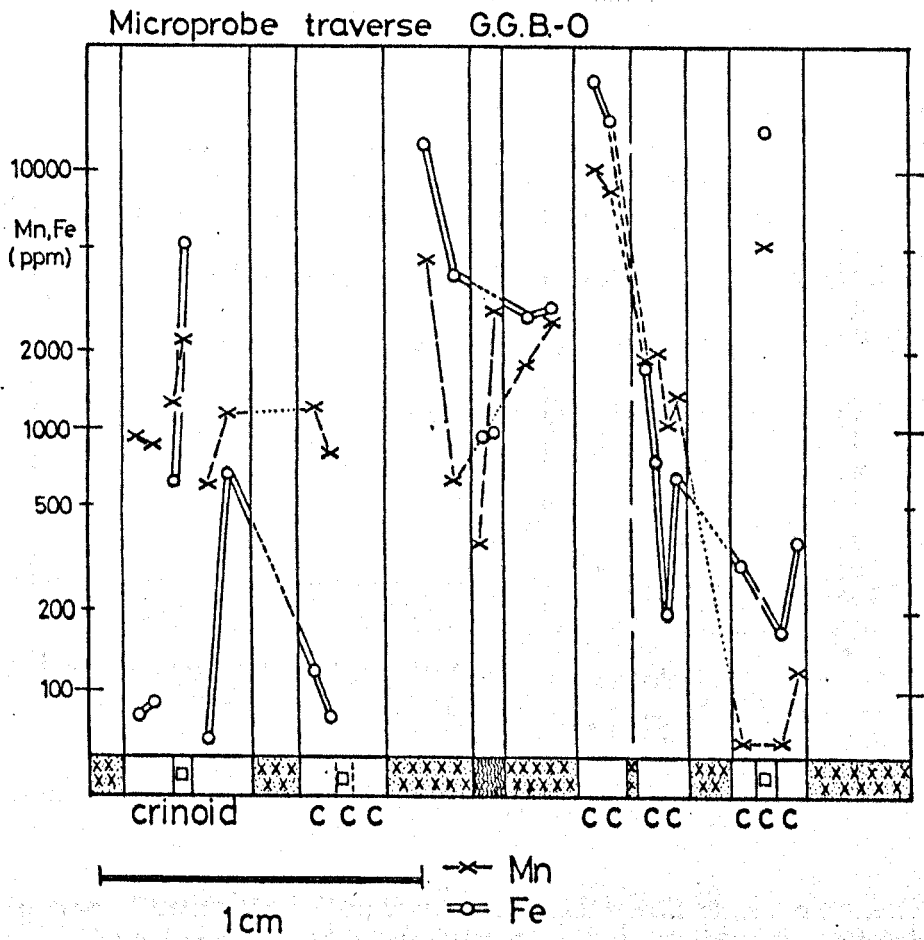


Figure 5.9m: Electron microprobe traverse of sample G.G.B-0 (Silvermines).
For key see Figure 5.9a.

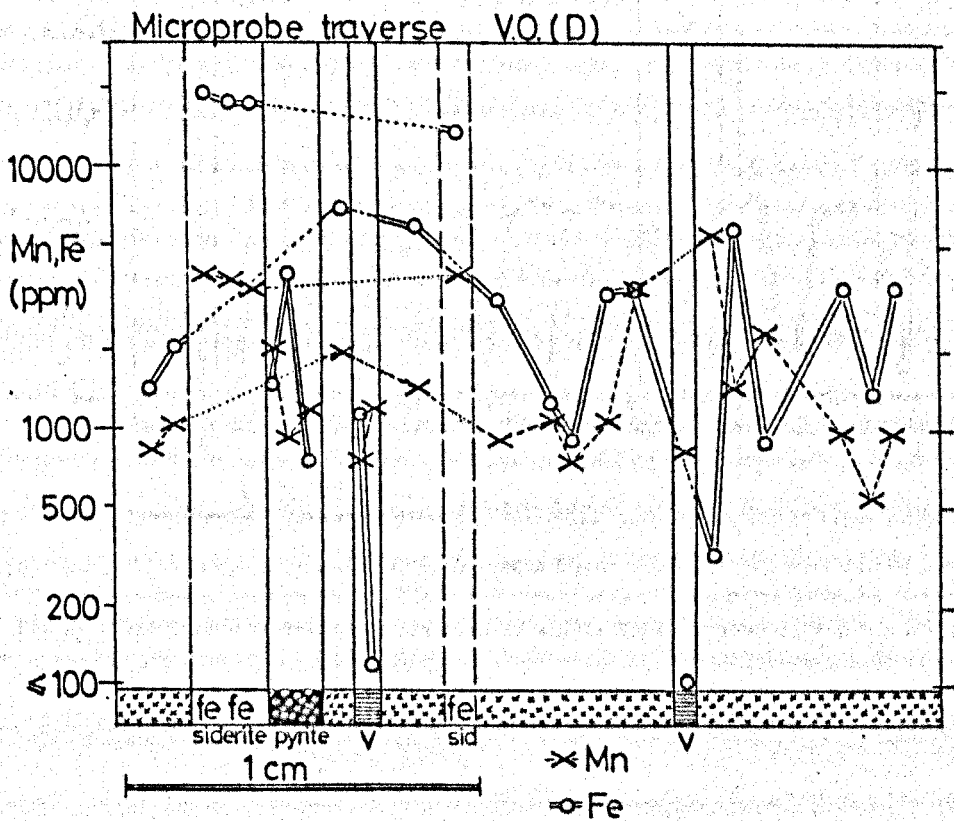


Figure 5.9n: Electron microprobe traverse of sample V.O.(D) (Silvermines).
For key see Figure 5.9a.

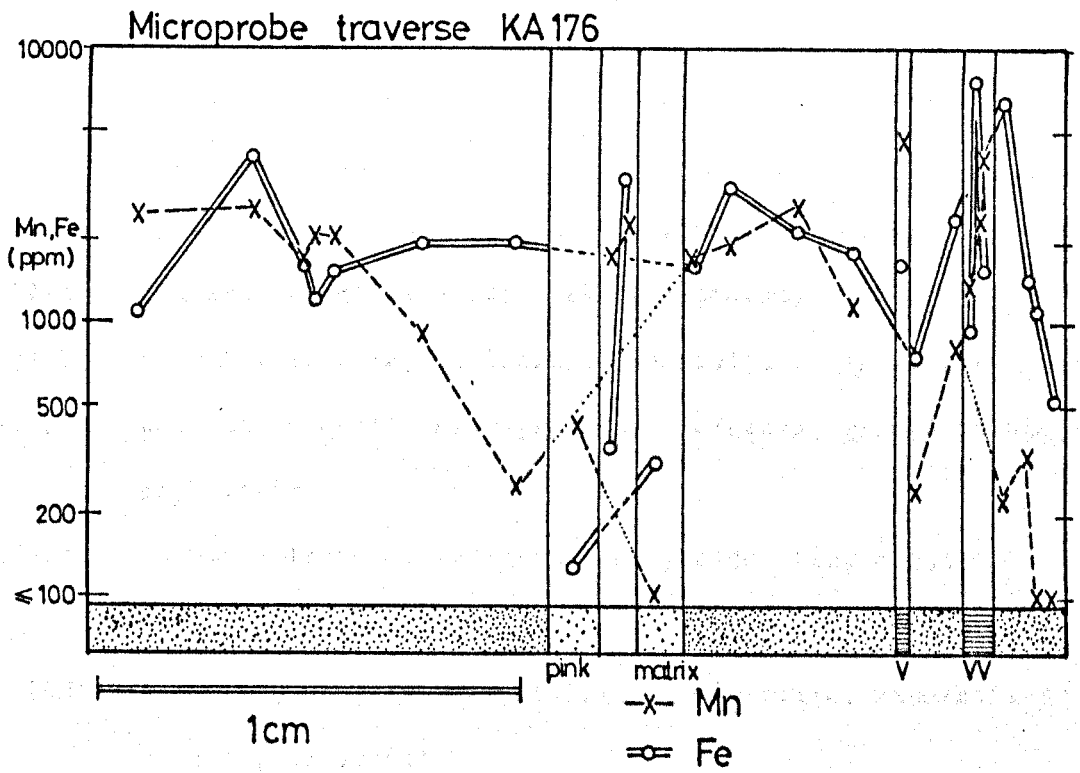


Figure 5.9o: Electron microprobe traverse of sample KA176 (Keel). For key see Figure 5.9a.

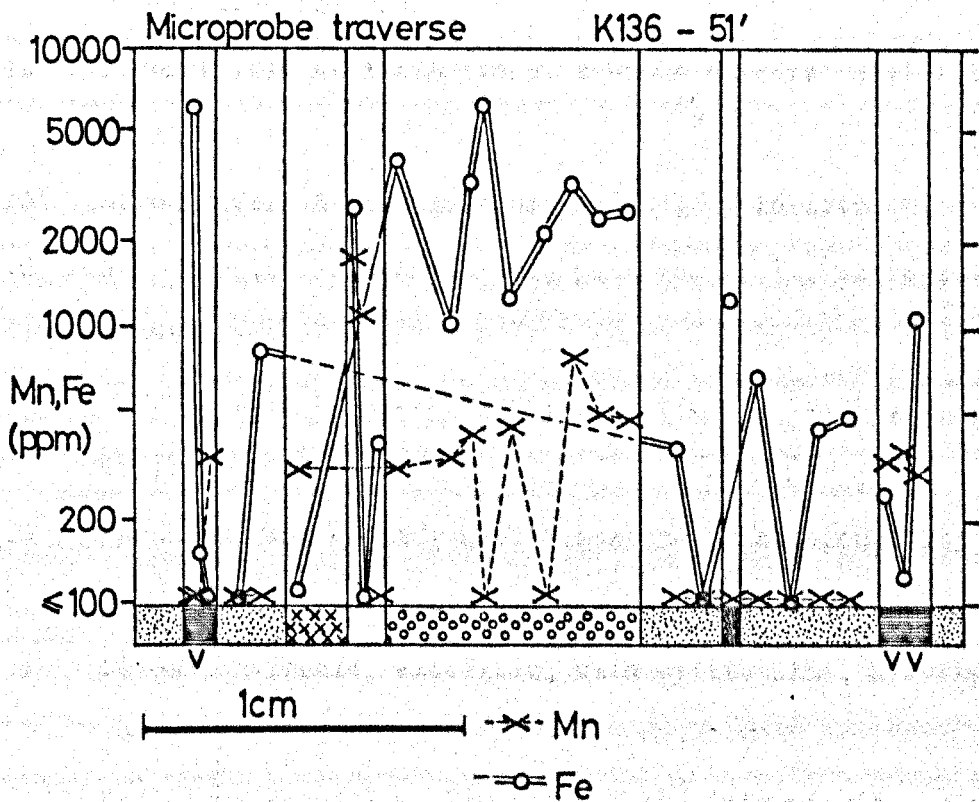


Figure 5.9p: Electron microprobe traverse of sample K136-51' (Keel). For key see Figure 5.9a.

Microprobe Sections

- *LF43 Limestone groundmass, geopetal cavity-fill dolomite and spar.
- B 147-610' 'pseudobrecciated' breccia, trace pyrite, dolomitic.
- S.O.241 Red Marble, heavily stylolitic, crinoidal.
- B 87-100' Dolomite Breccia, stylolitic, veinlets, murky matrix.
- W4-167' Dolomite Breccia, Fine-grained, laminated, graded turbidite, stylolitic.
- B 147-605' Dolomite Breccia, recrystallised, sideritic, argillaceous matrix
- V51-490' Dolomite, heavily recrystallised, sideritic, mineralised breccia, stylolitic
- V19-800' Stromatactis Reef Limestone, with dolomitic/sideritic/mineralised breccia
- V19-810' Stromatactis Reef Limestone, fibrous calcite, stylolites, veinlets.
- V19-820' Stromatactis Reef Limestone, veined, stylolitic.
- V19-840' Stromatactis Reef Limestone, part dolomitic, variegated, mineralised
- V19-940' Stromatactis Reef Limestone, shattered, veinlets, geopetal infil.
- G.G.B.O Basal mudbank - Muddy Reef Limestone transition, very crinoidal, stylolitic, buff weathered.
- V.O.(D) Dolomite Breccia, sideritic, with pyrite rims, heavily recrystallised.
- *KA176 Keel Iron Formation, laminated, hematitic micrite, with fine grained pyrite.
- *K136-51' Micrite with geopetal infil, sparry dolomite/calcite infil, minor hydrocarbon.

Note: * denotes Keel sample, all others from Silvermines.

5.6.1 Summary.

The data presented in this chapter illustrates the inhomogeneous nature of much of the host rocks to the Silvermines deposit, in terms of trace element distribution. Apart from the obvious inhomogeneity created by secondary calcite or dolomite, and patches of siderite or sulphide mineralisation, considerable heterogeneity may be present within individual phases of micritic or recrystallised matrix. This reinforces the need, as outlined in Chapter 2, to avoid such visible secondary contaminants during sampling, something which may not always be possible in the field, or indeed with simple hand-picked separation. Very fine scale intermixing of phases with contrasting geochemistry may be present, introducing the requirement of some care in interpretation of absolute trace element levels.

Because of possible matrix inhomogeneity, the use of very small samples, e.g. single chips of mudbank limestone, would be inadvisable, indeed the larger the sample the better. Not included in this part of the study, however, are samples of distal, relatively pure Waulsortian Mudbank Limestone. Therefore, these conclusions on sample inhomogeneity can only be tentatively applied to distal samples.

Simple correlation between trace element data from A.A. and X.R.F. analyses indicates that anomalous Mn and Fe levels in distal mudbank samples are generally associated with higher levels of 'impurity-related' constituents,

whereas in the mine area samples, any direct correlation between insoluble material and elevated trace element levels is obscured by other controls.

Use of the electron microprobe is insufficiently sensitive to reveal the levels of Zn incorporation into CaCO_3 (or dolomite), if at all, and any zinc recorded in Waulsortian and equivalent carbonates, is probably present largely as fine-grained sulphide phases.

CHAPTER SIX - Discussion and Genetic Implications.

Part One - Depositional Processes.

- 6.1.1. Introduction.
- 6.2.1 Ore Fluid Generation, Subsurface Transport and Composition.
- 6.2.2. Source Rocks and Hydrothermal Fluid Generation in the Irish Lower Carboniferous.
- 6.2.3. Subsurface Mineralisation and Dolomitisation.
- 6.3.1. Depositional Processes and Modification of Fluid Chemistry in a Submarine Environment.
- 6.3.2. Hydrothermal Plume Behaviour.
- 6.3.3. Development of Brine Pool Conditions.
- 6.3.4. Formation of Siderite.
- 6.3.5. Dispersion of Hydrothermal Components.
- 6.3.6. Oxidation of Iron and Manganese.
- 6.3.7. Trace Metal Scavenging by Iron and Manganese Oxides.
- 6.3.8. Sedimentary Features - Brecciation.
- 6.4.1. Trace Element Incorporation into Carbonate Rocks.
- 6.4.2. Trace Element Intake into Irish Waulsortian Limestones.

CHAPTER SIX - DISCUSSION AND GENETIC IMPLICATIONS.

Part One: Depositional Processes.

6.1.1. Introduction.

Iron and manganese oxide facies may be developed to a considerable lateral extent around both active and fossil hydrothermal exhalative centres (e.g. Afar Rift, Bonatti et al (1972); Santorini, Whitehead (1973); 21°N East Pacific Rise, Haymon and Kastner (1981)), and also around some stratiform syngenetic base metal deposits (e.g. Tynagh, Russell 1975). The greater areal extent of oxide facies makes their occurrence of interest to exploration geologists, as sulphide and sulphate deposition is generally restricted to the vicinity of venting sites. Of greater interest still, are more laterally extensive, but generally cryptic, trace element haloes, which may be developed beyond the oxide facies. The fact that the chemical haloes are essentially cryptic, means that a method of detecting various trace metals substituting in the crystal structures (with little or no mineralogical representation) is required.

Lithogeochemistry is defined by Govett and Nicholl (1979) as "the determination of the chemical composition of bedrock material with the objective of detecting distribution patterns that are spatially related to mineralisation". Application of lithogeochemistry in this study is largely limited to examination of simple trace element dispersion patterns around

individual centres, essentially without the use of multivariate statistical techniques to enhance weak anomalies. These patterns provide evidence for primary exhalative origin, and a simple but effective tool in mineral exploration.

Iron and manganese are generally the two most important minor element constituents of a hydrothermal fluid (Table 6.1), and both readily substitute for Ca in the CaCO_3 structure in sedimentary carbonate environments. In mildly reducing or oxidising conditions, Fe and Mn may precipitate together in the carbonate phases, and the two elements are most likely to migrate together and coprecipitate within the limits of their carbonate stability fields (Lepp 1963). Under normal seawater conditions, Mn:Fe ratios are much higher in carbonate rocks (average 0.29), compared to most other sedimentary rock types (average 0.02) which reflect closely the average crustal abundance of Mn and Fe (Lepp op cit).

The data presented in Chapters 3 to 5 indicate that Mn and Fe enrichments are present in the carbonate rocks around most (if not all) of the deposits examined in this study. This chapter is concerned with evaluating what information the trace element patterns divulge as to their origin, and of the genesis of their associated deposits. Application of this knowledge to the use of the technique of lithogeochemistry in exploration is discussed in the following chapter.

This discussion centres mainly on the dispersion

System	Average Seawater	Salton Sea Geothermal Brine	Atlantis II Deep, Red Sea	Matupi Harbor	21°N East Pacific Rise
References	A	B	C	D	E
Metals Deposited	-	Cu Ag Fe As Sb Bi	Zn Cu Pb As Sb Bi	Zn Cu Pb Mn Fe	Fe Ba Zn Cu Mn Pb
Temperature °C	~23	> 300	56	65	350
Element content (g/l)					
Cu	2×10^{-6}	0.010	0.00026	0.0005	0.0014
Pb	3×10^{-8}	0.104	0.00063	0.0009	0.000054
Zn	5×10^{-6}	0.3	0.0054	0.00253	0.00554
Ag	28×10^{-8}	0.001	-	-	n.a.
As	26×10^{-7}	0.015	-	0.0002	n.a.
Mn	1×10^{-6}	2.0	0.082	0.111	0.0486
Fe	1×10^{-5}	3.2	0.081	0.097	0.0798
Ba	15×10^{-6}	0.2	0.009	0.097	0.00137
Na	10.8	64	92.8	13.6	10.48
K	0.39	32	1.87	0.765	0.938
Ca	0.41	51	5.15	0.395	0.649
Mg	1.30	0.92	0.764	1.34	0
SO ₄	2.72	0.071	0.84	5.42	0
Cl	19.5	234	155.5	22.5	18.3
SiO ₂	6.2	~ 0.1	0.059	-	1.05
Al	0.001	0.45	-	-	0.00012

Table 6.1: Concentrations of selected elements in various hydrothermal systems. References: A - Turekian (1969), Miller et al (1966); B - White (1965); C - Craig (1969); D - Ferguson and Lambert (1972); E - Averaged from Von Damm et al (1985).

Fluid	T°C	T.D.M. (ug kg ⁻¹)
Black Smoker Fluid	350	310
White Smoker Fluid	~330 ?	240
Diluted Vent Fluid	< 330	4.7
Ambient Seawater	1.6	0.2

Table 6.3: Temperature and total dissolved manganese (T.D.M.) content of brine waters at 21°N, East Pacific Rise. Source - Lupton et al (1980).

System	Mn (ppm)	Mn:Fe
Estimated (Lyle 1976)	1 - 4	
Observed		
Matupi Harbor	2.7 - 111	0.19 - 1.14
Atlantis II 56°C Brine	82	1.22
Banu Wuhu, Indonesia	16 - 21	
*Heimay, Iceland	0.01 - 0.059	0.16 - 4.2
*Deception I. Antarctica	0.6 - 2.4	0.33 - 7.7
Experimental		
Bischoff and Dickson (1975)	6	1.0
Mottl et al (1974)	0.85 - 284	
Hajash (1975)	0.26 - 90	0.042 - 3.2
Bischoff et al (1981)	0.05 - 95	0.01 - 4.03

Table 6.2: Manganese concentrations and Mn:Fe ratios in selected hydrothermal and experimental systems, based on Lyle (1976). Those marked * reflect significant surface mixing with seawater.

patterns of trace elements, particularly Mn and Fe, around the Silvermines exhalative centre, with brief reference to the other Irish deposits where relevant. Considerations will be given to the various controls which may have operated on their outward migration and incorporation into actively forming carbonate sediments, which resulted in the formation of a primary trace element aureole.

The processes operating on these trace metals in solution, which account for the different distribution patterns in host rocks around fossil hydrothermal vents, may be divided into three main categories, as follows:-

- 1) differential concentration during generation and subsurface transport, leading to different concentrations in the exhaled fluids;
- 2) differential precipitation due to fractionation processes in a submarine environment;
- 3) differential solution and precipitation during diagenesis and post-depositional modification.

The discussion of the genetic processes operating on the Silvermines host rocks, and those of other Irish base metal deposits, will continue under these three headings.

6.2.1. Ore Fluid Generation, Subsurface Transport and Composition.

Circulation of seawater through thermal contraction features in axial zones of oceanic spreading centres permits exchange of elements between seawater and basaltic rocks at elevated temperatures. Channelling of these solutions upwards through major faults and expulsion of metalliferous fluid on seafloor locations may result (Bischoff and Dickson 1975, Seyfried and Bischoff 1977, Mottl and Holland 1978). Similar exchange is permitted when hot fluids percolate through greywacke or shale (Bischoff et al 1981), even at temperatures below 100°C (Long and Angino 1982).

During these processes, Mn and Fe follow roughly parallel geochemical paths. Hajash (1975) has shown that a solution derived by leaching of igneous rock will have a Mn:Fe ratio that is dependant on a number of factors, especially temperature and water-rock ratio. Bischoff et al (op cit) demonstrate the importance of fluid salinity and composition in greywacke leaching experiments, and show that unmodified seawater is comparatively ineffective in leaching sufficient metals at temperatures below 350°C, unless very high water-rock ratios are involved. They also demonstrate that, compared with basalt, greywacke provides more metal in solution during hot brine leaching, of which Fe and Mn are the most important constituents.

From experimental reactions in the temperature range

up to 300°C, Hajash (op cit) obtained Mn:Fe ratios in leach solutions of approximately 0.2 to 1. Iron greatly exceeds manganese in the leachate by a factor of about 20 in higher temperature experiments (Mottl et al 1979). Similarly, Bischoff et al (op cit) show how a large decrease in Mn:Fe ratio may arise if reaction temperature rises above 350°C in brine or seawater-greywacke interactions, such that Fe becomes a major constituent of the hydrothermal fluid.

Actual measured ratios in some present day hydrothermal systems are shown in Table 6.2. The wide range of observed values indicates that a wide range of initial solution ratios may have existed, or that some process of separation may have already begun by the time the solutions reached the surface.

Solubilities of the ore forming metals Zn and Cu, in hydrothermal leach solutions, are shown by Russell et al (1981) to be largely a function of fluid temperature, oxidation state and acidity. Lead behaves in a very similar manner to Zn, except that it is rather less soluble, especially at lower temperatures (Bischoff et al (1981)).

To produce an ore forming solution, the chloride complexing ability of a more saline brine is essential for sufficient metal transport in hydrothermal systems (see Finlow-Bates 1980). Solubility of iron and manganese during fluid transport will depend on a number of factors, including fluid chemistry.

High sulphate concentrations in solution will reduce iron solubility, but leave manganese relatively unaffected, thereby raising the Mn:Fe ratios in the final exhaled solution.

Lupton et al (1980) consider the 350°C fluids exhaling on the East Pacific Rise at 21°N to approximate to undiluted hydrothermal fluids, unlike those of other systems (e.g. Galapagos Spreading Centre), which have suffered sub-seafloor dilution with normal seawater.

Normally, some degree of subsurface mixing will prevent direct observation of pure, high temperature, end-member, ore transporting fluids (Edmond 1981). The 'black smokers' of 21°N provide the exception, in which 350°C fluids at a pH of 4.7, enriched in H₂S, Fe, Zn, Cu, Mn, Ba, Si, Li, Rb, Ca, and K, but devoid of Mg or SO₄, precipitate sulphides by rapid mixing with ambient bottom waters. However, dissolved manganese concentrations at 21°N may have been lowered by scavenging onto particulate matter (Table 6.3), being only a fraction of the totals measured in the Red Sea brines (55 - 82 mg/kg), which Lupton et al (op cit) suggest correspond to the upper limit for deep sea hydrothermal vent fluids. These levels are comparable with concentrations achieved in laboratory experiments (Mottl et al 1979).

6.2.2. Source Rocks and Hydrothermal Fluid Generation in the Irish Lower Carboniferous.

The structural regime during early Carboniferous times in Central Ireland was one of extensional stress (Russell 1973, Haszeldine 1984). This gave rise during mid to late Tournaisian times, to rapid subsidence of small second order basins, allied to tensional fracturing of the crust (Russell 1978). This in turn may have permitted access of saline waters from the transgressive Carboniferous sea, downwards into the thick Lower Palaeozoic metasedimentary pile and Caledonian granite plutons. Higher than normal seawater salinities are indicated by the presence of evaporite minerals at numerous localities in mid Tournaisian sediments (McDermott and Sevastopulo 1972, Sevastopulo 1979). Alternatively, tensional strain allowed the escape of high temperature metamorphic pore waters (Kozlovsky 1984).

Thick Caledonian geosynclinal metasediments underlie the central Irish Plain, comprising mainly greywacke, shale and siltstone, with volcanic horizons becoming prominent towards the southeast. These are intruded by granitic massifs of Lower Devonian age, such as the Leinster Granite (Holland 1981). Towards the south of the country, a very thick (over 6000 metres) Devono-Tournaisian sequence of entirely shallow water character (non-marine to shallow marine) was present below the Carboniferous cover, possibly bounded on

its northern side by a series of basin-margin faults (Naylor and Jones 1967, Clayton et al 1980).

The Lower Palaeozoic succession provided the metals for much of the Lower Carboniferous mineralisation in Ireland (Samson 1983), the regional compositional variation in the former perhaps contributing to the apparent regional chemical variation present within the deposits from north to south (Radtke et al 1977).

The result of deep penetration of saline fluids into heated crustal rocks and/or the escape of metamorphic pore waters, was the production of a reduced, hot, weakly acidic, metal and silica-bearing hydrothermal brine. The metals, chiefly barium, iron and manganese, but also significant amounts of base, alkali earth, and precious metals were held in solution mainly by chloride complexing. The fluids were also enriched in Ca, K and CO₂, but depleted in Mg and SO₄ (Samson 1983), similar to the experimental results of Bischoff et al (1981).

The heated fluids migrated from depth towards the sea floor along lines of structural weakness, such as active Lower Carboniferous fault zones, allowing them to bypass several hundred metres of relatively impermeable muddy carbonate sediments of the Lower Tournaisian (Sevastopulo 1979). At Silvermines, the main Silvermines Fault Zone and related northwest-trending cross-structures provided the conduit for fluids rising from depth (Taylor and Andrew 1978).

A steadily evolving hydrothermal fluid composition may have been generated by progressive deepening of crustal convection, and resulting increase in temperature and vigour of the circulative system (Russell 1978). Some of these processes of evolution, and their geochemical imprints, are considered throughout this chapter.

6.2.3. Subsurface Mineralisation and Dolomitisation.

Upon ascent, the hydrothermal fluids encountered cooler, saline fluids in the subsurface feeder zones, and were subjected to a sudden drop in temperature, combined with an increase in pH and Eh on mixing. Some reduced sulphur was carried by the hydrothermal solution, and precipitation of sulphides (with baryte and carbonate) in the fracture zones occurred on mixing with more alkaline brines. Very fine grained sulphides were formed by more rapid, turbulent mixing of the two fluids. Increased pH, brought about by reactions with carbonate wall rocks, may also have played a part in mineral deposition, as the host rocks were the first significant carbonate horizon encountered by the rising hydrothermal fluid.

Fluid temperatures in this feeder zone reached 220°C or more, with salinities of about 12 eq. wt. % (Samson and Russell 1983). Because of the wide range of temperatures and salinities recorded, and stable isotope evidence, Samson (1983) points towards the

mixing of perhaps more than two solutions. These would have been:-

- i) the original hydrothermal solution (hot, low to moderate salinity);
- ii) the cooler, high salinity fluids of the feeder zone (perhaps derived from an overlying brine pool);
- iii) possible components from connate, formation waters or meteoric sources.

The source of the denser, saline fluids in the overlying brine pool at this stage, may have been either from early (pre-main ore phase) hydrothermal exhalations, or from a hypersaline environment in shallower water some distance to the south (cf. the downward movement of dense, hypersaline bank waters to form lenses in troughs at Tongue of the Ocean, Bahamas (Schlager and James 1978)).

Extensive dolomitisation of the carbonate sediments is associated with the footwall epigenetic feeder zone ore-bodies at Silvermines (Taylor and Andrew 1978). Samson (op cit) favours primary dolomitising processes in their formation, based on relatively low Mg/Ca ratios in fluid inclusion leachates and some textural observations. He also cites the alternative that dolomitisation took place after the entire mineralising event, but neglects the possibility that other fluids may have been involved (e.g. circulating saline Carboniferous seawater or brine pool water), or that dolomitisation may have taken place between sediment deposition and mineral

emplacement.

Attenuation of the footwall succession, which hosts the Lower G and K Zone replacement ore at Silvermines, is noted close to the main fault zone (Taylor and Andrew op cit, Samson op cit). The ore is hosted in dolomitised portions of argillaceous limestone units in the succession (BrUck 1982). Moreover, considerable thinning of most of the Old Red Sandstone and Lower Carboniferous sequence in the mine area, relative to the neighbouring areas, is described by BrUck (op cit), Emo and Grennan (1982) and Philcox (1984).

Thinning of the footwall limestone sequence adjacent to the fault is just as likely a result of volume reduction during dolomitisation, and structural attenuation by later dip-slip fault movements, as it is due to differential subsidence rates during sedimentation.

Introduction of Mg rich, saline Carboniferous seawater by downward percolation into the feeder zone, aided by tectonic and hydrothermal fracturing, may have accelerated the growth of dolomite in place of calcite, through interactions with hot, Mg poor, Ca rich hydrothermal solutions. The analogy may be drawn here with the formation of Mg-chlorite and talc in footwall alteration pipes to massive sulphide orebodies such as Mattagami, Quebec (Roberts and Reardon 1978), where thermally induced convection may be intense.

Of the other Irish Carboniferous deposits, only Tynagh and Gortdrum feature subsurface, feeder-zone

type mineralisation in economic concentrations. Feeder-zone sulphides form all, or the bulk of sub-economic mineralisation at Keel, Moate, Moyvore, the Ballyvergin area, Aherlow and Mallow (see Section 6.3.5.). At each of these deposits, base metal sulphide mineralisation infills veins and fractures in predominantly limestone strata (except at Keel, where conglomerate and sandstone are dominant), often with severe recrystallisation, dolomitisation and replacement of adjacent host rocks.

Prior to seafloor exhalation, modification of the fluid chemistry had taken place as a result of mineral precipitation and subsurface reactions between the rising solutions, the wall rocks, and locally derived solutions. Precipitation of pyrite and dolomite in the subsurface environment would have played the greatest part in modifying the Mn and Fe levels of the exhaled hydrothermal fluids.

6.3.1. Depositional Process and Modification of Fluid Chemistry in a Submarine Environment.

Fractionation of the various trace metals in the submarine environment commenced immediately upon exhalation of the hydrothermal solutions at the vent sites. A number of processes were involved in determining the distribution and sedimentary incorporation of metallic effluents, and these may be divided into two main categories. Firstly, those affecting the distribution of metals in the immediate environment of ore deposition, including: i) hydrothermal plume behaviour; ii) brine pool formation; iii) metal oxidation and scavenging; iv) dispersion of trace metals and separation of Mn from Fe; v) sedimentary features; vi) waning hydrothermal activity; and secondly, those affecting the intake of trace metals into carbonate rocks and minerals on the surrounding sea floor.

The overall result of the processes acting in the environment of the vents will influence the 'export' of trace metals to the surrounding sea floor environment, although considerable overlap will clearly exist between the two environments.

6.3.2. Hydrothermal Plume Behaviour.

Characteristics of the fluids involved at the moment of exhalation, such as density or temperature contrasts and degree of mixing with surrounding ambient waters, and

the flow rate from the vents, determines the initial buoyancy behaviour. Sato (1972) describes a number of possible situations, ranging from a bottom-hugging current to a rising, buoyant plume, with combinations of the two in between. "Double diffusion" effects, caused by the different diffusion rates of heat and salt in solution, also have an influence on fluid behaviour (Turner and Gustafson 1978). The end result will determine to a considerable extent the nature of any accumulations of ore formed, as well as the lateral dispersion of related hydrothermal material.

We may infer much about the behaviour of exhaled hydrothermal solutions at Silvermines by considering the physical dispersion of material from present day exhalative systems on the ocean floor. Above the Galapagos hydrothermal field, plumes of hot vent waters with densities as low as 0.62gcm^{-3} , rise quickly and are diluted rapidly by ambient seawater (Enright et al 1981). Hot waters may be diluted 70-fold to within 0.3°C of ambient water temperatures within 10 metres vertically above the vent source. Lupton et al (1980) describe the behaviour of warm brine waters above the 21°N East Pacific Rise vents which, although rapidly diluted with ambient waters, rise about 200 metres upwards from the vents as buoyant plumes. On reaching density equilibrium, they spread laterally, detected by elevated Mn and ^3He concentrations and very weak temperature anomalies.

Klinkhammer (1980) demonstrates that hydrothermal emanations from the Galapagos field produce extensive areas of anomalously high Mn content in ocean waters, extending over one kilometre above the ocean floor (Figure 6.1^a) and many kilometres laterally from the vents. Manganese concentrations are as high as fifty times normal background levels, and perhaps even higher in anomalously warm waters associated with the vent areas.

Balance between the upward flowing plumes and particle size or settling rate will help determine the amount of physical dispersion of sulphide or other material, entrainment of sphalerite or galena to considerable heights above the sea floor being feasible (Solomon and Walshe 1979). Rapid precipitation of very fine grained sulphides, on or before exhalation, facilitates entrainment of metal sulphides with Mn and Fe species.

Vertical and horizontal movement of the plume will slow down, eventually resulting in its stagnation and settling of particulate matter. Thus, barring the possibility of current action, physical dispersion will be replaced by chemical diffusion. Solomon and Walshe (op cit) determine that the average velocity of an outwardly migrating brine plume declines by an order of magnitude every kilometre.

Though initially buoyant on entering the sea, entrainment of seawater may reverse this situation, and result in the relatively cool, saline solutions sliding

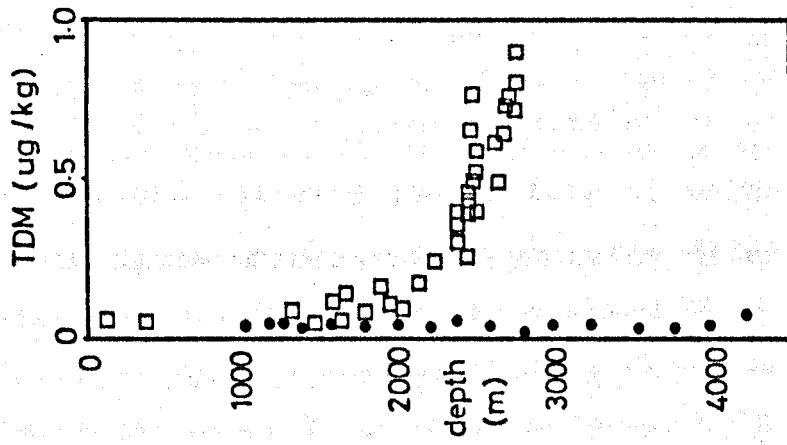


Figure 6.1a: Changes in total dissolved manganese (TDM) concentration with depth from two Pacific locations, simplified from Klinkhammer et al (1977).
 □ - Galapagos Rift area, ● - 'background' area, (Geosecs station 343).

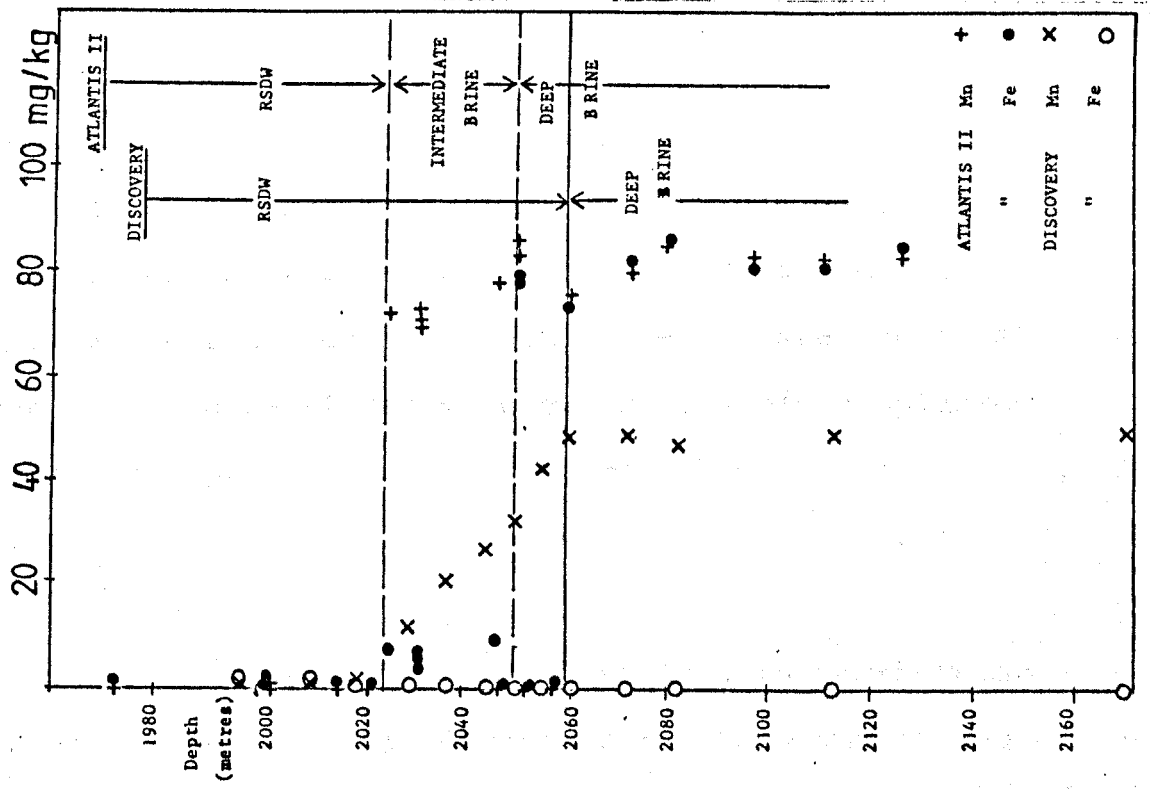


Figure 6.1b: Changes in Mn and Fe concentrations with depth in both Atlantis II and Discovery Deep, Red Sea. After Danielsson et al (1980).

downslope as a bottom-hugging current until they come to rest in a suitable hollow. Turner and Gustafson (1978) show by experimentation how physical movement (akin to turbidity flow) of the denser component of a double diffusive plume can permit great distances to be covered by mineral-laden waters. This would complement the outward spread and diffusion of a hotter, less dense, rising plume, which could eventually lose much of its metallic content by oxidation.

Particulate matter entrained within the bottom-hugging current may be deposited during downslope movement and will settle with newly precipitated sulphide when ponding has occurred in a seafloor depression. Accumulations of brines in irregular sub-basins may result in stratification of different components, according to density, as displayed by the Red Sea Brine Pools (Shanks and Bischoff 1980). Danielsson et al (1980) compare density profiles of Red Sea waters through the Atlantis II and Discovery Deeps, and observe a linear correlation between calcium content and salinity in the former, which indicates that intermediate brines arise by mixing of the hot, primary brine and Red Sea Deep Water (RSDW). A compound density profile, with step-like increases, reflects the brine stratification in Atlantis II, contrasting with the Discovery Deep, where ponding of a single, mixed brine occurs (Figure 6.1b). Chemical composition of the brines is a function of the interplay between each contributory component: hydrothermal input; buried evaporites; RSDW;

O₂ content; adsorption processes.

Wide dispersion patterns of various trace metals around the Red Sea Brine Pools (Bignell et al 1976) may be attributed to lower oxygen levels in and around the brine pools, slowing down oxidation and precipitation. Low sulphide contents in bottom waters would allow greater residency times of chalcophile species in solution, resulting in wider dispersion patterns by outward diffusion. Low sulphide levels in the Red Sea Brine Pools, and the apparent absence of bacterial activity, are envisaged by Mossman and Heffernan (1978) as being responsible for the relative scarcity of sulphide minerals in the muds. This is reinforced by the presence of minerals such as atacamite (hydrated copper chloride), which require extremely low H₂S concentrations to stabilise.

Behaviour of Exhaled Fluids at Silvermines.

Although moderately high temperatures of 200 - 220°C (salinity about 12 eq. wt. % NaCl) are indicated for fluids in the Silvermines feeder zones (Samson 1983), these were probably much lower on seafloor exhalation (less than 100°C, Boyce et al 1983), and the fluids would not readily have formed a buoyant plume on exhalation. More likely they would have developed double-diffusive characteristics, similar to the conditions envisaged by Solomon and Walshe (1979) for the Rosebery deposit. In this way, a denser, base metal rich brine may have flowed into topographic hollows on the seafloor

to form a brine pool, while a buoyant plume, charged mainly with dissolved constituents and colloidal Mn and Fe complexes, rose and spread over a much wider area than the brine pool.

Evidence from the study of fluid inclusions (Samson op cit) and sedimentological control (especially Waulsortian Mudbank growth, Boyce et al, op cit), point towards water depths of at least 100 metres in the vicinity of the fault zone, and even greater depths over the sedimentary orebodies forming in the adjacent sedimentary-structural basins. Although much shallower than the ocean floor hydrothermal systems described before, this is still sufficient depth to allow considerable separation of the two components of a double diffusive plume.

Discharge of large volumes of reduced, metal bearing brine onto the seafloor in a restricted basin allowed precipitation of the concordant sulphide lenses near the vents.

Taylor (1984) favours the growth of pre-existing (i.e. before the principal mineralising events and tectonic disturbances) Waulsortian mud mounds on structural highs in the footwall Muddy Reef Limestone (Figure 6.2). These structural highs run approximately parallel to one another, trending NNW-SSE, and developed in response to stress created by movements on the Silvermines Fault Zone. Taylor (op cit) observes that ore zones are thickest in the intermound depressions and thinnest, or absent, over the crests. Waulsortian Mudbanks of similar age and character in Tennessee, are shown by Macquown and Perkins (1982) to

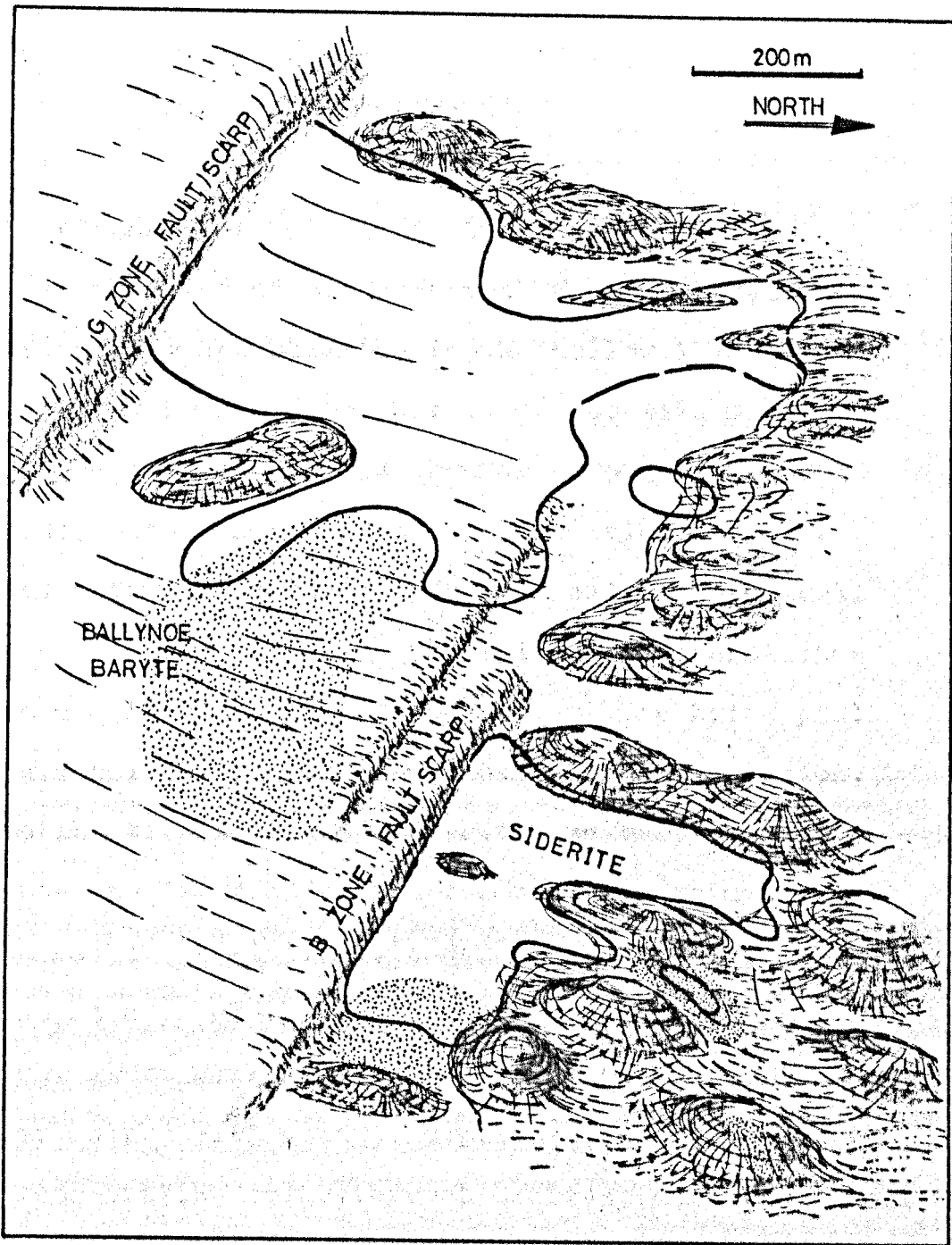


Figure 6.2: Sketch diagram of seafloor topography and outline of principal stratiform ore zones at Silvermines, viewed obliquely from above and to the east. Mounds are footwall mudbanks (Stromatactis Reef Limestone), stipple is stratiform baryte. For location of feeder zones and massive pyrite, see Figure 6.5.

have formed in localised, slightly elevated, sub-mound seafloor highs in a transgressing sea.

6.3.3. Development of Brine Pool Conditions.

Spatial arrangement of ore host rock facies (baryte on flanks, pyrite and siderite in the hollows) is closely related to the distribution of footwall mounds (Taylor op cit). This points towards strong brine pool development, with relatively anoxic conditions below a halocline, between the fault scarp and existing footwall mounds. Exhalation of fluids took place at several locations into different sub-environments of the brine pool system (Russell 1983). On the flanks of the depression, nearer to the main fault zone, pyrite and baryte were precipitated in low mounds with recognisable chimney features (Larter et al 1982), under relatively oxidising conditions at a pH of about 7.5. Deeper into the depression, where more anoxic conditions prevailed, galena and silver sulphosalts were precipitated around the vents and in cross-cutting veins through existing mudbanks, where fractured by NW trending faults (S.Taylor, personal communication 1982).

Abundant sulphur was present in the vicinity of the brine pool, both sulphate from seawater, and sulphide from hydrothermal sources as well as bacterially reduced sea water sulphate. The absence of significant pyrrhotite in the upper stratiform zone sulphides (Taylor and Andrew 1978) implies the presence of abundant reduced sulphur,

conditions favouring the formation of pyrite (Plimer and Finlow-Bates 1978). This is in spite of the relative abundance of primary pyrrhotite in parts of the feeder zone sulphides (Rhoden 1960), where conditions were much more strongly reducing.

Sulphur isotope studies by Boyce et al (1983) indicate intense bacteriogenic activity within the brine pool and underlying sediments, with much of the sulphide originating by reduction of seawater sulphate. This is in contrast to the sediments of the Red Sea Atlantis II Deep, which are virtually sterile with respect to bacterial activity (Zhabina and Sokolov 1982), H_2S being almost entirely of hydrothermal origin.

The overall size of the Silvermines exhalative site is approximately six kilometres long (from West Shallee to the C Zone, Figure 6.3), by a kilometre or so wide, closely comparable to the present day exhalative site in the $21^{\circ}N$ East Pacific Rise hydrothermal field (6.2km by 0.5km, with at least 12 separate vent clusters of chimneys and mineralised mounds, MacDonald 1982).

Although the individual sedimentary ore zones are fairly restricted areally (G Zone - 1000m by 700m, B Zone - 600m by 500m, Ballynoe baryte - 600m by 300m), the overall dimensions of the recognisable stratiform sulphide - sulphate horizon is about 2.5 kilometres long by 1.5 kilometres wide. In addition, small quantities of zinc and lead sulphide and pyrite mineralisation are present at an equivalent stratigraphic position some five kilo-

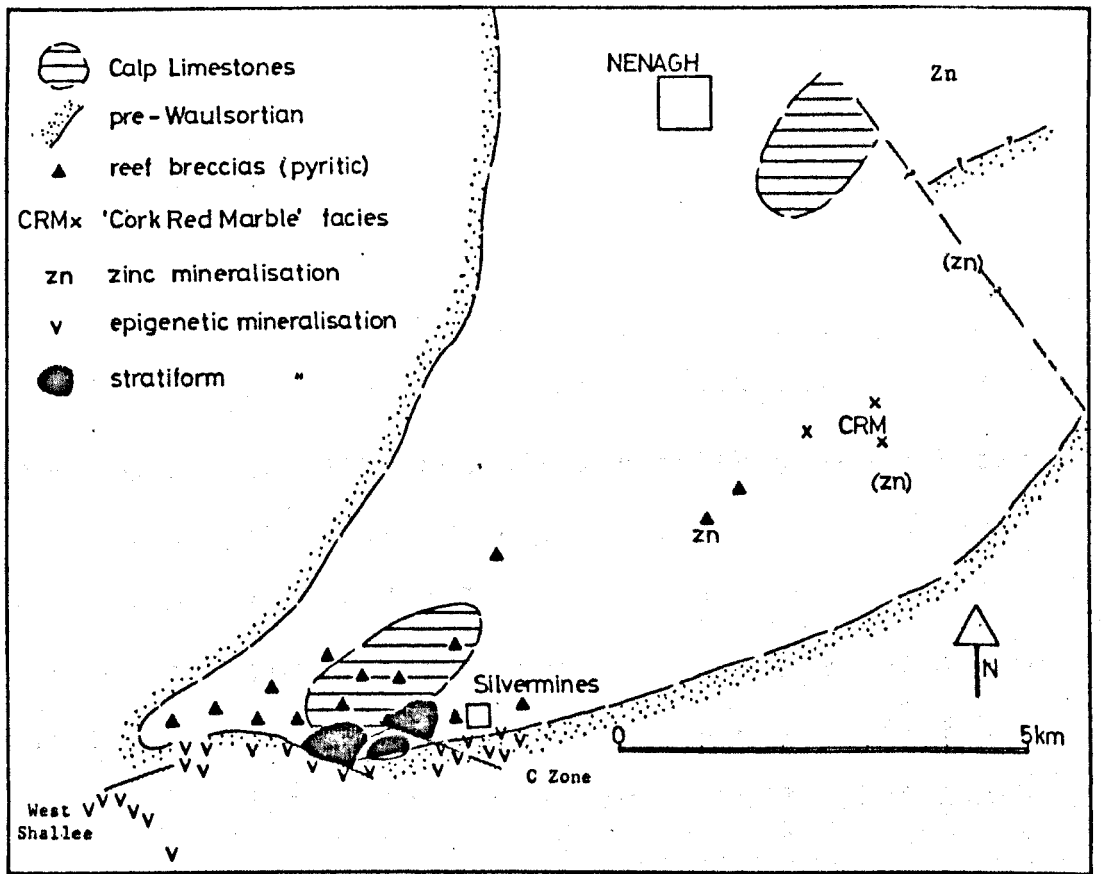


Figure 6.3: Sketch map of Silvermines - Nenagh Basin, showing location of Red Marble and zinc mineralisation mentioned in text.

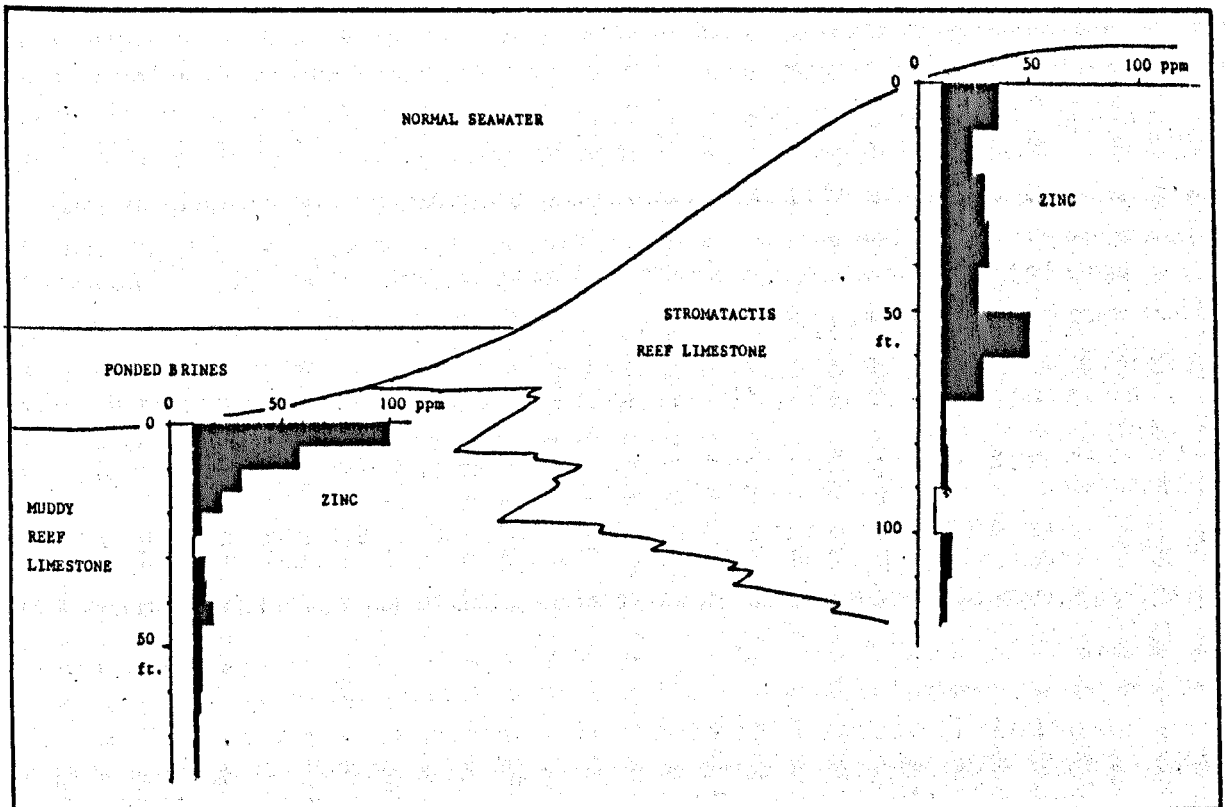


Figure 6.4: Comparison of vertical profiles of (average) zinc content in footwall Stromatolite Reef and Muddy Reef Limestones at Silvermines (from data in Figures 4.13 and 4.18). Note how elevated zinc values (above 10 ppm, shaded black) are developed over greater thickness in reef mounds, but to lower levels of enrichment.

metres to the northeast (Figure 6.3), intersected in two boreholes (S. Taylor, personal communication 1982). This suggests a certain amount of periodic entrainment of sulphide material by the rising plume, allowing greater distances to be covered in base metal dispersion.

Alternatively, one might speculate that they are related to another, as yet undiscovered, exhalative centre much closer by (see Section 6.3.5).

Rapidly changing conditions, marking the onset of hydrothermal input and brine pool formation are indicated by trace element profiles through footwall Muddy Reef Limestones, into ore horizon sediments and their stratigraphic equivalents (Section 4.2.2.). Geochemical profiles reveal increasing manganese concentrations upwards, coupled with decreasing acid-soluble iron (possible reflecting increased incorporation into pyrite), especially in the top 30 metres of footwall sediments (Figures 4.14 to 4.19).

The presence of extensive footwall enrichments of Fe, over 100m into the underlying limestones (Figure 4.14), may indicate that early hydrothermal solutions were free of appreciable H_2S concentrations. The Fe concentrations in the exhaled solutions were then reduced quite dramatically because of a buildup of H_2S , rendering the Fe more insoluble (coinciding also with increased Mn concentrations).

Zinc values show increases in the top 7 metres, indicating early hydrothermal input into the immediate footwall sediments. Local silicification is observed in close

relationship with sedimentary sphalerite or siderite accumulations, especially in the deeper parts of the depressions (Taylor and Andrew 1978, Taylor 1984).

Paralleling some of the geochemical changes, early hydrothermal activity is indicated by faunal flourishing and mass extinction towards the top of the Muddy Reef Limestone (Barrett 1975). Increase in crinoid size and density represents optimum conditions of nutrient and heat supply for growth, followed by metal or sulphide toxicity. The stimulative influence of hydrothermal fluid emanations on biological activity is exhibited in the discharge areas of present day submarine thermal springs (Corliss et al 1979, Karl et al 1980). In the absence of brine pool development, flourishing marine organisms reflect the abundance of sulphur-oxidising bacteria at the base of the food chain, which feed on H_2S expelled by the hot springs.

Comparison between the immediate footwall geochemical profiles where Stromatactis Reef Limestone is present and where it is absent, reveals some differences, even though the majority of the boreholes examined all occur within a short distance of one another (see Figures 4.13 and 4.14 - 18).

One reason for this may be the different rates of sedimentation of the two rock types, with reef mounds growing much faster than the argillaceous limestone of the Muddy Reef. For example, zinc enrichments in the Stromatactis Reef Limestone mounds extend down to about 20 metres

below the ore horizon, but only 7 metres into the Muddy Reef Limestone. Also to be taken into account is the fact that the reef mounds protude up to at least 30 metres above the basin floor in places, possibly leaving the growing surfaces beyond the influence of bottom-hugging or ponded, dense, hydrothermal solutions (Figure 6.4).

Profiles of Mn:Fe are broadly similar in the two lithologies,, with steadily rising Mn, relative to Fe throughout, except in the top 10 metres in the Stromatactis Reef Limestone, and the top 5 metres in the Muddy Reef Limestone (Figures 4.13, 4.15).

6.3.4. Formation of Siderite.

Siderite formation normally requires conditions of low oxidation potential (see Figure 6.10a), very low sulphide activity and restricted water circulation (Curtis and Spears 1968). Although normally restricted to a diagenetic environment, such conditions may develop within a brine pool. High HCO_3^- activity in solution (or CO_2 rich waters) would serve to enlarge the siderite stability field (Hem 1972), and balance the inhibiting effect of higher sulphide activities in hydrothermal brine waters. Alternatively, conditions just below the sediment surface may have favoured siderite precipitation. Klein and Bricker (1977) record the development of very localised, extreme conditions with highly reducing, Fe rich assemblages forming only centimetres below a highly

oxygenated medium.

Early stages in the brine pool history at Silvermines may have been characterised by relatively low sulphide concentrations from the hydrothermal source, or insufficient sulphide forming by bacterial reduction of seawater sulphate. This, combined with the high CO_2 contents of the hydrothermal fluids (Samson 1983), and already high CO_2 activities in the brine pool vicinity (caused by the instability of CaCO_3), favoured precipitation of siderite rather than pyrite. Close association of massive pyrite and siderite however, suggests that sulphide was not in short supply. Instead, we can perhaps envisage a situation where multiple layering of the brine pool had developed, with an upper brine favouring pyrite precipitation ($a\text{CO}_2 < aS_t$ (t=total sulphide)), and a lower brine or subsurface sediment waters favouring siderite precipitation ($a\text{CO}_2 > aS_t$), both environments characterised by high Fe concentrations (Figure 6.6). This setting would also account for the physical arrangement of pyrite relative to siderite, apparently overlying it, and on topographically higher parts of the depression (Figure 3.28). Blocks of siderite material incorporated into debris flows within the orebody testify to the relatively early formation of siderite, on or just below the sediment surface.

Siderite is the only carbonate mineral forming in-situ, in the brine pool (except, perhaps for some base metal carbonate, as reported by Kucha and Weiczorek (1984)

from Navan). The precipitation of calcite or dolomite is inhibited by the Eh-pH conditions brought about by the influx of hot, acidic, reducing, CO₂-rich, and metal chloride bearing solutions. Instability of calcite and dolomite may be promoted by the mixing of these solutions with cooler, more neutral or alkaline solutions, and resulting Zn-Pb precipitation, as described by Anderson (1973) for subsurface Mississippi Valley-type mineralisation.

Taylor (1984) shows how footwall carbonate mudbank growths are thinner or absent beneath significant ore developments in the stratiform orebodies (Figure 6.5), the only carbonate material present within or above these ore zones other than siderite, is in allochthonous sedimentary breccias. Within these debris flows, individual clasts are rimmed by reaction haloes of pyrite or other sulphide minerals.

One significant factor, concerning trace element geochemistry, is that siderite precipitation allows much greater amounts of Fe and Mn to enter the carbonate fraction of the sediment around the vents. Up to 40% MnCO₃ is recorded in naturally occurring siderites (Deer et al 1966), although analysis of siderite from the stratiform zones at Silvermines indicates around 10% MnCO₃ in solid solution with FeCO₃ (and varying amounts of CaCO₃ and MgCO₃ also).

Much greater quantities of Fe than Mn are removed from solution by the precipitation of pyrite and siderite,

SILVERMINES - ORE HORIZON GEOLOGY

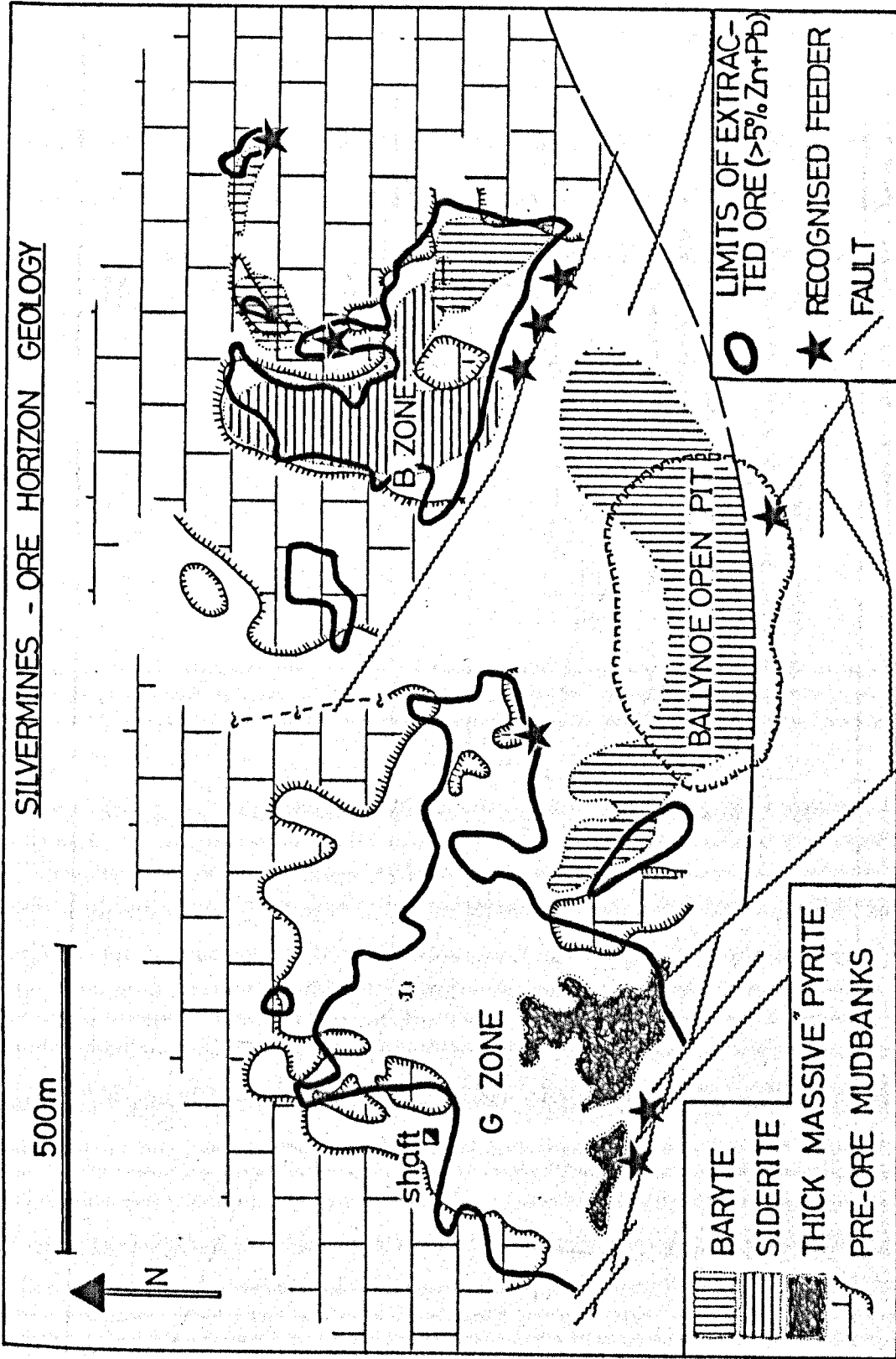


Figure 6.5: Plan of stratiform mineralisation at Silvermines, showing arrangement of major host lithologies, outline of economic mineralisation, postulated feeder zones and extent of footwall reef mudbank development, after Taylor (1984).

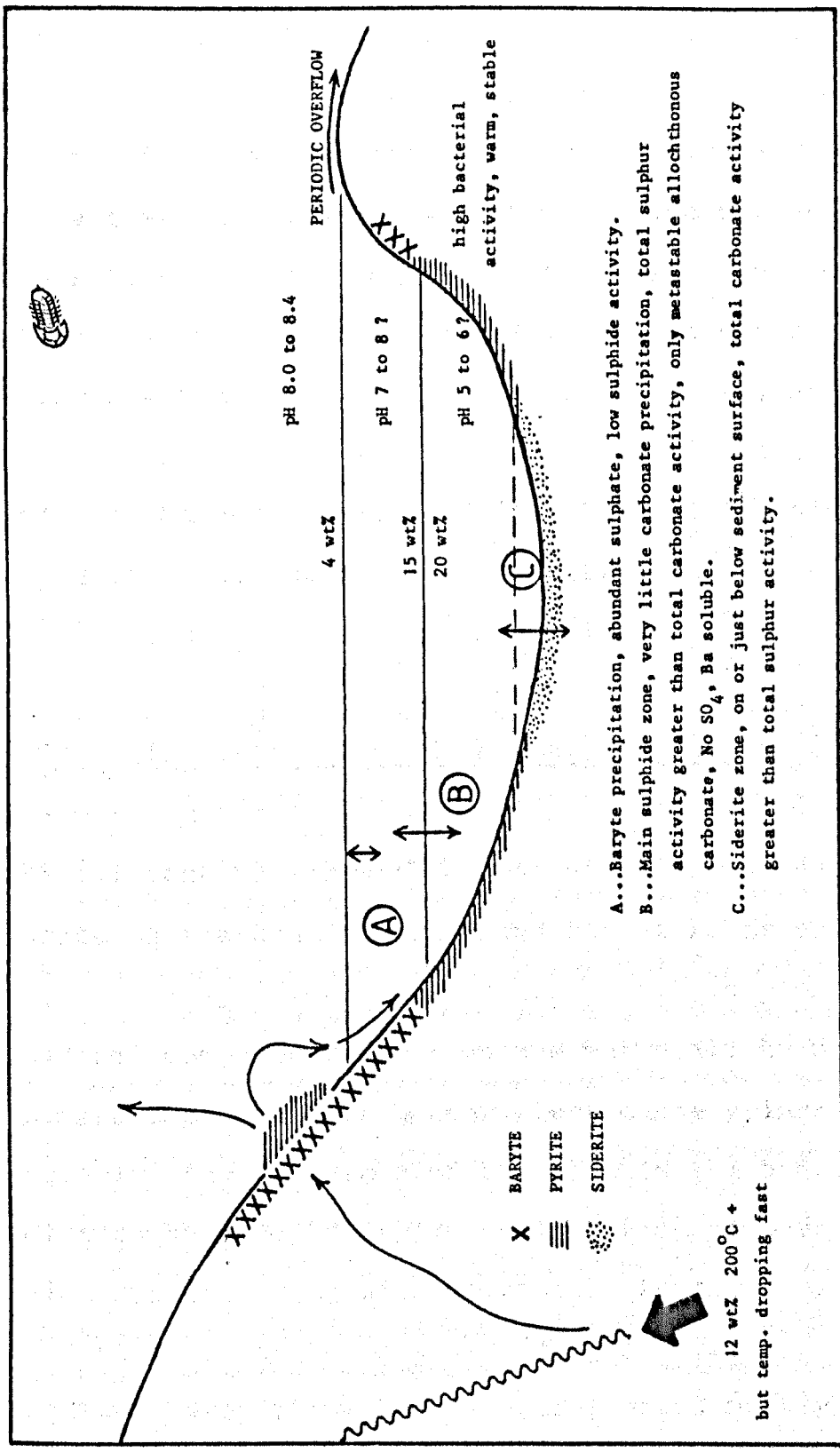


Figure 6.6: Diagrammatic cross section of 'mature' Silvermines brine pool. Vertical exaggeration about 3x. Interfaces between stratified layers fluctuate, hence overlap of different facies (Pb and Zn sulphide deposition overlaps all three). Note also that periodic overflow of brines would not,ally be composed of upper brine fluids only.

with rough estimates of about 10mt of massive pyrite and 1mt of siderite hosting the stratiform ores. Using these figures, and an average ratio of Mn to Fe of 1 to 4 in the siderite, and negligible Mn in the pyrite, over fifty times as much Fe is located in the pyrite and siderite host rocks than Mn. The ratio of Mn to Fe in the remaining host rocks (pyritic dolomite and limestone breccias) is of the order of 1 to 2.7, averaged from 86 ore horizon samples. Because of this, the quantities of Mn and Fe exported from the local basin of ore deposition did not necessarily reflect their relative proportions in the hydrothermal fluids.

6.3.5. Dispersion of Hydrothermal Components.

The mode and extent of metal dispersion around a hydrothermal vent source will depend on numerous characteristics of the exhaled fluid and the seafloor environment. Physical dispersion of effluents (metal complexes, oxidised components, particulate material) by plume flow is more important for hotter, less dense brines, particularly if the presence of sulphide in the hydrothermal solution has led to rapid precipitation of particulate sulphides on mixing with seawater. Physical dispersion in denser, lower temperature (sulphide-free) solutions, such as those of the Red Sea, is limited mainly to gravitational sliding and overflow of ponded fluids from seafloor depressions (Carne 1979). Chemical dispersion (diffusion) will play a more important role in

the latter case (Danielsson et al 1980).

Double diffusive systems are characterised by plume convection and gravitational brine movement, with both chemical and physical processes of dispersion facilitating the outward spread of metalliferous components.

The seawater chemistry will largely be responsible for continued stability of each dissolved component, and the resulting degree of dispersion around the vent, ranging from rapid dumping immediately around the vent, to complete dispersal to background seawater levels.

Seawater depth, current (and wave) activity and seafloor topography will also influence the physical behaviour of dispersing hydrothermal fluids.

The solution chemistries of iron and manganese are very similar, both remaining stable as divalent ions in hydrothermal solutions of low Eh and pH. Both are oxidised in normal surface conditions to give insoluble oxides, although the oxidation of the manganese ion requires a higher oxidation potential than that of the ferrous ion (Krauskopf 1957). The difference in solubility between Fe and Mn is greater in the oxides, resulting in a more efficient separation of the two in a more oxidising environment. Comparison of the stability fields of individual iron and manganese compounds (Figure 6.7a) shows that the Mn^{2+} ion is stable over a larger area of natural environmental conditions compared to Fe^{2+} , partly also because of the eagerness with which iron forms pyrite or siderite at

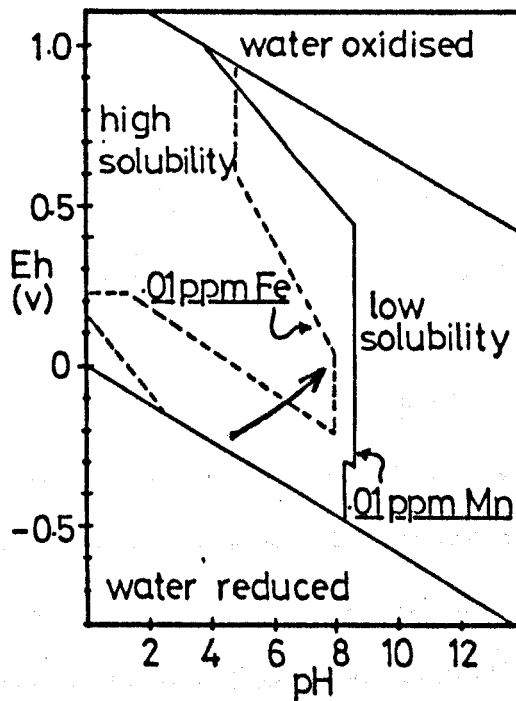


Figure 6.7a: Comparative solubility of Mn and Fe in the system $\text{H}_2\text{O-Mn-Fe-CO}_2\text{-S}$ at 25°C and 1 atm. Total CO_2 species activity 2000 mg/l as HCO_3^- ; total sulphur species activity 2000 mg/l as SO_4^{2-} ; after Hem (1972). Arrow indicates approximate composition of fluids in Silvermines seafloor hydrothermal system.

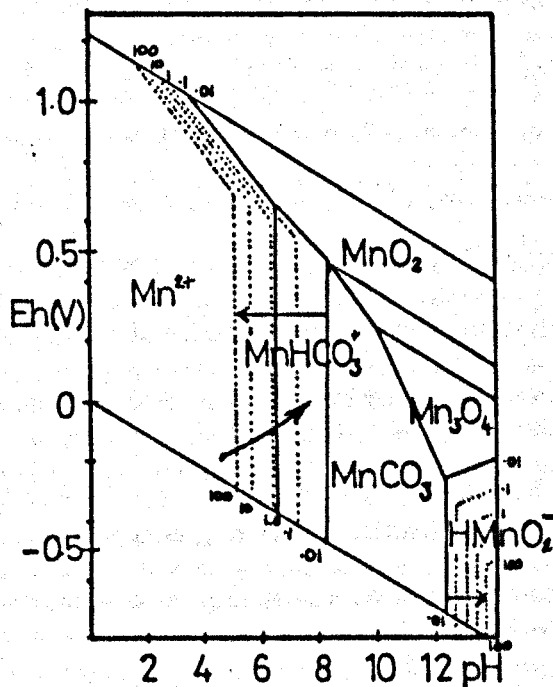


Figure 6.7b: Stability fields of solids and solutes, and solubility of manganese as functions of pH, redox potential and dissolved Mn concentration at 25°C and 1 atm. in the system $\text{Mn-CO}_2\text{-H}_2\text{O}$. Bicarbonate species activity 2000 mg/l as HCO_3^- , dissolved Mn activity from 0.01 to 100 ppm (see dotted lines).

lower Eh conditions.

The strong negative correlation of Mn and Fe in many hydrothermal deposits (Zantop 1978, 1981) is indicative of the efficient fractionation processes operating on the two elements.

In a carbonate environment, with lime mud forming rapidly on the sea bottom, neutralisation of acidic hydrothermal solutions would take place at a much faster rate, telescoping any outward fractionation of iron and manganese. The MnCO_3 stability field is enlarged by high CO_2 activities (Figure 6.7b), and Mn^{2+} readily enters the carbonate phase without oxidation, its mobility increased because of complexing with bicarbonate (Hem 1972). Unlike zinc (and iron to some extent), chloride complexing is of little significance in the natural solution chemistry of manganese (Hem op cit).

Virtually all of the manganese, and most of the iron, exhaled into the submarine environment, whether into the brine pool or upwards as a rising plume, would have been present initially in the divalent state. Low Eh conditions in the brine pool favoured continued solubility of Mn (II), whereas high sulphide activities encouraged rapid precipitation of Fe as pyrite.

Conditions beyond the brine pool contrasted with those prevailing in its depths, and transitional zones between the two would have existed. These may have been either stratified developments within the pool itself (with pronounced interfaces between each), or a diffuse zone

caused by periodic overflow and mixing of brine with seawater on the surrounding seafloor.

Overflow of dense brines from a brine pool onto the surrounding seafloor sediment allows development of an oxidising facies around a reducing one. Accumulation of oxidised manganese species around the edge of the Red Sea Brine Pools in a 'manganite facies' is documented by Bignell et al (1976). This occurs where mixed, intermediate zone brines first come into contact with the sediment surface, without anoxic primary brines below. Otherwise, precipitated Mn (IV) species would again be reduced on sinking into the primary brine (Danielsson et al 1980). No comparable oxidised manganese zone is present, at Silvermines, although oxidised iron minerals are significant in the baryte zone.

Beyond the influence of the Silvermines brine pool waters, the carbonate environment of the relatively shallow and turbid Waulsortian sea ensured rapid neutralisation of outwardly migrating hydrothermal fluids, and telescoping of any outward fractionation of Mn and Fe. The comparable behaviour of Mn and Fe is demonstrated by the good correlation between the elements in the surrounding mudbank limestones. Manganese to iron ratios in all distal outcrop in Ireland average 1.0 (Table 3.2), although this value is slightly higher (about 1.2) in the Silvermines - Nenagh area (Table 3.4). Little fractionation between Mn and Fe is observed, except perhaps for slightly higher Mn levels immediately to the north

and east of the stratiform orebodies, compared to the area close to the fault (Figures 3.39 and 3.48). This suggests that the respective domains of the brine pool environment and the carbonate basin environment were relatively clear cut with little overlap. A similar situation appears to have existed at Keel (Figure 3.60b).

The low Mn:Fe ratios in the vicinity of the stratiform ore zones at Silvermines effectively highlight the approximate extent of the local basin, where Mn solubility was perhaps slightly greater than Fe. In the carbonate-hosted Renison Bell deposit in Tasmania, Mn:Fe ratios also increase laterally from the massive sulphide and siderite host, outwards into the carbonates (Hutchinson 1979).

The elevated Mn and Fe levels present in the carbonate fraction of surrounding host rocks at Tynagh and Silvermines, may have arisen by direct incorporation into precipitating carbonate minerals in the divalent state, or by initial deposition in oxidised form, followed by post-depositional reduction and redistribution into carbonate minerals during diagenesis. Factors governing the entry of Mn and Fe into carbonate minerals are examined more closely in Section 6.4.1.

That Mn:Fe ratios are slightly higher in the Silvermines - Nenagh distal samples is perhaps a result of the removal of large quantities of hydrothermal iron (compared to manganese), incorporated into the ore host rocks (Section 6.3.4.).

Host rocks to the Silvermines deposit carry primary enrichments of several trace elements up to at least 4 kilometres from the economic mineralisation. Almost 80% of samples in this zone carry enriched levels of Mn and Fe, whereas over 60% carry enriched levels of Zn (Table 3.6). These enrichments arose from one or more of a number of possible mechanisms during the formation of the stratiform ore:

- i) precipitation or 'fall-out' from outwardly migrating fluids forming part of a buoyant plume;
- ii) periodic overflow of dense, metalliferous fluids from a brine pool onto the surrounding sea floor;
- iii) outward diffusion of the metals along concentration gradients, from the hydrothermal vents and associated brine pools.

An analogy can be drawn here with the Red Sea hydrothermal system, where anomalous concentrations of trace elements (Fe, Mn, Zn, Cu) in bottom waters and suspended particulate matter, arise because of diffusion of metals across the interface between hydrothermal fluids in the brine pools, and overlying Red Sea Deep Water (Holmes and Tooms 1973). Outward migration of metal ions takes place in both particulate and dissolved forms, influencing the composition of surrounding bottom waters and sediments. Bignell et al (1976) record lateral enrichments of Cu, Zn, Fe, Mn and Hg up to 10 kilometres from the metalliferous sediments of the Atlantis II and Nereus Deeps (Figure 6.8). Some overflow of ponded hydrothermal brines

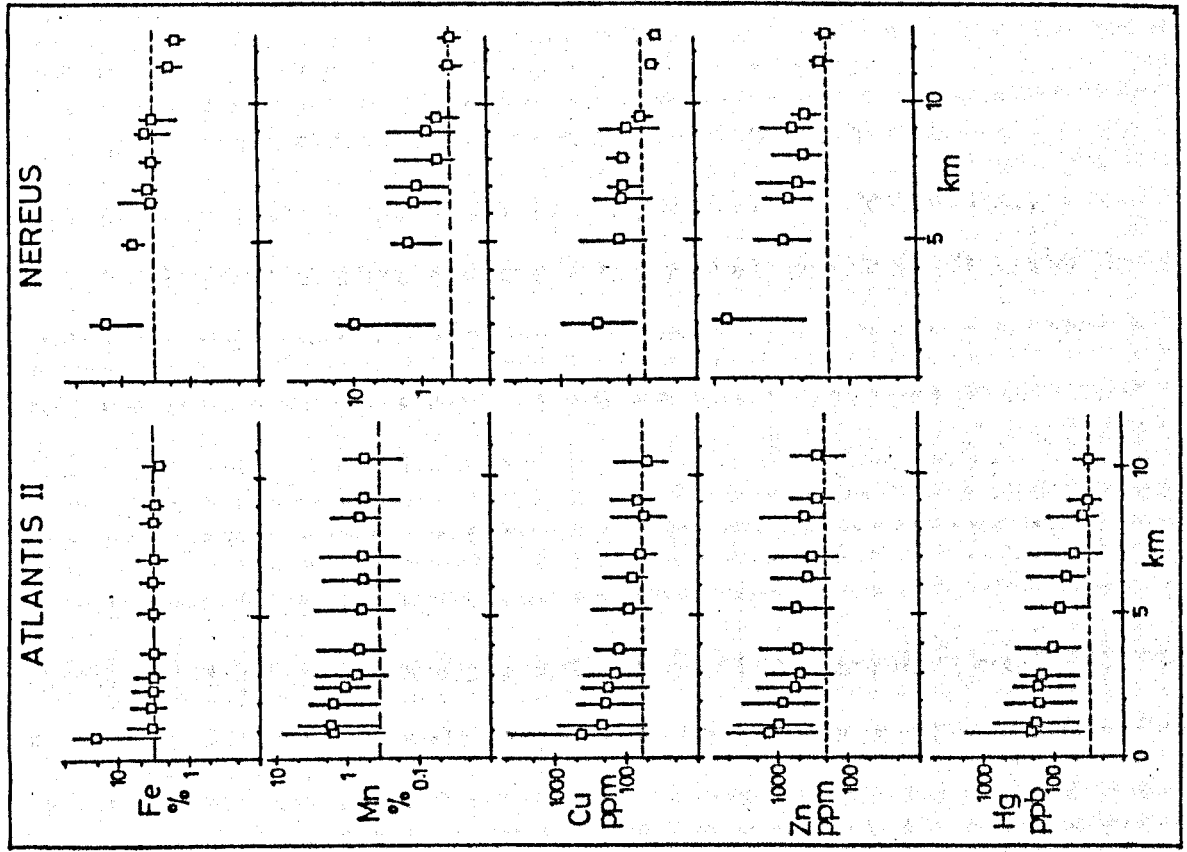


Figure 6.8a: Large scale variations in seafloor sediment composition across the Red Sea from marginal shelf to axial valley, after Bignell et al (1976).

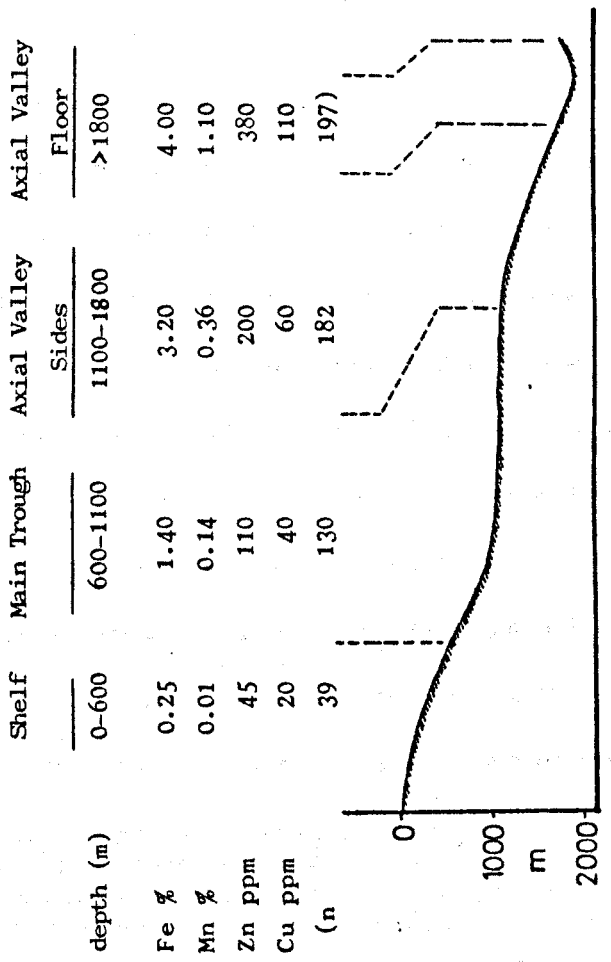


Figure 6.8b: Mean and range of selected metals in sediment cores from around the Atlantis II and Nereus Deeps in the Red Sea. Broken line represents background values measured from axial valley-side sediments. Redrawn from Bignell et al (1976).

also takes place onto the surrounding seafloor (Rona 1984).

Manganese and iron appear to be strongly fractionated in the Atlantis II sediments, perhaps reflecting slightly higher Eh conditions, and reduced mobility of Fe (and hence a less pronounced fractionation from Mn) and generally wider dispersion of each metal (Figure 6.8). In addition, lower background values of each metal may indicate less trace metal scavenging by precipitating Mn oxide phases. Higher levels of Mn, Fe, Zn and Cu are recorded in sediments from progressively deeper parts of the Red Sea, demonstrating the large scale influence of metalliferous exhalations along its axis (Figure 6.8a).

Tynagh.

In apparent contrast to Silvermines, separation of Mn and Fe compounds took place in the oxide facies at Tynagh, represented by iron-rich and peripheral manganese-rich samples in the Tynagh Iron Formation, laterally equivalent to the base metal orebody (Russell 1972). A suggestion of weak Mn enrichment relative to Fe, towards the northern flank of the Waulsortian outcrop near Tynagh (Figure 3.23) may indicate slight fractionation of Mn and Fe, beyond the edge of the Iron Formation, within the carbonate domain.

Tynagh displays a number of other differences from Silvermines, one result of which is the fact that trace

element enrichments appear to be more widely developed around the hydrothermal centre. At Tynagh, both ore and associated trace element enrichments are found throughout the Waulsortian and equivalent succession, whereas at Silvermines, both are focussed near to the basal part of the same succession. This testifies to the longer duration of hydrothermal processes at Tynagh.

The comparative lack of well developed stratiform ore, and the presence of an extensive, cogenetic, sedimentary iron formation close to the Tynagh Fault indicates reduced brine pool conditions were poorly (if at all) developed, allowing oxidising conditions to prevail throughout the local basin. As this would presumably reduce trace element mobility in solution generally, the implication arises that more efficient movement of trace metals by plume dispersal took place.

Taking such conditions to the extreme, complete absence of brine pool development in an oxidising environment leads to very sudden and thorough mixing of hydrothermal solutions with strongly oxygenated (and/or turbulent) waters. The resulting abrupt changes in Eh and pH leads to prevention of any fractionation between Mn and Fe, all of the components of a metalliferous fluid being rapidly precipitated or 'dumped' as hydroxides or adsorbed ions on the hydroxides of other elements (Marchig et al 1982). This situation is perhaps typical of ocean floor exhalative centres in an oxidising environment, such as those of the Gulf of California (Badham 1979, Lonsdale et al 1980).

Keel.

The stratiform Ba+Fe+Zn mineralisation preserved at Keel (Section 3.4.3) is localised at the base of the mudbank limestone, some 2 kilometres from the main subeconomic sulphide deposit (Zn with Pb), which is hosted mainly in epigenetic fracture zones in older clastic rocks (Figures 3.58 - 59).

The trace element enrichments recorded in the host mudbanks are also confined mainly to the basal part of the mudbank formation, but these are weakly developed, and consist of subtle Mn and Fe enrichments, with only minor Zn enrichments (Figures 3.60, 4.38 - 43).

The fact that mudbank growth appears to have been unaffected by hydrothermal exhalation indicated that normal seafloor conditions were relatively unchanged, and brine pool conditions did not develop. Metalliferous exhalations at Keel were probably relatively weak and short-lived, and the effluents largely dispersed to near-background levels in surrounding seawaters, with the result that only minor increases in host rock trace element levels were developed around the vent areas.

At Keel, iron tenors in surrounding mudbank limestones are noticeably higher than manganese, reflected in lower Mn:Fe ratios compared to Silvermines and Tynagh (Figure 3.60b). The absence of any significant development of sedimentary iron formation or extensive massive pyrite (both are present, but are only minor in

extent) may have led to large scale dispersion of iron, and increased incorporation into sedimentary carbonate in the vicinity of the hydrothermal vents.

Ballinalack.

The presence of manganese and iron enrichments in the micrite phases of mudbank limestones around the Ballinalack mineralisation (Figure 3.55), indicates that some syngenetic introduction of metals took place, although evidence for seafloor, base metal mineralisation is lacking.

At least two possible situations present themselves here. Firstly, that the growth of the mudbanks preceded the main exhalative event, and took place during early, base-metal-poor stages of hydrothermal activity, when Mn and Fe were the dominant metals carried by the solution. Metalliferous solutions then invaded the mudbanks, precipitating base metals and baryte in primary cavities (stromatactis) and secondary, fault-induced fractures or cavities, on mixing with connate SO_4 -rich brines. Any sedimentary ore zones, if preserved, would therefore be located in overlying argillaceous limestones, and would most likely be accompanied by enrichments of Mn, Fe and Zn in laterally equivalent strata. Alternatively, the metalliferous exhalations occurred during mudbank growth, but were relatively weak, and due to current winnowing and/or lack of any local stagnant depressions (and resulting brine pool development), no stratiform

mineralisation was preserved in the mudbank limestone. On the seafloor, any base metals were rapidly dispersed and oxidised, and deposition of sulphides was limited to subsurface cavities and fractures. Hydrothermal Mn and Fe were still present locally in the seawater, to become incorporated into the growing mudbanks at elevated levels.

The infilling of stromatactis cavities by sulphide suggests that passage of the mineralising solutions occurred soon after growth of the mudbank framework, before the precipitation of early diagenetic calcite, or geopetal lime mud (Halls et al 1979).

Core sections examined in this study did not include any complete profiles of the supra-reef limestones to affirm the first hypothesis, but work by R. Graham (personal communication 1982) indicates that no appreciable enrichments of Mn are present in the Upper Argillaceous Bioclastic Limestone or Calp Limestone.

The evidence here points towards more or less contemporaneous growth of mudbanks and introduction of metalliferous fluids, with the overall weakness of the hydrothermal system, and resulting failure of any brine pool to develop, the principal reasons for the absence of stratiform mineralisation.

One other significant difference between Ballinalack and Silvermines is in the comparison between ore isopachytes of ore thickness and mudbank thickness. At Ballinalack, the two are closely related, and thickest ore inter-

sections tend to coincide with maximum mudbank development (Jones and Bradfer 1982). The converse is true at Silvermines, where highest ore grades and thickness coincide with minimum mudbank (footwall Stromatactis Reef Limestone) development, and a general thinning of the overall Waulsortian-equivalent succession (Taylor and Andrew 1978, Taylor 1984). This reflects the fact that at Silvermines, deposition of sulphides took place on the seafloor, essentially controlled by mudbank topography, whereas at Ballinalack, it was confined to the subsurface environment within the mudbanks, and controlled by local permeability barriers.

Ballyvergin.

Locally enriched Mn and Fe levels in mudbanks which host the minor Cu+Pb+Zn deposits of the Ballyvergin area (Figure 3.67) suggest that the emplacement of the mineralisation coincided with the growth of the mudbanks.

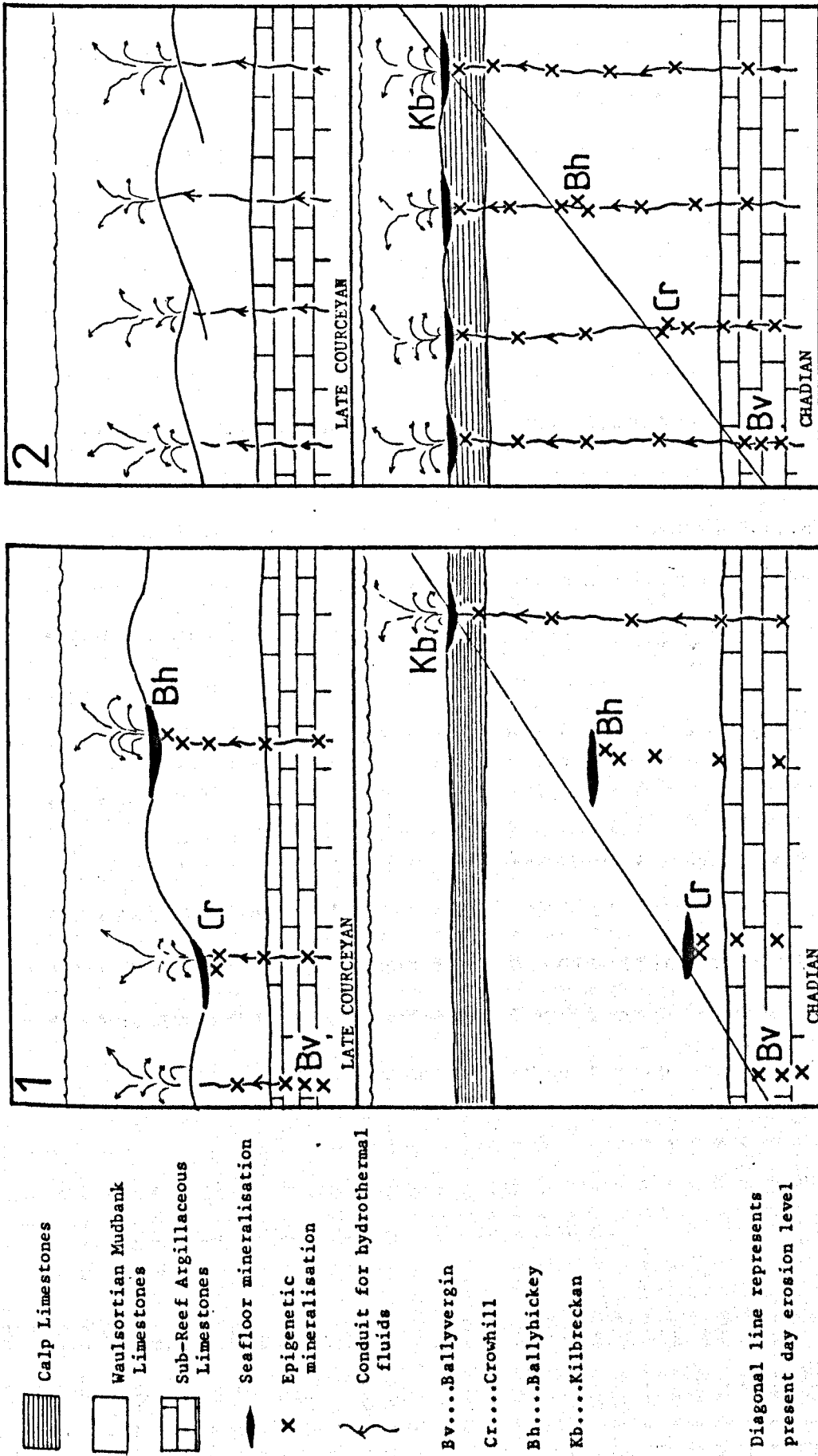
Those deposits hosted within the mudbank complex itself (Carrahin, Crowhill, Ballyhickey, Milltown) may therefore show greater affiliation to sedimentary exhalative type mineralisation (with considerable diagenetic and later Hercynian modification), even if genetic style is indicative of apparently epigenetic emplacement.

The localisation of at least one of the deposits (Kilbreckan) in supra-reef limestones requires that the hydrothermal processes were relatively long-lived, and continued after the cessation of mudbank growth.

Alternatively, and in the light of the lack of any appreciable zinc enrichments in the mudbank, the main hydrothermal event may have climaxed after mudbank deposition, and the Mn and Fe enrichments in the mudbank are effectively part of a footwall aureole, formed by early, base-metal-free exhalation. This situation would require that the deposits hosted in the mudbank complex (as well as those in older rocks, such as the Ballyvergin deposit itself) were some form of feeder zone mineralisation (Figure 6.9).

The absence of any sizeable stratiform sulphide zone most likely points towards the lack of any single, major 'plumbing' structure to focus the upward movement of hydrothermal fluids onto one seafloor location, possibly combined with the absence of any suitable local depression (e.g. fault-controlled) to allow brine pool development. It also remains a possibility that erosion has removed a major stratiform zone, either high up in the mudbank complex or in overlying limestones, and the existing deposits are remnants of its feeder zones. However, the fact that the existing trace element anomalies are not strongly developed suggests that large scale exhalation of metals did not take place, either in the presence or absence of suitable brine pool locations.

Suggestions that the deposits are Hercynian in age (Sevastopulo 1984) are refuted on the basis of the host rock trace element patterns presented here.



Aherlow.

The Cu-Ag mineralisation at Aherlow is epigenetic in style, hosted mainly in sub-Waulsortian limestones and shales (Cameron and Romer 1970). However, the presence of a stratiform chert zone at the base of the Waulsortian nearby, and the localisation of Mn, Fe and Zn enrichments in the same formation (up to at least 1.5 kilometres distant, Figure 3.69), is suggestive of hydrothermal activity contemporaneous with mudbank growth. Reduced Mn:Fe ratios coincide with the trace element enrichments, implying either a relative increase in Mn solubility over Fe (caused by lowered Eh, for example), or a local increase in Fe supply over Mn, both of which could have arisen by metalliferous exhalations.

Mallow.

In contrast to Aherlow, the similarly styled Cu-Ag mineralisation at Mallow (Wilbur and Royale 1975) does not appear to be accompanied by significant enrichments of Mn, Fe or Zn in nearby Waulsortian outcrops (Figure 3.71). The implications here may be one of several:

i) that hydrothermal processes post-dated mudbank growth, allowing normal background levels of trace elements to develop in the mudbanks;

ii) that hydrothermal processes coincided with mudbank deposition, but increased levels of trace element incorporation were either very restricted areally or

stratigraphically (and therefore not detected by the sampling pattern in this study), or enrichments are very weak and close to normal background levels. This latter situation could have arisen either because of general weakness of the seafloor exhalative system, or local bottom conditions favouring more or less complete dispersal of the effluents.

Examination of drill core sections through the Waulsortian Limestones may help to determine which of these suggestions is the most likely explanation.

Courtbrown.

There are two possible explanations for the Mn and Fe enrichments in Waulsortian Limestones around the Courtbrown Pb+Zn prospect (Section 3.5.3.). Firstly, that metalliferous fluids were introduced onto the seafloor during early mudbank deposition, to form the mineralisation observed at the base of the mudbank, and the Mn and Fe enrichments in laterally equivalent mudbanks. Secondly, the distribution of enriched values appears to be centred on the inlier of pre-Waulsortian rocks to the east of Courtbrown (Figure 3.70), where several old trial workings for Pb, Zn and Cu are known. These minor occurrences of epigenetic base metal sulphides may in fact represent a remnant of the feeder zone to a more central exhalative system, the products of which are now largely removed by erosion.

As at Ballyvergin, however, the apparent lack of any

major structural conduit for upward passage of hydrothermal solutions may have led to a more diffuse 'plumbing' system. The syngenetic expression of this system is now represented by relatively minor occurrences of base metal sulphide at several localities, including Courtbrown and Rineanna Point (Figure 3.70), and laterally extensive, but stratigraphically restricted, trace element enrichments in the mudbanks.

6.3.6. Oxidation of Iron and Manganese.

Manganese is essentially insoluble in oxygenated sea water, measured concentrations being present largely as colloidal Mn IV suspensions. Landing and Bruland (1980) show that the concentration of dissolved Mn depends principally on oxygen content, the oceanic maximum levels of Mn (at mid-depth) coinciding with the minimum of dissolved oxygen. Other maxima occur where input is high - either deep water hydrothermal (at oceanic ridge axes, Lyle 1976), bottom water hydrogenous, or shallow water, near shore, detrital inputs. At low concentrations, Mn may remain stable in seawater as Mn^{2+} and become selectively incorporated into newly forming carbonate minerals. However, appreciable oxidation of Mn will take place under conditions of elevated temperatures or Mn concentrations (Figure 6.10), or high natural pH values (Hem 1972, Raiswell and Brimblecombe 1977).

In oxidising environments, Mn is scavenged from

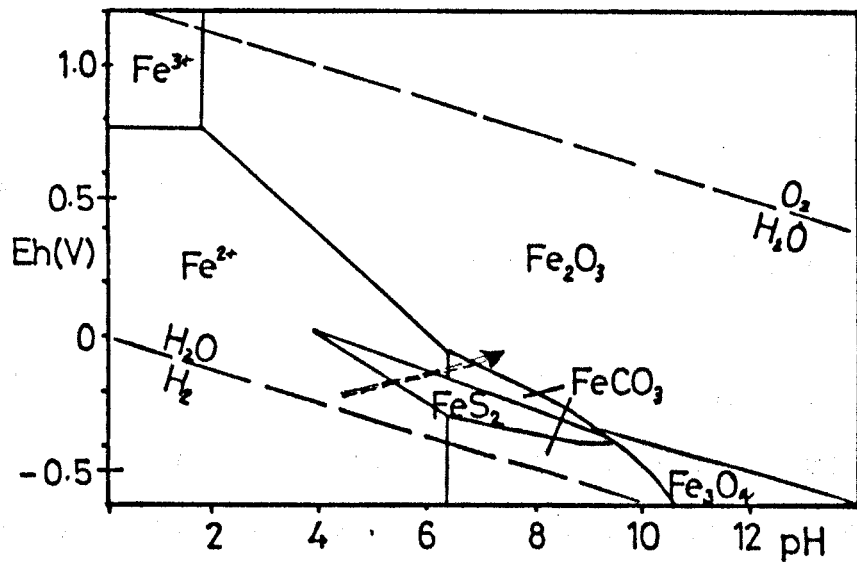


Figure 6.10a: Oxidation potential - pH diagram for the system Fe-H₂O-H₂S-CO₂ at 298^oK, 1 atm. Activity of Fe in solution 10⁻⁶ g-ion/l, activity of CO₂ in solution 10⁰ g-ion/l, activity of sulphur in solution 10⁻⁶ g-ion/l. Note FeCO₃ stability field is greatly enlarged by increase in Fe or CO₂ activity. (Source: Krauskopf 1979). Dotted arrow indicates approximate composition of fluids in and around the Silvermines brine pools.

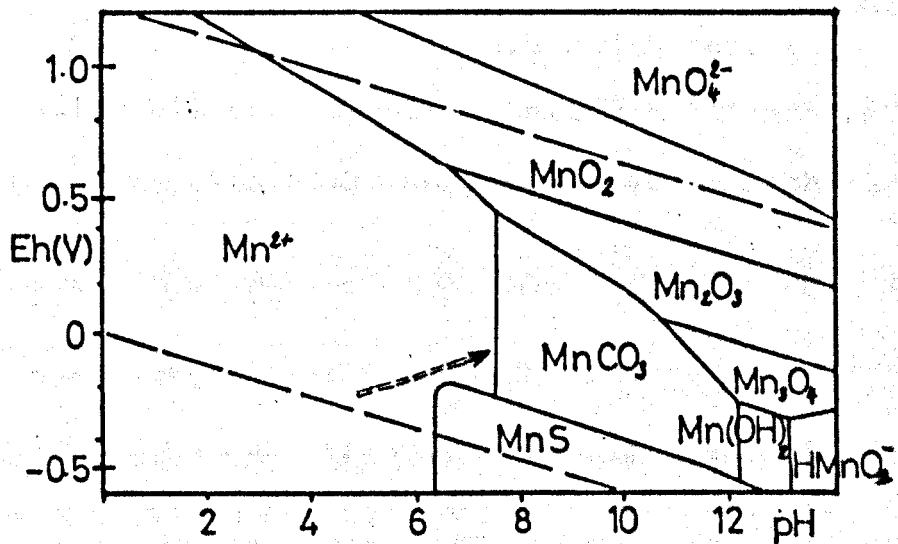


Figure 6.10b: Oxidation potential - pH diagram for the system Mn-H₂O-H₂S-CO₂ at 298^oK, 1 atm. Activity of Mn in solution 10⁻¹ g-ion/l, activity of CO₂ in solution 10⁻² g-ion/l, activity of sulphur in solution 10⁻¹ g-ion/l. (Source: Krauskopf 1979). Dotted arrow indicates approximate composition of fluids in and around Silvermines brine pools.

dissolved to particulate phases throughout the water column, and is only redissolved under suboxic conditions (Landing and Bruland op cit). Suspended particulate Mn oxide species settle at a much faster rate than precipitating colloidal phases.

At the 21°N East Pacific Rise site, the sluggish rate of oxidation reactions within the metalliferous deposits and overlying thermal plume, has led to development of millimetre-thick oxide coatings mantling the sea floor basalts up to 50 metres around the vents (Haymon and Kastner 1981). Iron-manganese oxyhydroxide crusts of similar origin, up to 20 kilometres distant, indicates the extent of areal dispersion of the slowly oxidising hydrothermal effluents. Precipitation of metal sulphide at 21°N is very rapid but inefficient, as 99% of the metal load is lost by dispersion from the rising plume into seawater oxidised species (Goldie and Bottrill 1981). Virtually all the soluble alkali metal ions are lost, and the base metal sulphide precipitates which collect on the seafloor around the vents are rapidly oxidised to form metalliferous ochres and umbers.

In a brine pool environment, the stability of manganese oxides will depend on how strongly reducing the bottom conditions are. Shanks and Bischoff (1980) indicate how sulphide accumulation and development of oxide or sulphide rich facies in the Atlantis II brine pool depends on the rate of brine influx and seawater mixing, and whether or not a stratified brine pool has developed.

Thick oxidic zones in present sediment profiles indicate prolonged deposition in oxidising conditions, in the absence of a brine pool, more akin to processes acting at 21°N or the Galapagos Spreading Centre (Corliss et al 1979, Hekinian et al 1980).

These are interbedded with sulphide rich zones which represent rapid influx of hot solutions, with minimal entrainment of seawater, in periods of more strongly reducing, brine pool conditions.

The comparative behaviour of Mn and Fe in stratified and unstratified brine pools is described by Danielsson et al (1980). In the stratified Atlantis II Deep, dissolved Mn concentrations are high throughout both deeper and intermediate brine (as well as being enriched in overlying waters), whereas dissolved Fe is concentrated only in the denser, lower brine. Higher O₂ concentrations in the intermediate brine cause Fe to oxidise to FeOOH in the mixing zone. In the unstratified Discovery Deep, initial mixing of hydrothermal fluids and Red Sea Deep Water (RSDW), with higher dissolved O₂ concentrations than the Atlantis II basal brine, leads to very low dissolved Fe levels throughout. Manganese is also much lower than in Atlantis II, although higher than in RSDW, and both elements are precipitated onto bottom sediments as oxides.

Elevated concentrations of Mn around the margins of a brine pool will occur where overflow of hydrothermal solutions and mixing with ambient seawater (at a pH of about 8.5) takes place (Rona 1984). Similarly, rising plume waters provide elevated Mn concentrations and temperatures above the vent source, with steadily rising pH values on mixing with seawater. These conditions may induce rapid Mn oxidation within the rising plume above the vents, or around the overflow zones of a brine pool, in spite of local reducing conditions within the pool or primary vent waters. This process may have given rise to the high Mn levels in baryte zones around the margins of the Meggen sulphide orebody (Gwosdz and Krebs 1977).

At Silvermines, increased concentrations of insoluble Mn within the deposit (Chapter 4.2.3) probably reflect the presence of authigenic clay minerals or feldspars, indexed by higher Al_2O_3 , SiO_2 and K_2O levels. It is unlikely that the normally sluggish oxidation of manganese to form insoluble hydroxides (and eventually MnO_2), would proceed any more rapidly, if at all, in the low Eh environment of the brine pool. Some of the insoluble Mn may have originated by resettling of suspended or particulate Mn from above, if rapid burial prevented its reduction into the divalent state (cf. Red Sea Brine Pools, Danielsson et al 1980).

Relatively unstable or fluctuating conditions, with

continued raising and lowering of halocline surfaces within the brine pool are indicated by interfingering of baryte and siderite zones in the lower (down-dip) parts of the baryte orebody (Barrett 1975). Reworking of baryte material by submarine debris flows also occurs to a small extent, giving rise to small nodules or clasts of jasperite or hematitic baryte in the pyrite or siderite zones of the stratiform sulphide orebody. These sometimes sport a reaction rim of pyrite, testifying to their metastable existence in the more reducing environment of the local basin.

Hematite - siderite assemblages are not generally found in nature because of the high partial pressures of CO_2 required (Klein and Bricker 1977). In hematite rich assemblages, carbonates are Ca-Mg rich because most of the iron present is in the trivalent state, which cannot readily be housed in the carbonate structure.

An extensive pyrite facies overlaps both the hematitic baryte and siderite zones in the Silvermines basin, similar to the situation at the Lady Loretta deposit in Australia (Loudon et al 1975).

Overflow of metal bearing solutions from the brine pool onto the surrounding sea floor may have resulted in development of a more oxidative mineral association around the siderite - pyrite of the anoxic hollows. Although the development of an iron formation is observed at Tynagh (Schultz 1966, Russell 1975), no

direct equivalent is known close to the Silvermines deposits. The Ballynoe baryte deposit, with strong hematite staining and jasperoid nodules (Barrett 1975), is perhaps the nearest equivalent where oxidised forms of iron are present in any quantity. Barrett (op cit) describes elevated Mn and Fe levels within the baryte horizon and immediate hanging wall and footwall, with out expanding on whether they are present in pyrite, oxide or carbonate, as oxidised or reduced species. The levels attained (a few percent) are much lower than Tynagh Iron Formation, where maxima of over 80% iron oxides and 79% manganese oxides are recorded in Fe-rich and Mn-rich samples respectively (Russell op cit).

The massive pyrite zones of the Upper G and parts of the B orebody at Silvermines, may represent the nearest equivalent to an iron formation. A rough estimate of 10 mt of pyrite forms these zones, to the virtual exclusion of Mn bearing phases, except for trace or minor quantities in carbonate clasts and mud seams.

One can speculate that more extensive oxidic facies may have existed up-palaesolope from the baryte orebody, now removed by erosion. The absence of reworked clasts of this in the breccia zones of the existing orebody (except for rare hematitic-jasperoid nodules and clasts in the B zone), would tend to preclude this suggestion.

Possible oxidation of Mn and Fe around the margins of

the brine pool is indicated by slight increases in the levels of insoluble Mn and Fe in several borehole sections through the ore horizon, beyond the economic mineralisation (Figures 4.26 - 27). Alternatively, these patterns may have arisen by settling of authigenic clay minerals or feldspars entrained by the buoyant hydrothermal fluids. The presence of visible pyrite and higher SiO_2 , Al_2O_3 and K_2O at this part of the succession supports this view (Figures 4.21 - 24).

A strongly hematitic facies of Waulsortian Limestone or 'off-reef', containing a few percent of Mn and Fe oxides, is present some 7 kilometres to the ENE of the Silvermines orebodies (Figure 6.3). These rocks bear strong resemblances to the Cork Red Marble (Neville 1959) and peripheral parts of the Tynagh Iron Formation (Schultz 1966). The origin of this occurrence of reddened 'reef' is unclear, but three possibilities may be considered:

- 1) development of an hematitic rich facies under oxidising conditions, related to the hydrothermal emanations in the Silvermines area. This seems unlikely due to the considerable distance between the two;

- 2) development of a similar oxide facies close to a more local hydrothermal source, unrelated to Silvermines, and as yet unidentified. Minor zinc mineralisation has been recorded nearby (C. Morrissey, personal communication 1981);

3) unrelated to hydrothermal sources, and due to eustatic phenomena such as re-emergence and subaerial weathering, later diagenetic dissolution under oxidising conditions, or some other process.

The significance and origin of this hematitic facies will be further discussed in the next chapter.

6.3.7.Trace Metal Scavenging by Manganese and Iron Oxides.

Manganese oxides precipitated from aqueous solutions often contain considerable proportions of trace metal impurities (Hem 1978). Although initial deposition of Mn oxides is dependent mainly on chemical parameters (such as Eh, pH, Mn supply), suitable sites for nucleation and growth are also required. There may be other mineral phases such as clay minerals, feldspars and oxides, which appear to have a catalytic effect on further precipitation (Hem 1963, 1978). Bacteria may be involved in the oxidation processes of Mn and Fe, by concentrating ferromanganese oxides from solutions containing only small quantities of these metals (Mustoe 1981), and especially in the oxidation of Mn (II) from seawater, where residence times are short, of the order of a few days (Emerson et al 1982).

Trace metal uptake is controlled by supply of individual element species and rate of manganese oxide formation, with rapidly precipitating oxides permitting a much reduced rate of metal scavenging by incorporating only into lattice defects (Hem op cit)

The availability of a wide variety of trace metals around a hydrothermal centre would ensure a plentiful supply of metals whose solubility may be influenced by surface redox mechanisms on manganese oxides. In addition, an abundant supply of suitable and varied catalysts (hydrothermal oxides, feldspars, clay miner-

als), and possibly intense bacterial activity, will promote a high level of Mn oxide formation. However, the relatively rapid precipitation rate of Mn oxides associated with the hydrothermal exhalative sites will most likely prevent high accumulation rates of trace metals by scavenging. Because of this, hydrothermal manganese deposits tend to be low in most trace metal species (e.g. Afar Rift, Bonatti et al 1972; Santorini, Whitehead 1973; Punta Banda, Vidal et al 1978, Gulf of California, Lonsdale et al 1980).

Any precipitation of Mn oxides at Silvermines (e.g. at the margins of the local basin or above the brine pool in a buoyant plume of hydrothermal fluid) would have taken place at a comparatively rapid rate, because of sudden mixing of hydrothermal solutions with oxidising seawater. This would have resulted in very limited scavenging effects on trace metals. Moreover, redistribution during burial and diagenesis, of the weakly held adsorbed metals (possibly into sulphide phases) would conceal their origin.

Silver is one metal which is particularly strongly influenced by Mn oxide scavenging (Hem 1978), and its concentration around possible hydrothermal vents on the seafloor, within the brine pool (Russell 1983, Taylor 1984) is suggestive of possible rapid scavenging effects on exhaled metals. Concentrations up to 3000 ounces per tonne of ore are recorded from the silver-rich zone, mainly in argentian sulphosalts (C. Andrew,

personal communication 1984). Electron microprobe analyses of material from this zone indicates around 1% Mn in dolomitic samples (R. Pattrick, personal communication 1979), probably present within the carbonate structure, rather than in oxide phases. Nevertheless, in the strongly reducing conditions of the brine pool bottom, Mn oxide precipitation would have been minimal, and the low solubility of Ag in reducing conditions (Hem 1978) played a greater influence in locating the higher concentrations around these feeder zones, than scavenging by manganese oxides.

In contrast to Silvermines, high trace metal concentrations in the Tynagh Iron Formation (Russell 1972, 1975) and perhaps more indicative of some concentration by adsorption onto newly precipitated Mn (and Fe) oxides, distally to the vents.

6.3.8. Sedimentary Features - Brecciation.

Much of the ore horizon and hanging wall succession at Silvermines is characterised by severe brecciation of host lithologies, now dominated by dolomitised breccias with varying composition of matrix and clast lithology (Taylor and Andrew 1978). These may be argillaceous, sulphide-bearing, coarse or fine grained, with generally very angular clast geometry, and a number of features of turbidite aspect, including graded bedding (Graham 1970). Boyce et al (1983) interpret their origin in terms of sediment gravity flow mechan-

isms, as distinct from early diagenetic or post-depositional 'in-situ shale breccias' (Taylor and Andrew op cit) or late-stage solution-collapse breccias (McArdle 1978).

Sediments in the basin of ore deposition were originally soft and water saturated (contrasting with the rapidly lithifying mudbanks elsewhere), and consequently were readily disturbed by continued fault movements and brine discharge to form 'density contrast' load and slump structures, on both a large and small scale (Boyce et al op cit). Moreover, fault movement-induced instability led to massive downslope redistribution of shallower water (up-scarp) material by sediment gravity flows, in which debris flow deposition played a major part. Localised layers of fine-grained graded carbonate indicate lower energy deposition by more fluid dominated flows, particularly in areas more distal to the main fault zone, towards the north (Graham op cit).

Instability on the fault scarp would be initiated by frequent tremors caused by rapid subsidence along the active Silvermines Fault Zone. Although very different in style and tectonic setting, the vents of the Galapagos spreading centre are associated with swarms (up to 80 per hour) of very shallow micro-earthquakes (MacDonald and Mudie 1974). In addition, the vents of the RISE field are characterised by shallow micro-earthquakes and harmonic tremors (MacDonald et al 1980).

Sedimentary textures in the seafloor sediments of the Silvermines ore basin would, to some extent, be obscured or destroyed by remobilisation and disruption during continued venting and associated hydrothermal-tectonic activity.

Although sedimentary gravity flows dominate much of the ore and hanging wall lithologies, massive down-slope reworking of sediment does not appear to have seriously affected the spatial arrangement of host rock lithologies on the ore horizon. The distribution of siderite, baryte and pyrite remain consistent with facies control, and indicate that most of the reworking took place after they had been deposited and preserved in a local basin. Baryte, pyrite, siderite and massive sulphide are displaced locally within the ore basin, but not sufficiently to mask the original extent of each facies.

Composition of breccia clasts along the fault scarp toe slope suggests that further extensive sulphide or sulphate deposition did not take place upslope from the preserved orebodies, with the possible exception of the G Zone massive pyrite, which may have extended further to the southwest, over the Shallee vein deposits. This is indicated by numerous pyrite clasts occurring in drill core to the west of the G Zone orebody (S. Taylor personal communication 1981).

The end result of the sudden, massive sediment influx during debris flow deposition was that the localised

development of brine pool conditions ceased upon infilling of the third order basin. Sediment influx outpaced basin downwarping and prevented development of strongly reducing, stagnant conditions, and inhibited development of associated facies (sulphide or sulphate). Even if exhalation of metalliferous fluids continued after deposition of the main sedimentary orebodies, no further thick accumulation of sulphides took place owing to rapid dispersal of metals in a more oxygenated, turbid, sediment-dominated environment.

Submarine debris flows are a characteristic feature of many sediment hosted base metal deposits like Silvermines (Russell et al 1981). Those of Tynagh (Schultz 1966, Hutchings 1979), McArthur River (Walker et al 1977) and Sullivan (Ethier et al 1977) are well described. At Navan, massive reworking of ore material is highlighted by an erosion surface slump scar, which truncates the orebody, and appears to have removed a portion of it to a position somewhere down the palaeoslope (Andrew and Ashton 1982, Boyce et al 1983).

6.3.9. Waning Stages of Hydrothermal Activity.

Weak hanging wall enrichments of Mn, Fe and Zn at Silvermines indicate that hydrothermal input of metals continued after deposition of the stratiform ore and infilling of the brine pool. Without the intense reducing conditions prevalent within the brine pool, increased incorporation of more Mn and Fe into insol-

uble oxide phases may have occurred, as suggested by the ratio between acid-soluble and total Mn and Fe in the hanging wall dolomites (Figures 4.26-29).

Alternatively, the concentration of oxidised and relatively insoluble minerals may have taken place after deposition of the carbonate rocks, during diagenesis and recrystallisation. This idea is investigated in Part Two of this Chapter.

The lower levels and reduced areal extent of the hanging wall enrichments, compared with those of the ore horizon, suggest either more efficient dispersal of exhaled metals to background levels (under more oxidising conditions), or reduced input of trace metals because of waning of the hydrothermal system.

The apparent greater vertical extent of the hanging wall enrichments of Mn, compared to the footwall, reflects either the differing rates of sedimentation between the two lithologies, or a longer waning stage of hydrothermal activity, compared to its early development. However, the possibility of more extensive development of footwall enrichments (Figure 4.14), suggests that pre-ore hydrothermal activity was at least as long lived as the waning stages.

In the immediate hanging wall to the orebody, in-situ carbonate precipitation appears to have been inhibited by a number of factors, with the result that the succession is particularly thin in the mine area (Taylor and Andrew 1978). The lithologies are dominat-

ed by allochthonous dolomite breccias, with much stylolite formation evident. Normal, in-situ Waulsortian Mudbank Limestones are absent above the Ballynoe baryte and G Zone sulphide orebodies, only appearing further to the north and east (Andrew 1984). The same factors responsible for mudbank inhibition in the brine pool environment (metal poisoning and low Eh conditions) may have contributed to their absence in the hanging wall. Seafloor instability and massive sediment influx may also have been involved, combined with selective post-depositional dissolution of certain fractions, leaving only the dolomite and other insoluble components.

Original trace element levels in the allochthonous carbonate of the hanging wall breccias may have been lower than local, in-situ carbonate, if the material originated more distally from the hydrothermal site.

Chert bearing breccias, deposited during continued instability, are followed by stratiform, layered cherts and cherty limestone, originating in a more stable structural environment (Taylor and Andrew op cit). These cherts may have been precipitated chemically by late stage of waning hydrothermal activity (Russell 1983). The stratiform cherts are localised only in the immediate area of fluid exhalation, directly overlying the stratiform sulphide and baryte orebodies. Dolomitic limestones associated with the chert carry elevated Mn and Fe levels (Section 4.2.1).

6.4.1. Trace Element Incorporation into Carbonate Rocks.

Trace elements present within a carbonate rock may have originated in a number of ways:

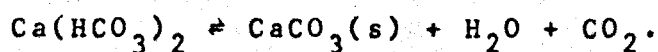
i) normal precipitation from seawater at background levels according to facies constraints on Eh and pH;

ii) incorporation to anomalously high or low levels via hydrothermal, terrigenous or hydrogenous input during sedimentation;

iii) post-depositional incorporation during recrystallisation, diagenesis, dolomitisation or other means.

The levels to which each individual trace element is incorporated will depend on the supply and chemical behaviour of that element during and after sedimentation. Conditions will obviously vary between one exhalative site and another, whether because of differences in hydrothermal source, sedimentary facies, scale or diagenetic history. The end result is a different trace element pattern around each centre.

Calcium carbonate precipitates chemically from waters carrying calcium bicarbonate in solution, if a loss of CO_2 from solution takes place:



This usually occurs at a pH above 7.8, as calcite tends to dissolve at a pH lower than this.

Many divalent ions may substitute for calcium in the calcite structure, most commonly magnesium, with up to 30% MgCO_3 in isomorphous series. Iron, manganese and strontium are also common, and small amounts of barium, zinc, lead, cobalt and sodium may also replace calcium, determined largely by dimensions of atomic radius (Table 6.4) relative to that of Ca^{2+} (Milliman 1974).

Solid solution between calcite (CaCO_3), dolomite ($(\text{Ca},\text{Mg})\text{CO}_3$), siderite ($(\text{Fe},\text{Mn})\text{CO}_3$) and ankerite ($(\text{Ca},\text{Mg},\text{Fe},\text{Mn})\text{CO}_3$) allows a more or less complete range of compositional differences in the carbonate minerals, with up to 40 wt.% FeCO_3 or MnCO_3 in iron and manganese rich varieties (Deer et al 1971, Richter and Fuchtbauer 1978). Trace elements which are incorporated to varying degrees into calcium carbonate, will do so in one of the following manners: i) diadochic substitution; ii) interstitial incorporation; iii) adsorption for unsatisfied charges; iv) filling of unoccupied lattice positions in lattice defects in the structure (Brand and Veizer 1980).

For the four main elements examined in this study (Mn, Fe, Zn, Mg), diadochic substitution is quantitatively the most important, and the principal controls in this process are outlined in the following pages.

The distribution coefficient ($k_{\text{calcite}}^{\text{M}}$) of a particular trace element (M) into calcite determines the rate of entry of that element into the calcite lattice

Ionic species	Partition Coefficient (Calcite)	Partition Coefficient (Aragonite)
Mn ²⁺	5.4 - 1700	0.86 (<u>±</u> 0.4)
Fe ²⁺	1 - 21	
Zn ²⁺	5.2 - 57	(0.21 - 2.85)
Sr ²⁺	0.055 - 0.27	
Na ⁺	$2 \times 10^{-5} - 3 \times 10^{-5}$	
Mg ²⁺	0.02 - 0.06	
Ba ²⁺	0.06 <u>±</u> 0.01	

Table 6.5: Partition coefficients of various trace elements into CaCO₃.
Source: Brand and Veizer (1980); Pingitore and Eastman (1984).

Element	Common Ionic State	Atomic Weight	Ionic Radius (Å)	Electro- negativity
Na	1+	22.99	0.95	0.9
Mg	2+	24.32	0.66	1.2
K	1+	39.10	1.33	0.8
Ca	2+	40.08	0.99	1.0
Mn	2+	54.94	0.80	1.5
	3+		0.66	
	4+		0.60	
Fe	2+	55.85	0.74	1.8
	3+		0.64	
Ni	2+	58.71	0.69	1.8
Co	2+	58.94	0.72	1.8
Cu	2+	63.54	0.72	2.0
Zn	2+	65.38	0.74	1.7
Sr	2+	87.63	1.12	1.0
Cd	2+	112.40	0.97	1.7
Sn	2+	118.69	0.93	1.8
Ba	2+	137.36	1.34	0.9
Pb	2+	207.21	1.20	1.8

Table 6.4: Ionic radii and electronegativities of selected cations,
from Krauskopf (1979).

during its growth. The partition coefficients for entry of Mn, Fe and Zn into calcite from solution are all greater than one (Table 6.5), meaning that all are effectively concentrated from solution by the precipitation of calcite. The opposite is true for elements with a partition coefficient of less than one (eg. Sr, Na, Mg, Ba). In laboratory experiments, distribution coefficients for intake of trace metals into CaCO_3 are dependent on a number of controls (Kitano et al 1980):

- 1) crystal form of carbonate precipitated;
- 2) precipitation rate;
- 3) chemical nature of the solution;
- 4) temperature and depth of water;
- 5) other controls, including chemisorption.

1) Crystal form of CaCO_3 precipitated.

Different levels of trace element incorporation are accommodated by different CaCO_3 polymorphs, for example, the partition coefficient for Mn and Zn entry into aragonite is much lower than for calcite (Milliman 1974, Kitano et al op cit).

Polymorph growth is itself controlled by numerous chemical and biological parameters. Depth and temperature are major influences, with aragonite and high-Mg calcite typically associated with shallow shelf environments, only forming in a deep sea environment under increased temperature or salinity. Low-Mg calcite is associated with inorganic precipitation in colder,

deeper water environments (Milliman op cit, Schlager and James 1978). Biological controls on organic precipitation of CaCO_3 polymorphs vary at taxonomic level. Chemical factors governing whether precipitation of calcite or aragonite takes place are complex, as the presence of certain elements tends to promote aragonite and inhibit calcite formation, or vice versa, depending on absolute concentration (Bathurst 1971, Milliman op cit, Barber et al 1975).

The principal factor governing trace element entry into Mg or Ca sites in calcite, aragonite or dolomite at trace concentrations, is ionic radius (Kretz 1982). Elements with larger ionic radius than Ca^{2+} (eg. Pb^{2+} , Ba^{2+} , Sr^{2+}) fit only into the larger calcium sites, and those smaller than Mg^{2+} (eg. Ni^{2+}) fit only into the smaller magnesium sites and are therefore usually absent in pure calcites. The entry of those cations with ionic radius between that of Ca^{2+} and Mg^{2+} (including Mn^{2+} , Fe^{2+} , Zn^{2+}) is controlled by the relevant partition coefficient (Tables 6.4, 6.5).

2) Precipitation rate.

Slower sedimentation rates increase the duration of exposure of sedimentary horizons to seawater circulation, enhancing cementation and the formation of hardgrounds or crusts (Bathurst 1979), affecting also the intake and fractionation of trace elements. This allows greater intake of elements with partition coefficients greater than one, and reduced intake of those with partition coefficients less than one (Lorens 1981).

The production and loss of CO_2 from the newly forming crystal surface is the principal rate-determining step in CaCO_3 precipitation. If slow, CO_2 buildup (and supersaturation) at the existing crystal surface inhibits further precipitation (Dreybrodt 1981).

3) Solution chemistry.

Intake of Mn^{2+} and Fe^{2+} into carbonate phases may be influenced by changes in Eh and/or pH via the availability in solution, of either element in the divalent state (Meyers 1974, Krauskopf 1979). Complexing of metallic cations with chloride or organic substances in solution may reduce their availability to precipitating carbonate minerals because of increased solubility or lowered partition coefficients (Crockett and Winchester 1966, Tsusue and Holland 1966). Manganese is unaffected by either of these influences, and Mn concentrations in calcite reflect more directly, the intensity of supply (Bodine et al 1965).

4) Depth and temperature.

The main effect of water depth or temperature on partition coefficients is via their influence in determining which CaCO_3 phase precipitates from that water (Kinsman and Holland 1969). Other effects on partitioning of Mn and Fe are minimal for the range of temperatures and depths envisaged for the Irish Lower Carboniferous (Bodine et al op cit).

5) Chemisorption.

In addition to coprecipitation of trace metals,

crystalline CaCO_3 effectively sorbs divalent ions from solution, particularly when fine grain sizes are involved (Bancroft et al 1977). Ions such as Mn^{2+} , Zn^{2+} and Ba^{2+} are strongly adsorbed onto CaCO_3 surfaces, and even more strongly onto MgCO_3 (MacBride 1979), effectively lowering the solubility of each metal below the level expected for its metal carbonate in solution.

The end result is that predicted entry of divalent cations such as Mn^{2+} into CaCO_3 (calcite or aragonite) may be exceeded because of chemisorption by rapidly forming lime muds. This may be especially important in the case of aragonitic muds, where enhancement of Mn:Ca ratios in solution by the precipitating phase, is not normally encouraged, according to partition laws. Later redistribution of chemisorbed ions into lattice-held sites during burial and diagenesis would mask their origin.

The interplay between each of these parameters during sedimentary CaCO_3 deposition is summarised in Figure 6.11.

Although information on primary sedimentary conditions can be obtained, the use of experimentally derived partition coefficients to deduce the chemistry of depositional fluids is adequate only in chemically simple solutions, a situation unlikely in natural systems. Cosubstitution of a variety of elements into the carbonate lattice, and microscopic heterogeneity

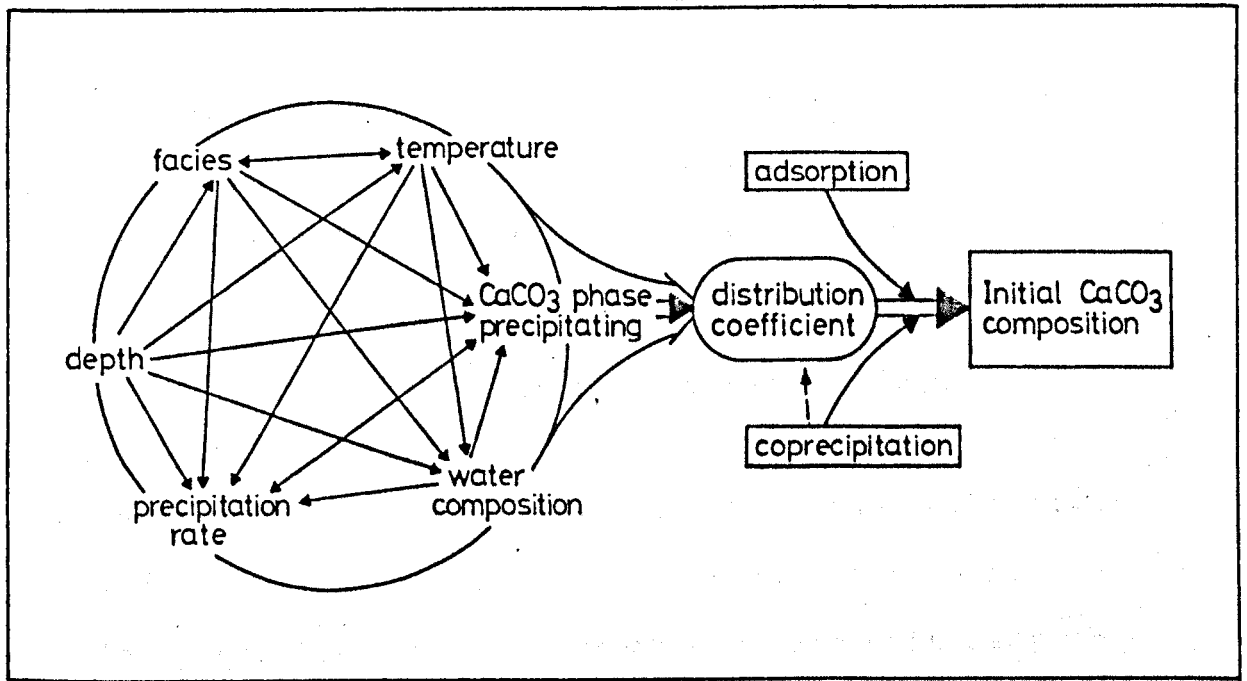


Figure 6.11: Relationships between interacting parameters which influence direct trace element intake into precipitating CaCO_3 phases in the sedimentary environment. Hydrothermal input will in turn influence virtually all of these directly or indirectly. The influence of different organic components (at taxonomic level) may be added to the circle of controls on the left.

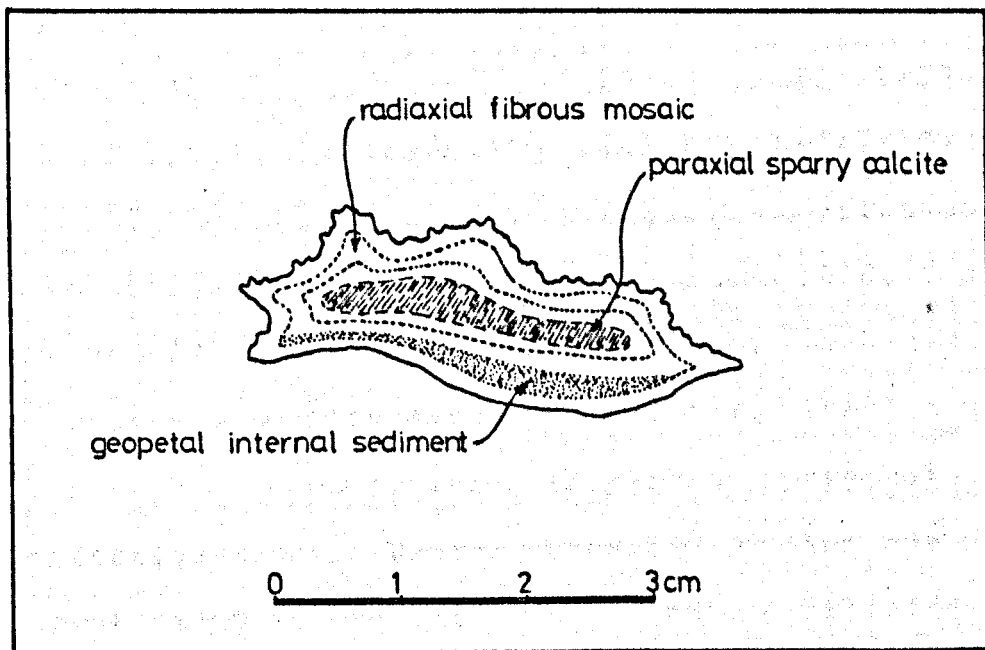


Figure 6.12: Component phases of typical stromatolite structure, sketched from an example from Ballinalack area.

in crystal composition further complicate matters, and some caution should be exercised when making genetic inferences from trace element concentrations in precipitated calcites (Angus et al 1977).

6.4.2. Trace Element Intake into Irish Waulsortian Limestones.

Initial mineralogical composition of the Waulsortian mudbanks may have played an important part in determining primary intake of trace elements both near to, and distant from, a hydrothermal centre. The environment of deposition envisaged for the growth of mudbank limestone is a tropical to subtropical shelf sea (water depth at least 100 metres), with little or no clastic sediment input (Wilson 1975, Bathurst 1982, Lees and Miller 1985). Initial inorganic carbonate mud accumulation would have been dominated by aragonite (Arag) or Mg-calcite (HMC) precipitation, mainly on account of the warmer water temperatures and presumed high Mg concentrations (Schlager and James 1978, Brand and Veizer 1980, Bathurst op cit). Recent work has shown that Waulsortian carbonate mud precipitation was dominantly HMC in composition (J. Miller, personal communication 1984). Visible biogenic calcium carbonate input is dominated mainly by crinoid debris (originally HMC), bryozoans (Arag, HMC) and brachiopods (LMC - Low Mg calcite).

A large proportion of ancient mudbank limestones now

consists of early diagenetic or later calcite phases, present as radiaxial fibrous mosaic and later, equant paraxial calcite. The radiaxial fibrous mosaic is an in-situ neomorphic alteration of an acicular precursor, either HMC (Bathurst 1982) or aragonite (Cotter 1966), whereas the paraxial calcite was precipitated in voids by diagenetic fluids. These voids (now represented by stromatactis structures) contain internal sediment which probably originated as inorganically precipitated HMC rosettes, on account of the uniform crystal size and lack of fossil debris (Bathurst op cit). This HMC internal sediment was precipitated into cavities from marine waters, some time after initial mud bank sedimentation, and predates the paraxial calcite (Figure 6.12).

Closer to the hydrothermal centre at Silvermines, a number of factors may have influenced CaCO_3 precipitation, favouring aragonite nucleation rather than calcite, as a precursor to the mud of the carbonate mounds. These include elevated temperatures, salinity and metal input, especially involving a range of minor and trace elements which inhibit the nucleation of calcite.

Within the immediate environs of the brine pool and exhalative centres, calcium carbonate was unstable, and its deposition was inhibited by high CO_2 concentrations, trace metal poisoning and low Eh conditions. Because of this, siderite was the only in-situ car-

bonate forming under the extreme conditions of the basin hollows.

Beyond the confines of the brine pool, primary enrichment of trace elements such as Mn and Fe (relative to seawater) in carbonate sediments forming on the surrounding seafloor, would depend to a large extent on which CaCO_3 polymorph was dominant. If HMC, rapid preferential incorporation of the elements would take place, whereas if aragonite, this would be much less pronounced.

With a relatively abundant and varied source of metals increased incorporation may be expected into CaCO_3 because of cosubstitution of two or more different cations into the Ca sites, eg. Mn together with Sr or Na. There is a suggestion of this being the case in the host rocks around Tynagh (Chapter 3.3.1), where both large and small cations occur together at increased levels, over a roughly similar area (Mn, Fe, Zn, Sr (Na also, see Figure 6.18) up to at least 5 kilometres from the deposit).

Local temperature and pH fluctuations were probably not significant in affecting Mn intake, as the partition coefficient for Mn into calcite is not particularly sensitive to these parameters within the ranges anticipated for subtropical shelf environments. Temperatures high enough to influence Mn intake would only be expected in the immediate vent areas (where CaCO_3 precipitation did not appear to be taking place) or

in the sub-surface feeder zones.

The relatively rapid growth of mudbank elsewhere on the seafloor would have prevented strong fractionation of trace elements between CaCO_3 and seawater in the sedimentary environment. To balance this, the fine grained nature of the rapidly forming mud may have encouraged strong chemisorption of some trace elements from seawater, particularly Mn and Ba (MacBride 1979), ensuring a wide possible range of trace element incorporation rates.

On a smaller scale, the varied sources of inorganic and organic CaCO_3 would have provided a variety of initial CaCO_3 polymorphs, a wide range of growth rates, and as a result differential trace element intake rates (Milliman 1974, Morrow and Mayers 1978, Nair and Hashimi 1981). In this way, compositional variations would also have arisen between the numerous different components, dominated largely by metastable aragonite and Mg calcite. In addition, because of fluctuating trace element supply levels (from hydrothermal sources), zonation may be expected within larger crystals or biogenic components, or on a larger scale between sediment layers. As only surface equilibrium is maintained between the precipitating phase and solution, constant changes in fluid composition are passed onto successive generations of CaCO_3 (Raiswell and Brimblecombe 1977). These anticipated inhomogeneities within host carbonates from near to the

mineralisation are borne out by electron microprobe examination of polished thin sections (Figures 5.9b-p).

Suggestions that Mn and Fe concentrations in carbonate rocks are a function of clay mineral content (Billings and Ragland 1968), or controlled primarily by coatings of oxide or clay minerals (Veizer 1978), may be applicable to very argillaceous limestones or dolomites, typical of environments other than the Waulsortian. Their proposals are not substantiated by the data presented in Chapter 4, except perhaps, to a limited extent in very muddy samples from the ore horizon or hanging wall. In the relatively pure mudbank limestones, which constitute the bulk of the distal outcrop samples (averaging over 97% CaCO_3 , about 1% MgCO_3 , and less than 0.5% $\text{SiO}_2 + \text{Al}_2\text{O}_3$), most, if not all, of the Mn and Fe is associated with the carbonate fraction of the rock.

Predicted Mn and Fe levels in calcites precipitated in equilibrium with normal seawater (20-30°C, 1.9ppb Mn, 3.4ppb Fe, 441ppm Ca; Turekian 1972) using available partition coefficients (Table 6.5), are 80 ppm or less for both elements, depending on the actual k value used (Michard 1968, Milliman 1974, Veizer 1977b, Rao 1981b). Manganese and iron levels in much of the Waulsortian Mudbank Limestone well away from the obvious influence of hydrothermal input, are still higher than the predicted levels from partition theory on present day seawater concentrations.

Expected zinc contents of limestones precipitated from normal seawater (11ppm. using 2ppb Zn in seawater (Turekian op cit) and a $k_{\text{calcite}}^{\text{Zn}^{2+}}$ of 5.5) are approximately three times higher than those found in nature (Hartree and Veizer 1982) and over twice as high as background zinc levels in the Irish Waulsortian Limestones. Measured zinc levels in Recent carbonate shell material are about 20 ppm (Milliman op cit).

These observed deviations from expected concentrations of Mn, Fe and Zn may indicate either:-

- 1) considerable modification of seawater concentrations by large scale hydrothermal input;
- 2) lowered Eh conditions throughout the Waulsortian basins, allowing increased Mn and Fe levels in solution (cf. Veizer 1977b);
- 3) increased trace element incorporation because of cosubstitution of more than one trace element species;
- 4) low or restricted depositional rates of mudbank limestone;
- 5) complexing of zinc with chloride in seawater (Tsusue and Holland 1966);
- 6) considerable modification of the trace element geochemistry during diagenesis.

Although the initial Mn:Fe ratio of the exhaled hydrothermal fluids may have ranged widely, probably dominated by Fe over Mn, the principal controls on the Mn:Fe ratio in the ore environment and surrounding

area were:-

a) precipitation of pyrite and siderite, which removed large quantities of Fe, leading to the 'export' of more balanced quantities of both elements from the brine pool area;

b) the carbonate-dominated geochemical environment of the distal areas, permitting comparable behaviour of Mn and Fe, and leading to approximately equal proportions of these elements in the host rocks.

Background Mn and Fe levels are approximately similar to one another throughout the Irish Waulsortian, although some differences are observed on a regional scale and in statistical comparison. These include the apparent regional gradient in background levels (Figure 3.9) and the slight contrast in statistical distribution of absolute values, with Fe displaying more extreme distribution than Mn (Figure 3.8).

The reasons for the regional variation in background Mn and Fe levels may be due to one or more of a number of factors. These include possible differences in water depth and bottom conditions across the country, different growth rates of mudbanks (possible faster accumulation in the southwest), greater hydrothermal input in the more enclosed part of the Waulsortian sea, to the northeast of the country (sufficient to affect overall seawater chemistry, cf. Solomon and Walshe (1979b) at Rosebery), or contrasting diagenetic histories (Gray and Russell 1984).

The lower levels of Fe, compared with Mn, in background samples, and the higher Fe levels in anomalous samples, may be accounted for by differences in supply around hydrothermal sites, the slightly lower solubility of Fe, and the slightly different partitioning behaviour of the two elements into CaCO_3 .

Before accepting predictions of the primary environment of deposition from patterns of trace element distribution around the Silvermines deposit, it should be borne in mind that virtually all the carbonate rocks preserved in the mineralised zone and immediate hanging wall are allochthonous. The exceptions are the Stromatactis Reef Limestone which predates most of the mineralisation, and the siderite, which hosts a portion of it. In addition, most of the host carbonate over a wider area has suffered extensive and severe recrystallisation and/or dolomitisation. For this reason, diagenetic alterations have played an important part in determining the eventual patterns of trace element distribution in the Silvermines area.

CHAPTER SIX - Discussion and Genetic Implications.

Part Two - Post-Depositional Modification.

6.5.1. Introduction.

6.6.1. Early Diagenesis.

6.6.2. Diagenesis in Waulsortian and Equivalent Carbonates.

6.6.3. Fluid Composition.

6.6.4. Redistribution of the Elements.

6.7.1. Later Diagenesis.

6.7.2. Texture and Neomorphism.

6.7.3. Trace Element Sinks.

6.8.1. Zinc.

6.8.2. Sodium.

6.8.3. Hydrocarbons.

6.9.1. Pressure Solution.

6.9.2. Volume Reduction.

6.9.3. Dolomitisation.

6.9.4. Summary.

Chapter Six - Discussion and Genetic Implications.

Part Two: Post-Depositional Modification.

6.5.1. Introduction.

Lithification of a sediment involves processes which ultimately convert a diverse array of particles into a thermodynamically stable mineral assemblage. From the moment a carbonate sediment is formed, interplay between that sediment and its pore water takes place, the rates and mechanisms of which constitute the study of diagenesis. These processes evolve with time and increasing burial depths, and further post-diagenetic modification may result from physical stresses brought about by orogenic events.

The three principal causes of diagenetic recrystallisation are:-

i) increasing pore pressure; ii) increasing temperature; iii) changing water chemistry; and the effects of these on the sediment are influenced by the physical and chemical characteristics of the sediment involved (Baker et al 1980).

Diagenesis of a carbonate sediment can be defined in terms of changes in the chemistry, structure, texture and mineralogy of the sediment (Brand and Veizer 1980). The chemical distribution of minor and trace elements in the resulting carbonate rock is obviously of great importance in this study, and is dependent on the influence of all four of these parameters during diagenetic reactions.

Minor and trace elements which substitute to varying degrees for Ca in the calcite or dolomite lattices (such as Mg, Sr, Fe, Mn, Pb, Zn) will all become involved in diagenetic reactions, whether they are present as direct diadochic substitutions, interstitial substitutions, adsorbed ions, or filling lattice defects.

Pingitore (1978) proposes that the chemistry of calcite during and after diagenesis is controlled by several factors, including:-

- i) chemistry of the original polymorph;
- ii) partition coefficient for the ionic species concerned;
- iii) openness of the water flow, or diffusion gradient to or from the diagenetic site;
- iv) externally fixed chemistry of the diagenetic fluid;
- v) non-carbonate reactions.

Obviously, the overall degree of diagenetic alteration will also determine how much change in trace element chemistry takes place. It may be possible to estimate the composition of the diagenetic solution by examining the trace element content of the diagenetic calcite and comparing it with the appropriate coefficient. Textural preservation and original trace element chemistry of sedimentary carbonate may survive if some degree of isolation is maintained from the bulk aquifer solution during diagenesis. As in primary

trace element intake, however, the situation is rarely so simple, and the interaction of numerous controlling parameters must be taken into account, and care exercised, before any predictions are made concerning the sedimentary or diagenetic environment of a particular rock.

1) Initial CaCO₃ polymorph.

Carbonate sediments dominated by low-Mg calcite will be subjected to less diagenetic alteration, because of its relative stability in diagenetic fluids, compared to high-Mg calcite and aragonite. They should therefore retain much of their original chemical characteristics (Brand and Veizer 1980, Rao 1981). On the other hand, sediments dominated by aragonite and high-Mg calcite are converted to more stable low-Mg calcite during diagenesis, with resulting chemical exchange during solution and reprecipitation, involving trace elements as well as Mg.

With an aragonitic parent, because of the volume increase (8%) generated by the transformation of aragonite to less dense calcite, some material may be effectively lost to the system, but is normally precipitated locally as cement (Wardlaw et al 1978). The proportion of metastable carbonate minerals in a carbonate sediment will determine to some extent, how much of the cement and resulting trace element chemistry in the stabilised carbonate rock is locally derived, assuming open system circulation (Veizer 1977a).

2) Partition coefficients.

During diagenesis, the trace element content of the initial solid phase is systematically partitioned through a liquid into the reprecipitated phase (Pingitore 1978). As in primary precipitation, this partitioning of different ionic species leads to enrichment of certain elements (eg. Mn, Fe, Zn) and depletion of others (Sr, Na, Mg, Ba) in the resulting phase, with a corresponding depletion or enrichment of the remaining solution. The greater the deviation from unity, of the partition coefficient for the element concerned, the stronger the depletion or enrichment for a given degree of diagenetic equilibration with meteoric water (Table 6.5).

3) Water Flow.

Most carbonate rocks appear to stabilise in fairly restricted diagenetic systems, in discrete zones, on solid-liquid interfaces. Pingitore (1982) stresses the importance of transport of dissolved constituents by aqueous diffusion in pore spaces much too confined (100μ) to permit normal hydraulic flow of aquifer solutions. Diffusive movement of ions in solution is a much slower process, is bidirectional (according to concentration gradients and charge balances), and takes place by both chemical and physical means. Within this regime, homeostasis is encouraged because diffusion counteracts excessive trace element buildup because of the higher gradients induced (Pingitore

op cit).

The 'messenger film water' is the medium through which transfer of chemical and textural information from dissolving to precipitating phase takes place, in the reaction zone (Brand and Veizer 1980). This transfer is controlled by the comparative rates of dissolution, and diffusion and flow transport rates between this film and surrounding meteoric bulk aquifer water (or macropore system) and the messenger film water (or micropore system), mainly by aqueous diffusion processes, will determine to a large extent, how open the overall system will be during diagenesis (Pingitore 1976, 1982). Thus, isolation of the micropore system from the macropore system will allow preservation of the original sedimentary trace element content, an event which happens only rarely in nature (Al-Aasm and Veizer 1982).

Early enrichment of Mn (and Zn) would perhaps indicate involvement of a single fluid, becoming progressively more depleted in these elements. In this way, considerable inhomogeneity in precipitated phases might arise during closed system diagenesis, caused by fractionation of elements with partition coefficients greater or less than one. Crystal nuclei or distinct early crystals would appear to be enriched in Mn and Zn relative to later generations of overgrowths, but the sediment would still retain the same bulk total content of Mn and Zn as its aragonitic precursor.

If the system is open, considerable enrichment of trace elements (Mn up to 15-fold, Zn up to 5-fold), relative to the original aragonitic parent, may take place (Pingitore 1978).

Early enrichment of Mn during aragonite-calcite transformation, involving Mn derived from the parent phase, is termed auto-enrichment, whereas Mn derived from an external source, under open system diagenesis, may lead to alloenrichment of the transformed phase (Pingitore op cit).

Physical properties of the carbonate sediment, such as permeability, sorting, texture and structure, all related to sedimentary facies, will obviously influence fluid movement in the bulk aquifer solution, and to the messenger film reaction zone (Brand and Veizer 1980).

Diffusion of dissolved material plays a role in any of the diagenetic processes occurring in the micro-pore system, whether mineral transformation, cement precipitation, stylolite formation or dolomitisation (Pingitore 1982).

4) Water Chemistry.

As in initial precipitation from seawater, changing water chemistry during diagenesis will influence secondary variation in Mn and Fe content, either via fluctuating Eh conditions, or supply of Fe(II) and Mn(II). Those cations with only a single valence state (eg. Mg^{2+}) are generally unaffected by oxidation

potential, and are controlled by supply alone (Meyers 1978). Unlike Mn, the Fe content of natural groundwaters is strongly bimodal, due to the presence or absence of sulphide (Richter and Fuchtbauer 1978). If sulphide is present, Fe concentrations are usually less than 1ppm, whereas if it is absent, Fe concentrations are usually between 20 and 300ppm.

The interactions between each of the parameters controlling aragonite-calcite transformation during early diagenesis are summarised in Figure 6.13.

Further modifications of a limestone under conditions of stress, whether physical compaction, deformation, neomorphism or solution, may take place. The last mentioned, in particular, will involve gain or loss of included trace elements by transportation of dissolved ions from recrystallisation sites by interstitial waters.

In this study, the effects of diagenesis on trace element composition will be considered under three main headings:-

- 1) early diagenesis, including mineral transformation;
- 2) later diagenesis, including recrystallisation, neomorphism and solution-reprecipitation;
- 3) pressure solution and dolomitisation (although dolomite formation may take place at any time from initial sedimentation onwards).

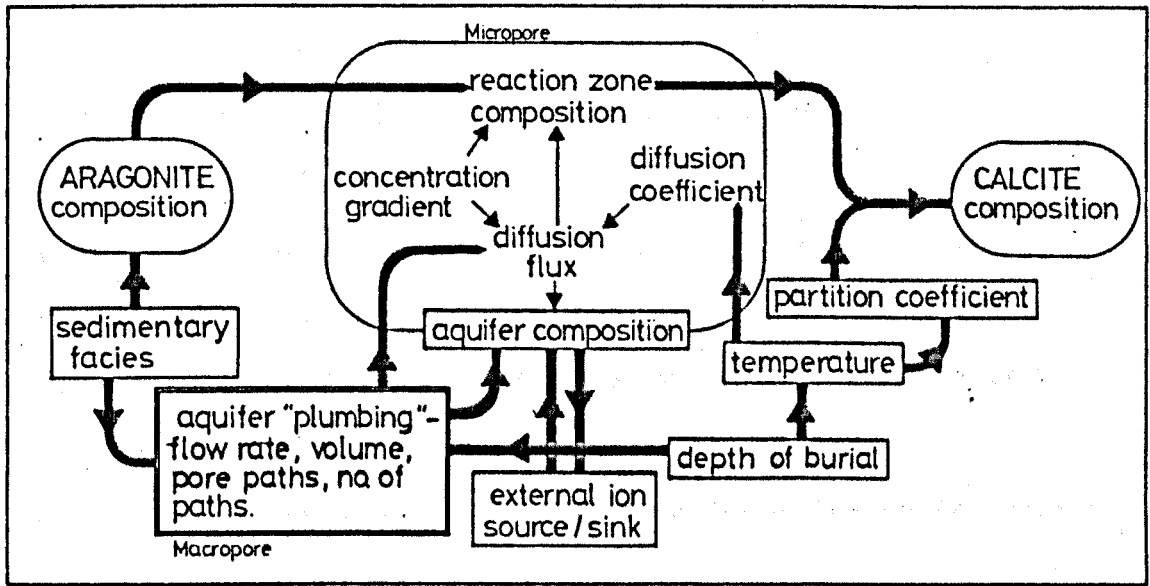


Figure 6.13: Flow diagram illustrating the interacting parameters that control the exchange of chemical information during aragonite - calcite transformation. Note the importance of micropore reaction (especially diffusion processes), which are particularly important in a relatively impermeable unit such as mudbank-type limestones. Modified from Pingitore (1982, Figure 3).

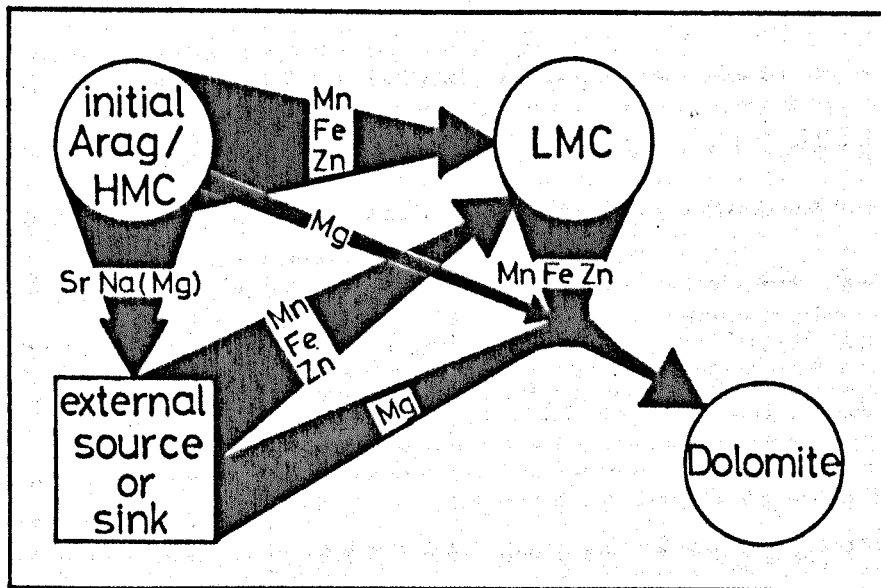


Figure 6.14: Simplified flow diagram illustrating the principal trace element exchange during initial diagenetic transformation of aragonite / high Mg calcite to low Mg calcite or dolomite. (Arag = aragonite, HMC = high Mg calcite, LMC = low Mg calcite).

6.6.1. Early Diagenesis.

The processes taking place during early diagenesis of a carbonate sediment are dominated by transformation of less stable polymorphs (aragonite and high-Mg calcite) to more stable low-Mg calcite.

Strontium contents reveal much about the geochemical controls operating during diagenesis of carbonate rocks. Ancient limestones tend to have lower Sr contents than their modern analogues because of diagenetic loss, although a wide range of contents are observed, from 50 to 1000ppm (Morrow and Mayers 1978). Several factors, each related to depositional facies, are responsible for this variation:-

- 1) primary mineralogy: original aragonite carbonate sediments contain from 5000 to 10000ppm Sr (Table 6.6), whereas sediments composed of inorganic calcite will contain considerably less than this (Kinsman 1969, Milliman 1974). These differences tend to become negated by diagenetic processes because of the greater stability of the latter (and therefore reduced susceptibility to loss) during diagenetic recrystallisation (Veizer and Demovic 1974);

- 2) textural differences: differences between carbonate rocks, in particular those affecting permeability, influence Sr behaviour principally by controlling the degree of exchange between bulk meteoric solutions and reaction zone pore waters. Relatively closed systems are typified by high Sr values, and open systems by

Phase		Sr (ppm)
Aragonite	cement	8300
	pelletoids	9000
	aggregates	9150
	Bryozoa	8600
High Mg calcite	cement	1300
	Bryozoa	2200
	Echinodermata	2050
Low Mg calcite	Brachiopoda	1500

Table 6.6: Measured strontium contents of various sedimentary carbonate components, from Milliman (1974).

Lithology	n	Sr (ppm)
All hanging wall	148	165
Limestones (under 3% Mg)	62	181
Dolomites (over 3% Mg)	86	153

Argillaceous dolomites	61	159
Non-argillaceous dolomites	25	140

Siderite	2	60

Footwall 'Muddy Reef'	21	384

Outcrop samples (distal)	54	168

Table 6.7: Mean strontium contents of Silvermines host rocks (X.R.F. analyses). Distal outcrop samples from beyond 4 kilometres, argillaceous dolomites with over 1% ($\text{SiO}_2 + \text{Al}_2\text{O}_3$), n = number of samples.

Lithology	n	Sr (ppm)
Core samples, L ₂ Reef	70	307
Ba rich	3	575
argillaceous	44	343
non-argillaceous	23	203

Reef outcrop within 2 km.	16	276
" " beyond 2 km.	70	166

Core samples, L ₁ , L ₃ limestones	8	277

Table 6.8: Mean strontium contents of Tynagh host rocks (X.R.F. analyses). L₁ and L₃ limestones are argillaceous bioclastic limestones above and below Waulsortian.

low values (Pingitore 1982);

3) depth and salinity: diagenesis in a fresh-water-dominated system leads to much lower Sr contents in limestones because of the much lower concentration of Sr in meteoric water (Morrow and Mayers op cit). Typical reef limestones contain from less than 100 to about 400 ppm Sr, whereas typical basinal limestones contain from 500 to 3000 ppm Sr, because deposition of the latter takes place far from the influence of fresh water, and much of the Sr is retained during diagenesis.

As Sr is lost during transformation of metastable phases to low-Mg calcite, successive volumes of meteoric water will each remove some Sr, causing a decline in the overall content within the limestones. An estimated tens to hundreds of thousands of pore volumes of solution must pass through typical shelf limestones to reduce their Sr content from around one percent to less than 200ppm. This is regardless of the number of dissolution-reprecipitation events which occur during the passage of each pore volume (Morrow and Mayers op cit).

6.6.2. Diagenesis in Waulsortian and Equivalent Carbonates.

At Silvermines, the original mineralogy of the carbonate mudbank sediments, both close to and away from the hydrothermal centres, was probably dominated

by aragonite and high-Mg calcite (HMC) of inorganic and organic origin, apart from some low-Mg calcite (LMC) of biogenic origin (Section 6.4.2). On burial, this metastable assemblage would have offered little resistance to diagenetic modification, allowing considerable release of Mg during HMC to LMC conversion.

During these reactions, widespread exchange of trace elements (Mn, Fe, Zn, Sr, Na) between the dissolving and reprecipitating carbonate phases and diagenetic fluids was permitted, leading to possible major modifications of primary trace element geochemistry.

The flow of diagenetic solutions in the vicinity of the deposit was facilitated by the heavily brecciated footwall and hanging wall sequence. This resulted in more intense recrystallisation and modification of the hanging wall succession (Filion 1973), in the same way that it focussed dolomitisation of the footwall sediments.

The low tenors of Sr (generally below 200ppm) throughout the Waulsortian Limestones and equivalent rocks in the vicinity of the Silvermines deposit (Table 6.7), indicate the considerable diagenetic modification undergone by the host carbonates. Low Sr and Mg concentrations (the latter generally below 1%) present throughout the Irish Waulsortian emphasise the widespread effects of thorough diagenetic alteration of original sedimentary carbonate material. This is in common with similar Palaeozoic carbonate buildups

from elsewhere in the world, including Waulsortian-type mudbanks in Northern England (Bathurst 1982).

The effects of diagenesis appear to be comparable both close to, and distant from the deposit, as no significant change is observed towards the mineralised Waulsortian sequence from distal, unmineralised mudbanks (Table 6.7). This contrasts with the situation at Tynagh, where elevated Sr levels are observed close to the mineralisation, within about 5 kilometres (Figure 3.22; Table 6.8).

Although generally low throughout the Silvermines area, average Sr values remain above 100ppm, indicating that the theoretical lower limit of Sr depletion has not been reached (Pingitore 1982).

Higher levels of Sr are only observed in the baryterich samples, where Sr substitutes for Ba in $BaSO_4$ to percent levels (Barrett 1975), or in the muddier parts of the succession, such as the footwall Muddy Reef Limestone, or argillaceous parts of the ore horizon and hanging wall dolomite breccias (Table 6.7). The excess Sr is either held within the clay mineral impurities, or a reduction in permeability of the more argillaceous limestones has inhibited normal diagenetic fluid circulation, resulting in reduced interchange between fluid and sediment, with corresponding retention of Sr in carbonate lattice sites.

Any inhibition of the normal processes of Mn and Fe enrichment, during diagenesis of the same muddy sed-

iments, may have been balanced out or masked by initially higher input from hydrothermal sources.

In effect, the argillaceous limestone units were subjected to a less open diagenetic system than the rest of the sequence, with more limited fluid circulation, and resulting trace element interchange (Pingitore op cit). Visible modification of these units, in the form of recrystallisation or dolomitisation, is less intense as a result. Slightly lower Sr values are observed in the hanging wall dolomites (Table 6.7), and a weak negative correlation is noted between Mg and Sr, compared with a strong positive correlation between Ca and Sr. Such a reduction in the Sr content of the dolomites is to be expected since fewer Ca lattice sites are available for substitution by Sr, as well as the greater degree of recrystallisation suffered by the dolomite during diagenetic fluid interchange. A number of analyses indicate comparable weak depletions of Ce and La in the dolomites (Table 6.12), elements which would similarly tend to occupy only the Ca sites. The strontium content of the sideritic samples, likewise is very low (Table 6.7) because of the reduction in available Ca lattice sites.

Strontium is generally enriched in hydrothermal solutions (Barnes 1981), yet in the host rocks surrounding the Silvermines exhalative centre (excluding the stratiform baryte) it shows no indication of increased primary intake into contemporaneous sediments; instead,

weak depletions of the element are observed in the dolomitic host rocks. This suggests that diagenetic controls are more important than hydrothermal input, in influencing the overall distribution of the element. One problem arising here is: how much of this is also true for the other elements involved in both primary hydrothermal intake and diagenetic reactions, such as Mn and Fe ?

At Tynagh, enrichments of Sr are detectable up to 5 kilometres from the hydrothermal centre, in Waulsortian carbonates (Figure 3.22). This would suggest that direct incorporation of exhaled Sr has occurred into newly forming carbonate sediments (perhaps co-substituting with Mn and Fe) around the vents. Alternatively, restricted circulation of fluids, brought about by the increased argillaceous content of the host mudbanks locally around the deposit, has reduced the degree of Sr depletion during diagenesis. As the extent of argillaceous impurity, indexed by anomalous Al_2O_3 content (Russell 1975) is much less widespread than the 5 kilometre-radius Sr enrichments, the latter argument seems less likely.

Anomalously high Sr contents recorded in host Waulsortian micrites from the Ballinalack deposit (Daly and Williams 1982) are suggestive of a hydrothermal influence on geochemical distribution, as no visible argillaceous impurity is present in the limestones locally.

6.6.3. Fluid Composition.

On the basis of fluid inclusion evidence, Samson (1983) proposes the involvement of at least three fluid components in the history of the Silvermines host rocks. These are the hydrothermal fluid, modified sea water, and a third, possibly meteoric component, of uncertain origin or composition. The generally low Sr contents in the Waulsortian mudbanks around the Silvermines imply continued involvement of large volumes of circulating waters during diagenetic reactions (Morrow and Mayers 1980). A number of possible local contributory sources may be considered for these waters.

Initially, connate waters (originally seawater) may have been released from clay minerals and carbonate grains in the reworked debris flow material, in the manner suggested by Bathurst (1979). These waters may have been modified locally by dewatering of sulphide muds and gels, producing a high salinity and anomalous trace element concentration during early diagenesis. Continued upward percolation of hydrothermal waters from the steadily weakening hydrothermal system took place, with entrainment of overlying brine pool or seawaters, so providing a continued source of trace element rich ground waters.

Later circulation of post-hydrothermal, marine or meteoric waters through the base metal sulphide-bearing sediments resulted in local modification of trace

element content of the diagenetic fluids. Any reduction in Eh or pH of the modified solutions would have resulted in increased dissolution of carbonate and increased trace element levels, whereas the presence of appreciable sulphide in solution would have considerably reduced the mobility of iron and zinc. The widespread occurrence of disseminated pyrite (and minor sphalerite) in the hanging wall suggests that sulphide was a significant component of the diagenetic fluids at some stage, possibly because of intense bacteriogenic sulphate reduction.

6.6.4. Redistribution of the Elements.

On a microscopic scale, irregular trace element distribution within the carbonate rocks may either have been accentuated or homogenised during diagenetic reactions. Martin and Zeegers (1969) document microscopic inhomogeneities in similar rock types from Belgium, which arise during diagenesis, particularly along matrix-bioclust contacts (manifested by concentrations of manganese), and in dolomite grains.

Relatively restricted diagenetic fluid circulation gives rise to later generations of calcite with different trace element contents than earlier ones, because of constant removal of certain species (Mn, Fe) and buildup of others (Sr, Mg) in the solution through time (Pingitore 1978). Such closed system transformation of unstable high-Mg calcite (HMC)

phases may have led to the growth of late dolomite crystals (as described by Bathurst (1982) in similar rock types), because of local buildup of Mg in a finite reservoir (Nair and Hashimi 1981). Much of the trace element inhomogeneities observed in electron microprobe traverses of Silvermines host rocks (Figures 5.9b-p) may have arisen because of continuous buildups of depletions of each element in the diagenetic fluid, rather than continually fluctuating external supply levels.

Some of the later generation, Fe rich calcites present in small quantities at Silvermines (Figures 5.9j,l) and Ballinalack (Jones and Bradfer 1982) may have been generated by recrystallisation of HMC under lowered Eh conditions, in the absence of significant sulphide concentrations (Richter and Fuchtbauer 1978).

On the other hand, more open system diagenetic circulation in the less muddy parts of the succession led to 'smoothing out' or homogenising of original microscopic inhomogeneities developed during sedimentation. In this way, trace element inhomogeneities caused by discrete inclusions of impurity cation phases (Angus et al 1977), reworked dolomite, siderite or calcite grains, or zonation caused by variable growth rates and supply, may all become dispersed or 'smeared' (Morrow and Mayers 1978). The end result is a general enhancement of primary enrichments of Mn and Fe, and loss of Sr (and Mg).

Once the transformation of a metastable assemblage to a stable one is achieved, porosity is often much reduced, and the rate at which diagenetic alteration or exchange takes place is also considerably reduced. Because of this, chemical changes that take place from original sediment to final product are ascribed principally to the early stages of diagenesis (Veizer 1977a).

6.7.1. Later Diagenesis.

By later stages of diagenesis, a large proportion of the originally metastable sedimentary carbonate would have undergone recrystallisation to more stable forms, unless some degree of isolation from meteoric solutions was maintained. As in earlier diagenetic reactions, low-Mg calcite (LMC) is only slightly altered by diagenesis compared with other phases, because of its relative stability in meteoric water.

With a reduction in porosity caused by growth of early diagenetic calcite cement, much greater reliance is placed on the processes of diffusion, for chemical transfer between the reaction zone and the aquifer solution during later diagenetic reactions (Pingitore 1982).

The only parameters which affect diffusion to any great extent (ie. those which vary by an order of magnitude) are: i) aquifer flow rate; ii) pore path and geometry (between reaction zone and aquifer); iii) external ion sources; iv) concentration gradients (Pingitore op cit). The first two parameters are largely facies dependent, reflecting sorting, mud content and degree of compaction, which in turn affect water movement through the sediment. Thus, in a compact lime mud or biomicrite of low permeability (such as the Waulsortian Mudbank Limestone), diffusion may become the principal transfer mechanism in the aquifer, physical flow being all but prevented.

The influence of temperature will become significant at greater depths of burial, improving diffusion rates and creating more efficient intake or expulsion of trace element species during diagenesis. Coefficients of diffusion between individual ionic species do not show such great variations to be of any real significance in determining their relative behaviour (Pingitore op cit). The influence of outward diffusion of CO₂ from crystal surfaces in the initial precipitation of calcite is recalled here, being the principal factor governing crystal growth rate (Dreybrodt 1981).

Concentration gradients of different strengths and directions may give rise to differing movements of one trace element relative to another, with the possible result that the system may be effectively open for one element and closed for another. This may be especially the case if widely differing partition coefficients are involved for each species, therefore invalidating the examination of single trace elements to determine diagenetic history.

6.7.2. Texture and Neomorphism.

The degree of diagenetic enrichment or depletion of trace metals is also a function of the texture of the original sediment, since for example, a porous, well sorted biosparite will allow a greater proportion of meteoric exchange than a pure micrite, for a given

sample volume. Brand and Veizer (1980) show that physical evolution of carbonate components of a limestone (micrite - microspar - pseudospar - sparite, in advancing textural maturity) may be accompanied by concomitant changes in trace element concentrations, especially strontium depletion and manganese enrichment.

Comparison of Mn and Fe data from a limited number of samples of different textural composition and facies, from a single locality (Ballybeg Quarry, see Philcox 1967), reveals that textural differences are accompanied by geochemical contrasts (Figure 6.15). Analyses for Sr were not performed on these samples.

Of note is the fact that the bryozoan facies (dominated essentially by later generations of sparitic calcite) contains much lower Fe tenors than the calcilutite ('off-reef') facies from which it was probably derived (mainly micritic mud, see section 6.4.2.). It is important to note that manganese levels are relatively unchanged, in apparent contradiction to Brand and Veizer (op cit), in the texturally 'mature' limestone.

Along similar lines, electron microprobe analyses of a sparry, recrystallised halo around a fine-grained dolomitic clast in the Silvermines host rock breccias, indicate markedly reduced Mn and Fe levels, compared to the parent dolomitic matrix (Figures 5.9d). This suggests that textural maturity is not always accompan-

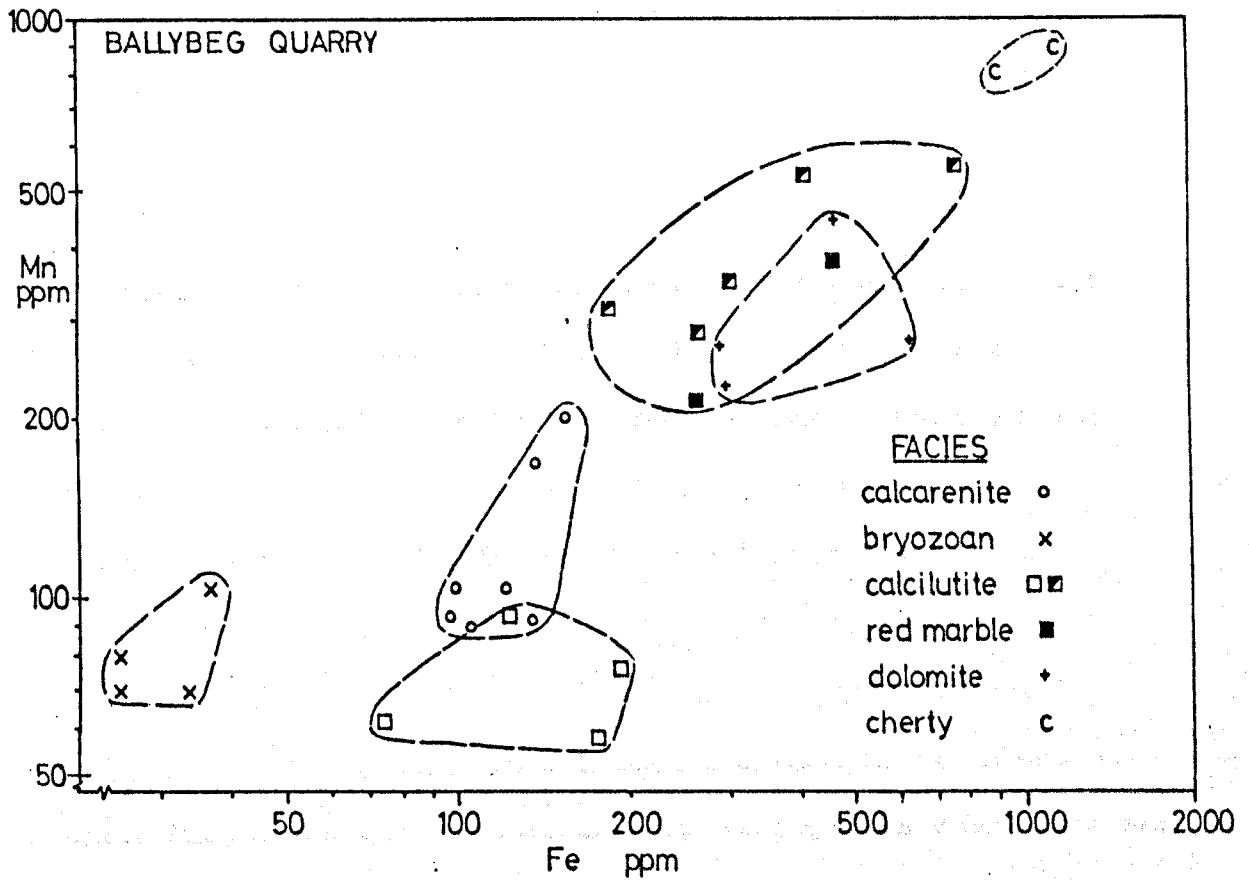


Figure 6.15: Manganese and iron contents of various components of the carbonate sequence at Ballybeg Quarry, County Cork (see Philcox 1965). Note the two very different calcilutite components: one (unfilled squares) from the north and west faces of the quarry, with low values of both elements; the other, from the south face of the quarry, with higher values of each. The latter calcilutites are associated with the Red Marble facies in the same part of the quarry (filled squares). Note also logarithmic scales.

ied by predicted geochemical changes, and many other controls may influence the redistribution of certain trace elements.

6.7.3. Trace Element Sinks.

Remobilisation of trace elements by diagenetic fluids, from whatever source, and migration into overlying zones of mineral transformation and recrystallisation (or even onto the sediment-water interface), may have resulted in the development of secondary or diagenetic patterns with apparent primary aspect.

Median values of $(\text{Mn}+\text{Fe})/2$ in the hanging wall dolomites at Silvermines are 570ppm, compared to less than 200ppm in the corresponding limestones (Table 6.9). Although several generations of dolomite are present (see Section 6.9.3), these figures suggest that preferential relocation of Mn and Fe has occurred into the dolomites, where both metals readily substitute for Mg, as well as for Ca. Strontium, on the other hand, only enters the Ca sites, and is therefore present at lower levels in the dolomitic samples (Table 6.8).

The openness of the overall diagenetic system at Silvermines has probably led to a net gain of Mn and Fe, and loss of Ca, Sr and Na in the resulting dolomite and calcite, involving external sources and sinks. Thus the net import of Mn and Fe resulted in alloenrichments of these elements in the host diagenetic carbonate, whereas the net removal of Sr, Na and Ca is

Lithology	Mean Values (ppm)			
	(n)	(Mn+Fe)/2	Mn	Fe
All samples	75	545	428	662
Limestone samples (under 3% Mg)	24	173	193	153
Dolomitic samples (over 3% Mg)	51	720	538	902

Lithology	Median (Mn+Fe)/2 Values (ppm)		
	(n)	Upper Hanging Wall	All Hanging Wall
All samples	161	450	582
Limestone samples (under 3% Mg)	47	170	240
Dolomitic samples (under 3% Mg)	114	570	740

Table 6.9a: Mean and median values of manganese and iron in the Silvermines hanging wall carbonates. Upper hanging wall is over 30 metres (100 ft.) above the top of the ore horizon. Median values are of (Mn+Fe)/2 only.

Lithology	Median zinc values (ppm)			
	(n)	A.A.	(n)	X.R.F.
Core Samples	426	38	150	88
Outcrop Samples	291	(5.4)	48	12.5
Core and Outcrop Samples	717	14	198	48
.....				
All Hanging Wall Samples	164	24	81	50
Upper Hanging Wall Samples	76	(5.8)	58	18
.....				
Borehole 77/36/1 (@ 2.5 km distant)	41	(5.4)	11	25

Table 6.9b: Median zinc values in Silvermines host rocks, comparing analytical results for both Atomic Absorption (A.A.) and X-Ray Fluorescence (X.R.F.) techniques. Upper hanging wall is over 30 metres (100 ft.) above the top of the ore horizon. Note much higher recorded values for X.R.F. analysis.

expressed in allodepletions of these elements in the same rocks. In addition, locally derived cement and trace elements involved in small scale redistribution and selective partitioning, formed autoenrichments which enhanced the original sedimentary levels of Mn and Fe in the hanging wall carbonates, albeit only locally into late diagenetic phases.

Following on from initial aragonite - calcite transformation, increases in Mn (and Zn) during this second cycle of autoenrichment may result in very high contents of these cations, especially manganese. Although a 100-fold increase for Mn is theoretically possible, a massive volume reduction would be required for this to happen, inversely related to the amount of Mn enrichment (Meyers 1974).

The diagenetic redistribution of magnesium may have involved both overall loss to the system, and local net gains, with conservation through volume reduction, and introduction from external sources (eg. seawater). These processes, and the resulting generation of 'pseudoprimary' trace element enrichments are discussed in Section 6.9.

6.8.1. Zinc.

Background zinc concentrations associated with the carbonate fraction of Waulsortian Limestones throughout Ireland remain below 10 ppm, lower than predicted values from partition theory (11 ppm or more, Hartree and Veizer 1982), and less than half that of Recent carbonate shell material (average 20 ppm Milliman 1974).

From this we may infer four possibilities:

i) lower than normal levels of zinc were present in Carboniferous seawater;

ii) higher salinities encouraged zinc complexing with chloride, rather than entry into the carbonate phase (Tsusue and Holland 1966);

iii) precipitation of aragonite rather than calcite reduced zinc intake to around one twentieth of the normal level (Kitano et al 1968);

iv) depletion of zinc has occurred during diagenesis (Morrow and Mayers 1978), in contradiction to the theoretical enhancement predicted by Pingitore (1978).

Low observed zinc contents beyond the immediate hanging wall aureole at Silvermines may be attributed to any of the above factors.

Most of the enriched zinc present in the Silvermines hanging wall carbonates (Table 6.9b) occurs as relatively insoluble, finely dispersed sulphide phases, rather than incorporated into the carbonate lattice structures. In spite of anticipated high zinc contents of seawater locally around the brine pools, high salinities, lowered

Eh conditions, and high sulphide activities led to very low levels of zinc incorporation into sedimentary carbonate minerals, most of the zinc being precipitated as sphalerite.

Continued low Eh conditions and high (bacterial) sulphide activity during diagenesis would have led to any zinc in diagenetic solutions being incorporated into ZnS phases. Alternatively, diagenetic redistribution may have served to reduce patchy enrichments to background levels throughout the mudbanks by 'smearing' or diluting the zinc during solution-reprecipitation events (Morrow and Mayers 1978). The same process would lead to more continuous, apparently primary enrichments with greater areal expression, if sufficient zinc was mobilised to permit adjusted levels to remain above background.

In the Navan deposit, Kucha and Weiczorek (1984) propose that the bulk of the sedimentary metal component was deposited as metastable base metal carbonate complexes, in a well oxidised intertidal environment, in the virtual absence of sulphide. Bacteriogenic conversion to sulphide minerals took place from early diagenesis onwards, with associated volume reduction.

A relatively complex explanation such as this is not required for the bulk of the Silvermines stratiform ore, because:

- 1) in-situ carbonate is relatively lacking;
- 2) a brine pool was developed;

3) sulphide was relatively abundant in the brine pool;

4) there appears to be little or no evidence for base metal rich carbonates.

However, pre-main ore phase deposition of iron and zinc-rich siderite under low Eh conditions, in the relative absence of sulphide, may have been obliterated by reaction with sulphide-bearing diagenetic solutions to yield the existing ZnS rich siderite zone, immediately below the B Zone orebody.

6.8.2. Sodium.

The ionic radius of Na^+ and Ca^{2+} in six-fold coordination (0.97\AA and 0.99\AA respectively), are sufficiently comparable to expect substitution of the former for the latter in CaCO_3 , in spite of the charge difference. Suggestions on the position occupied by Na occurring in carbonate minerals fall into one or more of the following categories:

- 1) carbonate lattice substitutions, in which the charge imbalance is accounted for by cosubstitution of hydroxide or bicarbonate radicals for carbonate (Billings and Ragland 1968, Land and Hoops 1973), or accompanying trivalent cations and/or anion lattice vacancies (White 1977);
- 2) association of Na with non-carbonate materials, either solid impurities such as clay minerals (Veizer et al 1977), or contamination by interstitial saline

inclusions (Land and Hoops op cit, Ragland et al 1979);

3) adsorption onto crystal surfaces, possibly as hydrate complexes (Mirsal and Zankl 1979, Ragland et al op cit).

A combination to two or more of these factors may be responsible, depending on the nature of the host carbonate rock.

Sodium concentrations in carbonates are most likely linked to the diagenetic history of the host rock, which modifies original sedimentary characteristics determined by palaeosalinity and facies control (Land and Hoops 1973, Veizer et al 1977, Ogorelic and Rothe 1979).

Under diagenesis, Na behaves in similar fashion to Sr, being concentrated in the diagenetic solution relative to precipitating calcite phases (Brand and Veizer 1980). As a result, concentrations are generally lower in rocks which have undergone severe diagenetic recrystallisation, and a reduction in Na content by an order of magnitude is observed in ancient carbonates compared to Recent sediments (Veizer et al op cit).

If partitioned into carbonate lattices according to theoretical constraints, genetic inferences could be made from Na concentrations in carbonate rocks, provided that the lattice-bound Na could be distinguished from Na trapped or adsorbed onto mineral surfaces.

Contrary to expectation from partition theory, hanging wall dolomites at Silvermines contain higher Na con-

centrations than undolomitised mudbank samples (cf. Sr levels), although a considerable overlap exists (Figure 6.16, Table 6.10). This is more in agreement with the work of Ogorelic and Rothe (1979), who record higher Na concentrations in dolostones over limestones. Sodium levels in the dolomites may therefore have either been increased by greater primary or diagenetic input, or normal diagenetic depletion of the element has been inhibited in some way.

The contrasting behaviour of Na and Sr suggests that diagenetic recrystallisation was not the only controlling factor in determining their final concentrations.

The slightly increased Na levels may be linked to primary dolomite formation in a strongly saline environment, or dolomitisation of the hanging wall sequence took place in the presence of very saline diagenetic fluids.

A weak correlation between Mn, Fe and Na in host Waulsortian and equivalent limestones and dolomites (Figure 6.16) is also suggestive of a link between increased salinity and trace element supply, involving a hydrothermal input of two, or perhaps three of these components. The existence of a similar correlation between Mn, Fe and Na away from any obvious hydrothermal source (Tralee area, Figure 6.19), is perhaps indicative of the influence of trace element cosubstitution. In this way, increased intake of one element (or group of elements) has led to higher intake of the

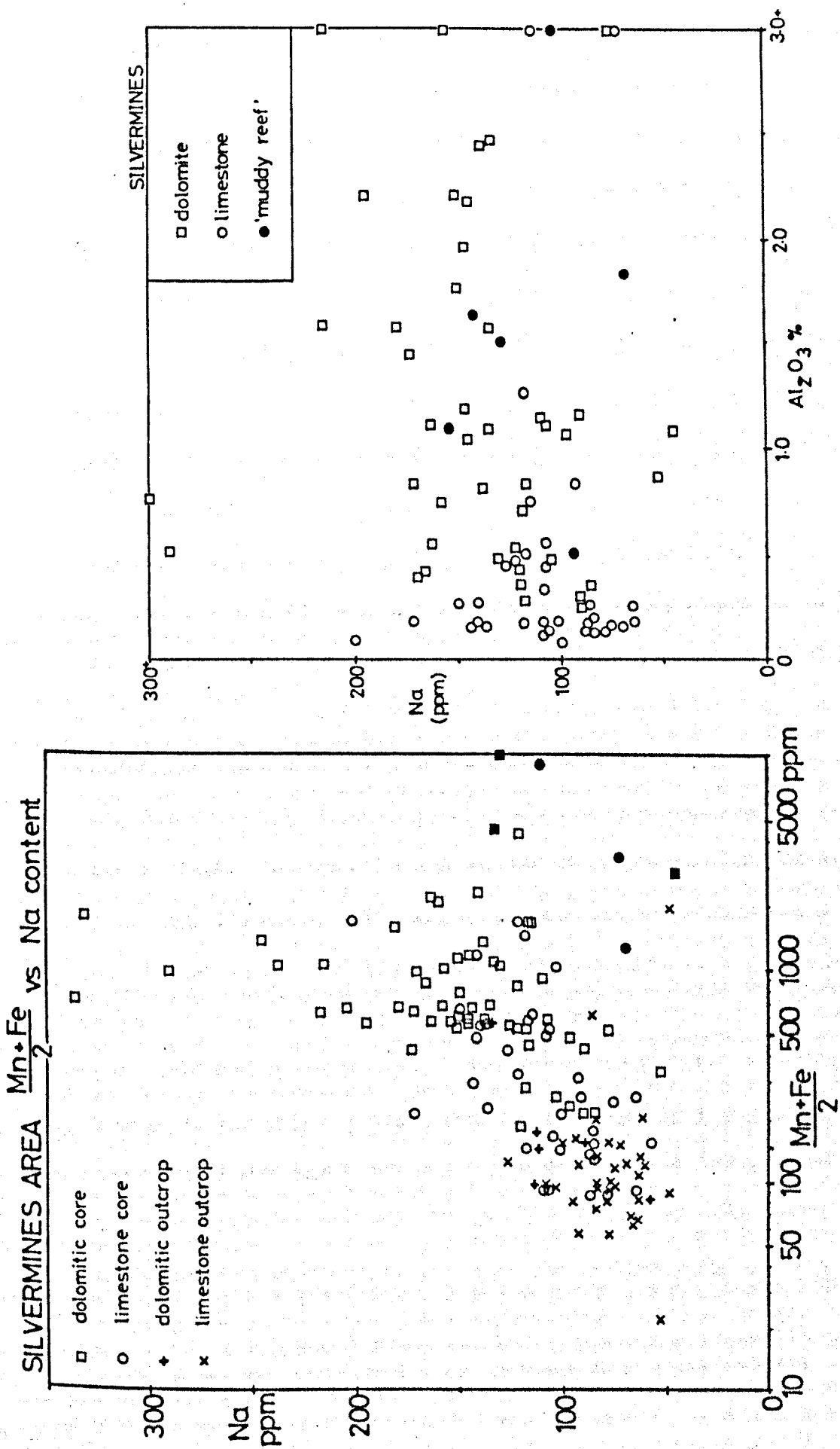


Figure 6.16: Comparison between Na and $(Mn+Fe)/2$ contents of Silvermines host carbonate rocks. Filled symbols (lower right) are samples from ore horizon.

Figure 6.17: Comparison of Na and Al_2O_3 content of host carbonates from Silvermines deposit.

other, although why this should happen in some samples and not in others still requires explanation.

An alternative suggestion involves clay mineral impurities (possibly also of hydrothermal origin) accounting for the anomalous Na concentrations within the domain of elevated trace element supply. Visible anomalous clay mineral impurities in mudbank limestones around the Tynagh deposit may thus account directly for enriched Na levels encountered there (Figure 6.18). More likely, the elevated Na (and Sr) contents arose indirectly via the inhibition of diagenetic circulation, caused by the more impermeable nature of the argillaceous mudbanks. No data was obtained to allow the direct comparison of Na with Al_2O_3 contents at Tynagh, but no direct correlation is observed between these two elements at Silvermines (Figure 6.17).

Higher Na levels are recorded in mudbank limestones around Ballinalack, relative to those (undolomitised) from Silvermines, although not as high as Silvermines dolomites (Table 6.10). Daly and Williams (1982) also record anomalously high Na in micrites from Ballinalack, compared to other areas. This may indicate possibly higher salinities presiding locally around Ballinalack, as no visible clay mineral impurities are observed in the host rocks. Limited data from nearby Keel and Ballymore (see Chapter 3.4.3) also suggestive of a vague correlation between $(Mn+Fe)/2$ and Na levels (Figure 6.20), with higher values associated with

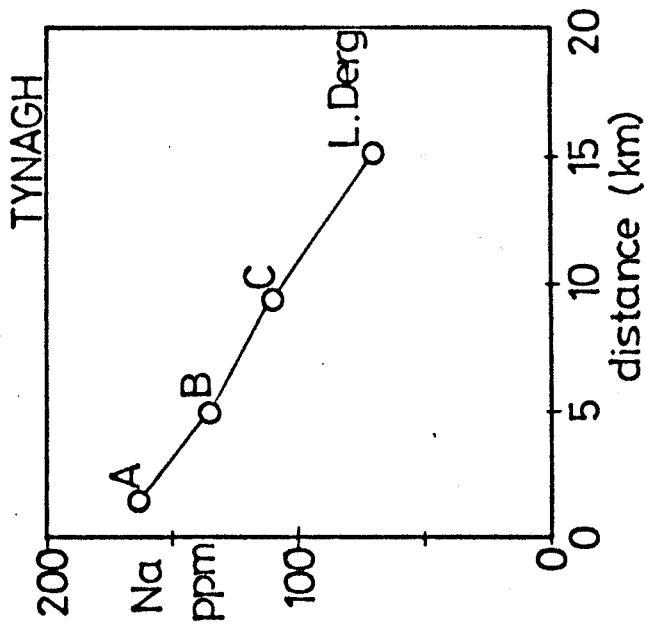


Figure 6.18b: Variation in Na content with distance from the Tynagh deposit, using data from samples in Figure 6.18a, and 11 other samples from more distal sites (Lough Derg).

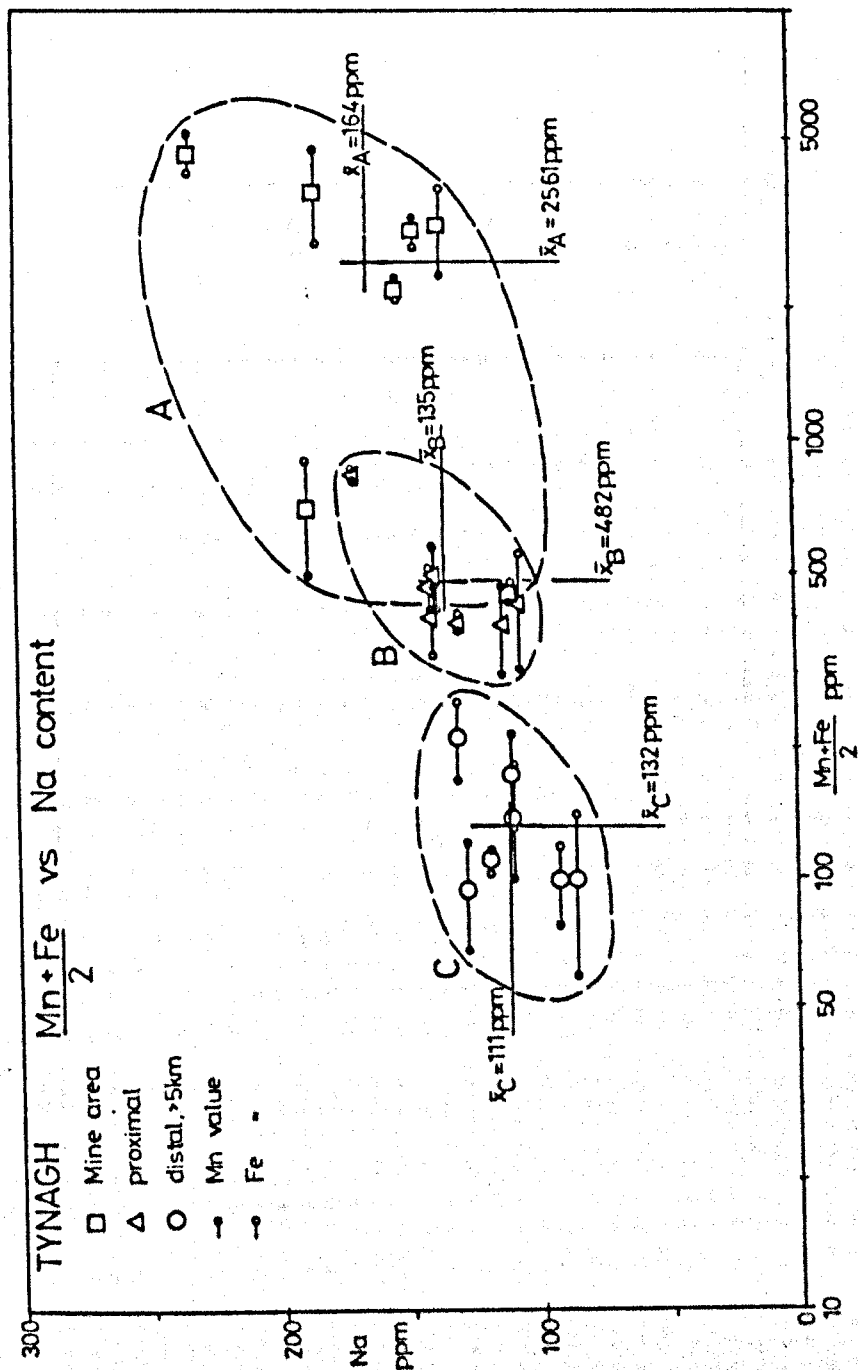


Figure 6.18a: Variation in Na content and $(Mn+Fe)/2$ content in Tynagh host rocks, showing also the compositional changes with distance from the deposit. Mean values for each grouping are also shown.

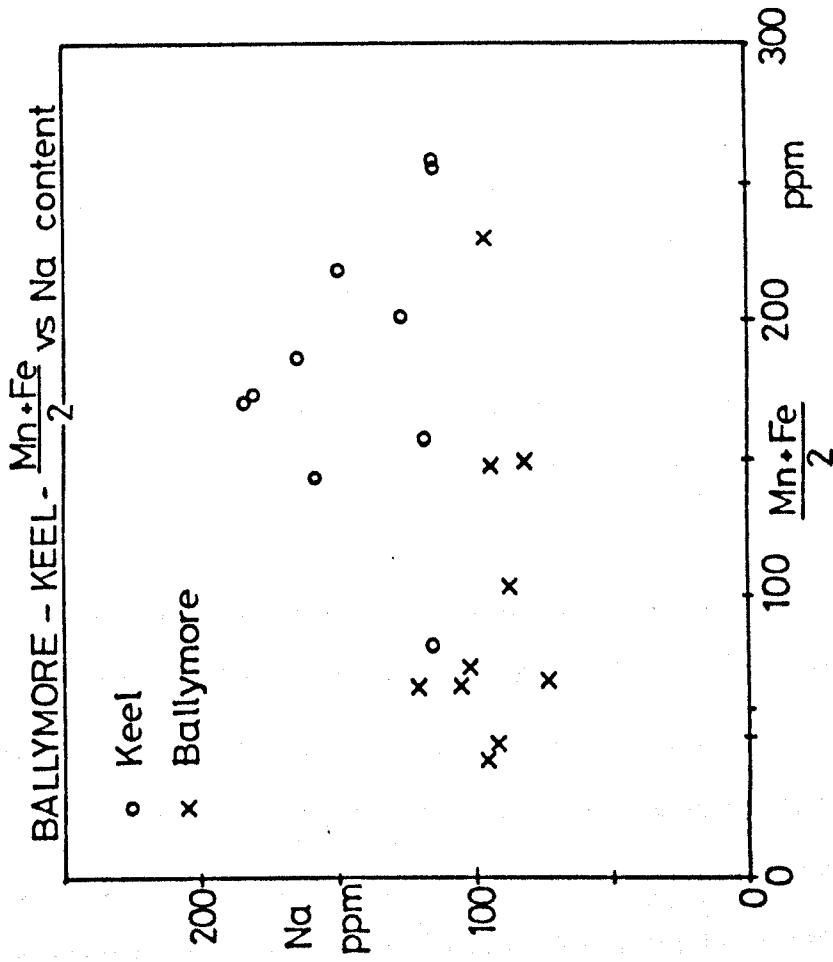


Figure 6.20: Comparison of Na and $(\text{Mn}+\text{Fe})/2$ content of samples from Keel and Ballymore areas, North Midlands.

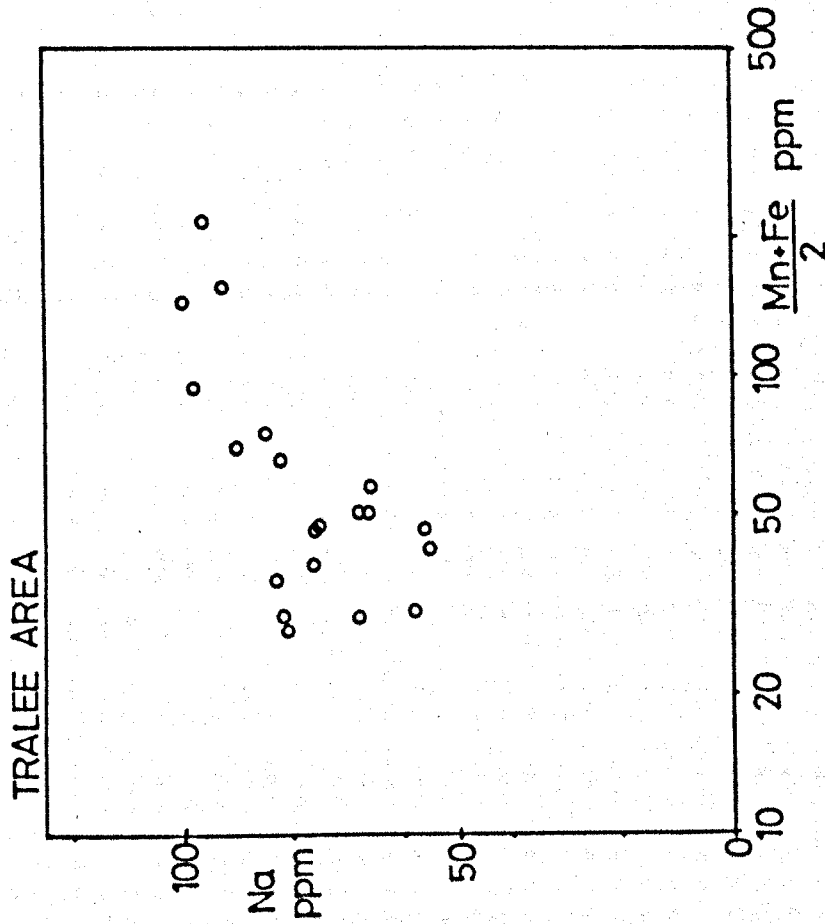


Figure 6.19: Comparison of Na and $(\text{Mn}+\text{Fe})/2$ content of samples from Tralee area, Co. Kerry. Note log scale for $(\text{Mn}+\text{Fe})/2$.

samples from near the Keel deposit (Table 6.10).

Comparison of Na contents from sample batches (distal samples only) from a number of areas throughout Ireland, reveals that a vague regional gradient of increasing Na from southwest to northeast may be present (Figure 6.21). This parallels the increase in background Mn and Fe values in the same direction (Gray and Russell 1984).

Any regional gradient or local enrichments developed close to individual deposits may reflect the direct or indirect influence of one or more of the following controls on the final trace element geochemistry: salinity of sea- or diagenetic waters; cosubstitution of a number of trace elements; the presence of clay minerals in the host rocks; and hydrothermal processes on a local or regional scale.

6.8.3. Hydrocarbons.

'Pyrobitumen' occurs as an accessory mineral in Waulsortian Mudbank Limestones and associated dark basinal limestone facies throughout much of central Ireland, possibly a relict of larger quantities of hydrocarbon (Morrissey 1972). Small amounts were observed during sampling of drill core and outcrop in the Ballinalack area, in apparent close association with late stage dolomite, in vuggy infillings of primary and secondary cavities within the mudbank limestone (Jones and Bradfer 1982).

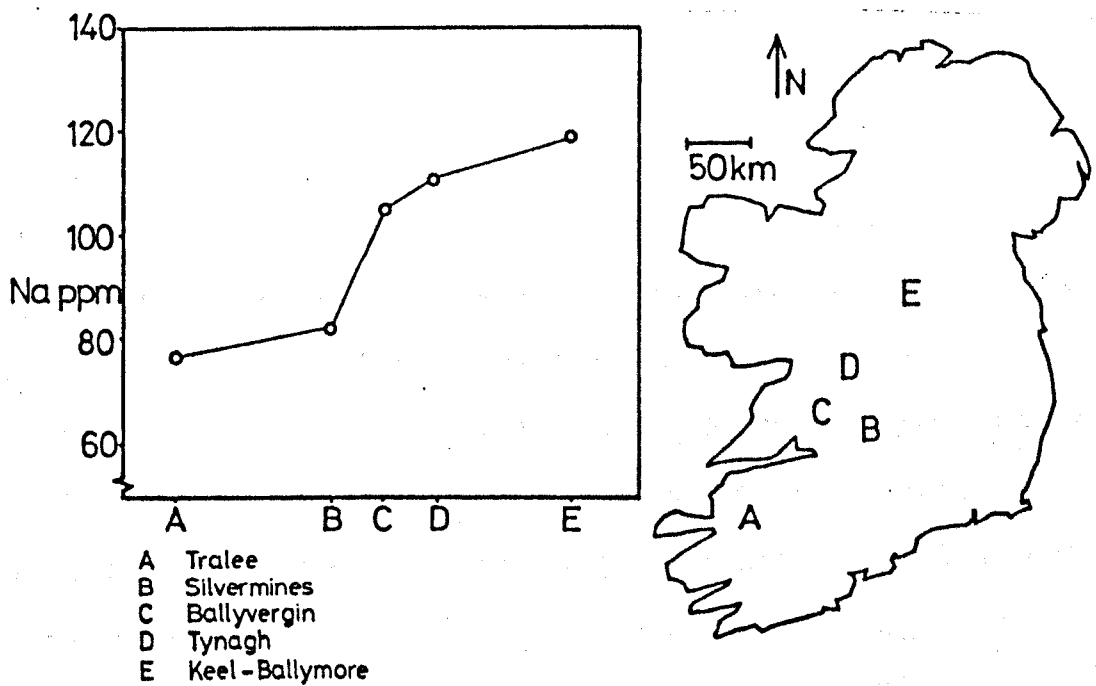


Figure 6.21: Regional variation in mean Na content of distal Waulsortian Limestone samples from throughout south and central Ireland.

location	description	(n)	mean Na content (ppm)
a Silvermines	all core	97	134
	dolomitic core	58	151
	limestone core	39	109
	Muddy Reef	19	103
	all outcrop	62	82
b Tynagh	all samples	21	137
	mine area (1.4 km)	7	164
	proximal (4.9 km)	7	135
	distal (9.3 km)	7	111
	Lough Derg (15.1 km)	11	71
c Tralee		20	77
	Ballyvergin proximal	10	127
	distal	10	105
	Ballinalack core	131	113
	Ballymore-Athlone	20	119
	Keel	10	143
	Ballymore	10	95

Table 6.10: Mean Na content of Waulsortian and equivalent carbonates from Tynagh, Silvermines and other areas. Dolomite samples = over 3% Mg.

Radke and Mathis (1980) suggest a common link between coexisting pyrobitumen and late stage 'saddle' dolomite in Mississippi-Valley type deposits, involving late epigenetic formation of sulphide by sulphate reduction and precipitation from a highly saline solution.

Morrissey (op cit) notes the occurrence of pyrobitumen at Tynagh, apparently of early diagenetic origin, principally hosted in late stage calcite veinlets, and elsewhere in common association with coarse epigenetic dolomite. However, no obvious relationship is observed between the occurrences of this hydrocarbon and the location of mineralisation, and he concludes that it is of no use as a guide in mineral exploration in Ireland.

Of more relevance in this study, is the possible effects of hydrocarbon during diagenesis, which can match those of high clay content in argillaceous limestones, slowing down solution-reprecipitation rate and acting as a permeability barrier (Morrow and Mayers 1978). This results in accumulations of hydrocarbon being associated with relatively high Sr contents in limestones, provided that the introduction of hydrocarbon preceded extensive diagenesis (Bathurst 1979).

Elevated values of Sr at both Tynagh (Figure 3.22) and Ballinalack (Table 6.10; also Daly and Williams 1982) in apparent close association with the occurrence of pyrobitumen, may indicate a genetic link between the two. Decreased permeability, brought about by the

presence of hydrocarbon, led to the inhibition of normal Sr depletion during diagenetic reactions.

At Tynagh, the influence of visible argillaceous impurities (Chapter 3.3.1) is more likely to have been the major cause of the anomalous Sr, whereas at Ballinalack, although visible argillaceous impurities are not characteristic of the mudbanks, higher contents of Na, Sc, Fe and Rb (Daly and Williams 1982) may indicate their presence.

The presence of hydrocarbon may have compounded the effect of clay mineral impurities on diagenetic circulation at one or both of these locations.

Recent work by Carter and Cazalet (1984) has found a strong link between mineralisation and trace quantities of hydrocarbon around the Tynagh, Silvermines, Navan and Mallow deposits. Haloes of increased methane proportions, relative to heavier hydrocarbons, are best developed around the larger deposits, extending perhaps 5 kilometres or more, seemingly irrespective of rock type. Although unclear, their origin appears to be related to the circulation of hydrothermal fluids associated with the emplacement of the deposits. However, the concentration levels of these trace amounts of hydrocarbon range from 100 ppb to 10,000 ppb, and at such levels would have limited effects on diagenetic reactions and trace element redistribution.

6.9.1. Pressure Solution.

During lithification, reduction of rock porosity takes place by compaction, deformation and dissolution-re-precipitation reactions, leading to pressure solution. Pressure solution may manifest itself by sutured or non-sutured seams, or pervasive non-seam solution (Wanless 1979).

A stylolite is defined as "any zone of relatively insoluble residue against which the original fabric elements of the rock are truncated by removal, rather than offset" (Geiser and Sansone 1981). Stylolites may be sutured (typically in rocks with less than 10% of insoluble materials) or undulose with branched terminations, typically in rocks with higher proportions (over 20%) of insolubles (Geiser and Sansone op cit). The former are typical of those seen in the Waulsortian mudbanks, whereas the latter are typically encountered in argillaceous footwall sediments (Muddy Reef Limestone and Muddy Limestone) at Silvermines.

Clearly any selective removal of constituent components of a carbonate rock will result in a readjustment of the overall trace element composition. An assortment of factors may control the degree and style of any stylolite development in carbonate rocks. For example, the location of solution surfaces may be defined by pre-existing structures, and growth catalysed by the presence of clay minerals in impure limestones (Wanless op cit). Clay minerals may induce or accelerate stylolite

growth by a number of physical or chemical processes (Weyl 1959, deBoer 1977, Robin 1978, Baker et al 1980). Sediment grain size is also critical, as is solution chemistry, which may cause accelerated loss of material to solution, either through elevated Mg concentrations or lowered Eh and/or increased salinity (Negebauer 1974, Wanless op cit, Baker et al op cit).

Stylolites are relatively abundant in the hanging wall carbonate sequence at Silvermines. Their presence was observed when sampling core and outcrop or underground exposures. They are present as:

i) sutured seams in mudbank limestones, especially the footwall Stromatactis Reef Limestone, both as thick (over 1mm) and thin, wispy seams;

ii) wispy or sutured seams in dolomite and limestone breccias, both within the clasts and the matrix (where they are also present as pervasive, thin-seam stylolites), and especially along the clast boundaries;

iii) thickly interwoven networks, sufficiently abundant in parts of the hanging wall to give the appearance of a breccia.

In addition, both the siderite of the B Zone, and the red marble facies occurring several kilometres to the northeast (Figure 6.3) are heavily sutured by stylolite networks, the latter also to the extent that it appears to be brecciated.

The majority of the stylolite seams in the Silvermines area, particularly in the autochthonous mudbank lime-

stones, are more or less sub-parallel to the bedding (R. Larter, personal communication 1982). This reflects the influence of lithostatic loading, initiated at, or catalysed by, vague bedding planes in the mudbank sediments, with little or no horizontal stress component.

During mudbank deposition, the presence of pore waters of extreme composition (eg. elevated Mg concentrations or salinities from overlying ponded brines, or lowered Eh or pH and increased metal content from continued percolation of hydrothermal fluids) may have led to rapid initiation of solution processes from early diagenesis onwards (cf. Geiser and Sansone 1981).

During pressure solution, dissolved constituents were either reprecipitated locally as cement and in veinlets (Rispoli 1981), or transported away and effectively lost to the system. The sizable overall reduction of the sequence at Silvermines suggests large scale removal of some components under open system diagenesis. This removal (of mainly carbonate material) was accompanied by continued fractionation of trace elements, especially loss of Sr, and possibly also by concomitant retention of Mn and Fe. Fractionation would have been less pronounced in those units where decreased permeability was brought about by higher mud contents.

The higher Mn and Fe contents of many veinlets in the Waulsortian equivalent carbonates (Figures 5.9b-p) suggest either lowered Eh conditions in the diagenetic fluids (and increased supply of Mn and Fe), or selective

removal of Mn and Fe rich phases during solution processes.

6.9.2. Volume Reduction.

The open system loss of dissolved constituents has resulted in an overall reduction in volume of the carbonate sequence at Silvermines. Comparison of the thickness of Waulsortian mudbank sequence in the centre of the nearby basins, with the Waulsortian equivalent sequence adjacent to the Silvermines Fault is made in Figure 6.22. Total estimated thickness of approximately 400 metres is present in higher ground near the town of Nenagh (BrUck 1982), and similar observed thickness (up to 370 metres) are present in borehole intersections (C1, C2) some 5 kilometres to the east of the mine. In the Silvermines section, however, less than 100 metres of largely allochthonous material is recorded above the upper G Zone orebody (Taylor and Andrew 1978). This thickness increases northwards and eastwards from the mine, with corresponding increase in proportions of in-situ mudbank, relative to dolomite breccias. As the upper G Zone lies adjacent to the Silvermines Fault at the point of maximum syndepositional throw (Russell 1979) thickness increases would be expected locally, not decreases.

The four- to seven-fold difference in thickness between the mine area (A) and the basin centre (D) implies either much faster downwarp of the latter during sed-

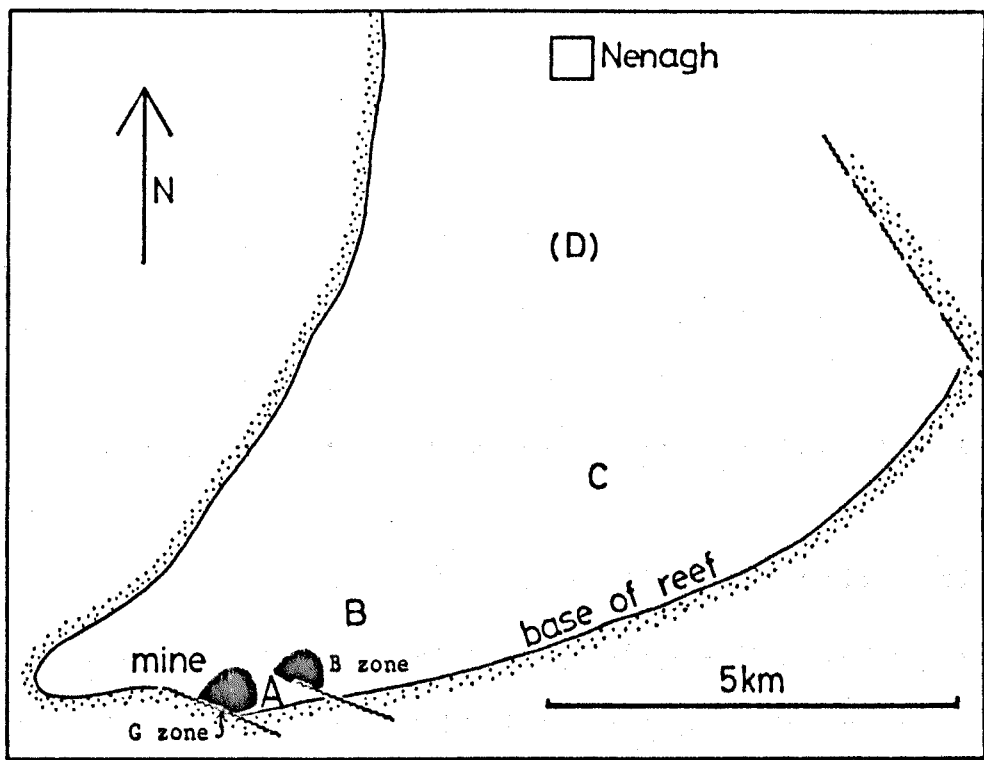


Figure 6.22a: Location of sections A to D discussed in Figure 6.22b and text, relative to stratiform mineralisation of Silvermines.

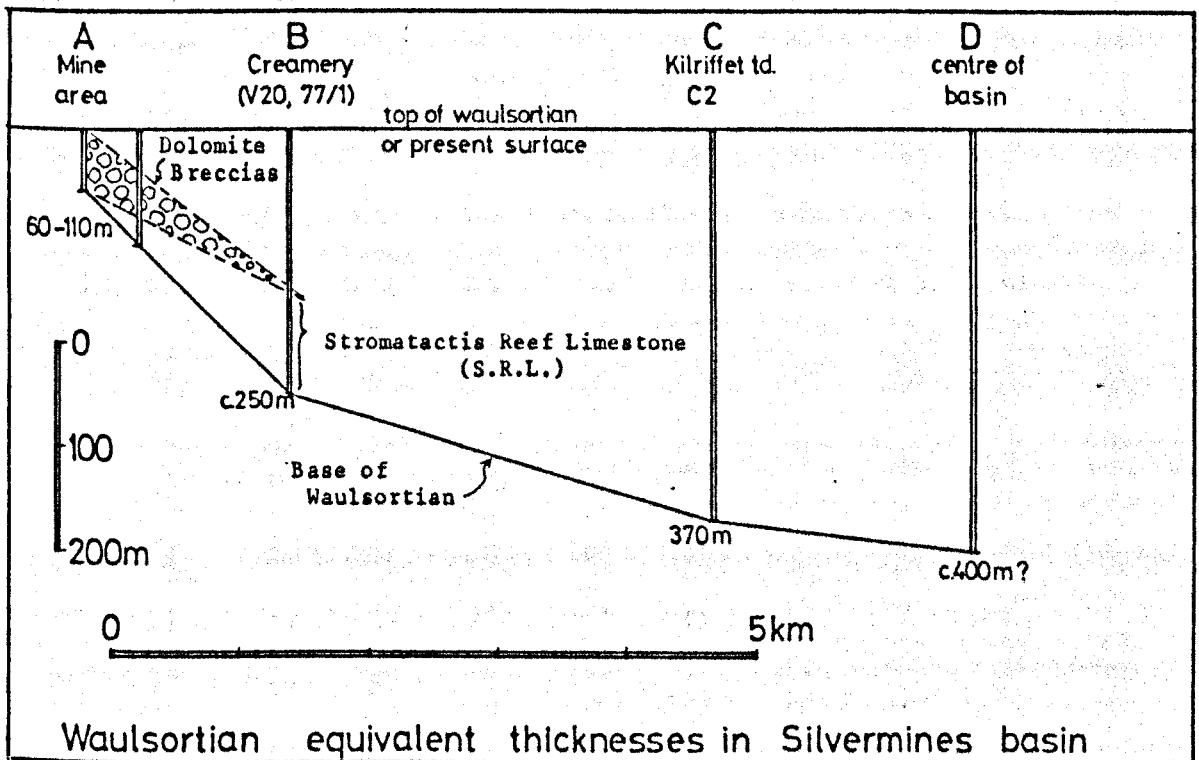


Figure 6.22b: Comparison of Waulsortian and equivalent thicknesses in Silvermines Basin (for locations, see Figure 6.22a). Upper limit is taken as the present suboutcrop level or the top of the Waulsortian equivalent succession (in the mine area, where up to 200 metres of Supra Reef and Calp Limestones are present). The dolomite Breccias of the mine area thin outwards into the basin. Source: Taylor and Andrew (1978); Brück (1982); Company logs (Mogul).

imentation, or non-deposition and/or post-depositional volume reduction near the Silvermines basin margin fault. The two to four fold difference in thickness between the mine area (A) and its periphery (B) - although only two kilometres apart - suggests that non-deposition and/or volume reduction were of importance locally.

Judging by the absence of footwall Stromatactis Reef Limestone below the ore horizon, which are present up to 30 metres thick in the peripheral area, local non-deposition played some part in the overall reduction in thickness. Volume reduction is also implied however, by the heavily stylolitic hanging wall sequence, perhaps totalling 50 to 70% loss:-

$$\frac{\text{Sequence B - S.R.L.}}{\text{Sequence A}} = 2.0 \text{ to } 3.7 \quad (\text{refer to Figure 6.22b}).$$

Let us now consider five features which affect the hanging wall sequence at Silvermines, and how their origins may be linked.

These are:-

- i) volume reduction;
- ii) anomalous insoluble content;
- iii) heavily stylolitic hanging wall sequence;
- iv) enriched Mn, Fe in hanging wall;
- v) dolomitised hanging wall.

Of these, ii) and iii) are obviously linked via the composition of the stylolites, originating by the pro-

cess of volume reduction (i). In proposing a common origin to explain these features, hydrothermal processes could feasibly account for four or all five of them, allowing for considerable post-depositional modification. However, it was demonstrated earlier in this chapter that diagenetic processes can produce Mn and Fe enrichments in carbonates, as well as causing volume reduction by pressure solution, thereby conserving insoluble material in the form of stylolites. Before any conclusions are drawn, let us first consider the possibility that all the features listed are wholly or partly diagenetic in origin.

A simple attempt to quantify the apparent concentration of insoluble material during volume reduction is shown in Table 6.11a. The 'insoluble' constituents of the rock are represented by SiO_2 , Al_2O_3 and K_2O (from XRF analyses), and average levels are shown for core samples from around the mine area (B), outcrop samples throughout the Silvermines Basin (A), and distal outcrop samples from beyond 5 kilometres only (C). By multiplying the average contents of these elements in outcrop samples by a factor of three (an approximation for the concentration factor during volume reduction), values very close to those in core samples (for SiO_2 , Al_2O_3 K_2O) are attained. Performing the same calculation of Mn, Fe and Mg levels from the outcrop samples fails to generate the required levels observed in the hanging wall drill core samples.

Element	Outcrop Samples			Core Samples		Distal Outcrop	
	(n)	A	(A x 3)	(n)	B	(n)	C
SiO ₂ (%)	45	0.34	1.02	59	0.95	6	0.11
Al ₂ O ₃ (%)	45	0.31	0.93	59	0.95	6	0.12
K ₂ O (%)	45	0.06	0.18	59	0.13	6	0.02
Mg (%)	45	0.95	2.85	59	6.00	6	0.95
Mn (ppm) (soluble)	27	172	516	57	784	6	99
Mn (ppm) (total)	27	178	534	57	1065	6	108
Mn (ppm) (insoluble)	27	6	18	57	281	6	9
Fe (ppm) (soluble)	27	205	615	57	1665	6	56
Fe (ppm) (total)	27	378	1134	57	6209	2	175
Fe (ppm) (insoluble)	27	173	509	57	4544	2	119

Table 6.11a: Comparison of insoluble (SiO₂, Al₂O₃, K₂O), Mg, Mn and Fe contents of Waulsortian and equivalent carbonates in Silvermines area. Core samples from hanging wall only (Holes B139, B144, V19, all close to the orebody). 'Soluble' is A.A. result, 'total' is X.R.F. result, 'insoluble' is total minus soluble. Distal samples from beyond five kilometres.

Sample	(n)	1	2	3	4	5	
		Hanging Wall Thickness (m)	average Insolubles (%)	Mg content (average) (%)	Insolubles Mg	'Total' insoluble content	
A. { Orebody	G217	55	4.76	4.17	9.73	0.49	262
	B139	17	3.57				
B. { Periphery	V19	110	1.62	2.83	4.44	0.36	178
	B144	17	3.04				
C. { 1 to 3km	V20	10	0.99	1.10	2.47	0.40	248
	77.36.1	6	1.22				
.....							
D. { Outcrop (Nenagh Basin) Distal Outcrop	45	(300)	0.74	0.95	0.78	(222)	
	6	(400)	0.27	0.95	0.29	(109)	

Table 6.11b: Comparison of 'insoluble' content, Mg content and thickness of hanging wall carbonates at Silvermines. Insoluble content (2) is SiO₂+Al₂O₃+K₂O+(Fe_{XRF}-Fe_{AA}). 'Total' insoluble content is represented by (thickness x average content). For locations of each hole, see Figure 4.1. Note the steady decrease in average insoluble content away from the mine (A to D), see also Figure 4.31.

The supposition to be made from this quantitative comparison is that SiO_2 , Al_2O_3 and K_2O are all conservative elements during diagenetic recrystallisation and volume reduction caused by pressure solution. They are therefore effectively concentrated by the substantial removal of other components, notably CaCO_3 . Manganese and iron, however, must have had higher initial levels locally in the hanging wall, prior to volume reduction, unless external sources were actively supplying them during recrystallisation. Likewise, Mg levels are indicative of higher initial values, or considerable introduction during diagenesis (eg. by seawater circulation).

Although higher initial background Mg concentrations would have been associated with an HMC parent phase, pressure solution and dolomitisation would have had to commence at a very early stage (before or during initial transformation to LMC) to preserve the Mg in the system. The origins of the dolomite are further discussed in the next section.

Note that the distal outcrop samples (C) contain much lower values of each element than the average background values from outcrop throughout the basin (A), suggesting that, although the latter were not subjected to volume reduction, they were not outwith the influence of hydrothermal input during sedimentation.

Electron microprobe data (Chapter 5) supports the idea

that insoluble Mn is not concentrated by pressure solution. Excess Mn is not recorded within the insoluble portion (ie. along the stylolite seams, eg. Figures 5.9c,d,e,f,g,m,p), even though higher insoluble Mn is recorded in the hanging wall dolomite breccias (Table 6.11a).

Further data on elements removed or concentrated by the selective dissolution of more soluble carbonate material is provided by a limited number of ICP analyses performed on 55 samples from the same area, summarised in Table 6.12. A reduction in the available Ca sites, caused by the destruction of calcite, is matched by reduced levels of Sr, Ce and La, whereas increased proportion of stylolitic insolubles has led to increased Fe_2O_3 , SiO_2 , K_2O , Na_2O , P_2O_5 , Rb, Li, Y and V levels.

Fast aquifer flow rates, rapid diffusion in micropore spaces, and involvement of large amounts of diagenetic water, as indicated by the low Sr concentrations, may have yielded as a side effect, the gross rapid dissolution of the carbonate sediments, in the manner suggested by Pingitore (1982). The apparent concentration of insoluble components by a factor of 3 in the remaining portion of stylolitic carbonate reinforces the possibility of hanging wall attenuation by up to 70%.

The origin of higher insoluble contents in the hanging wall sequence by solution processes is not un-

Lithology	(n)	ppm																											
		CaO	MgO	Fe ₂ O ₃	Z	Al ₂ O ₃	Na ₂ O	K ₂ O	TiO ₂	P ₂ O ₅	Mn	Sr	Pb	Zn	Ce	La	Li	Sc	Y	Ag	As	Bi	Co	Cr	Cu	Ba	Ni	Sb	V
Distal	7	34.98	1.11	.02	.03	-.02	.02	.01	.04	63	116	48	4	24	51	4	1	2	1	20	22	6	24	16	2	11	38	4	10
Proximal	6	15.50	17.44	5.60	.15	.02	.05	.01	.04	1910	110	1256	3797	16	29	5	1	6	3	105	41	13	40	26	44	26	61	16	15
77.36.1	41	31.29	5.20	.09	.05	.01	.02	.02	.01	151	108	54	37	22	47	4	1	2	1	*	21	6	27	15	3	12	40	6	10
Muddy Reef	1	25.77	1.15	.78	.34	-.09	.02	.03	.03	912	105	47	22	27	44	8	3	9	1	18	21	10	24	15	20	13	35	6	13

Table 6.12: Analytical results of I.C.P. Spectrometry on 55 samples of host carbonate rocks from the Silvermines area. Distal limestone samples from beyond 5 kilometres distant; proximal samples (all dolomitic) from boreholes V1, G217, close to the ore horizon; 77.36.1 approximately 2.5 kilometres from centre of orebody (both dolomitic and limestone samples); Muddy Reef sample also from 77.36.1.

equivocally backed by this data, as a number of other possible input sources may have existed. Initial insoluble concentrations may have been higher in the hanging wall rocks proximally to the vents, because of:-

- 1) greater argillaceous content of sediments near to the vents (possible direct hydrothermal input), as appears to be the case at Tynagh (Chapter 3.3.1);
- 2) oxidation of exhaled material under more oxidising conditions, in the absence of a brine pool;
- 3) reworking of sedimentary material from shallower, more oxidising flanks of the basin to the south, where higher concentrations of Mn and Fe oxide minerals may have been present in the carbonate.

6.9.3. Dolomitisation.

Dolomitisation of the hanging wall sequence is a distinctive feature of the rocks at Silvermines, with more than one generation of dolomite present in the breccias and mudbanks. Textural expressions range from those with almost complete preservation of original sedimentary textures, through hazy recrystallisation, to almost total destruction, leaving a saccharoidal and vuggy mosaic. Small, dispersed euhedra of dolomite are occasionally observed in otherwise normal mudbank sediments, and other varieties present include late stage veins of coarse, pinkish dolomite.

Clearly, more than one process was involved in the

origin of the varying textural and genetic styles of dolomite observed. These may have included:-

- 1) primary or very early, seafloor dolomitisation;
- 2) post-depositional circulation of modified seawater;
- 3) release of Mg from earlier carbonate phases, or from non-carbonate phases, during diagenesis and pressure solution.

Primary dolomitisation: Russell (1983) suggests that dolomite clasts in the sedimentary debris flow material originated as shallower water primary dolomite in the basin flanks to the south. Recent textural examination suggests that primary to very early dolomitisation is a major feature of much of the hanging wall dolomite breccia, especially the muddy component of the matrix (C.J. Andrew, personal communication 1984).

Conditions thought to favour primary, seafloor dolomite growth include high Mg^{2+}/Ca^{2+} ratios, increased salinities and temperatures, increased CO_3^{2-} ion concentrations (particularly in excess of Ca^{2+}), and either abnormally low or high pH conditions (Davies et al 1977, Tucker 1982, Morrow 1984).

Bottom conditions during and after brine pool development in the Silvermines Basin may have been sufficiently extreme to permit the direct seafloor, or very early diagenetic, precipitation of dolomite. Evidence for increased salinities, lowered pH condit-

ions from hydrothermal input, higher CO_3^{2-} activities (generation of CO_3^{2-} as a byproduct of extensive bacterial sulphate reduction, and indicated by the development of massive siderite) has been presented in this study, and elsewhere (Samson 1983, Boyce et al 1983, Russell 1983) to reinforce this possibility.

Seawater circulation: Continued circulation of saline, Mg rich seawater through the heavily brecciated and relatively porous hanging wall sequence provides one obvious source of Mg for post-depositional dolomite formation. In addition, late stage hydrothermal solutions may have borne higher Mg concentrations due to complete chloritisation of source rocks along fluid channelways, and therefore less efficient removal from circulating seawaters.

To the north and east of Silvermines, away from the heterogenous breccias and fault-induced fracturing, dolomite is a comparatively unimportant component of the host carbonate sequence (Taylor 1984, Andrew 1984), indicating the influence of local 'plumbing' systems on dolomitisation.

Following deposition of the hanging wall sediments, circulation of fluids through the still porous medium took place, aiding exchange of Mg and Ca, and initiating the growth of stylolites in the presence of high Mg concentrations and salinities (Negebauer 1974, Geiser and Sansone 1981).

Local derivation of Mg: Wanless (1982) observes the coincidence of lateral thinning of a limestone layer

and change in composition (actual increase in dolomite content) and uses it as evidence for pervasive (non-seam) pressure solution. His evidence is substantiated by the fact that the total (absolute) amount of insoluble residue remains the same in both the thicker and adjacent thinned zone.

Both pervasive and non-sutured seam solution modify the character of ancient limestones, with dolomite growing concomitantly on solution surfaces or zones of dissolution. Wanless (op cit) stresses the relative unimportance of physical compaction in volume reduction of carbonate rocks, and proposes that stratigraphic dolomite may form during pressure solution in the absence of stylolites or seams. He cites an example from New Mexico in which 100 volumes of limestone evolved into 13 volumes of dolomite, without requiring an external source for the necessary amount of Mg for the process.

Distinction of the dolomite formed during pressure solution from other types, can be made by a number of features, including cloudiness (because of included clay particles), occurrences of large rhombs along clay seams, higher Fe contents in later rhombs, and formation of intergrowth mosaics in thinned horizons.

If not entirely primary in origin, the growth of dolomite at Silvermines, coincident with volume reduction of the sequence, may have arisen by effective concentration of initial Mg levels through wholesale

loss of Ca from calcite. Wanless (op cit, p331) states that "magnesium should be a conservative element in rocks that have formed as a local byproduct of pressure solution." In this way, following burial of the carbonate sediments, Mg released during early mineral transformation may have been retained locally, sufficient to form dolomite in the hanging wall succession. Bathurst (1982) considers that the Mg released during HMC - LMC conversion is the source of dispersed grains of microdolomite, often present throughout the fine grained matrix of similar carbonate mudbanks in other areas.

However, the total volume reduction at Silvermines appears to be much greater than the theoretical 6 to 13% reduction brought about by the mole for mole replacement of calcite or aragonite by dolomite. Assuming a threefold reduction in volume of the sequence (and a 50% original porosity, zero final porosity), magnesium levels of approximately 8% in the original sediment would be required to form a completely dolomitised sequence, and approximately 4% to produce the average Mg levels recorded in the present hanging wall (Table 6.11b). Thus, if no external Mg source was involved, diagenetic LMC (with less than 1% Mg, as preserved elsewhere in the basin) is effectively ruled out as the only source of Mg, implying that the parent carbonate was an Mg-rich calcite, and that dolomitisation commenced early in the diagenetic history.

In more argillaceous members of the sequence, Mg released from clay minerals during diagenesis (along with quantities of Fe, Ca, Na, Si) may have built up in pore solutions (MacHargue and Price 1982). This may then have given rise to growth of late stage ferroan dolomite, present as small quantities in microspar grains and sparry cement (eg. Figures 5.9f,j,m).

If any of the hanging wall dolomite originated by concentration of local Mg in the manner suggested above, those elements which are favourably incorporated into precipitating calcite and dolomite phases (Mn and Fe in particular) should likewise have been concentrated in the resulting carbonate. This is backed up by the data presented in Table 6.9, which indicates higher values of Mn and Fe in dolomitic rocks, rather than limestones, from higher up in the hanging wall sequence. The limestones from over 30 metres (100ft.) above the ore horizon contain Mn and Fe at more or less background levels (similar to distal limestone samples), whereas the dolomitised rocks from the same part of the sequence still carry apparently anomalous values.

A quantitative comparison between total insoluble content (represented crudely by $\text{SiO}_2 + \text{Al}_2\text{O}_3 + \text{K}_2\text{O} + \text{Fe}_2\text{O}_3$) and total Mg content, suggests that a vague relationship exists between the two variables (Figure 6.23). A gradual decrease in the ratio (total insolubles / Mg content) is also apparent from the centre of the mineralised host

rocks outwards, paralleling the increase in thickness of the sequence. However, before any significant correlation can be made between the different variables under discussion, pressure solution would have to be quantified somehow, perhaps by measuring total stylolite thickness and density over a given part of the succession. Meanwhile, assumptions would have to be made that the movements concerned (involving CaCO_3 and trace element redistribution) were only local in scale, and that (difficult to measure) pervasive or non-seam solution phenomena were minimal.

6.9.4. Summary.

That trace element distribution in the Silvermines area has suffered considerable post-depositional modification is in no doubt. The overall extent and influence on individual trace elements is not clear cut, however. Much inhomogeneity in distribution of each element can be observed on both large and small scales, which may lead to problems in lithogeochemical sampling and errors in interpretation.

A direct genetic link may exist between the widespread dolomitisation, pressure solution and reduction in volume of the carbonate sequence. These processes, along with the selective partitioning (and resulting fractionation) of trace element species during mineral transformation and recrystallisation, were the main influences on modification of original primary sedimentary patterns of

distribution.

The range of possible sinks for dissolved material (CaCO_3 and trace elements) that existed in the Silvermines diagenetic system during post-depositional processes (solution-reprecipitation and stylolite formation) are summarised in Figure 6.24).

Upward transport of dissolved constituents, and incorporation into newly forming sediments on the seafloor (D), or diagenetically re-equilibrating sediments at depth (B) or just below the sediment surface (C), may have led to enrichment of new carbonate minerals in the elements Mn, Fe (and Zn?). In this way, secondary enrichment with apparent primary or hydrothermal aspect may have arisen. In other words, 'pseudo-primary' enrichments may have formed on or near the seafloor, even though hydrothermal emanations had waned or ceased altogether.

Diagenetic processes may thus have served to magnify or 'smear' an existing, albeit more subtly or stratigraphically confined, primary aureole, creating a more easily detectable anomaly. Existing enrichments may have been distorted, either by concentration (Mn, Fe) or by dilution to background levels (Zn?) or negative anomalies (Sr, and possibly Na).

In general, diagenetic redistribution may take the form of fractionation of certain trace elements, such as the enhancement of Mn and loss of Sr, at worst leading to the creation of 'false' or artificial anomalies, unrelated to any primary

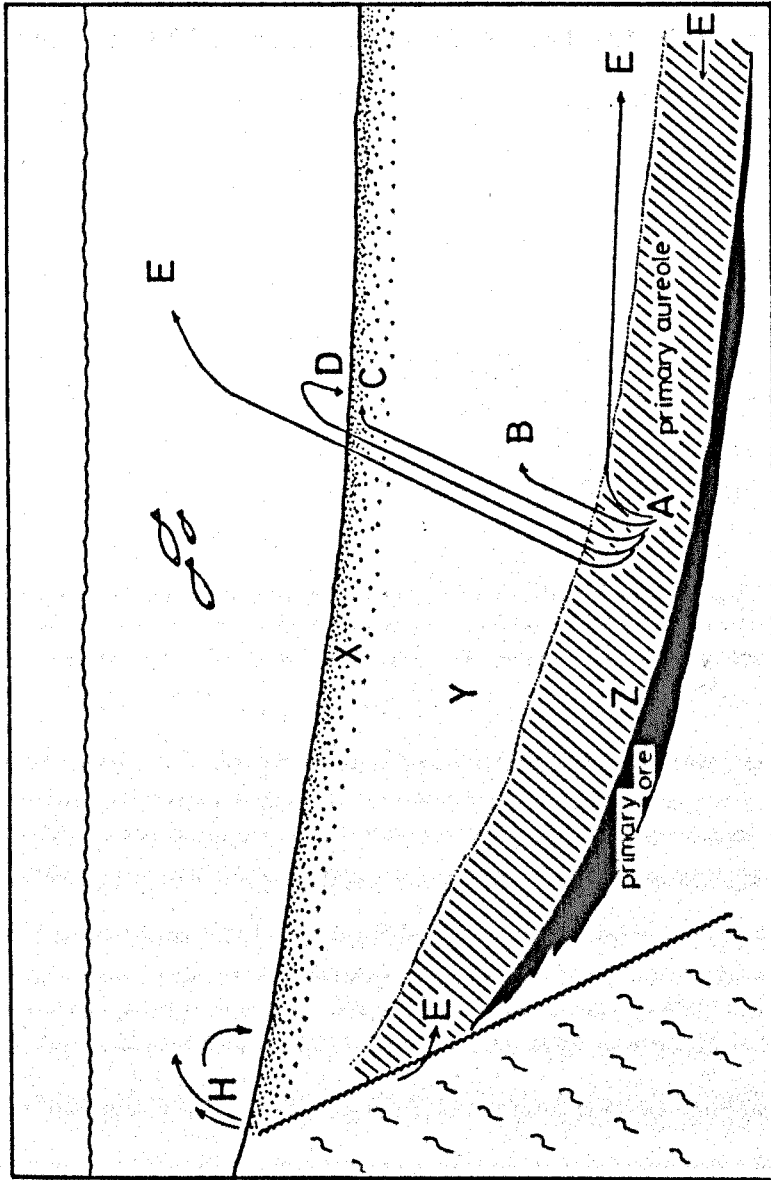


Figure 6.24: Diagrammatic representation of Silvermines host rocks during diagenesis, summarising the various potential sources and sinks for fluids and dissolved constituents involved in diagenetic exchange. The diagonal shading represents rocks with genuine primary syngenetic enrichments of trace elements from hydrothermal sources. The hydrothermal input displayed here represents late-stage, weak emanations.

Sources abbreviated:

- E - external (eg. meteoric, basinal);
- H - hydrothermal, deep-seated;
- X - initial mineral transformation reactions;
- Y - solution-precipitation reactions;
- Z - pressure solution.

Sinks abbreviated:

- A - gash veins, late cements, cavity fills;
- B - solution reprecipitation reactions;
- C - mineral transformation reactions;
- D - primary sediment;
- E - external (loss to seawater, dispersal).

hydrothermal processes.

Figure 6.25 attempts to summarise the pathways of (exhaled) manganese in a shallow marine hydrothermal system, based on the various reactions and sinks outlined in this chapter, for the Silvermines (and related) deposits.

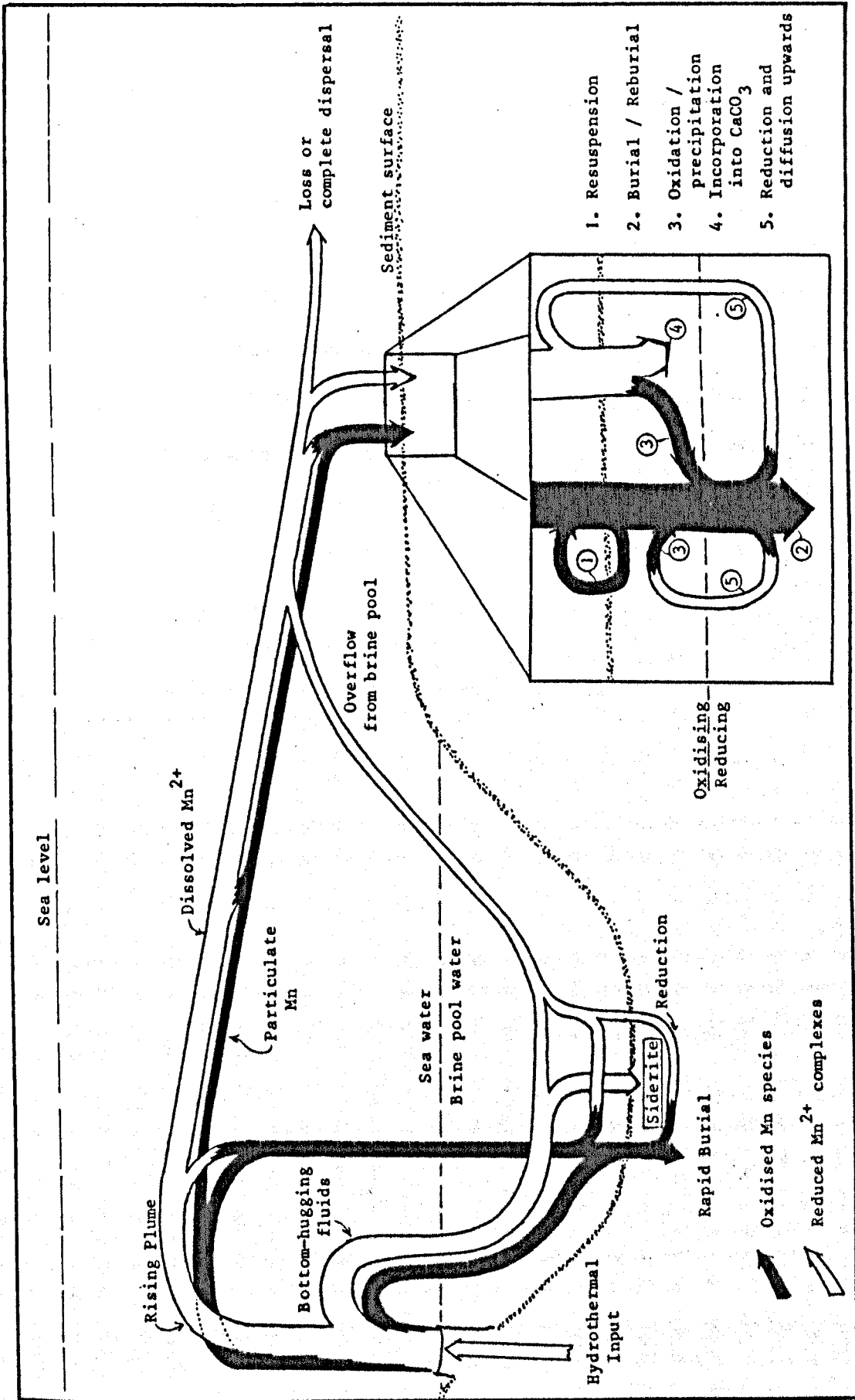


Figure 6.25: Summary of the pathways of hydrothermal manganese in a shallow marine hydrothermal system (such as the Irish deposits). This does not account for all the possible post-depositional recycling that may occur (see Figure 6.24) and excludes existing seawater or terrestrial (particulate or dissolved) manganese. Behaviour of iron would be similar but with greater tendency to oxidise (or precipitate as sulphide in brine pool). In Silvermines, oxidised species (in black) appear to be relatively unimportant.

CHAPTER SEVEN - Lithogeochemistry in Exploration.

7.1.1. Introduction.

7.1.2. Syngenetic Trace Element Enrichments around Sedimentary
Exhalative Orebodies.

7.1.3. Suitability of Waulsortian Limestones as a Host Rock
to Mineralisation.

7.1.4. Red Limestone Facies.

7.2.1. Application to Other Areas.

7.3.1. Discussion.

Chapter Seven - Lithogeochemistry in Exploration.

7.1.1. Introduction.

Discussion in the previous chapter has outlined a number of different genetic types of trace element dispersion pattern which may arise in carbonate rock formations.

The classification of geochemical aureoles, according to mode of formation, may be summarised as follows:

- 1) primary syngenetic patterns, formed by direct sedimentary incorporation of metals around a hydrothermal source, whether dispersed by chemical diffusion of dissolved metal complexes, or physical movement of particulate and dissolved metals;
- 2) primary epigenetic patterns, formed by wall rock alteration and epigenetic modification of host rock chemistry by the passage of hydrothermal fluids in a subsurface environment;
- 3) 'pseudo-primary' patterns, with apparently primary aspect, but formed essentially by non-hydrothermal processes. Post depositional modification by diagenetic interchange and recrystallisation, pressure solution, dolomitisation or even metamorphism, may be responsible. These patterns may have been generated around a locus of hydrothermal activity, or completely unassociated with one (ie. a 'false aureole');
- 4) secondary patterns, due to post-depositional processes of weathering and oxidation.

Overlap of these different types of pattern is possible, for example, if diagenetic processes significantly modify

pre-existing syngenetic (or epigenetic) patterns of primary origin, as appears to be the case at Silvermines.

The nature of geochemical dispersion patterns recorded around known mineralisation will obviously vary between different deposit types, and between similar types of deposit with different geochemical settings and post-depositional histories. The resulting patterns will show great diversity in metal content and lateral extent, and may be distinguished on the basis of recognisable mineral assemblages, whole rock analyses, or by subtle variations in the form of statistical populations.

Govett and Nicholl (1979) describe lithogeochemistry as "the study of the chemical composition of bedrock with particular reference to the search for ore deposits." In their reviews, primary dispersion patterns are those which may be attributed either to syngenetic or epigenetic processes, and thus may include subsurface or wall-rock alteration zones. Secondary dispersion processes include those influenced or arising by ground water movement, weathering or electrochemical diffusion, essentially unrelated to any hydrothermal processes. Following this reasoning, diagenetic modifications would be classified strictly as secondary in nature.

Rocks enclosing volcanic exhalative ore deposits have commonly undergone hydrothermal alteration to produce geochemically recognisable footwall alteration pipes and hanging wall envelopes. Alteration zones associated with

volcanogenic massive sulphide deposits are generally characterised by depletion of Na, Sr, Ca and enhancement of Fe, Mg, (K), S, Rb and a wide range of trace elements (Plimer and Elliot 1979). Mineralogical expression of these changes may be present, typified by the appearance of minerals such as sericite, chlorite and K-feldspar.

Govett and Nicholl (op cit) outline regional patterns of primary epigenetic dispersion around mineralisation associated with magmatic intrusions, and more locally around porphyry style Cu-Mo deposits.

In the epigenetic domain, vein wall rock alteration on the centimetre to metre-scale may effect whole rock geochemistry near to vein mineralisation, characterised by logarithmic decrease or increase in trace element contents outwards from the vein. The principle elements involved are Sr, Cu, Pb, Zn, Ag, Mn, Sb, As, Hg, Co and Ni, dispersed by diffusion-controlled migration of mineralising fluids from the vein, possibly along cleavage surfaces (Boyle 1965, Ineson 1969, Lavery and Barnes 1971, Bailey and McCormick 1974).

This study has concerned itself primarily with trace element enrichments around syngenetic mineralisation hosted within, or closely associated with, the Irish Waulsortian Limestones. The enrichments themselves are essentially of sedimentary origin, but may display ^{substantial} post-depositional modification. Care has been extended to eliminate contamination from secondary sources.

The scale of lithogeochemical investigation may be consider-

ed at three main levels, although considerable overlap exists between each:-

- 1) regional scale - to discriminate between productive and barren terrain, and delineate favourable formations or local basins;
- 2) intermediate or local scale - to identify individual exploration targets or horizons within a single basin;
- 3) mine scale - essentially to develop or extend known or postulated mineralisation.

The limits of these scales of investigation represent perhaps an order of magnitude difference, and could approximate the dimensions of first order (c. 100 km or more), second order (c. 10 km), and third order (c. 1 km) basins respectively, as described by Large (1980).

The present study is concerned essentially with the intermediate scale of investigation, that is, to seek local haloes (of dimension 1 to 10 km) associated with individual targets or deposits, within a single favourable horizon (the Waulsortian Mudbank Limestone and its immediately enclosing rocks). As the Irish Lower Carboniferous is a known metallogenic province and the Waulsortian Limestone a favourable target horizon, the larger regional scale of investigation is bypassed. Use of lithogeochemistry to predict local ore concentrations within individual deposits would require a greater sample density than is undertaken here, and is largely beyond the scope or aims of this study.

7.1.2. Syngenetic Trace Element Enrichments Around Sedimentary Exhalative Orebodies.

Europe (excluding Ireland).

Gwosdz and Krebs (1977) propose that extensive Mn enrichments in the host rocks (Lagerkalk) to the Meggen sulphide-baryte orebody are of similar hydrothermal origin as the economic minerals. The Mn enrichments peak in the margin of the local palaeobasin (coinciding with the baryte orebody), and are lower within the sulphide zone itself (Figure 7.1). Manganese concentrations return to background levels at between 2km (to the SW) and 5km (to the NE), with a lateral zonation in the form of primary separation of Fe from Mn, but no recognisable vertical zonation. Footwall sediments (Meggen Beds) carry distinct Mn enrichments which match the distribution of those in the Lagerkalk, though slightly less extensive in areal dimensions (Gwosdz et al 1974). Significantly higher Mn levels in basinal limestones downdip to the south, are associated more with facies control than hydrothermal enrichment and led to much wasted effort by exploration geologists seeking further mineralisation.

Badham (1982) describes extensive metal enrichments in host rocks to the Rio Tinto ores in Spain, also associated with syndepositional tectonics and instability. High background values of several metals are encountered throughout the area, due to their wide dispersion during metalliferous exhalations. Barium enrichments are recorded in the footwall throughout the ore basin, with Ba and Mn in the hanging

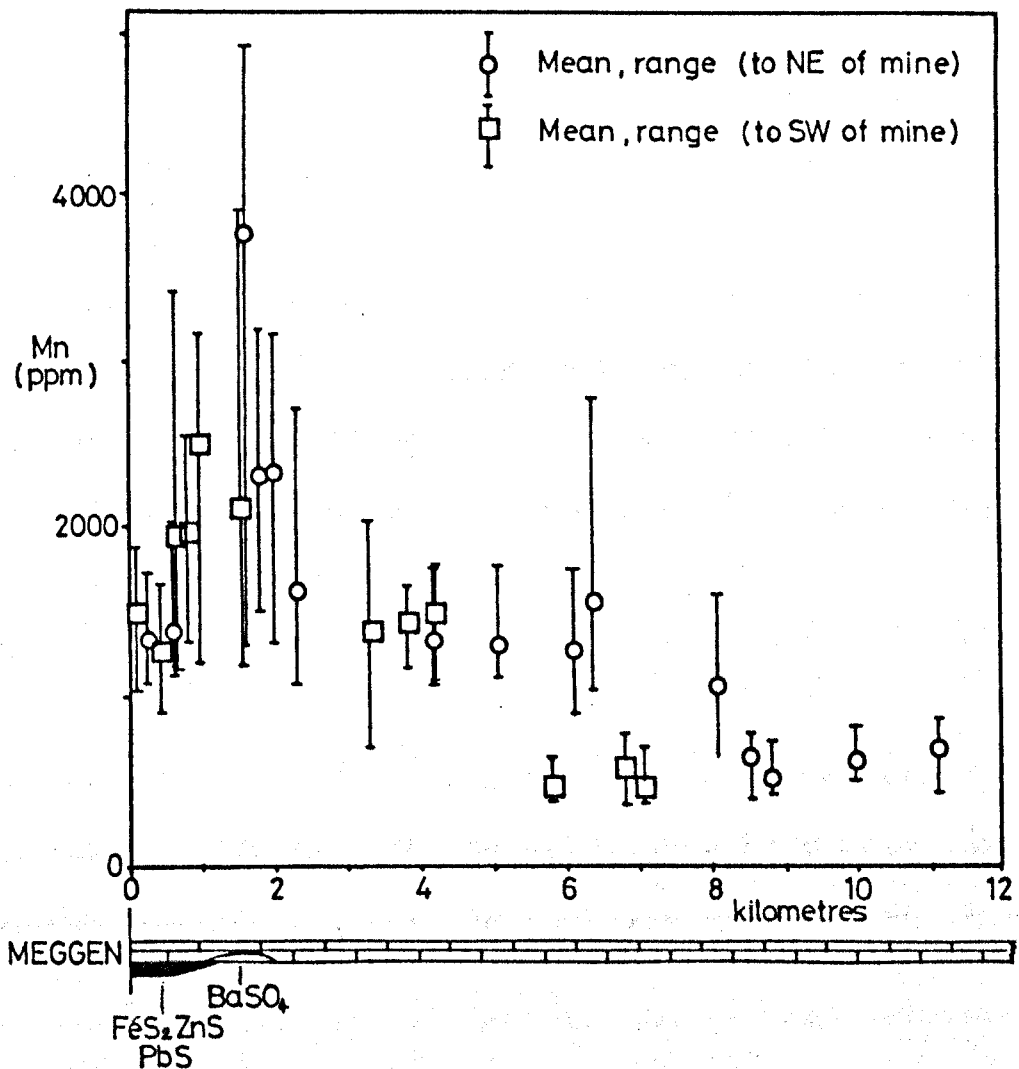


Figure 7.1: Manganese content of carbonate host rocks (Lagerkalk) either side along strike of the Meggen base metal-baryte deposit, Germany. This illustrates how manganese enrichments (comparable with those at Tynagh, but with apparently higher background levels, see Figure 3.14) are present up to 5 kilometres or more from the deposit. Redrawn from Gwosdz and Krebs (1977).

wall, and more locally developed anomalous Sn, As, Pb and Zn.

Barbier (1979) records anomalous Mn levels (2000 to 8000 ppm against a background of less than 1500 ppm) coinciding with basin-wide Zn mineralisation in the French Hettangian. More local, erratic zinc enrichments are recorded near the Figeac and Bois-Madame deposits, although even within 1 km of mineralisation, Zn values may still remain very low. A pronounced negative correlation between Mn and Sr is perhaps indicative of a strong diagenetic control on these trace element patterns.

Increased contents of Pb, Zn, Ag, Ba, Mn and Fe are observed in laterally equivalent strata around the base metal deposits in the North Bayaldyr district of the U.S.S.R. (Lur'ye 1957).

North America.

Anomalous Mn contents are present up to 10 km southwards and 5 km eastwards of the Sullivan orebody, in the host Aldridge sediments (Edmunds 1982). Within the domain of enriched Mn values however, only 36% of samples are considered anomalous (over 400 ppm Mn). Iron enrichments accompany the manganese, and numerous other elements show increasing tenors towards the orebody, notably Pb, Zn, Cu, S, Ni, Co and Ca. The Mn content is also controlled by the lithology, as higher overall contents are recorded in argillites, independent of proximity to the orebody. Enriched Mn values are present in the hanging wall, up to 200 metres above the ore horizon, detectable up to 5 kilometres from the orebody, although 'barren' layers with no anomalous contents are

also present. Mineralogical expression of the excess Mn contents also occurs, in the form of more prolific spessartine garnet in the mine area.

In the Howard's Pass area, weak Mn enrichments accompany high Pb, Zn, Cd, S, Ag, and V in the ore bearing facies of the Active Member, in the local basin of ore deposition (Morganti 1979). Barium tenors are very high on a basin-wide scale, but appear to decrease markedly towards the local ore basin.

On a regional scale, Goodfellow et al (1980) use stratigraphic geochemistry throughout the Misty Creek Embayment of Northern Canada, to recognise periods of volcanicity associated with carbonaceous, metalliferous shales and cherts. These 'active periods' are not easily detectable by direct lithological examination, but may be highlighted by anomalous TiO_2 , Na_2O and MgO , present as leucoxene, plagioclase and chlorite respectively. The active periods may in turn be associated with more locally enriched values of hydrothermally derived Zn, Cu, Ni, Ag, Mn, As, Hg, Sb and V in the sediments, of greater exploration significance.

Australia.

Anomalously high contents of Zn, Pb, Fe, Mn, Cu, As and Hg are present in the pyritic base of the HVC Member, laterally equivalent to the McArthur River base metal deposit. These values decrease outwards from the deposit, except where close to other subeconomic deposits (Lambert and Scott 1973), and are detectable as much as 20 kilometres distant from

the main deposit. Manganese levels peak in the immediate footwall sediments, where they are concentrated in a dolomitic argillite (the W-Fold Shale), along with anomalous Fe. In the hanging wall, significant enrichments of Zn, Pb, Fe, Mn, Cu, As and Hg are recorded in carbonaceous shales for at least 250 metres above the main ore horizon.

Manganese and iron enrichments have also been recorded in host rocks around the Broken Hill (Stanton 1976) and Mount Isa (Lambert and Scott op cit) deposits, and in carbonate and pelitic rocks enclosing the stratiform submarine-exhalative pyrrhotite-cassiterite deposits of Tasmania (Plimer 1980).

Ireland.

In addition to the work of Russell (1973, 1974, 1975), much of which is incorporated into this study, a number of parallel investigative studies have been undertaken in host rocks around known Lower Carboniferous mineralisation in Ireland.

In the host rocks around the Navan Zn+Pb deposit, widespread trace element haloes of Zn, Mn, As (and irregular Fe, Mg) have been identified within the hanging wall Pale Beds and overlying Upper Dark Limestones (Finlay et al 1984). Manganese enrichments extend over 300 metres or more into the hanging wall, and up to 2.5 kilometres from the deposit in boreholes, whereas the remaining elements are more restricted in their vertical and lateral distribution.

At Ballinalack, Daly and Williams (1982) record elevated Na, Sc, Fe, Rb, Sr, Sb, Cs, Ba and Th along with distinct-

ive Rare Earth Element signatures in host micrites to sub-economic Pb+Zn mineralisation, relative to unmineralised micritic mudbank samples from 'barren' localities.

Martin and Chabot (1981) recognise enrichments of Mn and Fe associated with ferro-dolomite, at several stratigraphic horizons close to the epigenetic Moate Pb+Zn prospect, which is hosted in fractures in sub-Waulsortian lithologies.

As well as the laterally equivalent Mn, Fe and Zn enrichments described by Russell (1974, 1975), anomalous levels of Cu, Pb, Zn, As, Sb and Hg are recorded in footwall sediments around the Tynagh deposit (J.Clifford, personal communication 1982). These anomalies are encountered in rocks to the north of the Tynagh Fault, but apparently not in the equivalent rocks to the south. The fact that the economic mineralisation at Tynagh is hosted in the former area (the North Tynagh Basin), and no significant mineralisation is known in the latter (the South Tynagh Basin), has led Clifford to propose the concept of the early trace element enrichments signifying that the North Tynagh Basin is 'fertile' with respect to potential mineralisation. The enrichments perhaps indicate a long history of weak hydrothermal activity prior to the main exhalative events, whereas the South Tynagh Basin is 'infertile' or barren, and contains neither enrichments of trace elements nor significant mineralisation.

Steed and Tyler (1979) describe local enrichments of Hg, As, Cu, Pb and Zn within a kilometre of the Gortdrum Cu+Ag+Hg orebody, associated with traces of sulphide mineralisation.

These formed by epigenetic dispersion from the mineralising solutions through the host rocks, facilitated by intense fracturing.

Van Orsmael et al (1980) undertook preliminary lithogeochemical investigations in carbonate rocks of the Belgian Dinant Basin, beds equivalent to (and of similar age as) the Irish Waulsortian Limestones. Anomalous levels of Mn, Fe, Zn and Pb in one section of core are associated with increased organic carbon and insoluble residue, a feature they attribute to organic complexing under reducing conditions, during sedimentation.

7.1.3. Suitability of Waulsortian Limestones as Host Rocks to Mineralisation.

Examination of the principle occurrences of base metal mineralisation hosted in Waulsortian-type limestones in Ireland indicates that, although this formation has been a prime focus of exploration for stratiform orebodies (Morrissey et al 1971, McArdle 1978), the mudbanks themselves are not good hosts to mineralisation. Waulsortian Mudbanks in the vicinity of two of the largest deposits (Silvermines and Tynagh) are characterised by pronounced physical and/or chemical changes, exemplified by brecciation, dolomitisation, attenuation or impurity. It seems that mudbank growth and sulphide deposition are incompatible, except where only minor quantities of sulphide (Keel, Courtbrown) or post-depositional, cross-cutting styles of mineralisation (Ballinalack, Ballyvergin) are concerned. Either

the normal Waulsortian Mudbank environment is too well oxygenated to permit metal sulphide stability, or exhaled hydrothermal fluids inhibit normal inorganic CaCO_3 precipitation on the seafloor and prevent organic CaCO_3 growth by excessive H_2S or metal contents. The incompatibility between the two 'facies' is well demonstrated by the relationship between mudbanks and ore host rock facies (and especially ore isopachs) at Silvermines (Taylor 1984; and this study, Chapter 6).

Because of this apparent incompatibility between normal mudbank growth and seafloor sulphide accumulation, exploration should therefore be focussed on areas where the Waulsortian is locally poorly developed, atypical or absent.

7.1.4. Red Limestone Facies.

One facies of Waulsortian Limestone which deserves some special attention is the 'red marble' which occurs sporadically throughout Ireland, particularly in the south. Elevated Fe (and Mn) values are associated with both the red limestone facies and the surrounding unreddened mudbank limestones (Figure 7.3).

The Cork Red Marble (Nevill 1962) and equivalent Castle-island Red Breccia (Hudson et al 1966) are two examples, comprising massive, weakly bedded to unbedded limestone breccias, up to about 20 metres thick, with ungraded, unsorted fragments of calcite mudstone (creamy white to pink, hematite stained, often mottled and porcellanous), up to 20 centimetres in size. The matrix is a red clay (occasion-

ally green, if reduction of iron has occurred), with minor silicification and fossil debris limited to rare crinoid and brachiopod fragments.

Considerable modification by pressure solution around fragment surfaces has yielded irregular stylolitic contacts, and further emphasises the brecciated appearance of the rock.

Theories on the origin of the red marble involve uplift and emergence of reef or back-reef sediments, with re-deposition by turbidity currents, and a terrestrial origin for the hematitic mud content (Nevill op cit; Hudson op cit; C. Andrew, personal communication 1984). However, the description of similar lithologies in the outer edge of the Tynagh Iron Formation by Schultz (1966) suggests a possible genetic link with hydrothermal processes, also bearing in mind the outcrop of similar red marbles within 6 kilometres of the Silvermines deposits (Chapter 6.3.6). The possible genetic link between the Tynagh orebody and laterally equivalent hematitic limestone (and Iron Formation) led to considerable exploration interest being focussed on the occurrence of the red limestone facies in the sixties.

Occurrences of hematitic reef facies known to the author are shown on Figure 7.2a, and their concentration is observed towards the southern half of the country, between Tralee and Cork (Nevill 1962), where they appear to form a seemingly continuous zone within the mudbank sequence. This includes a thick intersection (around 30% of a total thickness of almost 500 metres of mudbank) in the Meelin bore-

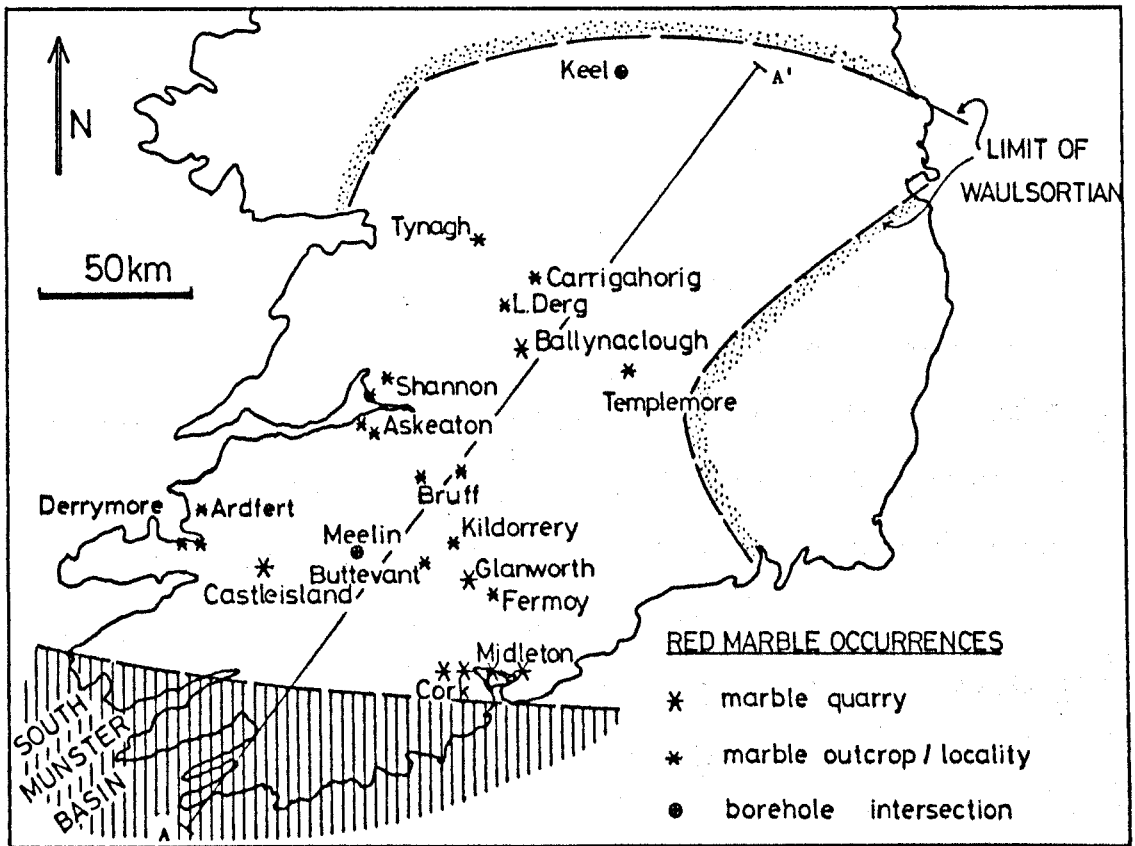


Figure 7.2a: Map showing localities of Red Marble known to author, approximate limits of Waulsortian and line of section A - A' in Figure 7.2b.

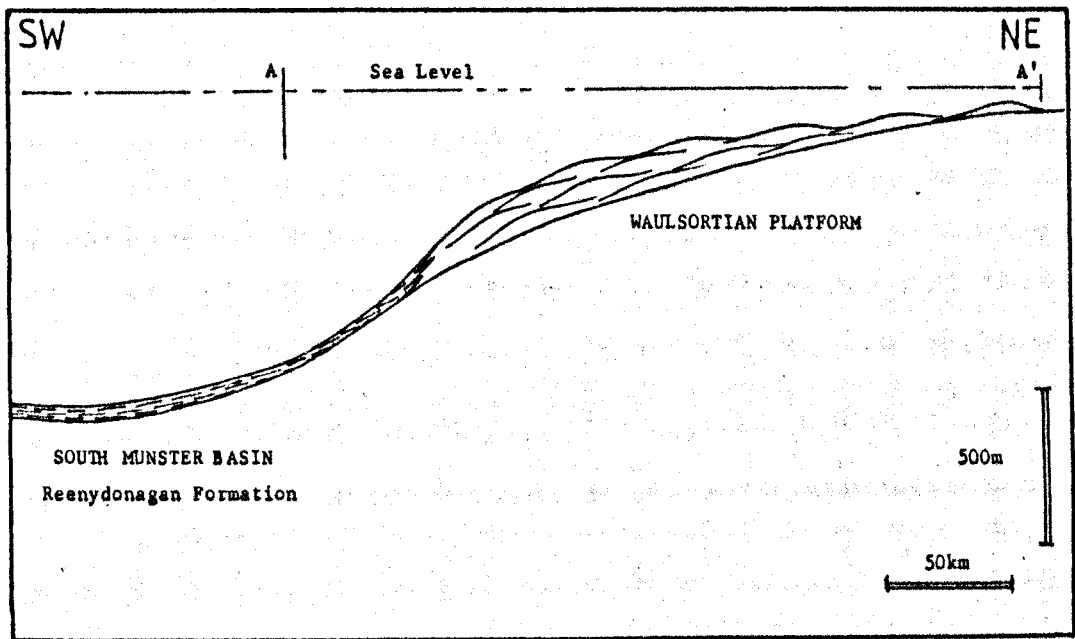


Figure 7.2b: Diagrammatic cross section of Waulsortian Shelf and South Munster Basin during Late Courcayan times. See Figure 7.2a for location of section A - A'. Note extreme vertical exaggeration.

hole (Sheridan 1977). North of this zone, sporadic occurrences are known from various stratigraphic levels in the mudbank formation.

Origin of the oxidised facies by shallowing and emergence seems unlikely, in view of the depth of water envisaged for Waulsortian mudbank deposition (perhaps 200 metres or more, Miller and Lees 1985), particularly in the south of the country. Alternatively, oxidation of Fe and Mn bearing waters of hydrothermal or other origin, on a widespread scale, may be envisaged to form the extensive development of hematitic limestone present throughout the south of the country.

If hydrothermal in origin, either no significant base metals accompanied the Fe and Mn, or the base metals were completely oxidised and dispersed into seawater on exhalation. This would help to explain the apparent lack of base metal (zinc) enrichments associated with the hematitic facies (Figure 7.3b).

Immediately to the south of the most extensive red marble development lies the Culm or South Munster Basin (Figure 7.2a). During Upper Courceyan times, when mudbank growth reached a climax, euxinic conditions, with starvation of sediment input, were dominant in this basin, to the west of the Glandore High, leading to the deposition of the black, pyritic mudstones of the Reenydonagan Formation (Naylor et al 1981, Sevastopulo 1981). This euxinic basin represents one possible source of reduced Fe and Mn bearing waters in the south of the country, which may be responsible for the

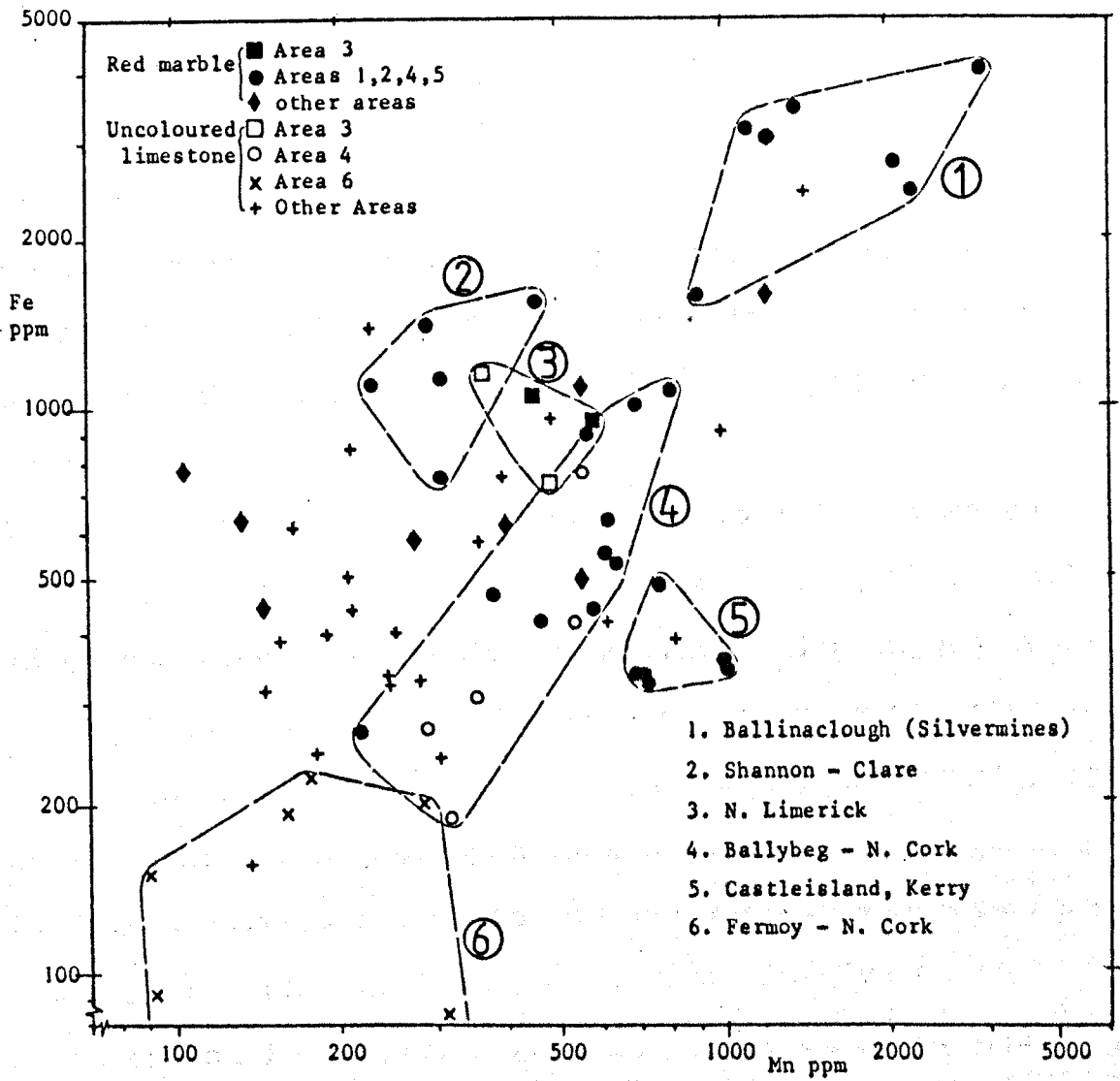


Figure 7.3: Manganese and iron contents of 73 samples of hematitic mudbank (red marble) and associated uncoloured mudbank limestones from numerous locations in Ireland (see Figure 7.2). Note the distinct groupings of samples from certain areas. Note also the logarithmic scales.

Sample medium	(n)	median (Mn+Fe)/2 (ppm)	Anomalous Zn (%)		High Mg (%)
			>10ppm	>20ppm	>1%
Red Marble	46	635	10.9	4.3	6.5
Uncoloured Limestone	27	305	18.5	3.7	11.1

Table 7.1: Median (Mn+Fe)/2 contents of samples in Figure 7.3, and percentage of either type with anomalous Zn and Mg levels.

reddening of the mudbank limestones, if they were exposed to the more oxidising conditions of the shallower limestone shelf environment.

However, many questions arise about the possible method of introduction of reduced fluids from the depths of the basin onto the carbonate ramp, whether by upwelling or some other process.

Oxidation may have arisen because of locally increased alkalinity of sea bottom or diagenetic waters, which would render hematite more stable at relatively low oxygen fugacities (Figure 6.10a). Red marble occurrences may thus indicate abnormally saline or alkaline conditions developing locally during mudbank deposition or diagenesis.

One alternative explanation for the anomalous Mn and Fe values post-dating sedimentation, would involve auto-enrichment during pressure solution (loss of CaCO_3 and residual concentration of trace elements), in the same way suggested for some of the hanging wall carbonates at Silvermines (Chapter 6.9.1).

Figure 7.3a graphs the Mn and Fe contents of each of the red marble and associated uncoloured mudbank limestone samples collected in this study. One feature of note is that samples appear to be grouped distinctly according to source area.

Clearly, the fact that uncoloured samples from near to known red marble localities may contain elevated Mn and Fe levels, may mislead exploration geologists utilising litho-geochemistry in the search for ore deposits.

No further insight is given into the origin of the hematite

facies of mudbank by the data presented here, but a number of avenues for further investigation are opened up, which might hopefully ascertain what relationship, if any, exists between the red marble and hydrothermal exhalative processes.

7.2.1. Application to Other Areas.

No scientific proposition is complete without some form of practical test. For this purpose, three areas of extensive Waulsortian Mudbank outcrop of relatively unknown mineral potential were examined on a reconnaissance basis, to investigate whether or not any syngenetic exhalations were indicated locally. These areas, in Counties Cork, Kerry and Limerick, were sampled according to availability of outcrop (and time constraints), at an average minimum density of approximately one sample site per square mile. Analysis for Mn, Fe, Zn and Mg was then undertaken following the principles outlined in Chapter Two.

1) North County Cork.

The location of this area is indicated on Figure 3.1, and the mudbank outcrops occur along the centre and flanks of a complex double syncline structure. As in much of the southern part of the Carboniferous shelf area, both Waulsortian and Upper Reef complexes are present in the sample area. Both have been sampled as a single unit, being difficult to distinguish apart, particularly since low grade metamorphism during Hercynian N-S compression has given rise to a weak E-W tectonic fabric. The assumption is made here that the trace element characteristics of the two are comparable, and the lack of any obvious stratigraphic changes in distribution of any of the elements examined would appear to substantiate this.

The intervening darker cherty limestone, between the two reef complexes, is visible in a few places towards the centre

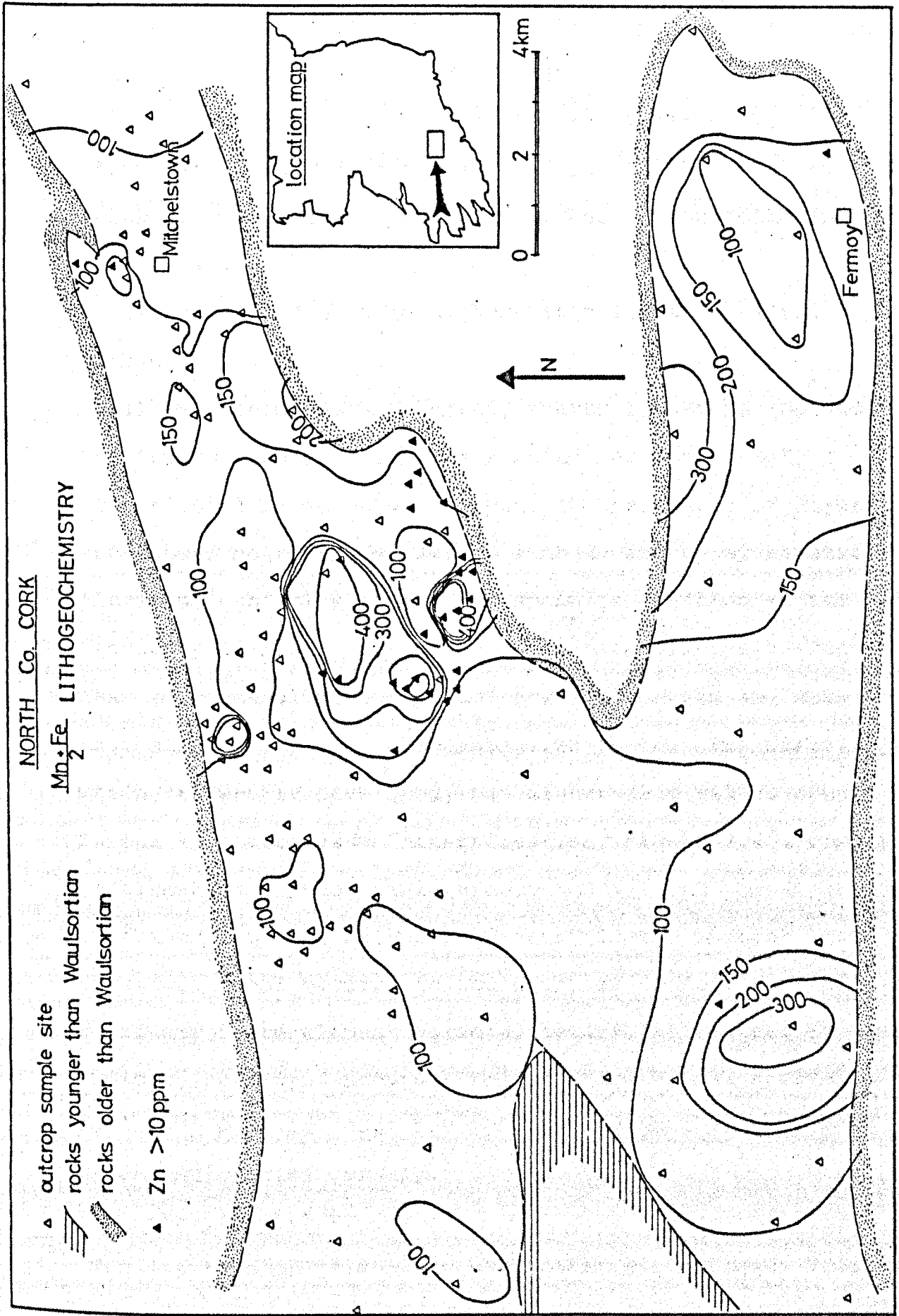


Figure 7.4: (Mn+Fe)/2 lithochemistry of Waulsortian and Upper Reef Limestones of North Co. Cork, contoured using a rolling mean. Also shown are sample sites with anomalous zinc (over 10 ppm).

of the synclinal structure.

In total, 489 samples were collected, and the results portrayed in contoured map form for $(\text{Mn}+\text{Fe})/2$, the median value of which was computed at 90 ppm (Table 3.4).

A number of $(\text{Mn}+\text{Fe})/2$ anomalies exist in the area, of which several can be attributed to one of the following influences:-

i) associated with local hematitic limestone ('red marble');

ii) associated with off-reef, cherty limestone (possibly the interval between the Waulsortian and Upper Reef).

The cluster of anomalous samples in the centre of Figure 7.4 showed neither association with the cherty or hematitic limestone, and closer ground inspection resulted in the discovery of minor galena and sphalerite mineralisation, near to the faulted contact of the Waulsortian and sub-reef strata. Recognisable anomalies in the zinc distribution are weakly developed, but higher zinc values occur in the same area as the mineralisation (Figure 7.4), compared to elsewhere in the sample area.

The anomalous Mn, Fe and Zn content in the mudbank around this base metal occurrence would appear to form part of a primary trace element aureole, several kilometres in dimensions, developed around a relict hydrothermal source. Follow-up work is currently being undertaken in this area by an exploration company.

2) County Limerick.

The location of this area is illustrated in Figure 3.1,

and the extensive Waulsortian Mudbank developments outcrop along an E-W trending, saddle-shaped synclinal structure, flanked by two inliers of older strata to the north and south. To the west lies a large area of younger Namurian strata, and to the east is the Limerick Volcanic centre, which post-dates the Waulsortian Complex.

In total, 217 samples were collected, and results for $(\text{Mn}+\text{Fe})/2$ are displayed on Figure 7.5 (see also Figure 3.70) in contoured form. Two main areas of elevated $(\text{Mn}+\text{Fe})/2$ levels are observed. One of these flanks the sub-reef inlier on the north side of the basin, whereas the other flanks the inlier to the south. The anomalous content to the north appears to be associated with the Courtbrown Pb+Zn prospect, at the western end of the inlier (Chapter 3.5.3), where the highest levels are measured, at 400 ppm or more. In addition, the location of minor epigenetic mineralisation (represented by old trials for Cu, Pb and Zn) throughout the inlier, suggest a more extensive root zone or feeder zone, more central to the observed aureole (see Section 6.3.5).

There is no significant mineralisation recorded in or around the southern inlier to account for primary enrichments in the mudbanks in the same way.

Zinc distribution in the Limerick Basin is virtually featureless, as nearly all the samples contain less than 10 ppm Zn, with the exception of a few from the vicinity of Courtbrown Point, within a kilometre of the known mineralisation.

Minor post-Waulsortian mineralisation (epigenetic in style)

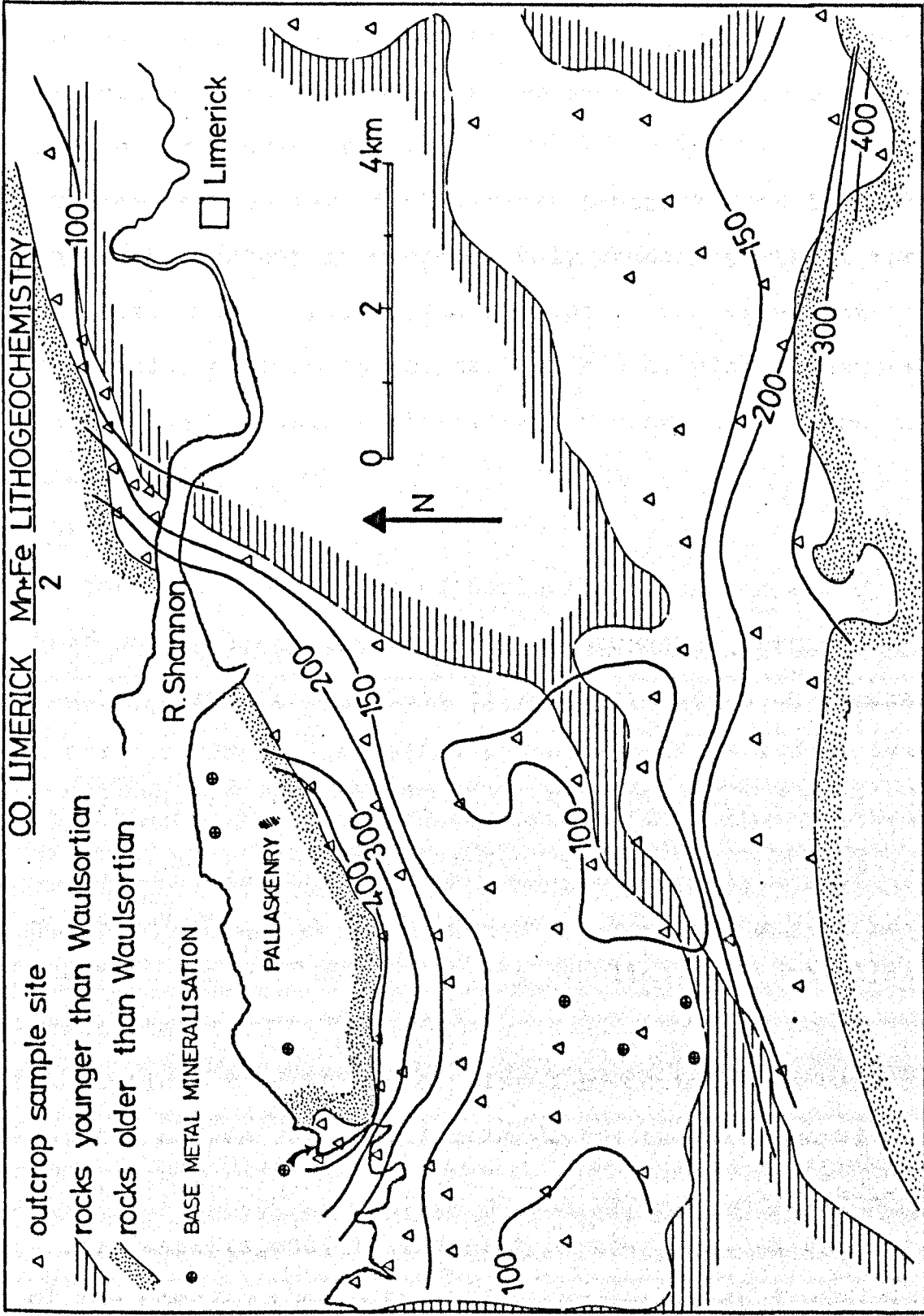


Figure 7.5: $\frac{(Mn+Fe)}{2}$ lithochemistry of Waulsortian Limestones of Co. Limerick, contoured using a rolling mean. Also shown are known base metal occurrences.

in mudbank and younger rocks in the centre of the syncline (marked by a number of old trials for Pb and Zn) is not associated with any apparent increase in Mn or Fe content in the surrounding rocks.

The general pattern in the North Limerick area is of lower Mn and Fe content in progressively younger parts of the Waulsortian, dropping below 100 ppm in the very centre of the basin, near to the contact with overlying limestones, suggesting a possible stratigraphic control on geochemical distribution.

3) County Kerry:

A total of 234 samples of Waulsortian Mudbank and Upper Reef were collected from three stretches of outcrop in County Kerry, the locations of which are shown on Figure 3.1. Rocks here are folded along E-W or ENE-WSW trending axes, and (as in the North Cork area) have suffered some degree of low temperature metamorphism, with development of an E-W cleavage. The three main belts of mudbank outcrop occur on limbs of complimentary synclinal and anticlinal structures.

Analytical results are displayed by contours in Figure 7.6, and the median value of $(\text{Mn}+\text{Fe})/2$ for the area is 84 ppm (Table 3.4). Three areas of enrichment are observed:-

- 1) Castleisland, to the east of the area, on the nose of the most southerly anticline, and associated with a development of hematitic mudbank (the Castleisland Red Breccia, Hudson et al 1966). The enrichments here are more extensive than the hematitic facies;

ii) The Maharees, to west of the area, on the peninsula in the middle of Tralee Bay. The elevated levels appear to be associated with an outcrop of pyritic mudbank near the harbour;

iii) on the south shore of Tralee Bay, where elevated trace element levels appear to be associated with outcrops of both red marble and pyritic facies of mudbank.

Zinc distribution in this area is also virtually featureless, with only 4 samples containing over 10 ppm.

No direct link can be drawn between trace element distribution patterns and base metal occurrences in this area, of which only two are known to the author, both very minor in nature (Figure 7.6).

7.3.1. Discussion.

From the three examples described, it can be seen how the application of Mn, Fe and Zn litho-geochemistry can assist in early stages of reconnaissance exploration, allowing select areas to be approached in more detail, and bypassing the time-consuming and expensive 'blanket' soil geochemistry. The chip sampling of mudbank outcrops can be undertaken during geological mapping, with little inconvenience to the geologist concerned (in the form of bulky samples to be carried around).

An even quicker method of reconnaissance sampling would be to utilise roadside sampling of farmers' walls and field boundaries, which are normally built from locally quarried limestones. This would necessitate a greater sample density to allow for reduced control of source location, and some care in interpretation of results because of the possibility of encountering transported (glacially or otherwise) boulders. In areas of thick, continuous drift cover (or bogland), the unavailability of locally derived rock on the surface would render this technique ineffective. Instead, the use of lightweight drilling equipment could provide sufficient core from suboutcrop, to yield one or more chip samples of 'uncontaminated' mudbank for litho-geochemical analysis. This could be done at regular intervals to allow more complete areal coverage, as well as providing valuable geological information.

Geochemical profiling of deeper exploration boreholes may outline prospective horizons within the mudbank complex,

even if no mineralisation is visible.

One problem that often arises is that of sample composition and heterogeneity. Many areas of mudbank outcrop have suffered severe weathering or alteration, or are composed dominantly of later diagenetic phases of sparry calcite (eg. the 'veines bleues' facies of Lees and Conil 1980). Other areas may contain significant argillaceous or other detrital components. This is where selective (but objective) chip sampling becomes important.

One inherent problem of relying upon surface outcrop sampling is that available outcrop may present a ready-made sample bias. This is because the different facies of Waulsortian Mudbank do not necessarily retain comparable resistance to the processes of weathering. Data from Ballybeg Quarry (Figure 6.15) illustrates the possible geochemical differences that may exist between different facies of mudbank, by utilising drill core (or quarry face) samples, where the problem of uneven weathering is avoided.

If sufficiently good control is available on sample medium, ie. matrix purity, and freedom from other possible contaminants, then a quicker dissolution technique (eg. stronger acid, such as HCl) could be applied without significantly affecting the final results. However, even pure Waulsortian Mudbank comprises an assortment of facies of differing biogenic and textural component phases, apart from any possible abnormality in composition. Brand (1981) advises against the use of multicomponent and multiphase matrix

material for interpretative geochemical investigations, instead favouring the use of monomineralic components, such as fossil tests.

One means of bypassing the possible effects of diagenetic modification on trace element geochemistry would be to utilise those components of the rock that were initially composed of low-Mg calcite, which remained relatively unaffected by recrystallisation and diagenetic interchange. An example here would be to examine the trace element content of brachiopod shells (al-Aasm and Veizer 1982, Morrison and Brand 1983). Problems arising from this, however, would relate to the relative scarcity of brachiopod remains in the Waulsortian, the difficulty of obtaining a sufficiently large sample without time-consuming separation techniques, or the need to apply electron microprobe examination, with associated problems of preparation, expense and reduced analytical sensitivity.

Some potential exists for the use of cathodoluminescence in carbonate litho-geochemistry, mainly for microexamination of trace element distribution (eg. in studies of diagenesis) or in very localised studies of trace element dispersion in vein wall rocks close to mineralisation (Chen et al 1978), rather than in regional reconnaissance programmes.

Certain elements (notably Mn^{2+} and Fe^{2+}) produce luminescence characteristics, either activation or suppression, in limestones and dolomites (Meyers 1978), but a number of others may also be involved (eg. Pb^{2+} , Ce^{2+} , Ni^{2+} , Machel 1983). Frank et al (1982) quote a figure of 280 ppm Mn as

the critical threshold level required to induce luminescence. This would be very convenient for application to litho-geochemistry, being very close to the threshold values of Mn used in this study. More information would be required first, about the effects of Fe and other trace elements in suppressing luminescence, and balancing out the effects of elevated Mn levels. Apart from the ambiguities that may arise in interpretation of results, the need for relatively sophisticated equipment and elaborate preparation requirements are further drawbacks which impinge on the use of cathodoluminescence in litho-geochemistry.

The application of litho-geochemistry to rocks other than Waulsortian Mudbanks may require a restructuring of methodology, from sampling and analytical techniques, to interpretation of results. In sediments with lower (or non-existent) carbonate contents, Mn and Fe will more likely be present in less soluble forms, requiring a different analytical technique from that used in this study, for example, a more powerful dissolution method for atomic absorption analysis, or else X-ray fluorescence. One problem arising then, would be the need to discriminate between trace elements associated with the detrital fraction of the rock, and any trace elements originating from hydrothermal sources. Variable proportions of detrital constituents of a sediment would lead to very fuzzy or erratic background levels, and possible failure in recognising subtle anomalies arising from hydrothermal input.

Comparison between the percentage of anomalous samples

around each deposit examined (for both $(\text{Mn}+\text{Fe})/2$ and Zn) illustrates the relatively poor definition of some of the aureoles, particularly towards the North Midlands (Table 7.2a,b). This may reflect a general weakness of the sea-floor hydrothermal activity, or mechanisms of dispersal of hydrothermal effluents, in that area. It may also be a result of the higher background levels of Mn and Fe in the same area (Figure 3.9), reducing the contrast between anomalous and background levels.

Tynagh appears to have, statistically, the best defined $(\text{Mn}+\text{Fe})/2$ and Zn aureoles, with the highest proportion of anomalous samples. This is particularly true in outcrop patterns (Table 3.5). By comparison, Silvermines outcrop samples are very inefficient in defining the extent of trace element enrichments developed around the mineralisation (Table 3.6).

Of the deposits examined in this study, surface outcrop sampling on a reconnaissance basis (with the same sample density) would have probably incited further interest in the vicinity of the Tynagh, Ballinalack, Ballyvergin, Moate and Courtbrown deposits, but not at Keel, Aherlow and Silvermines. The reliance on core samples to locate enrichments at the latter three deposits is one weakness of the technique.

A number of potential pitfalls await the exploration geologist utilising lithogeochemistry in carbonate terrains, which also apply to non-carbonate terrains. These are summarised as follows:-

Location	$\frac{\text{Mn+Fe}}{2}$	Distance (km)	Threshold (ppm)	Anomalous samples (%)	
				Proximal	Distal
Tynagh		6	250	94	10
Silvermines		4	200	79	15
(Nenagh)		4	200	68	15
Ballinalack		(5)	300	76	9.3
Keel		4	300	35	13
Moate/Moyvore		6	300	35	7.5
Ballyvergin		6	250	26	0
Aherlow		(2)	250	86	0
Courtbrown		*	250	91	8.2

Table 7.2a: Comparison of (Mn+Fe)/2 aureoles (as % anomalous samples) around each deposit examined. From data given in Chapter 3.

Location	Zn	Distance (km)	Threshold (ppm)	Anomalous samples (%)	
				Proximal	Distal
Tynagh		6	10	82	4
Silvermines		4	10	63	16
(Nenagh)		4	10	41	16
Ballinalack		(5)	10	28	0
Keel		4	10	7.5	0
Moate/Moyvore		6	10	4.3	1.1
Ballyvergin		6	10	(3)	0
Aherlow		(2)	10	52	0
Courtbrown		*	10	0*	4.1

Table 7.2b: Comparison of Zn aureoles (as % anomalous samples) around each deposit examined. From data given in Chapter 3. * For Courtbrown, limits of aureole are 1 km from the edge of the inlier, and anomalous Zn in proximal samples is 21% if core samples of Russell (unpublished data) are included.

1) Failure to recognise genuine background levels because of too restricted sample coverage. For example Barrett (1975), who stated that no Mn aureole was present around the Ballynoe baryte deposit, and geologists at Tynagh (J. Clifford pers. comm. 1982), who stated that no Mn aureole was present around the deposit there, after sampling only core (ie. proximal) samples;

2) Failure to locate stratigraphically restricted anomalous horizons, because of insufficient sample density or restricted areal coverage. For example, Russell (unpublished work) failed to locate appreciable Mn enrichments around Silvermines, and possibly also Al-Kindi (1979), whose samples failed to indicate primary enrichments around the Mallow deposit (see Section 3.5.4 and 6.3.5);

3) Generation of misleading patterns, linked more to lithological changes than hydrothermal input, because of contamination from 'detrital' and other sources, and non-selective sampling and analytical techniques (eg. geologists at Keel, see Section 5.3.1).

This also includes misleading patterns generated by including samples from two or more non-comparable lithological units, with distinctly different geochemistry, in the same study. For example, Finlay et al (1984) at Navan, and geologists at Meggen, who were misled by high Mn values in down-dip, basinal limestones of different character to the along-strike, shelf limestones (M.J. Russell pers. comm. 1985);

4) Generation of 'artificial' anomalies from non-hydrother-

mal sources, such as diagenetic processes (probably signified by substantial Sr loss, hence the need to analyse routinely for Sr), or intense pressure solution (which may be responsible for some of the anomalous values of Mn and Fe associated with red marbles, for instance).

These potential pitfalls should be borne in mind when planning a lithogeochemical survey of any area.

CHAPTER EIGHT - Conclusions.

Examination of the trace element distribution patterns around some Irish Lower Carboniferous base metal deposits substantiates the hypothesis set up in Chapter One of this thesis, and a number of the proposed aims of this study are achieved in the process. Firstly, as trace element aureoles appear to be a common feature around synsedimentary Irish-type mineralisation, lithogeochemistry has a useful potential as a tool in mineral exploration in the Irish Carboniferous. Also, valuable information on genetic aspects of the mineralisation is revealed by examination of the trace element patterns, (much of which has significant influence on the application of the technique in exploration. Some of these points are summarised in the following paragraphs.

The sampling technique favoured utilises selective chip sampling of mudbank limestone outcrops, to avoid secondary or epigenetic contamination, or visible mineral impurities such as sulphide, dolomite or mud seams. This has the advantage of being undertaken during reconnaissance (eg. mapping) stages of exploration, and if anomalies are produced, allows more intense activity to be focussed on more local areas of interest.

The principal analytical technique applied in this study utilises atomic absorption spectrophotometry analysis of samples for Mn, Fe, Zn and Mg, following dissolution by weak acid (2M acetic) at elevated temperature (90°C) for 1 hour. This technique has the advantages of relative

simplicity and rapidity, without loss of precision. It also has some ability to discriminate from those trace element patterns associated purely with facies or lithological changes, or secondary or impurity-related contaminants. Nevertheless, because of small-scale inhomogeneity, particularly in the vicinity of known mineralisation, some care in interpretation is required when attempting to identify primary trace element patterns associated with syngenetic hydrothermal processes.

Analysis of approximately 1600 samples from throughout the Irish Waulsortian reveals that background levels of Mn and Fe, well away from obvious hydrothermal influence, are not consistent. Instead, they vary from below 100 ppm in the southwest, to over 250 ppm in the north Midlands. Background levels for zinc are below 10 ppm throughout the country.

The Tynagh deposit is surrounded by a pronounced Mn and Fe aureole to at least 6 km distant, with elevated Zn (and Sr) values to about 5 km. Over 80% of samples from within these aureoles are considered anomalous, relative to background values. The enrichments appear to extend throughout the Waulsortian sequence with no obvious stratigraphic control.

Enriched Mn, Fe and Zn levels occur throughout much of the Nenagh-Silvermines Basin, but those associated with the Silvermines deposit are present up to at least 3 km distant, in Waulsortian and equivalent carbonates. These enrichments, however, display poor surface expression, because

of limited outcrop near the mine, and their confinement largely to basal mudbank sediments.

Examination of vertical borehole profiles of host rocks at Silvermines allows an insight into the early development and later, waning stages of hydrothermal activity, with peak Mn, Fe and Zn values coincident with the ore horizon. In the vicinity of the stratiform deposits, enrichments of Mn, Fe and Zn extend about 100 m into the hanging wall carbonates, with Mn and Fe especially concentrated in the dolomite breccias. Over 60% of Waulsortian and equivalent samples from within 4 km of the deposits retain anomalous Mn, Fe and Zn. Elevated levels of Mn, Fe and Zn also extend into the footwall sediments, with zinc to 6 metres, Mn to 30m and Fe possibly to as much as 100m below the base of the ore horizon, although further work is required to delineate their overall extent. The ratio Mn:Fe increases steadily upwards from less than 0.1 (over 30m below) to around 0.5 in the ore horizon and immediately underlying sediments, and finally averages about 10 in the hanging wall above 30m from the top to the ore horizon.

The principal controls on areal distribution of Mn and Fe around Silvermines are: original Mn and Fe levels in the exhaled hydrothermal fluids; local precipitation of large tonnages of massive pyrite and siderite (removal of large amounts of Fe relative to Mn); and the carbonate-dominated geochemical environment of the surrounding shelf (telescoping any lateral fractionation of Mn and Fe).

Another possible hydrothermal source is centred a few kilo-

metres to the east of Nenagh, with enriched Mn, Fe and Zn values covering a radius of about 4 km. Two-thirds of the samples from this zone carry anomalous levels of Mn and Fe, and sulphide mineralisation has been discovered near its centre.

Within 5 km of the Ballinalack deposit, over 75% of mudbank samples contain elevated levels of Mn and Fe, in the micrite phase of the limestone. Discontinuous outcrop precludes the definition of the overall lateral extent of the trace element aureole. Anomalous Zn levels account for 28% of samples within 5 km, most of these occurring more proximally to the mineralisation, in drill core. Borehole profiles reveal no apparent vertical distribution trends in the mudbanks.

The Keel deposit is associated with weak enrichments of Mn and Fe in surrounding mudbank limestones, occurring in 35% of samples from within 4 km of the stratiform mineralisation. Enriched zinc is recorded only in a few borehole samples, and both outcrop patterns and drill hole profiles are suggestive of a concentration of anomalous Mn and Fe values towards the base of the mudbank sequence. A similar proportion (35%) of mudbank samples within about 6 km of either the Moate and Moyvore prospects yield anomalous Mn and Fe levels.

Enrichments of Mn and Fe in mudbanks around the deposits of the Ballyvergin area suggest that exhalative processes were active during Waulsortian deposition. However, only a quarter of samples collected within a 6 km radius of the

centre of the deposits yielded anomalous Mn and Fe levels relative to background, with even fewer anomalous Zn values.

Core samples from within 2 km of the Aherlow prospect contain anomalous Mn, Fe and Zn levels, although the overall lateral extent of these enrichments is unclear because of the lack of outcrop in the vicinity.

Enrichments of Mn and Fe at the base of the mudbank limestone extend for a considerable distance (at least 6 km) along strike from the Courtbrown prospect. This pattern is suggestive of a more central exhalative source, some where to the east of the existing prospect, possibly represented by a number of old base metal trials in the sub-reef inlier. Anomalous zinc appears to be confined to core material from Courtbrown itself.

Mudbank limestone samples collected from around the Mallow prospect failed to delineate any appreciable primary enrichments associated with the mineralisation.

X-ray fluorescence data from Silvermines indicates a close relationship between high absolute Mn and Fe content, high insoluble trace element content (SiO_2 , Al_2O_3 , K_2O and acid-insoluble Mn and Fe), dolomite, and clay mineral impurities in host rock carbonates to the stratiform ore. This highlights the influence of post-depositional processes, including recrystallisation, dolomitisation, pressure-solution and volume reduction, which have severely modified the distribution patterns of trace elements around the mineralisation at Silvermines. One result is the enhancement of Mn

and Fe values, particularly in dolomite samples, although the post-depositional patterns are probably based on previously existing primary (hydrothermal) patterns in the host rocks. This brings to light, however, the possibility of encountering 'pseudo-primary' enrichments (entirely diagenetic in origin, and with no connection to hydrothermal processes) when exploring in relatively poorly known areas. To help identify these, routine analysis for Sr might be useful, since the diagenetic processes which magnify Mn and Fe levels in carbonates usually lead to depletion of Sr.

Application of the lithogeochemical techniques in exploration of areas with unknown potential has resulted in the discovery of minor Pb and Zn mineralisation in Waulsortian carbonates, surrounded by extensive Mn, Fe and Zn enrichments in two areas, one in north Co. Cork, the other in the Nenagh area.

APPENDIX I - Analytical Techniques.

Introduction.

As set out in Chapter 2, the problem of analysing impure carbonate samples for trace elements associated with the carbonate ('non-detrital') phase requires a dissolution technique which is potent enough to break down the more stable or resistant carbonates, whilst leaving intact the non-carbonate fraction. Trace elements such as Mn and Fe may be released from non-carbonate minerals in the rock by even weak acid attack (Martin and Chabot 1981). This must be minimised to prevent severe distortion of apparent Mn and Fe levels in the carbonate minerals.

There is a general lack of agreement in published work on a suitable analytical technique for application to this problem (as outlined in Chapter 2), due partly to the often very different nature of the samples involved. Because of this, a number of experiments were conducted on representative samples of relatively pure Waulsortian Mudbank Limestone, and impure and dolomitic equivalents, to determine a suitable dissolution technique for application to this study.

Which acid?

Preliminary experimentation with varying acetic acid concentrations, both heated and unheated, on pure calcium carbonate and dolomite powders, indicated that increased temperatures were required to break down dolomite within a reasonably short time. Digestion with more concentrated acid took place much more quickly in both hot and cold experiments.

Stronger (2M) acetic acid dissolved CaCO_3 effectively whether heated or not, but fully dissolved the dolomite only when heated. The weaker acid attack (0.2M) was generally insufficient to digest either carbonate powder fully, particularly at room temperature, and the reaction with dolomite was still taking place after four days (Table A.1).

As a continuation of this experiment, a number of samples of dolomite breccia and footwall argillaceous limestone from Silvermines were subjected to a range of acid attacks, this time quantitatively, by analysing for Mn in the resulting solutions. Comparison was made also with hydrochloric (0.5M and 3M), and concentrated nitric - perchloric acid mixture. (X-ray fluorescence analyses were performed on the same samples to allow comparison with a total value of Mn in both acid-soluble and insoluble portions of the rock. Hot 2M acetic acid gave the best overall extraction rates in both rock types, at over 90% extraction of total Mn (Table A.2).

In a similar experiment, the results for zinc were examined (Table A.3), and zinc extraction improved (as did analytical precision) in the order:- cold 0.2M < hot 0.2M < cold 2M < Hot 2M acetic acid.

Although higher extraction rates were obtained using both hydrochloric and nitric-perchloric acids (as would be expected if a sulphide was the principal source of zinc), poorer analytical precision was achieved. Even with the most dilute, weak acid digestion, leaching of the sulphide content was most likely taking place (Martin and Chabot 1981).

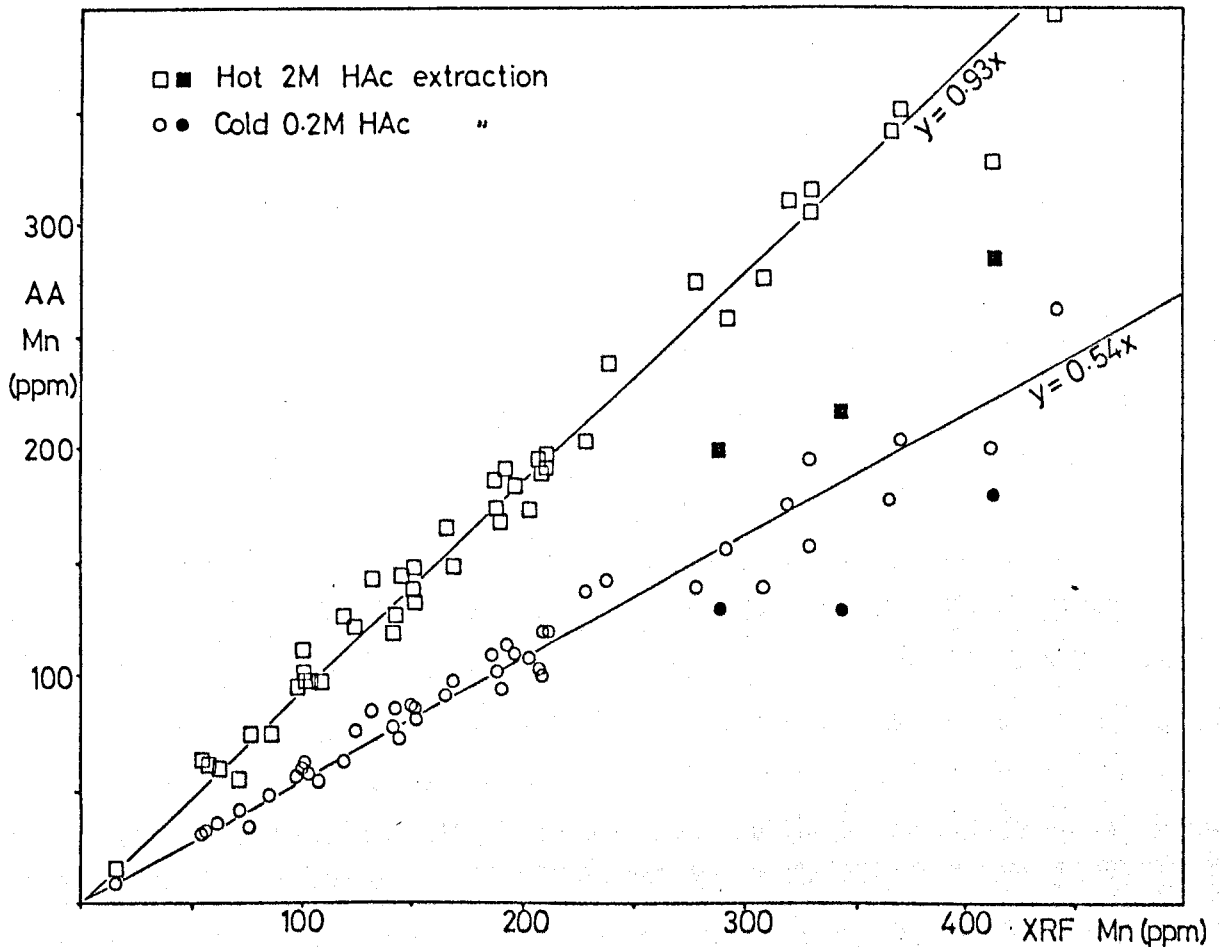


Figure A.1: Comparison of Manganese extraction by weak acid for A.A. analysis against X.R.F. analysis ('total content'). Undertaken on 48 samples from the Nenagh Basin, using both hot 2M and cold 0.2M (Russell 1974) acetic acid digestion. Filled symbols represent muddy or dolomitic samples.

Acid Used	Sample medium	Cold Digestion + Overnight	Hot Digestion + Overnight
Acetic Acid 0.2M	CaCO ₃	incomplete	incomplete?
" "	dolomite	incomplete*	incomplete
Acetic Acid 2.0M	CaCO ₃	complete	complete
" "	dolomite	incomplete?*	complete

* after four days ? effervescence ceased, much insoluble residue

Table A.1: Results of overnight acetic acid digestion of calcite and dolomite powders.

<u>ACID USED (AND CONCENTRATION)</u>	<u>PERCENTAGE EXTRACTION ON A.A.</u>		
	A	B	C
Cold Acetic (0.2M)	28	65	40
Hot Acetic (0.2M)	55	84	64
Cold Acetic (2.0M)	80	92	84
Hot Acetic (2.0M)	88	97	91
Cold Hydrochloric (0.3M)	84	90	86
Hot Hydrochloric (3.0M)	75	78	76
Cold HNO ₃ /HClO ₄ (25%)	73	80	76

Table A.2: Manganese extraction by different acid digestion, on Atomic Absorption. Expressed as a percentage of 'total' value (measured on X-Ray Fluorescence).

A = Dolomite Breccia samples (n = 6)

B = Muddy Reef Limestone samples (n = 3)

C = Average of A and B (n = 9).

<u>ACID USED (AND CONCENTRATION)</u>	<u>PERCENTAGE EXTRACTION ON A.A.</u>		
	A	B	C
Cold Acetic (0.2M)	(<4)	(<7)	(<5)
Hot Acetic (0.2M)	(<7)	(<8)	(<7)
Cold Acetic (2.0M)	7	17	11
Hot Acetic (2.0M)	12	24	15
Cold Hydrochloric Acid (0.3M)	30	58	38
Hot Hydrochloric Acid (3.0M)	(75)*	(80)*	(76)
Cold HNO ₃ /HClO ₄ (25%)	(74)*	(83)*	(76)

* including samples with A.A. result greater than X.R.F. result

Table A.3: Zinc extraction by different acid digestion, on Atomic Absorption. Expressed as a percentage of 'total' value (measured on X-Ray Fluorescence).

A = Dolomite Breccia and Siderite samples (n = 8)

B = Muddy Reef Limestone samples (n = 3)

C = Average of A and B (n = 11).

Experimentation with a batch of 45 powdered samples of pure Waulsortian limestone from the Nenagh - Silvermines area was undertaken using both cold, dilute (0.2M), and hot, more concentrated (2M) acetic acids, to compare the extraction of Mn from pure mudbank limestone samples with X.R.F. analyses of the same samples. Three muddy and dolomitic samples were also included, and the results are depicted in Figure A.1.

Although pure Waulsortian limestones contain less than 2% Mg, manganese is still not fully leached by the cold, weaker acid attack. On average, 54% of the total Mn (by X.R.F.) was released from each sample, compared with 93% by the hot 2M acetic digestion. This is in spite of the fact that the cold samples were left overnight, and the heated samples digested for only one hour. The percentage extraction of manganese is lowered by the presence of argillaceous impurity or dolomitisation, in both methods of leaching, as indicated by the three impure, dolomitic samples. In these, more Mn is locked up in relatively insoluble minerals.

Repeated analyses for Mn and Zn were performed on three representative samples of 'reef-equivalent' rocks from around the Silvermines deposit to determine precision levels for the techniques under scrutiny. A minimum of twelve analyses were performed on each sample for each technique. A variety of acid strengths and temperatures were investigated, similar to previous experiments, on one dolomitic sample with low Mn content, one dolomite with high Mn con-

tent, and one argillaceous limestone ('Muddy Reef'), also with high Mn content.

In this experiment, analytical precision was seen to improve, sometimes considerably, when the samples were heated during digestion, in both dilute and concentrated acid attack. This was the case for both Mn and Zn (Table A.4).

For routine application to mudbank and equivalent samples from around Silvermines, the use of stronger acids (HCl or $\text{HNO}_3/\text{HClO}_4$) was avoided, because of their effect on non-carbonate minerals, and the poorer precision levels obtained by experiment. In addition, reduced breakdown of carbonate by stronger mineral acids is indicated by lower extraction rates for manganese in the nitric - perchloric digestion.

The more powerful leaching capabilities of the two stronger acid digestions on non-carbonates (sulphides in particular), were considered inappropriate for application here, partly because of the increased sulphide concentrations present in the host rocks close to the Silvermines deposits.

Of the four acetic acid digestions experimented with, the hot 2M leach was preferred because of its ability to break down the more resistant minerals rapidly, with apparently improved analytical precision over the other three.

How hot, how long?

A number of simple leaching experiments with hot 2M acetic acid were then conducted on a sandbath, to determine the optimum duration and temperature of heating required for sample digestion. The conditions sought after were those

MANGANESE (PPM)		N	\bar{x}	μ	$\mu/\bar{x} \times 100$
B139 1	Cold 0.2M Acetic	12	156	10.0	6.4
	Hot 0.2M Acetic	12	265	8.8	3.3
	Cold 2.0M Acetic	15	470	7.6	1.6
	Hot 2.0M Acetic	15	508	6.1	1.2
	Cold 0.5M HCl	15	509	8.7	1.7
	Cold 3.0M HCl	15	473	21.7	4.6
	Cold HNO ₃ /HClO ₄	14	480	13.7	2.9
B139 6	Cold 0.2M Acetic	12	788	17.0	1.7
	Hot 0.2M Acetic	12	2299	17.3	0.75
	Cold 2.0M Acetic	15	3116	44.0	1.4
	Hot 2.0M Acetic	15	3466	24.8	0.72
	Cold 0.5M HCl	15	3263	53.4	1.6
	Cold 3.0M HCl	15	2957	31.3	1.1
	Cold HNO ₃ /HClO ₄	14	2351	55.1	2.4
ZINC (PPM)					
B139 1	Cold 0.2M Acetic	9	12.3	3.2	25.7
	Hot 0.2M Acetic	9	39.1	2.9	7.5
	Cold 2.0M Acetic	14	41.1	3.1	7.5
	Hot 2.0M Acetic	14	54.5	3.9	7.2
B139 6	Cold 0.2M Acetic	9	133	3.6	2.7
	Hot 0.2M Acetic	9	208	5.4	2.6
	Cold 2.0M Acetic	14	208	5.1	2.4
	Hot 2.0M Acetic	14	263	5.6	2.1

SAMPLE	DESCRIPTION	Z EXTRACTION				TOTAL CONTENT (XRF)					
		Mn	Fe	Zn		ppm Mn	ppm Fe	ppm Zn	% CaCO ₃ Al+Si		
1	KL696 Pure Limestone	80.2	84.6	70.0		192	350	17.8	1.70	96.2	0.59
2	KL729 Impure Limestone	89.4	32.7	35.5		329	700	32.3	0.26	97.4	1.80
3	V19.1 Impure Dolomite	65.7	35.6	28.7		632	1540	24.4	7.98	75.0	2.41
4	V19.6 Impure Limestone (trace zinc)	95.3	37.9	(17.9)		892	4060	(799)	0.53	95.0	1.32
5	B139.1 Impure Dol. Brecc. (trace zinc)	66.7	34.0	(12.9)		735	3080	587	10.1	71.1	1.42
6	B139.5 Impure Dol. Brecc. (FeS ₂ , ZnS)	74.6	(4.1)	(8.4)		1175	55720	7932	7.78	53.7	0.93
			4.5*	13.3*							

* denotes value after 90 minutes, and still rising

Table A.5: Percentage extraction of Mn, Fe and Zn after 1 hour at 90°C, 2M acetic acid, in a variety of Silvermines carbonates. X.R.F. value is taken as 100%. Mg, CaCO₃ and Al+Si (Al₂O₃+SiO₂) levels are included as indices of the dolomite, calcite and 'insoluble' content.

Table A.4: Comparison of Mn and Zn extraction and precision levels for different acid attacks, using two impure dolomitic samples from Silvermines. Zinc precision levels (though not shown) are much poorer for HCl and HNO₃/HClO₄ digestions because of their relative potency in breaking down sphalerite.

favouring most complete dissolution of carbonate minerals with minimum leaching of non-carbonate.

Identical aliquots of selected powdered samples of varying composition were subjected to hot acid attack for varying lengths of time, from 0 (ie. cold attack) up to 120 minutes, on the sandbath. After the required duration of heating was reached, the samples were immediately quenched under cold water, filtered, and analysed for Mn, Fe, Zn and Mg. The experiment was also carried out on relatively pure samples of massive pyrite, sphalerite and argillite from Silvermines, to compare their leaching behaviour under the same conditions, with impure samples of host carbonate. The results are summarised in Figures A.2 to A.13.

One set of experiments was conducted at a lower temperature of 50°C (Figures A.6-9), while the remainder were conducted at 90°C (Figures A.10 to 13). Solution temperatures within the digestion tube do not stabilise until after 45 minutes at either setting (Figure A.2).

The results show that breakdown is not quite complete in the lower temperature digestion, as continued weak release of Mg, Mn and Fe is still taking place after 75 minutes in the dolomite, and possibly also the limestone samples (Figure A.5,6,7).

At the higher temperature attack, Mg is fully released from the limestone samples after 15 minutes, and from dolomites after 30 minutes (Figure A.4,5). Manganese and iron are released in approximately the same time, indicating more or less complete breakdown of carbonate minerals within

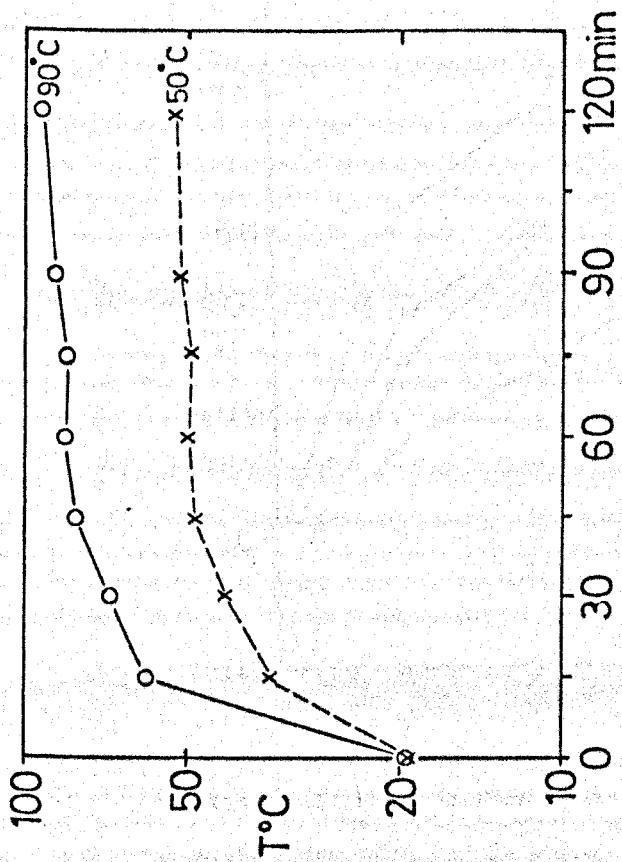


Figure A.2: Temperature of reactants on sandbath during hot acid digestion. These readings averaged from two or more trials.

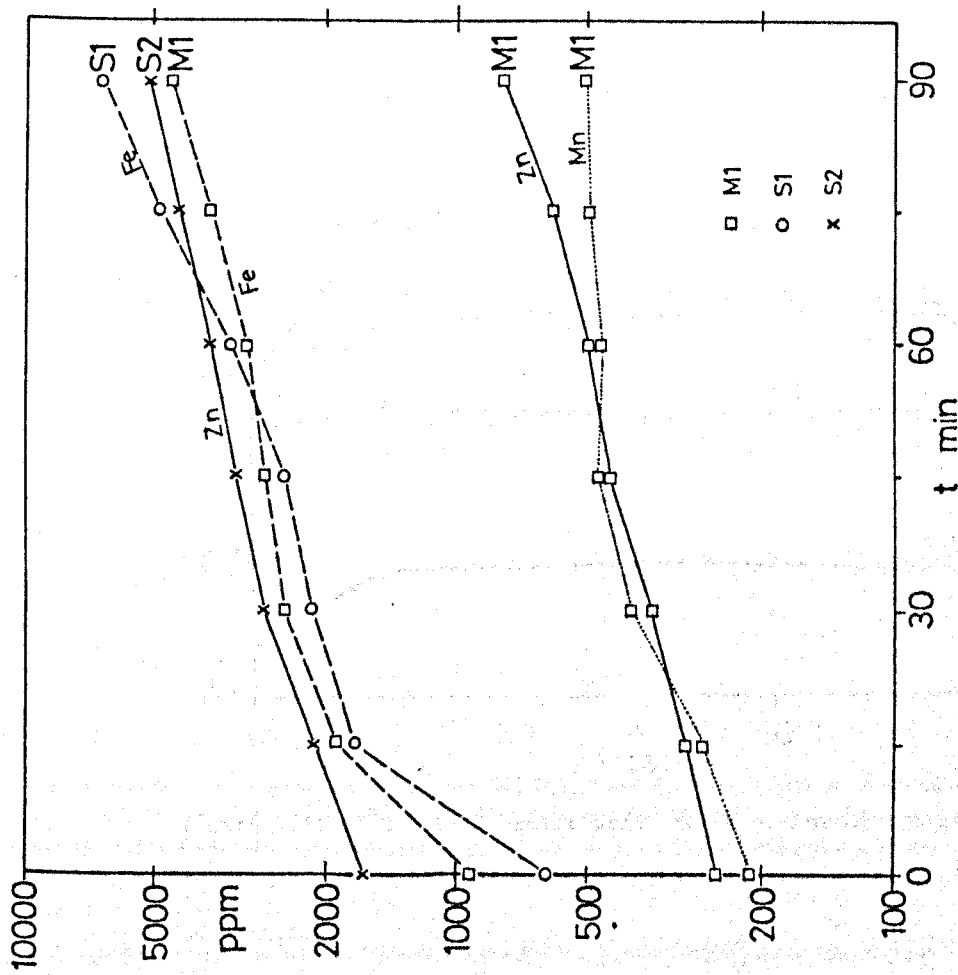


Figure A.3: Release of Mn, Fe and Zn from clay mineral- and sulphide rich carbonates from Silvermines.

M1 = Very muddy carbonate (with much f.g. pyrite also)

S1 = Very pyritic carbonate

S2 = Dolomitic carbonate with f.g. sphalerite.

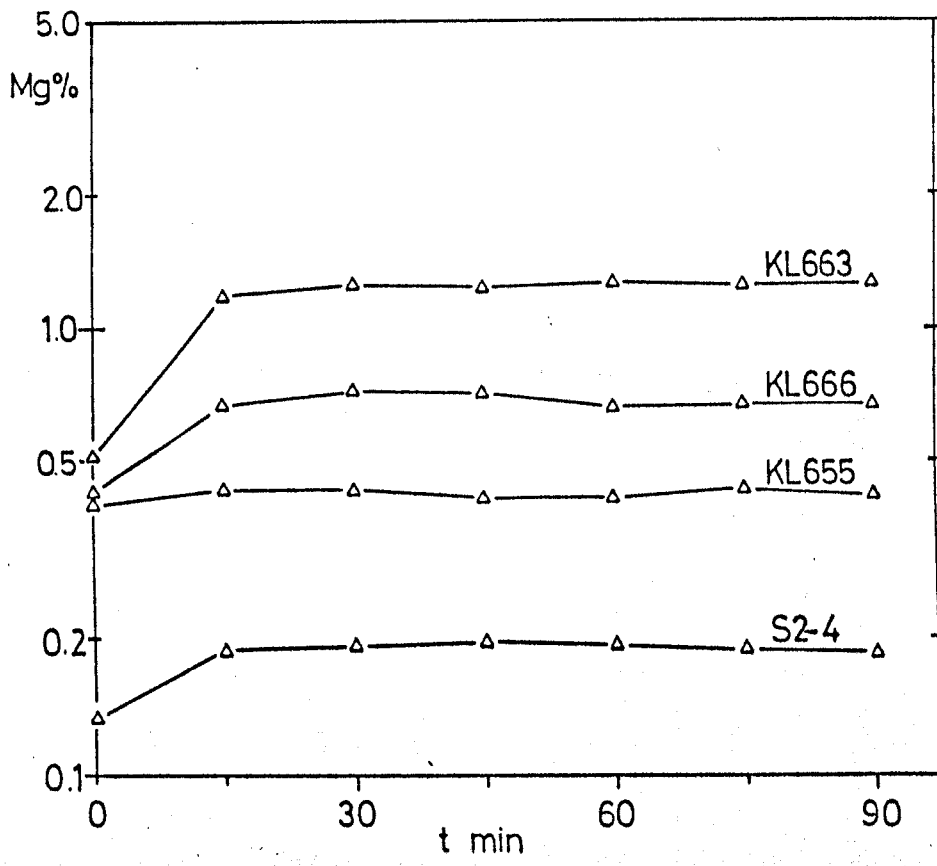


Figure A.4: 90°C hot 2M acetic acid leach of low Mg limestone samples, showing rapid release of Mg, and levels stabilising after less than 30 minutes.

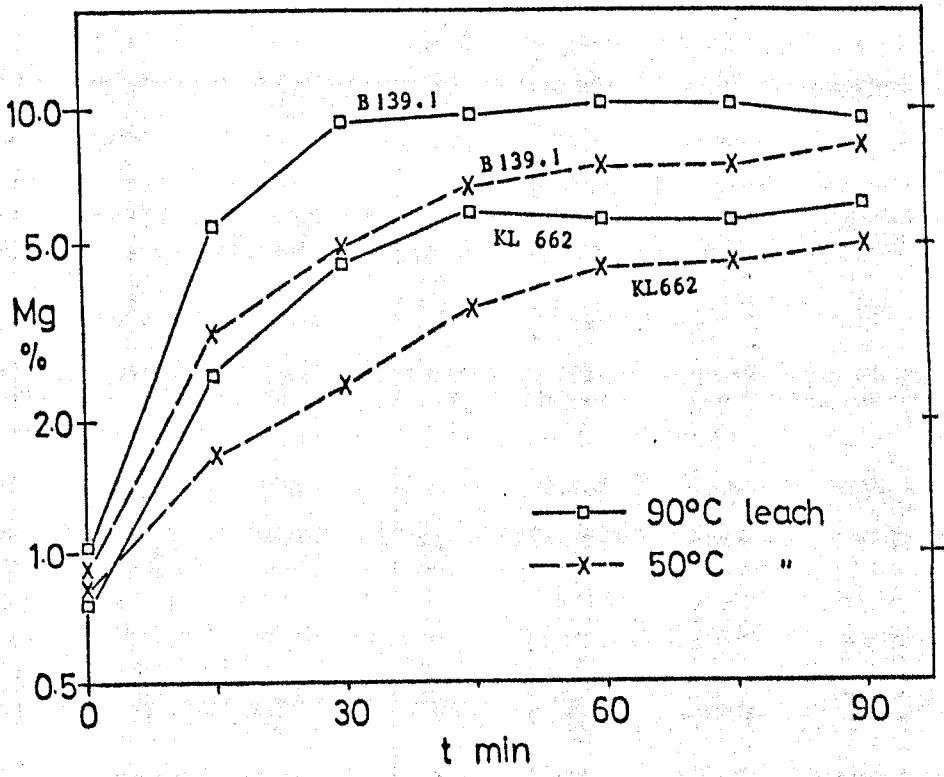


Figure A.5: Comparison of Mg release from two Silvermines dolomite samples at 50°C and 90°C, hot 2M acetic acid digestion. (B139.1 = impure dolomite breccia with 10.0% Mg, KL662 = fairly pure dolomitic limestone with 6.5% Mg).

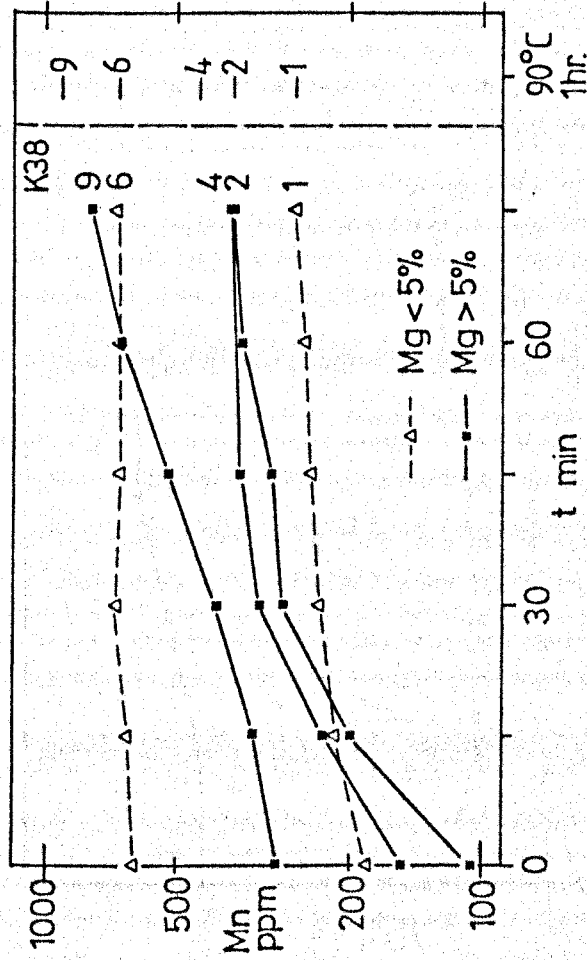


Figure A.6: Manganese release from Silvermines carbonate samples at 50°C digestion (2M Acetic acid). Also shown for comparison, is the analytical result for each sample after 1 hour at 90°C.

Samples K38.1 = Weakly dolomitic limestone

K38.2 = Dolomite Breccia, trace pyrite

K38.4 = " " "

K38.6 = Limestone

K38.9 = Dolomite Breccia, trace pyrite, minor ZnS.

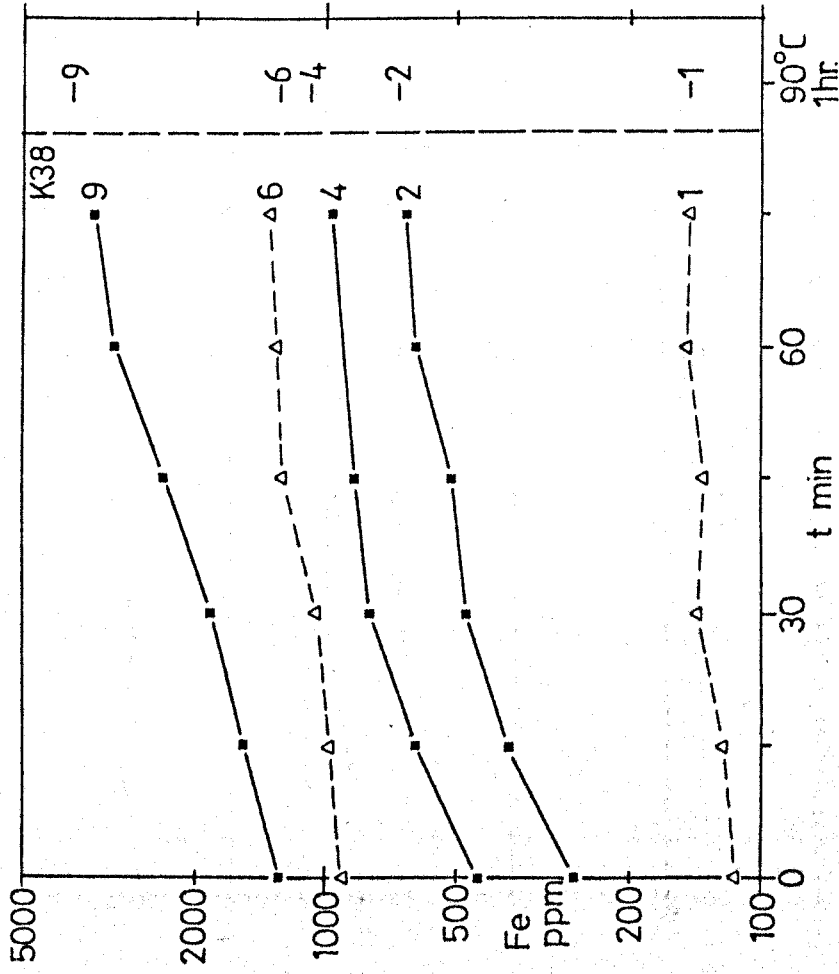


Figure A.7: Iron release from Silvermines carbonate samples at 50°C digestion (2M acetic acid). Key as for Figure A.6.

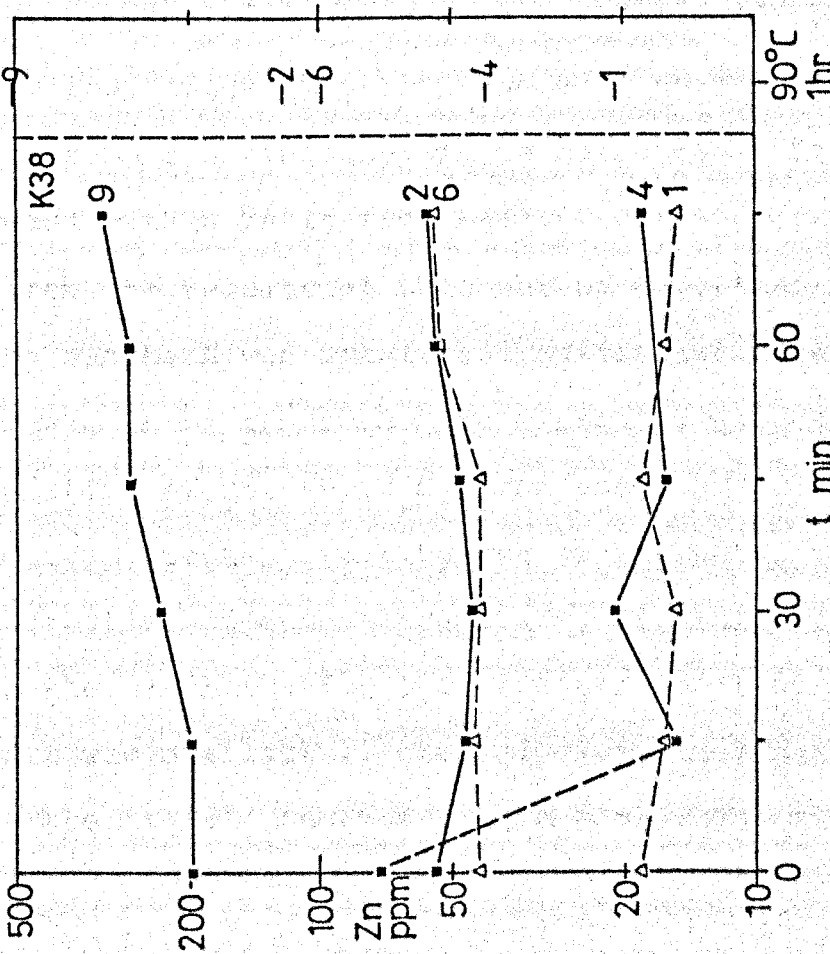


Figure A.8: Zinc release from Silvermines carbonate samples at 50°C digestion (2M acetic acid). Spurious result for K38.4 at 0 min. is probably due to contamination during analysis. Key as for Figure A.6.

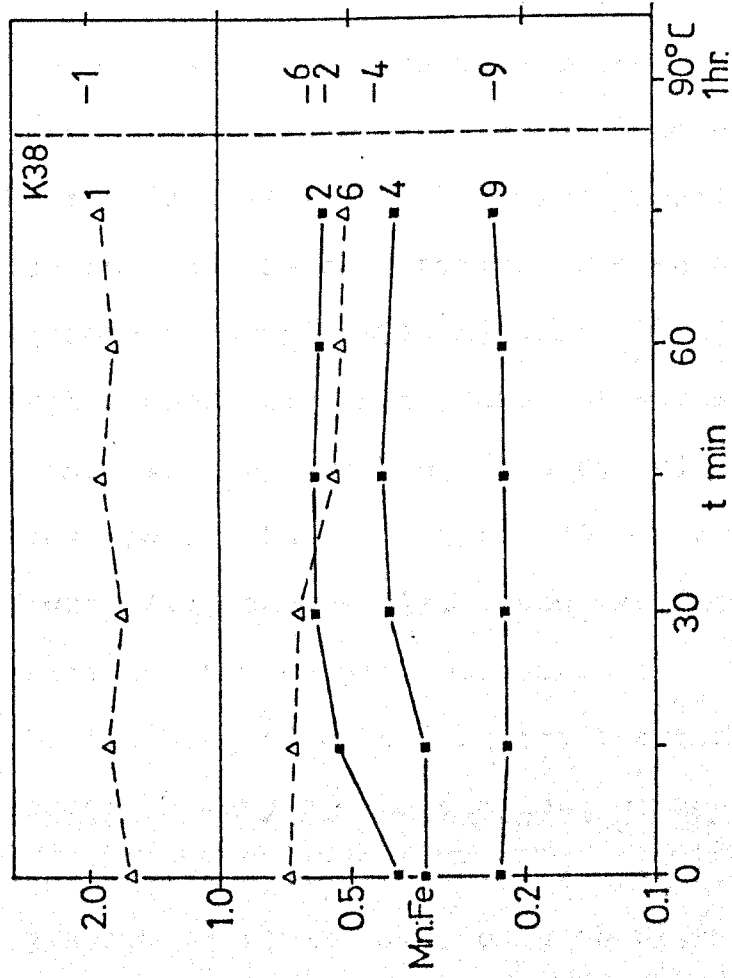


Figure A.9: Comparison between Mn and Fe release from Silvermines carbonate samples at 50°C digestion (2M acetic acid). The ratio Mn:Fe is shown. Key as for Figure A.6.

30 minutes, at the 90°C setting.

The presence of pyrite in a sample leads to significant contributions of Fe after about 30 minutes, by which time the temperature in the solution appears to be sufficiently high to leach Fe from pyrite (Figure A.11, samples m,n; Figure A.3, samples S1, M1).

Argillaceous carbonate does not appear to contribute Mn in this way, by leaching from eg. clay minerals, unless it takes place within the first 30 minutes of digestion (Figure A.3, sample M1). Iron is leached from fine-grained pyrite in this sample, however.

The leaching of zinc from small amounts of sphalerite, present in many of the samples, commences at relatively low temperature (Figure A.8, sample 9; Figure A.12, samples i,j,k,l,m,n; Figure A.3, samples M1, S2). Zinc levels in solution only remain static with time if absolute values are low, suggesting that there is no sphalerite present in the sample. Zinc appears to be released from ZnS more readily than Fe is from FeS₂.

From the results of this set of experiments, one hour on the sandbath was considered sufficient time to allow complete breakdown of the carbonate minerals, without substantial addition of Mn, Fe or Mg from the supposedly insoluble fraction. To further quantify the experiments, the percentage extraction of each element (Mn, Fe, Zn) after 60 minutes on the sandbath, for 6 of the samples (those for which X.R.F. data was available), was calculated using the X.R.F. results as the 'total' content (Table A.5). The six samples in-

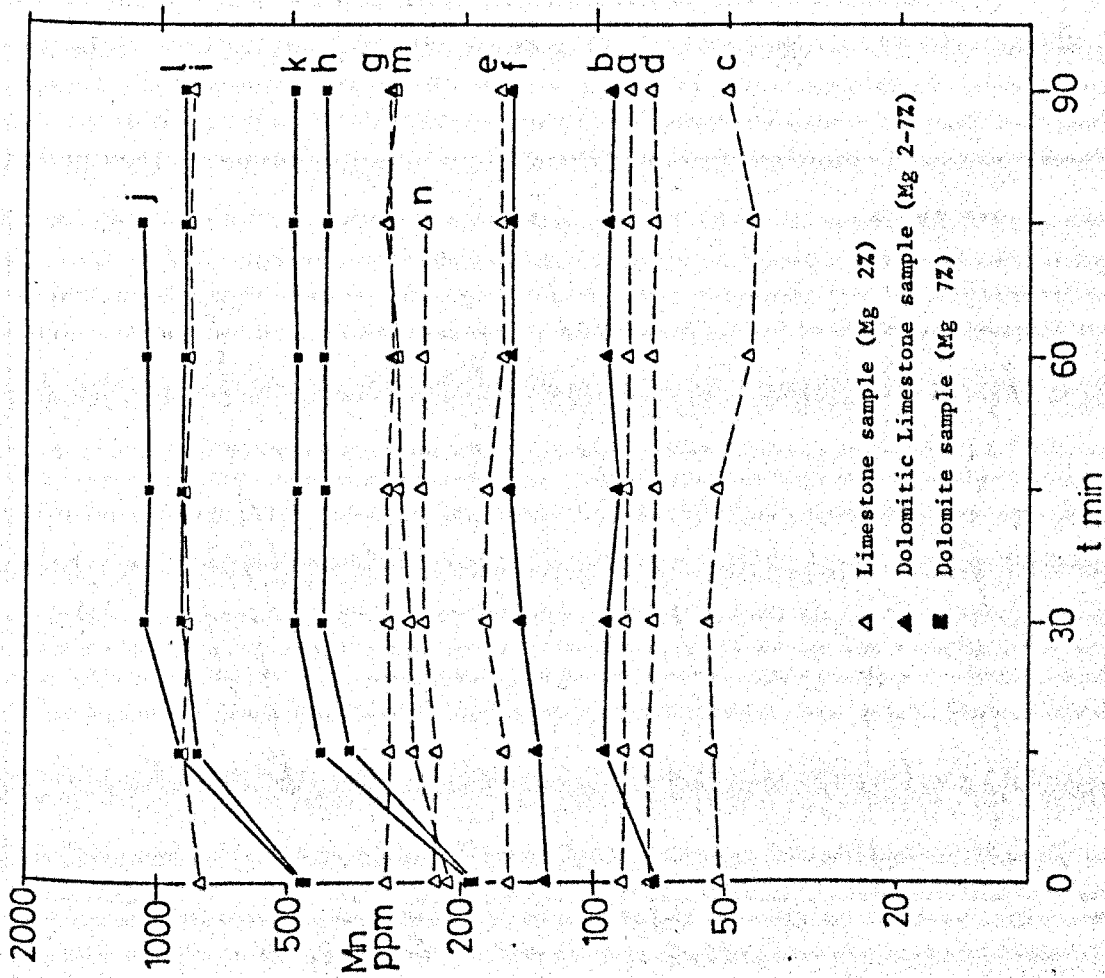


Figure A.10: Manganese released from various Silvermines carbonate samples at 90°C digestion (2M acetic acid). For key see next page.

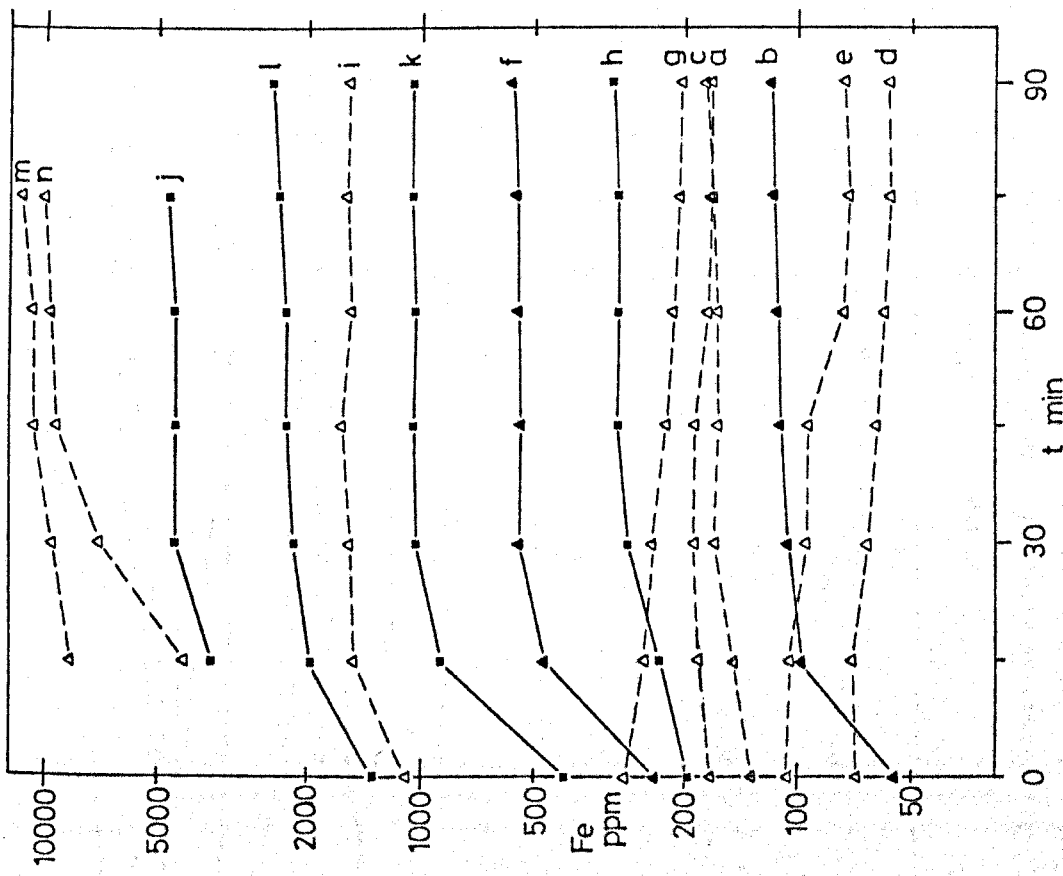


Figure A.11: Iron released from various Silvermines carbonate samples at 90°C digestion (2M acetic acid). For key see next page.

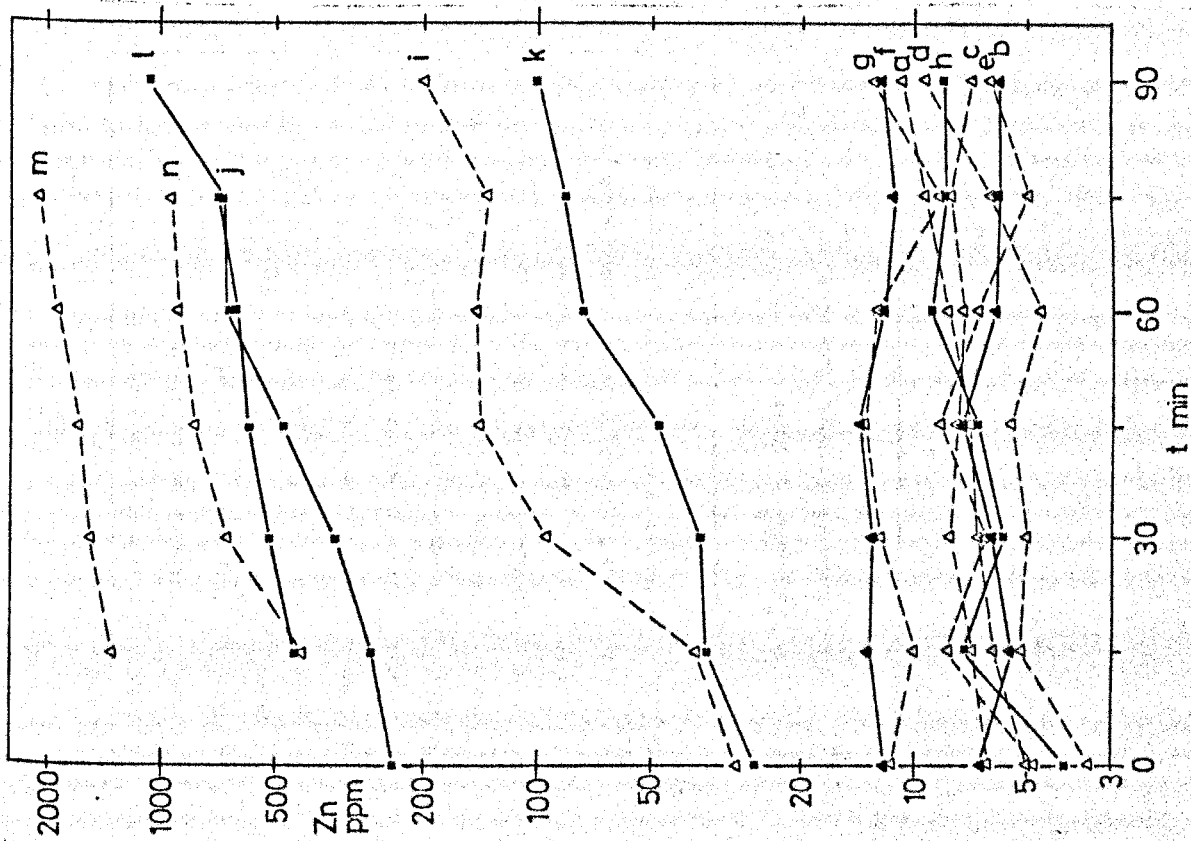


Figure A.12: Zinc release from Silvermines carbonate samples at 90°C digestion (2M acetic acid). For key see next page.

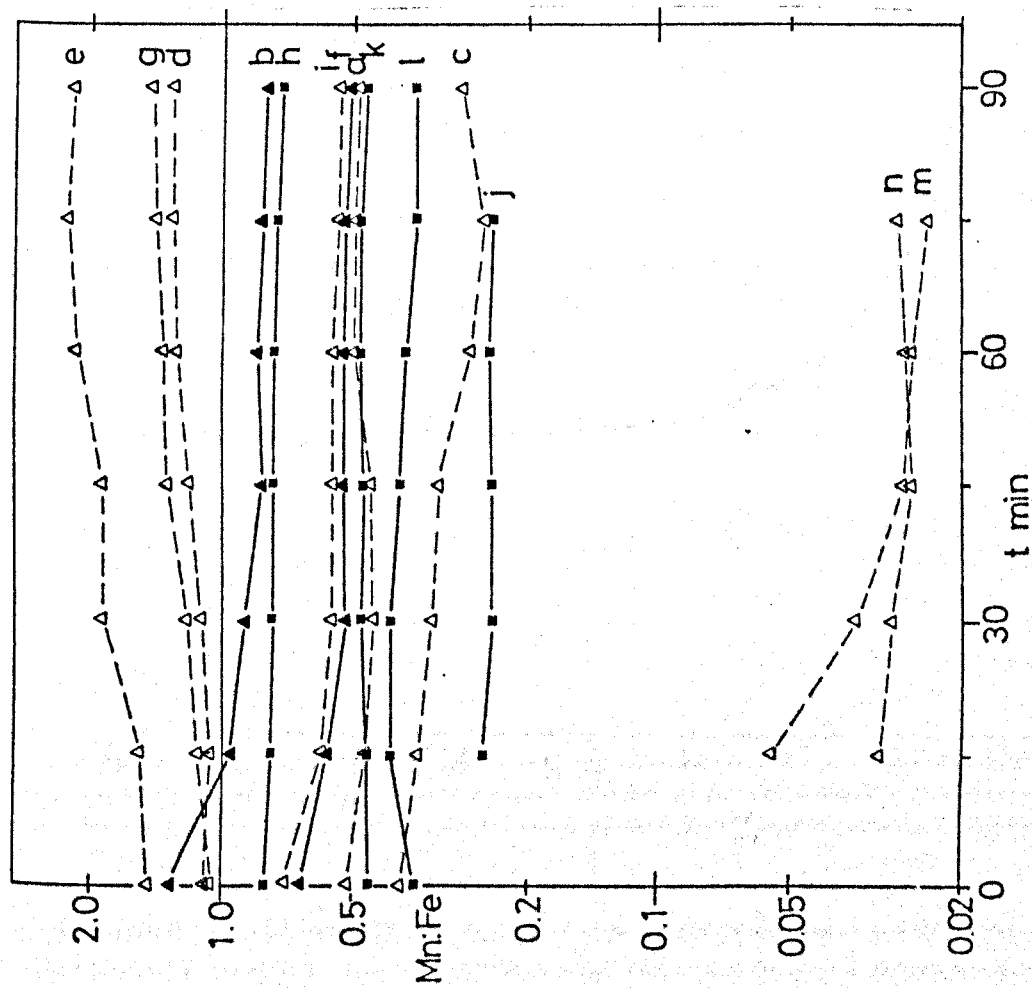


Figure A.13: Comparison between Mn and Fe release from Silvermines carbonate samples at 90°C digestion (2M acetic acid). The ratio Mn:Fe is shown. For key see next page.

SAMPLE	DESCRIPTION
a KL655	Pure mudbank limestone
b KL656	Dolomitic mudbank limestone
c KL659	Pure mudbank limestone
d KL663	" "
e KL666	" "
f KL696	Dolomitic mudbank limestone
g KL729	Impure mudbank limestone
h V19.1	Dolomitised mudbank limestone
i V19.6	Stromatolitic Reef Limestone (trace pyrite, ZnS)
j V21.5	Dolomite Breccia (minor ZnS, pyrite)
k B139.1	Pyritic Dolomite Breccia (trace ZnS)
l B139.5	Pyritic Dolomitic Breccia (muddy, minor ZnS)
m S2.4	Massive Pyrite, ZnS (only minor carbonate)
n S2.5	" " " " " "
Δ	Limestone (2% Mg)
▲	Dolomitic Limestone (2 - 7% Mg)
■	Dolomite (7% Mg)

Key for Figures A.10 to A.13.

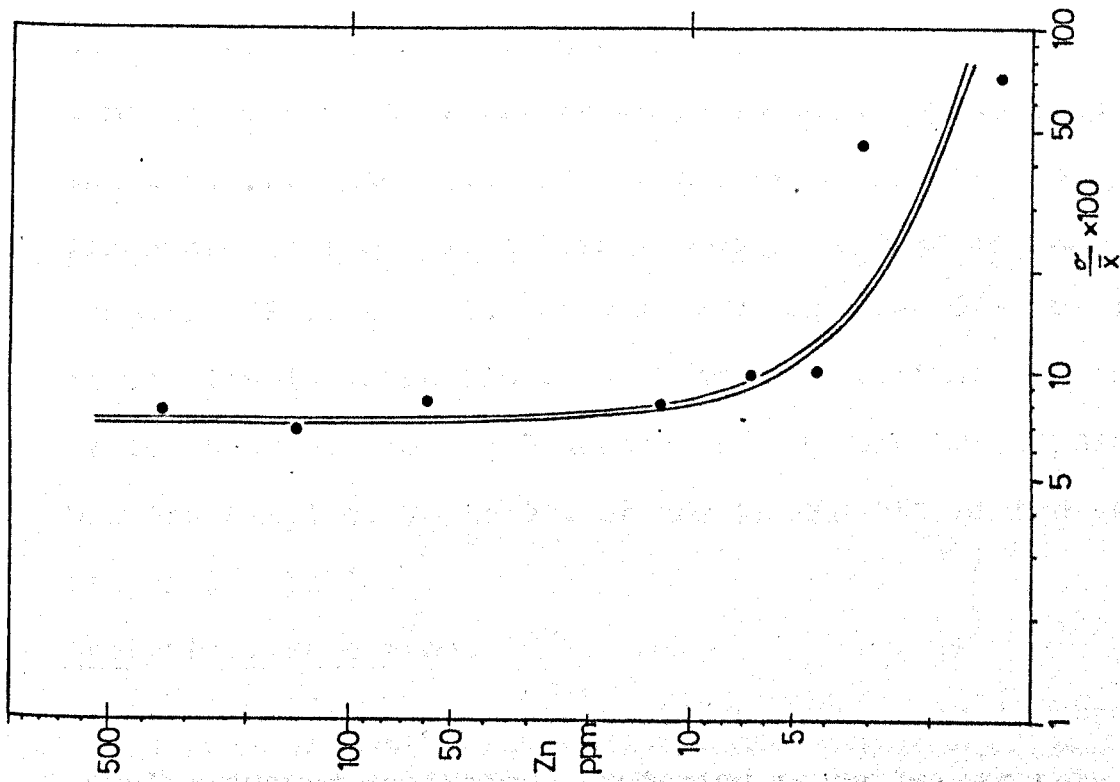


Figure A.14: Plot of zinc concentration against $\frac{o}{\sigma} \times 100$, showing poor precision levels below 5 ppm, for hot 2M acetic acid digestion. Data from Table A.7.

cluded dolomitic, non-dolomitic, impure, pyritic and zinc-rich examples. Of the limestone samples (1,2,4), 80 to 90% of the total Mn is leached, whereas in the dolomitic samples (3,5,6) this figure drops to 65 to 70%. Iron and zinc are also quite thoroughly leached in the pure limestone sample (1), but only weakly leached in the impure samples, (2 to 6), with between 60% and over 90% remaining in the insoluble portion. Even after a further 30 minutes of leaching of the argillaceous and Fe- and Zn-sulphide bearing samples, 70 to 90% of the Zn and 95% of the Fe remain insoluble.

Analytical Precision.

Initial tests on Mn content of 8 dolomite and limestone samples showed analytical precision to be better than 10% at 95% confidence limits, for the 1 hour leach, hot 2M acetic acid, digestion technique (Table A.6). Further repeats on a number of representative samples were carried out to determine the precision levels for Fe, Zn and Mg, as well as for Mn (Table A.7). For Mn, Fe and Mg, precision is generally better than 10% at 95% confidence limits. If pyrite is present in the sample, however, Fe precision levels deteriorate because of weak leaching from the sulphide in the high temperature attack.

Analytical precision for zinc is poorer because of its presence largely as a sulphide, only partially leached by the dissolution technique. At low levels of zinc in the rock (below 10 ppm), precision is very poor, because of proximity to the lower limit of detection of the analytical method (Figure A.14).

Sample	Type	n	\bar{x}	σ	$\frac{\bar{x}}{\sigma}$	X 100	range
V17.1	Dol	10	238	5.1	2.14	230 - 244	
V17.9	Lst	10	3931	66.5	1.69	3831 - 4024	
V20.6	Lst	10	1048	10.3	0.98	1031 - 1063	
V23.1	Lst	10	142	4.2	2.94	133 - 148	
V28.7	D/Lst	10	2897	23.7	0.82	2864 - 2951	
S6.1	Dol	10	1305	30.6	2.34	1259 - 1364	
B141.3	Lst	10	528	9.9	1.88	518 - 542	
B144.6	Dol	10	1392	11.7	0.84	1372 - 1402	

Dol = dolomite
D/Lst = dolomitic limestone
Lst = limestone

Table A.6: Initial analytical precision tests for manganese, using 2M hot acetic acid, 1 hour digestion, on carbonate samples from the Silvermines area. All concentrations in ppm.

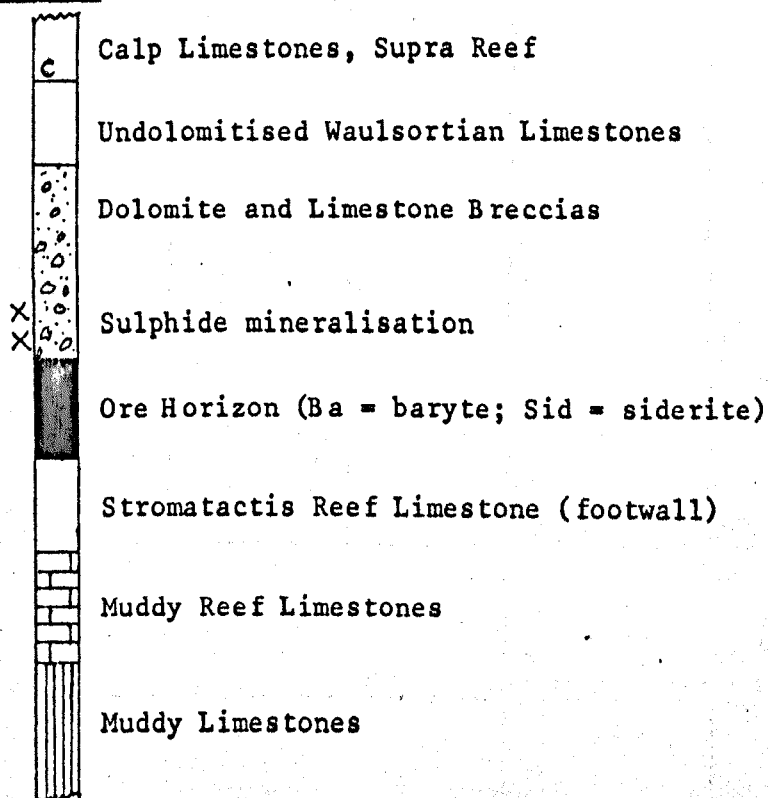
SAMPLE ELEMENT	N	\bar{x}	μ	$\frac{\mu}{\bar{x}} \times 100$	SAMPLE NATURE
KL655 Mn ppm	7	92.3	3.2	3.47	Pure limestone
Fe ppm	7	195.4	6.1	3.11	
Zn ppm	7	6.6	0.65	9.86	
Mg %	7	0.372	0.007	1.88	
KL660 Mn ppm	8	95.8	2.82	2.95	Dolomitic limestone
Fe ppm	8	98.9	5.77	5.83	
Zn ppm	8	4.2	0.42	10.0	
Mg %	8	3.63	0.074	2.04	
KL696 Mn ppm	8	161.6	3.11	1.92	Dolomitic limestone
Fe ppm	8	292.6	7.37	2.52	
Zn ppm	8	12.4	1.00	8.07	
Mg %	8	6.60	0.109	1.65	
B139.1 Mn ppm	8	493.8	6.61	1.34	Dolomite Breccia
Fe ppm	8	1029.1	25.3	2.46	
Zn ppm	8	141.1	9.64	6.83	
Mg %	8	11.01	0.136	1.24	
AP100 Mn ppm	13	91.6	8.14	8.89	Pure limestone
Fe ppm	13	175.6	16.5	9.40	
Zn ppm	12	3.14	1.44	45.9	
Mg %	9	0.42	0.012	2.91	
AP101 Mn ppm	10	68.4	2.37	3.46	Pure limestone
Fe ppm	10	116.8	6.56	5.61	
Zn ppm	10	1.23	0.881	71.6	
Mg %	10	0.402	0.006	1.57	
B139.B Mn ppm	10	529.3	38.9	7.35	Dolomite Breccia
* Fe ppm	10	1041	49.5	4.57	
Zn ppm	10	56.8	4.57	8.05	
B139.6 Mn ppm	10	3361	236.8	7.04	Dolomite Breccia
* Fe ppm	9	5010	339.1	6.77	
Zn ppm	9	346	27.5	7.96	

Table A.7: Analytical precision tests on carbonate samples from Silvermines area, using 2M hot acetic acid, 1 hour digestion. The two samples marked * were analysed without topping up loss due to evaporation on the sandbath, hence the poorer precision.

APPENDIX III - Hanging Wall and Footwall Profiles.

In these diagrams, $(Mn+Fe)/2$ and $Mn:Fe$ are plotted on logarithmic scales.

Figure A.0: Key for Figures A.1 to A.15.



Sections arranged in approximate E-W sequence, followed by footwall sections in same order:

Figure A.1 - W4, W5, W6, W7.

Figure A.11 - V1, B 139.

A.2 - V41, V42.

A.12 - M1.

A.3 - S2, S8, S6.

A.13 - B8.

A.4 - V21, V28.

A.14 - B4.

A.5 - 75/2, V23, V24.

A.15 - 76/3.

A.6 - G217.

A.7 - V17, M5.

A.8 - Y1, K38, K37.

A.9 - B 141, B 143.

A.10 - 77/1, 76/3.

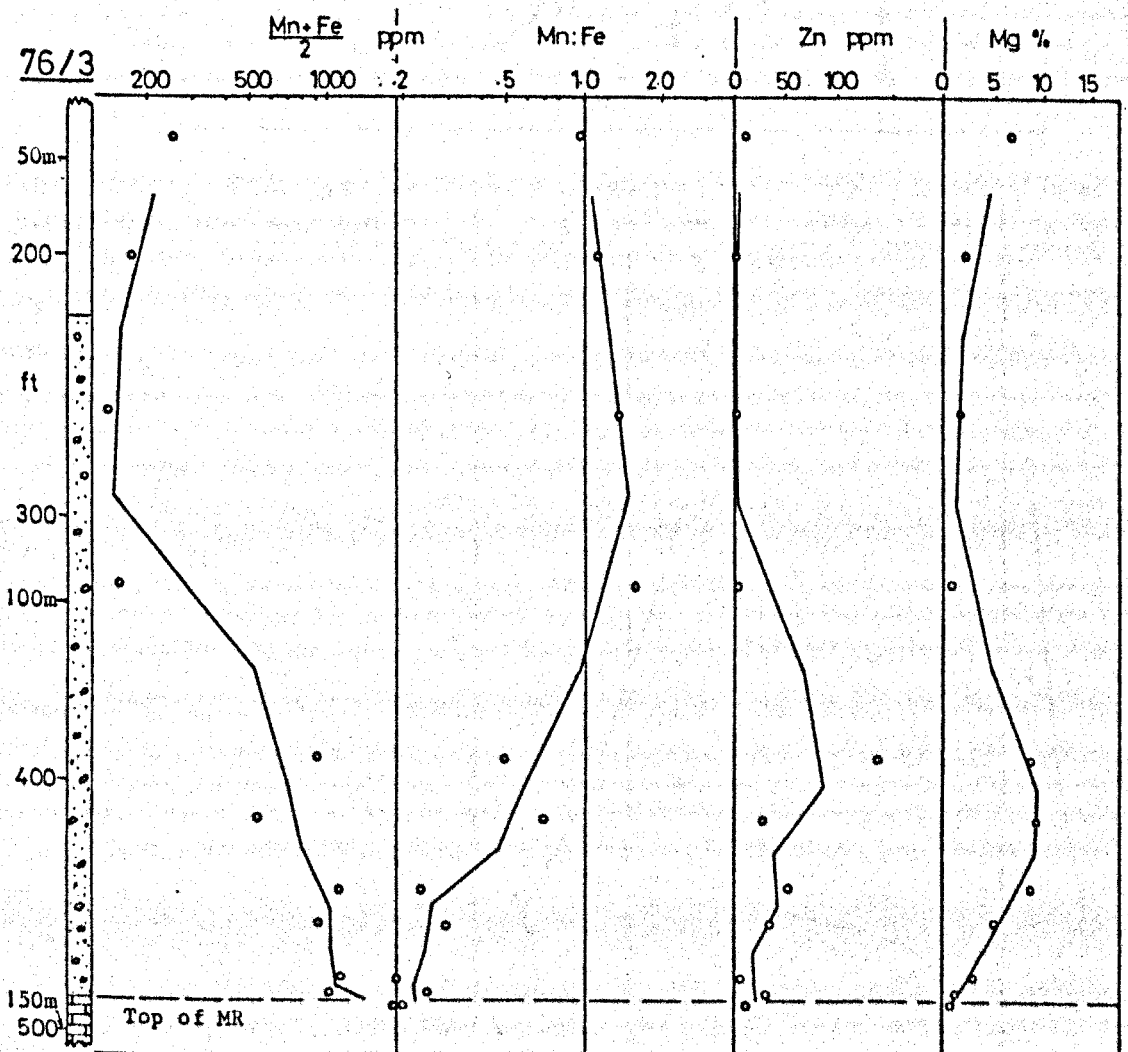
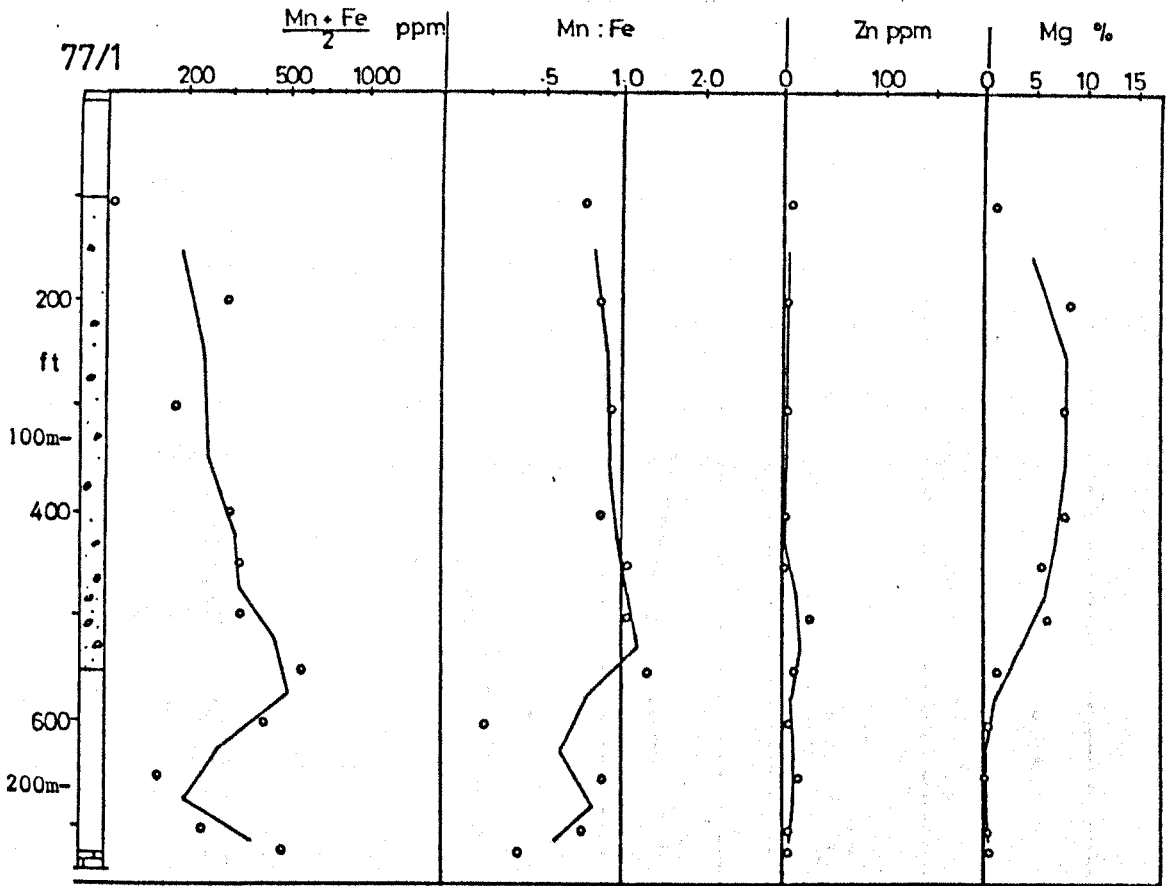


Figure A.10: Vertical profiles of boreholes 77/1 and 76/3 at Silvermines. Solid lines join mid-points between adjacent samples. For key see Figure A.0.

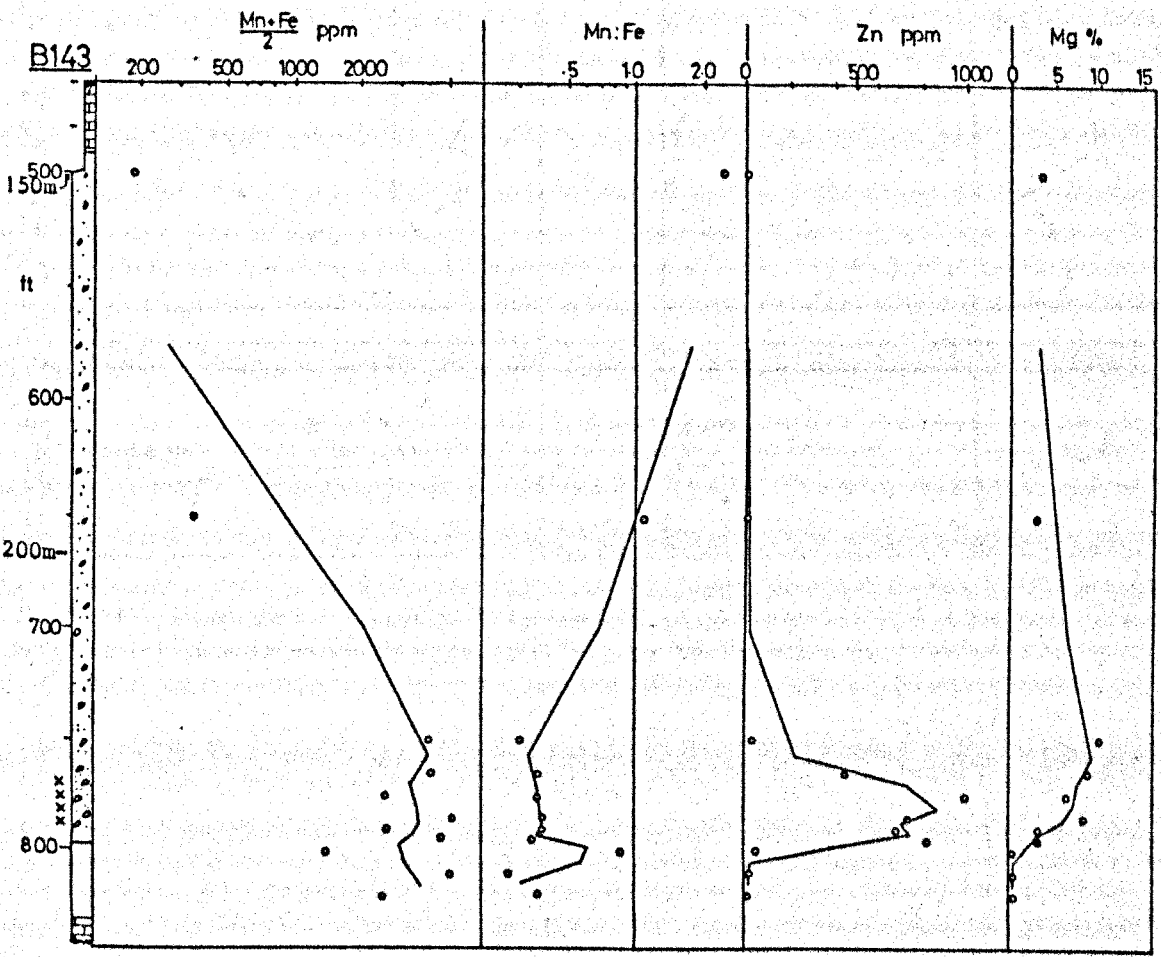
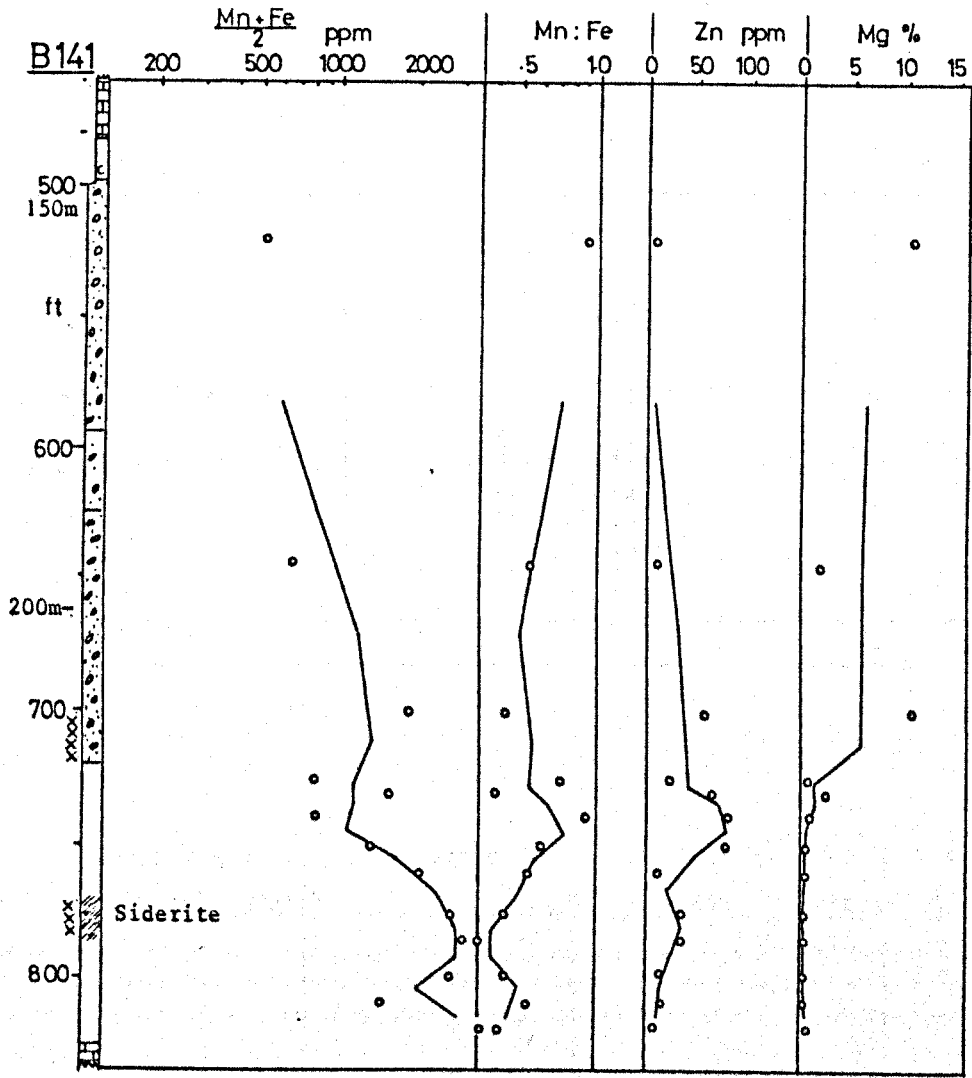


Figure A.9: Vertical geochemical profiles of boreholes B141 and B143 at Silvermines. Solid lines join mid-points between adjacent samples. For key see Figure A.0.

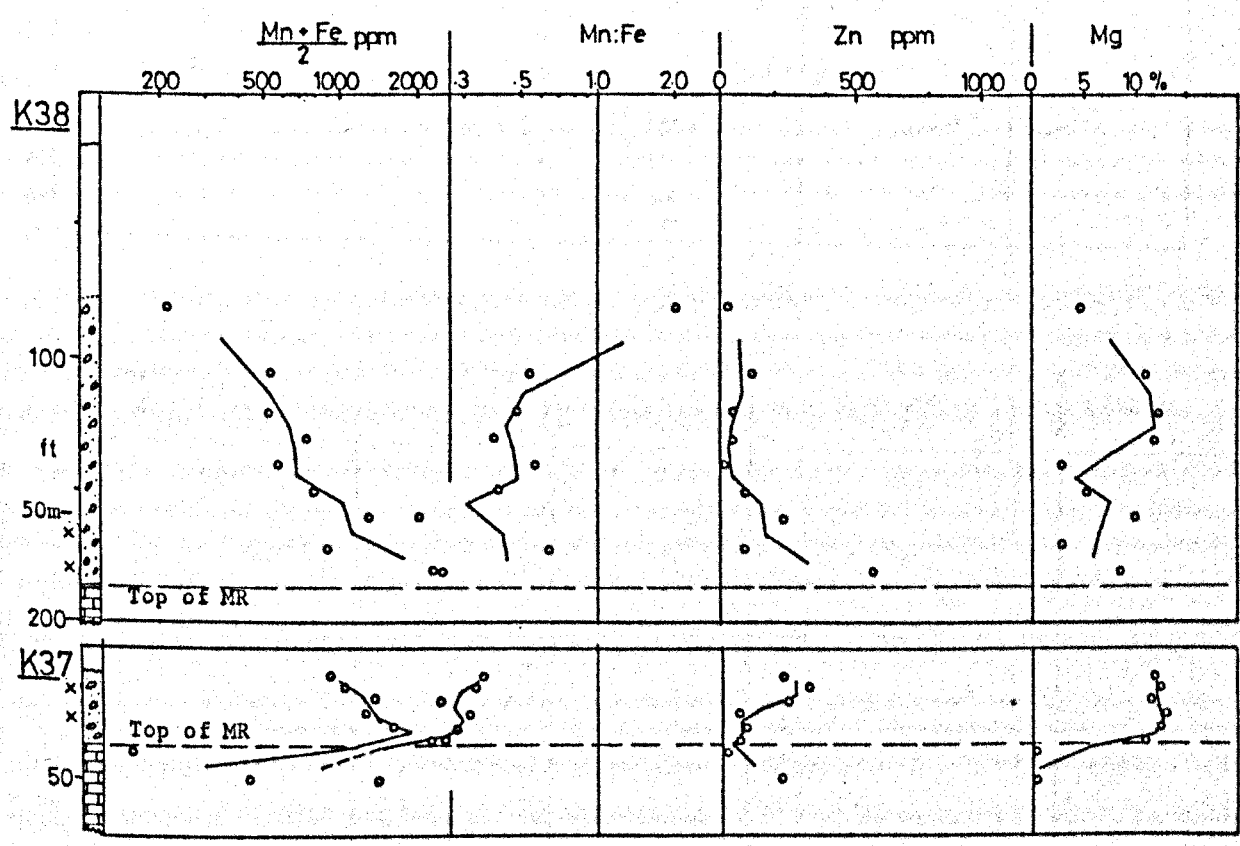
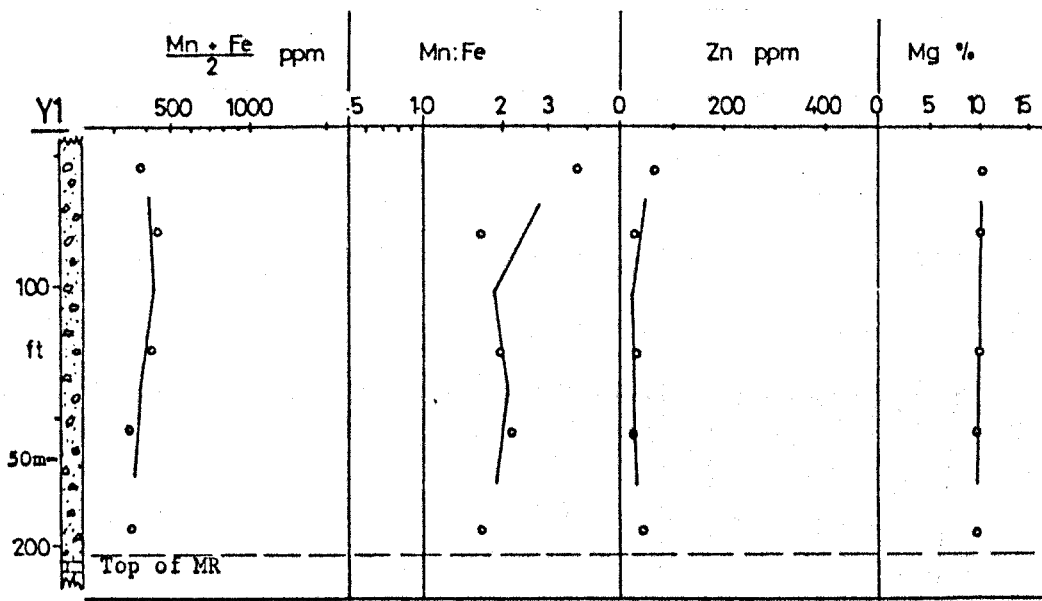


Figure A.8: Vertical geochemical profiles of boreholes Y1, K38 and K37 at Silvermines. Solid lines join mid-points between adjacent samples. For key see Figure A.0.

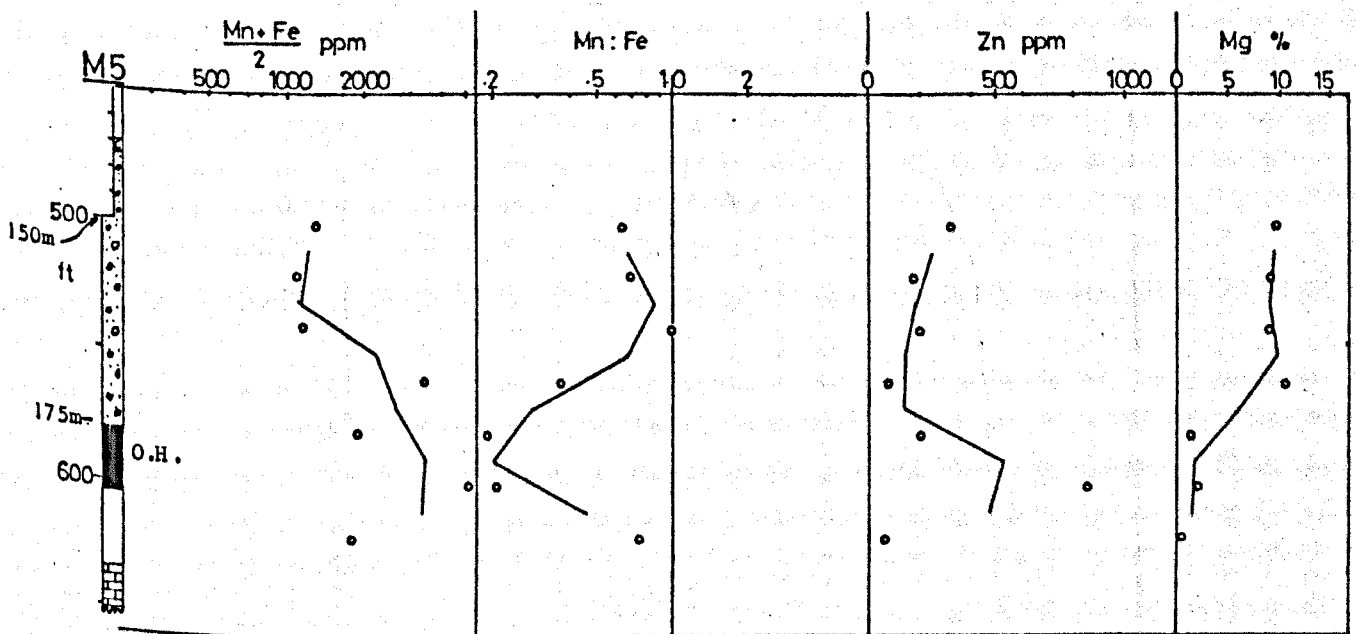
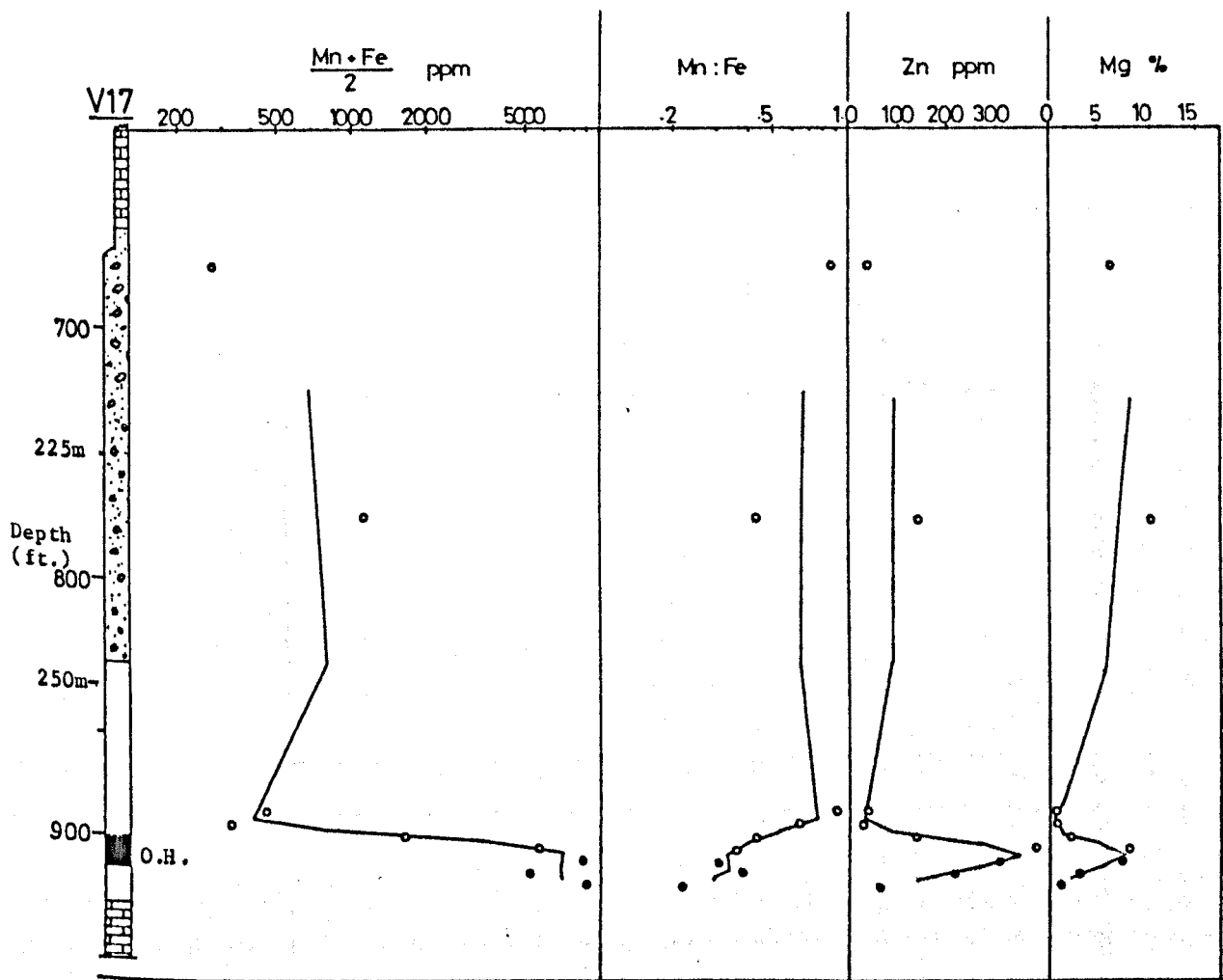


Figure A.7: Vertical geochemical profiles of boreholes V17 and M5 at Silvermines. Solid lines join mid-points between adjacent samples. For key see Figure A.0.

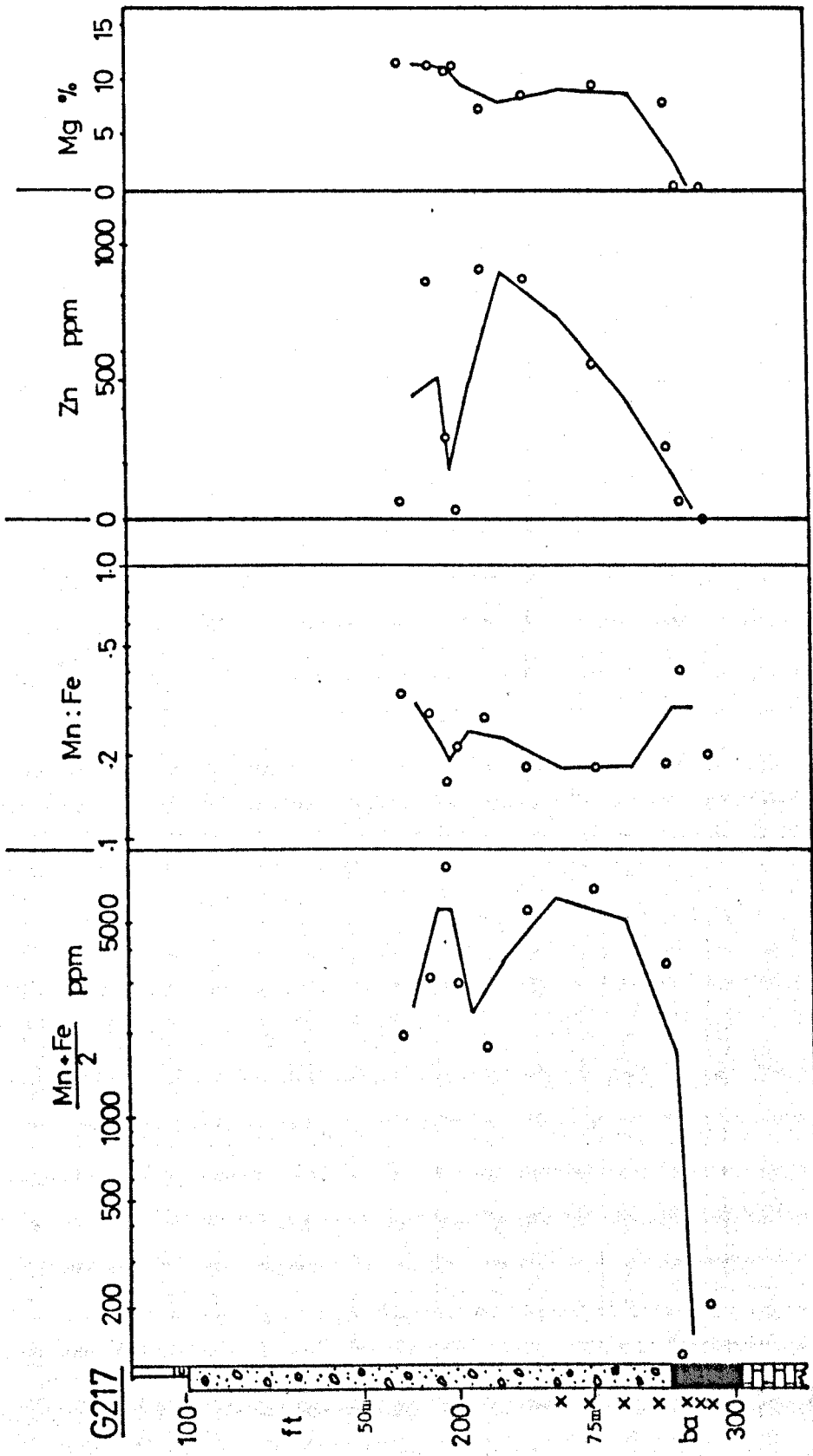


Figure A.6: Vertical geochemical profile of borehole G217 at Silvermines. Solid lines join mid-points between adjacent samples. For key see Figure A.0.

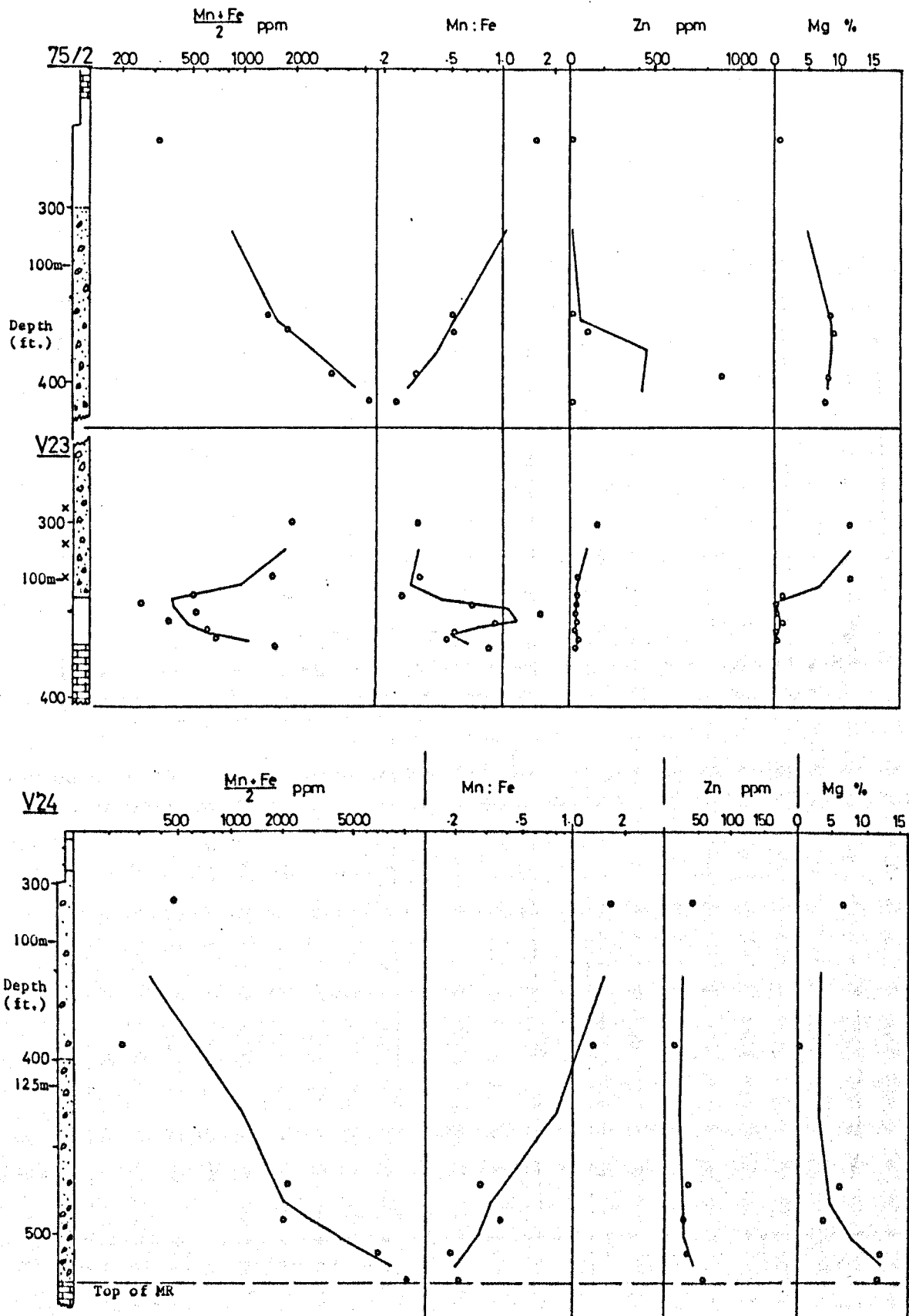


Figure A.5: Vertical profiles of boreholes 75/2, V23 and V24 at Silvermines. Solid lines join mid-points between adjacent samples. For key see Figure A.0.

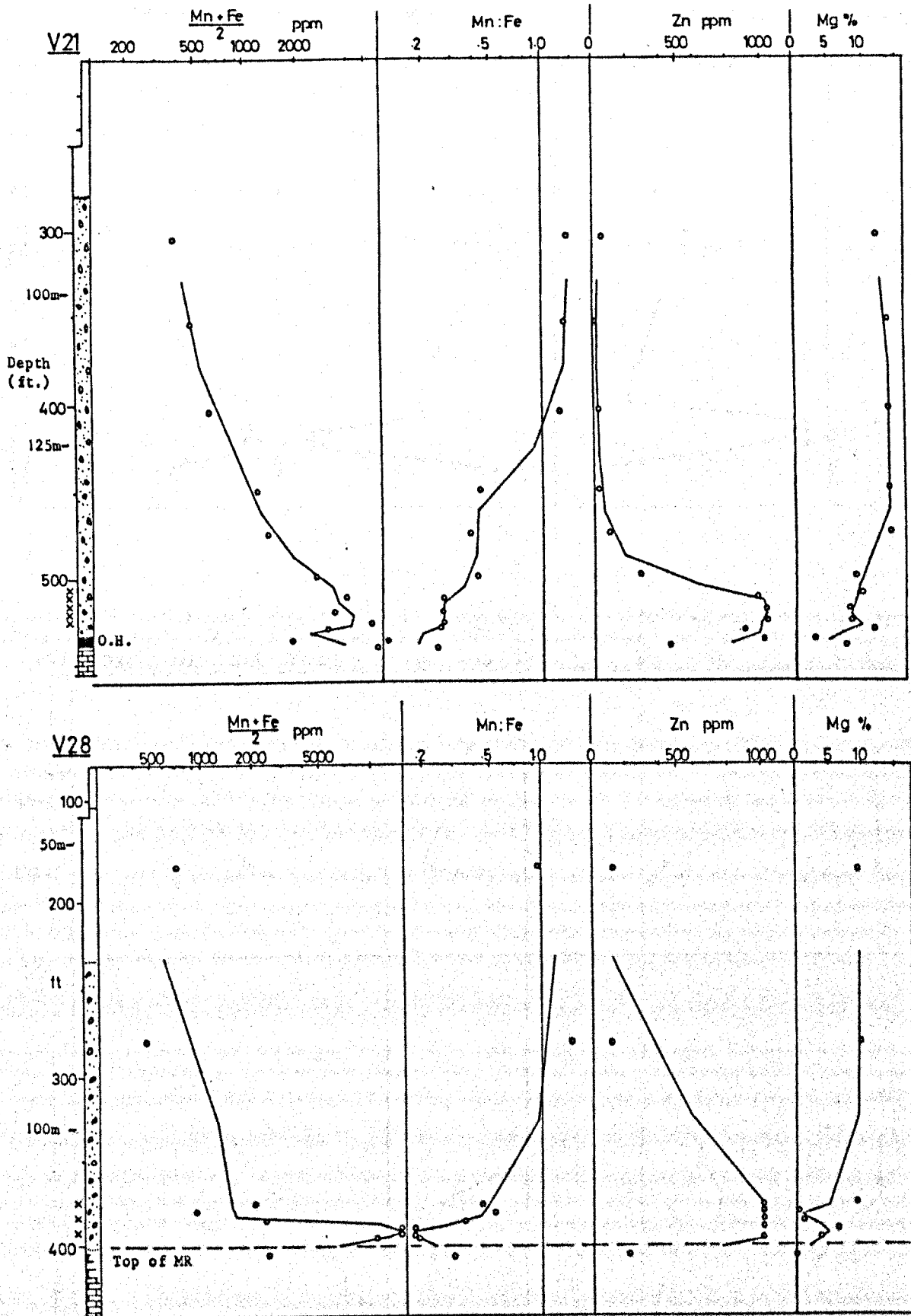


Figure A.4: Vertical geochemical profiles of boreholes V21 and V28 at Silvermines. Solid lines join mid-points between adjacent samples. For key see Figure A.0.

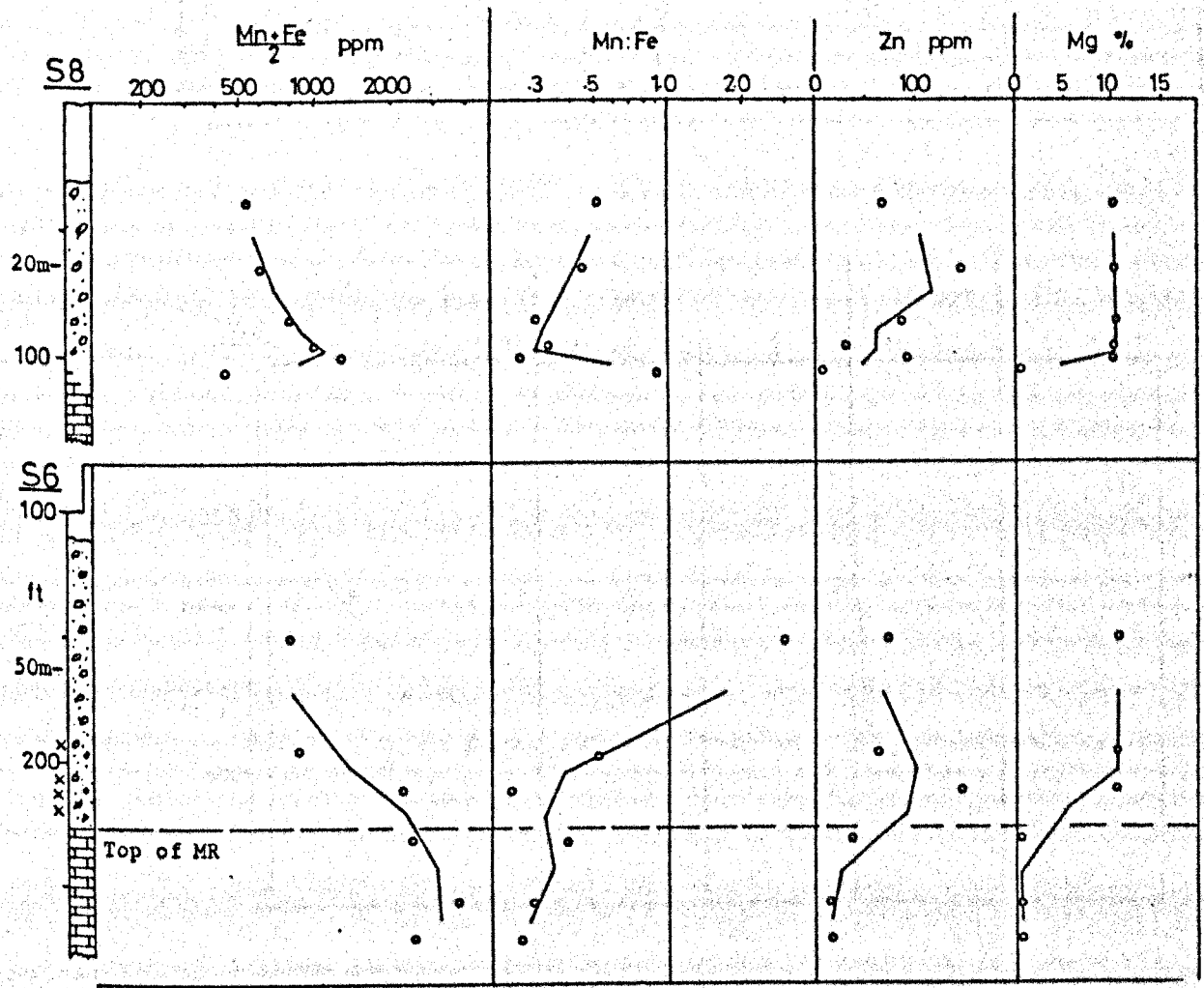
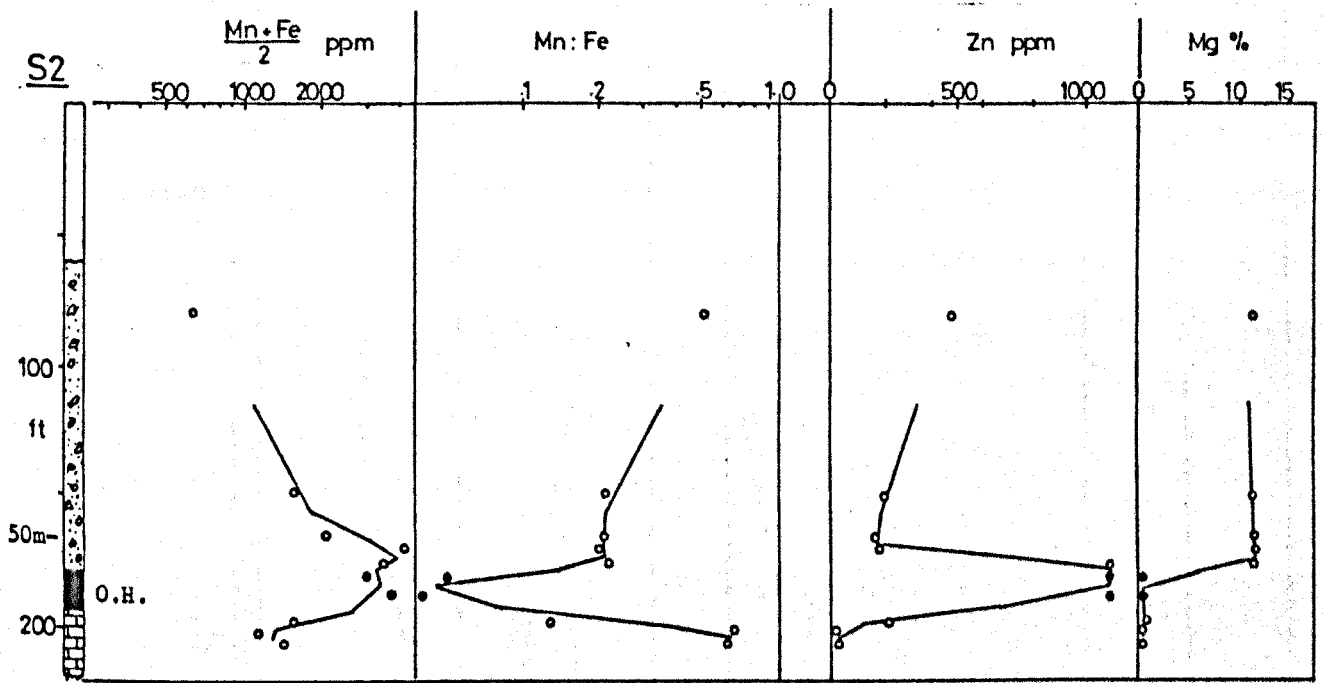


Figure A.3: Vertical geochemical profiles of boreholes S2, S8 and S6 at Silvermines. Solid lines join mid-points between adjacent samples. For key see Figure A.0.

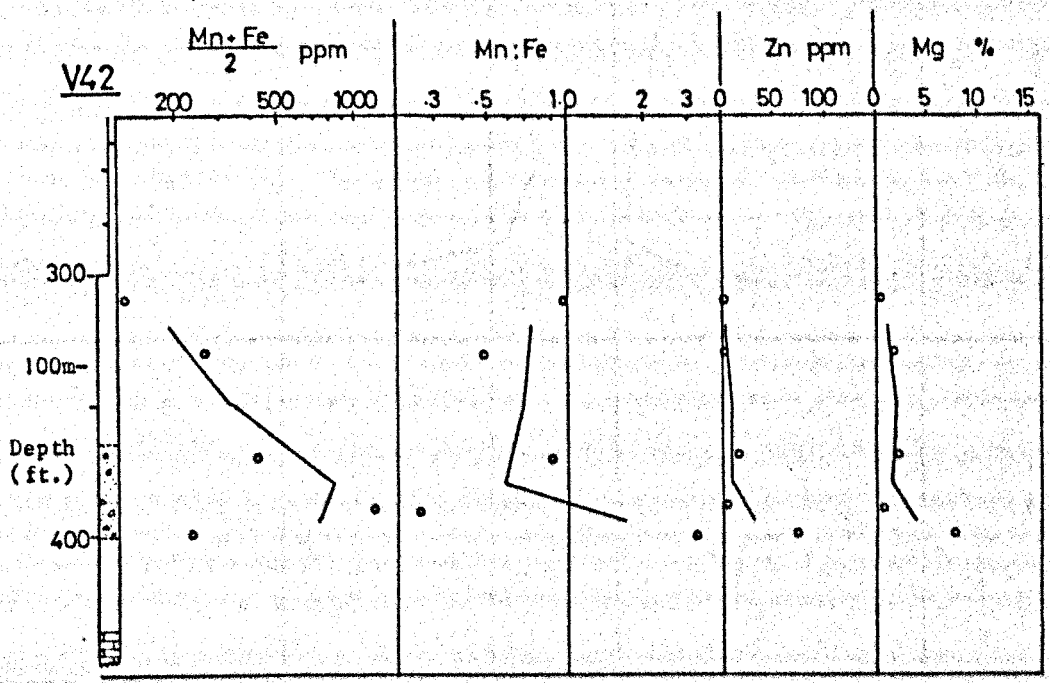
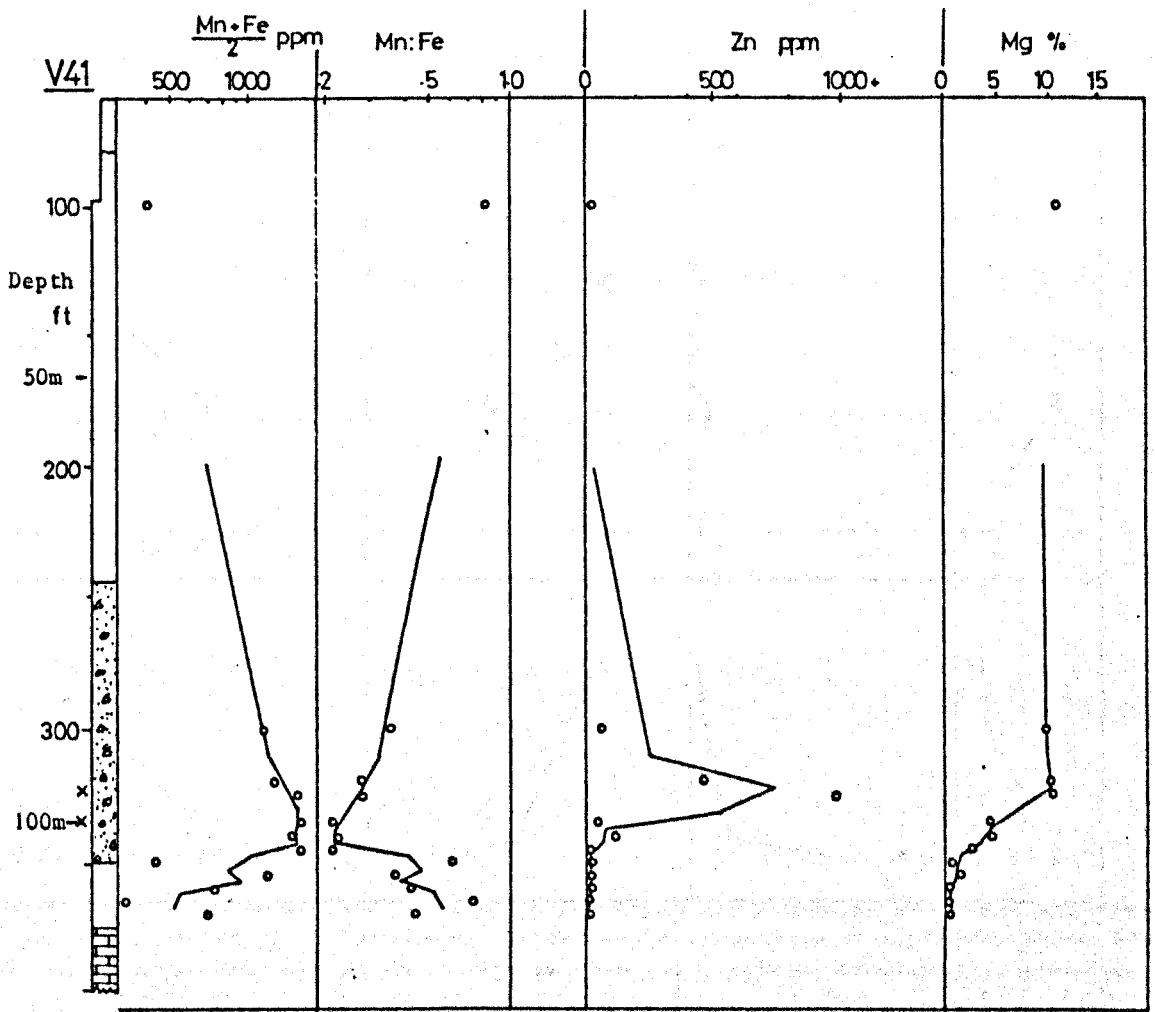


Figure A.2: Vertical geochemical profiles of boreholes V41 and V42 at Silvermines. Solid lines join mid-points between adjacent samples. For key see Figure A.0.

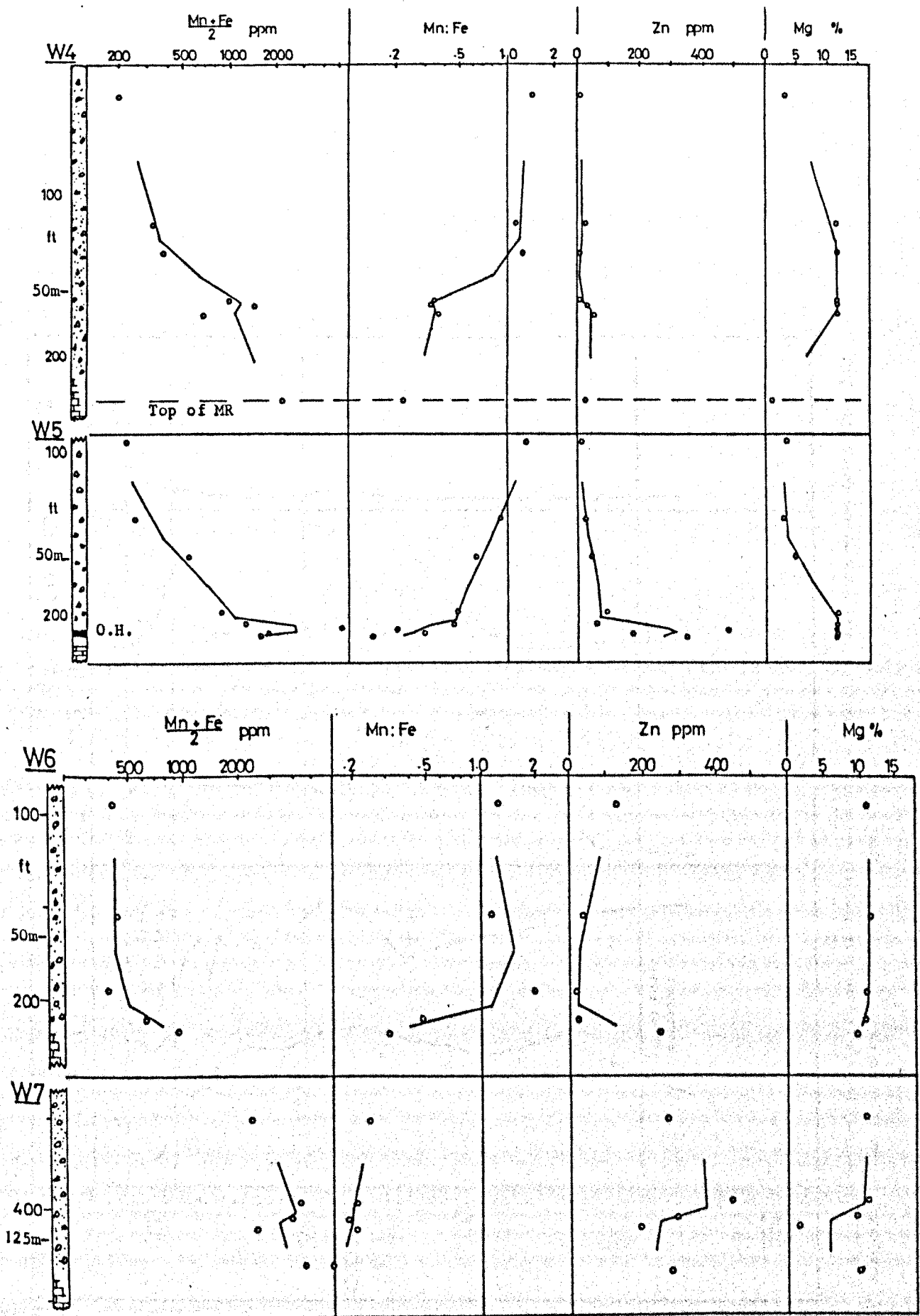


Figure A.1: Vertical geochemical profiles of boreholes W4, W5, W6, and W7 at Silvermines. Solid lines join mid-points between adjacent samples. For key see Figure A.0.

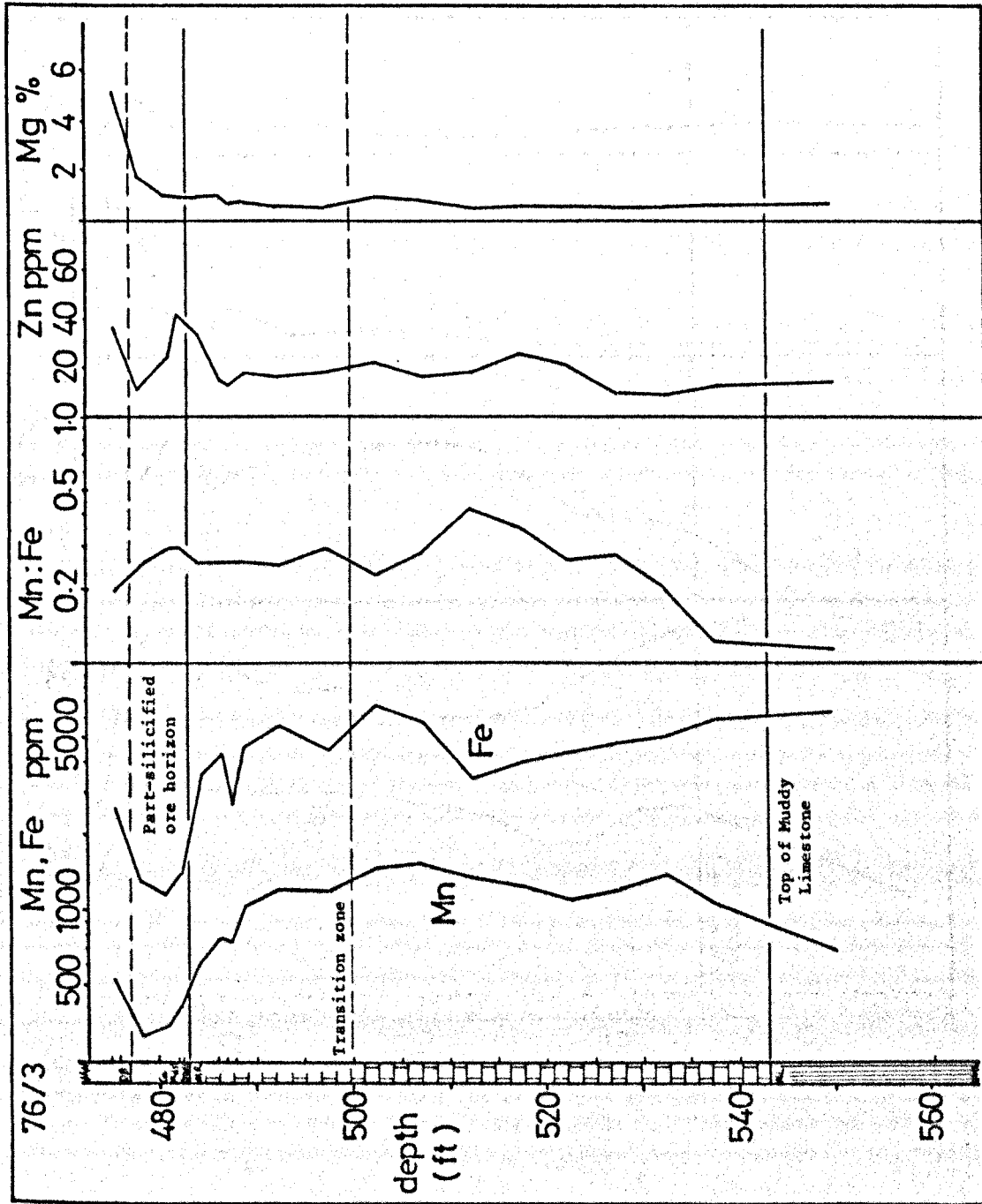


Figure A.15: Vertical profile of immediate footwall sediments in borehole 76/3 at Silvermines. Solid lines join mid-points between adjacent samples. For key see Figure A.0.

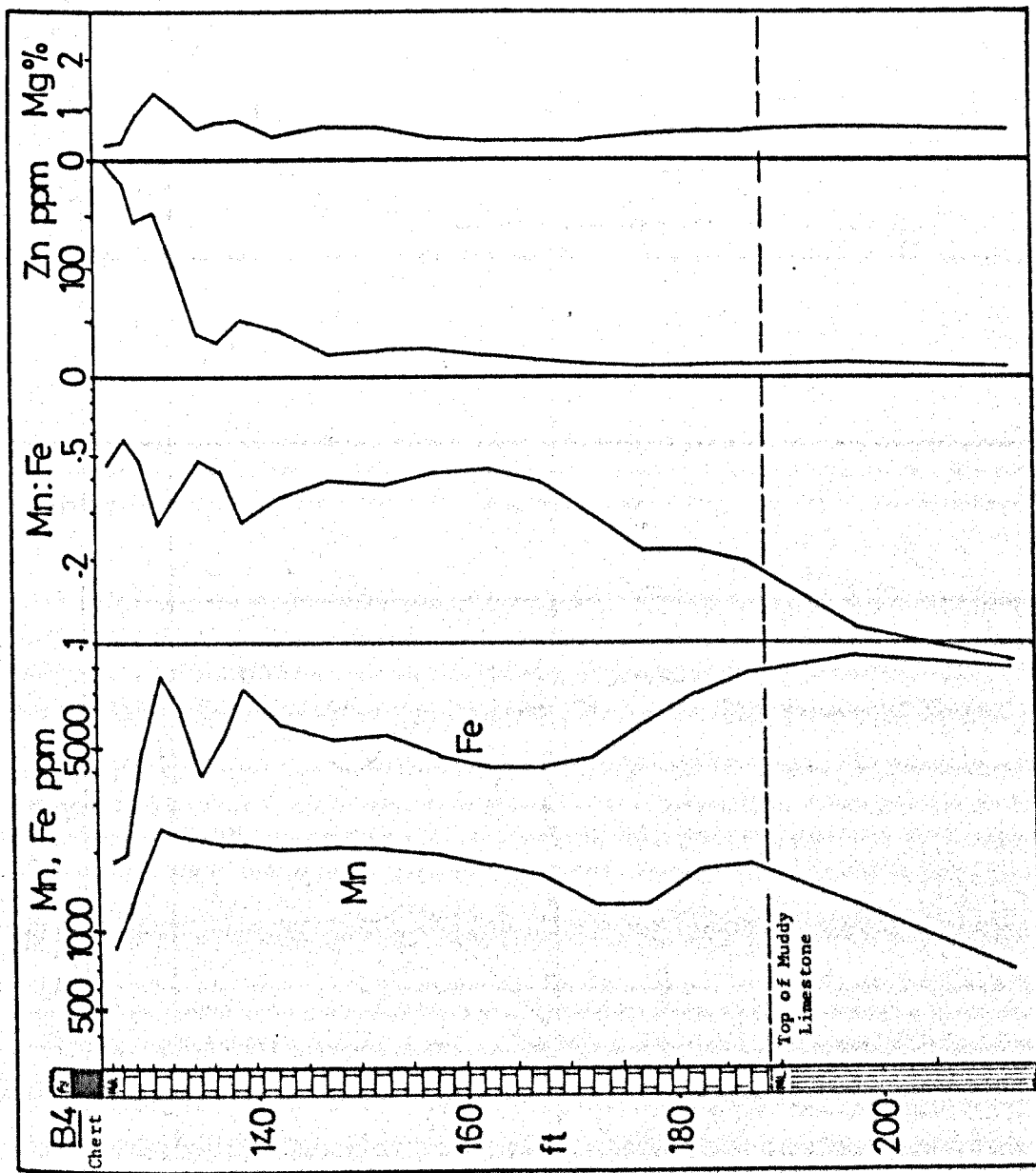


Figure A.14: Vertical profile of immediate footwall sediments in borehole B4 at Silvermines. Solid lines join mid-points between adjacent samples. For key see Figure A.0.

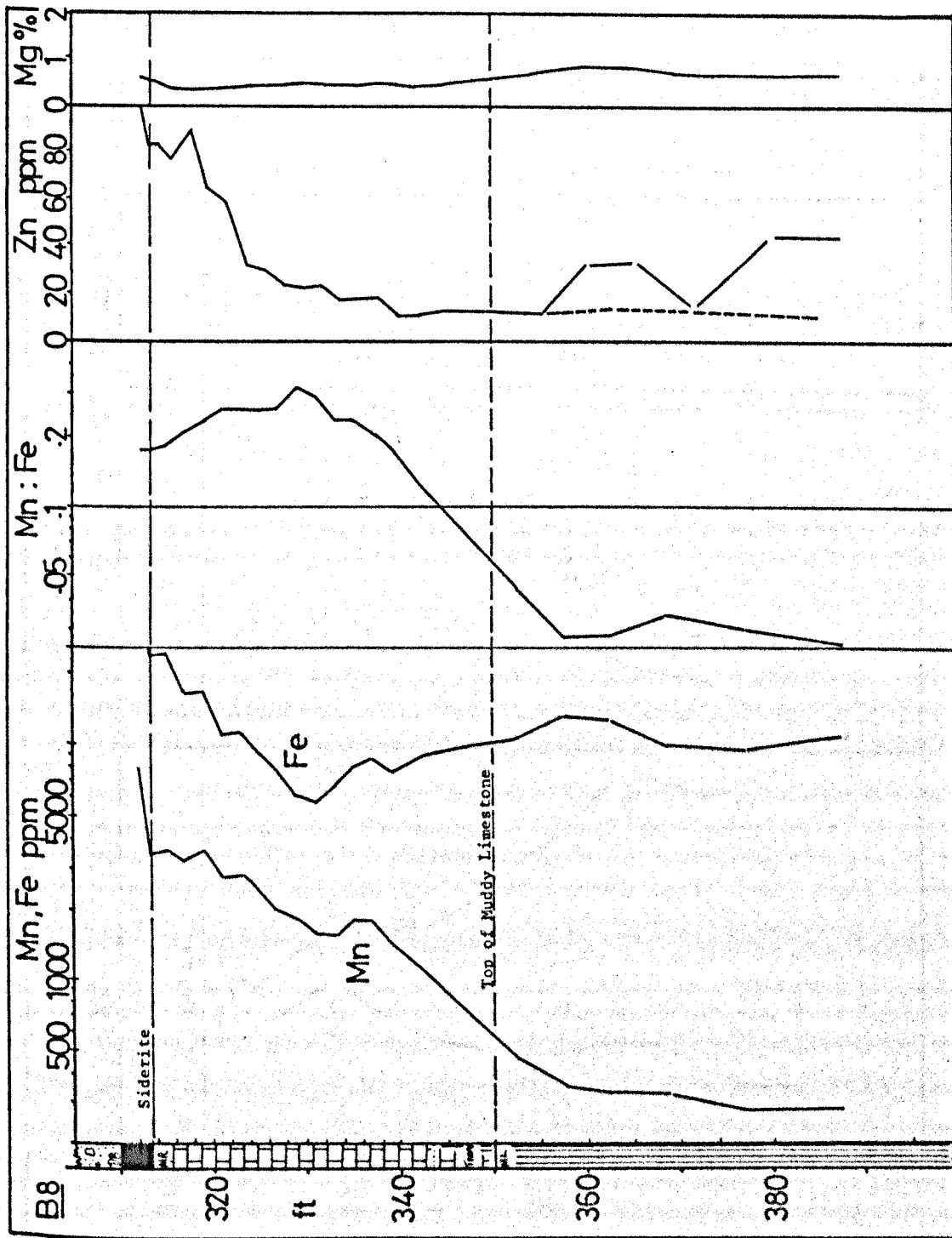


Figure A.13: Vertical profile of immediate footwall sediments in borehole B8 at Silvermines. Solid lines join mid-points between adjacent samples. For key see Figure A.0.

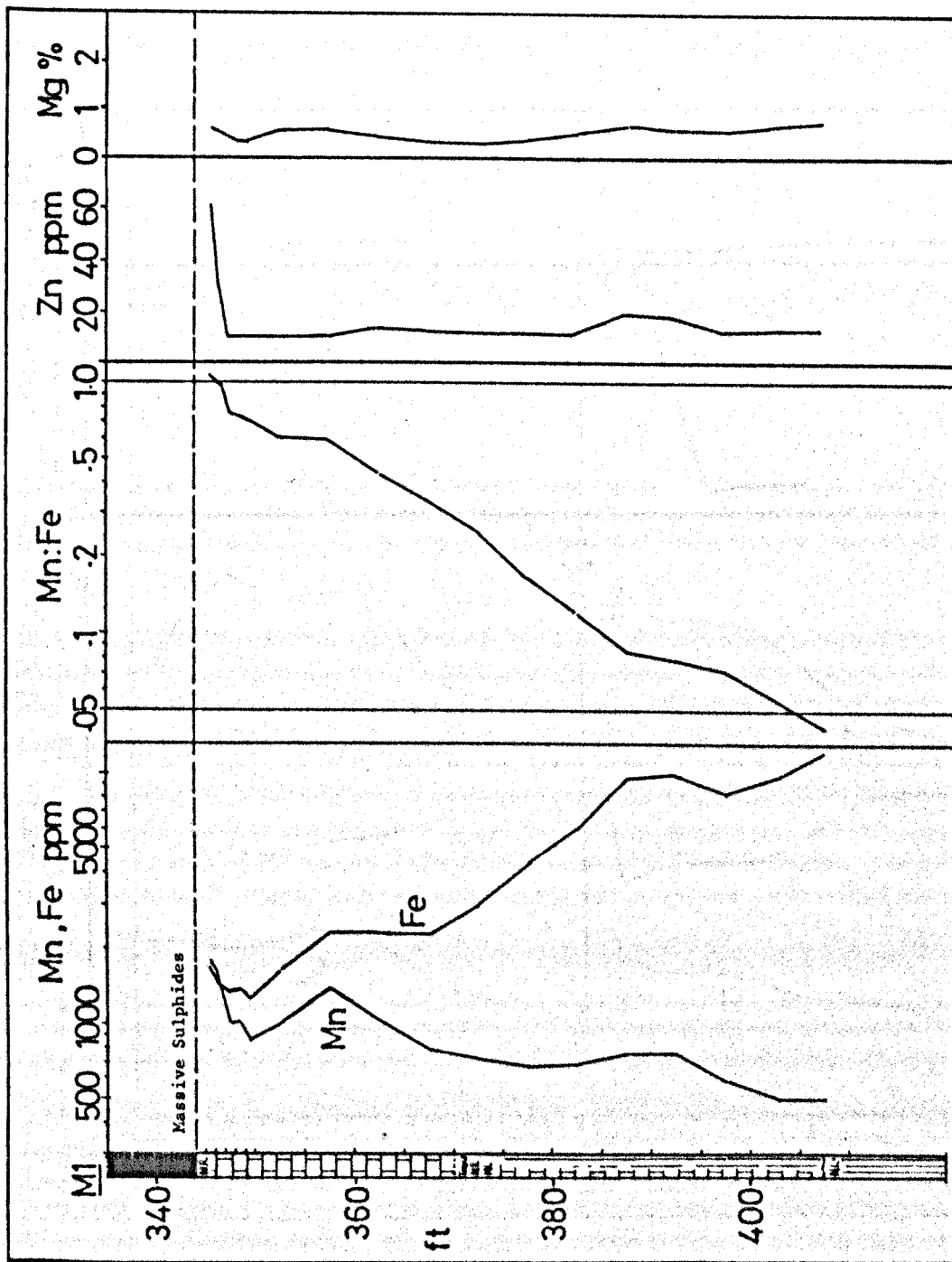


Figure A.12: Vertical profile of immediate footwall sediments in borehole M1 at Silvermines. Solid lines join mid-points between adjacent samples. For key see Figure A.0.

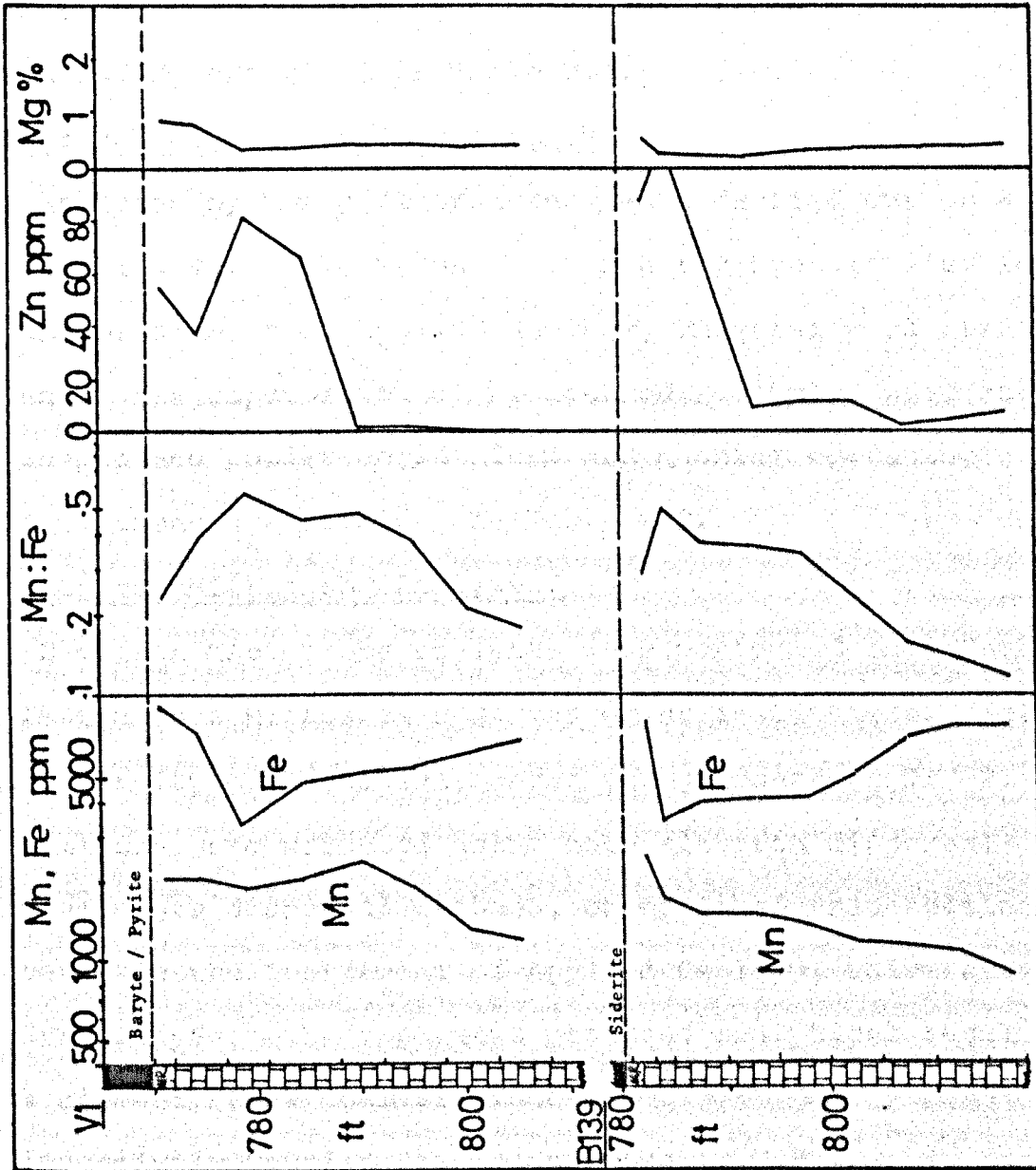


Figure A.11: Vertical profiles of immediate footwall sediments in boreholes VI and B144 at Silvermines. Solid lines join mid-points between adjacent samples. For key see Figure A.0.

APPENDIX II - Machine Operating Conditions.

Atomic Absorption Spectrophotometry.

Sample preparation and dissolution techniques are outlined in Chapter 2 and Appendix I. Analyses were performed on an Instrumentation Laboratories I.L.251 Spectrophotometer at the Department of Applied Geology, University of Strathclyde. Operating conditions for the elements Mn, Fe, Zn and Mg are given in Table B.1.

X-ray Fluorescence Spectrometry.

Analyses by x-ray fluorescence were carried out on a Phillips P.W. 1410 Manual Vacuum X-ray Spectrometer in the Department of Applied Geology, University of Strathclyde, under the supervision of M. MacLeod. Samples were analysed in pressed powder pellet form and machine operating conditions are outlined in Table B.2.

Electron Microprobe Analyses.

Electron Microprobe analyses were performed on a Cambridge Instruments Microscan 5 at the Grant Institute of Geology, University of Edinburgh, under the guidance of Dr. P. Hill. Analyses were produced using both electron dispersal and wavelength dispersal methods, on polished thin sections prepared in the Department of Applied Geology, University of Strathclyde. The apparatus produced analytical results as % element, to 4 decimal places.

Inductively Coupled Plasma Analyses (I.C.P.).

Analyses were conducted at King's College, London, on a Phillips 54-Channel Inductively Coupled Plasma Emission Spectrometer, by Dr. N. Walsh, following aqua-regia dissolution of rock powder (Programme B1).

Element	Wavelength (nm)	Lamp Current (mA)	Slit Width (u)	P.M. Voltage (mV)	Lamp B
Mn	403.1	2.5	160	530	no
	279.3	2.5	160	620	no
Fe	248.3	5.0	80	800	no
Zn	213.9	4.0	320	700	yes
Mg	285.2	3.5	160	460	no

Table B1: Machine operating conditions for atomic absorption analysis.

Element/ oxide	Line	$2\theta^{\circ}$ (+background)	Tube	kV	mA	Counter	Collimator	Crystal	Counting time (sec)
SiO ₂	Ka	109.21 \pm 2.0	Cr	45	25	flow	coarse	PE	40 (4)
Al ₂ O ₃	Ka	145.13 \pm 2.0 -1.5	Cr	45	20	flow	coarse	PE	40 (10)
K ₂ O	Ka	58.67 \pm 1.0	Cr	45	20	flow	fine	PE	100 (20)
CaO	Kb	100.23 \pm 1.5	Cr	40	12	flow	fine	LiF ₂₀₀	20 (2)
MgO	Ka	44.50 \pm 2.0	Cr	45	20	flow	coarse	RAP	100 (40)
Mn	Ka	95.2 \pm 2.0	W	50	25	flow	fine	LiF ₂₂₀	40 (20)
Fe	Ka	85.73 \pm 2.0	W	30	10	flow	fine	LiF ₂₂₀	40 (20)
Ba	(Lb ₁ , Lb ₄)	128.95 \pm 2.7	W	50	40	flow/ scint	coarse	LiF ₂₂₀	100 (40)
Sr	Ka	35.85 \pm 1.0	W	50	25	scint	fine	LiF ₂₂₀	40 (20)
Na ₂ O	Ka	54.25 \pm .75	Cr	45	30	flow	coarse	RAP	100 (100)
Pb	(Lb ₁ , Lb ₄)	40.41 \pm .41	W	50	25	scint	fine	LiF ₂₂₀	40 (20)
Zn	Ka	60.58 \pm 1.0	W	50	25	scint	fine	LiF ₂₂₀	40 (20)
S	Ka	75.85 \pm 1.5	Cr	45	20	flow	coarse	PE	40 (20)
Kb	Ka	37.99 \pm 1.0	W	50	25	scint	fine	LiF ₂₂₀	40 (20)

Table B2: Machine operating conditions for X-ray fluorescence analysis.

ACKNOWLEDGEMENTS.

This study has been made possible by input from a large number of colleagues, friends, institutions and exploration companies.

Firstly, I wish to thank my supervisor, Mike Russell, for instigating the research, and for his guidance and encouragement throughout.

Funding for the research studentship was provided by the Natural Environment Research Council.

Fieldwork was supported by several exploration companies: N.L. Petroleum Services; Mogul of Ireland; Riofinex; Noranda; and also by the Institution of Mining and Metallurgy. In particular, I would like to thank Blake Johnson, Ken Snyder, Robert Boyle, Arthur Williams, Stewart Taylor, Viv Byrne and Chris Morrissey.

Laboratory work was ably assisted by Murdo MacLeod, Jackie Wiles, Dougie Turner, Tom Crosbie, Peter Wallace, John Gilleece, Pete Hill, and Mike O'Neill.

Much advice and discussion was provided by my colleagues at the University of Strathclyde, Department of Applied Geology, in particular, Alan Hall, Iain Samson, Adrian Boyce, Richard Larter, Richard Patrick, Keith Nicholson, Saffron Fisk, Henry Allen, Paul Duller and Stuart Haszeldine.

I would also like to thank my parents for their encouragement, Glynis Ainsworth and Janette Forbes for their assistance, and Michele Spearman for assistance in typing the manuscript.

Finally, I wish to extend my gratitude to the people of Ireland for their warmth and cooperation during my many visits to their country - Tipperary for the All-Ireland!

REFERENCES.

- S.O. Akande and M. Zentilli (1984). Geologic, fluid inclusion and stable isotope studies of the Gays River Lead-Zinc deposit, Nova Scotia, Canada. Economic Geology Vol. 79, (1187-1211).
- I.S. Al-Aasm and J. Veizer (1982). Chemical stabilisation of low-Mg calcite: an example of brachiopods. Journal of Sedimentary Petrology Vol. 52, (1101-1109).
- G.A.K.A. Al-Kindy (1979). Trace element aureoles around some base metal mineralisation in Ireland. M.Sc. dissertation, University of Strathclyde.
- G.M. Anderson (1973). The hydrothermal transport and deposition of galena and sphalerite near 100°C. Economic Geology Vol. 68, (480-492).
- C.J. Andrew (1984). The tectono-stratigraphic controls to mineralisation in the Silvermines area, Co. Tipperary (Abstract). In: The geology and genesis of mineral deposits in Ireland, Irish Assoc. Econ. Geol. Dublin (1984).
- C.J. Andrew and J.H. Ashton (1982). Mineral textures, metal zoning and ore environment of the Navan orebody, Co. Meath, Ireland. In: Mineral Exploration in Ireland: Progress and Development, 1971-1981, Irish Assoc. Econ. Geol. Dublin 1982, (35-46).
- E. Angino and G.K. Billings (1972). Atomic Absorption Spectrophotometry in Geology. Elsevier, Amsterdam, (191pp).
- J.E. Angus, J.B. Raynor and M. Robson (1979). Reliability of experimental partition coefficients in carbonate systems: evidence for inhomogeneous distribution of impurity cations. Chemical Geology Vol. 27, (181-205).
- J.H. Ashton, D.T. Downing and S. Finlay (1984). The geology of the Navan Zn-Pb orebody, Co. Meath (Abstract). In: The geology and genesis of Mineral deposits in Ireland, Irish Assoc. Econ. Geol. Dublin (1984).
- J.P.N. Badham (1979). Sulphide ore deposits. Nature Vol. 277, (513-514).
- J.P.N. Badham (1982). Further data on the formation of ores at Rio Tinto, Spain. Transactions of the Institution of Mining and Metallurgy Vol. 91, Section B (Applied Earth Science), (26-32).
- G.B. Bailey and G.R. McCormick (1974). Chemical haloes as a guide to lode deposit ore in the Park City District, Utah. Economic Geology Vol. 69, (377-382).
- P.A. Baker, M. Kastner, J.D. Byerlee and D.A. Lockner (1980). Pressure solution and hydrothermal recrystallisation of carbonate sediments - an experimental study. Marine Geology Vol. 38, (185-203).
- G.M. Bancroft, J.R. Brown and W.S. Fyfe (1977). Quantitative X-ray Photoelectron Spectroscopy (ESCA): studies of Ba²⁺ sorption on calcite. Chemical Geology Vol. 19, (131-144).
- D. Banks (in preparation). Ph.D. Dissertation, University of Strathclyde.
- C. Barber (1974). Major and trace element associations in limestones and dolomites. Chemical Geology Vol. 14, (273-280).
- D.M. Barber, P.G. Malone and R.J. Larson (1975). The effect of cobalt ion on nucleation of calcium carbonate polymorphs. Chemical Geology Vol. 16, (239-241).

- J. Barbier (1979). *Geochemie en roches autour de quelques gites ou indices de Pb-Zn en milieu carbonate*. Bulletin Bureau Recherches Geologie et Minieres II, (1-22).
- H.L. Barnes (1979). *Geochemistry of Hydrothermal Ore Deposits*, 2nd edition, John Wiley and Sons, New York, 1979, (798pp).
- J.R. Barrett (1975). *Genesis of the Ballynoe baryte deposit, Ireland, and other British stratabound baryte deposits*. Ph.D. Dissertation, University of London.
- R.G.C. Bathurst (1971). *Carbonate sediments and their diagenesis*: Elsevier, Amsterdam, (658pp).
- R.G.C. Bathurst (1979). *Diagenesis in carbonate sediments: a review*. Geol. Rundsch. Bd. 68 (848-855).
- R.G.C. Bathurst (1980). *Stromatactis - origins related to submarine-cemented crusts in Palaeozoic mud mounds*. Geology Vol. 8, (131-134).
- R.G.C. Bathurst (1982). *Genesis of stromatactis cavities between submarine crusts in Palaeozoic carbonate mud buildups*. J. Geol. Soc. London, Vol. 139, (165-181).
- P.M.E. Beale (1976). *A litho-geochemical study at Ballinalack, Co. Westmeath, Ireland*. M.Sc. Dissertation, University of Leicester.
- A. Bencini and A. Turi (1974). *Manganese distribution in the Mesozoic carbonate rocks from Lima Valley, Northern Apennines*. Journal of Sedimentary Petrology Vol. 44, (774-782).
- R.D. Bignell, D.S. Cronan and J.S. Tooms (1976). *Metal dispersion in the Red Sea as an aid to marine geochemical exploration*. Transactions of the Institution of Mining and Metallurgy Vol. 85, Section B (Applied Earth Science), (274-278).
- G.K. Billings (1965). Atomic Absorption Newsletter, No. 4, (357).
- G.K. Billings and P.C. Ragland (1968). *Geochemistry and mineralogy of the Recent reef and lagoonal sediments south of Belize*. Chemical Geology Vol. 3, (135-153).
- J.L. Bischoff and F.W. Dickson (1975). *Seawater and basalt interaction at 200°C and 500 bars; implication for origin of seafloor heavy metal deposits and regulation of seawater chemistry*. Earth and Planetary Science Letters Vol. 25, (385-397).
- J.L. Bischoff, A.S. Radtke and R.J. Rosenbauer (1981). *Hydrothermal alteration of greywacke by brine and seawater: roles of alteration and chloride complexing on metal solubilization at 200°C and 500°C*. Economic Geology, Vol. 76, (656-676).
- D.F. Blake, D.R. Peacor and B.H. Wilkinson (1982). *The sequence and mechanism of low temperature dolomite formation: calcian dolomite in Pennsylvanian echinoderm*. Journal of Sedimentary Petrology, Vol. 52, (59-70).
- A.M. Boast, M.L. Coleman and C. Halls (1981). *Textural and stable isotopic evidence for the genesis of the Tynagh base metal deposit, Ireland*. Economic Geology, Vol. 76, (27-55).
- M.W. Bodine, H.D. Holland and M. Borcsik (1965). *Coprecipitation of manganese and strontium with calcite*. Symposium Vol. 2, Problems of Post-magmatic Ore Deposition, Prague, (401-406).
- E. Bonatti, D.E. Fisher, O. Joensuu, H.S. Rydell and M. Beyth (1972). *Iron-manganese-barium deposit from the Northern Afar Rift, Ethiopia*. Economic Geology, Vol. 67, (717-730).
- A.J. Boyce, R. Anderton and M.J. Russell (1983). *Rapid subsidence and early Carboniferous base metal mineralisation in Ireland*. Transactions of the Institution of Mining and Metallurgy Vol. 92, Section B (Applied Earth Science), (55-66).

- E.A. Boyle (1981). Cadmium, zinc, copper and barium in foraminifera tests. Earth and Planetary Science Letters, Vol. 53, (11-35).
- R.W. Boyle (1965). Geology, geochemistry and origin of the lead-zinc-silver deposits of the Keno Hill-Galena Hill area, Yukon Territory. Bulletin of the Geological Survey of Canada, No. 11, (302pp).
- U. Brand (1981). Mineralogy and chemistry of the Lower Pennsylvanian Kendrick fauna, eastern Kentucky: 1. Trace elements. Chemical Geology, Vol. 32, (1-16).
- U. Brand and J. Veizer (1980). Chemical diagenesis of a multicomponent carbonate system - 1: trace elements. Journal of Sedimentary Petrology, Vol. 50, (1219-1236).
- P.M. Brück (1982). The regional lithostratigraphic setting of the Silvermines zinc-lead and Ballynoe baryte deposits, Co. Tipperary. In: Mineral Exploration in Ireland: Progress and Developments, 1971-1981, Irish Assoc. Econ. Geol. Dublin, (162-170).
- D.E. Cameron and D.M. Romer (1970). Denison copper-silver deposit at Aherlow, Co. Limerick, Ireland. Transactions of the Institution of Mining and Metallurgy, Vol 79, (B171-B173).
- W.C. Campbell and J.M. Ottaway (1974). Determination of lead in carbonate rocks by atomic absorption spectrometry with carbon furnace atomization. Transactions of the Institution of Mining and Metallurgy, Vol. 83, (B 68-69)
- R.C. Carne (1979). Geological setting and stratiform lead-zinc-baryte mineralisation, Tom Claims, MacMillan Pass, Yukon Territory. Dept. of Indian and Northern Affairs, Report E.G.S. 1979-4.
- J.S. Carter (1982). The origin of the Irish lead-zinc deposits: a discussion. In: Mineral Exploration in Ireland: Progress and Developments, 1971-1981, Irish Assoc. Econ Geol. Dublin, (173-174).
- J.S. Carter and P.C.D. Cazalet (1984). Hydrocarbon gases in rocks as pathfinders for mineral exploration. In: Prospecting in Areas of Glaciated Terrain, 1984. Institute of Mining and Metallurgy, London, (11-20).
- C.C. Chen, R.J. Holmes, P.J. Ypma and P.W. Levy (1978). Radiation-induced thermoluminescence of limestones and dolomites containing lead-zinc deposits in Toggenburg, S.W. Africa; Charcas, Mexico; and Bisbee, Arizona. Unpublished manuscript.
- R. Chester (1965). Geochemical criteria for differentiating reef from non-reef facies in carbonate rocks. Am. Assoc. Petroleum Geol. Bull. Vol. 49, (258-276).
- R. Chester and M.J. Hughes (1967). A chemical technique for the separation of ferro-manganese minerals, carbonate minerals and adsorbed trace elements from pelagic sediments. Chemical Geology Vol. 2, (249-262).
- G. Clayton, G.R. Graham, K. Higgs, C.H. Holland and D. Naylor (1980). Devonian rocks in Ireland: a review. J. Earth Sci. Royal Dublin Soc. Vol. 2, (161-183).
- D. Collier (1982). Lecture to Irish Association for Economic Geology, Dublin 1982).
- P.G. Coomer and B.W. Robinson (1976). Sulphur and sulphate-oxygen isotopes, and the origin of the Silvermines deposits, Ireland. Mineralium Deposita, Vol. 11, (155-169).
- J.B. Corliss, J. Dymond, L.I. Gordon, J.M. Edmond, R.P. von Herzen, R.D. Ballard, K. Green, D. Williams, A. Bainbridge, K. Crane and T.H. van Andel (1979). Submarine thermal springs on the Galapagos Rift. Science, Vol. 203, (1073-1082).

- E. Cotter (1965). Waulsortian-type carbonate banks in the Mississippian Lodgepole Formation of central Montana. Journal of Geology, Vol. 73, (881-888).
- H. Craig (1969). Geochemistry and origin of the Red Sea brines. In: Hot brines and recent heavy metal deposits in the Red Sea; (E.T. Degens and D.A. Ross, Eds.), Springer-Verlag, New York, (208-242).
- J.H. Crockett and J.W. Winchester (1966). Coprecipitation of zinc with calcium carbonate. Geochim. et Cosmochim. Acta, Vol. 30, (1093-1109).
- C.D. Curtis and D.A. Spears (1968). The formation of sedimentary iron minerals. Economic Geology, Vol. 63, (257-270).
- J.S. Daly and C.T. Williams (1981). Trace element discrimination between barren and mineralised Carboniferous limestones (Abstract). Geochemical methods in mineral prospecting, Utrecht meeting, April 1981.
- L.G. Danielsson, D. Dyrssen and A. Graneli (1980). Chemical investigations of Atlantis II and Discovery brines in the Red Sea. Geochim. et Cosmochim. Acta, Vol. 44, (2051-2065).
- P.J. Davies, B. Bubela and J. Ferguson (1977). Simulation of carbonate diagenetic processes: formation of dolomite, huntite and monohydrocalcite by the reactions between nesquehonite and brine. Chemical Geology, Vol. 19, (187-214).
- R.B. deBoer (1977). Stability of Mg-Ca carbonates. Geochim. et Cosmochim. Acta, Vol. 41, (265-270).
- D.E. Deeny (1981). An Irish Carboniferous metallogenic model. Transactions of the Institution of Mining and Metallurgy, Vol. 90, (B183-185).
- W.A. Deer, R.A. Howie and J. Zussman (1966). An Introduction to the Rock-forming Minerals. Longman, London, (528pp.).
- E.T. Degens, H. Okada, S. Honjo and J.C. Hathaway (1972). Microcrystalline sphalerite in resin globules suspended in Lake Kivu, East Africa. Mineralium Deposita, Vol. 7, (1-12).
- D.R. Derry, G.R. Clark and N. Gillat (1965). The Northgate base metal deposit at Tynagh, Co. Galway, Ireland. Economic Geology, Vol. 60, (1218-1237).
- R. Deurer, U. Förstner and G. Schmoll (1978). Selective chemical extraction of carbonate-associated trace metals from recent lacustrine sediments. Geochim. et Cosmochim. Acta, Vol. 42, (425-429).
- W. Dreybrodt (1981). Mixing corrosion in $\text{CaCO}_3 - \text{H}_2\text{O}$ systems and its role in the karstification of limestone areas. Chemical Geology, Vol. 32, (221-236).
- J.M. Edmond (1981). Hydrothermal activity at mid-ocean ridge axes. Nature, Vol. 290, (87-88).
- F.R. Edmunds (1982). Lecture to Dept. of Applied Geology, University of Strathclyde, 1982.
- S. Emerson, S. Kalhorn, L. Jacobs, K. Neelson and R. Rosson (1982). Environmental oxidation rate of manganese II: Bacterial catalysis. Geochim. et Cosmochim. Acta, Vol. 46, (1073-1079).
- G.T. Emo and E.F. Grennan (1982). A review of mineralisation in the Old Red Sandstone and its significance to Irish exploration. In: Mineral Exploration in Ireland: Progress and Development, 1971-1981, Irish Assoc. Econ. Geol. Dublin, (27-34).
- J.T. Enright, W.A. Newman, R.R. Hessler and J.A. McGowan (1981). Deep-ocean hydrothermal vent communities. Nature, Vol. 289, (219-220).

- V.G. Ethier, F.A. Campbell, R.A. Both and H.R. Krause (1976). Geological setting of the Sullivan orebody and estimates of temperatures and pressures of metamorphism. Economic Geology Vol.71 (1570-1588).
- J. Ferguson and I.B. Lambert (1972). Volcanic exhalations and metal enrichments at Matupi Harbour, New Britain, T.P.N.G. Economic Geology, Vol. 67, (25-37).
- M. Fillion (1973). Economic geology and geostatistics of base metal mineralisation at Silvermines, Ireland. Ph.D. Dissertation, University of London.
- S. Finlay, D.M. Romer and P.C.D. Cazalet (1984). Litho-geochemical studies around the Navan Zn-Pb orebody, Ireland. In: Prospecting in Areas of Glaciated Terrain, Institution of Mining and Metallurgy, London, (35-56).
- T. Finlow-Bates (1980). The chemical and physical controls on the genesis of submarine exhalative orebodies and their implications for formulating exploration concepts: a review. Geol. Jahrb. Vol. 40, (131-168).
- U. Förstner and P. Stoffers (1981). Chemical fractionation of transition elements in Pacific pelagic sediments. Geochim. et Cosmochim. Acta, Vol. 45, (1141-1146).
- J.R. Frank, A.B. Carpenter and T.W. Oglesby (1982). Cathodoluminescence and composition of calcite cement in the Taum Sauk Limestone (Upper Cambrian), S.E. Missouri. Journal of Sedimentary Petrology, Vol. 52, (631-638).
- P.A. Geiser and S. Sansone (1981). Joints, microfractures and the formation of solution cleavage in limestone. Geology Vol. 9, (280-285).
- R. Goldie and T.J. Bottrill (1981). Seminar on seafloor hydrothermal systems. Geoscience Canada Vol. 8, (93-104).
- W.D. Goodfellow (1975). Major and minor element haloes in volcanic rocks at Brunswick No. 12 sulphide deposit, New Brunswick, Canada. In: Geochemical Exploration 1974, (Editors: I.L. Elliott and W.K. Fletcher). Elsevier, Amsterdam, (279-295).
- W.D. Goodfellow, I.R. Jonasson and M.P. Cecile (1980a). Nahanni Integrated Multi-Disciplinary Pilot Project Geochemical Studies, Part I: Geochemistry and mineralogy of shales, cherts, carbonates and volcanic rocks from the Road River Formation, Misty Creek Embayment, Northwest Territories. Geol. Surv. Canada, Paper 80-1A, (149-161).
- W.D. Goodfellow, I.R. Jonasson and M.P. Cecile (1980b). Nahanni Integrated Multi-Disciplinary Pilot Project Geochemical Studies, Part II: Some thoughts on the source, transportation and concentration of elements in shales of the Misty Creek Embayment, Northwest Territories. Geol. Surv. Canada, Paper 80-1B, (163-171).
- G.S. Govett (1976). The development of geochemical exploration methods and techniques. In: World Mineral Supplies - Assessment and Perspective, (G.J.S. Govett and M.H. Govett, Eds.), Elsevier, Amsterdam, (343-376).
- G.S. Govett and I. Nicholl (1979). Litho-geochemistry in mineral exploration. In: Geophysics and geochemistry in the search for metallic ores, Geol. Surv. Canada, Econ. Geol. Report No. 31, (Ed. P.J. Hood), (339-362).
- R.A.F. Graham (1970). The Mogul base metal deposits, Co. Tipperary, Ireland. Ph.D. Dissertation, University of Western Ontario.

- G.J. Gray (1982). Unpublished report to Dresser Minerals, Sept. 1982.
- G.J. Gray and M.J. Russell (1984). Regional Mn-Fe lithogeochemistry of the Lower Carboniferous Waulsortian 'Reef' Limestones in Ireland. In: Prospecting in Areas of Glaciated Terrain 1984, Institution of Mining and Metallurgy, London, (57-68).
- D.A. Grieve and W.K. Fletcher (1976). Heavy metals in deltaic sediments of the Fraser River, British Columbia. Canadian Journal of Earth Science, Vol. 13, (1683-1693).
- E.F. Grennan (1979). Ballynoe baryte deposit. In: Prospecting in Areas of Glaciated Terrain, 1979. Excursion Handbook (Editor A.G. Brown), Irish Assoc. Econ. Geol. Dublin, (66-72).
- E.F. Grennan (1984). The geology and mineralisation of the Courtbrown prospect, Co. Limerick (Abstract). The Geology and Genesis of Mineral Deposits in Ireland, Irish Assoc. Econ. Geol. Dublin.
- J.E. Gunton and I. Nicholl (1975). Chemical zoning associated with the Inger-belle - Copper Mountain mineralisation, Princeton, British Columbia. In: Geochemical Exploration 1974, (I.L. Elliott and W.K. Fletcher, Editors), Elsevier, Amsterdam, (297-312).
- W. Gwosdz and W. Krebs (1977). Manganese halo surrounding the Meggen ore deposit, Germany. Transactions of the Institution of Mining and Metallurgy, Vol. 86, (B73-77).
- W. Gwosdz, H. Kruger and P. Dietmar (1974). The beds underlying the Devonian pyrite and baryte deposits of Eisen (Saarland), Meggen and Rammelsberg, Germany. Geol. Rundsch. Vol. 63, (74-93).
- A. Hajash (1975). Hydrothermal processes along mid-ocean ridge axes: an experimental investigation. Contrib. Mineral. Petrol. Vol. 53, (205-226).
- P.G. Hallof, R.W. Schultz and R.A. Bell (1962). Induced polarisation and geological investigations of the Ballyvergin Copper deposit, Co. Clare, Ireland. Transactions of the American Institute of Mining Engineers, Vol. 223, (312-318).
- C. Halls, A.M. Boast, M.L. Coleman and I.G. Swainbank (1979). Contributed remarks to discussion of Silvermines orebodies. Transactions of the Institution of Mining and Metallurgy Vol. 88 (B129-30).
- R. Hartree and J. Veizer (1982). Lead and zinc distribution in carbonate rocks. Chemical Geology, Vol. 37, (351-365).
- R.S. Haszeldine (1984). Carboniferous North Atlantic palaeogeography: stratigraphic evidence for rifting, not megashear or subduction. Geol. Mag. Vol. 121, (443-463).
- R.M. Haymon and M. Kastner (1981). Hot spring deposits on the East Pacific Rise at 21°N: preliminary description of mineralogy and genesis. Earth and Planetary Science Letters, Vol. 53, (363-381).
- R.M. Hekinian, J.L. Fevrier, J.L. Bischoff, P. Picot and W.C. Shanks (1980). Sulphide deposits from the East Pacific Rise near 21°N. Science, Vol. 207, (1433-1444).
- J.D. Hem (1963). Increased oxidation rates of manganese ions in contact with feldspar grains. U.S. Geol. Surv. Prof. Paper 475-C, (216-217)
- J.D. Hem (1972). Chemical factors that influence the availability of iron and manganese in aqueous systems. Bull. Geol. Soc. America, Vol. 83, (443-450).
- J.D. Hem (1978). Redox processes at surfaces of manganese oxide and their effects on aqueous metal ions. Chemical Geology, Vol. 21, (199-218).

- D.M. Hirst and G.D. Nicholls (1958). Techniques in sedimentary geology: (1) Separation of the detrital and non-detrital fractions of limestones. Journal of Sedimentary Petrology Vol. 28, (468-481).
- C.H. Holland (1981). The geology of Ireland. Scottish University Press, Edinburgh, 1981.
- R. Holmes and J.S. Tooms (1973). Dispersion from a submarine exhalative orebody. In: Geochemical Exploration 1972, (Ed. M.J. Jones), Institution of Mining and Metallurgy, London, (193-202).
- R.R. Horns (1975). Possible transverse fault control of base metal mineralisation in Ireland and Britain. Irish Nature Journal, Vol. 18, (140-144).
- R.G.S. Hudson, M.J. Clarke and T.P. Brennand (1966). The Lower Carboniferous (Dinantian) stratigraphy of the Castleisland area, Co. Kerry, Ireland. Sci. Proc. Royal Dublin Soc. Vol. A2, (297-317).
- J. Hutchings (1979). The Tynagh deposit. In: Prospecting in Areas of Glaciated Terrain, Ireland 1979, Excursion Handbook. (Editor A.G. Brown), Irish Assoc. Econ. Geol. Dublin, (34-46).
- R.W. Hutchinson (1979). Evidence of exhalative origin for Tasmanian tin deposits. C.I.M. Bull. Vol. 72, (90-104).
- M. Ichikuni (1973). Partition of strontium between calcite and solution: effect of substitution by manganese. Chemical Geology, Vol. 11, (315-319).
- P.R. Ineson (1969). Trace element aureoles in limestone wallrocks adjacent to lead-zinc-baryte-fluorite mineralisation in the northern Pennines and Derbyshire orefields. Transactions of the Institution of Mining and Metallurgy, Vol. 78, (B29-40).
- Irish Association for Economic Geology (1979). Mineral exploration in Ireland, Dublin, 1979, (92pp).
- G.V. Jones and N. Bradfer (1982). The Ballinalack zinc-lead deposit, Co. Westmeath, Ireland. In: Mineral Exploration in Ireland: Progress and Developments, 1971-1981, Irish Assoc. Econ. Geol. Dublin, 1982, (47-62).
- D.M. Karl, C.O. Wirsen and H.W. Jannasch (1980). Deep sea primary production at the Galapagos hydrothermal vents. Science, Vol. 207, (1345-1347).
- D.J.J. Kinsman (1969). Interpretation of Sr^{2+} concentrations in carbonate minerals and rocks. Journal of Sedimentary Petrology, Vol. 39, (486-508).
- D.J.J. Kinsman and H.D. Holland (1969). The coprecipitation of cations with $CaCO_3$: IV. The coprecipitation of Sr^{2+} with aragonite between 16° and $96^\circ C$. Geochim. et Cosmochim. Acta Vol. 33, (1-17).
- Y. Kitano (1959). State of manganese in calcium carbonate deposits in thermal springs. Journal of Earth Sciences, Nagoya University, Vol. 7, (65-79).
- Y. Kitano, M. Okumura and M. Idogaki (1980). Abnormal behaviours of copper (II) and zinc ions in parent solution of the early stage of calcite formation. Geochemical Journal, Vol. 14, (167-175).
- C. Klein and O.P. Bricker (1977). Some aspects of the sedimentary and diagenetic environment of Proterozoic banded iron formation. Economic Geology, Vol. 72, (1457-1470).
- G.P. Klinkhammer (1980). Observations of the distribution of manganese over the East Pacific Rise. Chemical Geology, Vol. 29, (211-226).
- G.P. Klinkhammer, M.L. Bender and R.F. Weiss (1977). Hydrothermal manganese in the Galapagos Rift. Nature, Vol. 269, (319-320).
- Y.A. Kozlovsky (1984). The world's deepest well. Scientific American, Vol. 251, (98-104).

- K.B. Krauskopf (1957). Separation of manganese from iron in sedimentary processes. Geochim. et Cosmochim. Acta, Vol. 10, (61-84).
- K.B. Krauskopf (1979). Introduction to Geochemistry. McGraw-Hill, New York, (617pp).
- R. Kretz (1982). A model for the distribution of trace elements between calcite and dolomite. Geochim. et Cosmochim. Acta, Vol. 46, (1979-1981).
- H. Kucha and A. Weiczorek (1984). Sulfide-carbonate relationships in the Navan (Tara) Zn-Pb deposit, Ireland. Mineralium Deposita, Vol. 19, (208-216).
- I.B. Lambert and K.M. Scott (1973). Implications of geochemical investigations within and around the MacArthur River zinc-lead-silver deposit, Northern Territory. Journal of Geochemical Exploration, Vol. 2, (307-330).
- L.S. Land and G.K. Hoops (1973). Sodium in carbonate sediments and rocks: a possible index to the salinity of diagenetic solutions. Journal of Sedimentary Petrology, Vol. 43, (614-617).
- W.M. Landing and K.W. Bruland (1980). Manganese in the North Pacific. Earth and Planetary Science Letters, Vol. 49, (45-56).
- D.E. Large (1980). Geological parameters associated with sediment hosted, submarine exhalative Pb-Zn deposits: an empirical model for mineral exploration. Geol. Jahrb. Vol. 40, (59-129).
- D.E. Large (1983). Sediment-hosted massive sulphide lead-zinc deposits; an empirical model. In: Sediment-hosted stratiform lead-zinc deposits (Ed. D.F. Sangster), Short Course Handbook No. 9, (1-29).
- R.C.L. Larter (in preparation). Ph.D. Dissertation, University of Strathclyde.
- R.C.L. Larter, A.J. Boyce and M.J. Russell (1981). Hydrothermal pyrite chimneys from the Ballynoe baryte deposit, Silvermines, Co. Tipperary, Ireland. Mineralium Deposita, Vol. 16, (309-318).
- N.G. Lavery and H.L. Barnes (1971). Zinc dispersion in the Wisconsin zinc-lead district. Economic Geology, Vol. 66, (226-242).
- A. Lees (1961). The Waulsortian 'reefs' of Eire: a carbonate mudbank complex of Lower Carboniferous age. Journal of Geology, Vol. 69, (101-109).
- A. Lees (1964). The structure and origin of the Waulsortian (Lower Carboniferous) 'reefs' of west-central Eire. Phil. Trans. Royal Soc. Vol. B247, (483-531).
- A. Lees (1982). The palaeoenvironmental setting and distribution of the Waulsortian facies of Belgium and southern Britain. In: Symposium on the Environmental Setting and Distribution of the Waulsortian Facies; El Paso Geol. Soc. and University of Texas, El Paso, (1-16)
- A. Lees and R. Conil (1980). The Waulsortian reefs of Belgium. Geobios Mem. Special. Palaeont. Stratigr. Paleocol. No. 4, (35-46).
- A. Lees and M. Hennebert (1982). Carbonate rocks of the Knap Farm Borehole at Canning Park, Somerset. Report of the Institute of Geological Sciences 82/5, (18-36).
- A. Lees and J. Miller (1985). Facies variation in Waulsortian buildups, Part 2; Mid-Dinantian buildups from Europe and North America. Geological Journal, Vol. 20, (159-180).
- A. Lees, B. Noel and P. Bouw (1977). The Waulsortian 'reefs' of Belgium: a progress report. Mem. Inst. Geol. Louvain, No. 29, (289-315).
- H. Lepp (1963). The relation of iron and manganese in sedimentary iron formations. Economic Geology, Vol. 58, (515-526).

- D.T. Long and E.A. Angino (1982). The mobilisation of selected trace metals from shales by aqueous solutions: effects of temperature and ionic strength. Economic Geology, Vol. 77, (646-652).
- P.F. Lonsdale, J.L. Bischoff, V.M. Burns, M. Kastner and R. Sweeney (1980). A high temperature hydrothermal deposit on the seabed at a Gulf of California spreading centre. Earth and Planetary Science Letters, Vol. 49, (8-20).
- R.B. Lorens (1981). Sr, Cd, Mn and Co distribution coefficients in calcite as a function of calcite precipitation rate. Geochim. et Cosmochim. Acta, Vol. 45, (553-561).
- D.H. Loring (1979). Geochemistry of Co, Ni, Cr and V in the sediments of the estuary and open Gulf of St. Lawrence. Canadian Journal of Earth Science, Vol. 16, (1196-1209).
- A.G. Loudon, M.K. Lee, J.F. Dowling and R. Bourn (1975). Lady Loretta silver-lead-zinc deposit. In; Economic Geology of Australia and Papua New Guinea (Editor C.L. Knight), Monogr. Australas. Inst. Min. Metall. No. 5, Melbourne, (377-382).
- J.S. Lovell, M. Hale and J.S. Webb (1979). Soil-air disequilibria as a guide to concealed mineralisation at Keel, Eire. In: Prospecting in Areas of Glaciated Terrain, 1979. Institution of Mining and Metallurgy, London, (45-50).
- J.E. Lupton, G. Klinkhammer, W.R. Normark, R. Haymon, K. MacDonald, R. Weiss and H. Craig (1980). Helium-3 and manganese at the 21°N East Pacific Rise hydrothermal site. Earth and Planetary Science Letters, Vol. 50, (115-119).
- A.M. Lur'ye (1957). Certain regularities in the distribution of elements in sedimentary rocks of the Northern Bayaldyr District in Central Karatau. Geochemistry, Vol. 5, (470-479).
- M. Lyle (1976). Estimation of hydrothermal manganese input into the oceans. Geology, Vol. 4 (733-736).
- P. McArdle (1978). Tectonic framework of limestone hosted base metal deposits in the Lower Carboniferous of Ireland. Mineral Deposits Studies Group meeting, St. Patrick's Coll. Dublin, Sept. 1978.
- M.B. McBride (1979). Chemisorption and precipitation of Mn^{2+} at $CaCO_3$ surfaces. J. Soil Sci. Soc. America, Vol. 43, (693-698).
- C.V. MacDermot and G.D. Sevastopulo (1972). Upper Devonian and Lower Carboniferous stratigraphical setting of Irish mineralisation. Geol. Surv. Ireland Bull. No. 1, (267-280).
- K.C. MacDonald (1982). Geophysical observations in an active hydrothermal area: the East Pacific Rise at 21°N (Abstract). EOS, Trans. American Geophysical Union, Vol. 62, (912-913).
- K.C. MacDonald, K. Becker, F.N. Speiss and R.D. Ballard (1980). Hydrothermal heat flux of the 'black smoker' vents on the East Pacific Rise. Earth and Planetary Science Letters, Vol. 48, (1-7).
- K.C. MacDonald and J.D. Mudie (1974). Microearthquakes on the Galapagos Spreading Centre and the seismicity of fast spreading ridges. Geophys. J. Royal Astron. Soc. Vol. 36, (245).
- T.R. McHargue and R.C. Price (1982). Dolomite from clay in argillaceous or shale-associated marine carbonates. Journal of Sedimentary Petrology, Vol. 52, (873-886).
- W.C. McQuown and R.C. Price (1982). Stratigraphy and petrology of petroleum producing Waulsortian-type carbonate mounds in the Fort Payne Formation (Lower Mississippian) of North Central Tennessee. Am. Assoc. Petroleum Geol. Bull. Vol. 66, (1055-1075).
- H.G. Machel (1983). Cathodoluminescence in carbonate petrography: some aspects of geochemical interpretation (Abstract). Am. Assoc. Petroleum Geol. Bull. Vol. 67, (507).

- T.R. Marchant and G.D. Sevastopulo (1980). The Calp of the Dublin District, J. Earth Sci. Royal Dublin Soc. Vol. 3, (195-203).
- V. Marchig, H. Gundlach, P. Moller and F. Schley (1982). Some geochemical indicators for discrimination between diagenetic and hydrothermal metalliferous sediments. Marine Geology, Vol. 50, (241-256).
- H. Martin and A. Chabot (1981). Search for new geochemical metallotects in carbonate environments (Abstract). Geochemical Methods in Mineral Prospecting, Utrecht Meeting, April 1981.
- H. Martin and H. Zeegers (1969). Cathodoluminescence et distribution du manganese dans les calcaires et dolomies du Tournaisien Superieur au sud de Dinant (Belgique). Compte Rendu Acad. Sci. Paris, Vol. 269, Series D, (1922-1924).
- W.J. Meyers (1974). Carbonate cement stratigraphy of the Lake Valley Formation (Mississippian), Sacramento Mountains, New Mexico. Journal of Sedimentary Petrology, Vol. 44, (837-861).
- W.J. Meyers (1978). Carbonate cements: their regional distribution and interpretation in Mississippian limestones of Southwestern New Mexico. Sedimentology, Vol. 25, (371-400).
- W.T. Meyers and D.S. Evans (1973). Dispersion of mercury and associated elements in a glacial drift environment at Keel, Eire. In: Prospecting in Areas of Glaciated Terrain 1973, Institution of Mining and Metallurgy, London, (127-138).
- G. Michard (1968). Coprecipitation de l'ion manganoux avec le carbonate de calcium. Compte Rendu Acad. Sci. Paris, Vol. 267, Series D, (1685-1688).
- A.R. Miller, C.D. Densmore, E.T. Degens, J.C. Hathaway, F.T. Manheim, P.F. McFarlin, R. Pocklington and A. Jokela (1966). Hot brines and Recent iron deposits in the deeps of the Red Sea. Geochim. et Cosmochim. Acta, Vol. 30, (341-359).
- J. Miller and R.F. Grayson (1982). The regional context of Waulsortian facies in Northern England. In: Symposium on the Environmental Setting and Distribution of the Waulsortian Facies; El Paso Geol. Soc. and University of Texas, El Paso, 1982, (17-33).
- J.D. Milliman (1974). Marine Carbonates. Springer-Verlag, New York, (375pp).
- I.A. Mirsal and H. Zankl (1979). Petrography and geochemistry of carbonate void-filling cements in fossil reefs. Geol. Rundsch. Bd. 68, (920-951).
- J.M. Moore (1975). Fault tectonics at the Tynagh Mine, Ireland. Transactions of the Institution of Mining and Metallurgy, Vol. 84, (B141-145).
- J.M. Morganti (1979). The geology and ore deposits of the Howards Pass area, Yukon and Northwest Territories; the origin of basinal sedimentary stratiform sulphide deposits. Ph.D. Dissertation, University of British Columbia.
- C.J. Morrissey (1977). Reflections on ores and the apparent scarcity of oil in Irish Carboniferous sediments. In: Proceedings of the Forum on Oil and Ore in Sediments, Imperial College, London, (147-166).
- C.J. Morrissey, G.R. Davis and G.M. Steed (1971). Mineralisation in the Lower Carboniferous of central Ireland. Transactions of the Institution of Mining and Metallurgy, Vol. 80, (B174-185).
- J. Morrisson and U. Brand (1983). Chemical diagenesis of Pennsylvanian Brush Creek (Pennsylvania) carbonate components: trace elements (Abstract). Am. Assoc. Petroleum Geol. Bull. Vol. 67, (520).

- D.W. Morrow (1984). Diagenesis 1. Dolomite - Part 1: The chemistry of dolomitisation and dolomite precipitation. Geoscience Canada, Vol. 9, (5-13).
- D.W. Morrow and I.R. Mayers (1978). Simulation of limestone diagenesis - a model based on strontium depletion. Canadian Journal of Earth Science, Vol. 15, (376-396).
- D.J. Mossman and K.J. Heffernan (1978). On the possible primary precipitation of atacamite and other metal chlorides in certain stratabound deposits. Chemical Geology, Vol. 21, (151-159).
- M.J. Mottl and H.D. Holland (1978). Chemical exchange during hydrothermal alteration of basalt by seawater - I. Experimental results for major and minor components of seawater. Geochim. et Cosmochim. Acta, Vol. 42, (1103-1115).
- M.J. Mottl, H.D. Holland and R.F. Corr (1979). Chemical exchange during hydrothermal alteration of basalt by seawater - II. Experimental results for Mn, Fe and sulfur species. Geochim. et Cosmochim. Acta, Vol. 43, (869-884).
- G.G. Mustoe (1981). Bacterial oxidation of manganese and iron in a modern cold spring. Bull. Geol. Soc. America, Vol. 92, (147-153).
- R.R. Nair and N.H. Hashimi (1981). Mineralogy of the carbonate sands - western continental shelf of India. Marine Geology, Vol. 41, (309-319).
- P.E. Nawrocki and D.M. Romer (1979). A buried anomaly associated with a float train in central Ireland. In: Prospecting in Areas of Glaciated Terrain 1979. Institution of Mining and Metallurgy, London, (40-44).
- D. Naylor and P.C. Jones (1967). Sedimentation and tectonic setting of the Old Red Sandstone of Southwest Ireland. In: International Symposium on the Devonian System, Vol. II, Alberta Soc. Petroleum Geol. Calgary, (1089-1099).
- A.C. Neumann, J.W. Kofoed and G.H. Keller (1977). Lithoherms in the Straits of Florida. Geology, Vol. 5, (4-10).
- J. Negebauer (1974). Some aspects of cementation in chalk. In: Pelagic sediments on land and under the sea. International Assoc. Sedimentologists, Spec. Paper 1, (149-176).
- W.E. Nevill (1958). The Carboniferous knoll-reefs of east-central Ireland. Proc. Royal Irish Acad. Vol. 59B, (285-303).
- W.E. Nevill (1962). Stratigraphy and origin of the Cork Red Marble. Geol. Mag. Vol. 49, (481-491).
- V. Ogorelic and P. Rothe (1979). Diagenetische entwicklung und fazies bhängige Na - Verteilung in Karbonat-Gesteinen Sloweniens. Geol. Rundsch. Bd. 68, (965-978).
- M.A. Olade and W.K. Fletcher (1976). Trace element geochemistry of the Highland Valley and Guichon Creek Batholith in relation to porphyry copper mineralisation. Economic Geology, Vol. 71, (733-748).
- P.P. Parekh, P. Möller, P. Dulski and W.M. Bausch (1977). Distribution of trace elements between carbonate and non-carbonate phases of limestone. Earth and Planetary Science Letters, Vol. 34, (39-50).
- M.E. Philcox (1963). Banded calcite mudstone in the Lower Carboniferous 'reef' knolls of the Dublin Basin, Ireland. Journal of Sedimentary Petrology, Vol. 33, (904-913).

- M.E. Philcox (1967). A Waulsortian Bryozoan Reef ('cumulative biostrome') and its off-reef equivalents, Ballybeg, Ireland. Compte Rendu, XI International Congress, Stratigraphy and Geology of the Carboniferous, Sheffield, England, (1359-1372).
- M.E. Philcox (1984). Lower Carboniferous lithostratigraphy of the Irish Midlands. Irish Assoc. Econ. Geol. Dublin, (89pp).
- W.E.A. Phillips (1983). Correlation of geological, geochemical and geophysical data with satellite imagery, west-central Ireland. E.E.C. Seminar on Geophysical Methods, University College, Dublin, Oct. 1983.
- W.E.A. Phillips, C.J. Stillman and T.A. Murphy (1976). A Caledonian plate tectonic model. Journal of the Geological Society of London, Vol. 132, (579-609).
- N.E. Pingitore (1976). Vadose and phreatic diagenesis: processes, products and their recognition in corals. Journal of Sedimentary Petrology, Vol. 46, (60-67).
- N.E. Pingitore (1978). The behaviour of Zn^{2+} and Mn^{2+} during carbonate diagenesis: theory and applications. Journal of Sedimentary Petrology, Vol. 48, (799-814).
- N.E. Pingitore (1982). The role of diffusion during carbonate diagenesis. Journal of Sedimentary Petrology, Vol. 52, (27-39).
- N.E. Pingitore and J. Eastman (1984). The experimental partitioning of Ba^{2+} into calcite. Chemical Geology, Vol. 45, (113-120).
- I.R. Plimer (1980). Exhalative Sn and W deposits associated with mafic volcanism as precursors to Sn and W deposits associated with granites. Mineralium Deposita, Vol. 15, (275-289).
- I.R. Plimer and S.M. Elliott (1979). The use of Rb/Sr ratios as a guide to mineralisation. Journal of Geochemical Exploration, Vol. 12, (21-34).
- I.R. Plimer and T. Finlow-Bates (1978). Relationship between primary iron sulphide species, sulphur source, depth of formation and age of submarine exhalative sulphide deposits. Mineralium Deposita, Vol. 13, (399-410).
- B. Pomerol (1977). Le probleme du levissage des phyllites dans le dosage par Absorption Atomique des elements traces dans les carbonates. Chemical Geology, Vol. 19, (61-71).
- A. Poustie and H. Kucha (1984). The style and setting of Pb-Zn mineralisation in the Moyvoughly area, Co. Westmeath (Abstract). In: The Geology and Genesis of Mineral Deposits in Ireland, Irish Assoc. Econ. Geol. Dublin 1984.
- B.R. Pratt (1982). Stromatolitic framework of carbonate mudmounds. Journal of Sedimentary Petrology, Vol. 52, (1203-1227).
- L.C. Pray (1958). Fenestrate bryozoan core facies, Mississippian bioherms, southwestern United States. Journal of Sedimentary Petrology, Vol. 28, (261-273).
- L.C. Pray (1969). Micrite and carbonate cement: Genetic factors in Mississippian bioherms. Journal of Palaeontology Abstracts, Vol. 43, (895).
- R.M. Pytkowicz (1965). Rates of inorganic calcium carbonate nucleation. Journal of Geology, Vol. 73, (196-199).
- B. Radke and R.L. Mathis (1980). On the formation and occurrence of saddle dolomite. Journal of Sedimentary Petrology, Vol. 50, (1149-1168).

- A.S. Radtke, M.J. Russell and F.W. Dickson (1977). Relationships between minor elements in Palaeozoic sedimentary rocks and the distribution and chemical composition of base metal deposits in Ireland. Geol. Soc. America Annual Meeting, Seattle, Washington (Abstracts).
- R. Raiswell and P. Brimblecombe (1977). The partition of manganese into aragonite between 30° and 60°C. Chemical Geology, Vol. 19, (145-151).
- C.G. Rao (1981). Carbonate/clay mineral relationships and the origin of protodolomite in L-2 and L-3 carbonate reservoir rocks of the Bombay High Oil Field, India. Sedimentary Geology, Vol. 29, (223-232).
- C.P. Rao (1981). Geochemical differences between tropical (Ordovician) and sub-polar (Permian) carbonates, Tasmania, Australia. Geology, Vol. 9, (205-209).
- S. Ray, H.R. Gault and C.G. Dodd (1957). The separation of clay minerals from carbonate rocks. American Mineralogist, Vol. 42, (681-686).
- A. Reay (1981). The effect of disc-mill grinding on some rock-forming minerals. Mineral Magazine, Vol. 44, (179-182).
- M. Renard and P. Blanc (1972). Influence des conditions de mise en solution (choix de l'acide, temperature, duree d'attaque) dans le dosage des elements en traces des roches carbonatees. Compte Rendu Acad. Sci. Paris, Vol. 274, (632-635).
- H.N. Rhoden (1960). Mineralogy of the Silvermines District, Co. Tipperary, Ireland. Mineral Magazine, Vol. 32, (128-139).
- D.K. Richter and H. Fuchtbauer (1978). Ferroan calcite replacement indicates former magnesian calcite skeletons. Sedimentology, Vol. 25, (843-860).
- D. Riedel (1980). Elektronenmikroskopische untersuchungen an sphäroiden aus dem erz der Pb-Zn lagerstätte Tynagh, Irland. Mineralium Deposita, Vol. 15, (101-110).
- D. Riedel (1980). Ore structures and genesis of the lead-zinc deposit, Tynagh, Ireland. Geol. Rundsch. Vol. 69, (361-383).
- R. Rispoli (1981). Stress fields about strike-slip faults inferred from stylolites and tension fractures. Tectonophysics, Vol. 75, (T29-T36).
- G. Riverin and C.J. Hodgson (1980). Wall-rock alteration at the Millenbach Cu-Zn Mine, Noranda, Quebec. Economic Geology, Vol. 75, (424-444).
- R.G. Roberts and E.J. Reardon (1978). Alteration and ore-forming processes at Mattagami Lake Mine, Quebec. Canadian Journal of Earth Science, Vol. 15, (1-21).
- P.Y.F. Robin (1978). Pressure solution at grain to grain contacts. Geochim. et Cosmochim. Acta, Vol. 42, (1383-1390).
- P. Robinson (1980). Determination of Ca, Mg, Mn, Sr, Na and Fe in the carbonate fraction of limestones and dolomites. Chemical Geology, Vol. 28, (135-146).
- P.A. Rona (1984). Hydrothermal mineralisation at seafloor spreading centres. Earth Science Reviews, Vol. 20, (1-104).
- R.J. Ross, V. Janusson and I. Friedman (1975). Lithology and origin of Middle Ordovician calcareous mudmounds at Meiklejohn Peak, Southern Nevada. U.S. Geol. Surv. Prof. Paper 871, (48pp).

- M.J. Russell (1968). Structural controls of base metal mineralisation in Ireland in relation to continental drift. Transactions of the Institution of Mining and Metallurgy, Vol. 87, (B168-171).
- M.J. Russell (1971). North-south geofractures in Scotland and Ireland. Scottish Journal of Geology, Vol. 8, (75-84).
- M.J. Russell (1972). The geological environment of post-Caledonian base metal mineralisation in Ireland. Ph.D. Dissertation, University of Durham.
- M.J. Russell (1973). Base metal mineralisation in Ireland and Scotland and the formation of the Rockall Trough. In: Implications of Continental Drift to the Earth Sciences (D.H. Tarling and S. Runcorn, Eds.), Academic Press, Vol. 1, (581-597).
- M.J. Russell (1974). Manganese halo surrounding the Tynagh ore deposit, Ireland: a preliminary note. Transactions of the Institution of Mining and Metallurgy, Vol. 83, (B65-66).
- M.J. Russell (1975). Lithochemical environment of the Tynagh base metal deposit, Ireland, and its bearing on ore deposition. Transactions of the Institution of Mining and Metallurgy, Vol. 84, (B128-133).
- M.J. Russell (1976). Incipient plate separation and possible related mineralisation in lands bordering the North Atlantic. Geol. Assoc. Canada Special Paper 14, (339-349).
- M.J. Russell (1978). Technical note: Downward excavating hydrothermal cells and Irish-type ore deposits: Importance of an underlying thick Caledonian prism. Transactions of the Institution of Mining and Metallurgy, Vol. 87, (B167-171).
- M.J. Russell (1983). Major sediment-hosted exhalative zinc+lead deposits: formation from hydrothermal convection cells that deepen during crustal convection. In: Sediment-hosted stratiform lead-zinc deposits (D.F. Sangster, Ed.), Min. Assoc. Canada Short Course Handbook 8, (251-282).
- M.J. Russell, M. Solomon and J.L. Walshe (1981). The genesis of sediment-hosted exhalative zinc+lead deposits. Mineralium Deposita, Vol. 16, (113-127).
- I.M. Samson (1983). Fluid inclusion and stable isotope studies of the Silvermines orebodies, Ireland, and comparisons with Scottish vein deposits. Ph.D. Dissertation, University of Strathclyde.
- I.M. Samson and M.J. Russell (1983). Fluid inclusion data from Silvermines base metal - baryta deposits, Ireland. Transactions of the Institution of Mining and Metallurgy, Vol. 92, (B67-71).
- T. Sato (1972). Behaviour of ore forming solutions in seawater. Mining Geology, Vol. 22, (31-42).
- W. Schlager and N.P. James (1978). Low-magnesian calcite limestone forming at the deep-sea floor, Tongue of the Ocean, Bahamas. Sedimentology, Vol. 25, (675-702).
- R.W. Schultz (1966). Lower Carboniferous cherty ironstones at Tynagh, Ireland. Economic Geology, Vol. 61, (311-342).
- R.W. Schultz (1971). Mineral exploration practice in Ireland. Transactions of the Institution of Mining and Metallurgy, Vol. 80, (B238-258).
- W. Schwarzacher (1961). Petrology and structure of some Lower Carboniferous reefs in N.W. Ireland. Am. Assoc. Petroleum Geol. Bull. Vol. 45, (1481-1503).
- G.D. Sevastopulo (1979). The stratigraphic setting of base metal deposits in Ireland. In: Prospecting in Areas of Glaciated Terrain 1979. Institution of Mining and Metallurgy, London, (8-15).

- G.D. Sevastopulo (1981). The Lower Carboniferous. In: A Geology of Ireland, (Ed. C.H. Holland), Scottish Academic Press, Edinburgh, (147-171).
- G.D. Sevastopulo and W.E.A. Phillips (1984). The stratigraphic and structural setting of Irish base metal deposits in Upper Palaeozoic rocks. In: The Geology and Genesis of Mineral Deposits in Ireland. Irish Assoc. Econ. Geol. Dublin, (Abstract).
- W. Seyfried and J.L. Bischoff (1977). Hydrothermal transport of heavy metals by seawater: the role of seawater/basalt ratio. Earth and Planetary Science Letters, Vol. 34, (71-77).
- W.C. Shanks and J.L. Bischoff (1980). Geochemistry, sulfur isotope composition and accumulation rates of Red Sea geothermal deposits. Economic Geology, Vol. 75, (445-459).
- D.J.R. Sheridan (1977). The hydrocarbons and mineralisation proved in the Carboniferous strata of deep boreholes in Ireland. In: Proceedings of the Forum on Oil and Ore in Sediments, Imperial College, London, (114-146).
- E.D. Slowey (1984). The Keel Zn-Pb deposit, Co. Longford: a review and update (Abstract). In: The Geology and Genesis of Mineral Deposits in Ireland; Irish Assoc. Econ. Geol. Dublin, 1984.
- M. Solomon and J.L. Walshe (1979). The formation of massive sulphide deposits on the seafloor. Economic Geology, Vol. 74, (797-813).
- M. Solomon and J.L. Walshe (1979). The behaviour of massive sulphide ore solutions entering seawater and the development of zoned deposits. Bulletin Mineralogie, Vol. 102, (463-470).
- R.L. Stanton (1976). Petrochemical studies of the ore environment at Broken Hill, New South Wales: 1 - Constitution of 'banded iron formation'. Transactions of the Institution of Mining and Metallurgy, Vol. 85, (B33-41).
- G.M. Steed and P. Tyler (1979). Lithogeochemical haloes about Gortdrum copper-mercury orebody, Co. Tipperary, Ireland. In: Prospecting in Areas of Glaciated Terrain 1979; Institution of Mining and Metallurgy, London, (30-40).
- E.F. Stumpfl (1979). Manganese haloes surrounding metamorphic stratabound base metal deposits. Mineralium Deposita, Vol. 14, (207-217).
- B. Sundby, N. Silverburg and R. Chesselet (1981). Pathways of manganese in an open estuarine system. Geochim. et Cosmochim. Acta, Vol. 45, (293-307).
- F.M. Sygne (1979). Quaternary Glaciation in Ireland. In: Prospecting in Areas of Glaciated Terrain, 1979; Institution of Mining and Metallurgy, London, (1-7).
- S. Taylor (1984). Structural and palaeotopographic controls of lead-zinc mineralisation in the Silvermines orebodies, Ireland. Economic Geology, Vol. 79, (529-548).
- S. Taylor and C.J. Andrew (1978). Silvermines orebodies, Co. Tipperary, Ireland. Transactions of the Institution of Mining and Metallurgy, Vol. 87, (B111-124).
- A. Tsusue and H.D. Holland (1966). The coprecipitation of ions with CaCO_3 : III. The coprecipitation of Zn^{2+} with calcite between 80 and 250°C. Geochim. et Cosmochim. Acta, Vol. 30, (439-453).
- M. Tucker (1982). Precambrian dolomites: petrographic and isotopic evidence that they differ from Phanerozoic dolomites. Geology, Vol. 10, (7-12).
- K.K. Turekian (1972). Chemistry of the earth. Holt, Reinhart and Winston. New York, (131pp).

- J.S. Turner and L.B. Gustafson (1978). The flow of hot saline solutions from vents in the sea floor - some implications for exhalative massive sulphide and other ore deposits. Economic Geology, Vol. 73, (1082-1100).
- J.N. Valette (1973). Distribution of certain trace elements in marine sediments surrounding Vulcano Island (Italy). In: Ores in Sediments (Ed. G.C. Amstutz and A.J. Bernard), Springer-Verlag, New York, 1973, (321-337).
- J. vanOrsmael, W. Viaene and J. Bouckaert (1980). Lithogeochemistry of Upper Tournaisian and Lower Viséan carbonate rocks in the Dinant Basin, Belgium: A preliminary report. Meded. Rijks. Geol. Deinst. Vol. 32, (96-100).
- J. Veizer (1977). Geochemistry of lithographic limestones and dark marls from the Jurassic of Southern Germany. Neues Jahrb. Geol. Palaont. Abh. Vol. 153, (129-146).
- J. Veizer (1978). Secular variations in the composition of sedimentary carbonate rocks II: Fe, Mn, Ca, Mg, Si and minor constituents. Precambrian Research, Vol. 6, (381-413).
- J. Veizer and R. Demovic (1974). Strontium as a tool in facies analysis. Journal of Sedimentary Petrology, Vol. 44, (93-115).
- J. Veizer, J. Lemieux, B. Jones, M. Gibling and J. Savelle (1977). Sodium: palaeosalinity indicator in ancient carbonate rocks. Geology, Vol. 5, (177-179).
- J. Veizer (1977). Diagenesis of preQuaternary carbonates as indicated by tracer studies. Journal of Sedimentary Petrology Vol. 47, (565-581).
- V.M.V. Vidal, F.V. Vidal, J.D. Isaacs and D.R. Young (1978). Coastal submarine hydrothermal activity off Northern Baja California. Journal of Geophysical Research, Vol. 83, (1757-1774).
- G.H. Wagner, R.H. Konig, D.A. Smith, K.F. Steele and D.L. Zachry (1979). Geochemistry of Carboniferous limestone units in Northwest Arkansas. Chemical Geology, Vol. 24, (293-313).
- R.N. Walker, R.G. Logan and J.G. Binnekamp (1977). Recent geological advances concerning the H.Y.C. and associated deposits, McArthur River, N.T. Journal of the Geological Society of Australia, Vol. 24, (365-380).
- H.R. Wanless (1979). Limestone response to stress: pressure solution and dolomitisation. Journal of Sedimentary Petrology, Vol. 49, (437-462).
- H.R. Wanless (1982). Limestone response to stress: pressure solution and dolomitisation. Reply to discussion by B.R. Pratt. Journal of Sedimentary Petrology, Vol. 52, (323-332).
- N. Wardlaw, A. Oldershaw and M. Stout (1978). Transformation of aragonite to calcite in a marine gastropod. Canadian Journal of Earth Science, Vol. 15, (1861-1866).
- R.J. Watling (1976). Trace element distribution in primary sulphide minerals from the Keel prospect, County Longford. Proc. Royal Irish Acad. Vol. B76, (241-262).
- P. Weyl (1959). Pressure solution and the force of crystallisation - a phenomenological theory. Journal of Geophysical Research, Vol. 64, (2001-2025).
- A.F. White (1978). Sodium coprecipitation in calcite and dolomite. Chemical Geology, Vol. 23, (65-72).
- D.E. White (1965). Metal contents of some geothermal fluids. In: Symposium, problems of post-magmatic ore deposition, Prague 1963, Vol. 2, (432-443).

- D.E. White (1968). Environments of generation of some base-metal ore deposits. Economic Geology, Vol. 63, (301-335).
- R.E. Whitehead (1973). Environment of stratiform sulphide deposition; variation in Mn:Fe ratio in host rocks at Heath Steel Mine, New Brunswick, Canada. Mineralium Deposita, Vol. 8, (148-160).
- R.E. Whitehead and G.J.S. Govett (1974). Exploration rock geochemistry - detection of trace element haloes at Heath Steel Mines (New Brunswick, Canada), by discriminant analysis. Journal of Geochemical Exploration, Vol. 3, (371-396).
- D.G. Wilbur and J.S. Carter (1984). Two aspects of copper and silver mineralisation at Mallow, Co. Cork (Abstract). In: The Geology and Genesis of Mineral Deposits in Ireland; Irish Assoc. Econ. Geol. Dublin 1984.
- D.G. Wilbur and J.J. Royale (1975). Discovery of the Mallow copper-silver deposit, County Cork, Ireland. In: Prospecting in Areas of Glaciated Terrain 1975; Institution of Mining and Metallurgy, London, (60-70).
- C.E. Williams and P. McArdle (1978). Ireland. In: Mineral Deposits of Europe, Vol. 1: Northwest Europe, (Eds. S.H.U. Bowie, A. Kiralheim and H.W. Haslam), Institution of Mining and Metallurgy, London, (319-345).
- J.L. Wilson (1975). Carbonate facies in geologic history. Springer-Verlag, Berlin, (471pp).
- H. Zantop (1978). Geologic setting and genesis of iron oxides and manganese oxides in the San Francisco manganese deposit, Jalisco, Mexico. Economic Geology, Vol. 73, (1137-1149).
- H. Zantop (1981). Trace elements in volcanogenic manganese oxides and iron oxides - The San Francisco manganese deposit, Jalisco, Mexico. Economic Geology, Vol. 76, (545-555).
- N.N. Zhabina and V.S. Sokolov (1982). Sulphur compounds in the sediments of the Atlantis II Deep, Red Sea. Marine Geology, Vol. 50, (129-142).

ADDENDUM.

- K.L. Von Damm, J.M. Edmond, B. Grant, C.I. Measures, B. Walden and R.F. Weiss (1985). Chemistry of submarine hydrothermal solutions at 21°N, East Pacific Rise. Geochim. et Cosmochim. Acta, Vol. 49, (2197 - 2220).